TRANSPORTATION RESEARCH
RECORD

No. 1268

Materials, Construction, and Maintenance

Highway Maintenance Operations and Research 1990

A peer-reviewed publication of the Transportation Research Board

Transportation Research Record 1268

Contents

Foreword

Maintenance organizations are being asked to maintain the nation's aging transportation infrastructure with fewer maintenance dollars and fewer maintenance employees than they have had in the past. The papers in this Record contain information on innovative maintenance techniques and materials, and management programs used in the United States and several other countries to assist the maintenance engineer in meeting the challenges of the 1990s.

Renault and Allez describe the development and use of MEDITER, an expert computer system for assessing the cost of deferring pavement rehabilitation. MEDITER was integrated with ERASME to determine the cost of rehabilitating flexible pavements at selected times in the future, and thus can be used to evaluate the effect of funding constraints on a pavement rehabilitation program.

Chong discusses the cost-effectiveness of route and seal treatments of cracks in flexible pavement as a preventive maintenance procedure. The author provides information on cost-effectiveness of the rout and seal procedure, effects on pavement life, and optimum timing for application to achieve maximum cost benefit.

Failure modes in portland cement concrete (PCC) pavement joints and requirements for development of improved joint sealant systems are described by Belangie. At the time of failure, individual joint failure modes are distinctive, but wear and weather-related deterioration can alter their characteristics. The loss of these characteristics can result in misinterpretation of the cause of joint failure and may lead to inappropriate remedial actions.

El-Sheikh et al. describe the results of Indiana's efforts to reduce reflective cracks in asphalt overlays over deteriorated concrete pavements using cracking and seating. The researchers provide data on the effectiveness of cracking and seating after 5 years of service and on the performance of the asphalt overlay mixture with fibers added.

Results of a national study investigating the performance of sawing and sealing of joints in asphalt overlays on existing PCC pavements are presented by Kilareski and Bionda. Condition surveys, roughness measurements, and deflection measurements were taken on overlays with up to 10 years of service life. The authors describe changes in rideability and in the amount of transverse reflection cracking.

Darter and Hall describe an evaluation of the effect on ride quality of diamond grinding of jointed concrete pavements. The researchers surveyed and analyzed data from 76 diamond-grinding projects in 19 states. Information on the effects of diamond grinding on pavement life and the cost-effectiveness of repairs is also provided.

Thomas and Anderson report on a field evaluation of five experimental binders used to produce cold-stockpiled patching materials for repairs in cold, wet weather. The experimental mixes used a latex-modified MC–800 cutback and four high-float, medium-set emulsion binders. Information is provided on the operational and economic effectiveness of the experimental patching materials.

Harper et al. present the methodology and procedures used in selecting maintenance strategies in a network-level bridge management system (BMS). The authors describe the condition and maintenance and repair modules of the seven modal BMSs. These modules were used to record bridge condition data, identify corrective maintenance strategies, and determine the resulting condition for each strategy. In a companion paper, Harper et al. describe the prediction and stochastic optimization modules of the BMS. The prediction model generates estimates of the condition of bridge segments across time, and the optimization model determines the minimum cost subject to management's performance objectives.

Saito and Sinha describe the timing for bridge replacement, rehabilitation, and maintenance activities. Input variables to this process are timing and cost of activities, and effect of the activities on bridge condition. The results of life-cycle cost analysis are sensitive to the timing of future bridge repairs.

Chen and Johnston describe a method for evaluating optimum bridge management decisions for maintenance, rehabilitation, and replacement. The authors used an equivalent annualized cost approach with user and owner costs to forecast the optimum time and cost for maintenance actions on bridges. By summing these costs, the future funding needs and number of improvements can be predicted.

Al-Subhi et al. present an overview of OPBRIDGE, an integrated bridge budget forecasting and allocation module at the state level. This system has the capability of predicting funding requirements to achieve bridge system objectives or to allocate limited budgets optimally and of predicting performance of the bridge system. In a companion paper, Al-Subhi et al. describe a resource-constrained capital budgeting model for bridge maintenance, rehabilitation, and replacement. The optimal alternatives are selected on the basis of the criterion of maximizing reductions in equivalent uniform annual costs to the user-taxpayer.

An overview of a statewide underwater bridge inspection program for the state of Mississippi is provided by Avent and Whitmer. The authors provide information on inspection methodology, types of equipment, and the evaluation process used.

Graber provides a summary of bridge inspection efforts on the Chesapeake Bay Bridge-Tunnel. The author describes visual inspection methods used on all substructure elements, hands-on inspection methods for selected bents, and in-depth evaluation methods for selected piles.

The results of a repetitive load test conducted on a laboratory model to study the deterioration of connections in precast decked-steel bridges are presented by Osegueda and Noel. The researchers recorded loads, deflections, strains, and relative deck-beam displacements at several time windows.

Ghorbanpoor reports use of an acoustic emission (AE) technique to locate and characterize initiation fatigue crack signals in bridge structural components. The author conducted tests on welded and rolled beams, and an in-service bridge. The results are described in terms of detection within the fatigue crack life and the characteristics of the AE signals received.

The use of the p-median model to determine the best number of field maintenance offices and their optimum locations is described by Turner et al. If optimized on lane-miles served, the model minimizes the distance between the facilities and the maintenance work sites. The model can also be adapted to optimize two levels of maintenance offices.

Markow et al. present the results of an analysis of the Highway Maintenance and Operations Cost Index published annually by FHWA. The authors evaluate the procedures used to develop the cost index and propose alternatives to improve its effectiveness.

The development of a maintenance management system for a network of gravel roads is reported by Männistö and Tapio. This Finnish system uses an optimization model based on semi-Markovian models, and is divided into 1-year and multiyear submodels. The system can be used to divide funds between maintenance districts and to set up objective maintenance standards.

McElroy et al. report a laboratory study of ice undercutting and disbondment characteristics of deicer chemicals. Ten chemical deicers were studied—six discrete deicing chemicals and four blends. The results are reported in terms of the percent of undercutting necessary for ice removal by the force of a plow blade.

Experimental procedures and measurement techniques used in the evaluation of corrosion inhibitors for reinforced concrete are described by Beaudoin et al. Results obtained with the selected inhibitor, which can be applied as a curative or a preventive means to protect reinforced concrete, are presented.

Buchholz reports the use of lignosulfonates in deicing salts to reduce corrosion of rebars in concrete. The author observed reductions in chloride levels when a small percentage of lignosulfonate was added to sodium and magnesium chloride solutions.

Corrosion characteristics of straight and bent epoxy-coated reinforcing steel are described by Sohanghpurwala and Clear. Variables included suppliers, bend diameter, coating thickness, coating application before and after fabrication of the bar, rate of bending, temperature of steel during bending, and patching of damaged areas before installation. The results are reported in terms of measurable macrocell corrosion currents.

Livneh and Craus report use of economic models for setting priorities for road maintenance and rehabilitation in Israel. The authors assessed the existing condition of the road network, determined the cost to improve the service level, and evaluated the effect on the national economy to justify the investment in road maintenance. These models were then used to establish priority rankings for pavement overlays.

MEDITER, A Model for Assessment of Rehabilitation Delay Cost in ERASME

DANIEL RENAULT AND FRÉDÉRIC ALLEZ

An expert system was developed to assess maintenance delay opportunity. This project relied on previous works in the field of pavement condition prediction, particularly those of the Highway Design and Maintenance Model. MEDITER is a model that mixes theoretical and experimental results. It is integrated into the ERASME project, the aim of which was to build a multiexpert system for pavement rehabilitation. An application of MEDITER to an actual example is presented, and conclusions are drawn.

Under funding constraints, pavement managers are interested in delaying needed rehabilitation on some network sections. However, no tool is available to enable pavement managers to assess pavement rehabilitation delay cost. Such cost is linked to

- Curative maintenance before actual rehabilitation, and
- Rehabilitation cost increase when delayed.

Although some theoretical works and experimental results have been published, no explicit information is available in France for predicting future pavement conditions without rehabilitation.

The research objectives were to

1. Elicit knowledge in the field of pavement condition prediction using results from the Highway Design and Maintenance (HDM) Model concepts (*1*), mechanistic rational analysis, and experimental results, particularly those given by the Laboratoire Central des Ponts et Chaussées (LCPC, France) Circular Test Track (CTT) (*2*);
2. Create a model for rehabilitation delay cost; and
3. Encode elicited knowledge into an expert system integrated in ERASME (*3*) architecture.

STATE OF THE ART

Many flexible pavement distress prediction models exist in the world, most of them in the United States.

Empirical Models

The AASHTO model was developed from the AASHO Road Test and incorporated into the AASHTO Interim Guide (*4*). This model is based on empirical observations and provides the predicted loss of serviceability, which is closely related to roughness, over a given range of values.

Large empirical studies conducted in Kenya and Brazil led to the HDM Model, which is probably the most comprehen-

sive model at the present time, because it yields prediction of

- Cracking with initiation and progression phases, during which the cracking increases in extent and severity. Initiation and progression are predicted in two categories, all cracking (width not less than 1 mm) and wide cracking (spalled cracks).
  - Rutting with mean rut depth and standard deviation.
  - Ravelling initiation and progression.
  - Potholing initiation and progression.
  - Roughness progression.

HDM 3 Concepts

The growth of the cracking area of a given severity is a bell-shaped function with respect to time. As bell-shaped functions are awkward for modeling purposes, a cumulative total is defined, which represents the sum of all cracking areas of a severity not less than a given class of severity. The extent of cracking increases monotonically and presents a sigmoidal shape. The model takes into account uncertainty in the predictions because of variability of structural properties, drainage characteristics, construction quality, etc., over nearly homogeneous sections of pavement. The model automatically divides each section into three subsections identified as weak, medium, and strong to yield, for example, the ages at which the cracking of the three subsections (representing early, medium, and late failures) are expected.

Probabilistic Model

An original approach, developed by the Arizona Department of Transportation (*5*), takes into account the probabilistic aspect of road deterioration. This approach is derived from an Arizona data base that describes roughness and cracking progression. This process is Markovian and annually recursive, predicting indicator changes in 1 year as functions of previous values and environmental factors.

Mixing Empirical and Mechanistic Approaches

Mechanistic or theoretical methods based on the mechanical properties of materials and structural analysis of the pavement are invaluable for identifying the key variables and appropriate functional forms of distress evolution. When calibrated and validated to real conditions, the quality of predictions obtained by these methods appears better than that given by purely empirical methods.

C.E.T.E. Mediterranée, B.P. 39, 13762 Les Milles Cédex, France.

HDM 3 and VESYS (*6*) mix empirical and mechanistic approaches. VESYS is an FHWA structural subsystem that has been used by various agencies and universities throughout the United States. VESYS computes stresses, strains, deflection, rutting, cracking damage, and roughness.

State of the Art in France

There is one currently nonvalidated distress prediction model in France which consists of empirical laws concerning changes in deterioration, derived from the analysis of a data bank. This model was implemented in a pavement management system (PMS) for road networks (*7*). Normal cumulative distribution functions were established that yield percentages of pavements for several distress levels. Investigation continues according to these empirical laws.

Some prediction capability is available as follows:

1. The CTT has provided evolution curves of cracking and rutting on different pavement types. Cracking fatigue results are in accordance with those expected by elastic theory (*8*).
2. The unbound granular material and soil behavior study and the associated creation of a numerical analysis model (*9*) using finite elements have enabled a nonlinear elastic modelization of unbound aggregate materials and soils to be derived from experimental laboratory tests on several such materials. Knowing certain behavior laws, the rutting of a flexible pavement versus cycle number at different depths of the pavement can be obtained. Low-cost devices are currently under development in France to assess behavior laws of field pavement materials.
3. A satisfactory connection has been obtained between pavement distress condition in terms of cracking and repairs and the theoretical risk derived from elastic and fatigue theory at a known cumulative traffic level on a test section of a highway network (*10*). The pavement test section had three layers of asphalt materials with a total thickness of 30 cm built on 40 cm of unbound, well-graded aggregate.

Knowledge for building a model such as MEDITER does exist.

MEDITER MODEL

MEDITER includes two functions:

1. Forecasting evolution of key flexible pavement distress in the case of a rehabilitation or reconstruction delay, using the flexible pavement distress prediction (FPDP) model; and
2. Assessing maintenance cost increases caused by a rehabilitation or reconstruction delay (for which maintenance includes surface dressings, pothole patching, rehabilitation, and reconstruction).

In the same way as ERASME, MEDITER treats homogeneous sections whose significant parameters are sufficiently alike along their length.

FPDP Model

The FPDP model does not claim to improve knowledge, but to aggregate available knowledge. FPDP is based on seven ideas:

1. Mechanistic analysis of a flexible pavement relies on two main parameters, the horizontal tensile strain at the bottom of the bituminous surface layer and the vertical compressive strain at soil surface level;
2. Flexible pavements have two key distress types—cracking and rutting—which are related to the two previous parameters;
3. Homogeneity is an inadequate concept for pavement, so, as in the HDM model, the variability of homogeneous section concept is introduced;
4. Along the length of a section, distress evolution depends on the variability of pavement structure, layer thicknesses, asphalt and unbound materials characteristics, soil characteristics, environmental factors, and drainage characteristics;
5. In flexible pavement engineering, variability of deflection is a good parameter for tracking variability of pavement structure and soil characteristics. Homogeneous sections are divided into three subsections: weak, medium, and strong, associated with characteristic, medium, and low deflections, respectively.
6. Along one subsection, some variability still occurs and is dependent on asphalt mix fatigue law dispersion and environmental factors. Variability on each subsection is small compared with section variability. To assess variability, two evolution curves, namely optimistic and pessimistic, of the whole section were drawn up and calibrated on several field experiments; and
7. The two key distresses are depicted by two characteristics: extent expressed in percentage of length or surface and severity related to cumulative length of cracks by surface unit (m/m²) for cracking, and rut depth (mm) fur rutting.
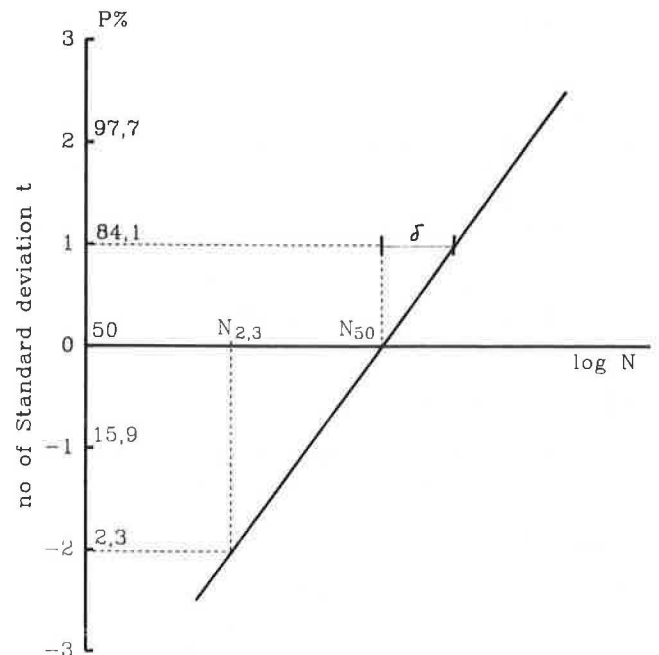
Probability corresponding to number of standard deviation t is also figured on Y−axis
Value of standard deviation δ is read directly on the graph

FIGURE 1 Cumulative normal distribution in a plane (*x* = log *N*, *y* = *t*) and correspondence between *t* and probability *P*.

Three prediction submodels have been created which forecast cracking, rutting, and deflection evolution.

Cracking Model

The following steps are performed:

1. Three subsections are defined as weak, medium, and strong, associated with a characteristic, medium, and low deflections, respectively;

2. For each subsection, a mechanistic assessment is carried out by computing elastic strains and stresses with ALIZE (*8*), and by using the bituminous concrete fatigue relationship with cumulative numbers of axle loads that leads to a 50 percent risk of cracking, to obtain three characteristic parameters, $N_{50}^{\text{weak-subsection}}$, $N_{50}^{\text{medium-subsection}}$, and $N_{50}^{\text{strong-subsection}}$.

3. It is asssumed that the log N distribution on the entire section is a normal statistical distribution defined by

$$N_2^{\text{section}} = N_{50}^{\text{weak-subsection}}$$

$$N_{50}^{\text{section}} = N_{50}^{\text{medium-subsection}}$$

$$N_{98}^{\text{section}} = N_{50}^{\text{strong-subsection}}$$

where N_2, N_{50}, and N_{98} stand for cumulative axle loads that lead to 2, 50, and 98 percent cracking risk, respectively, on the homogeneous section. (Cracking variability on each subsection is ignored at this step.)

4. The standard deviation δ of that distribution is (see Figure 1)

$$\delta_{\text{cracking}} = \frac{1}{2} (\log N_{50} - \log N_2) \tag{1}$$

or, more generally,

FIGURE 2 Relation between failure probability P and cracking extent E.

$$\log N' = \log N + \delta_{\text{cracking}}(t' - t) \tag{2}$$

where t and t' are the fractiles of the log normal distribution law associated with given probabilities of failure P and P' at N and N' cycle numbers, respectively.

5. It is assumed that extent (E) of cracking and probability (P) of failure are strongly correlated (see Figure 2). Experimental results on a highway section (*10*) can be described by
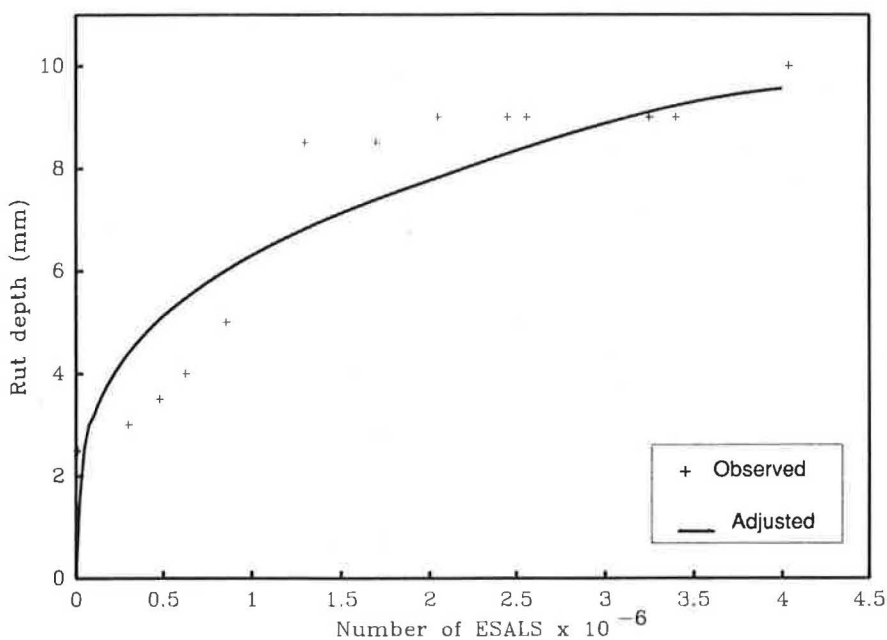
$$E = 2P - 10 \tag{3}$$

FIGURE 3 Example of rut depth evolution versus N on one cross section (LCPC CTT results).

and the results obtained on the CTT are

$$E = 0.15P^{1.5} \qquad (4)$$

These two results define an area of expected cracking as

$$0.15P^{1.5} < E < \max$$
$$(2P - 10; 0.15P^{1.5}), \text{ with } E_{max} = 100 \qquad (5)$$

This step allows variability at the whole section level, previously ignored on each subsection, to be taken into account.

6. This area is associated with the extent of all cracking; i.e., cracks that are at least perceptible (0.1 to 0.2 m/m²).

7. Other areas can be defined for severe cracking and potholes. It is assumed that, for a given extent

$$N_{severe-cracking} = 2.5 N_{perceptible-cracking} \qquad (6)$$

$$N_{pothole} = 3.5 N_{perceptible-cracking} \qquad (7)$$

where $N_{perceptible-cracking}$, $N_{severe-cracking}$, $N_{pothole}$ stand for cumulative axle loads relative to perceptible cracks, severe cracks, and potholes, respectively. Equation 6 has been calibrated with CTT results. The mean size of severe cracking pattern is about 20 cm. It is assumed that extent E of severe cracking and potholing is related to the probability of emergence P by Equation 5. Potholing extent $E_{potholing}$ is computed as

$$E_{potholing} = \text{percent of 100-m lengths of section} \qquad (8)$$
$$\text{containing at least one pothole.}$$

Rutting Model

Rutting forecasting is a difficult engineering task; behavior laws of unbound materials and soils cannot be assessed at a low cost (9). Experimental results from CTT (3,11) have shown that rut depth increases as $N^{0.4}$ (see Figure 3) (N is the cumulative number of 13-tonne single-axle loads). At a given cumulative N, the log RD (rut depth) distribution may be adjusted to a normal statistical distribution (see Figure 4), from which log N also presents a normal statistical distribution for a given rut depth.

To take into account pavement structure and soil quality, it was assumed that RD increases as $(N/N_{allowable})^{0.3}$. $N_{allowable}$ is obtained by using a Dormond-like rule applied to the vertical compressive strain on soil bearing the pavement, in such a way that deflection has the mean value d_m of the deflection distribution. Furthermore, it is assumed that for $N = N_{allowable}$, RD is between 20 and 30 mm when its extent is 50 percent.

Therefore,

$$20(N/N_{all})^{0.3} \; 10^{-0.3 t \delta_{rutting}} < RD$$
$$< 30 \; (N/N_{all})^{0.3} \; 10^{-0.3 t \delta_{rutting}} \qquad (9)$$

where $\delta_{rutting}$ is the log N dispersion for a given rut depth and t is the fractile of the log N distribution associated with probability P of having rut depth RD. P is then assumed to be the extent of rutting of which the depth is RD. Equation 9
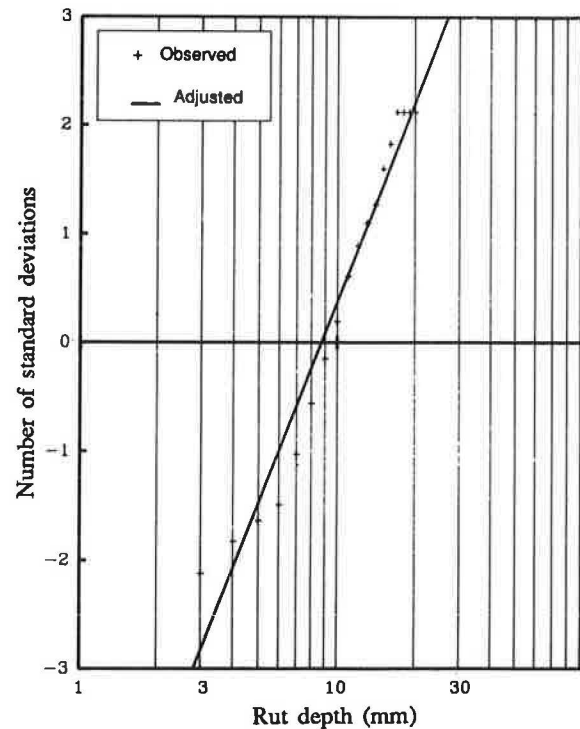
FIGURE 4 Example of rutting dispersion along length for 4 × 10⁶ repetitions (LCPC CTT results).

gives pessimistic and optimistic evolution curves of rutting extent versus N, for given RD.

To calculate $\delta_{rutting}$, similar steps were performed to those concerning cracks, by calculating for weak and medium subsections the cumulative number of axle loads that are assumed to lead to 2 and 50 percent occurrence probability, respectively, of at least 20 to 30 mm rut depth. Thus,

$$\delta_{rutting} = \frac{1}{2} (\log N_{50} - \log N_2) \qquad (10)$$

where N_{50} is the same as $N_{allowable}$ in Equation 9.

Deflection Model

Throughout pavement life, deflection has three ranges. For $N < N_{allowable-for-deflection}$, deflection is constant. Then, for $N_{allowable-for-deflection} < N < N_{disallowable-for-deflection}$ deflection may increase about 10 percent. Finally, for $N_{disallowable-for-deflection} < N$, deflection increase can be strong, up to 100 percent, and random. In these inequalities, $N_{allowable-for-deflection}$ and $N_{disallowable-for-deflection}$ are two MEDITER-calculated cumulative numbers of axle loads.

In flexible pavement engineering, deflection evolution primarily depends on surface layer permeability, which is the ability of water to pass through surface layers and to increase soil moisture content. This ability being related to the extent and severity of cracking implies that the two previous terms are calculated as

$$N_{allowable-for-deflection} = N_{perceptible-cracking}^{weak-section} \qquad (11)$$

$$N_{disallowable-for-deflection} = N_{severe-cracking}^{medium-section} \qquad (12)$$

Deflection stays constant until a 0.5 percent extent of perceptible cracking, and then increases to 10 percent when severe cracking extent reaches 53 to 90 percent.

Conclusions for FPDP Model

Pavement evolution is broken down into three simpler subelements, and can be summarized by cracking, rutting and deflection evolution. An FPDP model constitutes a simple modelization of complex interactions in which, among other relationships, cracking increases the permeability of the surface layer, affects the amount of rutting, cracking of the surface layer, and the permeability of the surface layer determines the amount of rutting.

Although the cracking and deflection prediction models seem well developed, some work needs to be done on rutting prediction.

Maintenance Delay Assessment

Because of funding constraints, pavement managers sometimes delay rehabilitation work. MEDITER will help them to assess rehabilitation delay costs, which can be broken down into four parts:

1. User costs linked to road deterioration (which are not evaluated by MEDITER, a section level tool).
2. Patching costs on severely cracked areas and potholes. Patching does not prevent an increase in cracking but it delays moisturizing of structure pavement and soil. It was assumed that patching is carried out each year on areas that become severely cracked the previous year, and patching durability decreases from 5 years for an average daily traffic (ADT) of less than 1,000 to 2 years for an ADT of more than 15,000.
3. Road shape correction costs caused by rutting. In France, it is estimated that for ruts greater than 25 to 30 mm user's comfort and security are put at risk and pavement resurfacing has to be carried out.
4. Rehabilitation cost increases because of loss of strength of pavement structure. This increase is directly linked to increase in deflection.

INTEGRATION OF MEDITER IN ERASME

Diagnosis, Design, and Prediction

Evaluation of a pavement and development of feasible rehabilitation alternatives are performed according to the following steps:

1. Evaluation of present condition,
2. Prediction of future condition without rehabilitation,
3. Rehabilitation designs,
4. Prediction of future condition on each design,
5. Cost analysis of each design, and
6. Physical testing as needed.

ERASME V8.0 performs Steps 1, 3, and 5. MEDITER integration will bring in Step 2.

Multiple Diagnoses

For some pavement problems, when the ERASME diagnosis expert system detects inconsistencies between several data, it proposes several concurrent diagnoses. Each of these diagnoses is associated with certain hypotheses; for example, mistakes in data.

For each obtained diagnosis, ERASME will perform Steps 2, 3, and 5. During Step 2, MEDITER will assess several rehabilitation delay opportunities associated with concurrent diagnoses.

EXAMPLE OF APPLICATION

Case Description

A 30-km section of RN 104, located in Ardèche, France, was surveyed in 1978, and rehabilitation was found to be needed. Four years later, rehabilitation work had still not been undertaken, so a new survey was carried out.

The pavement condition on a 1.5-km homogeneous section was as follows:

Pavement Condition	1978	1982
Mean deflection (mm/100)	55	55
Characteristic deflection (mm/100)	100	100
All cracking (percent of area)	55	84
Severe cracking (percent of area)	8	22
Perceptible rut depth (percent of length)	63	70
Severe rut depth (percent of length)	0	0.5

Pavement structure was given as

1. 6-cm bituminous concrete layer dated 1969,
2. Old successive surface dressings,
3. 50-cm old granular subbase, and
4. Clay and coarse-gravel soil.

Its two-way ADT as found to be 3,400 with 5 percent truck traffic in 1969. Traffic growth was about 6 percent per year. By 1978, 3×10^5 ESALs (130 kN) by lane had been accumulated.

Predicted Performance Since 1969

Since RN 104 was rehabilitated in 1985, it was not possible to compare 1989 predicted and measured conditions. However, two measured conditions in 1978 and 1982 were used. As shown in Figures 5 and 6, predicted and measured values were closer for cracking than for rutting.

Rehabilitation Delay Cost

The 1985 rehabilitation consisted of an 8-cm bituminous concrete overlay, the cost of which was $70,000/km—the cost of bituminous concrete being about $50/ton (these costs are in 1979 dollars).

Patching From 1979 to 1985, cumulative predicted cost of patching on severe cracking ($10/m²) was between $25,000/km and $50,000/km, i.e., $4,200/year-km to $8,400/year-km. Predicted potholes were between 0/km and 1/km in 1978,
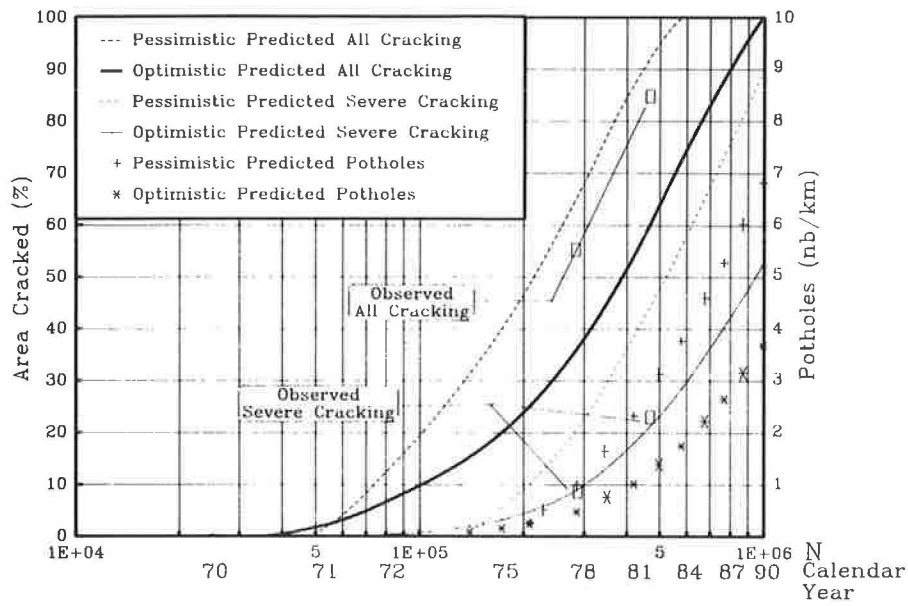
FIGURE 5 Observed and predicted cracking and potholes.

between 2/km and 4/km in 1984. Pothole patching is not expensive: from $10 to $20 for one pothole. However, they cannot be left because of user security.

Rutting   Rutting was not a real problem on this road section because less than 1 percent of the section length presented a severe (about 30-mm) rut depth in 1982. Resurfacing cost was between $20/m and $40/m of rut, which is less than $400/km.

Rehabilitation Cost Increase   Between 1978 and 1985, increase of deflection was less than 2 percent and had a negligible effect on rehabilitation cost.

To sum up, total discounted cost in 1979 value at 8 percent discount rate of 1985 rehabilitation plus interim cost for maintenance, leads to an estimation between $65,000/km and $86,000/km, compared with a $70,000/km cost for 1979 rehabilitation. Comparisons should have been made by adding maintenance costs subsequent to the 1979 rehabilitation, but on this new overlay distress over 6 years is negligible.

Of the total discounted cost, rehabilitation cost was $44,000 and interim maintenance between $21,000 and $42,000, or between half and total of the discounted rehabilitation cost (difference between higher and lower estimation results from prediction model). To avoid a decrease in user security because of potholes and rutting, and to avoid the risk of spending up to 20 percent more than the 1979 rehabilitation cost, it would
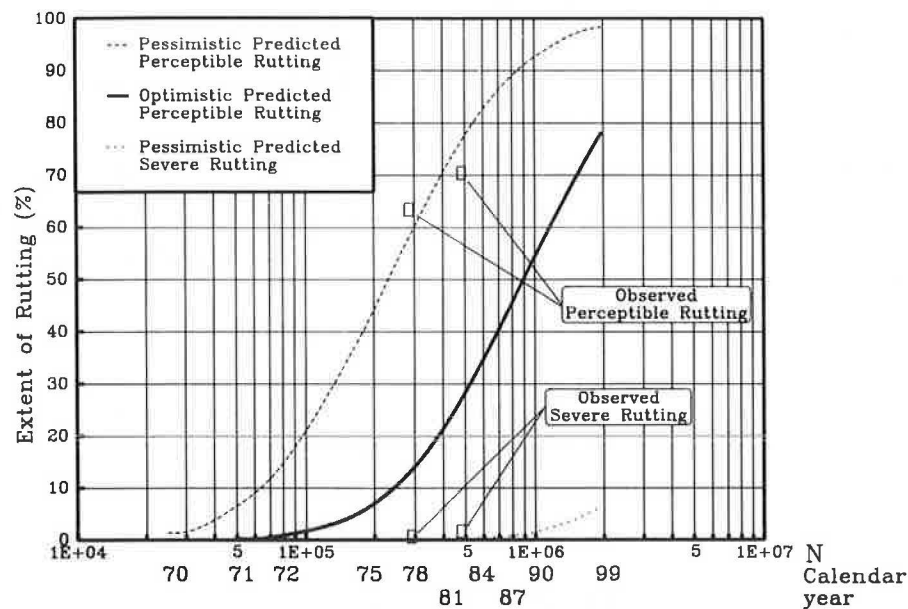
FIGURE 6 Observed and predicted rutting.

have been more advisable to carry out rehabilitation as early as 1979.

CONCLUSION

1. MEDITER is the first approach in France at designing a model for the assessment of rehabilitation delay opportunity. This model uses distress prediction laws built from theoretical and experimental results, and assesses interim routine maintenance costs and increases in rehabilitation work costs because of rehabilitation delay.

2. At present, MEDITER works only for flexible pavements, when the main distress is fatigue of the asphalt mix surface course and structural weakness. Surface dressing distress is not treated, nor is thermal cracking of asphalt mix. Bituminous and hydraulic bounded pavements will be studied in the future.

3. Calibration and validation are needed to improve the quality and reliability of MEDITER. In 1990, it will be implemented on validation sites with this aim in view.

4. User costs are not taken into account in economic comparisons, but serviceability takes place by means of trigger threshold for routine maintenance.

5. MEDITER operates at the section level, not at the network level, unlike a PMS. However, applied to several sections of a network, it could define a priority range among these sections, and thus might find a place in a PMS.

6. Hence, MEDITER constitutes a long-awaited tool, which will enable the asessment of rehabilitation delay consequences for pavement managers, who are so often subjected to funding constraints.

REFERENCES

1. W. D. O. Paterson. Road Deterioration and Maintenance Effects. *The Highway Design and Maintenance Standard Series*, The World Bank, Washington D.C., 1987.
2. P. Autret, A. De Boissoudy, and J. C. Gramdsammer. The Circular Test Track of LCPC. Presented at 6th International Conference on Structural Design of Asphalt Pavements, Ann Arbor, Mich., 1987.
3. F. Allez, M. Dauzats, P. Joubert, M. Puggelli, and D. Renault. ERASME: A Multi Expert System for Pavement Assessment and Rehabilitation. Presented at 68th Annual Meeting of the Transportation Research Board, Washington D.C., 1989.
4. *Interim Guide for Design of Pavement Structures*. AASHTO Washington D.C., 1981.
5. G. B. Way, and J. Eisenberg. *PMS for Arizona, Phase 2: Verification of Performance Prediction Models and Development of Data Base*. Arizona Department of Transportation, 1980.
6. W. J. Kenis. *Predictive Design Procedures VESYS: User Manual*. Report 77-154, FHWA, U.S. Department of Transportation, 1978.
7. C. Peyronne, J. L. Aubert, and D. Renault. Presentation of a PMS for a Network of Departmental Roads. Planning and Transportation Research and Computation, Bath, England, 1987.
8. P. Autret, A. De Boissoudy, and J. P. Marchand. ALIZE 3—Practice. *Proc., 5th International Conference on Structural Design of Asphalt Pavements*, Delft, Netherlands, 1982.
9. P. Jouve, J. Martinez, J. L. Paute, and E. Ragneau. Rational Model for the Flexible Pavement Deformations. In *Proc., 6th International Conference on Structural Design of Asphalt Pavements*, Ann Arbor, Mich., 1987.
10. J. Chabrol, D. Duran, J. P. Marchand, and F. Prudhomme. Road Mechanics in Highway Management. In *Proc., 6th International Conference on Structural Design of Asphalt Pavements*, Ann Arbor, Mich., 1987.
11. P. Autret, G. Caroff, and B. Miet. Comportement des Structures Inverses—Chaussées d'Autoroute Infos No. 9. SCETAU-ROUTE, Saint Quentin en Yvelines, France, Oct. 1987.

Rout and Seal Cracks in Flexible Pavement—A Cost-Effective Preventive Maintenance Procedure

GEORGE J. CHONG

The Ministry of Transportation of Ontario conducted a comprehensive study on the feasibility of a rout and seal treatment of cracks in flexible pavement as a preventive maintenance procedure. The objectives of this study were to ascertain the cost-effectiveness of this procedure on the basis of the successful treatment of the distress, the resultant extension of pavement service life, and the optimum timing for application to achieve maximum cost benefit. Implemented in 1986 across the province of Ontario, the study ensures complete coverage of different climatic and environmental conditions. Monitoring of the treatment performance and pavement conditions has been completed for a period including three winters. From the data, it has been established that (a) certain rout configurations are more effective in different regions in the province, (b) the rout and seal treatment effectively delays or even stops progressive distress deterioration, and (c) the treatment is essential to achieve maximum cost benefit, with the optimum time being from the 3rd to 5th years for initial treatment, and the 8th to 9th years for follow-up treatment.

The Ministry of Transportation (MTO) uses two maintenance treatments for cracks in flexible pavement and composite pavement; (a) the traditional spray patching with emulsified asphalt and sand or stone chips and (b) the method commonly known as rout and seal (1). Time has demonstrated that sealing with emulsified asphalt is not only ineffective but can create undesirable side effects (2,3). On the other hand, rout and seal has shown success in effective maintenance of cracks, although the question of how cost-effective this particular maintenance treatment is has not been answered (4,5).

In 1981, a small experimental study was initiated by MTO Pavements and Roadway Office and the Ottawa District Maintenance Office. This study provided significant, though limited, cost-effectiveness data (2,4,5). In 1986, the MTO's Highway Operations and Maintenance Division initiated a comprehensive study program on rout and seal treatment of cracks as a preventive maintenance procedure, with the Pavements and Roadway Office as the appointed coordinator. The scope of this later study is an extension of the 1981 study, but is now province-wide to ensure complete coverage of the different climatic and environmental conditions that exist in Ontario (4,5).

PROVINCIAL PROGRAM

The program's proposed course of action was to select pavement sections for study from age groups of less than 3 years,

4 to 6 years, and 7 to 9 years. Each group was to have a minimum of two test sections. Each test section was to have a minimum of five subsections of 150 mm each. These subsections were to be laid out with the control section located between the four remaining sections of rout and seal treatment. Two of the subsections were to have rout size of 40×10 mm. Two subsections were to have rout sizes of 19×19 mm, if the pavement was located in Districts 5, 7, 8, 9, 10, and upward; 12×12 mm if the pavement was located in Districts 1, 2, 3, 4, and 6. Low-modulus polymer sealants of Hydrotech 6165 and TREMCO THC200 were to be used in Districts 5, 7, 8, 9, 10, and upward; Hydrotech 6165 and standard Hydrotech 6160 sealants were to be used in Districts 1, 2, 3, 4, and 6. A standard crew with standardized equipment from the MTO Ottawa District was to be used to minimize installation variables. The study was to be coordinated and monitored by the Pavements and Roadway Office of the Research and Development Branch of MTO.

Program Objectives

The main objective of the program was to determine the definitions and standards for rout and seal operational specifications for both in-house and contract work in terms of the equipment, methodology, materials, and rout size for different climatic and environmental conditions.

Other objectives were to study the effectiveness of treatment, extension of pavement service life, importance of treatment timing for cost effectiveness, and consequences of deferred treatment.

Test Section Selection

A total of 37 test sections were selected from the three different age groups and from four different regions of the province as follows:

- Age Group
  —1 to 3 years, 10 sections;
  —4 to 6 years, 13 sections; and
  —7 to 9 years, 14 sections.
- Regions
  —Northern region, 6 sections;
  —Eastern region, 9 sections;
  —Central region, 2 sections; and
  —Southwestern region, 20 sections.

Research and Development Branch, Ministry of Transportation of Ontario, Downsview, Ontario, Canada M3M 1J8.

Procedures

Monitoring

A condition survey was to be carried out using the Condition Survey of Pavement Surface form shown in Figure 1. The same form will be used for subsequent monitoring during the successive winters (months of January or February, or both).

The pavement sections under study were to be identified from completion of the following form:

Item	Explanation	
1.	Highway No.	Number of highway.
2.	Location	Proximity to the nearest town or city, major highway interchanges, or any other prominent landmarks.
3.	Date of survey	Date the condition survey is taken.
4.	Section	Test section number on the basis of predetermined number provided. For example, if test section number is 20, then section number should be 20–1, 20–2, 20–3, or 20–4. The control section where no rout and seal work is to be carried out will be labeled "Control."
5.	Rout size	Size of rout designated and used on the section, that is, 12 × 12 mm, 19 × 19 mm, or 40 × 10 mm.
6.	Material	The sealant material used for sealing of the rout crack. Brand name and type designation must be given, for example, Hydrotech 6165.
7.	Crack mapping	The form is set up for a 200-m, 2-lane section, in 10-m increments. The cracks should be drawn as accurately as possible on the form.
8.	Transverse crack (total length)	The total length of transverse cracks (sealed and unsealed) in the section will be measured (to the nearest meter) with a measuring wheel.

FIGURE 1   Condition Survey of Pavement Surface form.

9.	Longitudinal crack (total length)	The total length of cracks (sealed and unsealed) other than transverse cracks in the section will be measured (to the nearest meter) with a measuring wheel.
10.	Total length of cracks	Combined length in meters of all cracks, from Items 8 and 9.
11.	Transverse crack, cupping/lipping	If present, check either slight, moderate, or severe, on the basis of the general condition of the transverse cracks with cupping or lipping.
12.	Crack spalling	If present, check either few, frequent, or extensive, for all cracks in the section. Percentage is based on the number of cracks that have spalled.
13.	Crack opening	For unsealed cracks only. Check the appropriate square for transverse crack openings and for longitudinal crack openings on the basis of the general condition of the section.
14.	Sealant bond failure	For sealed sections only. Check the appropriate square for bond failure of the sealant. Failure includes one-side debonding, both-side debonding, and sealant splitting. Percentage is based on proportion of total length of all sealed cracks in the section.

Roughness Measurement

The roughness (ride quality) measurement was to be made by the MTO Pavement Design and Evaluation Office with the Mays Meter at the original position. The measurement was taken in summer, and was to be repeated 5 years after or at termination of the study, and in the same time frame as the original measurement.

Treatment Operation

Crew Complement	Number
Foreman/woman	1
Router operator	2
Hot lance operator	1
Kettle operator	1
Tow vehicle operator	1
Total	6

Safety personnel are to be supplied by local patrol where work is located.

Equipment Complement	Number
Router	2
Hot lance	1
Kettle	2
Tow vehicle	2
Crew cab, 1 ton	1
Total	8

Safety personnel are to be supplied by local patrol where work is located.

Work procedures are as follows:

1. Both kettles are to be used at the same time, each specifically for one designated sealant material;
2. One router is set up permanently for 40 × 10 mm;
3. One router is set up for 12 × 12 mm or 19 × 19 mm, depending on locality of work; and
4. Hot lance is used just ahead of kettle.

SUMMARY OF FIELD OPERATIONS

The field operation began in June 1986 and was completed in September 1986, a month behind schedule because of a record-breaking rainy summer, the worst experienced by the province in the last 50 years.

Test Sections 5 and 24 were deleted because major maintenance was performed on Section 5 before rout and seal treatment, and Section 24 exhibited massive multiple cracking with spalling, making it impractical to use for the study purpose. Section 36 was simplified to a 40 × 10 mm test section, and Hydrotech sealed under a postconstruction arrangement for a rehabilitation contract.

Although low-modulus polymer sealant TREMCO THC200 was ordered, the manufacturer supplied the standard TREMCO THC205 in error. Sections 31 to 34, inclusive, in District 8 were also sealed with Hydrotech 6160 because not enough TREMCO was available.

Between 1986 and 1989, Sections 16 and 31 were lost because of major maintenance or rehabilitation.

MONITORING RESULTS FOR 1986 TO 1989

Monitoring of the rout and seal test sections and their corresponding control sections was conducted between January and March of 1987, 1988, and 1989. All three winters experienced a similar pattern: below-average snowfalls and prolonged periods of above-average temperatures with short durations of intense cold days.

Equipment and Methodology

The equipment and work procedures developed by the Pavements and Roadway Office and the Ottawa District Maintenance Office used for the study proved to be highly efficient and productive in successfully waterproofing the cracks in the pavement surface. Details were provided by Chong and Phang (5).

Materials and Rout Configuration

After three winters of monitoring, the performance evaluation on the basis of bond failure occurrences, gave the following ranking orders:

Materials Performance (see Figure 2)

1. TREMCO 205.
2. HYDROTECH 6160.
3. HYDROTECH 6165.

Material Matched With Rout Configuration (see Figure 3)

1. 12 × 12 mm with TREMCO 205.
2. 12 × 12 mm with HYDROTECH 6165.
3. 40 × 10 mm with TREMCO 205 or HYDROTECH 6160, 12 × 12 mm with HYDROTECH 6160.

4. 40 × 10 mm with HYDROTECH 6165.
5. 19 × 19 mm with TREMCO 205.
6. 19 × 19 mm with HYDROTECH 6160.
7. 19 × 19 mm with HYDROTECH 6165.

Rout Configuration (All Ontario) (see Figure 4)

1. 12 × 12 mm and 40 × 10 mm.
2. 19 × 19 mm.

Rout Configuration (Cold Region) (see Figure 5)

1. 40 × 10 mm.
2. 19 × 19 mm.

Rout Configuration (Milder Region) (see Figure 6)

● Equal for 12 × 12 mm and 40 × 10 mm.

Crack Development

Crack development was assessed on the basis of the value of the crack factor F_c—the total linear length L_c (in meters) of transverse cracks and longitudinal cracks on the pavement surface divided by the total surface area (in square meters) of the pavement section. That is,

$$F_c = \frac{L_c}{A} \times 100 \qquad (1)$$

Figure 7 shows the crack factor for various pavement ages from 1 to 12 years. It appears that crack development begins from Year 1 of the pavement service life and increases steadily until Year 6. It then becomes static until the 11th year, when the increase becomes quite dramatic.

Figure 8 shows the crack factor for transverse and longitudinal cracks separately for various pavements from 1 to 12 years old. It appears that transverse cracks develop fully in the 1st year of the pavement service life and remain quite static until the 11th year, when a sharp increase begins to take place.

Figures 7 and 8 also show that the initial crack factor is generated nearly solely by transverse cracks, and that increases between Year 1 and Year 6 are from longitudinal crack development. The figures also show that pavement with a low crack factor will remain static in crack development over its service life.
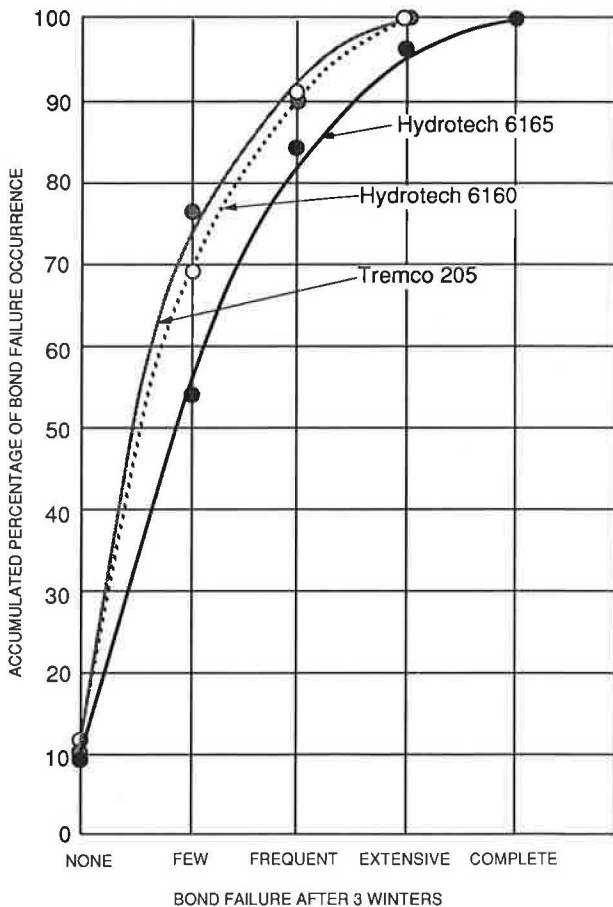
FIGURE 2 Ranking of materials on bond performance.
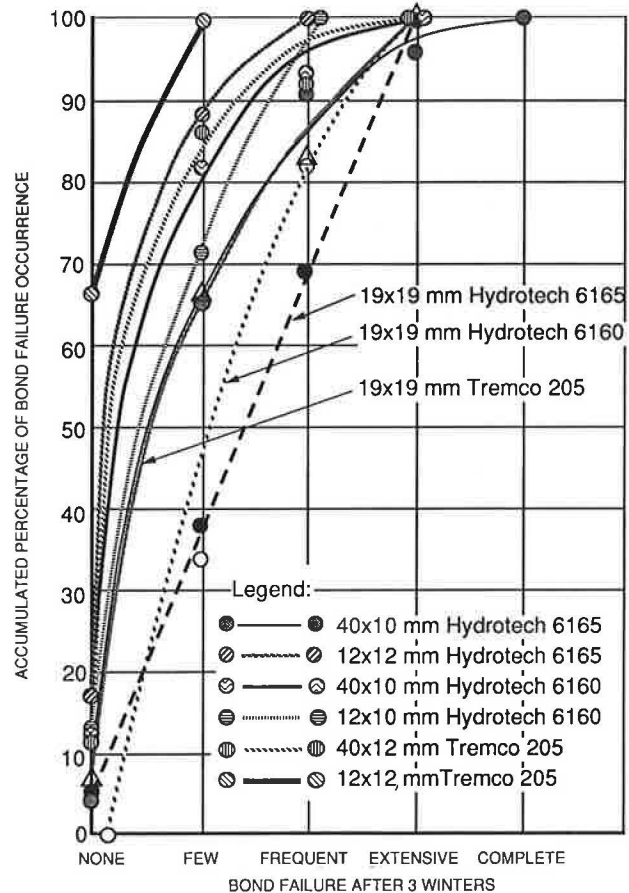
FIGURE 3 Ranking of material/rout configuration on bond performance.
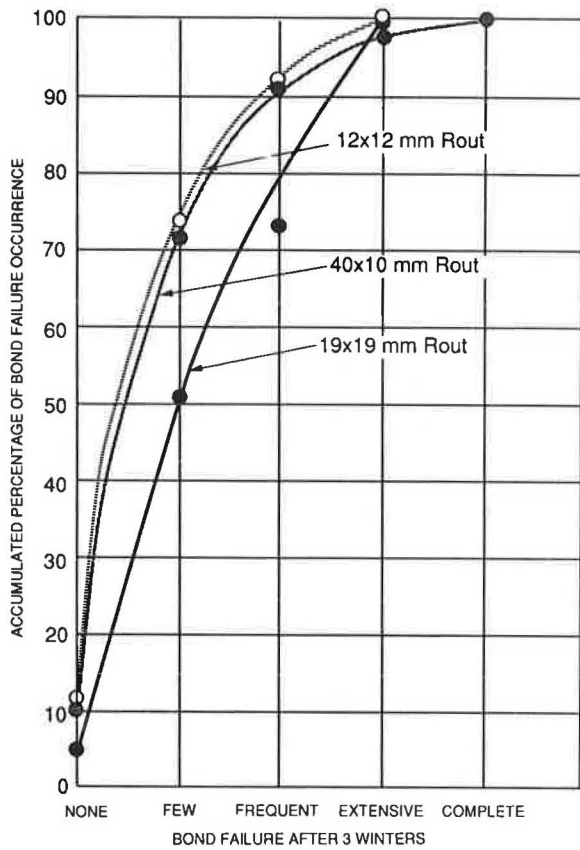
FIGURE 4 Ranking of rout configuration on bond performance (all Ontario).
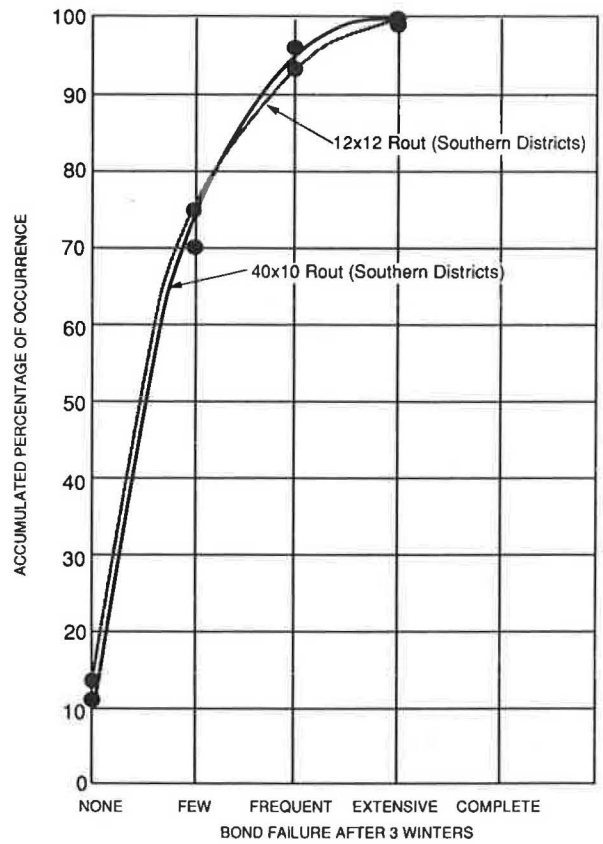
FIGURE 6 Ranking of rout configuration on bond performance (southern districts only).
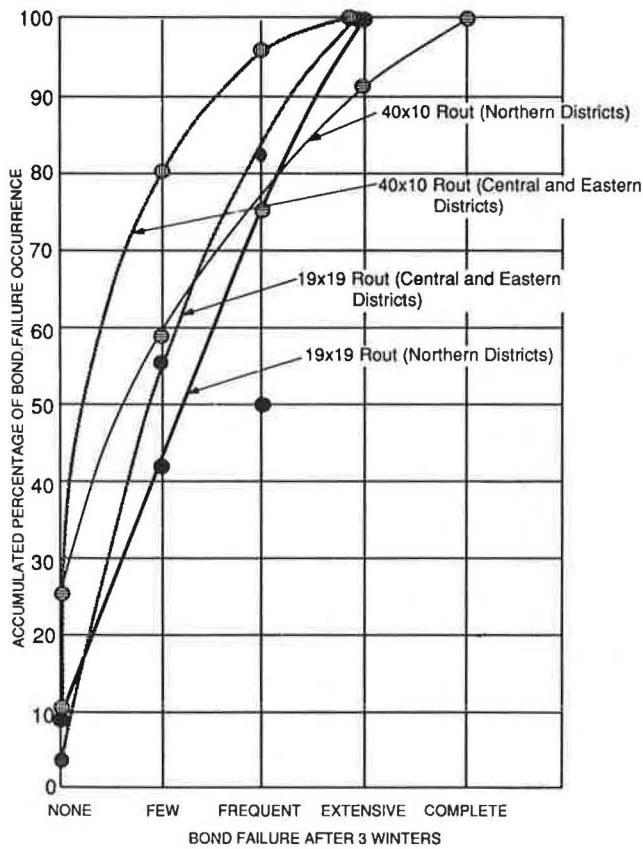
FIGURE 5 Ranking of rout configuration on bond performance (central, eastern, and northern districts).
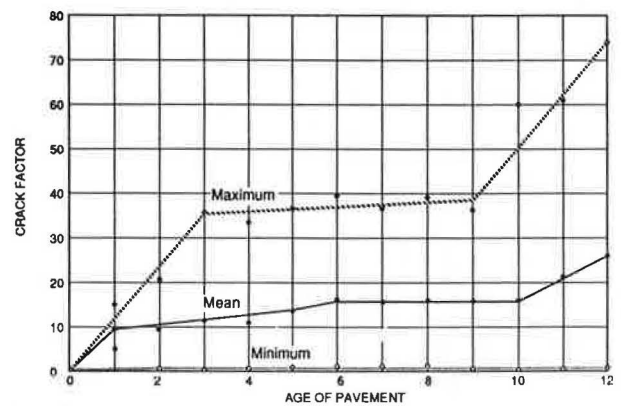
FIGURE 7 Crack factor for transverse and longitudinal crackings combined.
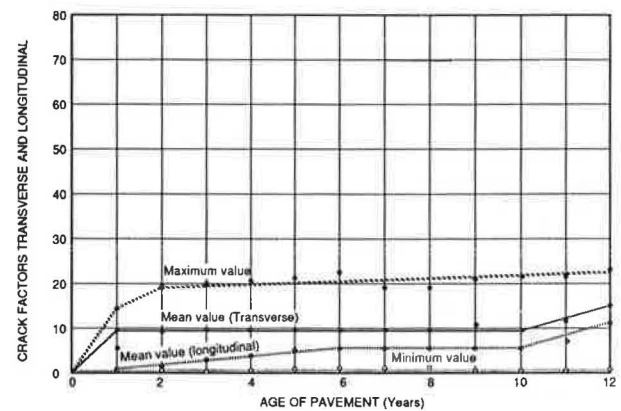
FIGURE 8 Crack factors for transverse and longitudinal crackings only.
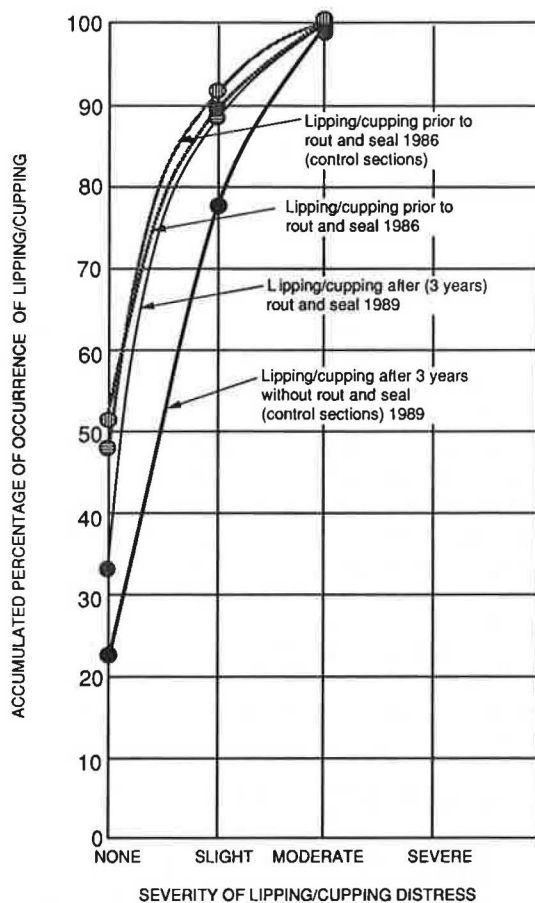
FIGURE 9 Crack deterioration after three winters.

Crack Deterioration by Lipping and Cupping

Crack deterioration is assessed on the basis of evaluation of deformations in the form of lipping or cupping. Figure 9 shows the different rates of deterioration for rout and seal treated cracks and nonsealed cracks from the control sections after three winters of service life. The rout and seal cracks remain static in performance, whereas the cracks in the control sections show significant increase in lipping and cupping deterioration after three winters.

DISCUSSION OF RESULTS

Cost-Effectiveness of Maintenance Treatment

The cost-effectiveness of a maintenance treatment depends on

1. How the treatment changes the existing condition; that is, how effectively it corrects the existing distress.
2. How well the treatment effectively delays the distress deterioration process, thereby extending the pavement service life.
3. Whether there is a particular condition or time during the progression of the cracking distress when appropriate maintenance can be most effective.

The information needed to establish cost-effectiveness must therefore quantify

1. The effectiveness of treatment—that is, (a) performance of sealant materials over time, and (b) performance of various rout width and depth sizes over time to establish the most efficient rout configuration.
2. The extension of pavement service life—that is, (a) retarding of additional crack development and (b) delaying the deterioration process of the existing distress.
3. The influence of time—the point in the pavement's life cycle at which the treatment is applied most cost-effectively.

Effectiveness of Treatment

Material Performance

All three materials are approved and included in the Ministry Designated Sources List. Performance, on the basis of the criteria of bond failure, indicates that TREMCO 205 and Hydrotech 6160, which both conform to ASTM D–1190, are similar and better than the low-stiffness modulus Hydrotech 6165, which conforms to ASTM D–3405 (see Figure 2).

This evidence appears to contradict the previous assumption that the low-modulus materials will perform better in a harsher climate than the standard D–1190 formulation. However, it should be noted that overall performance for all three sealant materials is exceptionally good because after three winters of service life, less than 10 percent of the sealant suffered a bond failure rating of "extensive."

Material/Rout Configuration Performance

All three sealant materials are matched with rout configurations of 12 × 12 mm and 40 × 10 mm for the southern part of the province and 19 × 19 mm and 40 × 10 mm for central, eastern, and northern areas.

Performance based on the criteria of bond failures indicates that regardless of materials, rout configuration of 19 × 19 mm is the poorest performer. There is virtually no difference in performance between 12 × 12 mm and 40 × 10 mm in southern Ontario, where the climatic condition is considered milder (see Figures 3–6).

The results definitely reinforce the previous assumption that rout configuration of 19 × 19 mm for asphalt concrete pavement is the least desirable and should be discarded. For uniformity, rout configuration of 40 × 10 mm should be the standard province-wide. For southern Districts 1, 2, 3, 4, and 6, rout size of 12 × 12 mm can be used as the optional standard, especially for urban expresssways.

Extension of Pavement Service Life

Crack Development

Evaluation of crack development during the pavement service life, on the basis of the criteria of crack factor, shows that cracking increases from the 1st to the 6th year, when it becomes more or less static until the 10th year. From the

11th year onward, crack development appears to accelerate (see Figure 7).

The most interesting aspect is that transverse cracking developed almost immediately from Year 1 to its full potential and thereafter remained fairly static until the Year 10. From the 11th year onward, transverse cracking appears to again accelerate. In addition, cracks other than transverse appear to begin their development in the 2nd year of pavement service life and reach a peak in the 6th year, which accounts for the trend of increasing crack factor from Year 1 to Year 6 (see Figure 8).

Rout and seal treatment of cracks does not appear to have a great deal of influence on crack development, because there is no discernible trend in crack development between the sealed test sections and the unsealed control sections.

Crack Deterioration

The criterion used to determine crack deterioration is the degree of deformation at the transverse crack, commonly known as either lipping or cupping. Treatment is considered to be effective when it either retards or stops the deformation process, thus extending pavement service life. An increase in deformation results in increased roughness in the pavement surface and reduced serviceability.

Figure 9 shows the static condition of the rout and seal test sections after three winters of the treatment's service life. The unsealed control sections indicate a marked increase in the severity of lipping and cupping distress.

Timing

The data on crack development indicates that rout and seal treatment should be applied between the 3rd and 5th year for maximum cost benefit (see Figures 7 and 8). For pavement with low crack factor less than 2.0 by the 4th year, there is no benefit to rout and seal cracks as the crack factor will remain static and low (see Figures 7 and 8).

A second rout and seal treatment can also be cost effective in prolonging or extending pavement surface life if it is carried out at the 8th or 9th year, before crack development begins to accelerate.

MINIEXPERIMENTAL STUDY

In 1981, a small-scale study was launched by the Pavements and Roadway Office and the Ottawa District Maintenance Office to look into the consequence of sealing pavement cracks with rout and seal treatment versus deferred maintenance (2,4,5).

A second of Highway 17 near Ottawa was selected that was originally constructed in 1965 with 115 mm (4½ in.) of hot-mix asphalt, and rehabilitated in 1979 because of extensive cracking with 65 mm (2½ in.) of hot-mix asphalt. In 1981, 2 years after resurfacing, extensive transverse cracks reappeared and the pavement was routed and sealed as a preventive maintenance measure. Part of this pavement was used for the miniexperimental study.

In 1985, an investigation was made of the deferred maintenance control section and the rout and seal test sections.

Results proved that rout and seal treatment prevented secondary crack development on the sealed cracks and also stopped or retarded internal deterioration, which was reflected on the surface as cupping deformation (5).

In 1989, as part of the winter monitoring program, a performance evaluation was made of the experimental test sections. The performance data are presented in Table 1.

Material Performance

Hydrotech 6160 and Meadow 164R had been approved as sealant materials at the same time. The third material, which had just been placed in the marketplace, was the Shell Cariphalte, a low stiffness modulus polymer material that Shell Canada hoped would be accepted by the Ministry on the Designated Sources List. (Shell Canada has now discontinued the manufacturing and sale of this product.)

After eight winters of service life, the sealants are still effective in their designed function, which is waterproofing the pavement surface. This includes Meadow 164R, which has the worst performance record for bond failure and was subsequently withdrawn from the market by its manufacturer. Figure 10 shows a typical rout and seal crack using Hydrotech 6160, Figure 11, using Shell Cariphalte, and Figure 12, using Meadow 164R.
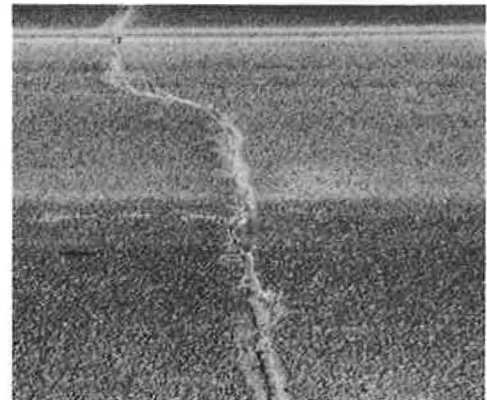
FIGURE 10   19- × 19-mm rout and seal with Hydrotech 6160 Test Section 1, 1981 (February, 1989).
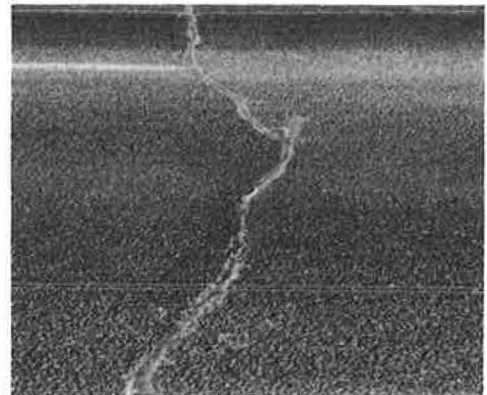
FIGURE 11   19- × 19-mm rout and seal with Shell Cariphalte Test Section 3, 1981 (February, 1989).

Pavement Performance

The sealed test sections, Meadow 164R included, were definitely in better condition than the control section (see Table 1). The sealed cracks remained sealed with little secondary crack development. New crack development for sealed sections was also less than in the control section, which in 1989 was estimated as approximately 30 percent more than in 1981.

There was no spalling with the sealed cracks, whereas spalling did occur in numerous unsealed cracks in the control section (see Figure 13).

The new crack development, after the sealing in 1981, has had no maintenance in the sealed test sections or in the control section. These unsealed cracks have now progressed to openings of as much as 19 to 25 mm. It will be beneficial to have a follow-up rout and seal treatment in the eighth or ninth year to extend the pavement service life before accelerated deterioration takes place.

FIGURE 12   19- × 19-mm rout and seal with Meadow 164R Test Section 7, 1981 (February, 1989).

TABLE 1   MINIEXPERIMENTAL STUDY—HIGHWAY 17, OTTAWA DISTRICT

SECTION NO.	CHAINAGE (km)	MATERIAL	ROUT	SEALANT BOND CONDITION
1	0 - 1.0	Hydrotech	19 mm	<10% bond failure, about 5 cm sealant missing from <10% of crack <15% new cracks developed, Average crack width 13-19 mm
2	1.0 - 2.0	Control		<30% new cracks developed Most transverse crack width 13-19 mm, some 19-25 mm Most longitudinal crack width 6-13 mm, some 13-19 mm
3	2.0 - 2.5	Shell	19 mm	No bond failure, no sealant missing <10% new cracks developed Average transverse crack width 6-13 mm, C\L crack >25 mm
4	2.5 - 3.0	Shell	10 mm	No bond failure, no sealant missing <10% new cracks developed Average crack width 6-13 mm, some longitudinal cracks 19-25 mm
5	3.0 - 4.0	Hydrotech	10 mm	<10% bond failure, no sealant missing <10% new cracks developed Average crack width 6-13 mm, some longitudinal cracks 19-25 mm
6	4.0 - 4.5	Meadows	10 mm	>50% bond failure, about 5 cm sealant missing from most cracks <15% new cracks developed Average crack width 6-13 mm, some longitudinal cracks 19-25 mm
7	4.5 - 5.0	Meadows	19 mm	>50% bond failure, about 5 cm sealant missing from 50% of cracks <15% new cracks developed Average crack width 6-13 mm, some longitudinal cracks >25 mm
8A	7.4 - 7.9	Meadows	Flat	>40% bond failure, about 5 cm sealant missing from 25% of cracks <15% new cracks developed Average crack width 6-13 mm, some longitudinal cracks >25 mm
8B	7.9 - 8.4	Meadows	Bead	>40% bond failure, about 5 cm sealant missing from 10% of cracks <15% new cracks developed Average crack width 6-13 mm, some longitudinal cracks >25 mm
8C	7.9 - 8.4	Hydrotech	Bead	<10% bond failure, no sealant missing <15% new cracks developed Average crack width 6-13 mm, some longitudinal cracks >25 mm
8D	7.4 - 7.9	Hydrotech	Flat	<10% bond failure, no sealant missing <15% new cracks developed Average crack width 6-13 mm, some longitudinal cracks >25 mm
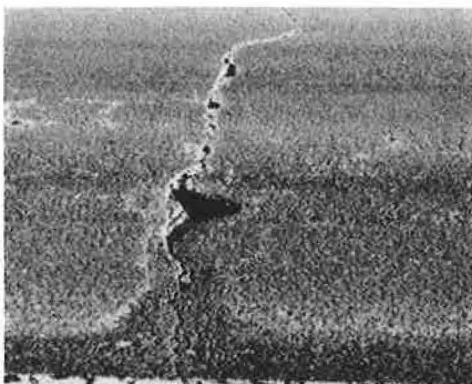
FIGURE 13 No maintenance, test section 2, control, 1981 (February, 1989).

SUMMARY

Rout and seal treatment is designed to seal asphalt concrete pavement cracks to prevent water from entering and damaging the pavement structure. It is important for pavements in cold areas because of the combination of low-temperature-induced crack opening and the winter maintenance practice of snow and ice removal with salt.

This experimental study, evaluating the effectiveness of rout and seal treatment and its cost benefit, has achieved good results, which lead to the following conclusions:

1. The equipment and methodology presently used by the ministry are efficient and highly successful and should be the specified standard.

2. All three approved materials on the Ministry Designated Sources List perform satisfactorily whether they are formulated to meet ASTM D–1190 or D–3405.

3. Standard rout configuration for the province of Ontario should be 40 × 10 mm.

4. Rout configuration for southern Ontario (Districts 1, 2, 3, 4, and 6) should have 12 × 12 mm as the optional choice. The 12 × 12 mm will present a neater appearance, less material usage than 40 × 10 mm, and will be especially suitable for urban expressway systems.

5. Rout and seal treatment will either stop or retard the deformation commonly known as lipping and cupping, which is detrimental to pavement serviceability and, therefore, pavement service life.

6. The initial rout and seal treatment must be performed between the third and fifth year of the pavement service life to achieve maximum cost effectiveness.

7. The second rout and seal treatment, which is a follow-up operation, should be performed between the eighth and ninth years of the pavement service life to extract the maximum benefit of the initial treatment in extending pavement service life.

8. For pavement with an initial low crack factor (2.0 or less) at the 4th year of pavement service life, rout and seal treatment has doubtful benefit.

9. Deferred maintenance, particularly on transverse cracks, is not an acceptable engineering or economical option.

RECOMMENDATIONS

Three winters of monitoring have been completed. Monitoring must continue until the sealant reaches extensive failure or, at minimum, for an additional 2 years. The Pavement Design and Evaluation Section of the Highway Design Office should be the agency designated to continue further monitoring of this project.

ACKNOWLEDGMENTS

REFERENCES

1. *Maintenance Operation Instruction: M-1005-A Crack Sealing Flexible Pavements*. Ontario Ministry of Transportation and Communications, Ottawa, Sept. 1981, Interim Revision, May 1984.
2. G. J. Chong. Sealing Cracks in Flexible Pavements in Cold Areas. In *Proc. Ontario Ministry of Transportation and Communications, PICA Mini-Workshop*, Vancouver, Oct. 1982.
3. G. J. Chong and W. A. Phang. *Sealing Cracks in Flexible Pavements in Cold Areas—An Audio-Visual Script*. Report PAV-83-01. Ontario Ministry of Transportation and Communications, Ottawa, Jan. 1983.
4. G. J. Chong. Consequences of Deferred Maintenance on Transverse Cracks in Cold Areas. In *Proc. Ontario Ministry of Transportation and Communications, PICA Workshop III*, Ottawa, July 1987.
5. G. J. Chong and W. A. Phang. *Improved Preventive Maintenance: Sealing Cracks in Flexible Pavements in Cold Regions*. Report PAV-87-01, Ontario Ministry of Transportation, Ottawa, Jan. 1988.

Factors Affecting Joint System Performance

M. C. BELANGIE

Identification of failure modes occurring in portland cement concrete pavement joints is a critical element in correction of joint-sealant failures and a key requirement for development of improved joint-sealant systems. Specific failure modes associated with the application, concrete surround, concrete-sealant interface, design, sealant material, moisture, and cold temperatures are identified and discussed. Effects of inadequate quality control and lack of performance tests are addressed. Individual failure modes at the time of failure are distinctive and usually unique; however, wear and weather-related deterioration can erase these unique characteristics. Loss of characteristics results in misinterpretation of the cause of failure and inappropriate remedial actions. As a result, failures are frequently replicated.

Failure modes observed on Utah test sites are summarized. Space requirements have severely limited the number of failure modes discussed and precluded the use of detailed illustrations and representative photographs. Most of the failure modes discussed have been given minimal exposure in the literature. Lack of discussion of a failure mode does not indicate that the missing failure mode is not important. There is need for a comprehensive, evolving reference on evaluating joint-sealant system performance.

The presentation is based largely on field performance evaluations of concrete joint-sealant test sites (1,2) and asphalt concrete crack sealant test sites (3). It includes some supporting information from other sources (4–7). The Utah field evaluations included one or more sealants from five field-cured sealant groups: RTV (room-temperature-vulcanized) silicone, PVC-Coaltar, polymer-modified liquid asphalt rubber, crumb rubber, and rubber nitrile. Sealants were placed in $\frac{3}{8}$-in.-wide transverse joints on plain jointed concrete pavements with 12.5-ft average panel lengths. The polymer-modified asphalt rubber materials were also placed in $\frac{1}{8}$-in.-wide transverse joints to simulate performance of joint systems used in Utah before 1975. Load transfer at joints is by aggregate interlock. Field-cured joint-sealant systems placed in these designs have and are showing unacceptable levels of failure within 1 to 3 years of placement.

FAILURE ANALYSIS

Joint-sealant system failures can be separated into horizontal and vertical failures. Horizontal system failures are commonly reported in miles of failure. Vertical failures are determined in fractions of an inch. An understanding of both concepts is essential to the evaluation of joint-sealant failure modes.

Vertical failures may be classified into partial-depth failures and full-depth failures. Partial-depth failures are failures that extend below the top surface of the sealant but do not penetrate into the joint area below the bottom surface of the sealant, as shown in Figure 1a. Full-depth failures are failures that penetrate below the bottom surface of the sealant and allow liquids or solids to enter the joint below the sealant, as shown in Figure 1b. All partial-depth failure modes observed on the Utah test sites were progressive and either have become, or eventually are expected to become, full-depth failures.

Horizontal failure may be divided into two categories, localized failures and general failures. Localized failures and general failures include both partial-depth and full-depth failures.

Localized failure is defined as a specific failure or group of failures that either delineate a specific failure mode or help identify the causal mechanisms of that failure mode. Localized failures may vary from a fraction of an inch to several feet in length. On the Utah test sites, most of the joints developed localized failures within 1 year of placement. By the 3rd year after placement, all joints were displaying localized failures.

General failures are defined as extended failures involving significant segments of a project or the entire project. General failures involving the concrete surround or concrete-sealant interface appear to be largely from design or procedural causes. General failures involving the sealant appear to be primarily from procedural or material-related causes.
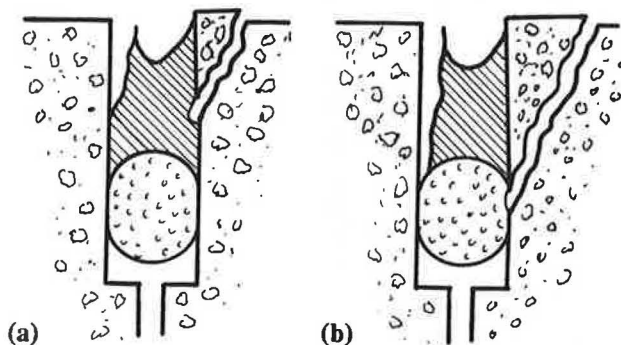
FIGURE 1 Vertical failures, a, partial-depth failures, b, full-depth failures.

27 Q Street, Salt Lake City, Utah 84103.

PRINCIPAL FAILURE LOCATIONS

Portland cement concrete (PCC) field-cured, joint-sealant system failures are located in one or more of three locations: (a) the concrete surround, (b) the concrete-sealant interface, or (c) the sealant, as shown in Figure 2.

VISIBLE AND NONVISIBLE FAILURE ANALYSIS

Failures may be visible or nonvisible. Visible failures are failures that can be visibly examined with the sealant in place. Nonvisible failures may require removal of the sealant or a concrete core to verify the failure mode.

Visible failures are frequently hidden. In many instances, it is necessary to probe the interface or the surface of the sealant to expose the failure. Minute concrete cracks may be exposed by the application of water. Visibility of a sealant or interface failure and the degree of the failure, particularly the first year of the failure, depends on the sealant, the period in which the observation is made, and the amount and size of incompressible material available to enter the separation.

Nonvisible failures are failures that have occurred below an intact joint surface. Nonvisible failures frequently may be examined indirectly by pressing or twisting the surface of the sealant with various types of probes and noting the characteristics of the resistance to the applied forces. Verification of the interpretation of failure usually requires the removal of the sealant and visual examination of the failed portions of the system.

Whether the failure is visible or nonvisible, laboratory analysis of a failed sealant (and if appropriate, the backer rod and concrete core of the failed channel section) may be necessary to corroborate the investigator's interpretation of the cause of the failure.

FAILURE MODES—CONCRETE SURROUND

Failures in the concrete surround (Figure 2) contributed significantly to overall failure on the various Utah sites. Five failure modes were identified: concrete defect failure, torque-shear failure, groove (tine) failure, vertical compression failure, and horizontal compression failure.
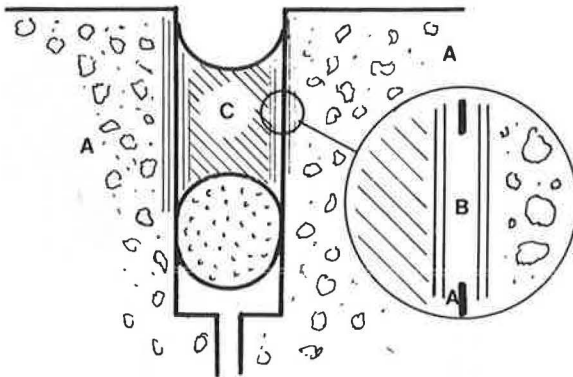
FIGURE 2 Principal failure locations in joint-sealant systems.

Each failure mode had characteristic indicators that helped to identify the probable cause of a concrete failure. They include

● Angles of fracture at the channel face and the pavement surface,
● Intersection points of the fracture with the pavement surface and the channel face,
● Surface characteristics of the principal fracture face, and
● Comparative surface characteristics of the failed and intact adjacent pavement surfaces.

Concrete defect, torque-shear, and groove (tine) failures are causing unacceptably high rates of failure in Utah. A major concern is that these three failure modes do not appear to be correctable with existing joint designs. The depth of the joint designs appears to be the underlying cause of saw shear forces' being transmitted into the concrete adjacent to the joint channel faces resulting in stress cracking.

Concrete Defect Failure

Concrete defect failures include loss of aggregates, defective or inadequate aggregates, foreign matter (clay or organic particles), or mortar deficiencies. Failures may be initiated by saw action, surface loadings, water, lack of water, wet-dry cycling, temperature changes, or freezing and thawing.

Individual Aggregate Failure

Loss of individual aggregates from the channel-pavement corner edge was fairly common. Loss from the channel face was less common. Individual aggregate failures had the appearance of a pop-out. Failure characteristics include a smooth failure face, mirroring the aggregate contours. The angle A (Figure 3) of the failure face either with pavement or channel surface was usually greater than 45 degrees. In some instances, the void would undercut the surface. The intersect of the fracture line with the pavement surface had little relationship to surface deformities or grooving. Cracking or rupture in the intact concrete adjacent to the fracture face was rare. Other failure indicators were usually not present.

Fractured-Aggregate and Deficient-Mortar Failure

Fractured-aggregate or deficient-mortar failures usually had a bulky, angular, somewhat trapezoidal, cross section. The fracture face was rough, but may have had smooth areas mirroring a segment of lost aggregate. The usual angle A of failure with either the channel or pavement surface was between 45 and 90 degrees; however, more acute angles occasionally occurred on the vertical channel surfaces. There was normally only one failure face. The intersect of the fracture line with the pavement surface had little relationship to surface deformities or grooving. Cracking or rupture in the intact concrete
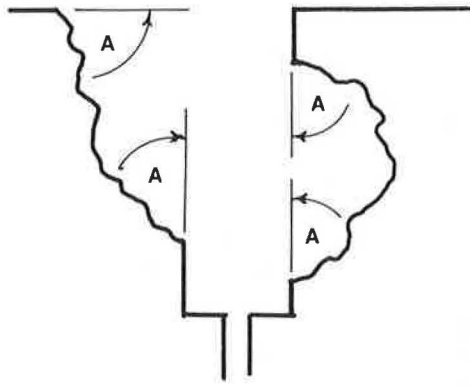
FIGURE 3 Angle of failure.

adjacent to the fracture face was rare. Other failure indicators were usually not present.

Foreign Matter

Channel surface failures caused by foreign matter were less common. Failures had characteristics similar to the other concrete defect failures, including cavity overhangs and retention of the pattern of the lost material. There was normally only one failure face. The intersect of the failure face with the pavement surface had little relationship to surface deformities or grooving. There was rarely any significant degree of cracking or rupture in the intact concrete adjacent to the fracture face. The surrounding pavement surface commonly had a large number of foreign-matter cavities. Other failure indicators were usually not present.

Torque-Shear Failure

Torque-shear failures were the most common concrete surround failure observed on Utah joint channels. Utah concretes contain hard to moderately hard aggregates; whether these failures will be as common in softer aggregates is not known.

Torque-shear failures were characterized either by individual or a connected series of thin triangularly shaped failures resembling flint or chert pressure-flaked arrowheads. They usually occurred on the upper half of the vertical channel surfaces, and rarely extended into the lower third of the channel. Torque-shear failures tended to occur randomly, or in random groups, with the effected horizontal channel segment varying from a fraction of an inch to over 1 ft in length. Failure groups did not occur opposite each other. On new construction, torque-shear failures were about equally distributed on both sides of the joint. On the one joint rehabilitation project evaluated, the rate of torque-shear failure was much lower on the older concrete. Patches, however, had failure rates similar to or higher than new construction.

The individual failure was thin and usually longer than it was wide. The arrowhead shape was distinctive and rarely associated with other failure modes. (Arrowhead shapes associated with other failures tended to be thicker and bulkier.) The angle *A* of the failure with the channel surface was usually

between 15 and 30 degrees; and between 60 and 90 degrees at the intersect with the pavement surface. The fracture face was generally rough. Shallow failures tended to be closely interlocked and have the appearance of a raveled edge. This appearance of raveling became more pronounced over time as the high points between the failures deteriorated. On the deeper failures, other failure indicators were usually not present.

Torque-shear failures occurred over a number of years; the lack of early failures did not reflect the extent of the eventual failure. Early appearance of failures was more likely with sealants that did not stress and relax, such as RTV silicones. Early appearance also seemed to be initiated by a deformity in the pavement surface (see groove-tine failure). There was also some evidence that torque-shear failures will be less, or their formation may be delayed longer with sealants that stress and relax, such as the more ductile polymer-modified asphalt rubber materials.

Torque-shear failure appears to be caused by uplift saw forces acting on the concrete immediately adjacent to the channel face. The shear forces are transmitted to the concrete face by friction when a force acting at a right angle to the joint is applied to the saw. The most common source of transverse forces is the operator, who uses side pressure to maintain the alignment of the joint channel over the shrinkage cut. A second source of transverse force may be blade or shaft misalignment. However, misalignment-related failures would probably tend to be fairly continuous, whereas most of the failures observed on the Utah sites were random. Individuals familiar with misalignment-related problems are requested to comment.

Groove (Tine) Failure

Groove, or tine, failures appear to be a subcategory of torque-shear failure, the tine groove acting as a failure initiator for the torque-shear failure. If this case occurs, torque-shear-related failures are more likely to appear earlier on a grooved pavement than on pavement with a less pronounced finish.

Groove (tine) failure is indicated when the failure resembles the torque-shear failure but intersects the invert or lower portion of the tine groove. On the Utah sites, groove failures rarely occurred beyond the invert closest to the joint. Failures extending farther into the concrete surround were usually caused by other factors. The literature indicates the use of various protective devices, (e.g., canvas or metal strips) to prevent the intersection of the tine groove with the joint channel has apparently reduced the frequency of early tine failure. However, if in fact these failures are caused by saw-related, torque-shear stresses, then the problem has been deferred and failure will be occurring later in the joint-sealant system's life. Investigators who have experience with the various protective devices are requested to comment on delayed failure.

Vertical Compression Failure

Vertical compression failures were a result of running steel-rimmed or metal-tracked equipment on the concrete. The

failures usually resembled fractured aggregate or deficient mortar failures, having a bulky, angular, somewhat trapezoidal, cross section. The fracture face was usually rough, but occasionally had smooth areas. The angles A of failure with both the channel and pavement surfaces were between 45 and 90 degrees; however, angles approaching 15 degrees occurred on a few vertical channel surfaces. Unlike fractured aggregate or deficient mortar failures, there were often multiple fracture faces. The fracture line frequently intersected the invert of a tine groove. Vertical compression failures normally had fine rupture cracks radiating from the fracture faces. Spider-web cracking was not typically present. If the failure section was present, it normally contained a number of fractures. A path of crushed high points was usually present on the recently damaged pavement surface between joints. On older pavements, wear usually erased this evidence.

Horizontal Compression Failure

Horizontal compression failures are caused by incompressibles lodging in the joint channel. Incompressibles lodged in the channel when the top surface of the sealant was placed too low or when there was a failure of the joint-sealant system that permitted incompressibles to enter the system.

Horizontal compression failures resembled fractured-aggregate or deficient-mortar failures. They usually had a bulky, angular, trapezoidal, cross section with a single fracture face. The intersects of the fracture face had little relationship to pavement surface deformities or grooving. The fracture face was generally rough, but occasionally had smooth areas.

Unlike fractured aggregate or deficient mortar failures, the usual angle A of failure at the pavement surface was between 30 and 60 degrees. Although angles of failure with the vertical channel surfaces were normally between 90 and 60 degrees, steeper angles of channel failure to about 30 degrees did occur. Often some cracking or rupture occurred in the concrete channel adjacent to the fracture face. The concrete adjacent to the pavement surface intersect often had spiderweb cracking. Shallow failures tended to be longer in the horizontal plane than in the vertical plane.

FAILURE MODES—CONCRETE-SEALANT INTERFACE

Concrete-sealant interface failures are usually described as adhesion or bond failure. The common terms have come to imply a sealant or preparation-related deficiency. This implication is unfortunate because it directs attention away from other causes. Concrete-sealant interface failures may be classified into four groups: preparation-related failures, application-related failures, sealant-related failures, and moisture- and cold-related failures.

Preparation-Related Failure

Ineffective preparation is the failure to provide a concrete channel bond surface with an adequate level-of-cleanliness. There are at least four physical sources of preparation failures: dirt, laitance, dust, and oil. These failure modes are well known and will not be discussed further. The fifth source is

tacitly acknowledged and ignored. But until the communication problem is resolved, preparation failures will be routine.

Ineffectual Communication

Neither a generally acceptable definition of what is an adequate level-of-cleanliness, nor a generally acceptable procedure for obtaining it are available. The immediate consequence is that none of the individuals involved in joint preparation operations have a consistent, explicit method of determining what is clean. As a result, specification, preparation, and enforcement vary greatly and premature failures are ensured.

Also, some sealants may require a higher level-of-cleanliness to achieve acceptable bond. Without a repeatable standard and method for measuring it, the determination of what level-of-cleanliness is required for a given sealant is impossible.

A similar, much less understood problem exists regarding the determination and measurement of acceptable level-of-moisture.

FAILURE MODES—APPLICATION-RELATED

Application-related failures include inadequate depth control, inappropriate design depth, inadequate backer rod installation, inappropriate backer rod, inadequate tooling, pavement surface overlap, and overheating of hot pours. The first four are reasonably well known but will be briefly summarized.

Inadequate Depth Control

Inadequate depth control is primarily caused by a lack or incorrect use of depth gauges. Nonadjustable T-gauges are preferred for inspectors and installers; adjustable gauges are appropriate for administrative personnel.

Inappropriate Design Depth

Inappropriate design depth occurs when the top surface of the sealant is placed too low, permitting incompressibles to lodge in the joint above the sealant.

Inadequate Backer Rod Installation

Backer rod depth determines the lower boundary of most field-placed sealants. Inaccurate placement results in inappropriate sealant thicknesses that usually result in premature failure. Torn, cut, or broken backer rods may interfere with adhesion or cause cohesion failures. Selection of inappropriate backer rod may cause sealant dissolve or bubble caused by chemical reactions or heat reactions.

Inadequate Tooling

Tooling has three functions: to provide the desired recess configuration, distribute the sealant over the bonding surface, and obtain adequate pressure for adhesion.

Sealant distribution and adequate adhesion pressure require tooling device down-pressure sufficient to mold the sealant

into the designed configuration (outlined by the backer rod and the channel) and obtain an adequate bond. The difficulty is that the information available both to the individual doing the tooling (tooler) and to the wand operator (placer) is inadequate. The tooler has insufficient feedback to determine whether the pressure being exerted on the tool is adequate to achieve molding the bond. The placer has to determine whether sufficient material is being placed in the channel, but the visible surface may not provide sufficient information to ensure that enough material has been delivered.

Visual inspection procedures emphasize obtaining the desired recess shape and eliminating any overlap onto the pavement surface. These constraints cause the tooler, placer, and inspector to err on the side of the visible desired result and to neglect the invisible desired result. The problem is further complicated because inspection to determine adequate molding and adhesion is judgmental. The removal of the sealant from the joint provides the installers with minimal information that has little relationship to the need for consistent information feedback.

Identifying this failure mode is difficult. The inadequate placement is hidden; and the failure may take a number of years to occur. Once the failure occurs, the cause may be difficult to assign. In part, because the inadequate placement failure mode can be mistaken for at least two other failure modes: inadequate preparation and surface moisture.

There are two definitive indicators of inadequate tooling; both require removal of the sealant. Cold-pour sealant pumps usually produce a pulsed placement pattern. If the down force is insufficient to mold the sealant to the bond faces of the channel then a ripple pattern is left on the bond face of the sealant. The other indicator is a lack of molding into the area between the backer rod and the channel face. However, the lack of the ripple pattern and good conformance to the channel does not necessarily confirm adequate placement pressure.

Excessive down-pressure may force the backer rod deeper into the channel, deform the rod, or cause the sealant to overlap onto the pavement surface.

Pavement Surface Overlap

Overlap of the sealant onto the pavement surface is a cause of early failure for some materials; for other materials overlap of the material onto the pavement surface may significantly improve performance.

RTV Silicones

When some RTV silicones overlap onto the surface, traffic action causes the trafficked portion to loosen. The loosened flap functions as a lever and may cause a fissure to form in the concrete-sealant interface at the top of the channel. Over a period of time, the fissure fills with contaminants causing further breakdown of the interface, eventually resulting in premature failure.

Polymer-Modified Asphalt Rubbers

Overlapped, trafficked, low-modulus asphalt rubber hot-pours performed much better than nontrafficked portions of the

sealants on the Utah test sites. The bond to the pavement surface remained intact. Equally important, the materials exposed to tire action retained their ductile, elastic, and adhesive characteristics significantly longer than the same materials in either the joint channel or on the overlapped, untrafficked shoulders. This performance reflected similar observations of equivalent sealant materials used on Utah asphalt crack sealant test sites (*3*). However, the wear characteristics of these materials are insufficient to handle moderate-to-high average daily traffic when the sealant is placed in an exposed band on the surface of the pavement. Significant differences can occur in the wear characteristics of different brands meeting the same ASTM/AASHTO specifications.

Solvent-Related Failure

Solvent-related failures are usually associated with hot-pours. However, there is evidence that cold-pours may be failing because of solvents effecting cure. In 1987, one RTV silicone exhibited an apparent cure problem in Utah. The characteristics of the Utah failure were good adhesion but unacceptably low resilience. Events and failure characteristics indicated a possible nonsealant-related cause. Dust control water had been obtained from a source polluted by a petroleum product; the failures were most pronounced near where the water trucks entered the roadway; there was a pattern of reduced failure as distance from the entry point increased.

FAILURE MODES—SEALANT-RELATED

Sealant-related failure is defined as a material deficiency that results in inadequate performance. Sealant-related failures can be divided into acceptance of incompressibles, cohesion failure, and bond deterioration. Acceptance of incompressibles and cohesion failure have received extensive attention in the literature; bond face deterioration, particularly, of polymer-modified asphalt rubbers has not.

Bond Face Deterioration

On the Utah test sites, apparent decomposition of the sealant bond face was observed in all polymer-modified asphalt rubber sealants, and to a lesser degree on PVC coaltar sealants. Bond deterioration caused by sealant bond face decomposition was not identified with RTV silicone materials.

Polymer-Modified Asphalt Rubber Failure Modes

For better-performing polymer-modified asphalt rubber sealants, sealant bond face deterioration is indicated when the following conditions exist:

1. There is no full-depth interface failure the first winter,
2. Other failure modes are not present or do not adequately explain the interface failure, and
3. The failed portion of the sealant bond face shows signs of weathering similar to untrafficked surface weathering.

First-year bond separations are usually not open long enough or wide enough to acquire a sufficient number of fines to keep the separation open when the joint closes in the spring. The failure identification is complicated because many materials soften, may absorb the fines, and may readhere to the joint face. This adherence can begin early in the spring; and with some materials, depending on weather, may be complete within a few weeks. The bond associated with this readherence is weak and will fail soon after the joints begin to open in cold weather. Failure can be determined by lightly probing the interface with a thin, narrow blade. The blade will easily penetrate a readhered bond; whereas the same pressure on a good bond will achieve little if any penetration. When a failed interface is opened up by a probe, it will reveal fines embedded in the sealant surface.

Partial-depth failures begin at the top of the channel-sealant interface. In appearance, the sealant failure closely resembles the deterioration of the untrafficked sealant at a similar stage of failure development. Like the untrafficked sealant failure, the sealant bond face failure appears to be related to oxidation (e.g., the deterioration appears to be related to exposure to water, ultraviolet, and air). Failures may also be occurring at the bottom channel-sealant interface, but observations were insufficient to confirm the existence of this failure mode. The partial-depth failure generally takes 2 to 3 years to become a full-depth failure. A full-depth failure the first year is usually related to another failure mode.

Partial-depth failures are frequently attributed to poor preparation. However, when poor preparation does occur high in the channel it will also occur lower down, resulting in a full-depth failure the first year.

Concrete-Related Failure—All Sealants

Characteristics of concretes may influence both bond development and longevity of bond regardless of sealant type. Concretes consist of diverse materials having different chemical properties. Void structures, permeability of mortar, fractures, and aggregate defects provide openings for water, oxidants, and reducing agents to infiltrate the channel-sealant interface. Frequently, materials with different chemical characteristics adjoin. The presence of moisture and oxygen facilitates the development of a wide variety of acids and bases either from the infiltrating materials or from the pavement structure itself. Wetting and drying effects have received little attention in the literature and may not be well understood for this environment, but their effects on adhesion between other materials are known to cause breakdown of the bond.

The effect of these factors on sealant adhesion, particularly long-term bond, has been generally neglected. A few states require sealants to adhere to concretes typical of their region; some still use ASTM mortar block bond tests that rarely reflect actual conditions; whereas others do not test. The bond tests themselves are short-term tests and do not provide information regarding longevity of bond. Early bond failures in some instances have resulted in the use of primers that appear to have reduced or eliminated early bond failure. The long-term effects of the primers on joint-sealant performance, however, has received inadequate attention.

FAILURE MODES—MOISTURE- AND COLD-RELATED

Presence of surface water, rain, snow, and ice are obvious sources of failure. Moreover, sealant installation frequently occurs when equivalent conditions exist because of condensation or cold weather.

Cold-Weather Failure Modes

Hot-pour failures because of cold weather were originally isolated in evaluations of asphalt concrete crack sealant failures. Neither hot-pour nor cold-pour failures caused by cold alone have been observed on the Utah concrete joint sealant test sites. However, the asphalt pavement sealant failures indicate that cold is inducing similar failures in concrete joint systems.

Asphalt Concrete Crack Sealant Failure Indicators

Characteristics of asphalt concrete sealant failures related to cold weather can be seen by removing the intact sealant from the asphalt and examining the bond surface. If the pavement or sealant was too cold during application, the sealant will have skinned rapidly. The sealant bond surface will not accurately replicate the surface pattern of the asphalt, but will display a blurred pattern or in extreme cases, no pattern. Bond strength is reduced but typically fairly uniform. In extreme cases, there may be no bond.

Cold-bond sealant failures on asphalt concrete are frequently accompanied by dirt- and moisture-related failure modes. Both dirt- and moisture-related failure modes result in irregular bond strength. If the failure is related to inadequate cleaning, the bond surface will contain dirt particles. If the failure is moisture related, the wearing surface of the sealant (band configurations) will contain small holes, each frequently surrounded by a small crater-like depression. The bond surface below the crater will show a smooth area with little or no surface pattern.

Concrete Joint Sealant Failure Indicators

Concrete sealant failures related to cold weather will be difficult to isolate. The concrete channel and backer rod provide texture-free, smooth bond faces, eliminating one of the principal failure mode indicators (some backer rods do provide texture). Reduction of bond strength is an indicator. But reduction in bond strength is also connected with other failure modes and does not provide a definitive indicator by itself. Weather records, equipment application temperature logs, and knowledge of the heat loss characteristics of the equipment used in sealing may provide enough supportive data to indicate cold weather related failure.

Equipment-Related Causes of Failure

Cold weather reduces or prevents sealant equipment from achieving or maintaining the required application tempera-

tures. With reacted material, underheating may prevent development of adequate bond. With unreacted material, other performance attributes in addition to bond may be affected. (Any material that requires being held at temperature for a given time before application is considered to be an unreacted sealant.)

Temperature gauges may contribute to the problem. A significant number of temperature gauges tested by the Utah Department of Transportation in 1982 to 1984 had substantial inaccuracies. Evaluation of temperature gauges on a random selection of Utah DOT sealant machines indicated that 1 in 3 gauges can be expected to be in error by at least 50°F, and that 1 in 6 gauges may be in error by at least 100°F.

Even if product tanks can achieve and maintain application temperatures, heat losses in the product pipe circuit, hose, and wand can reduce sealant temperature at the wand tip significantly below the desired application temperature. If these heat losses are coupled with a cold pavement, early failure is almost ensured.

Moisture-Related Failure Modes

Concrete is a permeable material whose moisture level tends to follow the humidity level of the surrounding environment. Sawing operations (and water blast cleaning) saturate the area surrounding the joint. Under hot-weather conditions, this additional moisture apparently has little adverse effect on sealing operations.

Joint Channel Microclimate

The joint channel, however, has its own microclimate. The existence and potential effects of the microclimate on sealants has been largely overlooked.

Two aspects of the microclimate are of particular importance, humidity and the temperatures of the air and channel faces. These two aspects determine dew point. When the dew point is reached, condensate can form on the joint channel faces. Dew point is a threshold reaction. Under supersaturated conditions, a minor drop in temperature can result in rapid formation of condensate.

The humidity of the joint channel during sealing will typically be quite high. This condition is caused in part by the reservoir of moisture at the base of the shrinkage crack, created by the joint saw's cooling water; and moisture drawn from the newly constructed concrete. The geometry of the joint channel may also be a factor in maintaining high channel humidity. The channel is narrow and deep. This geometry may prevent normal air circulation and contribute to a stagnant air volume.

If air temperatures are cycling below about 60°F (probable during spring or fall construction and in mountainous or desert locations), condensate related to dew point on the channel faces is likely. Clear skies will also increase the probability of condensate forming, because radiation heat loss at night from the pavement is increased.

Condensate-Related Failure

Condensate-related failure has not been definitively established. Evaluation of failures indicates that it is probable.

Characteristics of probable condensate failure can be divided into two groups: full-bond failure and partial-bond failure.

Full-depth condensate failure was observed on one of the Utah test sites. The failure occurred in the fall during a late evening RTV silicone sealing operation. Joints had been water blasted at least 24 hr prior to sealing. Both air blast before backer rod placement and brush and low-pressure air blast before sealing were being used. There had been no rain at this site for over 1 week. Temperatures during sealing were in the low 50s and may have dropped into the high 40s. The failure was observed the following morning while applying pressure to the sealant to check resilience. The characteristics of the failure were a total lack of bond, no fines or contaminants on bond face, and a light sheen of moisture on the bond face. The failure was total and included approximately 50 full-width joints. The critical indicator is the sheen of moisture. Condensate appears to have been the only valid source. It is pertinent to note that no dew or moisture was apparent on the pavement surface during the sealing operation or when the failure was first noted just after sunrise in the morning. Had this failure been found after the joint had opened significantly, the failure faces would likely have acquired sufficient superficially adhered debris that the failure would have been attributed to some other cause.

Hot-pours would be expected to cause the condensate to turn to steam, and bubbling may occur along the joint faces. Whether the bubbling is noticeable will depend on how much moisture is present and whether the sealant overlaps onto the pavement surface.

Partial-Depth Condensate Failure

This mode may be a fairly common failure mode, particularly with cold-pour materials such as RTV silicone. The characteristics of the failure are no visible surface failure. Surface resilience is adequate. The visible bond surface is intact but the sealant is easily forced downward. Movement of the probe (eraser tip of a wooden pencil) while the sealant is in the depressed condition results in feel of subsurface bond failure. This must be verified by removal of the affected sealant. If examination of the sealant bond faces shows bond failure, no rippling, adequate conformation to the lower channel and backer rod configuration, and no sign of contamination, then a possible cause of failure is condensation.

RTV Silicone

In addition to condensate failure, RTV silicone may have another moisture-related problem. The silicone bond peel test is conducted with oven-dried mortar blocks stored in a desiccated atmosphere. There is some indication that if the blocks are permitted to stand for 1 day or longer at higher humidities (more than 50 percent), there is a significant drop in peel strength. Considering that most pavement sealants are placed at relative humidities greater than 50 percent, this bond strength test may be misleading.

DETERIORATION OF FAILURE MODES

Individual failure modes were found to have distinctive, usually unique identifying characteristics. However, both dete-

rioration and multiple failure modes often interact to obscure the individual failure mode. Weather and traffic interact to wear away the distinguishing characteristics of the various failure modes. This loss of distinguishing characteristics can result in inaccurate conclusions as to cause of failure. Inaccurate conclusions misdirect the correction process and result in perpetuating the causes of the failure.

In order to identify failure modes accurately, inspection of joint-sealant systems during construction, immediately following construction, and at 6- to 12-month intervals for at least 5 years, is essential. Systematic multisealant, multiconfiguration, interlocked regional and national test sites would provide significant information that is presently not available from the one or two sealant test sites commonly placed by state experimental feature programs.

GENERAL FINDINGS

- The identification of failure modes is a key element in the correction of joint-sealant system failures.
- Failure modes were identified within the concrete adjacent to the joint channel, the sealant, and at the various interfaces between the sealant and its surround.
- Specific failure modes were associated with one or more of the evaluated sealants. The association of a failure mode with a given sealant does not necessarily have a causal relationship to that sealant.
- A number of failure modes appear to be inherent in existing joint designs, or construction and sealing practice. Similar failures may occur with other field-cured, preformed, elastic and preformed compression joint-sealant systems not included in the evaluations.
- Individual failure modes have distinctive, usually unique, identifying characteristics. However, both deterioration and multiple failure modes often interact to obscure the individual failure mode. In order to observe the individual failure modes as they develop, frequent, systematic evaluations are required.
- The loss of distinguishing failure mode characteristics can result in inaccurate conclusions as to cause of failure. Inaccurate conclusions misdirect the correction process and usually result in perpetuating the causes of the failure.
- A failure mode in one joint-sealant system may provide improved performance in another joint-sealant system.
- There is a need for nondestructive field evaluation equipment for the objective evaluation of joint-sealant system performance.

RECOMMENDATIONS

Systematic evaluation of multisealant, multiconfiguration, interlocked regional and national test sites would provide significant information toward the improvement of the performance and reduction in cost of these systems.

Inspection of representative joint-sealant systems and evaluation of failure modes should occur during construction, immediately following construction, and at 6- to 12-month intervals for a 5-year period thereafter.

Development of nondestructive field evaluation equipment for the objective evaluation of joint-sealant system preparation, installation, and performance should be given priority.

REFERENCES

1. M. C. Belangie, et al. *Evaluation of Concrete Joint Sealants, Clear Creek Summit to Belknap Interchange—Second Interim Report.* Utah Department of Transportation, April 1986.
2. M. C. Belangie. Evaluation of Concrete Joint Sealants—Nephi to Mills Jct. Draft report, Utah Department of Transportation, March 1987.
3. M. C. Belangie et al. *Crack Sealing—Methods and Materials for Flexible Pavement.* Second revision, Utah Department of Transportation, Oct. 1987.
4. R. C. Evers and D. F. Lynch. *Sealing Cracks in Asphaltic Concrete Pavements.* Ontario Ministry of Transportation and Communications, Oct. 1984.
5. G. J. Chong and W. A. Phang. *Improved Preventive Maintenance—Sealing Cracks in Flexible Pavements in Cold Regions.* Ontario Ministry of Transportation and Communications, Dec. 1987.
6. G. Loza and D. I. Anderson. *Evaluation of Concrete Joint Sealants—Clear Creek Summit to Belknap Interchange.* Second Interim Report, Utah Department of Transportation, June 1987.
7. G. Loza and D. I. Anderson. *Evaluation of Concrete Joint Sealants—Clear Creek Summit to Belknap Interchange.* Final draft, Utah Department of Transportation, May 1988.

Cracking and Seating of Concrete Pavement on I-74

Magdy El-Sheikh, Joseph J. Sudol, and Rebecca S. McDaniel

Cracking and seating is becoming a popular technique for reducing reflective cracks in asphalt overlays over deteriorated concrete pavements. Indiana initiated an experimental project on I-74 in the spring of 1984 to study the potential of cracking and seating. The performance of the asphalt overlay is described 5 years after implementing the technique. Cracking and seating prevented at least 75 percent of the reflective cracks that normally occur at 5 years of service life. Adding fibers to the asphalt overlay mixture over cracked and seated sections resulted in further prevention of reflective cracks, maintained the structural strengths both of the pavement and of its support, and may have reduced the formation of blowups. Furthermore, the number of blowups per mile in the cracked and seated sections was reduced by 50 percent over the control sections, which were not cracked and seated.

Many of the nation's highways are constructed with concrete pavements. These concrete pavements deteriorate with age, and resurfacing becomes necessary to restore rideability, structural strength, and skid resistance. Asphalt overlays have been a popular and practical choice for most resurfacing. However, experience has shown that an asphalt overlay usually develops a cracking pattern that reflects the one existing in the old concrete. Such cracks are referred to as "reflective cracks."

Reflective cracks are mainly initiated and propagated by thermally induced and traffic-induced stresses (1). Thermal contraction of the underlying concrete causes tensile strains in the asphalt overlay; cracks form whenever the tensile capacity is exceeded. The differential vertical deflections of the concrete pavement at cracks and joints under traffic loads also help propagate reflective cracks.

Preventing, or at least reducing, reflective cracks helps to prolong the service life of an asphalt overlay and reduces maintenance costs. Over the years, many techniques have been developed to try to control reflective cracks. One technique currently used by many states involves cracking and seating the old concrete pavement before overlaying it with asphalt. This technique has potential for reducing reflective cracks. The process of cracking and seating consists of breaking the old concrete slabs into small pieces and pressing these pieces down by rolling with heavy rollers.

The effectiveness of the cracking results from having smaller concrete slabs that undergo reduced thermal length changes and therefore induce smaller thermal strains in the asphalt overlay. Seating the cracked pieces also reduces the differential vertical deflections at cracks.

As a supplementary treatment to further reduce reflective cracks, part of this experiment contains polypropylene fibers

in the asphalt overlay. This addition of fibers to the overlay is intended to increase its tensile strength.

A description of roadway conditions following 5 years of service follows. Past experience indicates that development of reflective cracking in overlays, at this point in the pavement's life, has sufficiently stabilized so that the data obtained can be used to evaluate the merit of most crack reduction techniques. However, the previous five winters in Indiana were not severe and reflection cracking in general was slow to develop (2–4).

The original condition of the concrete pavement in this study was quite good between joints and cracks, but elsewhere it was in an advanced stage of deterioration because of D cracking. Pavement drainage did not appear to be a general problem, but localized areas with poor drainage did exist. Drainage was upgraded during construction of this contract and can be considered at this time to be good.

OBJECTIVES

The objectives of this experimental study are as follows:

1. To evaluate the effectiveness of the cracking and seating technique in reducing reflective cracks,
2. To determine the optimum asphalt overlay thickness for best crack control and pavement strength,
3. To study the effect of adding fibers to the asphalt overlay on reflective crack intensity and any resulting increase in strength, and
4. To investigate any negative aspects associated with these rehabilitation techniques.

SCOPE

The Indiana DOT initiated this experimental cracking and seating study in the spring of 1984. The project is located on I-74 and runs from SR-39 to 2.0 mi west of the Montgomery-Boone county line. It involves 12.2 mi of centerline concrete pavement originally constructed in 1974. The traffic volume is over 10,000 vehicles per day with about 30 percent trucks.

WORK PLAN

Eight different concrete pavement rehabilitation treatments were used in this study. The details of each treatment, as well as the layout of different sections rehabilitated, are shown in Table 1 and Figure 1, respectively. The two basic rehabilitation techniques used were

1. asphalt undersealing with an asphalt overlay, and
2. cracking and seating the concrete slabs with an asphalt overlay.

Indiana Department of Transportation, Division of Research, 1205 Montgomery Street, P.O. Box 2279, West Lafayette, Ind. 47906.

TABLE 1 REHABILITATION TREATMENTS

Treatment	Description	Overlay Thickness (in.)	Overlay Contents (lb./sq.yd.)		
			Surface	Binder	Base
A	asphalt underseal with asphalt overlay	4.25	70	150	250
A1	as A with fiber reinforced asphalt base layers	4.25	70	150	250
A2	as A with fiber reinforced asphalt base and binder layers	4.25	70	150	250
B	cracked and seated with asphalt overlay	5.00	70	150	330
B1	as B with fiber reinforced base layer	5.00	70	150	330
B2	as B with fiber reinforced asphalt base and binder layers	5.00	70	150	330
C	cracked and seated with asphalt overlay	6.50	70	150	510
D	cracked and seated with asphalt overlay	8.50	70	150	700

An asphalt overlay thickness of 4.25 in. was used for the control sections. These control sections were also undersealed with asphalt. Overlay thicknesses of 5.0, 6.5, and 8.5 in. were used on the cracked and seated sections. Fibers were added both to the base and binder mixtures on one control section and on one cracked and seated section. Fibers were also added to the base layer only for one control and one cracked and seated section.

To determine the performance of these treatments for various sections, the following actions were conducted:

1. Transverse reflective cracks were counted by visual survey each year for each section over a 5-year period (1985 to 1989).
2. Deflections were measured using the Dynaflect each year for all sections.
3. Blowups were counted for each section by visual survey.
4. Ruts in the wheel path were measured for all sections using a 4.0-ft straightedge.

RESULTS

Reflective Cracks

Reflective crack intensities for different treatments over the 5-year period were plotted in Figure 2. The reflective crack

development on the control sections was high in the beginning and increased at a fast rate. Most reflected cracks show considerable compounding and meandering, probably because of the D cracking in the old pavement. Adding fibers to the mixtures in the control sections did not help to control the occurrence of high crack reflection in the first 2 years; however, crack development progressed more slowly afterwards. Reflective crack development on the cracked and seated sections was low in the first 3 years and thereafter increased slowly. Cracking and seating reduced reflective cracks by at least 75 percent over those occurring in the uncracked control sections. A further reduction of reflective cracking on the cracked and seated sections was obtained by the addition of fibers to the asphalt mixture. It was observed that increasing asphalt overlay thickness on the cracked and seated sections from 5.0 to 6.5 in. reduced the number of reflection cracks by about 25 percent. As expected, overlaying with 8.5 in. of asphalt reduced reflective cracks even more. Also, adding the fibers to the asphalt mixture delayed the onset of reflective cracks and reduced their rate of development.

Road Structural Strength

Deflections for all the different sections were collected annually using the Dynaflect. In Figures 3 to 6, the maximum and minimum Dynaflect readings taken in 1984 and 1988 (or 1989)

KEY:

Underseal, 4¼ in. Overlay
Crack & Seat, 5 in. Overlay   1: Fiber Reinforced Base
Crack & Seat, 6½ in. Overlay   2: Fiber Reinforced Base
Crack & Seat, 8½ in. Overlay   and Binder
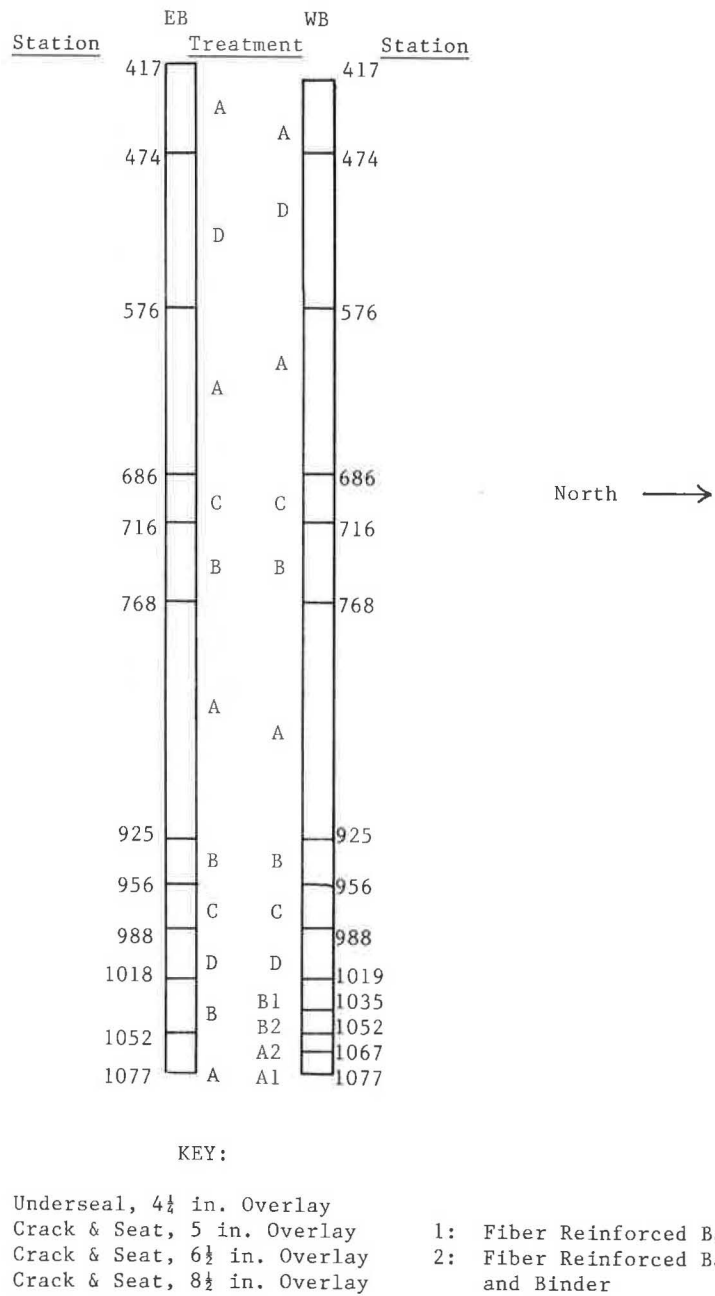
FIGURE 1 Treatment locations.

were plotted for all different treatments. The deflection data were adjusted to the standard temperature of 70°F according to Majidzadeh and Kumar (5). Maximum deflections indicate the relative strength of the pavement section, whereas minimum deflections give an indication of the relative strength of the pavement support. Satisfactory maximum deflection for overlaid concrete pavement is 0.50 mils, whereas the unsatisfactory value starts at 0.70 mils. Satisfactory minimum deflection is under 0.30 mils. Anything over 0.30 mils represents poor pavement support (5).

The 4.25-in. overlay on the uncracked control section is similar in strength to the 8.50-in. overlay on the cracked and seated section. Both of these sections have undergone less than 15 percent strength decrease in 5 years. However, the cracked and seated sections with 5.0- and 6.5-in. overlays have

deteriorated in strength as much as 50 percent. As can be seen in Figures 4 and 6, the addition of fibers to the overlay mix improved or at least maintained the total pavement strength and the pavement support strength with time. The addition of fibers to either the base (fb) or binder, or both (fbb), improved or maintained the pavement strength similar to uncracked pavement with 4.25 in. overlay or to the cracked and seated pavement with 8.50-in. overlay.

Ruts and Blowups

Ruts were measured in the wheel path on all pavement sections using a 4.0-ft straightedge in 1989. Ruts for all fiber mix overlay sections were approximately ¹⁄₁₆ in. and for all other
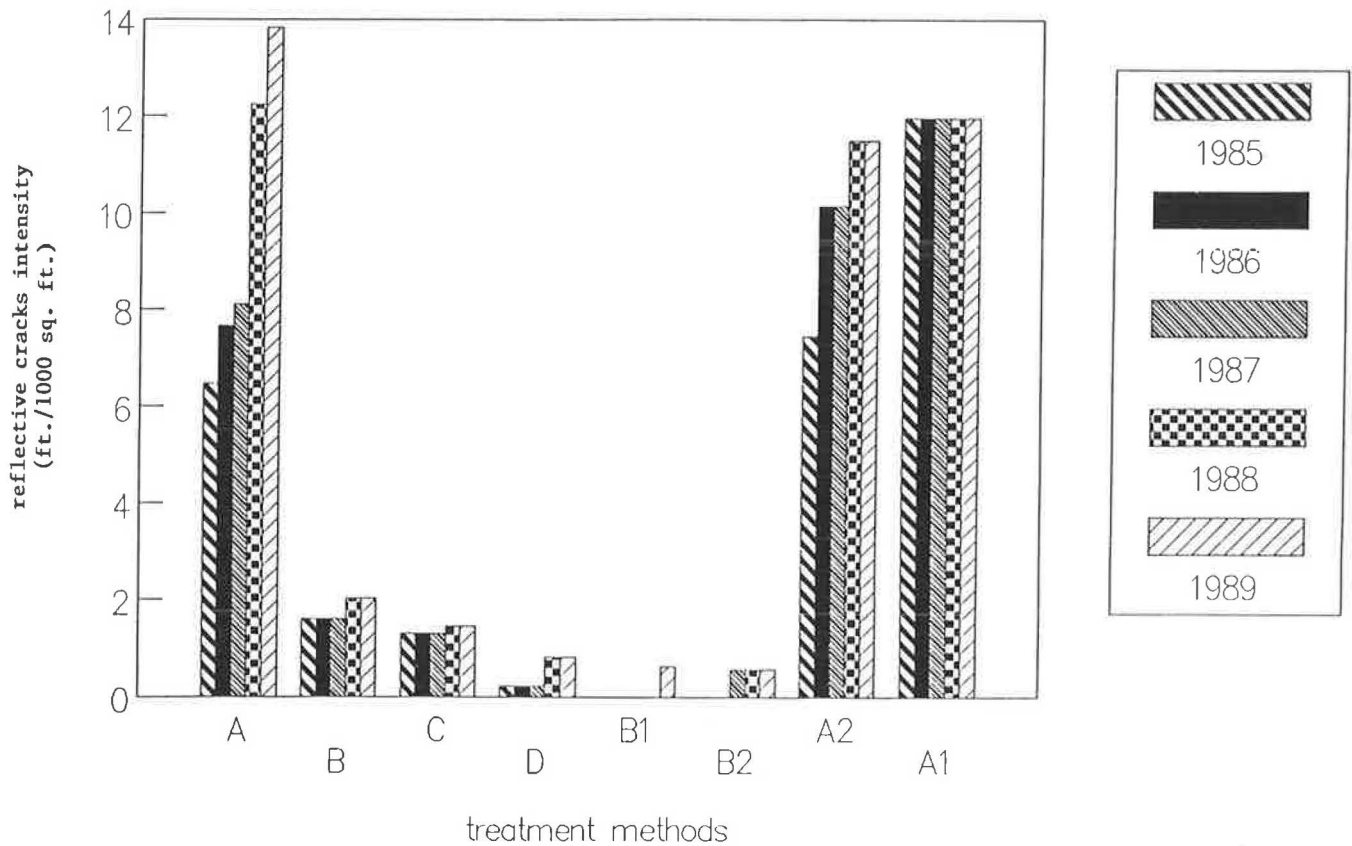
FIGURE 2 Development of reflective cracks with time for several treatments.

sections they were about ⅛ in. The slight difference in rutting is attributed to the fiber reinforcement of the overlay mix, as expected. In both cases, however, rut depths are lower than one would expect on bituminous pavements after 5 years of service.

Blowups were surveyed visually for different treatments in 1989. The blowup intensities (number of blowups per mile) are shown in Figure 7. Blowup intensities in cracked and seated sections are less than on the uncracked control sections by about 50 percent. Also, on the sections with added fibers, no blowups have been observed. Blowups, as defined here, are all sharp pavement protrusions that develop over the joints and which grow with time and eventually need to be milled or burned off. Blowups are relatively rare events, so the observed differences may not be significant.

VISUAL OBSERVATIONS

The severity of reflective cracks for the different treatments has been visually surveyed. Cracks in control sections containing fibers were compounded and more severe than those elsewhere, as shown in Figures 2 and 8.

Most blowups were not severe, except one that now is rough and should be milled or ground off to restore rideability. Several other blowups have been milled off during the past 5 years.

Some longitudinal surface cracks were observed in the wheelpath. The reason for the formation of such cracks is not understood. They appear to be related to the surface mixture only.

CONCLUSIONS

Cracking and seating techniques reduced reflective cracks by at least 75 percent over those occurring in the uncracked control sections.

Adding fibers to the asphalt overlay mix over cracked and seated sections reduced reflective cracking by 85 percent over cracks occurring in the control sections. The fibers also improved the pavement strength and support conditions by about 15 percent over sections without fibers. Fiber addition did not significantly reduce reflective cracking for sections that were not cracked and seated.

The 5.0-in. asphalt overlay with fibers gave the best performance among all treatment combinations with respect to reflective cracking and maintaining pavement strength.

Generally, blowup intensity on the cracked and seated sections was observed to be less than that in control sections by at least 50 percent. Reinforcing the asphalt overlay with fibers reduced rutting slightly and may have prevented blowups from developing.

Treatment: underseal, 4.25 in. overlay
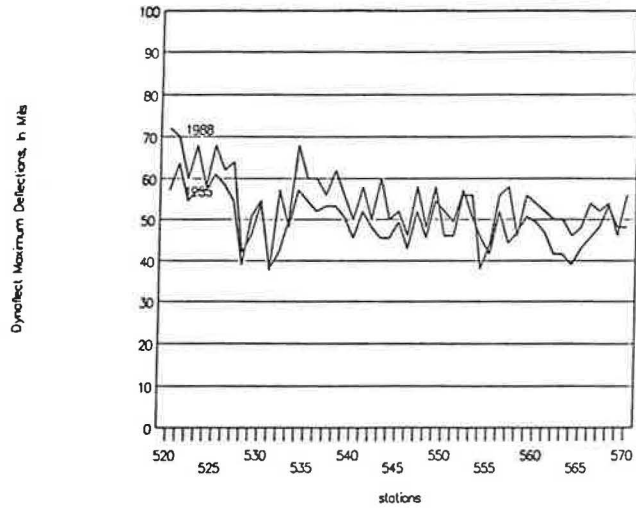
Treatment:Crack&Seat, 5 in. overlay
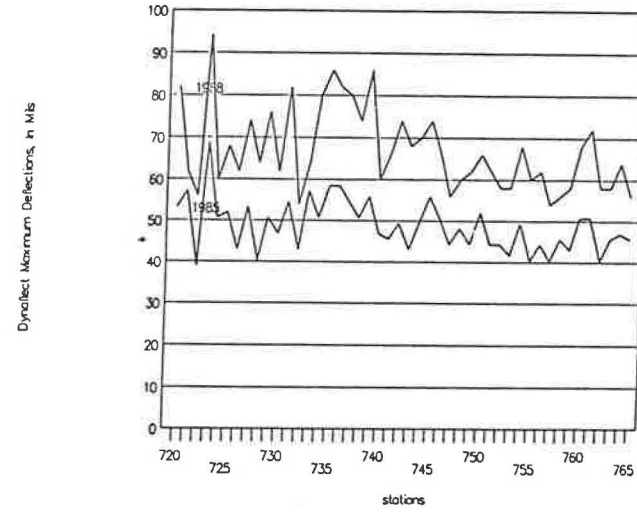
Treatment: Crack&seat, 6.5 in. overlay
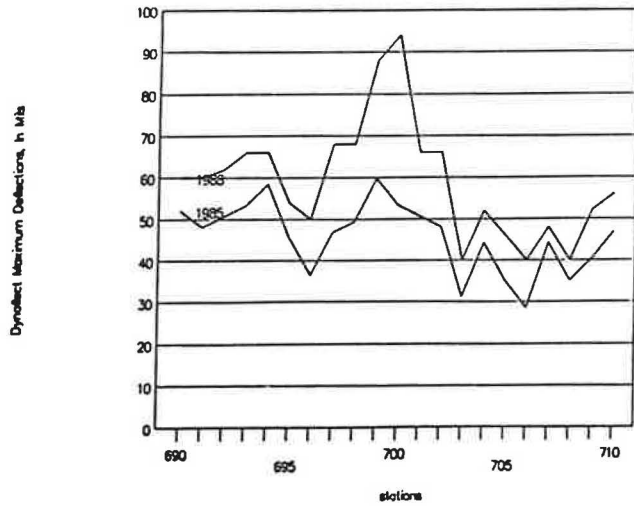
Treatment: Crack&seat, 8.5 in. overlay
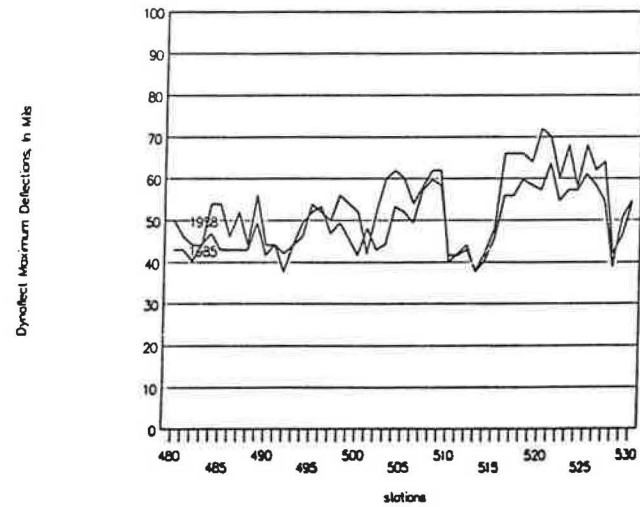
FIGURE 3   Dynaflect maximum deflections.

Treatment: Underseal-4.25 in. – fb

Treatment: Underseal-4.25 in. – fbb
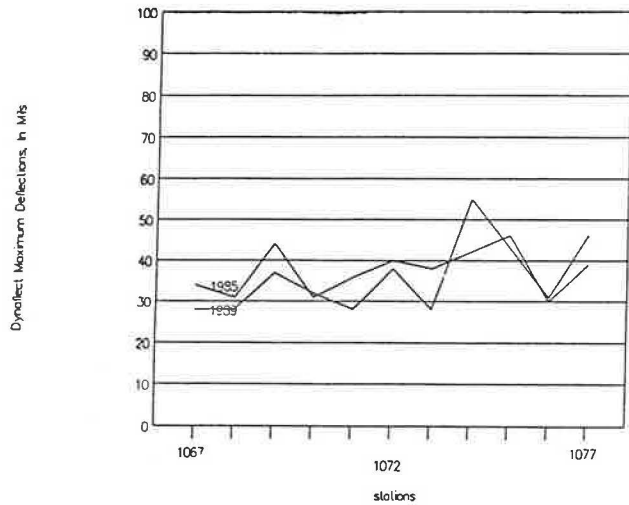
fb: fibers are added to asphalt base layer
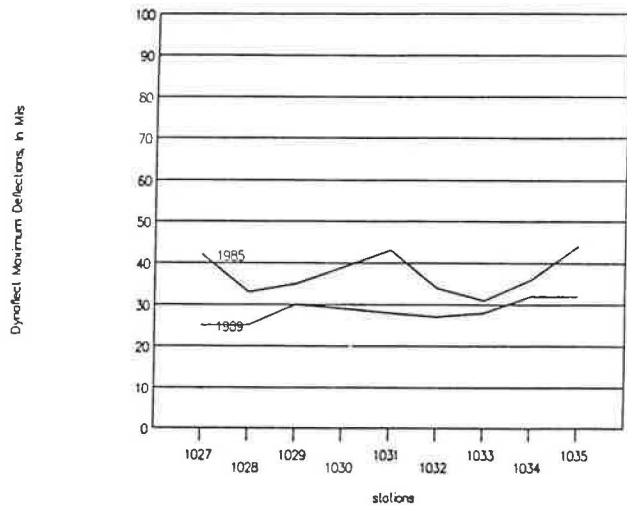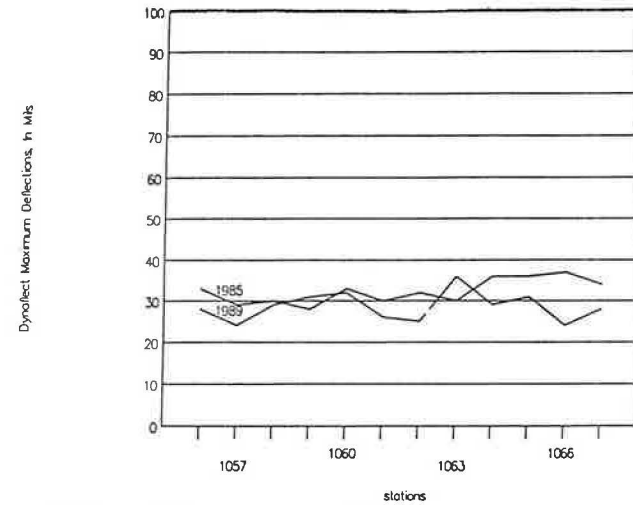
fbb: fibers are added to both asphalt base
and binder layers

Treatment: Crack&seat – 5.0 in. – fb

Treatment: Crack&seat – 5 in.– fbb
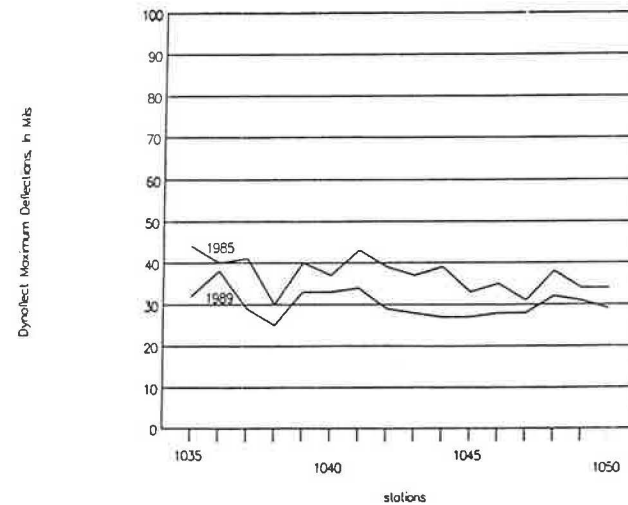
FIGURE 4 Dynaflect maximum deflections with fibers added.

Treatment: underseal, 4.25 in. overlay
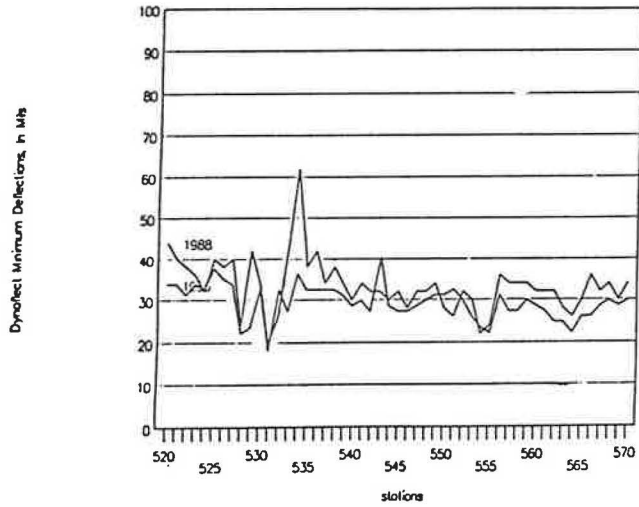
Treatment:Crack&Seat, 5 in. overlay
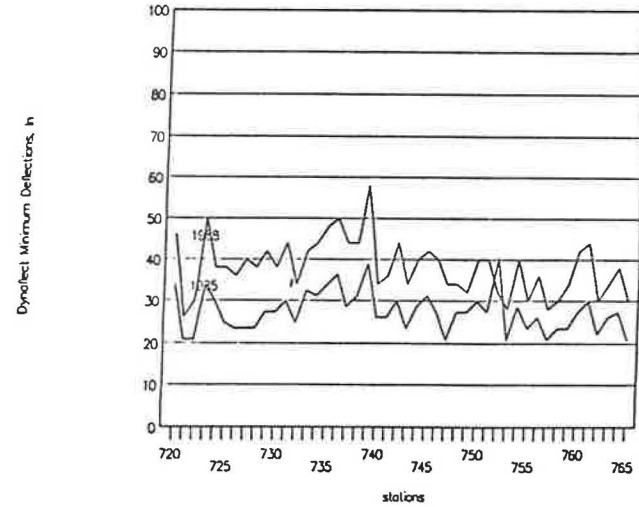
Treatment: Crack&seat, 6.5 in. overlay
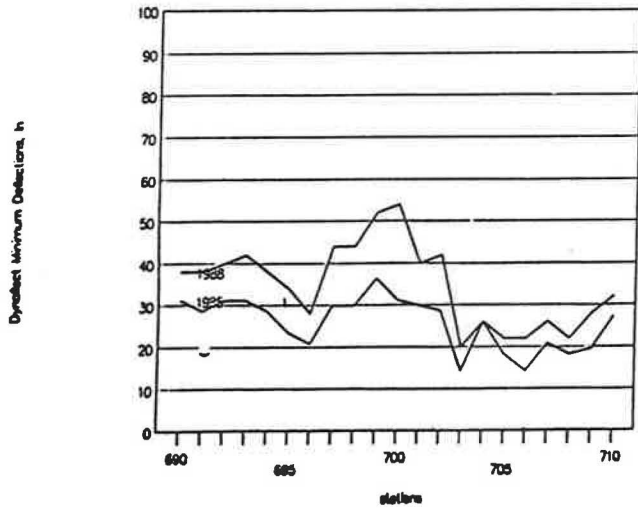
Treatment: Crack&seat, 8.5 in. overlay
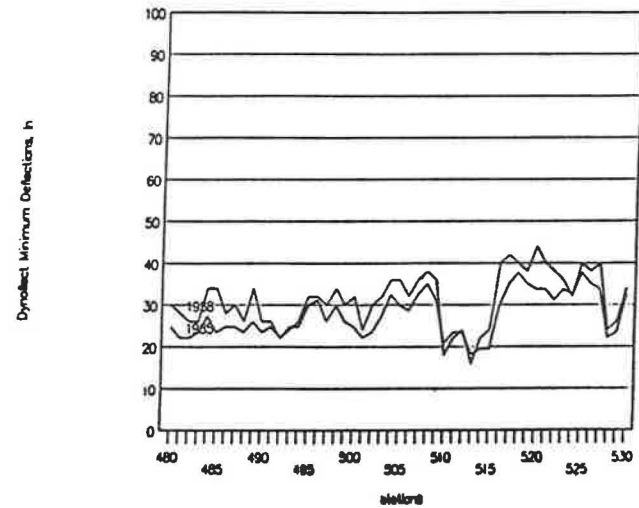
FIGURE 5   Dynaflect minimum deflections.

Treatment: Underseal-4.25 in. - fb
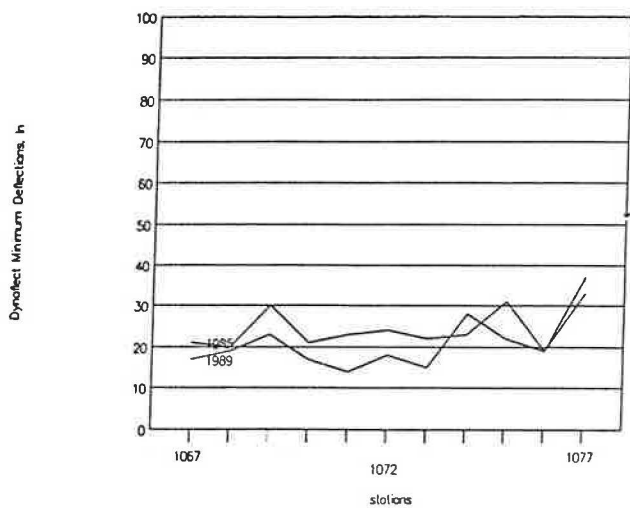
Treatment: Underseal-4.25 in. - fbb
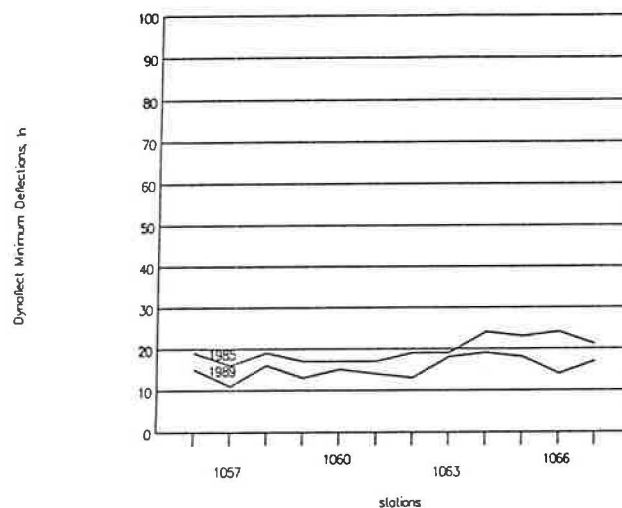
Treatment: Crack&seat - 5.0 in. - fb
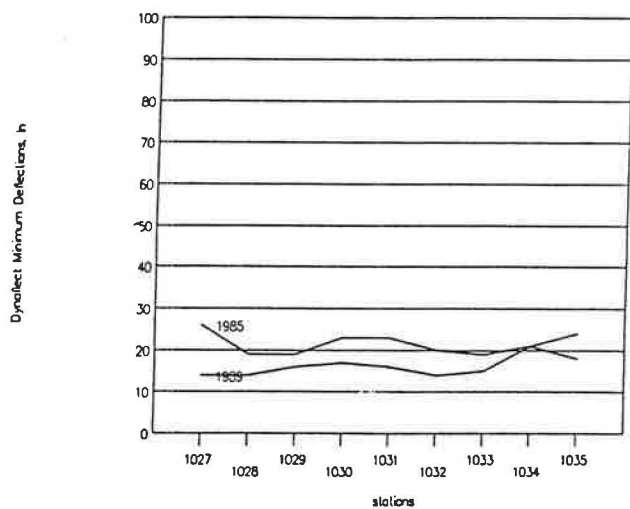
Treatment: Crack&seat - 5 in.- fbb
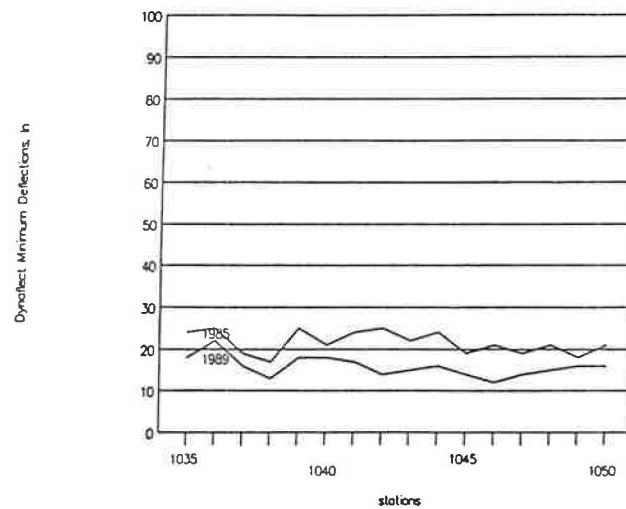
FIGURE 6 Dynaflect minimum deflections with fibers added.
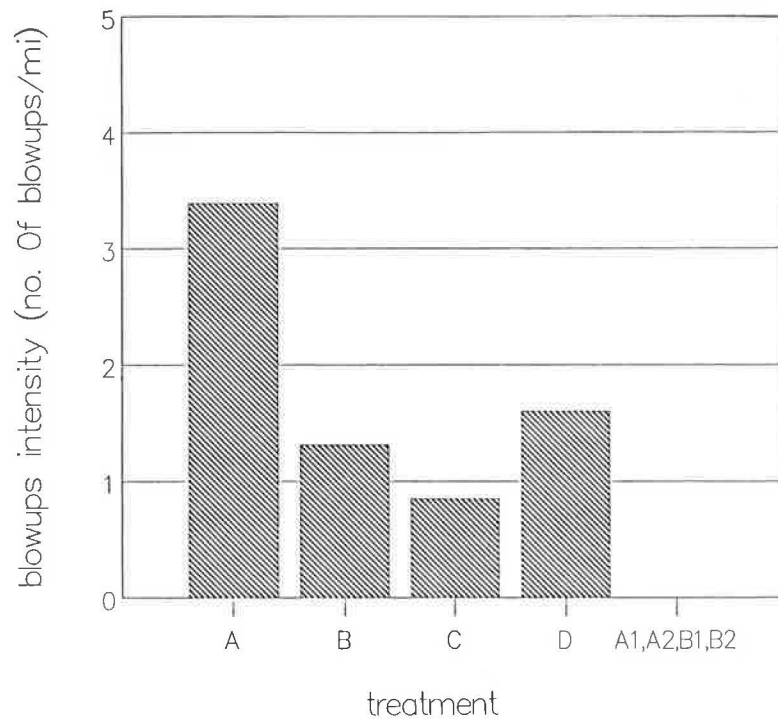
FIGURE 7   Blowup intensities (1989).
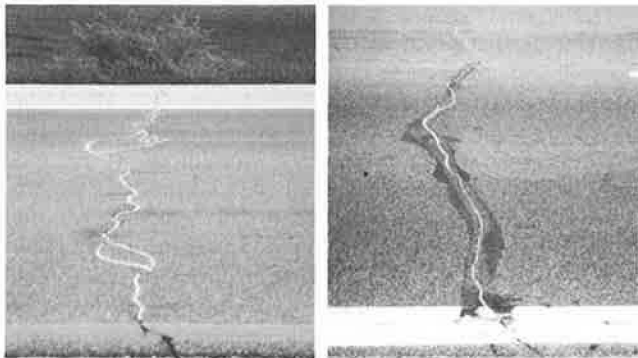
FIGURE 8   Typical reflective crack (*left*) in fiber section and (*right*) elsewhere.

REFERENCES

1. C. Crawford. *Cracking and Seating of PCC Pavements Prior to Overlaying with Hot Mix Asphalt: State-of-the-Art.* Information Series 98/89, National Asphalt Pavement Association, Riverdale, Md. 1989.

2. M. D. Harness. *Cracking and Seating of Concrete Pavement on I-74.* Report IN84-01A, Indiana Department of Transportation, Division of Research, West Lafayette, Ind., 1987.

3. M. D. Harness. *Performance of Bituminous Mixtures with Polypropylene Fibers.* Report IN84-01B, Indiana Department of Transportation, Division of Research, West Lafayette, Ind., 1987.

4. M. D. Harness and J. J. Sudol. *Initial Construction and Interim Report: Cracking and Seating of Concrete Pavement on I-74 and Performance of Bituminous Mixtures with Polypropylene Fiber.* Indiana Department of Transportation, Division of Research, West Lafayette, Ind., 1986.

5. K. Majidzadeh and V. Kumar. *Manual of Operation and Use of Dynaflect for Pavement Evaluation.* Resource International Inc., Ohio Department of Transportation, and FHWA, Department of Transportation, U.S. 1983.

Sawing and Sealing of Joints in Asphaltic Concrete Overlays

WALTER P. KILARESKI AND RICHARD A. BIONDA

One method used to rehabilitate portland cement concrete pavements is to place an asphaltic concrete (AC) overlay on the existing pavement. The overlay, which can improve the pavement's structural capacity and rideability, can also create maintenance problems. These problems result from reflection cracking at the location of joints and cracks in the underlying slab. A method used to control the reflection cracking problem is to saw a joint in the AC overlay above the existing joint and then seal the joint (i.e., sawing and sealing). The performance of AC overlays with sawing and sealing was the subject of a national study. Pavements with up to 10 years of service life were evaluated through condition surveys, roughness measurements, and deflection measurements. Both saw-and-seal pavements and control sections were evaluated. The analysis indicated that sawing and sealing improves the rideability of the AC overlay and significantly reduces the amount of transverse reflection cracking.

One method used to rehabilitate portland cement concrete (PCC) pavements is to place an asphaltic concrete (AC) overlay on the existing pavement. The overlays can help improve the structural capacity and rideability of the pavement. Although an overlay can improve the pavement performance, it can also create some maintenance problems. Generally, maintenance problems result from reflection cracking at the location of joints and cracks in the underlying slab. The reflective cracks can occur soon after the completion and placement of the overlay, thus reducing the cost-effectiveness of the overlay.

Numerous techniques and treatments have been tried to prevent or minimize the reflection cracking problem. Some of the treatments include the use of fabrics, stress-relieving interlayers, crack-arresting interlayers, and cracking and seating. The results of these treatments vary considerably. However, reflection cracking appears almost impossible to stop.

Because of this difficulty, some agencies have decided to control the problem rather than eliminate it. One method is to saw a joint in the overlay above all existing transverse joints immediately after its placement and completion, as shown in Figure 1. The joints are sealed with joint sealant material and subsequently maintained as typical pavement joints.

REFLECTION CRACKING FAILURE MECHANISM

Attempts to prevent the occurrence of reflective cracks in an AC overlay have been reported (1) as early as 1932. Since

that time, most of the advancements in the state of the art for reflective crack prevention have come primarily from experience gained through trial-and-error experiments on in-service pavements. Only in the last 10 to 15 years have theoretical studies of reflection cracking been conducted. Although these studies have not succeeded in developing a method that prevents reflection cracking, they have provided a better understanding of the mechanisms that cause an overlay to fail in this manner.

Pavement researchers generally agree that the primary mechanisms leading to the development of reflection cracks in an AC overlay are the horizontal and differential vertical movements at joints and cracks in the existing pavement, with horizontal movements considered more critical (2–6). Smith et al. (5) stated that these damaging horizontal movements are caused by three factors: traffic loadings, seasonal temperature changes, and daily temperature cycles.

Traffic loadings are responsible for differential vertical movements that occur at underlying joints with poor load transfer and at working cracks. Jayawickrama et al. (7,8) stated that three stress pulses occur as a moving wheel load travels across an underlying joint or crack, as shown in Figure 2. These stress pulses create stress concentrations that lead to reflection cracking.

Seasonal temperature changes and daily temperature cycles cause expansion, contraction, and curling in the existing slabs and overlay (Figure 3). A change in the moisture content (moisture differential) will also cause the slab to warp, creating stress concentrations in the overlay that can lead to cracking. The actual amount of movement is controlled by the temperature change, the thermal coefficient of expansion

W. P. Kilareski, Pennsylvania Transportation Institute, Pennsylvania State University, University Park, Pa. 16802. R. A. Bionda, Parsons, Brinckerhoff, Quade, and Douglas, 301 N. Charles Street, Baltimore, Md. 21201.
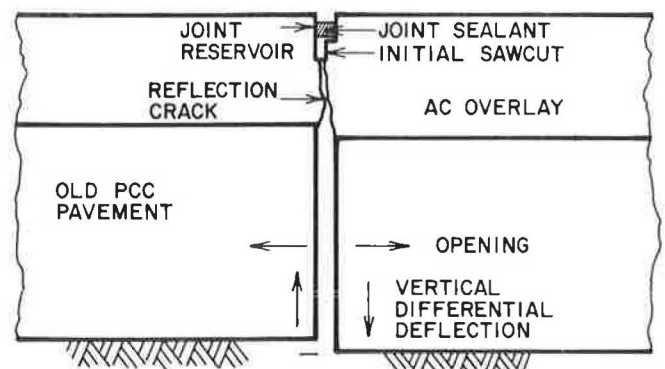
FIGURE 1 Schematic illustrating the saw-and-seal method of reflective crack control (17). (The sawed joint should be within 1 in. of the underlying PCC joint to prevent secondary cracking.)
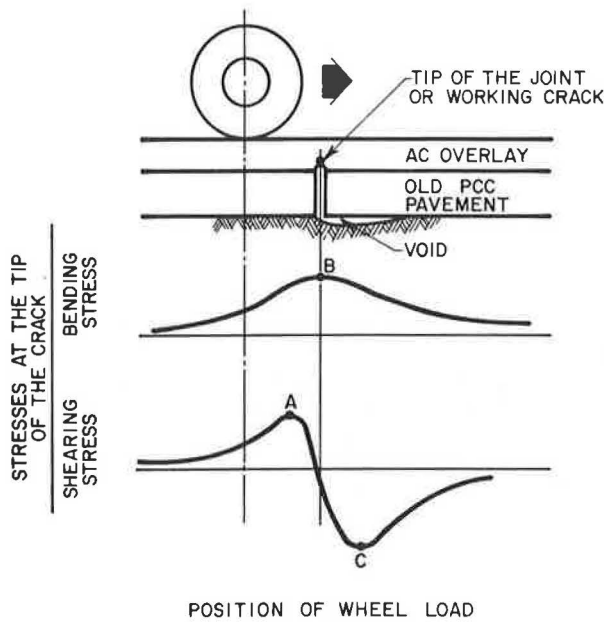
FIGURE 2 Shearing and bending stresses in an AC overlay resulting from a moving traffic load (7).
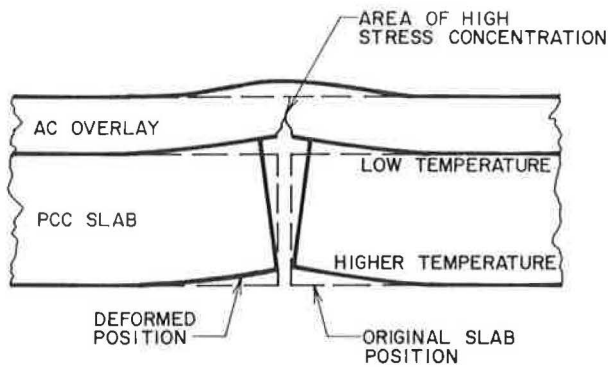
FIGURE 3 Stress concentrations in an AC overlay resulting from thermal curling of the pavement slab.

of the pavement materials, the joint or crack spacing, and the amounts of friction between the slab and base layer and between the overlay and PCC slab (8).

EARLY ATTEMPTS AT SAWING AND SEALING

The concept of sawing and sealing joints in an AC overlay as a method of controlling the location and severity of reflective cracks seems to have been first recommended in 1954 by Bone et al. (9). As a potential solution to the reflection cracking problem, they suggested the following:

> Accept the cracks and develop adequate means for maintaining them. To avoid the difficulty of filling narrow and crooked cracks, it has been suggested that grooves be sawed in the resurfacing over joints in the concrete and that these sawcuts be filled with elastic material.

Several states, particularly in the northeastern United States, have developed procedures for the design and construction of the saw-and-seal rehabilitation technique. Connecticut,

Massachusetts, and New York have used the technique for many years and consequently have the most experience with sawing and sealing. Massachusetts investigated grooving existing cracks in the asphalt overlay before adding sealer. This process resulted in improved sealer performance, which subsequently led to additional saw-and-seal treatments.

Wilson (10) reported on Connecticut's first experience with sawed joints in an AC overlay. His object was to determine whether sawing and sealing joints in the overlay would extend the maintenance-free life of the overlay enough to justify the additional construction cost. In 1958, researchers sawed joints in the overlay on two sections of highway: US-7 in Norwalk and US-1 in East Haven. Wilson stated that the sawed joints on these two projects performed well, but that adhesion failure of the sealer was a problem.

After testing such methods as bond breakers, reinforcing mesh, and fabrics for controlling reflection cracking, and obtaining poor or inconsistent results, the New York Department of Transportation (NYDOT) decided to investigate the sawing and sealing of joints in AC overlays. Noonan and McCullagh (11) and Vyce (12) reported on the construction of two experimental sections of roadway. Other studies were subsequently conducted by New York and, on the basis of the results, New York now saws and seals transverse joints on all new AC overlays on PCC pavements.

Although there have been numerous experiments with the sawing and sealing of joints in AC overlays, there has been little or no evaluation or documentation of the field performance of the technique on either a regional or a nationwide basis. An in-depth evaluation of sawing and sealing was initiated to provide information on the expected performance life of the technique.

A major FHWA project titled *Performance/Rehabilitation of Rigid Pavements* developed design and construction guidelines for the sawing and sealing of joints in AC overlays (13). These guidelines will become part of FHWA's *Pavement Rehabilitation Manual*.

SAW-AND-SEAL STUDY SECTIONS

Five categories of data were used in the analysis and development of improved design and construction procedures: measured field performance, original PCC pavement design factors, overlay design factors, traffic, and environmental data. These data were obtained from pavement condition surveys, state highway agency as-built plans and special provisions, and other agency records. In general, the procedures specified in the Strategic Highway Research Program (SHRP) *Data Collection Guide for the Long-Term Pavement Performance Studies* (14) were used.

Several criteria were used to identify a group of candidate saw-and-seal projects. The first criterion was to include study sections from each of the four major environmental zones of the country. This criterion could not be satisfied, because most of the saw-and-seal overlays identified were in the northeastern United States, a wet-freeze zone. Although one saw-and-seal overlay was identified in Arizona in the dry-freeze zone, and another was found in North Carolina in the wet-nonfreeze zone, these overlays had been in service less than 1 year at the time of the field surveys. Because it was

believed that no discernible performance trends would be observed on these pavements, they were not selected for the study. Other states, such as Georgia, Virginia, and Louisiana, have tried sawing and sealing but have not documented the performance of these projects.

The second criterion was to select pavement sections for which past field performance, original PCC pavement and overlay design details, and historical traffic volumes could be obtained from the appropriate state agencies.

Finally, special consideration was given to saw-and-seal overlays that had adjacent control sections available for comparison. Using these criteria, 10 projects with a total of 15 overlays were identified and selected for study. Table 1 lists the 15 selected pavement sections.

Two of the more important design variables considered when selecting the sections were the age and the thickness of the overlay. The age of the selected overlays varied from 2 to 10 years, and the thickness ranged from 2 to 4.5 in. The distribution of the overlays by age and thickness is shown in Figures 4 and 5, respectively.
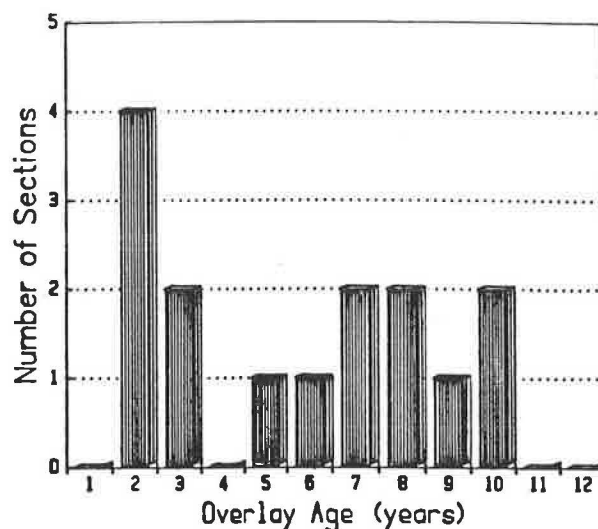
FIGURE 4 Age distribution of study sections.

TABLE 1 PAVEMENT SECTIONS SELECTED FOR INCLUSION IN THE STUDY

Project No.	Route	Location	Lane
1	I-91	Meridan, CT	NB
2	I-84	New Britain, CT	EB
3(A)	I-95	Falmouth, ME (control)	NB
3(B)	I-95	Falmouth, ME	NB
4(A)	US-22	Somerville, NJ	WB
4(B)	US-22	Somerville, NJ (control)	WB
5(A)	I-80	W. Paterson, NJ (control)	EB
5(B)	I-80	W. Paterson, NJ	EB
6(A)	Route 5	Caledonia, NY (control)	EB&WB
6(B)	Route 5	Caledonia, NY	EB&WB
7	I-81	Syracuse, NY	NB
8	I-87	Albany, NY	SB
9(A)*	I-70	Columbus, OH	EB
9(B)	I-70	Columbus, OH	EB
10	US-22	Huntingdon, PA	EB&WB

*Sections A and B due to different sealant materials.
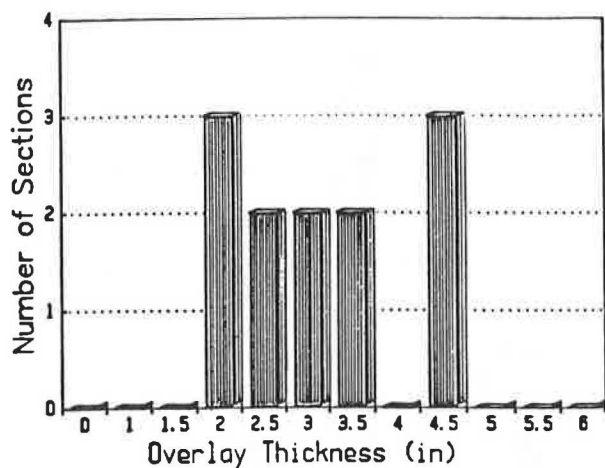
FIGURE 5 Overlay thickness distribution of the study sections.

FIELD DATA COLLECTION

A thorough condition survey of each pavement section was conducted during July and August 1987. The procedures used were those specified under the SHRP Long-Term Pavement Performance (LTPP) program. SHRP's standard *Distress Identification Manual for the LTPP Studies* (*15*) was used as a guide to identify the types, severities, and quantities of the various distresses.

The roughness of each pavement section was determined with a Mays ride meter. In addition, the survey crew rode each of the pavement sections to give a subjective present serviceability rating (PSR).

Pavement deflections on each saw-and-seal study section were measured to determine the joint load transfer efficiency and the stiffness of the pavement layers and foundation. The deflections were measured using a falling weight deflectometer (FWD) at three load levels: 9,000, 13,000, and 17,000 lb.

Traffic volumes, including percentage of truck traffic, were collected from the appropriate state highway agency for each study section. The state agencies were asked to provide the volumes from the time the pavement was opened to traffic to the date of survey. However, in some instances traffic counts were not available for every year in which the overlay experienced traffic.

Environmental data were taken from documentation of monthly temperatures and precipitation published by the National Oceanic and Atmospheric Administration. The nearest weather station was assumed to be representative of the environmental conditions at each study section. In addition, the U.S. Army Corps of Engineers freezing index contour map was used to determine the mean freezing indices of the study sections (*16*).

The raw data obtained from these sources were in several formats, such as field distress forms, construction plans, and research reports. After reduction, the data elements were entered into a data base (on a hard storage disk of an IBM personal computer). The PC software used to manage the

TABLE 2   MAYS RIDE METER ROUGHNESS MEASUREMENTS

Project	Section ID	Roughness (in/mi)
1	CT 1	78
2	CT 4	40
3(A)*	ME 1-1	55
3(B)	ME 1-2	38
4(A)	NJ 4-1	54
4(B)*	NJ 4-2	60.5
5(A)*	NJ 5-1	116.5
5(B)	NJ 5-2	69
6(A)*	NY 3-1	80
6(B)	NY 3-2	98
7	NY 4	50
8	NY 5	60
9(A)	OH 3-1	60
9(B)	OH 3-2	38
10	PA 2	90

*Control sections

data base was RBASE System V, which allowed for efficient data entry, retrieval, and management.

OVERVIEW OF SAW-AND-SEAL PERFORMANCE

Pavement Roughness

The longitudinal roughness of each pavement section, measured with a Mays ride meter, is presented in Table 2. The amount of surface roughness varied widely, from a low of 38 in./mi to a high of 116 in./mi. The two study sections with the least amount of roughness, 38 in./mi, were overlays with saw-and-seal joints on I-95 in Falmouth, Maine, and I-70, in Columbus, Ohio. The study section found to have the most roughness, 116 in./mi, was the control section on I-80 in West Paterson, New Jersey. The average roughnesses for the saw-and-seal and control sections were 60 and 78 in./mi, respectively.

Four projects had control sections available for comparing the roughness of an AC overlay with sawed joints to the roughness of an adjacent overlay without such joints. The roughness measurements taken on these eight overlays are shown in Figure 6. Three of the four saw-and-seal overlays exhibited from 10 to 21 percent less roughness than the control sections. The one saw-and-seal overlay with more roughness than its adjacent control section was the overlay built on Route 5 near Caledonia, New York, in 1980. The probable cause of this overlay's poor performance was the substandard design of the overlay joint configuration. Conversations with NYDOT personnel indicated that the joint reservoir width of ⅝ in. used in this overlay was too narrow to accommodate the temperature-induced horizontal movements experienced by the 90-ft-long PCC slabs. The large slab movement resulted in an adhesion failure of the joint sealant, that led to severe spalling and eventual failure of the joints in the AC overlay.

On the average, the saw-and-seal overlays exhibited 20.3 percent less roughness than the control sections. Because roughness is usually considered one of the primary indicators of pavement performance, sawing and sealing can be said to help extend the life of the overlay. However, determining the
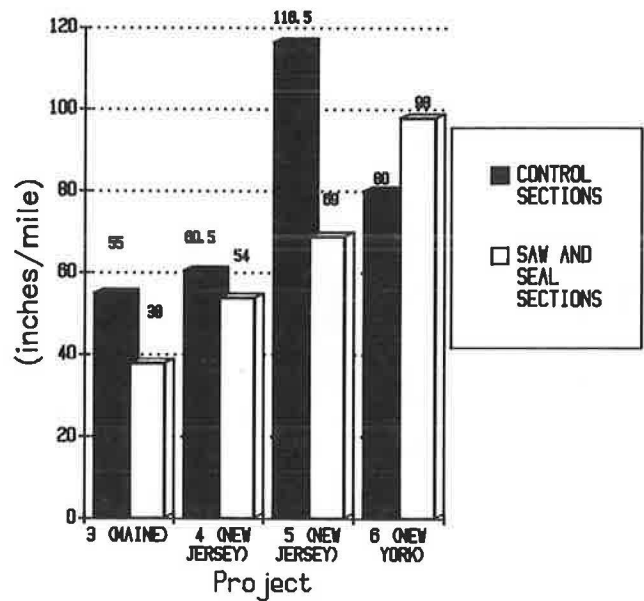
FIGURE 7 Pavement roughness versus overlay thickness divided by traffic since overlay.

approximate number of additional years of service that are caused by the saw-and-seal technique is difficult. A 20-percent difference in roughness (control versus saw-and-seal) does not imply a 20-percent increase in pavement life. Pavement life is a function of the magnitude in the change in roughness and the rate of change for each particular performance curve. From a subjective evaluation, however, the saw-and-seal sections performed better than the control sections. This implies that the saw-and-seal section should provide a better level of serviceability for a longer period of time. Because only four control sections were tested, drawing conclusions about extended pavement life is difficult.

The roughness data were then plotted against the actual field overlay thickness normalized for traffic. Figure 7 shows the roughness versus the normalized thickness divided by equivalent single-axle loads. Included in the figure are both control sections and saw-and-seal sections. Figure 7 shows a
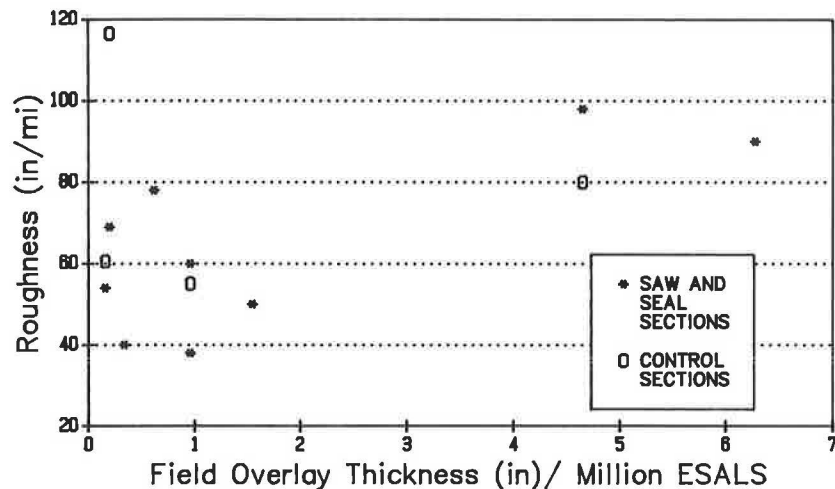
FIGURE 6 Comparison of roughness measurements taken on the four saw-and-seal overlays with control sections.
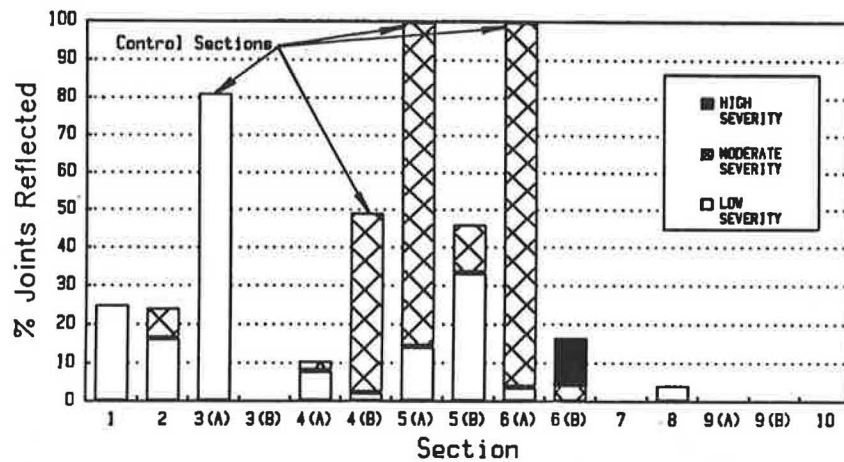
FIGURE 8   Distribution of transverse joint reflection cracking on the 15 pavement sections.

Transverse Joint Reflection Cracking

The amounts of transverse joint reflection cracking observed on each study section during the field surveys are shown in Figure 8. The amounts of reflection cracking on the overlays varied widely. Six of the saw-and-seal overlays experienced low- and medium-severity transverse reflection cracking of from 4 to 46 percent of the transverse joints. The five remaining saw-and-seal overlays were totally free of any transverse reflection cracking. The only section with high-severity cracking was the saw-and-seal overlay on Route 5 in Caledonia, New York, which experienced high-severity cracking on approximately 12 percent of its joints.

The amount of transverse reflection cracking measured on the four saw-and-seal overlays is compared with the amount measured on their control sections in Figure 9. As the figure shows, all of the control sections experienced more reflection cracking than the pavement sections with saw-and-seal joints. All of the underlying joints reflected through on two of the control sections, while the two remaining control sections experienced transverse reflection cracking on 81 and 49 percent of their joints. The percentage of transverse reflection cracking on the saw-and-seal overlays varied between 0 and 46.1 percent. The average percentage of transverse joints that had reflected through the control overlays was 83 percent, compared with 18 percent on the saw-and-seal overlays. Thus, the saw-and-seal overlays experienced approximately 65 percent less transverse reflection cracking than the control sections.

The conditions of the saw-and-seal and control overlays at the location of the underlying joints in the PCC slab are compared in Figures 10 and 11. The photographs show that the control sections developed transverse cracks with severe spalling. The saw-and-seal joints were in excellent condition and did not show any signs of spalling or raveling. In a subjective comparison, the photographs show that the saw-and-seal sections are performing much better than the control sections.

Variables such as age, joint spacing normalized by thickness, field thickness, and roughness were plotted against transverse reflection cracking to determine which, if any, trends were present. The plot of transverse reflection cracking versus age (Figure 12) shows that more cracking occurred in the control sections than on the saw-and-seal overlays, as was discussed previously. The amount of reflection cracking observed on the saw-and-seal overlays remained constant with age, suggesting that if reflection cracking is to occur on a saw-and-seal overlay because of missawed joints or secondary
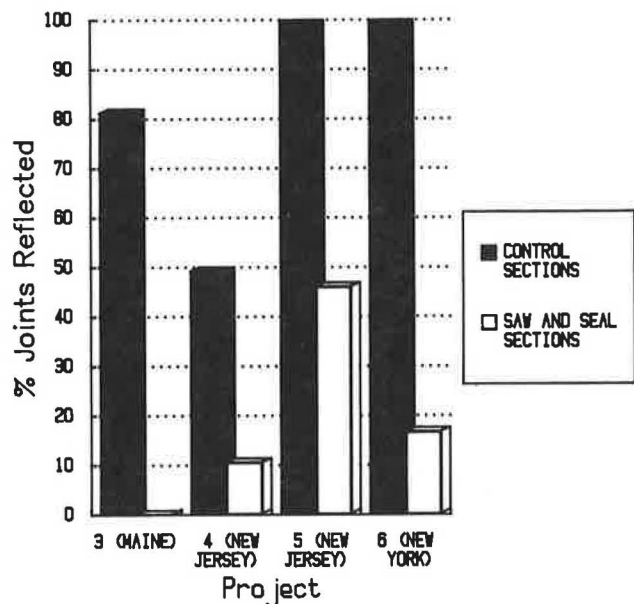
FIGURE 9   Comparison of transverse joint reflection cracking observed on the four saw-and-seal overlays with control sections.
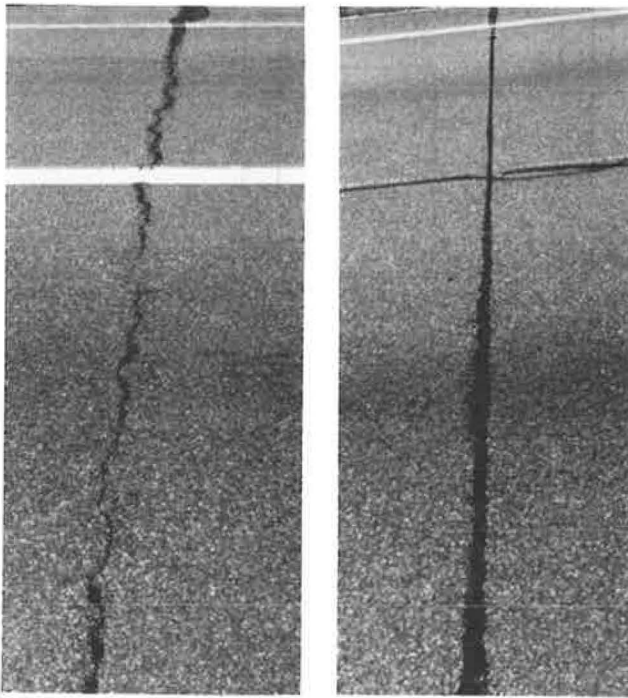
FIGURE 10 Overlay condition of control section (*left*), and of saw-and-seal section (*right*) on I-95, Falmouth, Maine.

cracking, it will occur shortly after the overlay is constructed and remain relatively constant throughout its life.

A plot of reflected joints versus overlay thickness is shown in Figure 13. The saw-and-seal sections had less reflection cracking than the control section, and thickness did not appear to have any effect on the amount of cracking on the saw-and-seal section. The sections with thick overlays (5 in.) performed better than the sections with the thinner overlays.

The construction of a joint in the AC overlay is supposed to alleviate the reflection cracking problem. During the field surveys, a problem related to the transverse reflection cracking became apparent. This problem was the appearance of secondary cracking adjacent to and paralleling the sawed joint. This type of distress appeared on many of the joints in the saw-and-seal overlays. The cause of the secondary cracking is not known for certain; it could be the result of a tear caused by low tensile strength because of poor mix design or other thermal-type cracking. In most cases, especially for cracks appearing several inches from the joint, the secondary cracking can probably be attributed to the improper location of the sawed joints above the underlying joints in the PCC. The observation of secondary cracks as close as 1 in. from the saw joint implied that it is critical to locate the saw cut directly above the joint. A saw cut more than 1 in. away can result in secondary cracking. An example of secondary cracking is shown in the photographs in Figure 14.

FINDINGS

● A total of 12 states were found either to have experimented with or to be using saw-and-seal AC overlays as a routine rehabilitation procedure. Most of these states are in
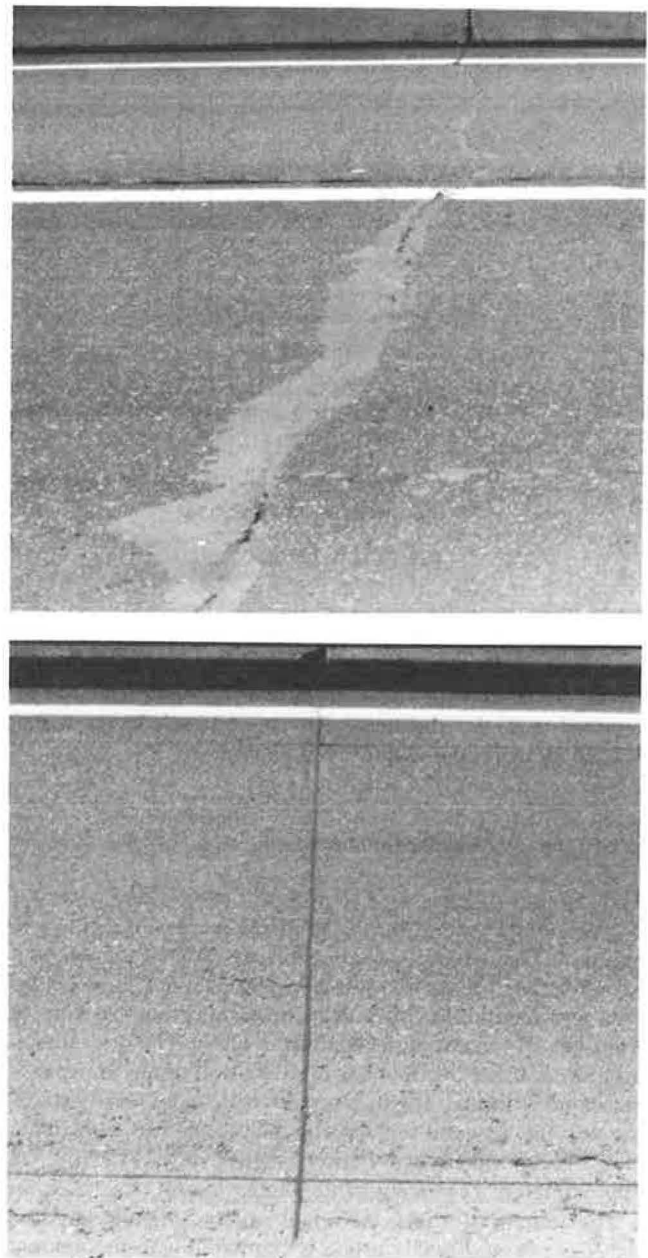
FIGURE 11 Overlay condition of control section (*top*), and of saw-and-seal section (*bottom*) on US-22, Somerville, N.J.
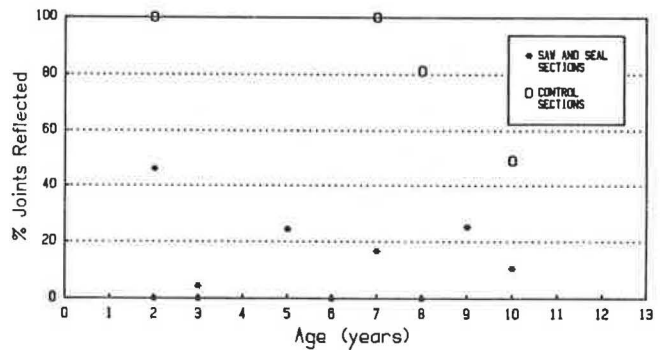
FIGURE 12 Percentage of transverse joints reflected versus overlay age.
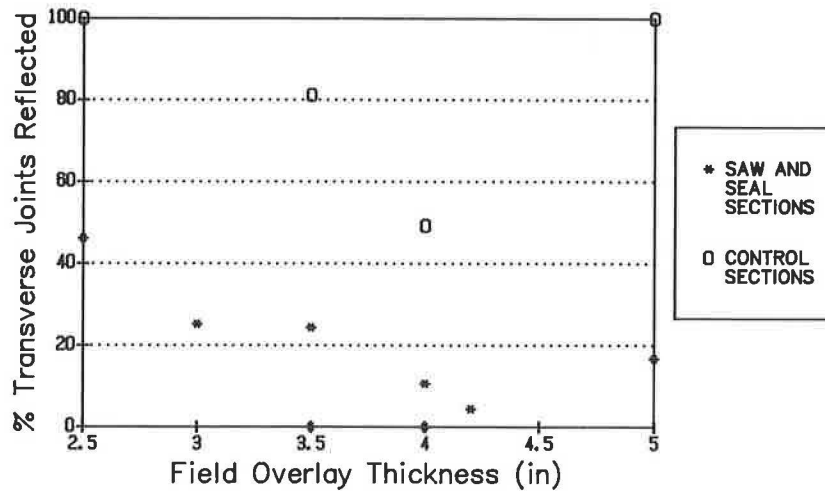
FIGURE 13 Percentage of transverse joints reflected versus overlay thickness.
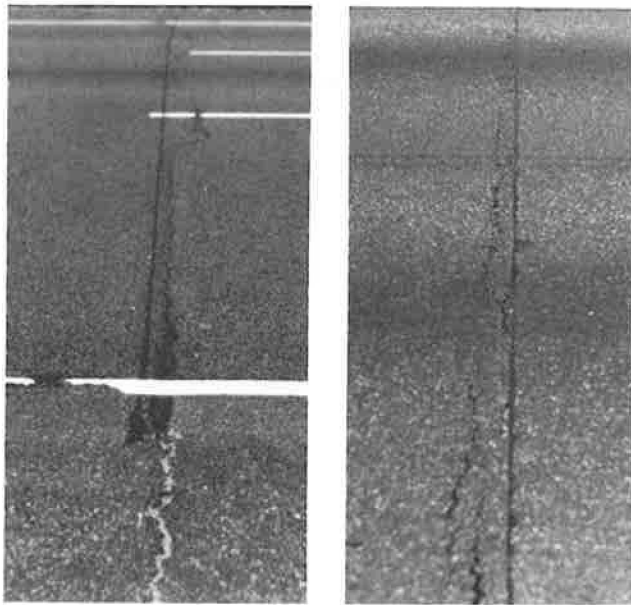
FIGURE 14 Secondary cracking: on I-84, New Britain, Conn. (*left*), and on I-80, West Paterson, N.J. (*right*).

the northeastern part of the country. Connecticut, New York, New Jersey, and Pennsylvania have had the most experience.

● An important step in the construction process is properly locating the saw cut above the existing joint. Secondary reflection cracking can occur unless a precise match (within 1.0 in.) of saw cut and existing joint is made.

● Saw-and-seal sections with thick (5.0 in.) overlays performed better (with respect to roughness and reflection cracking) than sections with thin (2.5 in.) overlays.

● If properly constructed, saw-and-seal joints in an AC overlay of jointed PCC can reduce the adverse effects of reflection cracking. For the pavement sections examined (control versus saw-and-seal), pavement roughness was reduced by 20 percent and transverse reflection cracking was reduced by 64 percent. Sawing and sealing joints in AC overlays on PCC pavements can extend the pavement life.

REFERENCES

1. B. E. Gray and G. E. Martin. A Symposium on Resurfacing of Pavements with Bituminous Mixtures. *HRB Proc.*, Vol. 12, 1932, pp. 177–192.
2. H. J. Treybig, B. F. McCullough, P. Smith and H. Von Quintus. *Development of New Design Criteria, Overlay Design and Reflection Cracking Analysis for Rigid Pavements, Vol. 1.* Report FHWA-RD-77-66. FHWA, U.S. Department of Transportation, 1977.
3. A. J. Bone and L. W. Crump. Current Practices and Research on Controlling Reflection Cracking. *Bulletin 123*, HRB, National Research Council, Washington, D.C., 1956, pp. 33–39.
4. G. Sherman. *NCHRP Synthesis of Highway Practice 92: Minimizing Reflection Cracking of Pavement Overlays.* TRB, National Research Council, Washington, D.C., Sept. 1982.
5. R. E. Smith, R. P. Palmieri, M. I. Darter, and R. L. Lytton. *Pavement Overlay Design Procedures and Assumptions, Vol. II: Guide for Designing and Overlay.* Report FHWA-RD-85-007. FHWA, U.S. Department of Transportation, 1984.
6. F. R. McCullagh. *Reflection Cracking in Bituminous Overlays on Rigid Pavements.* Special Report 16. Engineering Research and Development Bureau, New York State Department of Transportation, Albany, 1973.
7. P. W. Jayawickrama and R. L. Lytton. Methodology for Predicting Asphalt Concrete Overlay Life Against Reflective Cracking. In *Proc., 6th International Conference on the Structural Design of Asphalt Pavements*, Vol. 1, 1987, pp. 912–924.
8. P. W. Jayawickrama, R. E. Smith, R. L. Lytton, and M. R. Tirado. *Development of Asphalt Concrete Overlay Design Equations, Vol. I: Development of Design Procedures.* ERES Consultants, Inc., Champaign, Ill.: 1987.
9. A. J. Bone, L. W. Crump, and V. J. Roggeveen. Control of Reflection Cracking in Bituminous Resurfacing over Old Cement-Concrete Pavement. *HRB Proc.*, Vol. 33, 1954, pp. 345–354.
10. J. O. Wilson. Crack Control Joints in Bituminous Overlays on Rigid Pavements. *Bulletin 322*, HRB, National Research Council, Washington, D.C., 1962, pp. 21–29.
11. J. E. Noonan and F. R. McCullagh. *Reduction of Reflection Cracking in Bituminous Overlays on Rigid Pavements.* Research

Report 80. Engineering Research and Development Bureau, New York State Department of Transportation, Albany, 1980.

12. J. M. Vyce. *Reflection Cracking in Bituminous Overlays on Rigid Pavements.* Report FHWA/NY/RR-83/109. Engineering Research and Development Bureau, New York State Department of Transportation, Albany, 1983.

13. W. P. Kilareski and R. A. Bionda. *Improved Design and Construction Procedures for Sawing and Sealing Joints in AC Overlays Over Existing PCC Joints.* Report FHWA-RD-88-204. FHWA, U.S. Department of Transportation, 1988.

14. J. B. Rauhut, M. I. Darter, R. L. Lytton, P. R. Jordahl, and M. Gardner. *Data Collection Guide for Long-Term Pavement Performance Studies.* Strategic Highway Research Program, National Research Council, Washington, D.C., 1987.

15. K. Smith, M. I. Darter, J. B. Rauhut, and K. T. Hall. *Distress Identification Manual for the Long-Term Pavement Performance Studies.* Strategic Highway Research Program, National Research Council, Washington, D.C., 1987.

16. K. T. Hall, J. M. Conner, M. I. Darter, and J. H. Carpenter. *Rehabilitation of Concrete Pavements,* Vol. 4: *Concrete Pavement Evaluation and Rehabilitation System.* University of Illinois, Urbana, 1987.

17. *Technique for Pavement Rehabilitation—A Training Course.* FHWA, U.S. Department of Transportation, 1987.

Performance of Diamond Grinding

MICHAEL I. DARTER AND KATHLEEN T. HALL

Although diamond grinding of jointed concrete pavements has been used in the United States since 1965 to remove faults and improve rideability, no documentation of its performance nation-wide has been available until now. As part of a study of eight concrete pavement rehabilitation techniques conducted by the University of Illinois for FHWA, 76 diamond grinding projects in 19 states were surveyed and analyzed. Diamond grinding is an effective means of improving ride quality on pavements with faulted joints, cracks, and repairs. The rideability of a newly ground pavement is typically as good as or better than that of a newly constructed pavement. However, if no other restoration work except grinding is performed on pavements with poor subdrainage, slab support, and load transfer, faulting after grinding recurs at a faster rate than for newly constructed pavements. Other factors found to significantly affect the performance of diamond grinding include traffic, slab thickness, joint spacing, base type, subgrade type, and climate. Surprisingly, dowel bar diameter was not found to be significant to the prediction of faulting after grinding. By the time faulting reaches objectionable levels, dowels may already be so loose that they contribute little to load transfer. More than 20 percent of the grinding projects surveyed had large amounts of cracking (more than 825 ft/lane-mi), and probably should have been overlaid or reconstructed rather than restored. The full benefit of diamond grinding, in terms of pavement life extension and cost effectiveness of repair, is not likely to be achieved on such pavements, which are likely to require major structural rehabilitation long before appreciable faulting recurs.

This investigation of the performance of diamond grinding on jointed concrete pavements is part of a study entitled "Determination of Rehabilitation Techniques for Rigid Pavements," conducted between 1985 and 1988 by the University of Illinois for FHWA. The objective of the study was to improve procedures for evaluating and rehabilitating concrete pavements. Five concrete pavement restoration techniques (diamond grinding, load transfer restoration, edge support restoration, full-depth repair, and partial-depth repair) and three types of overlay (bonded concrete, unbonded concrete, and crack and seat AC overlay) were investigated. The results of this study are fully reported elsewhere (1–4).

DIAMOND GRINDING

Diamond grinding of jointed portland cement concrete (PCC) pavements has been part of experimental and routine restoration work since 1965 (5–7). The first major project ground in that year was recently reground to restore rideability. Within about the last 10 years, the amount of diamond grinding work

Department of Civil Engineering, University of Illinois at Urbana-Champaign, Champaign, Ill. 61801.

completed has increased. The capabilities of diamond grinding equipment have also improved during this time period (5).

To date there has been no nationwide documentation of the performance of diamond grinding. Several specifications exist and the technique has proven effective in several states. Diamond grinding has been effective in removal of faulting and surface wear; however, the overall effectiveness of the technique in terms of extending pavement life has not been determined and verified through country-wide field performance.

Available references on diamond grinding of jointed concrete pavements were reviewed. Some new publications are available that have added considerable knowledge to the design, construction, and performance of diamond grinding (5,6,8–12).

The development of an extensive data base containing information on original pavement design, traffic, environmental conditions, and performance was required to determine the effectiveness of grinding. This data base was developed to allow analysis of many factors that might affect performance.

To obtain all of the necessary data base elements, the following methods and sources were used:

● A field survey was conducted on each project to document its current condition. The surveys included crack mapping, faulting measurements, distress data collection, and subjective ratings of pavement condition and rideability.

● The design of each original pavement structure was determined from "as built" plans and verbal communication with state DOT personnel.

● Environmental data of temperature and precipitation were obtained from historical records kept by the National Oceanic and Atmospheric Administration.

● Traffic estimates, including average daily traffic and percent commercial trucks, were obtained from the state DOTs. For calculation of accumulated axle loads on each project, FHWA historical W–4 tables on axle load distributions for the corresponding states and pavement classifications were used.

Physical test data were not collected. The most useful tests would have been heavy load deflection testing, coring, and laboratory testing. These tests would have greatly increased the ability to analyze and interpret the pavement deterioration observed in the visual surveys. An understanding of the physical properties of the pavement layers, quality of support, load transfer, and base gradations would have permitted structural, material, and drainage evaluations.

DATA BASE AND DATA COLLECTION

A total of 76 diamond ground pavement sections in 19 different states were included in the data base. Two sample units about 1,000 ft in length were surveyed on as many sections as possible; so the data base contained a total of 114 sample units. Included in the data base are many of the projects on which diamond grinding was done after 1976, when this type of work began in earnest throughout the country. These pavements were field surveyed between June 1985 and July 1986. Figure 1 shows the general location of the diamond grinding projects. A fair distribution exists among the different geographic and climatic zones.

The field and office data collection procedures are described in detail by Reiter et al. (4). For the purposes of developing performance prediction models and improving design and construction procedures, the following types of data were necessary:

- Field condition data,
- Original pavement structural design and improvement data,
- Rehabilitation design data,
- Historical traffic volumes and classifications, W–4 load tables and calculated 18-kip equivalent single axle loads (ESAL), and
    - Environmental data.

A complete list of all of the variables considered in the field surveys are as follows:

- General
  —Sample unit,
  —Foundation of sample unit,
  —Condition of drainage ditches,
  —Subsurface drainage present and functional, and
  —Number of transverse joints in sample unit.
- Slab distress variables
  —Transverse cracking,
  —Transverse D cracking,
  —Longitudinal cracking,
  —Longitudinal D cracking,
  —Longitudinal joint spalling, and
  —Scaling, crazing, map cracking, shrinkage cracking.
- Joint distress variables
  —Transverse joint spalling,
  —Corner spalling,
  —Pumping,
  —Faulting (mean over sample unit),
  —Joint width (mean over sample unit),
  —Corner breaks,
  —D cracking along joint,
  —Reactive aggregate distress,
  —Joint sealant condition, and
  —Incompressibles in joint.

The following are design variables for the original pavement that are contained in the data base.

- General
  —Identification (highway, milepost, direction);

FIGURE 1   Location of diamond grinding sections included in the data base.

—Beginning and ending mile posts and stations;
—Number of through lanes;
—Type of original pavement, jointed plain concrete pavement (JPCP), or jointed reinforced concrete pavement (JRCP);
  —Layer descriptions, material types, thicknesses;
  —Date of original pavement construction; and
  —Dates and descriptions of major improvements.
* Joints and reinforcement
  —Average contraction joint spacing,
  —Skewness of joints,
  —Expansion joint spacing,
  —Transverse contraction joint load transfer system,
  —Dowel diameter,
  —Type of slab reinforcement,
  —Longitudinal bar/wire diameter, and
  —Longitudinal bar/wire spacing.
* Subgrade, shoulder, and drainage
  —Type of subgrade soil (fine-grained, coarse-grained),
  —Outer shoulder surface type,
  —Original subsurface drainage type, and
  —Original subsurface drainage location.

The data base is comprehensive, containing as many projects as could be included within available resources. This was done to provide a wide range of data to facilitate regression analysis for development of performance models.

Figures 2 and 3 show the distributions of age and accumulated 18-kip ESALs since grinding. The age distribution indicates the relative newness of the grinding technique, with a mean of 4 years and a range of 1 to 9 years. The ESAL distribution shows a mean of 2 million ESALs and a range of 0.22 to 7.81 million ESALs after grinding in the outer traffic

FIGURE 3 ESAL distribution of diamond grinding sections.

lane. The physical designs of the pavements are summarized as follows:

* Pavement type: 39 JRCP, 75 JPCP.
* Slab thickness: 7 to 12 in.
* Joint spacing: 15 to 100 ft.
* Base type: 54 percent granular, 46 percent stabilized.
* Load transfer: 38 percent dowelled, 62 percent undowelled.
* Shoulder type: 95 percent AC, 5 percent tied PCC.
* Subdrainage: 82 percent with none, 18 percent with edge drains.

Subgrade and climate variables had the following ranges:

* Subgrade type: 53 percent fine-grained, 47 percent coarse.
* Precipitation: 9 to 61 in. per year.
* Freezing Index: 0 to 1,750 freezing degree-days.

About 50 percent of the projects were diamond ground in both lanes, and the other 50 percent were ground in the outer lane only. For 29 percent of the projects, the age of the pavement at the time of grinding is unknown; in nearly all cases this is because the year of original construction is unknown. For the remaining projects, the range of ages was 11 to 32 years, and the average age was 19 years.

FIELD PERFORMANCE AND EVALUATION

Diamond grinding greatly improves the rideability of the pavement by removing faulting. Diamond grinding also

FIGURE 2 Age distribution of diamond grinding sections.

TABLE 1   SUMMARY OF DISTRESS TYPES IDENTIFIED FOR DIAMOND
GRINDING PROJECTS (OUTER TRAFFIC LANE ONLY)

Distress Type	Severity	Mean	Range
Transverse Cracking	Medium and High	459	0 to 2928 ft/mile
Longitudinal Cracking	Medium and High	91	0 to 1900 ft/mile
Corner Breaks	All	7	0 to 222 /mile
"D" Cracking	All	6 percent of sections	
Pumping	Low	99 percent of sections	
	Medium	1	
	High	0	
Joint Spalling	Low	96 percent of sections	
	Medium	4	
	High	0	

Notes: 1 mile = 1.609 km

1 ft/mile = 0.1894 m/km

increases the friction of the surface for a short time after grinding (*5,12–14*). An evaluation of distresses that may affect the structural capacity, rideability, and friction of ground pavements is presented in this section.

Distresses that may directly affect the structural integrity of the ground pavement are transverse and longitudinal cracking, corner breaks, joint spalling, joint faulting, pumping, and D cracking. Rideability is affected by most of these distresses. Friction is decreased by wear and polish of the surface texture. Table 1 presents a summary of the mean and range of major distresses measured in the grinding section outer lanes, expressed on a per-mile basis.

The severity levels used in describing distresses correspond to standard definitions given in the concrete pavement evaluation system (COPES) distress manual (*15*). For example, a low-severity crack is a hairline crack, a medium-severity crack is working (spalled and faulted), and a high-severity crack is badly spalled and faulted, in need of immediate repair.

Transverse Cracking

Deteriorated (medium- and high-severity) transverse cracks on jointed concrete pavements are largely caused by a combination of traffic loading fatigue damage and thermal curling stresses. For JRCP, an additional contributing factor may be lock-up of transverse joints caused by dowel bar corrosion or misalignment. The distribution of deteriorated transverse cracks in the outer lane for the ground pavements surveyed is shown in Figure 4. Of the pavement sections, 43 percent had no deteriorated transverse cracks. However, 21 percent had over 825 ft of deteriorated cracks per mile. This level of cracking is considered indicative of a pavement in need of structural rehabilitation. This value of approximately 825 ft/mi was found to be the average of all projects in the NCHRP 1–19 COPES data base that had a present serviceability rating less than 3.0. It corresponds to a working crack every 77 ft.

Without historical distress data, it is impossible to determine how much of the cracking on these sections was present at the time of grinding and how much developed afterwards. In either case, these sections were probably structurally inadequate before grinding and should have been overlaid or reconstructed rather than restored.

Longitudinal Cracking

Longitudinal cracking is usually caused by late sawing, shallow saw cuts, or the use of plastic inserts that do not create an adequate weakened plane for longitudinal joint. Figure 5 shows a distribution of the deteriorated (medium- to high-severity) longitudinal cracking on the diamond ground sections. Of the sections, 75 percent had no deteriorated longitudinal cracking. Only 5 percent had more than 500 ft of deteriorated longitudinal cracking per mile. Three sections had over 1,500
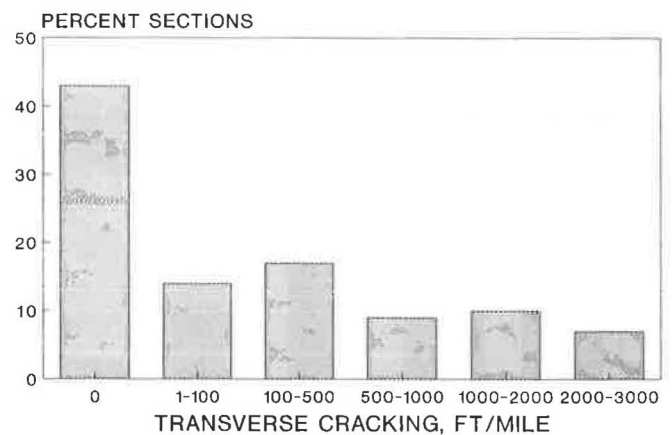
FIGURE 4   Transverse cracking distribution of diamond grinding sections.

PERCENT SECTIONS
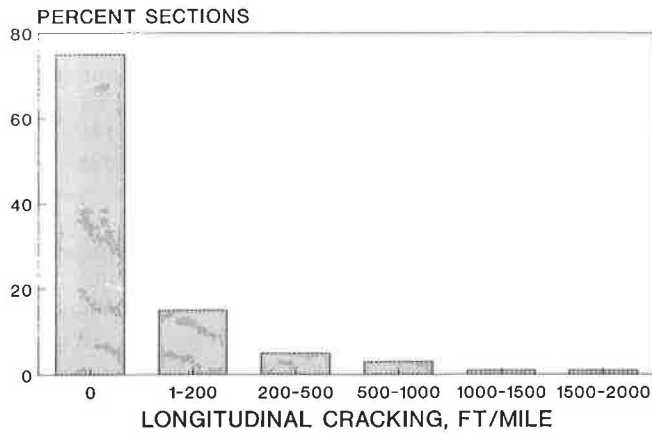
FIGURE 5 Longitudinal cracking distribution of diamond grinding sections.

ft/mi of deteriorated longitudinal cracking. It is impossible to determine whether this cracking occurred before or after grinding.

Corner Breaks

Corner breaks are the result of loss of support beneath the slab caused by erosion of the base course or subgrade. Projects that are diamond ground for faulting (which is indicative of pumping) frequently have some loss of support. Significant faulting cannot occur without some erosion of the underlying layers of the concrete pavement (*11*). Corner breaks are a good indicator of structural deficiency.

These breaks were observed on 19 percent of the sections. However, only 6 percent of the sections had more than 25 corner breaks per mile, a level that is considered serious. Three sections had more than 100 corner breaks per mile. Whether the breaks occurred before or after diamond grinding is not known. In either case, that many of the sections were diamond ground without consideration or determination of support conditions is evident.

Joint/Crack Faulting and Pumping

Faulting develops from pumping and erosion of underlying materials through the combination of factors:

1. The movement of heavy wheel loads across the joint or crack,
2. The presence of free moisture in either the base or subgrade, or both,
3. An erodible base or subgrade material (high in fines), and
4. Poor load transfer across joints and cracks (*9,13,14*).

If these factors are present, the base or subgrade materials, or both, have the potential to pump beneath the approach slab as wheel loads cross joints and cracks. Pumping forces water and fines from under the leave side and either deposits the fines under the approach side or force them out through the longitudinal joint. This action depends on the deflection of the slab corners, and is more severe on pavements that

exhibit poor load transfer. The accumulation of fines lifts the approach side and leaves a void under the leave side, resulting in faulting (*9*).

The distribution of transverse joint faulting for the diamond grinding sections is shown in Figure 6. The average faulting in the outer lane was 0.065 in., with individual sections ranging from 0.01 to 0.33 in. Faulting detracts significantly from ride quality on JPCP when it exceeds about 0.13 in., which occurred on 7 percent of the sections (*16*).

Low-severity pumping (water bleeding, blowholes, some pumped fines) was observed on many of the diamond grinding sections. However, only one section exhibited medium-severity pumping (substantial amount of fines pumped on to the shoulder). Edge drains and tied PCC shoulders on several sections probably reduced the occurrence of visible signs of pumping.

D Cracking

D cracking is caused by freeze-thaw damage to either the aggregates or the paste in PCC, and is evidenced by fine hairline cracks near and parallel to joints and cracks that eventually spall out. Only 6 percent of the diamond grinding sections exhibited D cracking.

Wearout of Grinding Texture

The texture developed by grinding provides good friction immediately (*5,12,17*). The ridges produced improve the surface macrotexture and provide an escape route for water under tires.

Data on friction numbers were not available for any of the sections. On some, wear of the grinding texture in the wheel paths was evident. This concern warrants further detailed study because loss of texture could result in loss in friction. The Georgia DOT has used the sand patch method to measure

PERCENT SECTIONS
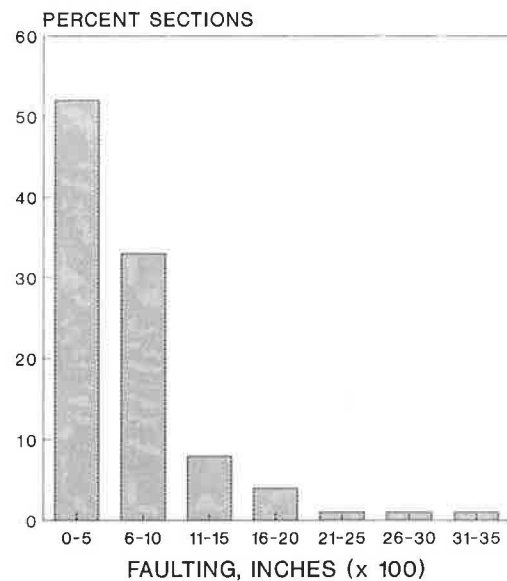
FIGURE 6 Faulting distribution of diamond grinding sections.

texture depths on grinding projects (*17*) and observed the effect of traffic on wearout of grinding texture. Texture depths between 0.04 and 0.06 in. have been measured on several projects shortly after grinding. These values compare favorably to the 0.035-in. depth required on newly constructed pavements. The texture depths on many projects dropped off to 0.03 in. or less after about 5 million vehicle passes, but decreased more slowly after that. They did not reach the specified minimum level requiring correction until after about 25 million vehicle passes (in the Georgia study a truck pass was considered to be approximately equal to 8 passenger car passes in terms of wearout of grinding texture). Most of the projects included in the Georgia study had granite aggregates; wearout of grinding texture on pavements with softer aggregates would probably be more rapid. The width of the land area between the grinding blades is also likely to be a factor in the rate of texture loss.

PERFORMANCE MODEL

Model Development

Faulting is a major distress type that develops after grinding on most jointed concrete pavements. A predictive model was developed for transverse joint faulting using nonlinear regression techniques available in the Statistical Package for the Social Sciences (SPSS) (*18*).

As a first step in analyzing the data, all independent variables that were believed to have a significant influence on the faulting of ground pavements were identified. These variables were then considered in the development of a nonlinear regression model for faulting.

In addition to the regular 114 diamond grinding sections, data from dowelled joint load transfer restoration sections were added so that this work, when done concurrently, could be considered. These sections were also diamond ground.

A great deal of time was spent trying to develop a faulting model for diamond ground pavements, with only limited success. As diamond grinding is applied in more states with differing climates and designs, the initial model can be revised to include more variables and wider ranges of applicability.

Faulting Model

The factors that entered into the faulting model included design, traffic, subgrade, climate, and additional restoration work. The model obtained is as follows:

$$
\begin{aligned}
\text{FAULT} = {}& -5.62(\text{ESAL} + \text{AGE})^{0.54} \, [5.85(1 \\
& + \text{DRAIN} + \text{SUB})^{0.0529} \\
& - 3.8 * 10^{-9}(\text{FI}/100)^{6.29} + 0.484 \, (\text{THICK} \\
& + \text{PCCSH})^{0.335} + 0.1554\text{BASE} \\
& - 7.163\text{JSPACE}^{0.0137} + 0.1136\text{LTR}]/100 \qquad (1)
\end{aligned}
$$

where

FAULT = outer-lane mean transverse joint faulting after grinding (in.),
ESAL = outer-lane accumulated 18-kip ESALs after grinding (millions),

AGE = time since diamond grinding (years),
DRAIN = 0 if no edge drains were present after grinding, 1 if edge drains were present after grinding,
SUB = 0 for fine-grained subgrade soil (A4 to A7), 1 for coarse-grained subgrade soil (A1 to A3),
FI = Freezing Index (mean Fahrenheit degree-days below freezing),
THICK = original slab thickness (in.),
PCCSH = 0 if no tied concrete shoulder was present, 1 if tied concrete shoulder was present,
BASE = 0 if existing base is granular material, 1 if existing base is stabilized material (asphalt, cement),
JSPACE = mean transverse joint spacing (ft),
LTR = 0 if no retrofit dowels were placed when ground, 1 if retrofit dowels were placed.

The statistics were as follows:

$$R^2 = 0.38,$$
Standard error $= 0.027$ in., and
$n = 114$ sections (diamond grinding without load transfer restoration plus 72 joints with diamond grinding and load transfer restoration).

The mean and ranges of factors are as follows:

Factors	Mean	Range
Faulting, in.	0.06	0.01 to 0.33
ESALs, millions	1.94	0.22 to 7.8
Age, years	4	1 to 9
Slab thickness, in.	9.0	7.0 to 12.0
Joint spacing, ft	38	15 to 100
Dowel diameter, in.	—	0 (no dowels) to 1.25
PCC shoulder	—	0 (no PCC shoulder), 1 (tied PCC shoulder)
Base type	—	0 (granular), 1 (stabilized)
Edge drains	—	0 (none), 1 (yes)
Subgrade type	—	0 (fine-grained), 1 (coarse-grained)
Freezing Index, degree-days	436	0 to 1,750
Annual precipitation, in.	33.5	9.3 to 61.1
Pavement type	—	JRCP, 39 sections JPCP, 75 sections

Several factors were identified that affect the rate of faulting of a ground pavement. Two typical or standard pavements were defined. Each factor was varied over a typical range and the change in faulting determined. The ratio of the higher faulting value to the lower value was computed. The results are as follows:

JRCP Factor	Range	High/Low Range
ESALs, million	1 to 10	5.9 Increase
Slab thickness, in.	8 to 12	1.6 Decrease
Joint spacing, ft	25 to 75	1.4 Increase
Base type	Granular, stabilized	1.2 Decrease
Subgrade soil	Fine, coarse	1.4 Decrease
Freezing Index	0 to 1,500	1.2 Increase
Concrete shoulder	No, yes	1.1 Decrease
Edge drains	No, yes	1.4 Decrease
Load transfer restoration	No, yes	1.6 Decrease

JPCP Factor	Range	High/Low Range
ESALs, million	1 to 10	6.0 Increase
Slab thickness, in.	8 to 12	3.0 Decrease
Joint spacing, ft	8 to 20	1.7 Increase
Base type	Granular, stabilized	1.2 Decrease
Subgrade soil	Fine, coarse	2.0 Decrease
Freezing Index	0 to 1,500	1.3 Increase
Concrete shoulder	No, yes	1.2 Decrease
Edge drains	No, yes	2.0 Decrease
Load transfer restoration	No, yes	1.6 Decrease

These results indicate that the variables in the faulting model are affecting faulting in the logical direction, and that some of them have a much larger effect than others. The variable having the greatest effect is traffic, and the design factor showing the most effect is slab thickness. The subgrade soil type also has a major effect, probably because of better subdrainage with a coarse-grained soil. One factor that did not enter the equation was the presence of dowels in the original pavement. It appears that after a pavement has faulted badly enough to require grinding, the dowels are too loose to have any impact on future faulting after grinding. Additional restoration work, including concrete shoulders, edge drains, and load transfer restoration, also has a significant effect on reducing faulting.

Figure 7 shows faulting development for the standard JRCP (see Table 2) over its initial life (using the NCHRP 1–19 faulting model) and after diamond grinding (Year 20) when no additional restoration work is done. The results show that the recurrence of faulting after grinding is more rapid than when the pavement is new.

Figures 8 and 9 show predicted faulting for the standard JRCP and JPCP designs respectively (see Table 2) after diamond grinding, with and without edge drains. The faulting of the pavement over its initial performance period, labeled "new," is also shown for comparison.

Figures 10 and 11 show faulting development for grinding alone, grinding with tied PCC shoulders, grinding with load transfer restoration (using dowels) and grinding with tied PCC shoulders and load transfer restoration.

The results clearly indicate the importance of concurrent restoration work to the success of a grinding project when deficiencies such as poor subdrainage and joint load transfer

TABLE 2 TYPICAL STANDARD PAVEMENT CHARACTERISTICS FOR FAULTING SENSITIVITY ANALYSIS

Factor	JRCP	JPCP
ESAL	0.5 million/year	0.5 million/year
Age (since grinding)	0 to 20 years	0 to 20 years
Edge Drains	None	None
Subgrade Soil	Fine grained	Fine grained
Freezing Index	250	0
Slab Thickness	9 in	8 in
Shoulder Type	Asphalt Concrete	Asphalt Concrete
Base Type	Granular	Stabilized
Joint Spacing	50 ft	15.5 ft
Load Transfer (retrofit dowels)	No	No

Notes: Sensitivity analysis was conducted by varying one factor at a time over the range of age with corresponding change in ESAL.
1 in. = 2.54 cm
1 ft = 0.3048 m

exist. These results are for only two standard or typical designs, and other design parameters would produce different results. Therefore, the designer should apply judgment when using the faulting prediction model for determining whether or not to do other restoration work.

CONCLUSIONS AND RECOMMENDATIONS

Overall Effectiveness

Diamond grinding has been successful in producing a smooth ride and extending the service lives of jointed concrete pave-

FIGURE 7 Projected faulting for standard JRCP section for new construction and after diamond grinding.
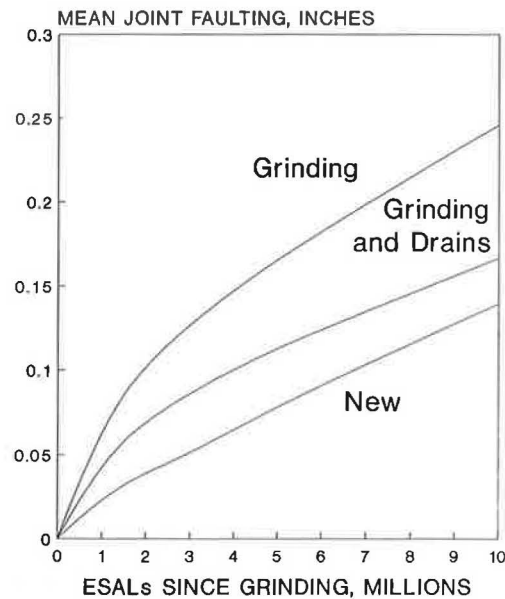
FIGURE 8 Effect of grinding and retrofit edge drains on JRCP faulting.
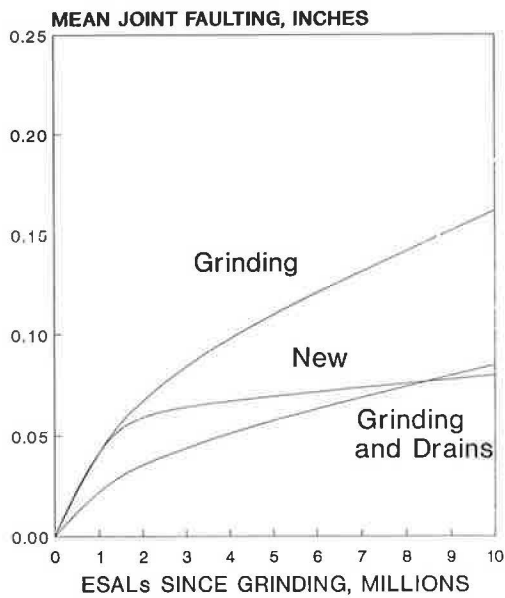
FIGURE 9 Effect of grinding and retrofit edge drains on JPCP faulting.

FIGURE 11 Predicted faulting of JRCP after grinding and other restoration work.

ments. About one out of five grinding projects surveyed in this study had substantial quantities of structural distress (cracking and corner breaks) and probably should have been overlaid or reconstructed rather than restored. Diamond grinding does not contribute to the structural capacity of a pavement, and its benefits will be short-lived on any pavement with extensive structural damage.

Longitudinal Cracking

About 90 percent of the ground sections showed little or no deteriorated longitudinal cracking. Only 2 percent of the sections showed a serious amount of longitudinal cracking (greater than 1,000 ft/mi).

Corner Breaks

About 19 percent of the ground sections showed minor corner breaks, and only 6 percent showed a serious amount (greater than 25/mi).

Transverse Cracking

About 21 percent of the ground sections showed a large amount of deteriorated transverse cracking (over 825 ft/lane-mi). This amount is for pavements having an average life after grinding of four years and 2 million accumulated 18-kip ESALs. Of the sections, 57 percent had minor amounts of deteriorated cracks.

Faulting of Transverse Contraction Joints

The rate of faulting after grinding generally is higher than for newly constructed pavements if no other restoration work is accomplished. However, this accelerated development of faulting can be largely overcome by reducing the pumping potentials with concurrent work such as load transfer restoration, sealing joints, and retrofitting tied PCC shoulders and subdrainage. Some key factors that affect faulting were determined to be the following:

● Future traffic—Truck traffic after diamond grinding (accumulated 18-kip ESALs) has a large effect on the amount of faulting that develops. Faulting after grinding develops rapidly at first and then levels off, similarly to faulting of new pavements (15).
● Existing pavement design—Pavements with thicker slabs, stabilized bases, and shorter joint spacings fault less after grinding.
● Drainage—Edge drains and coarse-grained subgrade soils reduce faulting after grinding.
● Climate—The colder the climate where the pavement is located, the greater the amount of faulting after grinding.
● Tied concrete shoulder—Tied concrete shoulders reduce faulting after grinding.
● Load Transfer Restoration—Retrofitting dowels to restore load transfer at transverse joints and working cracks reduces faulting after grinding.

FIGURE 10 Predicted faulting of JPCP after grinding and other restoration work.

• Prediction of Faulting After Grinding—The prediction model for faulting after grinding can be used with caution to estimate the life of the technique (number of years until faulting again reaches an unacceptable level) and to examine the potential impact of concurrent work such as edge drain installation, load transfer restoration, and tied concrete shoulders.

Wearout of Grinding Texture

The surveys revealed that there was some wear of the texture in the wheel paths. The rate of wearout and the factors involved could not be determined. It is likely that the hardness of the aggregate, the level of traffic, and the land area width are major factors involved. It is important to maximize the land area between grooves, while still providing an adequate number of grooves for surface drainage.

ACKNOWLEDGMENT

REFERENCES

1. M. B. Snyder, M. J. Reiter, K. T. Hall, and M. I. Darter. *Rehabilitation of Concrete Pavements, Volume 1—Repair Rehabilitation Techniques*. Report FHWA/RD-88/071, FHWA, U.S. Department of Transportation, 1989.
2. G. F. Voigt, S. H. Carpenter, and M. I. Darter. *Rehabilitation of Concrete Pavements, Volume 2—Overlay Rehabilitation Techniques*. Report FHWA/RD-88/072, FHWA, U.S. Department of Transportation, 1989.
3. K. T. Hall, J. M. Connor, M. I. Darter, and S. H. Carpenter. *Rehabilitation of Concrete Pavements, Volume 3—Concrete Pavement Evaluation and Rehabilitation System*. Report FHWA/RD-88/073, FHWA, U.S. Department of Transportation, 1989.
4. M. J. Reiter, G. F. Voigt, M. I. Darter, and S. H. Carpenter. *Rehabilitation of Concrete Pavements, Volume 4—Appendices*. Report FHWA/RD-88/074, FHWA, U.S. Department of Transportation, 1989.
5. L. G. Mosher. Restoration of Final Surface to Concrete Pavement by Diamond Saw Grinding. In *Proc., 3rd International Conference on Concrete Pavement Design and Rehabilitation*, Purdue University, 1985.
6. T. T. Trussell. Diamond Grinding of Concrete. *Concrete Construction*, Nov. 1986.
7. *Grinding Extends Pavement Life*. International Grinding and Grooving Association, New York, undated.
8. *Concrete Pavement Restoration Performance Review*, Pavement Division and Demonstration Projects Division, FHWA, U.S. Department of Transportation, 1987.
9. ERES Consultants, Inc. *Techniques for Pavement Rehabilitation*. Participant's Notebook, National Highway Institute/FHWA, U.S. Department of Transportation, third revision, Oct. 1987.
10. *Guide Specifications for Concrete Pavement Rehabilitation*. Association of State Highway and Transportation Officials, Association of General Contractors, and American Road and Transportation Builders Association, 1984.
11. M. I. Darter, E. J. Barenberg, and W. A. Yrjanson. *NCHRP Report 281*: Joint Repair Methods for Portland Cement Concrete Pavements. TRB, National Research Council, 1985.
12. R. D. Smith. *Longitudinal Grinding and Transverse Grooving to Improve Frictional and Profile Properties*. Iowa Department of Transportation, 1983.
13. W. H. Ames. Profile Correction and Surface Retexturing. *Proc., National Seminar on Portland Cement Concrete Pavement Recycling and Rehabilitation*, Transportation Research Board, St. Louis, Mo., 1981.
14. H. L. Tyner. Concrete Pavement Rehabilitation—Georgia Methodology. *Proc., National Seminar on Portland Cement Concrete Pavement Recycling and Rehabilitation*, Transportation Research Board, St. Louis, Mo., 1981.
15. M. I. Darter, J. M. Becker, M. B. Snyder, and R. E. Smith. *NCHRP Report 277: Portland Cement Concrete Pavement Evaluation System (COPES)*. TRB, National Research Council, Washington, D.C. 1985.
16. K. W. Heinrichs, M. J. Liu, S. H. Carpenter, M. I. Darter, and A. M. Ioannides. *Rigid Pavement Analysis and Design*. Report FHWA-RD-88-068. FHWA, U.S. Department of Transportation, 1989.
17. W. Gulden and J. B. Thornton. *Restoration Methods for Jointed Concrete Pavements*. Research Report 7504. Georgia Department of Transportation, 1985.
18. *Statistical Package for the Social Sciences*. McGraw-Hill, New York, 1981.

Evaluation of Experimental Cold-Stockpiled Patching Materials for Repairs in Cold and Wet Weather

H. Randolph Thomas and David A. Anderson

Results of the field evaluation of five experimental binders used to produce cold-stockpiled patching materials for repairs in cold and wet weather are described. The materials were compared against an MC–800 cutback control mix. The experimental mixes were made with a latex-modified MC–800 cutback and four high-float, medium-set (HFMS) emulsion binders. One of the HFMS binder mixes contained fibers. The procedures were specifically designed to minimize the likelihood that variables other than the binder were the proximate cause of repair failures. The failure criteria used are also described. Field evaluations were made from March 1986 to May 1987. Two HFMS mixes performed better than the companion control mix. Because the latex-modified cutback mix did not perform satisfactorily, no further development was recommended. An economic analysis showed that premium mixes need only extend the average service life by a modest amount to provide a lower annualized cost than conventional mixes. For example, a $120/ton mix lasting 2 years provides substantial savings compared to a $30/ton mix lasting 1 year. Extended field trials of stockpiled mixtures using HFMS binders are recommended. Field trials using fibers are also recommended.

Pothole repairs conducted by most highway agencies during the cold, wet winter and spring months are typically short-lived. Potholes that must be filled repeatedly are expensive to repair. A study of 1,000 repairs in Pennsylvania in 1979–1981 indicates that a patch repaired with a dump and run procedure has an annualized direct agency cost of $310/ton ($340/Mg) (1). A properly compacted repair made by cutting out the deteriorated pavement has an annualized cost of $100/ton ($72/Mg). The uniform annual cost of repairing a pothole correctly includes manpower, material, and equipment. These figures have been normalized to represent the cost on the basis of the unit weight of material placed in the pothole at the initial time of repair. The cost can also be translated to a cost per repair. For example, assuming an average pothole volume of 3 ft³ (0.086 m³) and a compacted density of 133 lb/ft³ (2.1 Mg/m³), 1 ton (0.91 Mg) of mix will repair five average potholes. Therefore, the cost of repairing a pothole with the approved procedure would be approximately $20/repair; with the dump and run procedure the cost would be $62/repair.

Repair longevity is the secret of a cost-effective procedure because repeated repairs cost almost as much as the initial repair. Material costs have been found to constitute less than 10 percent of the total cost of repair when the correct procedure is used. Thus, a more expensive material can be justified if it provides increased repair life.

The results of a research project sponsored by FHWA to evaluate various cold-mix patching materials that can be used in cold and wet weather are described (2). The research project involved the identification of failure mechanisms and performance requirements, laboratory testing to screen candidate binders, development of mix design procedures, field placement and documentation, evaluations for a 1-year period, and the economic comparison of materials on the basis of life-cycle costs. Field evaluations and life-cycle costing results are described.

PRODUCTION AND STORAGE

Five experimental mixes and one control mix were involved in the field study. PennDOT 485 patching material made with MC–800 cutback was used as the control mix. One experimental mix was produced using latex-modified MC–800 cutback as the binder. The remaining experimental mixes were produced using a high-float, medium-set (HFMS) emulsion binder. One of these was latex modified and another two were butyl modified. One of the butyl mixes contained fibers. The same crushed limestone aggregate was used for all mixes. The gradation of the aggregate is presented in Table 1. Additional details regarding the mixes and their selection can be found elsewhere (2).

All five experimental mixes were produced on the same day (November 14, 1985) in a conventional 100-ton/hr (91 Mg/hr) McCarter batch plant. An Etnyre Model M3384 double-boiler, crack-sealer unit was used to heat, mix, and pump the binder into the weigh hopper. To prevent binder contamination, the tank of the unit was cleaned with kerosene before and after the use of each binder. The aggregate was double-dried before it was conveyed to the weigh hopper. The fibers were separately weighed and dumped into the pugmill where they were dry-mixed with the aggregate for 30 sec before the binder was added. The mix data and the sequence in which the mixes were manufactured are presented in Table 1.

After mixing, the mixes were stockpiled on a bituminous concrete pad on the premises of the batch plant. The depth of the stockpiles was less than 2 ft (0.6 m) to facilitate cooling and minimize drainage. To protect the freshly made mix from the rain, the stockpiles were covered with polyethylene sheets. Although considerable rain fell on the piles during the stockpiling operation, no stripping or unacceptable drainage was observed.

The Pennsylvania Transportation Institute, The Pennsylvania State University, Research Building B, University Park, Pa. 16802.

TABLE 1 MIX DATA, NOVEMBER 14, 1983

| Mix Type | Residual Binder Content (%) | Temperature (°F) | | | No. of Batches | Total Quantity Manufactured (tons) |
		Aggregate	Binder	Mix		
MC-800L	5.2	140	175.	140	3	10.54
HFMS-2	5.5	90	110	75	3	8.02
HFMS-2L	5.5	140	140	112	2	7.39
HFMS-2B	5.5	150	115	140	3	8.55
HFMS-2BF	5.7	150	120	160	3	9.38
PennDOT 485 MC-800 (Control)	-	-	-	-	-	45.00

Mix Gradation

Sieve Size	Percent Passing (%)
3/8"	100
No. 4	85
No. 8	15
No. 200	1.0

Note: °F = 9/5 (°C) + 32; 1 ton = 0.9 Mg.

On November 18, 1985, the experimental mixes were shipped to Ebensburg, Cambria County, Pennsylvania, and stockpiled at the office of PennDOT Maintenance District 9–3. The stockpiles were then covered with tarps to prevent the infiltration of rain and snow.

FIELD PLACEMENT

Particular care was given to the monitoring of the field trials. A single-axle dump truck was partitioned with a sheet of plywood so that an experimental mix could be loaded into one side of the truck and the control mix loaded into the other side. The assignment of the control mix or an experimental mix to a given repair was done randomly, and the repair procedures were thoroughly documented. Thus, on a given day approximately the same number of experimental and control patches were placed.

Site Selection

In cooperation with Cambria County, Pennsylvania, maintenance personnel, roadways with high traffic levels [average daily traffic (ADT)], were selected for the field experiment. Another criterion for selection was that the roadways should not be candidates for overlay or mechanized patching for at least 2 years after the potholes were repaired. Unfortunately, many of the patches were unexpectedly overlaid in the fall of 1985 when the local PennDOT office decided to accelerate its overlay program. Both rigid-base and flexible-base pavements were included in the study. Cambria County lies on the peak of the Appalachian ridge in western, central Pennsylvania. The weather in this area is considerably colder than in many other parts of Pennsylvania, with late-season snowstorms and freeze-thaw cycles. Heavy coal-hauling trucks are also common in the area, which made the area an excellent one for the field trials.

Repair Procedure

The standard PennDOT procedure for manual patching with stockpiled mix was used during the study. This procedure is often referred to as the "do-it-right" method. In the standard procedure, the deteriorated pavement is removed with a mechanical cutting tool, leaving vertical edges. The debris is removed with a shovel and the hole is cleaned with a broom or compressed air (3).

Only one experimental mix was used on any given day. Repairs alternated between the experimental mix and the control mix. All repairs were located in the traffic wheel path.

Before compaction, enough patching material was placed in the hole so that the compaction device did not bridge on the surrounding pavement. The goal was to have the top of the compacted patch approximately ¼ in. (6 mm) higher than the surrounding pavement to ensure that the compaction device had fully compacted the patching mix. The compactive effort

consisted of six passes with a Model V30W2–R Essick vibrating roller. All repairs were done using a single lift of material regardless of the depth of the repair.

The objective of the study was to improve the effectiveness of mixes in cold, wet weather. Therefore, if the sides and bottom of the pothole were not damp, water was sprinkled into the hole before filling it with patching mix. No edge sealing or tacking material was used in any of the repairs.

Field Documentation

At the time of patching, each repair was thoroughly documented. Information collected for each repair included the repair number, date, location, hole size, traffic, environmental conditions, mixture characteristics, and surrounding conditions of the pavement. The procedure and equipment used in the repair, along with mixture type and an evaluation of the suitability of the mix, were recorded. Nuclear density readings were also obtained.

Summary of Repairs

A total of 288 repairs were made during the period from March 4 to April 25, 1986. Approximately one-half of the repairs were made with the experimental mix, and the other half with the PennDOT 485 control mix. All the mixes, including the control, performed well and were enthusiastically accepted by the crews.

Table 2 presents the number of potholes repaired with each mix, the pavement type, and the average ADT. As can be seen, the repairs were approximately equally divided between flexible and concrete composite pavements.

EVALUATION OF MIXTURE CHARACTERISTICS

At the time of placement, various measurements and subjective evaluations were made. These are discussed below.

Drainage Resistance

Drainage of the binder from the aggregate was evaluated visually during the temporary storage at the mix plant and the following spring (3 months later) at the PennDOT maintenance yard. None of the mixes showed evidence of any drainage. After another 3 months, in May 1986, there was some evidence of drainage for the MC–800L mix. It was concluded that although the styrene butadiene rubber (SBR) latex modifier increased the workability of the mixes at low temperatures, it did so at the expense of increased drainage. The effect of the latex modification on drainage was less pronounced for the HFMS–2L emulsion.

Workability

All mixes could be loaded satisfactorily from the stockpile; in no instance was the mix so lumpy that it did not break up during loading or shoveling. Workability was also rated subjectively at the time of placement in the field. In general, the workability of the mixes was rated as excellent for the entire placement temperature range, 25°F to 65°F. However, 13 observations for the HFMS–2B mix, which represent 32 percent of the repairs made with the mix, received a less-than-excellent workability rating. All five repairs, made when the HFMS–2B mix temperature was less than 42°F (6°C), received a less-than-excellent pass rating. The latex modification improved low-temperature workability, although the effect was more pronounced for the cutback (MC–800L) than for the emulsion (HFMS–2L). Addition of the fibers did not adversely affect the workability of the HFMS–2B mix. These results are in agreement with earlier laboratory workability tests.

Stripping Resistance

The susceptibility to stripping was determined at the time of placement by a subjective evaluation of the percentage of

TABLE 2 SUMMARY OF POTHOLES PATCHED WITH EACH MIX TYPE

Mix Type	No. of Potholes Repaired		Total No. of Repairs	Average ADT
	Flexible Pavement	Composite Pavement		
MC-800L	16	14	30	3853
HFMS-2	16	14	30	3406
HFMS-2L	14	14	28	7324
HFMS-2B	9	22	31	5812
HFMS-2BF	7	20	27	7821
PennDOT 485	61	81	142	6223
Total	123	165	288	

aggregate that was coated with bitumen. In all cases, more than 90 percent of the aggregate was coated, indicating no apparent susceptibility to stripping. These results agreed with the water resistance test results for the plant mixes.

Self-Tacking

In all cases, excellent self-tacking characteristics were observed. Even in cold weather, the mixes adhered to the old pavement. No tacking materials were used, and all the repairs were done in damp or wet holes.

EVALUATION OF DENSITY

A nuclear gauge was used to measure the density of the repairs. Readings between 104.8 lb/ft³ (1.69 Mg/m³) and 132.8 lb/ft³ (2.13 Mg/m³) were obtained. The average density reading was 120 lb/ft³ (1.93 Mg/m³). Table 3 presents the average density obtained for each material.

The density of a repair is potentially affected by a number of factors including hole depth and volume, type and condition of base, and type of pavement. All of these aspects, along with the number of passes, whether the compaction tool bridged on the surrounding pavement, and whether the hole was filled with a sufficient amount of material were documented. Several of these aspects are discussed below.

Hole Dimensions

The average hole depth was 2.5 in. (64 mm); the minimum depth was 0.9 in. (23 mm); and the maximum depth was 6.4 in. (163 mm). Five holes were less than 1.0 in. (25 mm) deep; 17 holes were deeper than 4.5 in. (114 mm). A plot of density versus hole depth showed no discernible relationship. An analysis of variance was used to test the hypothesis that the density of holes less than 4 in. (102 mm) in depth was equal to the density of holes deeper than 4 in. The average densities were as follows:

Depth (in.)	Sample Size	Avg Density (lb/ft³)	Standard Error
≤4	241	119.9	0.249
>4	32	118.3	0.686

These statistics indicate that, from an engineering point of view, hole depth does not significantly affect density. Similar results were obtained from an analysis of surface area. Therefore, it can be concluded that potholes as deep as 4 to 5 in. can be repaired in a single lift as long as proper compaction techniques are used.

Bridging of Compacting Device and Adequate Filling

If the hole is underfilled, it is impossible to obtain full compaction. Only if the compacted repair is slightly above the pavement surface can it be certain that full compaction has been achieved. Only 3 times out of 273 was the repair flush with the pavement. Thus, there are insufficient data to draw a statistically valid conclusion with respect to the effect of underfilling on density. However, in these three instances, the average density was 115.3 lb/ft³ (1.85 Mg/m³), whereas the average density when the repair was slightly above the pavement was 119.8 lb/ft³ (1.92 Mg/m³).

TABLE 3 SUMMARY OF DENSITIES MEASURED IN THE FIELD FOR DIFFERENT MIXES

Mix	Number of Repairs	Number of Density Measurements	Density (lb/ft³)		
			Avg.	Median	Std. Dev.
MC-800L	30	29	118.7	119.5	--
HFMS-2	30	28	120.5	120.4	--
HFMS-2L	28	28	120.5	119.8	3.9
HFMS-2B	31	31	119.5	120.0	--
HFMS-2BF	27	22	119.7	120.7	6.0
PennDOT 485	142	135	119.6	119.6	3.6
Total	288	273	119.8	119.9	3.9

1 lb/ft³ = 16 kg/m³.

Mix Temperature

The effect of mix temperature on density was evaluated using a simple linear regression. A significant relationship was found, although the correlation coefficient was small (0.19), indicating a weak relationship between the two variables. To further analyze the data, three levels of the independent variable (temperature) were established. The average densities for these levels were as follows:

Temperature (°F)	Sample Size	Avg Density (lb/ft³)
≤ 37	67	118.0
38 < T ≤ 47	140	120.5
> 47	66	119.6

Some decrease in density is shown for those repairs compacted at temperatures less than 37°F (3°C); however, the differences are small and probably not sufficient to affect repair longevity. These results imply that adequate compaction can be achieved with these mixtures at temperatures as low as 25°F.

MONITORING OF IN-SERVICE PERFORMANCE

The most commonly observed in-service failures are dishing, raveling, bleeding, and shoving. Each repair was rated with respect to these failure modes during four different evaluations from March 1986 to May 1987. The in-service rating criteria are presented in Table 4. A repair was considered to have failed if it had to be replaced or if any part received a rating of 3 or greater. Using the presence of a single 3 rating as a failure criterion imposed strict performance standards. Many agencies would probably consider the repair to have failed only when total or partial replacement was necessary.

RESULTS OF FIELD SURVEY

A summary of performance is presented in Table 5. The data indicate that during the first evaluation there were no failures in either the experimental mix or the control mix. During the second evaluation, the only repairs that had failed were those made with the HFMS–2 experimental mix. Two of the 30 repairs had failed by dishing even though they were still intact and serviceable. Data collected during the third and fourth evaluations are shown graphically in Figures 1 and 2, respectively. Given the different failure rates for the various control mixes, it is obvious that, overall, the placement and service conditions varied between the mixes. Therefore, it is important that the evaluations be made by comparing the experimental mixes with their respective control mix and not directly with each other.

Figure 1 shows that, at the time of the third evaluation, the failure rate for the emulsion-based mixes was still small. A higher failure rate was observed for the MC–800L mix and its control, but the difference between the experimental and control mix was not large (24 versus 18 percent). A better picture of potential performance emerged after the fourth evaluation. It can be seen in Figure 2 that over the winter there were no additional failures for the HFMS–2 mix (13 percent), but the failure rate for the control mix increased from 9 to 24 percent. At the time of the fourth evaluation, the failure rate for the latex-modified emulsion was equal to that of the control mix (23 percent). The failures increased from 8 to 23 percent for the HFMS–2L mix and from 4 to 23 percent for the control mix, indicating that a slightly greater percentage of the repairs made with the control mix failed over the winter. No failures were observed for the HFMS–2B or the HFMS–2BF mixes, and only one failure was observed for the control mix associated with the HFMS–2BF,

TABLE 4   IN-SERVICE RATING CRITERIA

Distress Condition	Rating			
	1	2	3	4
Dishing	None	⟨1/4 in	⟩1/4 in, but ⟨1/2 in	⟩1/2 in
Raveling	None	"pock marks" on surface due to loss of fine aggregate and binder	larger particles have come loose but damage limited to surface	damage no longer confined to surface
Bleeding	None	small, 1 1/2-in size bleeding	large patches of asphalt on surface	mass movement of asphalt to surface
Shoving	None	localized bulging ⟨1/2 in	localized bulging ⟩1/2 in but ⟨1 in	depth of corrugations ⟩1 in

TABLE 5 COMPARISON OF MIX PERFORMANCE USING THE STANDARD REPAIR PROCEDURE

Mixture Type		Evaluation 1 (1 month)		Evaluation 2 (3 months)		Evaluation 3 (8 months)		Evaluation 4 (14 months)	
		Expt. Mix	Control Mix	Expt. Mix	Control Mix	Expt. Mix	Control Mix	Expt. Mix	Control Mix
HFMS-2	Repairs Avail.	30	31	30	31	24	22	24	21
	No. Failed	0	0	2[d]	0	3[d]	2[d]	3[d]	5[c]
	% Failed	0	0	7	0	13	9	13	24
HFMS-2L	Repairs Avail.	33	40	30	37	26	28	26	27
	No. Failed	0	0	2[d]	0	2[d]	1[d]	6[s]	9[c]
	% Failed	0	0	7	0	8	4	23	33
HFMS-2B	Repairs Avail.	31	27	31	27	9	7	9	7
	No. Failed	0	0	0	0	0	0	0	0
	% Failed	0	0	0	0	0	0	0	0
HFMS-2BF	Repairs Avail.	28	22	28	22	23	18	23	18
	No. Failed	0	0	0	0	0	0	0	1[d]
	% Failed	0	0	0	0	0	0	0	6
MC800-L	Repairs Avail.	30	28	30	28	17	17	17	16
	No. Failed	0	0	0	0	4[c]	3[c]	8[c]	4[c]
	% Failed	0	0	0	0	24	18	47	25

d = patches failed due to dishing.
s = patches failed due to dishing or raveling.
c = patches failed due to dishing or raveling or unknown cause.

making it difficult to reach a conclusion regarding their potential long-term performance.

A different picture emerges with respect to the latex-modified cutback, MC–800L. After the fourth evaluation, the failure rate for the MC–800L mix had increased from 24 to 47 percent, nearly double that of the control mix (25 percent). The drainage problem encountered with the MC–800L mix has led the researchers to question the effectiveness of the latex modification. The incompatibility of the latex with the asphalt may be a possible explanation for the question-

able performance of the latex-modified cutback and emulsion. Such incompatibility would explain the relatively soft nature, drainage, and resulting larger failure rate for the MC–800L mix.

Raveling and shoving were the primary failure modes for all mixes. In no case was failure associated with stripping of the mix. In many cases, the failures occurred in locations where there was poor drainage or severe reflection cracking, and a recurrence of the pothole was inevitable. Other failure modes were not observed on a recurring basis.

Percent Failed, Evaluation No. 3, Standard Method
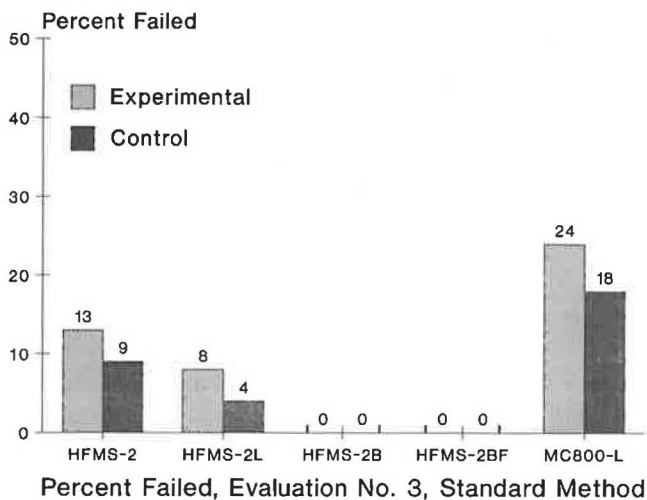
FIGURE 1 Performance of mixes, standard procedure, Evaluation 3.

Percent Failed, Evaluation No. 4, Standard Method
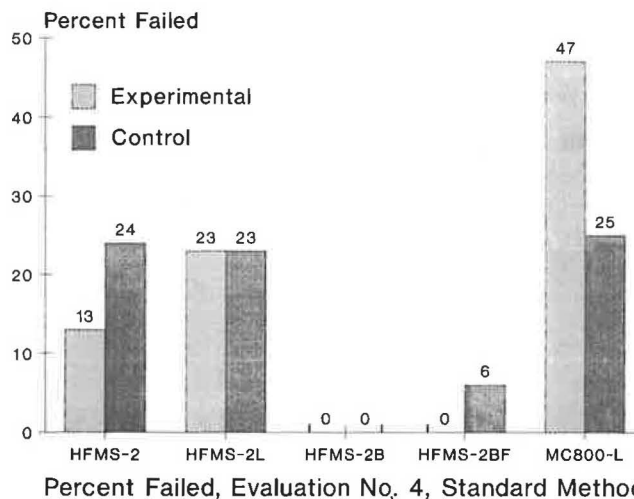
FIGURE 2 Performance of mixes, Evaluation 4.
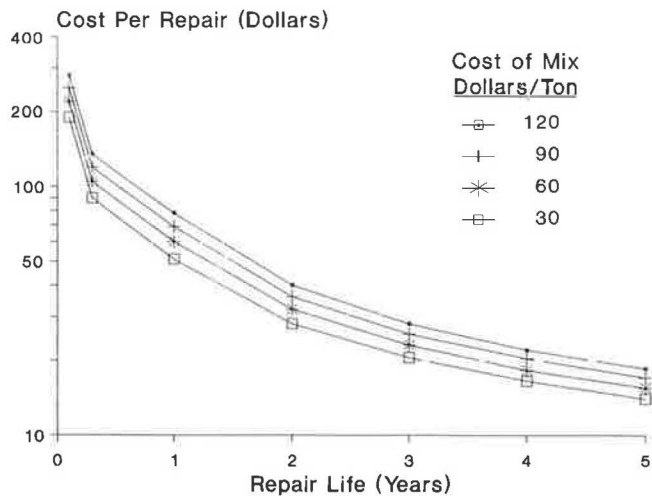
FIGURE 3 EUAC (dollars per repair) for the standard method when repairs can be conducted on a production basis.

COMPARISON OF MATERIALS ON THE BASIS OF ANNUALIZED COST

The cost per ton for the control mix was estimated at $30, and for the five experimental mixes, estimates ranged from $30/ton to $47/ton. Earlier research has shown that material costs represent about 15 to 25 percent of the total cost of repair. The important question is whether, on an equivalent uniform annualized cost (EUAC) basis, the more expensive materials will result in a lower overall cost.

The annualized cost per repair was calculated using procedures published from earlier research (1,3). Cost data include manpower, equipment, and user delays. Calculations were made for material costs ranging from $30/ton to $120/ton. An interest rate of 10 percent was assumed.

EUAC values per repair as a function of repair longevity is shown in Figure 3. As can be seen, the annualized cost differential for various materials, especially those in the range of $30/ton to $50/ton, is relatively small. The dominant influence on annualized cost is the longevity of the repair.

Figure 3 can be used to compare costs for hypothetical materials with varying costs and repair life. Suppose an agency is presently using a material that costs $30/ton, and the average repair life using the standard procedure is 1.0 year. From Figure 3, the cost of each repair is $52.58. Figure 3 clearly shows that if the average service life can be extended to 2.0 years, then the use of material costing as much as $120/ton would result in a significant cost saving. The HFMS–2BF, at $47/ton the most expensive mix in the study, is comparable in total annualized cost to the $30/ton mix if the average service life can be extended from 1.0 to 1.1 years or more. Thus, a 10 percent increase in repair life offsets an increase

in material costs from $30/ton to $47/ton. As another example, Figure 3 shows that a $30/ton mix lasting 2.0 years is comparable to a $120/ton mix lasting 3.0 years. The HFMS 2BF mix at $47/ton and lasting 2.2 years is comparable to the $30/ton mix with a service life of 2.0 years. Similarly, mixes costing about $73/ton or less that will last 5.0 years have a lower annualized cost than mixes costing about $30/ton that will last 4.0 years. It seems evident that to provide a lower annualized cost than conventional mixes premium mixes need only extend the average service life by a modest amount.

CONCLUSION

Several conclusions can be drawn on the basis of the results of this study:

● Two of the four experimental mixtures using HFMS emulsion binders performed better than companion control mixtures in the field trials. The other two HFMS mixtures showed no failures in the field, but definitive conclusions could not be reached because their companion controls had only zero and one failure, respectively.
● Experimental mixtures using the SBR latex-modified cutback binder did not perform as well as their companion controls and no further development is recommended.
● Extended field trials of stockpiled mixtures using the HFMS binders are recommended to interested highway agencies. Field trials using fibers is also recommended.
● A well-designed, cold, stockpiled patching mix can be effectively used in cold-wet weather without the need to heat the mix in a hot box.
● Premium mixes need only extend the average service life by a modest amount to provide a lower annualized cost than conventional mixes.

REFERENCES

1. D. A. Anderson, H. R. Thomas, and Z. Siddiqui. *A Comprehensive Analysis of Pothole Repair Strategies for Flexible and Rigid Base Pavements.* Report FHWA-PA-86-035-80-5. Pennsylvania Transportation Institute, The Pennsylvania State University, University Park, 1986.
2. D. A. Anderson and H. R. Thomas. *More Effective Cold-Wet Weather Patching Materials for Asphalt Pavements.* Report FHWA/RD-88/001. FHWA, U.S. Department of Transportation, Sept., 1987.
3. H. R. Thomas and D. A. Anderson. Pothole Repair: You Can't Afford Not To Do It Right. In *Transportation Research Record 1102.* TRB, National Research Council, Washington, D.C., 1986, pp. 32–40.

Selection of Ideal Maintenance Strategies in a Network-Level Bridge Management System

WILLIAM V. HARPER, ABDULAZIZ AL-SALLOUM, SAAD AL-SAYYARI, SAUD AL-THENEYAN, JENNY LAM, AND CHERYL HELM

A modular bridge management system (BMS) is being developed to select ideal scopes of maintenance work on the basis of the condition states of bridge segments. The maintenance and repair (M&R) scopes and condition modules, which are two of seven modules that make up the BMS are the major focus of this paper. A companion paper in this Record completes the overview of this network-level BMS. The condition module uses surveyed condition ratings to develop composite condition indexes (CCI) that characterize the condition of each structural element within a segment. The CCI values are further refined to derive condition states, which characterize the overall condition of each segment on the basis of the condition levels of its constituent elements (deck, substructure, and superstructure). When the condition state of a bridge segment is known, engineering judgment can be used to select ideal maintenance activities from the M&R scopes module. The M&R scopes describe the intensity level—routine maintenance, repairs, rehabilitation, or replacement—of various M&R actions, each with a defined effect on condition level. When the condition state and the M&R scope effects are provided, the condition state resulting from a certain scope of work can be determined, and the feasible M&R scopes can be ranked from the ideal (most recommended) to the least recommended course of action.

Many bridges are in urgent need of repair, rehabilitation, or replacement. Sudden catastrophic failures caused by unpredictable events (e.g., flooding) cannot be accurately predicted, and their prevention is difficult. However, bridges exhibiting normal, progressive structural damage can be maintained, repaired, rehabilitated, or replaced under an effective bridge management system (BMS), similar in concept to the widely used pavement management systems.

A modular network-level BMS is under development. The structure of this Markovian-based BMS is shown in Figure 1. The system uses surveyed condition ratings in the condition module and levels of maintenance strategies in the maintenance and repair (M&R) scopes module to define core condition states for each segment of a bridge. Ideal M&R scopes can then be selected to restore the segment to good condition. The prediction and optimization modules are described by Harper et al. in a companion paper in this Record.

This BMS is part of an overall highway maintenance management system, which integrates a pavement management system, a nonpavement management system, and a bridges and structures management system (B&SMS). The B&SMS

includes optimization of bridges, tunnels, and culverts. The BMS described here is the bridge portion of the B&SMS.

BMS METHODOLOGY

Various bridge systems (1–8) were reviewed. None of these systems completely satisfied the objectives for this BMS, which are as follows:

- Objective 1. To maximize information collection that could be used in a network-level BMS,
- Objective 2. To make provisions for the stochastic nature of bridge degradation,
- Objective 3. To provide a systematic mechanism for updating degradation models,
- Objective 4. To perform a multiyear optimization,
- Objective 5. To link the project-level plan (detailed individual bridge plan) to the guidance from a network-level optimization, and
- Objective 6. To provide feedback mechanisms that allow system performance and implementation to be reviewed.

Bridges are constructed of one or more spans that vary in length and width from bridge to bridge and can exhibit considerable variations in condition from span to span. To meet Objective 1, bridges are rated and modeled in segments (a superstructure span with an abutment or pier). The many components of a bridge are individually rated on a span-by-span basis and modeled as three structural elements (deck, superstructure, and substructure) at the network level. Functional deficiencies such as inadequate load capacity and insufficient deck width may also be included.

This approach maximizes the capture of data that accurately reflect structural conditions for which realistic, timely, and cost-effective corrective actions can be taken. Models that use some type of cumulative index to rate either the entire bridge or its structural elements (e.g., a bridge deck rating over the entire structure) can have misleading results, both in evaluating and predicting structural conditions and in determining the cost of the requisite maintenance. This BMS is not dependent on having network data on spans, but the system is designed to accommodate such data. If information is available only for the entire structure, which is common in the United States, the BMS will not have the same discrimination ability on the network level.
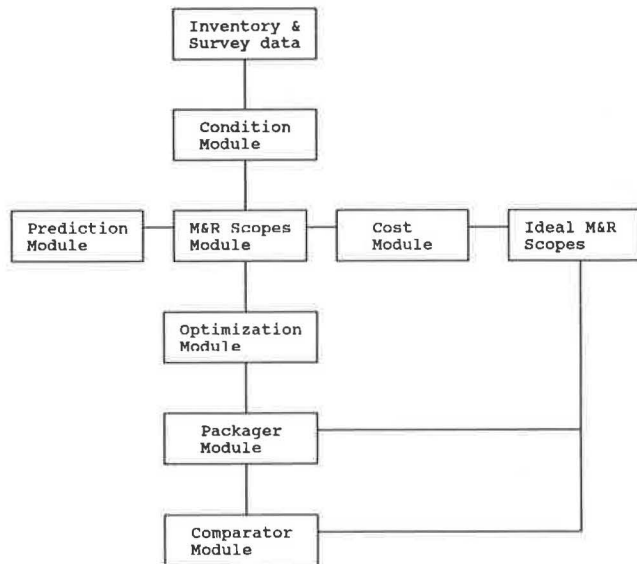
FIGURE 1 Structure of a modular bridge management system.

The prediction module that addresses Objectives 2 and 3 and the network-level optimization models that pertain to Objective 4 are described in the companion paper in this Record. A packager module provides the link between overall network-level guidance and the detailed project-level needs of the individual bridge (Objective 5). A comparator module provides the quality-control feedback to highlight areas of concern in either the system's predictions or its implementation (Objective 6).

CONDITION MODULE

Condition modeling begins with the surveyed condition ratings (SCRs) assigned to the various bridge features. The following scale is being used by the Kingdom of Saudi Arabia; however, any similar scale, such as the 0–9 scale used by FHWA, can be accommodated.

Rating	Definition
7	Like new
6	Good condition
5	Insignificant deterioration
4	Structurally adequate
3	Not functioning as designed
2	Structurally inadequate
1	Potentially hazardous
0	Beyond repair

The SCR values of the components of the deck, superstructure, and substructure are used to derive composite condition indexes (CCIs) for each structural element. The CCIs are then translated into condition levels. The various configurations of condition levels are used to construct the core condition states, for which feasible M&R scopes can be identified and selected from the M&R scopes module using some combination of engineering judgment and the BMS optimization module.

Equations such as the following convert the SCR values to CCIs. User-defined thresholds can be incorporated in order to modify the CCI or assign it the value of the lowest SCR. Different equations are used for certain bridge types.

For bridges with the deck separate from the superstructure, the deck index is calculated as

$$DI = 0.10A + 0.90B \tag{1}$$

where

DI = numerical CCI of deck,
A = numerical SCR of deck surface, and
B = numerical SCR of deck structure.

For bridges with separate decks and superstructures, the superstructure index is calculated as

$$SPI = 0.75C + 0.15D + 0.10E \tag{2}$$

where

SPI = numerical CCI of superstructure,
C = numerical SCR of primary members,
D = numerical SCR of secondary members, and
E = numerical SCR of bearing devices.

If the deck is part of the superstructure, the superstructure index incorporates the SCR value (A) of the deck surface:

$$SPI = 0.10A + 0.70C + 0.10D + 0.10E \tag{3}$$

If the substructure consists of a pier, the substructure index is calculated as

$$SBI = 0.10F + 0.30G + 0.30H + 0.30I \tag{4}$$

where

SBI = numerical CCI of substructure,
F = numerical SCR of pedestals,
G = numerical SCR of capbeam,
H = numerical SCR of column (stem), and
I = numerical SCR of footings.

If the substructure consists of an abutment, the substructure index is calculated as

$$SBI = 0.10F + 0.30I + 0.10J + 0.20K + 0.30L \tag{5}$$

where

J = numerical SCR of backwall,
K = numerical SCR of wingwall, and
L = numerical SCR of breastwall.

The various combinations of CCI ratings for the structural elements making up each segment are used to define core condition states that represent the overall condition of that segment. To reduce the number of condition states to a workable number, the numerical CCI values are translated into

one of four condition levels (good, fair, poor, and critical) for each of the three elements, according to the following scheme:

Range of CCI Values	Condition Level
6 to 7.00	Good
4 to 5.99	Fair
2 to 3.99	Poor
0 to 1.99	Critical

Core condition states are defined as possible combinations of condition levels for the elements that make up the structural segment. There are 64 (4^3) possible core condition states. To these three core condition state parameters (deck, superstructure, and substructure) are added additional parameters reflecting the needs of the organization implementing the BMS. Typical examples include element-age parameters (e.g., superstructure age) or various functional deficiency parameters (e.g., insufficient deck width). The selection of these parameters depends on the proposed use of the system. In Saudi Arabia, most bridges are new and functional deficiencies are rare. Element age was added to their system to enhance the prediction models. In the United States, where it is important to address functional deficiencies, the government agency would be more apt to include several parameters to capture the possible functional deficiencies, including inadequate load capacity and insufficient vertical clearance.

The following example demonstrates the procedures for deriving CCIs, condition level descriptors, and core condition states for Span 2 of a hypothetical bridge using a rating form such as that shown in Figure 2. From this figure, the SCR values for Span 2 are as follows:

Elements of Span 2	SCR Values
Deck surface, *A*	7
Deck structure, *B*	6
Superstructure primary members, *C*	7
Superstructure secondary members, *D*	7
Superstructure bearings, *E*	6
Substructure pedestal, *F*	7
Substructure cap beam, *G*	7
Substructure column stem, *H*	5
Substructure footing, *I*	U (Unknown)

The CCIs for this segment are calculated as follows:

Deck:

$$DI = 0.10A + 0.90B$$
$$= 0.10(7) + 0.90(6)$$
$$= 0.70 + 5.4$$
$$= 6.10 \tag{1}$$

Superstructure:

$$SPI = 0.75C + 0.15D + 0.10E$$
$$= 0.75(7) + 0.15(7) + 0.10(6)$$
$$= 5.25 + 1.05 + 0.60$$
$$= 6.90 \tag{2}$$

Substructure:
Because the footing is unknown, a change must be made in Equation 4.

$$SBI = 0.10F + 0.30G + 0.60H$$
$$= 0.10(7) + 0.30(7) + 0.60(5)$$
$$= 0.70 + 2.10 + 3.00$$
$$= 5.80 \tag{4}$$

The CCI values are translated to condition levels through the conversion table.

$$DI \text{ (deck)} = 6.25 \text{ (good)}$$
$$SPI \text{ (superstructure)} = 6.90 \text{ (good)}$$
$$SBI \text{ (substructure)} = 5.80 \text{ (fair)}$$

Condition State 17 from Table 1 describes this segment.

M&R SCOPES MODULE

The M&R scopes module contains 40 possible types of work for repairing, rehabilitating or replacing the structural elements of bridge segments. These are broad scopes of work, rather than specific M&R tasks. The M&R scopes are selected on the basis of their relationship to existing structural conditions and their implicitly defined effect on the improvement of these conditions. The following rationale is used to construct these M&R scopes.

Bridge maintenance strategies can be categorized by four generic descriptors: routine maintenance, repairs, rehabilitation, and replacement. These categories can be broadly defined as follows.

- Routine maintenance consists of tasks such as cleaning and lubricating bearings. The BMS assumes that all elements receive routine maintenance as well as any other maintenance that may be selected.
- Repairs are those activities that do not require relieving dead loads, which can be performed while maintaining traffic flow.
- Rehabilitation represents more advanced repairs requiring special efforts. Closure of the bridge to traffic may be required.
- Replacement is defined as a complete replacement of one or more major elements.

The repair, rehabilitation, and replacement scopes are coupled with each structural element, yielding the composite M&R scopes in the following list. The impact of each scope may be determined from Table 2.

- Routine maintenance,
- Deck repairs,
- Deck rehabilitation,
- Deck replacement,
- Superstructure repairs,
- Superstructure rehabilitation,
- Superstructure replacement,
- Substructure repairs,
- Substructure rehabilitation, and
- Substructure replacement (which is equivalent to segment replacement in most cases).

TABLE 1 RANKING OF FEASIBLE COMPOSITE M&R SCOPES FOR SEGMENTS OF BRIDGES WITH SEPARATE DECKS

CORE COND. STATE NO.	COND. LEVELS SUB.	SUP.	DECK	RANK	FEASIBLE COMPOSITE M&R SCOPES DESCRIPTION	SCOPE NO.	RESULTING CORE COND. STATE NO.	RESULTING COND. LEVELS SUB.	SUP.	DECK
1	G	G	G	1	Routine Maintenance	1	1 or worse	G	G	G
2	G	G	F	1	Deck Repairs	2	1	G	G	G
				2	Routine Maintenance	1	2 or worse	G	G	F
3	G	G	P	1	Deck Rehabilitation	3	1	G	G	G
				2	Deck Replacement	4	1	G	G	G
				3	Deck Repairs	2	2	G	G	F
				4	Routine Maintenance	1	3 or worse	G	G	P
4	G	G	C	1	Deck Replacement	4	1	G	G	G
				2	Deck Rehabilitation	3	2	G	G	F
				3	Routine Maintenance	1	4 or worse	G	G	C
5	G	F	G	1	Superstructure Repairs	5	1	G	G	G
				2	Routine Maintenance	1	5 or worse	G	F	G
6	G	F	F	1	Superstructure & Deck Repairs	6	1	G	G	G
				2	Deck Repairs	2	5	G	F	G
				3	Superstructure Repairs	5	2	G	G	F
				4	Routine Maintenance	1	6 or worse	G	F	F
7	G	F	P	1	Superstructure Repairs & Deck Rehabilitation	7	1	G	G	G
				2	Superstructure Repairs & Deck Replacement	8	1	G	G	G
				3	Deck Rehabilitation	3	5	G	F	G
				4	Deck Replacement	4	5	G	F	G
				5	Superstructure & Deck Repairs	6	2	G	G	F
				6	Deck Repairs	2	6	G	F	F
				7	Superstructure Repairs	5	3	G	G	P
				8	Routine Maintenance	1	7 or worse	G	F	P
8	G	F	C	1	Superstructure Repairs & Deck Replacement	8	1	G	G	G
				2	Deck Replacement	4	5	G	F	G
				3	Superstructure Repairs & Deck Rehabilitation	7	2	G	G	F
				4	Deck Rehabilitation	3	6	G	F	F
				5	Routine Maintenance	1	8 or worse	G	F	C
9	G	P	G	1	Superstructure Rehabilitation	9	1	G	G	G
				2	Superstructure Replacement	13	1	G	G	G
				3	Superstructure Repairs	5	5	G	F	G
				4	Routine Maintenance	1	9 or worse	G	P	G
10	G	P	F	1	Superstructure Rehabilitation & Deck Repairs	10	1	G	G	G
				2	Superstructure Replacement	13	1	G	G	G
				3	Superstructure Rehabilitation	9	2	G	G	F
				4	Superstructure & Deck Repairs	6	5	G	F	G
				5	Superstructure Repairs	5	6	G	F	F
				6	Deck Repairs	2	9	G	P	G
				7	Routine Maintenance	1	10 or worse	G	P	F
11	G	P	P	1	Superstructure & Deck Rehabilitation	11	1	G	G	G
				2	Superstructure Rehabilitation & Deck Replacement	12	1	G	G	G
				3	Superstructure Replacement	13	1	G	G	G
				4	Superstructure Repairs & Deck Rehabilitation	7	5	G	F	G
				5	Superstructure Repairs & Deck Replacement	8	5	G	F	G
				6	Superstructure Rehabilitation & Deck Repairs	10	2	G	G	F
				7	Superstructure & Deck Repairs	6	6	G	F	F
				8	Deck Rehabilitation	3	5	G	P	G
				9	Deck Replacement	4	5	G	P	G
				10	Deck Repairs	2	10	G	P	F
				11	Superstructure Rehabilitation	9	3	G	G	P
				12	Superstructure Repairs	5	7	G	F	P
				13	Routine Maintenance	1	11 or worse	G	P	P

TABLE 1 *(continued)*

CORE COND. STATE NO.	COND. LEVELS SUB.	SUP.	DECK	RANK	FEASIBLE COMPOSITE M&R SCOPES DESCRIPTION	SCOPE NO.	RESULTING CORE COND. STATE NO.	RESULTING COND. LEVELS SUB.	SUP.	DECK
12	G	P	C	1	Superstructure Rehabilitation & Deck Replacement	12	1	G	G	G
				2	Superstructure Replacement	13	1	G	G	G
				3	Superstructure Repairs & Deck Replacement	8	5	G	F	G
				4	Deck Replacement	4	9	G	P	G
				5	Superstructure & Deck Rehabilitation	11	2	G	G	F
				6	Superstructure Repairs & Deck Rehabilitation	7	6	G	F	F
				7	Deck Rehabilitation	3	10	G	P	F
				8	Routine Maintenance	1	12 or worse	G	P	C
13	G	C	G	1	Superstructure Replacement	13	1	G	G	G
				2	Superstructure Rehabilitation	9	5	G	F	G
				3	Routine Maintenance	1	13 or worse	G	C	G
14	G	C	F	1	Superstructure Replacement	13	1	G	G	G
				2	Superstructure Rehabilitation & Deck Repairs	10	5	G	F	G
				3	Superstructure Rehabilitation	9	6	G	F	F
				4	Routine Maintenance	1	14 or worse	G	C	F
15	G	C	P	1	Superstructure Replacement	13	1	G	G	G
				2	Superstructure & Deck Rehabilitation	11	5	G	F	G
				3	Superstructure Rehabilitation & Deck Replacement	12	5	G	F	G
				4	Superstructure Rehabilitation & Deck Repairs	10	6	G	F	F
				5	Superstructure Rehabilitation	9	7	G	F	P
				6	Routine Maintenance	1	15 or worse	G	C	P
16	G	C	C	1	Superstructure Replacement	13	1	G	G	G
				2	Superstructure Rehabilitation & Deck Replacement	12	5	G	F	G
				3	Superstructure & Deck Rehabilitation	11	6	G	F	F
				4	Routine Maintenance	1	16 or worse	G	C	C
17	F	G	G	1	Substructure Repairs	14	1	G	G	G
				2	Routine Maintenance	1	17 or worse	F	G	G
18	F	G	F	1	Substructure & Deck Repairs	15	1	G	G	G
				2	Deck Repairs	2	17	F	G	G
				3	Substructure Repairs	14	2	G	G	F
				4	Routine Maintenance	1	18 or worse	F	G	F

Abbreviations: Sup. = Superstructure
Sub. = Substructure
G = Good
F = Fair
P = Poor
C = Critical

TABLE 2   COMPOSITE M&R SCOPE DESCRIPTIONS AND IMPACTS ON CONDITION LEVEL

NO.	DESCRIPTION	IMPACT ON CONDITION LEVEL
1	Routine Maintenance	No improvement; condition may worsen
2	Deck Repairs	Improve Deck by one level: From Fair to Good, OR From Poor to Fair
3	Deck Rehabilitation	Improve deck by two levels: From Poor to Good, OR From Critical to Fair
4	Deck Replacement	Restores any deck to Good condition
5	Superstructure Repairs	Improves superstructure by one level: From Fair to Good, OR From Poor to Fair
6	Superstructure Rehabilitation	Improves superstructure by two levels: From Poor to Good, OR From Critical to Fair
7	Superstructure Replacement	Restores Critical superstructure to Good condition and replaces the deck at the same time.
8	Substructure Repairs	Improves substructure by one level: From Fair to Good, OR From Poor to Fair
9	Substructure Rehabilitation	Improves substructure by two levels: From Poor to Good, OR From Critical to Fair
10	Substructure Replacement (Segment Replacement)	Restores entire segment to Good condition since this scope constitutes replacement of all elements.

The various combinations of these scopes (e.g., deck repair plus superstructure rehabilitation) constitute the basis of the 40 possible M&R scopes that could be applied to a bridge segment. These scopes are input to the optimizer module and may be assigned to any segment to which they might feasibly apply. In the packaging module, the detailed actions under each scope are determined.

SELECTING IDEAL M&R SCOPES FOR CORE CONDITION STATES

The selection of an ideal M&R scope for each set of structural segment conditions is an integrative process linking the methodologies used to define core condition states for the segments and the feasible M&R scopes for the structural elements. The derived results can be readily modified to incorporate different additional condition state parameters such as those involving functional deficiencies. These two sets of information are now integrated to accomplish the following:

1. Derive a list of feasible scopes that could be applied for each core condition state;

2. Rank the feasible scopes for each condition state in preferential order, from the most recommended to the least recommended; and

3. Select the ideal M&R scope from the list of ranked feasible scopes.

The ideal M&R scope is defined as the scope that will restore a segment to Core Condition State 1 (all elements in good condition) for the lowest relative implementation cost. This definition is liberal; in practice, other considerations come into play (e.g., traffic loading and detour options, budget constraints, scheduling, user priorities, and agency policies). Some of these other considerations, however, may be incorporated into the selection process.

The information necessary to complete these tasks has been incorporated into the development of core condition states and feasible M&R scopes. The condition levels of each constituent element for that segment define the core condition

BRIDGE NO._____ INSPECTION DATE:_____

INSPECTED BY: _____

LOCATION:_____

CONDITION RATINGS	SPAN NUMBERS										
	1	2	3	4	5	6	7	8	9	10	-
DECK											
Surface	5	7	7	6	7	6	5	7	6	7	
Structure	4	6	6	5	6	6	6	7	7	6	
SUPERSTRUCTURE											
Primary members	6	7	7	5	5	6	6	7	7	5	
Secondary members	6	7	7	6	6	6	6	3	7	6	
Bearings	6	6	7	7	7	6	5	7	6	6	
SUBSTRUCTURE											
ABUTMENTS											
Pedestals	5										
Backwall	6										
Breastwall	6										
Wingwall	7										
Footing	U										
PIERS											
Pedestals	6	7	6	7	5	5	7	7	6	6	
Cap beam	5	7	7	6	7	7	6	7	7	6	
Stem/Column	5	5	5	4	3	7	6	5	4	7	
Footing											

RECOMMENDED FURTHER ACTION:

EVALUATE FOR MAINTENANCE REPAIRS:___YES____
EVALUATE FOR REHABILITATION/REPLACEMENT?___YES____

CURB: 6 inches UNDERCLEARANCE:_12 feet POSTED LOAD CAPACITY 20 tons

REMARKS:__1. Serious deterioration pier breastwall, span no. 5
_____2. Concrete girder shows serious cracks, span no. 8
_____3. Drainage system has failed in span no. 9

FIGURE 2 Sample bridge inspection and condition report.

states. In defining the composite M&R scopes, the effect of each scope on structural element conditions is defined. The feasible M&R scopes are the scopes that represent realistic alternatives for a given core condition state.

When the condition levels that define the condition state are known and the effect of each M&R scope on each condition level is determined, the effect of each feasible scope can be defined in terms of the condition state that could result if the scope were implemented. The extent to which a feasible M&R scope would improve a condition state can now be used as one of two criteria for comparing the scopes and selecting the ideal. The second criterion is the implementation costs of feasible M&R scopes, when two or more scopes would restore the segment to Core Condition State 1.

Two other criteria were used as part of the engineering assessment applied to rank the scopes that did not restore the segment to Core Condition State 1. These criteria evaluated which elements would contribute most to further degradation of the structure and would have the greatest effect on user inconvenience and safety.

If all elements cannot be restored to good condition by the selected M&R scope because of budget constraints or other priorities), the most important element to remedy is the one with the lowest condition level rating. User-defined priorities can be set to determine which element receives attention first.

The following precedence rules were employed in the ranking scheme. If two or more elements are in the same condition (less than good), the deck element will take precedence over the others. If the deck is not one of those elements, the substructure is more important, followed by the superstructure. Using these precedence rules, if the substructure, superstructure, and deck are in poor condition, deck improvement takes precedence over the substructure improvement. Improving the substructure, in turn, takes precedence over

the superstructure. The scope ranked first would remedy all three elements and is the ideal; the succeeding scopes to remedy these conditions would be ranked according to these precedents.

Some M&R scopes are not feasible for certain condition states and would not be selected. Scopes are considered infeasible (or inappropriate) when the condition levels do not warrant remediation, the cost-benefit considerations do not justify a particular scope, or the structural conditions are so severe that a low-level scope (e.g., repairs) would achieve little benefit.

For example, if a structural segment is in Core Condition State 1, all its elements are in good condition and require no maintenance. If a deck, superstructure, or substructure is rated as critical, repair activities would at most improve the element to poor condition; in these instances, rehabilitation (at a minimum) would logically be selected. The process for selecting an ideal M&R scope for a particular condition state is demonstrated in the following example.

Consider a bridge segment that has been assigned Core Condition State (Table 1). The condition levels of this condition state are good for the deck and substructure, poor for the superstructure. Only those feasible M&R scopes that would affect the superstructure need to be considered. The substructure and deck are in good condition and do not require any remedial work. The following feasible scopes for Core Condition State 9 would be drawn from Table 1.

1. Routine maintenance (M&R Scope 1). If this scope were selected, the segment would receive only routine maintenance. The condition state would remain at 9 (or worse if the segment deteriorates over time).
2. Superstructure repairs (M&R Scope 5). This scope could improve the superstructure by one level. If implemented, the resulting condition levels would be good for the deck and substructure and fair for the superstructure. This scope could restore the segment to Core Condition State 5.
3. Superstructure rehabilitation (M&R Scope 9). This scope would improve the superstructure condition by two levels. If implemented, the resulting condition levels would be good for all three elements. This scope could restore the segment to Core Condition State 1.
4. Superstructure replacement (M&R Scope 13). This scope would improve the superstructure condition by two levels. If implemented, the resulting condition levels would be good for all three elements. This scope could restore the segment to Core Condition State 1; however, it would (on the average) cost more to implement than rehabilitation.

On the basis of the precedence rules and the new condition states that might result if each of the M&R scopes were implemented, these scopes can be ranked from the most recommended to the least recommended as follows:

Original Condition State No.	Feasible Scope No.	Improved Core Condition State No.
9	9	1
9	13	1
9	5	5
9	1	9 (or worse)

If the segment actually deteriorates further in time, the core condition state number could become greater than 9.

All of the information obtained in the ranking process for Core Condition States 1 through 18 is presented in Table 1. The M&R scope listed first is the ideal scope; the remaining scopes are ranked using the decision process outlined previously.

USE OF IDEAL M&R SCOPES IN THE BMS

The procedures to derive ideal M&R scopes constitute the engineering-based selection of maintenance activities. The previously presented scopes are ideal when the budget is unrestricted. However, few agencies operate under such a scenario. The ideal M&R scopes can still be used by the BMS in several ways.

- The ideal engineering-based scopes can constitute alternative policy considerations to be accessed by the optimization, packaging, and comparator modules.
- The engineering-based solution can be compared with the solutions of the optimization module. If the optimized solutions and the engineering-based solutions are very different, which can result from insufficient budget or other modeling considerations, the optimized solutions can be reassessed.
- The ideal M&R scopes can be used in the comparator module for quality control and to cross check the optimized solutions and their performances.

Once the ideal engineering-based solutions have been selected, the M&R tasks necessary to implement them need to be specified. In the BMS, this is handled by the packaging module, using a variety of data not used by the optimization module, including data obtained during the condition surveys that evaluate the type and cause of damage, and recommend specific maintenance tasks.

SUMMARY

This BMS is being developed to address the six goals listed earlier. Formulas are used to transform the component survey ratings into element CCIs on a segment-by-segment basis to provide a more informative base for the network optimization models. The M&R scope module selects the feasible scopes for each core condition state. These feasible scopes are ranked, and the ideal scope is chosen on the basis of specific criteria. The network optimization models may select from any of the feasible M&R scopes (not just the ideal) for a given condition state.

REFERENCES

1. S. W. Hudson, R. F. Carmichael III, L. O. Moser, and W. R. Hudson. *NCHRP Report 300: Bridge Management Systems*. TRB, National Research Council, Washington, D.C., 1987.
2. D. W. Johnston and P. Zia. A Level-of-Service System for Bridge Evaluation. In *Transportation Research Record 962*, TRB, National Research Council, Washington, D.C., 1984, pp. 1–8.
3. K. M. I. Al-Subhi, D. W. Johnston, and F. Farid. *Optimizing System-Level Bridge Maintenance, Rehabilitation, and Replace-*

ment Decisions: Executive Summary. Research Project 88-1, Center for Transportation Engineering Studies, Department of Civil Engineering, North Carolina State University, Raleigh, 1989.

4. R. C. Arner, J. M. Kruegler, R. M. McClure, and K. R. Patel. The Pennsylvania Bridge Maintenance Management System. In *Transportation Research Record 1083*, TRB, National Research Council, Washington, D.C., 1986, pp. 25–34.

5. C. Boyce, W. R. Hudson, and N. H. Burns. *Improvements in On-System Bridge Project Prioritization*. Research Reports 439-1 and 439-2, Center for Transportation Research, Bureau of Engineering Research, The University of Texas at Austin, 1987.

6. K. M. Al-Subhi. *Optimizing System-Level Bridge Maintenance, Rehabilitation, and Replacement Decisions*. Ph.D. dissertation.

Department of Civil Engineering, North Carolina State University, Raleigh, 1988.

7. C. Chen and D. W. Johnston. *Bridge Management under a Level of Service Concept Providing Optimum Improvement Action, Time, and Budget Prediction*. Center for Transportation Engineering Studies, Department of Civil Engineering, North Carolina State University, Raleigh, 1987.

Stochastic Optimization Subsystem of a Network-Level Bridge Management System

William V. Harper, Jenny Lam, Abdulaziz al-Salloum, Saad al-Sayyari, Saud al-Theneyan, George Ilves, and Kamran Majidzadeh

The prediction and stochastic optimization modules are two of seven modules that make up a stochastic network-level bridge management system which is under development. An overview of major portions of the bridge management system is provided. The prediction model of structural degradation generates initial estimates of transition probabilities (tp values). A tp value is defined as the probability that a bridge segment will move from one condition state to another within 1 year given the maintenance scope assigned to it. The tp values are updated with new survey data using a Bayesian updating procedure. Methods are developed to account for the fact that structural surveys may be performed on a multiyear basis, while yearly tp values are needed for the optimization models. The optimization module, which minimizes cost subject to top management's performance objectives, is a Markovian-based linear program that stratifies the bridge network to improve degradation predictions. Rather than using single ratings for a major bridge element (e.g., bridge deck), the program optimizes on a bridge segment level to maximize the use of structural condition information. The condition state of a segment can include selected functional deficiencies as well as structural condition ratings.

A network-level bridge management system (BMS) based on the Markovian decision process is under development. Seven modules make up this BMS. The condition module uses surveyed condition-rating data to derive condition states that characterize the overall condition of each bridge segment. The use of this module to derive engineering-based maintenance solutions has been described by Harper et al. in a companion paper in this record.

The maintenance and repair (M&R) scopes module contains 40 possible levels of M&R intensity (under the categories of repair, replacement, rehabilitation, and routine maintenance) for the condition states. Each M&R scope has a defined effect on each condition level, so that improvements resulting from the application of these scopes can be modeled. The M&R scopes provide input to the prediction, cost, optimization, packaging, and comparator modules.

The prediction module estimates transition probabilities (tp) and uses Bayesian techniques to update them to predict the probability that a given segment will move from one condition state to another over time. The prediction module covers all M&R scopes, so that long-term segment changes can be predicted.

The cost module uses historical cost data, condition states, M&R scopes, and other inputs to estimate unit costs of the M&R scopes. This module includes a parametric equation that can be used to aid in the generation of user costs.

The optimization module consists of three network optimization solution models based on a Markovian decision model using linear programming techniques. A separate linear program is solved for each stratum. Bridges are stratified according to factors such as bridge type, climate, and functional class. The first year's solution (of the multiyear model) provides the network-level guidance used in the subsequent modules.

The packaging module packages the first year of the optimized network solutions into individual work projects in which the generalized M&R scopes are made specific. In the project-level analyses by the packager, maintenance costs identified by the optimizer will be more accurately assessed.

The comparator module performs a quality control role on the performance and implementation of the BMS and provides necessary comparisons of the cost and predictive capabilities of the models with actual experience when the BMS solutions are implemented.

BASIC UNIT OF MANAGEMENT

Network bridge optimization can be approached in two ways in terms of the basic unit being modeled. Either the bridge or a subset thereof can be the fundamental unit for the optimization model. This BMS can work on bridge segments as this subset. A segment is defined as one superstructure span with a unit of substructure (either a pier or an abutment).

The difficulty in using the bridge as the unit of optimization is that many M&R activities will apply only to a given segment, and not to the entire structure. Although tasks for a particular bridge can be determined given the survey information, it would be extremely difficult to predict future bridge maintenance needs without subdividing the structure into smaller units. Also, better cost estimations are possible when segments are the basic unit.

Each bridge segment is categorized by its condition state and the strata to which it is assigned. Core condition states are developed on the basis of the structural condition ratings. The core condition state assigns a condition level of good, fair, poor, or critical to the major bridge elements, the deck,

superstructure, and substructure. This level is based on the detailed ratings of the individual components that comprise each element. Supplementing the core condition state parameters are user-defined parameters, such as element age, or various functional deficiency parameters, such as insufficient deck width.

Strata have been created in this BMS for two reasons. The first is to develop groups of bridges that exhibit similar degradation patterns. The second is to form groups that have approximately the same costs for the various M&R scopes. Subject to the desired performance goals in the optimization module, the interaction of cost and transition probabilities determines the optimal policy. User-defined stratifying variables may include such items as bridge type, climate, and functional class.

PREDICTION MODULE

The prediction module is based on a Bayesian updating of tp values. These tp values are estimates of the probability of a segment moving from one condition state to another for the various M&R scopes. In the following paragraphs, the development of initial tp values is followed by a brief description of a direct Bayesian updating of the tp matrices that are generated for later input to the Markovian-based optimization models.

A Bayesian updating of the tp values necessitates assigning a prior probability distribution. This approach uses the multivariate Dirichlet distribution (*1*). Given the current condition state, the tp values for moving from that state to all possible states in the next year must add up to 1. The survey data updating the tp values is multinomial. The Dirichlet distribution is a conjugate prior for the multinomial and may be considered a multivariate generalization of the beta distribution, as the multinomial is a generalization of the binomial distribution. The Dirichlet distribution simultaneously updates each individual tp value for a given initial state and ensures that the resulting sum is 1. A separate Dirichlet distribution is used for each row of a given tp matrix.

Each prior tp estimate can be treated as coming from a beta distribution when a Dirichlet multivariate prior distribution is assumed for a given set of tp values. The beta prior distributions can be handled individually, and the probabilistic aspects of the posterior tp values are preserved (the sum of tp values for any row in the tp matrix equals 1).

Given a Dirichlet prior distribution and multinomial observed data, the resulting posterior distribution is a Dirichlet distribution. The tp values needed may be easily determined from the Bayesian updated matrix once all the new data have been used in the updating procedure (*2*).

INITIAL DEVELOPMENT OF TRANSITION PROBABILITIES

To develop initial tp values for each stratum is necessary. These tp values will provide the first prior distributions for the initial Bayesian updating. After implementation of the BMS, the Bayesian updating will result in self-adjustment of the tp values to the specific conditions for each stratum. However, during the first years of its operation the initial tp values will still influence the operation of the Markovian decision-based optimization models.

Expert opinion has been used to estimate the remaining useful life (RUL) of the deck, superstructure, and substructure for different bridge types on the basis of current condition ratings. This information is used to develop the initial tp values, which are updated annually with the actual survey data using Bayesian statistical methods. The initial tp matrix is made specific for each stratum. If sufficient historical data exist, they should be used to develop the initial tp values.

The following example generates the initial tp values for a bridge deck changing condition levels from good to the possible condition levels good, fair, poor, or critical in 1 year under routine maintenance. The same procedure will be used to develop the tp values for both superstructure and substructure. These tp values include adjustment for the dependence of the elements. The initial core tp matrix (based on element condition ratings) results from multiplication of the associated individual-element tp value.

Using the results of the analyzed expert opinion, the estimated RUL for an average deck in good condition results in a good RUL_{Deck} of 30 years (*2*). Similarly, the expected RUL for a top-of-the-range fair deck, (Top of fair RUL_{Deck}) equals 22 years. The difference between the expected RUL for a typical good deck and the top of the fair deck level results in an expected difference [Delta(RUL)] of 8 years.

A structural dependency table is then used to adjust the Delta(RUL), if necessary, to account for the condition of the structural elements. This procedure results in an Adj-Delta(RUL). Assuming the other elements are in good condition, this adjustment results in an AdjDelta(RUL) that is still 8 years. The resulting tp value for a deck going from good to fair, when the other elements are in good condition, may be estimated as ⅛, which equals 0.125. The general formula for converting an AdjDelta(RUL) to a tp value is as follows:

$$tp = [AdjDelta(RUL)]^{-1} \qquad (1)$$

This formulation results in the correct expected transition times from one level to another. In the development of the initial tp matrix, an additional assumption is made that under normal conditions, a structural element will not degrade more than one level in a 1-year time period. Thus, the tp values for a deck transitioning from good to each of the four levels (when the other elements are in good condition) are calculated as follows:

To Condition Level	tp Value
Good	$1.0 - 0.125 = 0.875$
Fair	$1.0/(30 - 22) = 0.125$
Poor	0.0
Critical	0.0

Using the same approach, the other deck tp values may be calculated. In a similar manner, the tp values will be calculated for superstructure and substructure. These tp values are combined to give the initial joint tp values for the core condition states under routine maintenance. From this tp matrix, all other M&R scope tp matrices are generated.

BAYESIAN UPDATING USING MULTIYEAR SURVEYS

The initial tp values are 1-year probabilities. Surveys performed in a given year may only cover part of the structures each year. The resulting data then reflect multiyear tp values instead of the needed 1-year tp values. Thus, the survey will represent different periods of time ($k = 1, 2, \ldots,$ years) since the last survey on various structures. In this section, the methodology is introduced for using the multiyear data to generate 1-year tp values. If all bridges are surveyed each year, these steps are not necessary.

After each year's survey, the prior tp values can easily be converted from 1-year tp value estimates to k-year (where k is a positive integer) tp value estimates by multiplying the tp matrix by itself as follows:

$$\mathbf{T}^{(k)} = \mathbf{T}^k \tag{2}$$

where

$\mathbf{T}^{(k)} = k$-year tp matrix,
$\mathbf{T} = $ 1-year tp matrix, and
$\mathbf{T}^k = \mathbf{T}$ multiplied by itself k times.

Using the matrix $\mathbf{T}^{(k)}$, the Bayesian updating algorithm presented in *B&SMS Conceptual Framework* (2) may be applied using Year k survey data (k years since last survey). Thus $\mathbf{T}^{(k)}$ represents the prior tp matrix that will be updated with the Year k survey data. A prior tp matrix is needed for each Year k that the current survey represents. For each Year k, there is a Bayesian updating step. Year $k = 1$ survey data will be used first, then Year $k = 2$ survey data, and so forth until all the survey data have been used in the tp updating. For example, if current survey data are available for bridges that were last surveyed 1, 2, 3, and 5 years ago, the mathematical process will generate the needed prior tp matrix for each of the 4 years represented in the survey.

The resulting updated tp values are k-year tp values. These tp values then need to be converted to $(k + 1)$-year tp values so that Year $(k + 1)$ survey data can be used for updating purposes. After all the survey data have been used, the final conversion to 1-year tp values is used for the Markovian decision linear program process. In the following, $\mathbf{B}_k$ represents the posterior k-year tp matrix (resulting matrix after the Bayesian updating using Year k data), and $\mathbf{A}_k$ represents the posterior 1-year tp matrix after updating with Year k data. The mathematics for this is as follows:

$$\mathbf{B}_k = \mathbf{U}_k \mathbf{D}_k \mathbf{U}_k^{-1} \tag{3}$$

where

$\mathbf{B}_k = k$-year updated (posterior) tp matrix,
$\mathbf{U}_k = $ eigenvector matrix of $\mathbf{B}_k$, and
$\mathbf{D}_k = $ diagonal matrix with eigenvalues on diagonal.

Then,

$$\mathbf{A}_k = \mathbf{U}_k \mathbf{D}_k^{1/k} \mathbf{U}_k^{-1} \tag{4}$$

where

$\mathbf{A}_k$ – annual (or 1-year) updated tp matrix after updating with Year k data,
$\mathbf{U}_k = $ eigenvector matrix of $\mathbf{B}_k$, and
$\mathbf{D}_k^{1/k} = $ diagonal matrix $\mathbf{D}_k$ replaced with kth roots of its diagonals.

It is easily seen that

$$(\mathbf{A}_k)^k = (\mathbf{U}_k \mathbf{D}_k^{1/k} \mathbf{U}_k^{-1})^k = \mathbf{U}_k \mathbf{D}_k \mathbf{U}_k^{-1} = \mathbf{B}_k \tag{5}$$

After all the survey data have been used, the desired Bayesian, updated, 1-year tp values are in the final tp matrix $\mathbf{A}_F$. There is a separate matrix $\mathbf{A}_F$ for each stratum. This posterior matrix $\mathbf{A}_F$ becomes the prior tp matrix $\mathbf{T}$ in the subsequent year. This approach using eigenvalues also eliminates the need to multiply the matrix $\mathbf{T}$ by itself k times to generate the matrix $\mathbf{T}^{(k)}$. Similarly, the steps can be reduced by moving directly from a posterior k-year tp matrix to a prior $(k + 1)$-year tp matrix without having to create an intermediate posterior 1-year tp matrix after each Year k Bayesian updating.

As an illustration of this procedure, assume that the recent survey provides data for bridges that were last surveyed 1, 2, 3, and 5 years ago. The prior matrix $\mathbf{T}$ will be updated using the methodology in *B&SMS Conceptual Framework* (2) with the Year $k = 1$ data, resulting in the posterior tp matrix $\mathbf{B}_1$. Obviously, $\mathbf{A}_1 = \mathbf{B}_1$. Following the mathematics illustrated with matrix $\mathbf{T}$, the matrix $\mathbf{A}_1$ becomes the prior 1-year tp matrix for updating with Year $k = 2$ data. Therefore the prior 2-year tp matrix is $\mathbf{A}_1^2 = \mathbf{A}_1 * \mathbf{A}_1$ (or could be generated using the eigenvalue approach). This tp matrix is updated with the Year $k = 2$ data, resulting in the posterior 2-year tp matrix $\mathbf{B}_2$. From this matrix, $\mathbf{A}_2$ is obtained, representing the posterior 1-year tp matrix after updating with Year $k = 2$ data. This in turn becomes the prior 1-year tp matrix for updating with Year $k = 3$ data. As a result, $\mathbf{A}_2^3$ is the needed prior 3-year tp matrix. (Another way to obtain $\mathbf{A}_2^3$ is to bypass generating the 1-year posterior tp matrix and go directly from the Year 2 posterior tp matrix $\mathbf{B}_2$ to the desired prior tp matrix, $\mathbf{A}_2^3$. Because $\mathbf{B}_2 = \mathbf{U}_2 \mathbf{D}_2 \mathbf{U}_2^{-1}$, $\mathbf{A}_2^3 = \mathbf{U}_2 \mathbf{D}_2^{3/2} \mathbf{U}_2^{-1}$.) $\mathbf{A}_2^3$ is updated, resulting in the posterior $\mathbf{B}_3$ (3-year posterior tp matrix). After Year $k = 3$ data have been used, $\mathbf{A}_3$ is the 1-year posterior tp matrix and is then the prior 1-year tp matrix for subsequent updating with the Year $k = 5$ data. $\mathbf{A}_3^5$ is the prior 5-year tp matrix that is updated to give $\mathbf{B}_5$, the posterior 5-year tp matrix. From this matrix, $\mathbf{A}_5$ is the desired 1-year tp matrix $\mathbf{A}_F$ that provides the tp matrix needed for the Markov-based linear programs. Of course, $\mathbf{A}_5$ will be the prior 1-year tp matrix $\mathbf{T}$ in the following year.

BMS OPTIMIZATION MODULE

The three optimization models are the long-term (steady state) goal-setting model, the multiyear (short-term) planning model, and the financial exigency planning model. The long-term model is used to establish the steady state goals that provide targets for the multiyear and financial exigency models. The multiyear model addresses the year-by-year maintenance needs

for the planning horizon. Both the long-term and multiyear models solve a separate linear program for each stratum. The financial exigency model imposes a network-wide budget constraint across all strata if the budget is insufficient to satisfy the sum of the multiyear models of the individual strata.

The optimization models can be used to develop a set of maintenance plans for a bridge system over the desired planning horizon. Various inputs are required to run each of the models. Management input, cost parameters, tp values, and condition survey data are necessary. This process is iterative. If satisfactory results are not obtained, looping backwards may be necessary. For example, if satisfactory budget estimates cannot be obtained from the short-term model, new performance objectives may need to be set. This would require running both the steady state and short-term models again.

The following planning steps are necessary:

Step 1. Survey the bridge system. The survey results are used to update the present estimates of tp values. They are also used to compute proportions of the bridges in each condition state to be used in the multiyear planning model and the comparator.

Step 2. Determine realistic long-term performance goals by solving the long-term model until an acceptable level of annual expenditures is achieved. This iteration may involve lowering performance objectives to obtain a satisfactory budget level. The final result becomes a goal to be reached in the final year of the planning horizon for the multiyear optimization.

Step 3. Determine performance objectives to be achieved for each year of the planning horizon. The present surveyed condition states describe the present performance level, and the long-term model solution indicates the performance objectives for the final year of the planning horizon.

Step 4. Solve the multiyear model to determine the optimal maintenance policy for each year in the planning horizon and to develop the expected expenditures. If budgeting requirements are too high between the first and last years of the planning horizon, the performance objectives can be revised.

Step 5. If the multiyear solution is satisfactory, the first-year maintenance policy is packaged into actual projects using the packager module. If the result is not satisfactory, Step 6 is required.

Step 6. If the multiyear solution does not provide satisfactory results because of inadequate fund availability for the first year, the financial exigency model is solved. This solution indicates the optimal first-year maintenance policy that stays within the first-year budget while computing the additional expenditures needed to successfully achieve the performance objectives for the remaining years in the planning horizon. Management must then decide whether this additional cost is excessive. If not, the solution may be considered as the plan for the entire planning horizon, and Step 5 is executed. If the additional cost is considered excessive, two options are (a) to request supplemental funds for the first year to relax the budget constraint, or (b) to reduce performance objectives (and subsequent costs) for succeeding years. As with the multiyear model, the financial exigency model may be used iteratively to revise performance objectives or to justify supplemental budget requests. Once an acceptable solution is found, Step 5 is performed. The final step is to implement the packaged projects.

The linear programs for each of the three network models minimize cost subject to meeting the desired performance goals of top management. The Markovian-based linear programs optimize the M&R scopes for bridge segments instead of the entire bridge, because this allows a more in-depth use of the available information. The system accommodates mandatory projects (in which specific actions are mandated for a given bridge) that have been determined on the basis of engineering or policy decisions. The mathematical structures of the linear programs are provided in the following section. More detailed explanation of all three optimization models are given in *B&SMS Conceptual Framework* (2). Modifying these models to include additional performance constraints is not difficult.

LONG-TERM OPTIMIZATION MODEL

The parameters of the long-term (or steady-state) model are defined as follows:

Input Parameters

I = index set $(1, 2, \ldots, n)$ of condition states;
D = index set $(i_1, i_2, \ldots, i_g)$ of desirable condition states;
U = index set $(i_1, i_2, \ldots, i_b)$ of undesirable condition states;
S = index set $(1, 2, \ldots, m)$ of bridge strata;
M_i = index set $(a_1, a_2, \ldots, a_{mi})$ of feasible maintenance scopes a for bridge segments in condition state i;
$C_{ia}(s)$ = average cost of maintenance scope a applied to one bridge segment in stratum s and condition state i;
$P_{iaj}(s)$ = the probability that a segment in stratum s and condition state i that has scope a applied to it will transition into condition state j in 1 year;
$\bar{p}(s)$ = maximum proportion of segments in stratum s that is allowed in an undesirable condition state;
$\underline{p}(s)$ = minimum proportion of segments in stratum s that should be in a desirable condition state; and
$N(s)$ = number of segments in stratum s.

Output Parameters (Decision Variables)

$w_{ia}(s)$ = proportion of the segments in stratum s that are in condition state i and should receive maintenance scope a; and
$C(s)$ = expected maintenance cost per segment in stratum s.

The long-term optimization model for stratum s requires minimizing the expression

$$C(s) = \sum_{i \in I} \sum_{a \in M_i} w_{ia}(s) C_{ia}(s) \tag{6}$$

subject to

$$w_{ia}(s) \geq 0 \qquad \text{for all } a \text{ in } M_i \text{ and } i \text{ in } I \tag{7}$$

$$\sum_{i \in I} \sum_{a \in M_i} w_{ia}(s) = 1 \tag{8}$$

$$\sum_{a \in M_j} w_{ja}(s) - \sum_{i \in I} \sum_{a \in M_i} w_{ia}(s) P_{iaj}(s) = 0 \qquad \text{for all } j \text{ in } I \tag{9}$$

$$\sum_{i \in D} \sum_{a \in M_i} w_{ia}(s) \geq \underline{p}(s) \tag{10}$$

$$\sum_{i \in U} \sum_{a \in M_i} w_{ia}(s) \leq \overline{p}(s) \tag{11}$$

Minimizing the objective function of Equation 6 minimizes the average cost per segment in stratum s. To get the total expected long-term cost for the stratum, the solution $C(s)$ must be multiplied by $N(s)$, the number of segments in the stratum. Constraints 7 and 8 ensure that solutions satisfy the probability axioms. The $w_{ia}(s)$ functions may be thought of as the elements of a discrete joint probability distribution. Constraint 7 ensures the nonnegativity of each individual element in this joint probability distribution, and Constraint 8 forces its sum over the possible sample space to equal 1. Constraint 9 provides the steady state equations for a Markovian process (forcing the proportion of the network in condition state i to remain fixed, i.e., at a steady state). Constraints 10 and 11 enforce the lower bound on the proportion of segments in desirable condition states and the upper bound on the proportion in undesirable states, respectively. Additional constraints to satisfy particular functional deficiencies can be easily added as desired.

MULTIYEAR OPTIMIZATION MODEL

The notation for the multiyear model is defined as follows:

Input Parameters

I = index set $(1, 2, \ldots, n)$ of condition states;
D = index set $(i_1, i_2, \ldots, i_g)$ of desirable condition states;
U = index set $(i_1, i_2, \ldots, i_b)$ of undesirable condition states;
S = index set $(1, 2, \ldots, m)$ of bridge strata;
M_i = index set $(a_1, a_2, \ldots, a_{m_i})$ of feasible maintenance scopes a for bridge segments in condition state i;
$C_{ia}(s)$ = average cost of applying maintenance scope a to one bridge segment in stratum s and condition state i;
$P_{iaj}(s)$ = probability that a segment in stratum s and condition state i that has scope a applied to it will change into condition state j in 1 year;
$\overline{p}^t(s)$ = maximum proportion of segments in stratum s allowed in an undesirable state in year t;
$\underline{p}^t(s)$ = minimum proportion of segments in stratum s that should be in a desirable state in year t;
$\hat{w}_{ia}(s)$ = lower bound on the proportion of segments in stratum s that is in condition state i and will receive maintenance scope a in Year 1, for mandatory projects;
$q_i(s)$ = proportion of the segments in stratum s in condition state i at the beginning of Year 1;
ϕ = parameter for uniformly relaxing minimum desirable condition state standards in Year 2;
f = parameter for uniformly relaxing maximum undesirable condition state standards in Year 2;
g, h = tolerances;
$w_{ia}^*(s)$ = optimal values for the steady state (long-term) problem;
r = discount rate for computing net present value; and

$C^*(s)$ = optimal cost per segment in stratum s from the steady state (long-term) model.

Output Parameters (Decision Variable)

$w_{ia}^t(s)$ = proportion of the segments in stratum s that are in condition state i and should receive maintenance scope a in year t,
$\hat{C}(s)$ = expected net present value of cost per segment in stratum s of a maintenance policy, and
$E^t(s)$ = expected expenditures in year t in stratum s.

The finalized multiyear (short-term) optimization model for stratum s requires minimizing the expression

$$\hat{C}(s) = \sum_{t=1}^{T} \sum_{i \in I} \sum_{a \in M_i} (1 + r)^{1-t} w_{ia}^t(s) C_{ia}(s) \tag{12}$$

subject to

$$w_{ia}^t(s) \geq \hat{w}_{ia}^t(s) \quad \text{for all } i \text{ in } I \text{ and } a \text{ in } M_i, \text{ for } t \\ \text{with known mandatory projects} \tag{13}$$

$$w_{ia}^t(s) \geq 0 \quad \text{for all } i \text{ in } I, a \text{ in } M_i, \text{ and } 2 \leq t \leq T \tag{14}$$

$$\sum_{i \in I} \sum_{a \in M_i} w_{ia}^t(s) = 1 \quad 1 \leq t \leq T \tag{15}$$

$$\sum_{a \in M_i} w_{ia}^1(s) = q_i(s) \quad \text{for all } i \text{ in } I \tag{16}$$

$$\sum_{a \in M_i} w_{ja}^t(s) - \sum_{i \in I} \sum_{a \in M_i} w_{ia}^{t-1}(s) P_{iaj}(s) = 0 \text{ for all } j \text{ in } I \\ \text{and } 2 \leq t \leq T \tag{17}$$

$$\sum_{i \in D} \sum_{a \in M_i} w_{ia}^2(s) \geq \underline{p}^2(s)\phi \tag{18}$$

$$\sum_{i \in D} \sum_{a \in M_i} w_{ia}^t(s) \geq \underline{p}^t(s) \quad \text{for } 3 \leq t < T \tag{19}$$

$$\sum_{i \in U} \sum_{a \in M_i} w_{ia}^2(s) \leq \overline{p}^2(s)f \tag{20}$$

$$\sum_{i \in U} \sum_{a \in M_i} w_{ia}^t(s) \leq \overline{p}^t(s) \quad \text{for } 3 \leq t < T \tag{21}$$

$$\sum_{a \in M_i} w_{ia}^T(s) \geq \sum_{a \in M_i} (1 - g) w_{ia}^*(s) \quad \text{for all } i \text{ in } I \tag{22}$$

$$\sum_{a \in M_i} w_{ia}^T(s) \leq \sum_{a \in M_i} (1 + g) w_{ia}^*(s) \quad \text{for all } i \text{ in } I \tag{23}$$

$$\sum_{i \in I} \sum_{a \in M_i} w_{ia}^T(s) C_{ia}(s) \leq (1 + h) C^*(s) \tag{24}$$

Minimizing the objective function of Equation 12 minimizes the average present cost per segment of maintenance over the time horizon of interest. To get the necessary (least) budget, $E^t(s)$, for stratum s for Year t, the following calculation is necessary:

$$E^t(s) = N(s) \sum_{i \in I} \sum_{a \in M_i} w_{ia}^t(s) C_{ia}(s)$$

Constraint 13 accommodates the mandatory projects for Year 1 and beyond, if planned. Constraints 14 and 15 are based on probability and are needed to satisfy the fact that $w_{ia}^t(s)$ constitutes a discrete joint probability distribution. Constraint 16 ensures that the optimal scopes associated with each condition state are assigned to the correct percentage of the network, a boundary condition that sets $q_i(s)$, the proportion of the network in each condition state in the first year, on the basis of survey results. Constraint 17 is a condition state balance equation from Year $t - 1$ to Year t based on the use of the transition probabilities $P_{iaj}(s)$.

Constraints 18 through 21 force the optimization to meet the performance objectives established by top management. Constraints 18 and 20 also allow a possible relaxation of the second-year performance objectives if desired, for instance, budget is insufficient. Constraints 22 and 23 allow a relaxation, if desired, in meeting the optimal steady state proportions. Constraint 24 allows a similar flexibility in meeting the optimal steady state average cost per segment in the last year (T) of the multiyear planning horizon. As with the long-term model, constraints can easily be added or modified to satisfy the goals of the organization.

FINANCIAL EXIGENCY MODEL

The multiyear model formulated in Equations 12 through 24 is actually a series of identical (in mathematical structure) and independent models, one for each stratum. The financial exigency model ties all the strata models together with a common budget constraint and has a combined objective function. Constraints 13 through 24 do not change in the financial exigency model. This combined model is too large to solve directly by the simplex method used in commercial linear programming packages, but it may be solved using Lagrangean methods. The model requires minimizing the expression

$$\sum_{s \in S} N(s) \sum_{i \in I} \sum_{a \in M_i} \sum_{t=2}^{T} (1 + r)^{1-t} w_{ia}^t(s) C_{ia}(s)$$

where S is the set of all strata indices, subject to Constraints 13 through 24 for all s in S and the condition

$$\sum_{s \in S} N(s) \sum_{i \in I} \sum_{a \in M_i} w_{ia}^1(s) C_{ia}(s) \leq B \qquad (25)$$

where B is the available budget for the first year.

This model seeks to minimize the present worth of the expected cost in Years 2 through T of the maintenance policies for Years 1 through T. Constraint 25 prevents expenditures in Year 1 from exceeding the budget. This constraint combines the problems of different strata into a single problem and destroys their independence. On the basis of work by Everett (*3*), the following modified version of the financial exigency model can be solved by selecting values for the Lagrange multiplier α (*2,4*) that minimize the expression

$$\sum_{s \in S} N(s) \sum_{i \in I} \sum_{a \in M_i} \left[\sum_{t=2}^{T} (1 + r)^{1-t} w_{ia}^t(s) C_{ia}(s) \right] + \alpha w_{ia}^1(s) C_{ia}(s)$$

subject to Constraints 12 through 24 for all s in S.

Because this version has no budget constraint, it may be separated into the independent strata problems. Once separated, it is exactly like the original multiyear models, Equations 12 through 24, except that the coefficient of the first-year expenditures is α. Different values of α will yield solutions that expend different amounts in Year 1.

Everett's (*3*) results applied to this problem indicate that the amount expended in Year 1 is a monotonic, nonincreasing function of α. Therefore, if, for a given α, the solution prescribes a policy that expends too much money in the first year, a new solution can be obtained for a larger value of α that will expend a smaller amount in Year 1. Everett also proves that if a given value of α produces a solution in which the total of all first-year expenditures among the strata is equal to the first-year budget (B), then such a solution is a globally optimal solution to the original financial exigency model. The results of the financial exigency model are a step function for different values of α. Thus the optimal solution is for the value of α that either results in a sum of B or is as close as it can get to B. An efficient searching procedure on α is used to find the requisite solution for the financial exigency model.

PACKAGING MODULE

The results of the optimization module are the proportions of the segments in a given stratum that should receive a particular M&R scope. The packaging module converts these figures to detailed bridge-by-bridge maintenance actions for the entire network for the first year of the planning horizon. Four major processes are involved: translation, specification, ranking, and aggregation. The packager focuses on a project-level analysis and uses the detailed bridge-by-bridge survey information.

The translation step converts the optimization output to specific M&R scopes for each segment in the network. The specification step uses the in-depth detailed survey information to further refine the M&R scopes into detailed activities for the entire bridge. The ranking step results in an ordered list of bridges that will guide the scheduling of the needed bridge work in the first year of the planning horizon. The aggregation step (if needed) consolidates all the bridge maintenance projects for a given district, geographical area, or other desired subset of the network.

COMPARATOR MODULE

The role of the comparator module is to perform a quality control check on both the BMS and its implementation. The comparator module is a means of evaluating and monitoring the performance of the BMS against established practices and engineering judgment.

The question of how well the BMS is performing and being implemented is addressed through items such as the following:

- Differences between planned and actual M&R activities,
- Differences between planned and actual costs, and
- Differences between planned and actual proportion of segments in desirable condition.

The comparator module also determines the cause for these deviations. Many additional questions are addressed in the comparator module, which provides the feedback necessary both to improve the actual BMS mathematical models and to ensure that its results are being properly implemented.

SUMMARY

The BMS is a modular network stochastic optimization model that also addresses project-specific needs. It provides automatic updating of the degradation models (transition probabilities) using Bayesian statistical procedures. If insufficient historical data are available, the system provides a methodology to generate initial degradation models using expert opinion. In the near future, organizations will find the advantages of such BMS network models as they have with pavement management systems.

REFERENCES

1. S. Kotz and N. L. Johnson. *Encyclopedia of Statistical Sciences*, *Vol. 2*. John Wiley and Sons, Inc., New York, 1982, pp. 386–387.
2. W. V. Harper, A. al-Salloum, J. Lam, S. al-Sayyari, and S. al-Theneyan. *B&SMS Conceptual Framework*. Report D3.1. Highways Maintenance Associates, 1989.
3. H. Everett. Generalized Lagrange Multiplier Methods for Solving Problems for Optimum Allocation of Resources. *Operations Research*, Vol. 8, 1960.
4. PMS Conceptual Framework. In *Highway Maintenance Management System*, Report C1, Highways Maintenance Associates (Resource International Inc.), Columbus, Ohio, 1989.

Timing for Bridge Replacement, Rehabilitation, and Maintenance

MITSURU SAITO AND KUMARES C. SINHA

Throughout its useful life, a bridge requires both routine and periodic maintenance and major rehabilitation work before being entirely replaced. Therefore, economic decisions on bridge replacement and rehabilitation need to be made with the future expenses in mind. For a life cycle cost (LCC) analysis to be realistic, three types of information must be supplied: timing, cost, and effect of bridge work. A reasonable estimate of the timing for future bridge repair work is especially critical because it strongly affects the results of LCC analysis. A statistical analysis examined the timing of various bridge activities performed by the Indiana Department of Transportation. The analysis indicates that bridges have been replaced for various reasons when bridge life is between 40 and 70 years, with 53 years being the average. Deck replacement has been done when bridges are about 45 years old, with no previous major rehabilitation work. Deck reconstruction and overlay, the most frequently recorded rehabilitation group, has been performed when bridges are about 22 years old. Timings of occasional routine maintenance works were not determined because the maintenance records available at the time of study did not contain specific locations of the bridges. Maintenance costs need to be included as an annual expenditure in an LCC analysis until more complete information is available.

Bridges last much longer than paved highways. Throughout its useful life, a bridge requires both routine and periodic maintenance and rehabilitation work before being entirely replaced. For a highway agency, bridges are a long-term, multiyear investment. A life cycle activity profile of a bridge includes a series of future improvements laid out in a cash flow diagram. Therefore, economic decisions on bridge replacement and rehabilitation must be made with these future expenses in mind (1). Comparisons of only initial investments in projects fail to reflect future funding needs.

For a life cycle cost (LCC) analysis to be realistic, three types of information must be supplied: timing, cost, and effect of bridge work. A reasonable estimate of the timing for future bridge repair activity is especially critical because it controls the outcome of an LCC analysis. A network-level analysis examined the timing of various bridge activities using data collected from bridge rehabilitation records (2) and bridge structural inventory and appraisal (SIA) records (3) maintained by the Indiana Department of Transportation (IDOT). Activities were divided into three groups: replacement, rehabilitation, and maintenance. Discussions for the costs and the effect of bridge work can be found elsewhere (4–6).

M. Saito, Civil Engineering Department, City College of New York, CUNY, New York, N.Y. 10031. K. C. Sinha, School of Civil Engineering, Purdue University, West Lafayette, Ind. 47907.

TIMING FOR BRIDGE REPLACEMENT

Bridges that were replaced by IDOT between 1981 and 1985 were examined for this analysis. The bridge rehabilitation records (2) provided information on (a) the year of construction, (b) bridge age at replacement, (c) bridge type (concrete and steel), (d) average daily traffic (ADT), and (e) rehabilitation types. Condition ratings of deck, superstructure, and substructure at the time of replacement or rehabilitation were extracted from the bridge SIA data file (3). In this analysis, replacement meant the replacement of the entire bridge structure. Timing for replacement was measured by the number of years passed before the entire replacement. For all statistical analysis, the SPSS statistical analysis package (7) was used.

Number of Years Passed Before Replacement

From the bridges replaced during this period, 105 were selected for subsequent analyses. All of these bridges were located on non-Interstate (other) highways; none of the Interstate bridges in Indiana were replaced during the given analysis period. Three management factors were used to assess their possible impact on bridge life: climatic region (north or south), bridge type (steel or concrete), and traffic level (average daily traffic—ADT). The state of Indiana was geographically divided into north and south regions approximately at the center of the state. Bridge type was determined by the material used for bridge superstructure. Because of the few repaired bridges, the number of groupings was kept small to maintain the reliability of the results.

Table 1 presents the average life of a bridge for the two climatic regions; Table 2 presents the two bridge types defined for this analysis. Only a small difference was seen in the average life of a bridge between the two groups. The average bridge life in the southern region was 52.96 years, and 52.53 years in the northern region (see Table 1). The difference was not statistically significant, implying that the regional difference would not be a factor in determining the timing of bridge replacement.

Similar results were found for the bridge-type grouping. Bridge life did not differ significantly between the concrete and steel bridge groups. Both groups had about 53 years of mean bridge life (see Table 2).

Prevailing traffic, especially truck traffic, was believed to affect bridge life. The life span of the sampled bridges was plotted against the 1985 ADT at the bridge sites. Figure 1 shows a scatter plot of these bridges. The data points were

TABLE 1   COMPARISON OF BRIDGE LIFE BY CLIMATIC REGION

Group	Count	Mean (yrs)	Standard Deviation (yrs)	Standard Error (yrs)	Min. (yrs)	Max. (yrs)	95%C.I.* (yrs)
North	53	52.53	5.81	0.798	39	65	50.92-54.13
South	52	52.96	5.74	0.796	41	71	51.36-54.56
All	105	52.74	5.75	0.562	39	71	51.63-53.86

Note: * 95%C.I. = 95% confidence interval of the mean

TABLE 2   COMPARISON OF BRIDGE LIFE BY BRIDGE TYPE

Group	Count	Mean (yrs)	Standard Deviation (yrs)	Standard Error (yrs)	Min. (yrs)	Max. (yrs)	95%C.I.* (yrs)
Conc.	75	52.91	5.84	0.674	39	65	51.56-54.25
Steel	30	52.33	5.61	1.024	45	71	50.24-54.43
All	105	52.74	5.75	0.562	39	71	51.63-53.86

Note: * 95%C.I. = 95% confidence interval of the mean
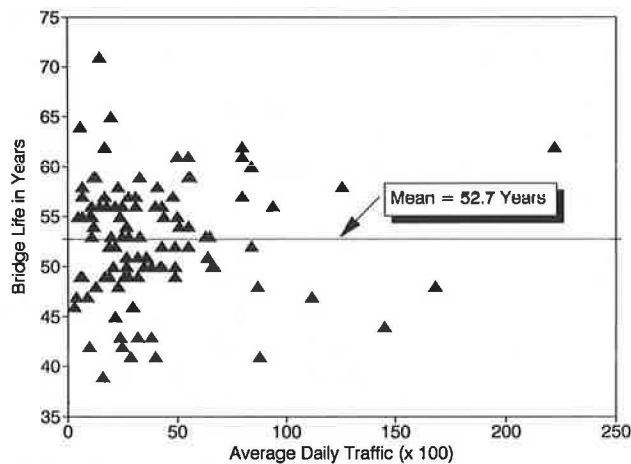
FIGURE 1   Bridge life versus ADT.

normally distributed around the overall mean value of approximately 52.74 years. A linear regression analysis on bridge life with ADT as a predictor variable showed that the slope of the regression was not statistically significant at a 5 percent significance level for this data set. This test implied that the level of traffic volume would not have a strong effect in the determination for bridge replacement. One probable reason

for this outcome is that bridges are designed primarily for heavy trucks.

The existence of previous major rehabilitation or widening work or both was believed to affect the decision of bridge replacement. A one-way analysis of variance (ANOVA) was performed to assess the difference between the mean bridge ages of the two groups: (a) a group of bridges that were rehabilitated only once, and (b) a group of bridges that had never been rehabilitated before their replacement.

For a statistical inference derived from the ANOVA to be correct, the assumption of homogeneity of variance in sample data must be met. The Cochran's C-statistic provided by the SPSS package (7) was used to test this assumption. The resultant C-statistic was 0.639 and its significance probability was 0.042. Therefore, this assumption was met at the significance level of 0.001, the significance level used for testing the homogeneity of variance (8).

The ANOVA presented in Table 3 indicates that the difference in the mean life of a bridge between the two groups was significant at the 5 percent significance level ($\alpha = 0.05$) with a significance probability of 0.0003; therefore, intermediate rehabilitation work did affect the bridge service life (see Table 4). Bridges that were rehabilitated once had a mean life of about 51 years, and bridges that had no history of major rehabilitation had a mean life of about 55 years. Although the difference was statistically significant, it was only 4 years,

TABLE 3   ANOVA TABLE

Source	d.f.	SS	MS	F-Ratio	Significance Probability
Between Groups	1	415.92	415.92	14.15	0.0003
Within Groups	103	3028.13	29.4		
Total	104	3444.05			

Cochran's C-Statistic = 0.6392 (Probability = 0.042 > α = 0.01)

Note: d.f. = Degree of freedom
           SS   = Sum of squares
           MS   = Mean squares

           Groups: 1. Bridges without major improvement
                   2. Bridges with major improvement

TABLE 4   DESCRIPTIVE STATISTICS ON SERVICE LIFE

Group	Count	Mean (yrs)	Standard Deviation (yrs)	Standard Error (yrs)	Min. (yrs)	Max. (yrs)	95%C.I.* (yrs)
Without Improvement	47	50.53	4.54	0.662	41	62	49.20-51.86
With Improvement	58	54.53	6.04	0.793	39	71	52.95-56.12
All	105	52.74	5.75	0.562	39	71	51.63-53.86

Note: * 95%C.I. = 95% confidence interval of the mean

implying that the existence of previous major rehabilitation work may not strongly affect the decision making of bridge inspectors in recommending bridge replacements. This result, however, does not necessarily mean that rehabilitation would not strengthen the bridge structure.

Condition Ratings at the Time of Replacement

Along with bridge life, condition ratings of the bridge deck, superstructure, and substructure at the time of replacement were examined separately for all the sampled bridges in both the concrete and steel types. Numerical ratings used in Indiana follow the definitions found in the structural inventory and appraisal guidelines prepared by FHWA (9). Figure 2 shows the ratings of the three bridge components within each bridge group. Not much difference was found. Nearly two-thirds of

the bridges had condition ratings less than or equal to 5 at the time of replacement. The remaining third of the bridges were rated as 6 or higher.

However, caution is needed in interpreting these condition-rating distributions, because the plots shown in Figure 2 include the effects of rehabilitation and maintenance work. Decisions for replacing bridges may not only be affected by the condition rating but by some other factors, such as bridge age and realignment of the approach road. It was difficult to establish a conclusive relationship between the condition rating and timing of replacement. Nevertheless, this analysis indicated that the current practice of assuming 50 years as the bridge service life may be appropriate for network-level bridge management to ensure the structural safety of bridges in the system. The mean life span of all the bridges in the data set was found to be approximately 53 years with 95 percent confidence interval between 52 and 54 years.

(a)

Number of Bridges

Condition Rating

■ Deck ▨ Superstructure ☐ Substructure

(b)

Number of Bridges

Condition Rating

■ Deck ▨ Superstructure ☐ Substructure
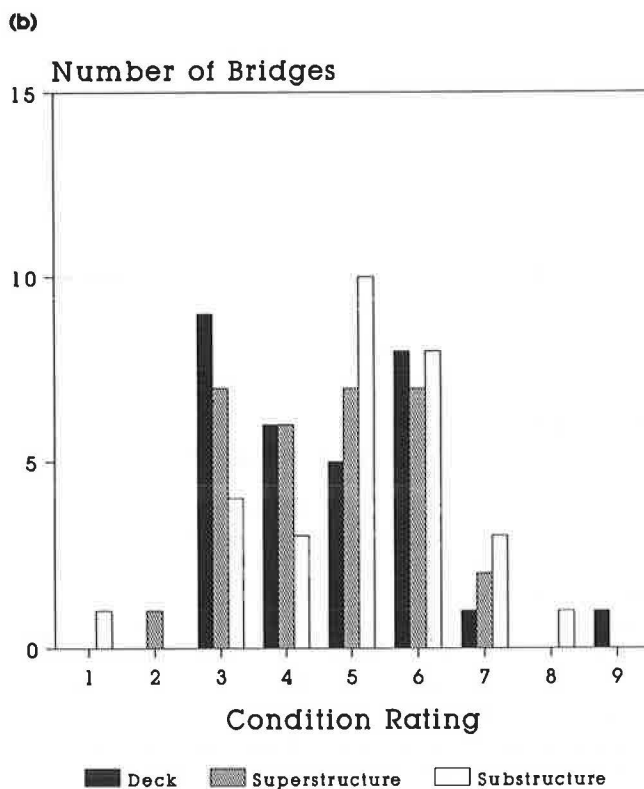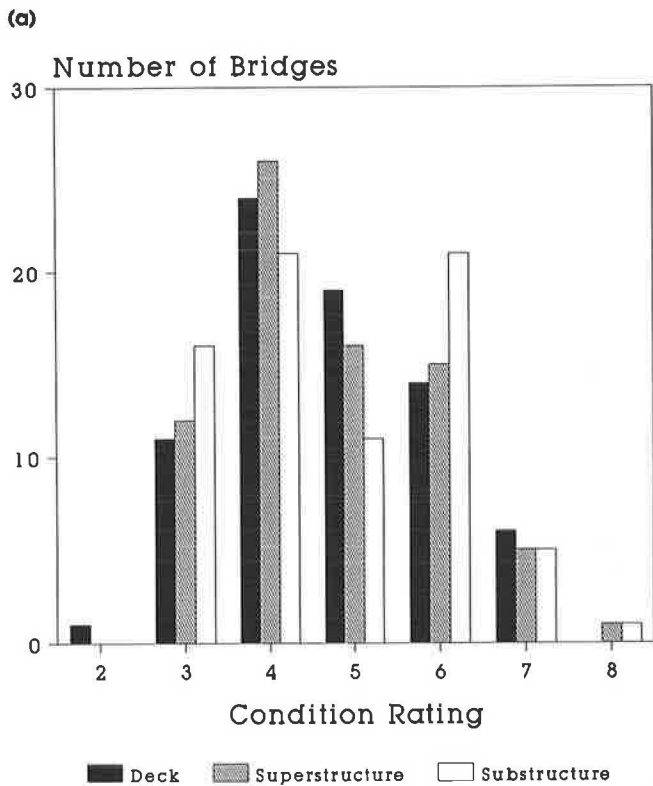
FIGURE 2 Distribution of condition ratings at the time of bridge replacement: a, concrete bridges; b, steel bridges.

TIMING FOR MAJOR REHABILITATION WORK

Two major rehabilitation groups (deck reconstruction and deck replacement) were used for the analysis because they were the groups most frequently used to identify rehabilitation work by the state bridge inspectors. Under the deck reconstruction group, part of the deck is repaired by shallow or deep patching, or both, and the surface is overlaid. Other items, such as expansion joints and railings, may be repaired as well. However, the entire deck is not replaced under this group. The deck replacement group, on the other hand, consists of the replacement of the entire deck with a completely new one. This work may be accompanied by some superstructure rehabilitation, partial or whole, and widening of the deck or superstructure, or both.

Deck Reconstruction

Two management parameters—the number of years passed before the time of the first deck reconstruction and the percentage of deck area in need of patching—were selected in this analysis because of their importance in recommending deck reconstruction. Classification factors, such as highway type, traffic volume, and climatic conditions, were tested for their effects on the inspector's decision to recommend deck reconstruction work. Bridges that had only one deck reconstruction since their initial construction were selected for the analysis; 237 bridges met this criterion.

Number of Years Passed Before Deck Reconstruction

One-way ANOVA tests on the three classification factors showed that only the regional classification had a significant effect on the number of years passed before the first deck reconstruction. Table 5 presents the result of this analysis. The resulting significance probability was 0.0004 (0.4 percent) and the regional effect was significant at the 5 percent significance level. This result indicated that there were statistically significant differences between the mean number of years passed by the time of the first deck reconstruction in the northern region (20.3 years) and that of the southern region (23.5 years). Therefore, on the average, state bridge inspectors were recommending the deck reconstruction activity about 3 years earlier for bridges in the northern region than for those in the southern region. This difference was primarily caused by the severe weather and the frequent use of deicing materials in northern Indiana.

Percentage of Deck Area Needing Patching

The extent of needed patching is considered to be an indicator of deck deterioration that is most obvious to the inspectors in evaluating deck conditions. Needed patching can be measured at the site and is, in fact, reported in the rehabilitation design plans. Using one-way and two-way ANOVAs, the effects of classification factors on the selection of the deck reconstruction and overlay alternative were examined for the percentage of deck area in need of patching. The three classification factors used in the preceding analysis were again used.

TABLE 5 COMPARISON OF THE NUMBER OF YEARS PASSED BEFORE FIRST DECK RECONSTRUCTION, BY CLIMATIC REGION

North	South	Total
N = 121	N = 116	N = 237
Mean = 20.3 yrs.	Mean = 23.5 yrs.	Mean = 21.9 yrs.
SE = 0.64	SE = 0.65	SE = 0.45
95%CI = 19.0-21.6	95%CI = 22.2-24.8	95%CI = 21.0-22.8

Homogeneity test significance level = 0.335 > α = 0.001

Significance probability of two groups (North & South)
      = 0.0004 < α = 0.05

Notes: N   = Number of samples in the group
       Mean   = Mean number of years passed from initial
                 construction
       SE   = Standard error of the mean (in years)
       95%CI   = 95% confidence interval of the mean
                 (in years)

The ANOVA indicated that the climatic region factor was not significant at the 5 percent significance level. Therefore, this factor may not be a statistically significant component when the percentage of deck area in need of patching is used as a decision factor. Thus, the state bridge inspectors are more concerned with factors other than the regional difference when they decide on deck reconstruction.

The highway type and the amount of traffic were, on the other hand, both significant (see Tables 6 and 7). The 95 percent confidence interval of the expected mean percent patching area for Interstate bridges was between 6.20 and 8.00 percent, when the first deck reconstruction and overlay were undertaken. The confidence interval of the mean for bridges on other state highways was between 10.56 and 13.41 percent. The state bridge inspectors tolerated less deterioration for bridges on Interstate highways than for bridges on other state highways.

For ADT, two factor levels were defined for this analysis: low (ADT < 10,000) and high (ADT ≥ 10,000). The mean percentage of deck area in need of patching was significantly different between the two factor levels, as presented in Table 7. Bridges with high traffic volumes were more likely than bridges with low traffic volumes to have the deck reconstruction work performed when the percentage of deck area in need of patching was low.

As highway type and traffic volume factors were found to be significant, a two-way ANOVA was performed to examine the interaction effect of these two factors on percent patching areas. Table 8 presents the model and results of this analysis. Both main effects and the interaction effect became significant at the 5 percent significance level. This result implies that when the percentage of deck area in need of patching is used as a decision variable, the combination of highway type and traffic volume should be considered in deciding on the timing of the deck reconstruction and overlay alternative. For instance, the mean percentage of the deck area in need of patching would be 7.35 percent for bridges on Interstate highways with ADT > 10,000, as presented in Table 8. The mean values

TABLE 6 PERCENTAGE OF DECK AREA IN NEED OF PATCHING AT TIME OF FIRST DECK RECONSTRUCTION, BY HIGHWAY TYPE

Interstates	Other State Highways
N = 111	N = 126
Mean = 7.04%	Mean = 11.90%
95%CI = 6.20-8.00	95%CI = 10.56-13.41

Homogeneity test significance level = 0.002 > α = 0.001

Significance probability of two groups = 0.000 < α = 0.05

TABLE 7 PERCENTAGE OF DECK AREA IN NEED OF PATCHING AT
TIME OF FIRST DECK RECONSTRUCTION, BY ADT

```
    ADT < 10,000                    10,000 ≤ ADT


         N = 144                        N =  93
     Mean = 10.31%                  Mean =   7.95%
     95%CI =  9.16-11.60            95%CI =   6.86-9.21


    Homogeneity test significance level = 0.110 > α = 0.001

    Significance probability of two groups = 0.007 < α = 0.05


Notes: N       = Number of samples in the group
       M       = Mean percent of deck area needing patching
                   at the time of the first deck reconstruction
       95%CI   = 95% confidence interval of the mean
```

TABLE 8 COMBINED EFFECTS OF HIGHWAY TYPE AND TRAFFIC VOLUME LEVEL ON
THE SECTION OF DECK RECONSTRUCTION BY PERCENTAGE OF DECK AREA IN NEED OF
PATCHING

		Traffic Volume (ADT)	
		Low	High
		ADT < 10,000	10,000 ≤ ADT
H i g h w a y	Interstate	N = 33 Mean = 6.36% 95%CI = 5.03-8.04	N = 78 Mean = 7.35% 95%CI = 6.31-8.56
	Other State Highway	N = 111 Mean = 11.90% 95%CI =10.47-13.52	N = 15 Mean = 11.94% 95%CI = 8.44-16.90

```
Homogeneity test significance level = 0.002 > α = 0.001

Notes: N       = Number of samples in the group
       Mean    = Mean percent of deck needing patching
                   at the time of the first deck reconstruction
       95%CI   = 95% confidence interval of the mean
```

obtained from this analysis can be used in a bridge management system to automatically select bridges that may need deck reconstruction.

Condition Ratings at the Time of Deck Reconstruction

This analysis was performed to examine the timing of deck reconstruction work in relation to condition rating. Condition ratings are seen as a reflection of the severity and extent of distresses that exist on bridge structures. Because deck reconstruction is closely related to the condition ratings of the deck and superstructure, these two condition ratings were checked. Figure 3 shows the difference in condition-rating distributions of the deck and the superstructure. Condition ratings of decks were mostly 5 and 6 when the deck was reconstructed. However, condition ratings of the superstructure were mostly 6 and 7 at the time of deck reconstruction, implying that the speed of deterioration of a superstructure would be slower than that of a bridge deck.

Number of Bridges
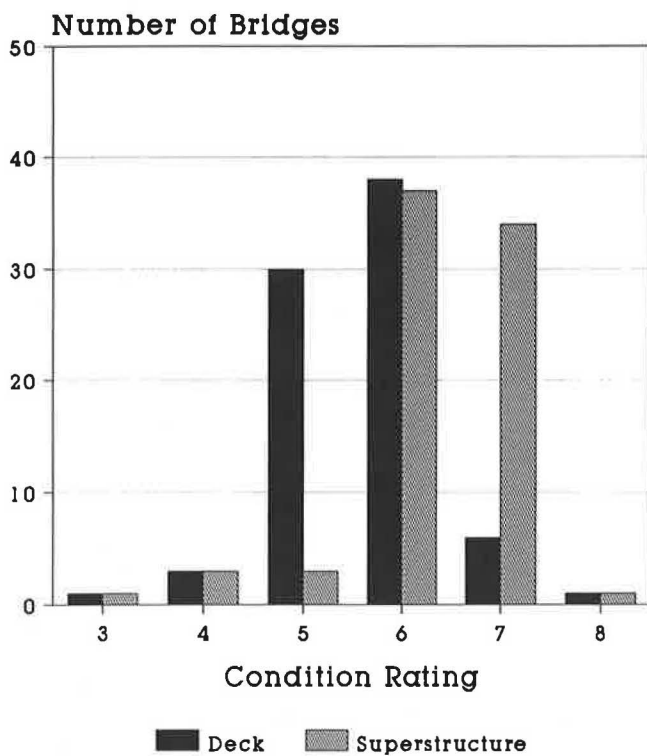
FIGURE 3   Condition ratings at the time of first deck reconstruction.

Number of Bridges

Summary Statistics for Deck Replacement:
Number of samples = 16
Mean = 44.6 years
Standard deviation = 6.0 years
Standard error = 1.5 years
95% Confidence interval = 41.4 years to 47.8 years

FIGURE 4   Number of years passed before the first deck replacement.

Deck Replacement

There were only a few bridges found in the deck replacement category. Within the 3-year period 1984–1986, only 16 bridges fit the description of this rehabilitation alternative. These bridges had only one deck replacement during their entire life and no other major rehabilitation work was performed.

Number of Years Passed Before Deck Replacement

Figure 4 shows the frequency of deck replacement for each 5-year range. Although there was one extreme case (deck replacement at the 26th year), this process seems to have been undertaken when bridge age was greater than about 40 years.

Figure 4 also shows the summary statistics of these bridges. The mean number of years passed before deck replacement was 44.6 years, and the 95 percent confidence interval level was 41.4 to 47.8 years. When the extreme case of 26 years was excluded from the data set, the mean value became 45.9 years with the 95 percent confidence interval being 44.2 to 47.7 years. This finding is important because deck reconstruction is recommended about 20 to 22 years after bridge construction. Clearly, there will be a trade-off between the deck reconstruction at an early stage of bridge life and the deck replacement at a later stage, because the unit costs of these two rehabilitation alternatives are substantially different. Unit costs of deck replacement were found to be about twice as much as the units costs of deck reconstruction (*6*).

Condition Ratings at the Time of Deck Replacement

Condition ratings at the time of deck replacement were plotted for the three components of the bridge structure (deck, superstructure, and substructure), as shown in Figure 5. Substructure condition ratings were plotted to compare with the ratings of the deck and superstructure. Deck replacement is recommended when the deck condition rating reaches a value of 6 or less. The superstructure may be at a similar condition level. However, the substructure may not be as deteriorated as the deck and superstructure, when the replacement work is recommended. By the time the substructure condition rating declines to Condition Rating 6 or lower, other parts of the bridge may become so deteriorated that the replacement of the entire structure may be warranted (see Figure 2 for comparison).

TIMING FOR MAINTENANCE WORK

Bridge routine maintenance activities are performed to maintain the structural integrity of a bridge structure, decrease the speed of its deterioration, and ensure the safe passage of traffic. Each maintenance activity may have a minimal effect

Number of Bridges
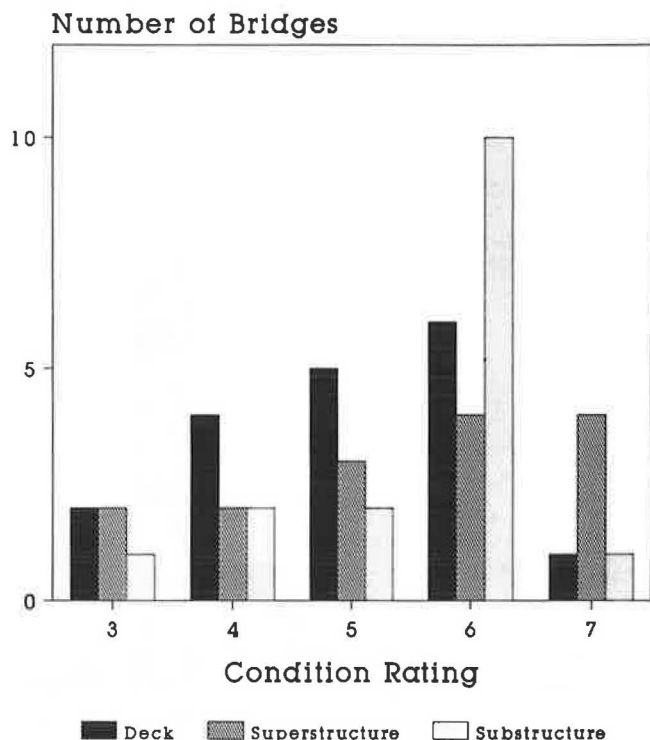
FIGURE 5 Condition ratings at the time of first deck replacement.

by itself but a group of well-planned maintenance activities may be able to achieve these goals. Maintenance work is conducted at any condition-rating level as long as it is needed.

The analysis of timing of maintenance activities became difficult because of the nature of routine maintenance and the lack of information in the maintenance activity records of IDOT available at the time of this study. Some works, such as deck cleaning and flushing, are annual events and need not be analyzed for timing. These tasks are performed, especially in the northern region of Indiana, to decrease salt contamination and possible future damages of the deck induced by debris collected in spots such as drainage pans and expansion joints. Records of other occasional maintenance activities, e.g., bridge repair and patching, were difficult to trace to individual bridges. The maintenance activity recording procedure available did not require the maintenance crew to include specific locations of bridges for which maintenance work has been performed.

For a life cycle cost analysis, the timing for occasional maintenance activities needs to be input based on engineering judgment at the moment. Expenditures for maintenance and repair work are often assumed to increase as the bridge age increases. However, the data showed no evidence for substantiating this assumption. Identifying maintenance activities with specific bridge structures so a data base can be developed is essential. A lack of data for the timing of maintenance activities may cause some difficulty in conducting a realistic LCC analysis. However, the use of the annual maintenance cost concept may not seriously jeopardize the validity of the LCC analysis. The outcome of LCC analysis was more sen-

sitive to large capital expenditures such as rehabilitation and replacement than to small expenditures for maintenance (10).

SUMMARY AND CONCLUSIONS

Estimates of the timing for future bridge improvement activities were made on the basis of historical records, and the relationship between condition ratings and recommended actions was examined. Consequently, the results indicate what was done, not what could be done. The timing used by bridge engineers may not have been optimal, and the results do not represent service lives that can be theoretically achieved. Nevertheless, findings from this study can be helpful in performing a realistic LCC analysis. However, the results apply primarily to bridges in Indiana, and analyses on bridges in other states may provide different results. In this analysis, changes in design, rehabilitation, and maintenance policies, if any, were assumed to be reflected in the data collected.

The average bridge service life of about 50 years used by the state is a reasonable assumption on which to conduct an LCC analysis. The state-wide average was found to be about 53 years. Climatic region, bridge type, and traffic volume factors did not significantly affect the decisions recommending bridge replacement. Such a decision is based on the overall structural safety of a bridge, as perceived by state bridge inspectors. The age of a bridge is one of their primary decision factors. A clear relationship between the condition rating at the time of replacement and the bridge life could not be established because condition ratings were affected by rehabilitation and maintenance activities performed during the life span of the bridge.

On the other hand, differences of service life of bridges with or without rehabilitation were found to be statistically significant. However, the average difference observed was only 4 years. The existence of previous rehabilitation work may have a small impact on current replacement decision making. Rehabilitation work done on bridges is often related to bridge deck and superstructure, and the life spans of these bridge components are shorter than the life span of the entire bridge structure. Deck and superstructure conditions seem to be the key element that causes bridge inspectors to recommend bridge replacement.

As for rehabilitation alternatives, two major activity categories, deck reconstruction and deck replacement, were evaluated. The first deck reconstruction took place approximately 22 years, on the average, after the initial construction of the bridge. The effect of climatic conditions was found to be present and the mean values were 20.3 years for the northern region and 23.5 years for the southern region. The frequent use of deicing materials in the northern region of Indiana may be the primary cause for this difference. Some bridges received second deck reconstruction work in their lifetime, but they rarely received third and fourth deck reconstruction work.

The deteriorated area in need of patching is often a sign of the need for deck reconstruction. The percentage of deck area in need of patching at the time of deck reconstruction was used as a parameter to express the level of deck deterioration. The amount of deck area in need of patching at the time of deck reconstruction varies by highway type and traffic volume. On the average, bridges on Interstates had smaller per-

centages of deteriorated deck areas when deck reconstruction was recommended, implying that bridge inspectors tend to place higher priority on bridges on Interstate highways when appraising them for the reconstruction.

The average life of a bridge before it received the first deck replacement was found to be approximately 45 years. Few bridges received deck replacement as compared with deck reconstruction. Those bridges that had their decks replaced did not receive any major deck rehabilitation before their replacement. Because the difference between the unit costs of deck reconstruction and replacement was large, a careful tradeoff analysis would be necessary to select a rehabilitation alternative.

No detailed analysis of timing of maintenance work was undertaken in the present study because the existing maintenance record-keeping procedure did not provide information on maintenance work for specific bridges. Record keeping of maintenance work needs to include information related to specific bridge locations in a data base for future statistical analyses. At the moment, engineering judgment needs to be used to enter future maintenance activities as annual expenditures in an LCC analysis.

ACKNOWLEDGMENT

REFERENCES

1. *Bridge Management Systems.* Report FHWA-DP-71-01. FHWA, U.S. Department of Transportation, March 1987.
2. *Bridge Rehabilitation Records Files.* Indiana Department of Highways, Indianapolis, 1978–1984.
3. *SIA Bridge Records.* Indiana Department of Highways, Indianapolis, 1978–1984.
4. M. Saito, K. C. Sinha, and V. L. Anderson. Statistical Models for the Estimation of Bridge Replacement Cost. Presented at 69th Annual Meeting of the Transportation Research Board, Washington, D.C., 1990.
5. M. Saito and K. C. Sinha. A Delphi Study on Bridge Condition Rating and Effect of Bridge Improvement Alternatives. Presented at 69th Annual Meeting of the Transportation Research Board, Washington, D.C., 1990.
6. M. Saito. *The Development of a Statewide Network Level Bridge Management System.* Ph.D. dissertation, School of Civil Engineering, Purdue University, West Lafayette, Ind., 1988.
7. C. H. Hull and N. H. Nie, eds. *SPSS Update 7-9: New Procedures and Facilities for Release 7-9.* McGraw-Hill, New York, 1981.
8. V. L. Anderson and R. A. McLean. *Design of Experiments: A Realistic Approach.* Marcel Dekker, New York, 1974.
9. *Recording and Coding Guide for the Structure Inventory and Appraisal of the Nation's Bridges.* FHWA, U.S. Department of Transportation, Jan. 1979.
10. T. J. Wonsiewicz. Life Cycle Cost Analysis: Key Assumptions and Sensitivity of Results. In *Transportation Research Record 1191*, TRB, National Research Council, Washington, D.C., Jan. 1988.

Forecasting Optimum Bridge Management Decisions and Funding Needs on the Basis of Economic Analysis

CHWEN-JINQ CHEN AND DAVID W. JOHNSTON

An analytic method is presented for evaluating optimum bridge management decisions for maintenance, rehabilitation, and replacement. The decision process is based on economic analysis of the alternatives using an equivalent annualized cost approach. Both user costs because of bridge level of service deficiencies and owner costs for maintenance and improvement are included in the analysis. By forecasting the optimum time and cost for actions on each bridge in the future, funding needs and number of improvements can be predicted. Results of an example bridge system analysis are presented.

In 1985, approximately 41 percent of the nation's bridges were classified as either structurally deficient or functionally obsolete (1). The backlog of needs on over 500,000 bridges is acknowledged to be substantial. Increasingly, local, state, and congressional elected officials have been requesting the responsible transportation agencies to predict those needs and make bridge management decisions on a cost-effective basis. However, rigorous approaches for estimating current and future needs and for making these decisions have not been available.

BACKGROUND

Under the current federally mandated inspection system, three empirical summary evaluations are made for each bridge to calculate a sufficiency rating (2). Depending on the rating, which can range from 0 to 100 points, a bridge may be eligible for federal funding for improvements. Bridges may be classified as structurally deficient for several reasons, but particularly if posted for low load capacity. A bridge may be classified as functionally obsolete if it has relatively narrow width, poor alignment, or low vertical clearance. The sufficiency rating considers these factors, element conditions, etc., but is relatively insensitive to the volume of traffic and the roadway functional classification.

Although any bridge deficiency is undesirable, the effect of the deficiency on the public may be different for bridges with differing traffic volumes and characteristics. Because the sufficiency rating places little emphasis on the traffic volume and the highway functional classification, the level of service deficiency point system was developed (3) to aid ranking of bridge improvements.

C-j. Chen, National Nankang Ilan Expressway Office, Ministry of Communications, Taipei, Taiwan, Republic of China. D. W. Johnston, Department of Civil Engineering, North Carolina State University, Raleigh, N.C. 27695-7908.

The deficiency point system compares the current width, load capacity, and vertical clearance of a bridge to the corresponding ideal user level of service goals for these characteristics to determine user level of service deficiencies. Deficiency points are calculated considering the level of service deficiencies and traffic volume as a measure reflecting user costs. Bridges can then be ranked for improvement in order of quantity of deficiency points.

Although these approaches have been helpful in setting priorities for bridge improvements, these two empirical systems have no capability for determining the optimum improvement alternative for a bridge or the optimum time for the alternative selected. To obtain adequate funds to maintain the bridge system at an acceptable level of service with minimum cost, there is a need to predict required funding. A rational system is needed for cost-effective decisions to determine the optimum time and alternative for maintaining, rehabilitating, or replacing an existing bridge. Future funding needs for the entire bridge system should be based on the optimum alternative selected for each individual bridge if adequate funds are available to undertake all the optimum alternatives. The objective is to develop such a system (4).

BRIDGE IMPROVEMENT UNDER A LEVEL OF SERVICE CONCEPT

With some special constraints, bridges can be evaluated for improvement or replacement in a manner similar to an item of equipment. Hanssmann (5) considers equipment replacement as a problem of minimizing total cost over the entire planning horizon. Assuming that the acquisition cost, final salvage value, and economic life of the new asset will not be influenced by the replacement time of the old asset, the cost C_r of maintaining the old asset, which has incremental decline of salvage value and incremental current expenses, was expressed by Hanssmann as

$$C_r = \sum_{t=1}^{r} (d_t + e_t) + (T - r)$$

$$* \left(\frac{A - S + E}{L} \right) \qquad r = 1, \ldots, T \qquad (1)$$

where

d_t = decline in salvage value of the old asset in Year t,
e_t = current expense of the old asset in Year t,

A = acquisition cost of the new asset proposed,

S = salvage value of the new asset at the end of service life,

E = total current expense of the new asset over the service life,

L = service life of the new asset,

r = projected replacement year, and

T = planning horizon.

The expression $(A - S + E)/L$ represents the average annual cost of the new asset over its lifetime. The optimal time T^* to replace the old asset can be found by minimizing Equation 1. From Figure 1, the value T^* can be found by inspection. Area $OABCT$ represents the minimum total cost C_T of Equation 1. If the old asset is replaced 1 year early or late, the total cost of maintaining it will be greater than that of being replaced at year T^*. The differences are the extra costs represented by the areas $A'B''B$ and $BB'C'$, respectively. Thus, when the annual cost of the old asset exceeds the average annual cost of the new asset for the first time, the time for replacement has come.

Characteristics of Bridge Service Life

A bridge starts its service life when construction is completed. Because of the effect of traffic and other spontaneous factors, bridge elements deteriorate. During inspection, elements such as the deck, superstructure, and substructure are rated numerically for condition from 0 to 9, with 9 indicating new condition. When these elements deteriorate, adequate maintenance is needed to keep the bridge in good service condition. Different elements have various deterioration rates, and the maintenance needs vary as a function of the element, material type, and condition. Minor repairs at a particular condition level do not necessarily improve the condition level of the element, but may extend the time before a drop occurs to the next lower level. Without reconstruction or rehabilitation, maintenance needs would increase with a decrease of the element conditions.

If the bridge has a narrow width, low vertical clearance, low load capacity, or poor alignment relative to the roadway, user costs related to bridge deficiencies will be incurred. For example, costs can be generated from time lost and extra mileage accumulated because of detours resulting from deficiencies in load capacity or vertical clearance. Because of deterioration of the materials and other factors, bridge load capacity may decrease with time. Correspondingly, the bridge

posting decreases and a higher proportion of the total vehicles desiring to use the bridge has to detour.

User costs are also generated because of accidents. Narrow, poorly aligned, and low-clearance bridges have higher vehicle accident probabilities. The number of accidents is directly correlated with the total number of vehicles using the bridge. Generally, the traffic volume increases with time, so the user costs generated by deficiencies that cause accidents also increase with time.

Roadway systems have various service purposes. Interstate highways are constructed mainly for long distance Interstate travel. Arterial roadway systems connect important towns located in adjacent counties within a state. Collector systems are constructed to provide the intracounty services with shorter traveling distances. Local routes provide access to farms, residences, and some abutting properties. As a result, different factors influence user costs generated by bridge level of service deficiencies on these roadway systems with different functional classifications. Thus, the user costs need to be determined considering functional classifications of the bridges.

Usually, there are three improvement alternatives for a deteriorated bridge. The first alternative is to replace the existing bridge with a new one having a desirable level of service. The elements of a new bridge have the highest condition level, and user costs would be reduced to zero at the beginning of its service life.

The second alternative is to rehabilitate the existing bridge using the optimum rehabilitation action under a given set of bridge element conditions. After rehabilitation, the condition level would be improved to a better, but generally less than new, level, and some additional years of service life would be gained. The user level of service would also be improved, but not generally to the highest level.

The third alternative is to only continue essential maintenance as a means of avoiding accelerated deterioration. The annual maintenance costs and user costs are the only sources for this alternative, and these costs will increase year by year because of bridge deterioration and traffic volume increase.

Optimum Improvement Action and Time Prediction

Because maintenance and user costs increase with age, the economic life increment for a deteriorated bridge may be taken as 1 year. From Equation 1 and Figure 1, the optimum time to rehabilitate or replace an existing bridge is the time when the year-by-year cost of the existing bridge exceeds the economic annual equivalent cost of the new bridge or the rehabilitation action. According to Smith (6), the year-by-year costs for a piece of deteriorated equipment can be expressed as

$$C_t = M_t + (S_{t-1} - S_t) + (S_{t-1}) * i \qquad (2)$$

where

C_t = year-by-year cost of the equipment at Year t,

M_t = maintenance and operating cost at Year t,

S_{t-1} = salvage value of the equipment at beginning of Year t,
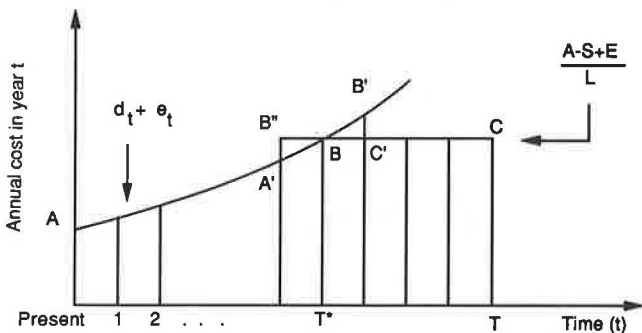
FIGURE 1 Optimal time to replace old asset.

S_t = salvage value of the equipment at end of Year t, and

i = interest rate.

Equation 2 can also be stated as C_t = (maintenance cost at Year t) + (decline in value at Year t) + (interest return if equipment is sold at beginning of Year t).

Smith (6) also stated the equivalent annual cost of the proposed replacement or rehabilitation as

$$EAC = \left[FC - S_T * (P/F,i,T) + \sum_{t=1}^{T} M_t * (P/F,i,t) \right] * (A/P,i,T) \tag{3}$$

where

EAC = equivalent annual cost of the proposed alternative,

FC = first acquisition cost of the proposed alternative,

S_T = terminal salvage of the proposed alternative,

M_t = maintenance costs of the proposed alternative at Year t,

T = service life gained,

$(P/F,i,t)$ = present worth factor $[= (1 + i)^{-t}]$,

$(A/P,i,T)$ = capital recovery factor $\left[= \dfrac{i * (1 + i)^T}{(1 + i)^T - 1} \right]$, and

i = interest rate.

Annual Cost of the Existing Bridge

One of the alternatives for bridge improvement is to keep the existing bridge for 1 year or more by providing adequate maintenance. Although some materials of various types of bridges can be reused, most have relatively small or no salvage value compared with their construction costs. Thus, it would not be appropriate to consider salvage decline and interest return from salvage in the economic analysis for bridge improvement. As a result, the annual cost from Equation 1 to keep the existing bridge for an additional year comes only from the possible element maintenance costs.

Although the user costs generated by a level of service deficiency are not paid or assumed directly by government, the public is both the user and the ultimate owner of a bridge. Thus, for a deficient bridge, the user costs should be considered as part of the annual cost. User costs, generated by deficiencies in width, vertical clearance, and alignment, increase with increase of traffic volume. User costs resulting from a bridge load capacity deficiency increase with increase of load capacity deficiency and traffic volume. As the bridge traffic volume increases with time, the annual user costs also increase with time. From Equation 1, the annual cost for the existing bridge can be stated as

$$ACEB(t) = ARMC(t) + AURC(t) \tag{4}$$

where

$ACEB(t)$ = annual cost for the existing bridge in Year t,

$ARMC(t)$ = annual regular maintenance cost of the existing bridge in Year t, and

$AURC(t)$ = annual user cost of the existing bridge in Year t.

Furthermore,

$$ARMC(t) = \sum_{j=1}^{M} MC_j(t) \tag{5}$$

for M types of element maintenance, and

$$AURC(t) = \sum_{k=1}^{N} URC_k(t) \tag{6}$$

where

N = number of types of level of service deficiencies,

$MC_j(t)$ = maintenance cost for Element Type j in Year t, and

$URC_k(t)$ = user cost for Deficiency Type K in Year t.

Equivalent Annual Cost for the New Bridge

Another alternative for bridge improvement is to replace the existing bridge with a new one having a desirable level of service. From Equation 3, the cost for a new proposed alternative comes from the first acquisition cost and all possible maintenance and operating costs over its service life. For a new bridge, the total cost over its service life includes construction costs, maintenance costs, and user costs caused by level of service deficiencies for width, vertical clearance, alignment, and load capacity. As in Equation 3, the cost components of the new bridge over its economic service life can be converted to equivalent annual cost as follows:

$$AERP = RPC * (A/P,i,N) + AEMNT + AEUSR \tag{7}$$

$$AEMNT = \left\{ \sum_{t=1}^{N} [ARMC(t) * (P/F,i,t)] \right\} * (A/P,i,N) \tag{8}$$

$$AEUSR = \left\{ \sum_{t=1}^{N} [AURC(t) * (P/F,i,t)] \right\} * (A/P,i,N) \tag{9}$$

where

$AERP$ = annual equivalent replacement cost,

RPC = actual replacement cost,

$AEMNT$ = annual equivalent maintenance cost,

$AEUSR$ = annual equivalent user cost, and

N = economic service life of the new bridge.

The annual regular maintenance cost $ARMC(t)$ and annual user cost $AURC(t)$ of the new bridge over its expected service life can be calculated using Equations 5 and 6, respectively.

Equivalent Annual Cost for Rehabilitated Bridge

The third alternative for improving the existing bridge is to rehabilitate it to a higher condition level. The cost components

for this alternative are the same as those of replacement. After rehabilitation, some additional years of service life can be gained. For a bridge with n_1 additional years of service life gained after rehabilitation, the equivalent annual cost for the rehabilitation alternative can be expressed as

$$AERH = RHC * (A/P,i,n_1) \qquad (10)$$
$$+ \ AEMRH + AEURH$$

$$AEMRH = \left[\sum_{t=1}^{n_1} ARMC(t) * (P/F,i,t) \right] * (A/P,i,n_1) \qquad (11)$$

$$AEURH = \left[\sum_{t=1}^{n_1} AURC(t) * (P/F,i,t) \right] * (A/P,i,n_1) \qquad (12)$$

where

$AERH$ = annual equivalent rehabilitation cost,
RHC = actual rehabilitation cost,
$AEMRH$ = annual equivalent maintenance cost over the extended period because of rehabilitation,
$AEURH$ = annual equivalent user cost over the extended period because of rehabilitation, and
n_1 = additional years of service life gained because of rehabilitation.

The annual regular maintenance cost $ARMC(t)$ and annual user cost $AURC(t)$ of the rehabilitated bridge can be calculated using Equations 5 and 6 over the additional service life gained after rehabilitation.

At any given time, a bridge can be rehabilitated to higher condition levels, as shown in Figure 2. Each of these different rehabilitation policies requires different efforts. The additional service lives gained and user costs reduced by these different policies also vary. The rehabilitation costs and user costs after rehabilitation for different policies can be converted to equivalent annual costs over the corresponding extra service lives gained. The one with the lowest equivalent annual cost is the optimum rehabilitation action, which should be chosen as the rehabilitation alternative and then compared with other alternatives for the bridge, such as replacement and regular maintenance.
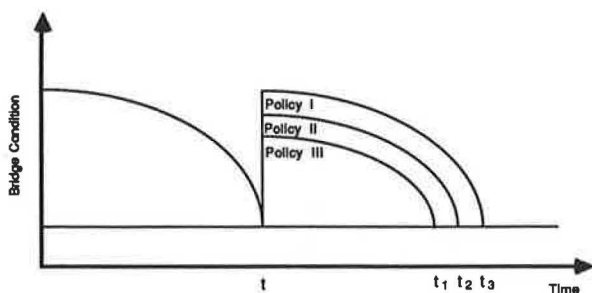
Analysis Procedure and Decision Rules

The equivalent annual costs of the three alternatives, calculated using Equations 4, 7, and 10, are compared to determine the optimum improvement action. The alternative with the lowest cost is the best alternative at that time. If the annual cost of the existing bridge is lowest, the bridge will be continued in service for an additional year with appropriate maintenance. The bridge will then be aged 1 year and its element conditions, load capacity, and ADT will also be estimated according to its structure and material types and geographic location. The annual maintenance, user, and rehabilitation costs of the existing bridge under the new predicted conditions will be calculated. The same evaluations will be repeated year after year until an improvement action other than maintaining the existing bridge for another year is favored. The improvement action selected in the final evaluation iteration and the time predicted will be considered as the optimum improvement action and life time for the bridge.

The annual maintenance costs for the existing bridge are determined in the evaluation iterations. By adding the maintenance costs of all the bridges in the system within each year, an annual maintenance budget can be determined. Similarly, the total needed actual replacement or rehabilitation costs in a given year are determined by adding such costs for all bridges selected by the analysis for the corresponding improvement.

Two types of level of service goals affect the results of the evaluation. First, the user level of service goals for bridge width, vertical clearance, load capacity, and approach roadway alignment are considered in terms of user costs. Specifying higher user level of service goals will decrease the annual user costs of the bridge after being rehabilitated but will increase the rehabilitation cost. Specifying lower user level of service goals for rehabilitation will not yield a dramatic decrease in the annual user costs but will result in lower rehabilitation costs.

The second type of level of service goal, related to maintenance condition level, also influences the improvement action selected in the analysis system. Different minimum or acceptable maintenance condition levels influence the rehabilitation frequency and efforts needed, as shown in Figure 3. A lower bridge condition level allowed in service reduces rehabilitation frequency but will accelerate deterioration and decrease the average condition level of the system. This maintenance level of service is different from the user level of service mentioned previously. In the evaluation iteration, if a bridge element reaches the predetermined minimum

FIGURE 2 Rehabilitating the bridge element to different higher condition levels.
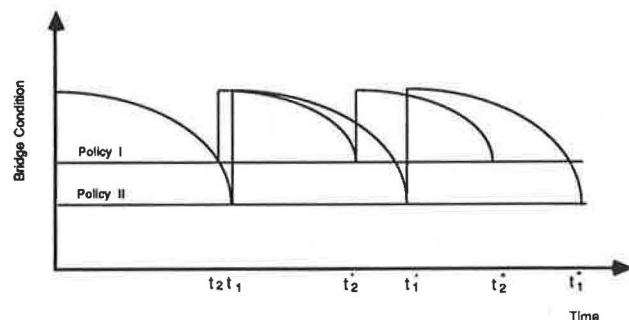
FIGURE 3 Rehabilitating the bridge element from different condition levels.

acceptable maintenance level of service, a rehabilitation action will be initiated to raise the condition to a higher, and perhaps desirable, level.

IMPLEMENTATION

A computer program (4) was created for analysis purposes. The program incorporates the analysis procedures described herein, and the parameters and relationships for bridge ownership costs, user costs, element condition deterioration rates, etc., also determined in this study.

For each individual bridge, the annual maintenance costs and user costs are calculated based on the bridge's current condition and user level of service deficiencies in relation to the desirable level of service goals. The bridge improvement alternatives for rehabilitation and replacement are generated, and equivalent annual costs for the alternatives are calculated. In any given year, if the annual cost of the existing bridge is the lowest cost, the bridge will be maintained for another year. The bridge element conditions in the subsequent year will then be predicted based on the deterioration rates applicable to the element, material, and environment. The traffic volume of the bridge will also be predicted on the basis of the ADT increase rate. The analysis will be repeated each year based on the new predicted conditions and traffic volume until one of the improvement alternative costs is favored.

When the optimum alternative is determined, the same analysis iterations will continue for the rehabilitated or new bridge. The analysis iterations will continue for as many years as the predetermined analysis horizon. Figure 4 shows the flow chart of the analysis program.
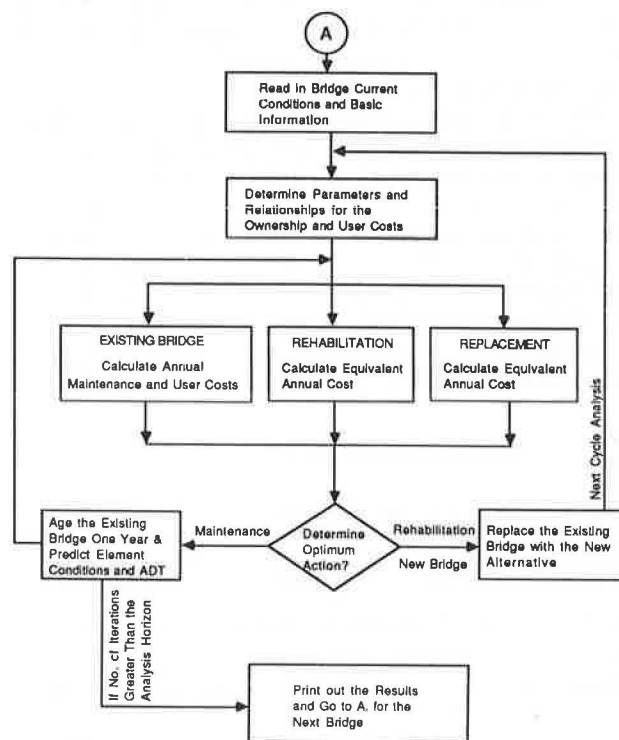
In addition to the replacement alternative, two types of bridge rehabilitation alternatives are provided in the analysis program. A rehabilitation alternative will be triggered for consideration if one of the deck, superstructure, or substructure ratings decreases to the acceptable minimum and the other two ratings are also relatively low. This rehabilitation action cost would be based on increasing all conditions to the level specified as desirable.

However, when some of the element conditions deteriorate to the minimum acceptable level and others still remain good, a second possible alternative is an interim rehabilitation. This would improve the element in poor condition to a higher condition level compatible with the good elements, as shown in Figure 5. The capability to generate an interim rehabilitation alternative has been incorporated into the analysis program. Two interim rehabilitation alternatives are available in the analysis as follows:

1. Rehabilitate the lowest condition among the three types of bridge elements to as high as the average condition of the two higher conditions if only one condition rating is less than 6, and the difference of the average of the two higher conditions and the lowest condition is greater than or equal to 2 points, or
2. Rehabilitate the lower two conditions to as high as the highest condition if only one of the three element conditions is greater than or equal to 6, and the difference of the highest condition and the lowest condition is greater than or equal to 2 points.

On the basis of these two alternatives, an interim rehabilitation alternative is considered only when there is an element condition rating of less than 6. An interim rehabilitation alternative always improves the lowest element condition at least 2 points.

For a bridge deficient in level of service, two different improvement policies are incorporated in the analysis program. The first policy selects the optimum improvement action for the deficient bridge on the basis of the engineering economic analysis. The second policy initiates an immediate improvement whenever a bridge becomes deficient in relation to a specified user level of service. If the second policy is specified by the program user, an appropriate improvement action, either a replacement or a rehabilitation, is selected for the faulty bridge on the basis of its user level of service deficiency. A bridge with load capacity deficiency will be replaced with a new bridge. A bridge with both width and

FIGURE 4 Flow chart of the bridge optimum alternative analysis program.
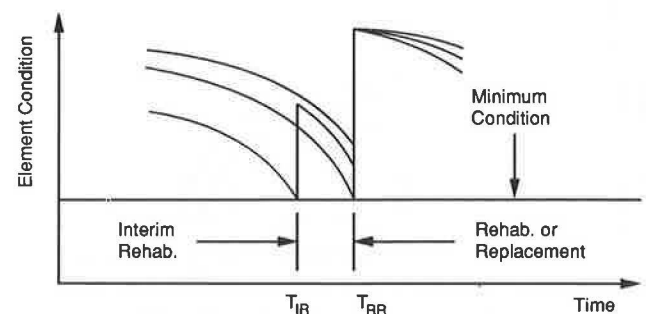
FIGURE 5 Interim rehabilitation evaluation.

vertical clearance deficiencies at the same time will also be replaced with a new bridge that will meet the desirable user level of service goals. A bridge with a width or a vertical clearance deficiency, but not both, will be rehabilitated to meet the user level of service goals specified by the program user.

On the basis of economic analysis, rehabilitation of bridges on rural, low-ADT routes for several cycles is often optimum. However, some types of bridges, for example timber bridges, cannot be practically rehabilitated after a long period because of decay or other general deterioration of the material. Thus, in the analysis, a replacement alternative is forced to be selected for a timber substructure or superstructure bridge over 40 years old and with a substructure or superstructure condition rating less than the minimum maintenance condition level of service specified.

During the analysis, the maintenance costs of all bridges in the system are accumulated for each year within the analysis horizon. The rehabilitation costs and replacement costs are also accumulated under the year determined as the optimum time for each respective alternative. The final total maintenance, rehabilitation, replacement, and user costs in each year within the analysis horizon are thereby predicted. Similar future yearly predictions are made for the average bridge element conditions, average bridge postings, and average level of service deficiencies on the basis of the assumption that funding needs and improvements predicted by the analysis are provided.

Although it is possible to set up intermediate level of service goals between the minimum acceptable and desirable level of service goals, only two goals, "Acceptable" and "Desirable," are used as the user level of service options in this program. These are the same goals numerically as those proposed by Johnston and Zia (3), which are presented in Tables 1–3.

The element condition rating in the National Bridge Inventory (NBI) Structure Inventory and Appraisal data file reflects current condition but not how long the element has been at that condition. For example, an element rated 6 may have just dropped from a 7 or may be about to drop to a 5. To provide a randomness in the first few years of evaluation, the initial condition rating was varied in increments of 0.1 point to a maximum of ±0.5 point using a random number generator. For example, a condition rating of 6 was randomly varied within the range 5.5 to 6.5.

Several controlling options are provided in the analysis program for users to select either all or subgroups of bridges in the inventory to be analyzed, and to specify acceptable and desirable maintenance condition levels, as well as user level of service goals. Subgroups of bridges can be selected to separate by federal-aid and non-federal-aid systems as well as

TABLE 1   BRIDGE LOAD CAPACITY GOALS

Functional Classification	Single Vehicle Capacity	
	Acceptable	Desirable
Interstate and Arterial	NP	NP
Major Collector	25 Tons	NP
Minor Collector	16 Tons	NP
Local	16 Tons	NP

NP : Not Posted (Maximum Legal Load = 33.6 Tons)

TABLE 2   BRIDGE VERTICAL CLEARANCE GOALS

Functional Classification	Vertical Clearance (Feet)	
	Acceptable	Desirable
Interstate and Arterial	14.0	16.5
Major and Minor Collectors	14.0	15.0
Local	14.0	15.0

TABLE 3 BRIDGE CLEAR DECK WIDTH GOALS

Functional Classification	Current ADT	Acceptable Width		Desirable Width	
		Lane (ft)	Shoulder (ft)	Lane (ft)	Shoulder (ft)
Interstate and Arterial	0 - 800	10	1	12	4
	801 - 2000	10	2	12	6
	2001 - 4000	11	2	12	8
	4000 - Over	11	3	12	8
Major and Minor Collectors	0 - 800	9	1	10	2
	801 - 2000	9	2	11	3
	2001 - 4000	10	2	12	3
	4000 - Over	10	3	12	3
Local	0 - 800	9	1	10	2
	801 - 2000	9	2	11	3
	2001 - 4000	10	2	12	3
	4000 - Over	10	3	12	3

Clear Deck Width = No. of Lanes x Lane Width + 2 x Shoulder Width

primary, secondary, and urban systems. The analysis horizon, interest rate, and percentage of the user cost considered in the analysis can also be specified.

ANALYSIS RESULTS

Data on the North Carolina bridge inventory for 1987 were used to demonstrate the Bridge Optimum Alternative Program.

Of the 16,813 state-owned structures on North Carolina highways, there are 14,460 bridges and 2,353 culverts and pipes. In the analyses, bridges with miscoded data for any entry, such as condition ratings, structural type, or single vehicle posting, were excluded. After the exclusions, 14,362 bridges (about 99.32 percent of the total state-owned bridges) were analyzed.

Three analysis cases will be mentioned. Each was for an analysis horizon of 50 years. Case 1 was based on all decisions being made on a purely economic basis. Case 2 was also based on optimum economic decisions, except that if a bridge did not meet acceptable criteria for levels of service, an improvement action was forced to be funded to eliminate the deficiency even if there were no economical alternatives. Case 3 was similar to Case 2, but desirable levels of service were imposed. Primary emphasis will be placed on Case 2. Additional details on these and other cases can be found elsewhere (4).

Analysis results for each of the cases include predictions of the optimum alternative, time, and improvement cost for each individual bridge, predictions of annual funding needs, number of bridges rehabilitated and replaced, average bridge element conditions, average single-vehicle posting, and average level of service deficiency for North Carolina bridges. Table 4 presents the analysis results of Case 2 for some example

bridges. Table 5 presents the backlog of needs determined for the three cases, that is, the estimate of 1st year needs. Table 6 presents the predictions of future funding needs and number of bridges rehabilitated and replaced over the 50-year analysis horizon for Case 2, as an example. Predicted average bridge element conditions and average single-vehicle posting for Case 2 are shown in Figure 6.

On the basis of the results of Case 2 presented in Table 6, the analysis indicates an immediate need to replace 4,638 bridges at a cost of $1,002 million and to rehabilitate 1,640 bridges at a cost of $170 million. After the 1st year, the predicted annual budget need for rehabilitation ranges from $14.3 to $170 million, and the number of bridges predicted for rehabilitation ranges from 178 to 1,701 bridges each year. After the 1st year, the predicted annual budget need for replacement ranges from $5.5 to $82 million and the number of bridges predicted for replacement each year ranges from 11 to 214 bridges. On the basis of the Case 2 analysis results presented in Table 6, the predicted annual budget for maintenance within the next 50 years ranges from $3.4 to $6.3 million in 1986 dollars.

Over the 50 years, 9,159 bridges or 63.8 percent of the inventory will require replacement. If the replacements are accomplished as indicated by the needs analysis, the 14,362 bridges in the inventory will require 24,930 minor-to-major rehabilitations over the next 50 years. This number averages slightly less than two rehabilitations per bridge to maintain or improve condition, strength, and width. Maintenance needs would be $4 to $5 million per year assuming the replacements and rehabilitation were accomplished.

Figure 6 traces the system-wide average condition ratings and posted capacity assuming that the recommended funding is available and that the recommended work is done on the basis of the results of Case 2. The average deck condition rating increases from 6.53 currently to 7.66 in the 1st year of

TABLE 4 ANALYSIS RESULTS FOR EXAMPLE BRIDGES ON THE BASIS OF CASE 2

BRIDGE NO. COUNTY FACILITY	DK SP SB	SPTY SUFF DPA	FC SY FA	RL DL TT	CG UG LENG	YR	AGE	ADT	SV	WG	CDW	VCLU	D K	S P	S B	MAIN $00	USER $00	EQUIV. $00	*	REPLACEMENT COST $000	EQUIV. $00	*	INTERIM D K	S P	S B	*	REHAB. COST $00	EQUIV $00	*	FINAL ACTION
42039	RC	T-BM	PA	25	33.6	88	31	5050	34	28	28.0	99.9	7	7	7	1	45	46	*	476	394	* N				*	538	172	*	
HARNETT	RC	80.0	U	1	14.0	04	47	8946	34	28	28.0	99.9	4	5	5	11	79	90	*	476	395	*					1100	247	*	
US421 & NC55	PS	0.0	OF	37	130	04	47	8946	34	28	28.0	99.9	8	8	8												1100			RH
						26	69	19649	34	28	28.0	99.9	4	6	6	5	174	179	*	476	395	*				*	957	328	*	
						26	69	19649	34	28	28.0	99.9	8	8	8												957			RH
42040	RC	M-BM	LO	8	16.0	88	33	300	26	20	24.0	99.9	6	5	5	11	9	20	*	368	303	* N				*	946	110	*	
HARNETT	ST	24.0	S	9	14.0	89	34	303	25	20	24.0	99.9	6	5	4	11	9	20	*	368	303	*				*	1020	117	*	
SR1213	TM	4.0	SR	37	142	89	34	303	26	20	24.0	99.9	8	8	8												1020			RH
						09	54	368	24	20	24.0	99.9	6	6	4	REPLACED DUE TO SUBSTRUCTURE CONDITION				368										
						09	54	368	34	24	27.0	99.9	9	9	9															NB
42041	TM	M-BM	LO	3	16.0	88	33	500	8	20	19.2	99.9	6	7	7	REPLACED DUE TO LOAD CAPACITY DEFICIENCY													
HARNETT	ST	22.0	S	7	14.0	88	33	500	8	20	19.2	99.9	6	7	8					282										
SR1215	TM	25.0	SR	12	158	88	33	500	34	24	27.0	99.9	9	9	9															NB
						24	36	710	34	24	27.0	99.9	4	5	5	9	0	9	*	384	317	*				*	1081	94	*	
						24	36	710	34	24	27.0	99.9	8	8	8													1081			RH
42044	CS	SLAB	LO	50	16.0	88	2	300	34	20	23.8	99.9	8	8	8	0	1	1	*	361	298	*				NOT AVAILABLE			*	
HARNETT	PS	63.0	S	7	14.0	15	29	390	34	20	23.8	99.9	5	4	6	4	1	5	*	361	297	*				*	960	87	*	
SR1222	ST	0.0	SR	37	137	15	29	390	34	20	23.8	99.9	8	8	8												960			RH
42045	RC	T-BM	MA	13	33.6	88	57	6500	34	28	20.0	99.9	6	4	5	67	559	626	*	2484	2064	* N				*	7725	837	*	
HARNETT	RC	16.0	P	1	14.0	88	57	6500	34	28	20.0	99.9	6	4	5	67	559	626	*	2484	2064	*				*	7725	837	*	
US401	RC	13.0	OF	37	739	88	57	6500	34	28	28.0	99.9	8	8	8												7725			RH
						10	79	14273	34	28	28.0	99.9	4	6	6	36	126	163	*	2484	2064	*				*	5709	748	*	
						10	79	14273	34	28	28.0	99.9	8	8	8												5709			RH
						32	**	31341	34	28	28.0	99.9	4	6	6	36	278	314	*	2484	2064	*				*	5709	900	*	
						32	**	31341	34	28	28.0	99.9	8	8	8												5709			RH
42046	RC	M-BM	MA	22	33.8	88	30	7000	34	28	28.2	99.9	5	7	7	27	59	86	*	2669	2223	* N				*	4677	639	*	
HARNETT	ST	79.0	P	1	14.0	89	31	7255	34	28	28.2	99.9	4	7	7	27	61	86	*	2669	2223	*				*	5252	660	*	
US401	ST	0.0	OF	37	608	89	31	7255	34	28	28.2	99.9	8	8	8												5252			RH
						11	53	15930	34	28	28.2	99.9	4	5	6	54	134	188	*	2669	2224	*				*	6759	865	*	
						11	53	15930	34	28	28.2	99.9	8	8	8												6759			RH
						33	75	34981	34	28	28.2	99.9	4	5	6	54	294	349	*	2669	2224	*				*	6759	1025	*	
						33	75	34981	34	28	28.2	99.9	8	8	8												6759			RH

Column header spanning groups: ******ANNUALIZED EQUIVALENT COSTS AND OPTIMUM ACTION********* — REGULAR MAINT. (MAIN $00 / USER $00 / EQUIV. $00) — REPLACEMENT (COST $000 / EQUIV. $00) — INTERIM (D K / S P / S B) — REHABILITATION (COST $00 / EQUIV $00).

TABLE 5 IMMEDIATE NEEDS BACKLOG FOR REHABILITATION AND REPLACEMENT CALCULATED IN YEAR 1 OF ANALYSIS HORIZON

Case	Rehabilitation Cost Millions	No. of Bridges Rehabilitated	Replacement Cost Millions	No. of Bridges Replaced	Total Cost Millions	Total Bridges
1	$96	831	$ 634	3,224	$ 730	4,065
2	$170	1,640	$1,002	4,638	$1,172	6,278
3	$570	2,666	$1,892	8,482	$2,462	11,148

TABLE 6   PREDICTED FUTURE FUNDING NEEDS AND NUMBER OF
BRIDGES NEEDING IMPROVEMENT FOR NORTH CAROLINA BRIDGES
ON THE BASIS OF CASE 2

YEAR	REGULAR MAINTENANCE	REHABILITATION COST	NO. OF BRIDGES	REPLACEMENT COST	NO. OF BRIDGES
1988	$3,453,228	$169,810,324	1,640	$1,002,027,427	4,638
1989	$3,521,687	$14,371,845	180	$74,119,002	214
1990	$3,465,007	$42,771,950	420	$36,896,427	146
1991	$3,413,397	$44,313,706	249	$38,137,689	185
1992	$3,809,075	$23,288,966	178	$38,095,226	143
1993	$4,731,794	$23,236,448	298	$34,057,057	156
1994	$4,995,947	$40,894,594	411	$40,827,131	176
1995	$4,846,521	$48,457,085	349	$45,726,961	177
1996	$4,623,498	$73,426,025	521	$46,207,728	166
1997	$4,665,805	$40,147,892	287	$22,332,234	87
1998	$4,298,914	$79,464,744	492	$45,788,396	142
1999	$4,436,700	$45,102,825	328	$22,273,012	94
2000	$4,617,824	$50,446,753	288	$23,946,979	76
2001	$5,246,990	$48,248,631	262	$19,452,033	72
2002	$5,418,347	$41,425,388	253	$15,240,776	61
2003	$5,590,677	$56,138,929	280	$22,060,570	70
2004	$5,761,262	$43,977,388	223	$24,463,425	44
2005	$5,652,957	$50,176,661	435	$38,572,873	180
2006	$5,636,052	$61,821,660	362	$20,552,068	121
2007	$5,799,569	$50,101,,857	565	$33,611,216	182
2008	$6,308,027	$32,301,487	235	$25,304,913	121
2009	$6,642,756	$35,610,136	268	$20,419,443	90
2010	$6,542,426	$90,831,529	444	$46,169,060	164
2011	$6,674,657	$55,331,475	307	$33,684,339	170
2012	$6,456,155	$67,239,975	318	$82,602,227	170
2013	$5,904,676	$110,763,038	1,585	$43,702,549	156
2014	$6,496,135	$37,033,165	330	$26,972,044	124
2015	$6,305,683	$112,888,741	643	$22,782,346	98
2016	$6,368,729	$61,795,122	323	$38,890,529	138
2017	$6,375,692	$56,786,581	355	$21,158,308	82
2018	$6,276,182	$92,522,611	340	$28,901,951	73
2019	$6,217,633	$77,919,700	618	$16,209,401	65
2020	$6,460,073	$70,789,526	399	$17,600,603	53
2021	$6,459,010	$73,918,030	494	$9,965,650	41
2022	$6,379,455	$71,017,189	477	$15,213,830	56
2023	$6,375,918	$90,726,726	471	12,026,037	47
2024	$5,690,122	$137,212,572	1,701	$9,324,668	38
2025	$5,559,507	$99,007,025	854	$9,187,693	34
2026	$5,657,634	$56,024,279	667	$7,677,802	28
2027	$5,628,827	$62,367,008	456	$9,495,396	30
2028	$5,802,782	$58,925,375	396	$10,376,827	33
2029	$5,853,021	$63,229,006	428	$8,284,458	28
2030	$6,082,422	$59,308,613	462	$55,817,048	32
2031	$6,325,683	$51,932,092	374	$57,567,694	23
2032	$6,303,827	$78,134,137	496	$25,294,525	45
2033	$6,316,126	$72,974,549	1,496	$12,011,712	30
2034	$6,265,332	$76,979,266	451	$8,774,314	17
2035	$6,371,723	$71,080,926	420	$8,027,687	18
2036	$6,735,725	$49,298,589	398	$7,639,179	14
2037	$6,300,694	$118,786,136	703	$5,492,801	11

the analysis horizon because of the large number of improvements. Average deck condition rating then decreases over about 20 years and thereafter averages about 6.6 through the end of the analysis horizon. The average superstructure and substructure condition ratings follow the same trend.

The average single-vehicle posting increases from 24.6 tons currently to 30.6 tons in the 1st year because of the large number of improvements. Thereafter, the average single-vehicle posting gradually continues to improve and stabilizes at a level between 32 and 33 tons within the analysis horizon.

From an examination of detailed results for the different cases, the purely economic approach of Case 1 resulted in the lowest cost but had one significant flaw. The purely economic approach results in allowing some low load capacity and
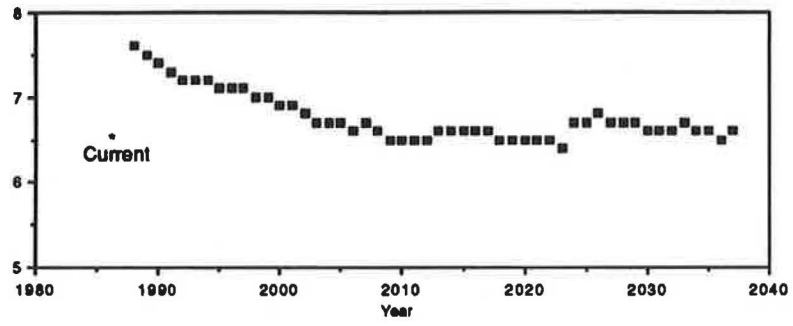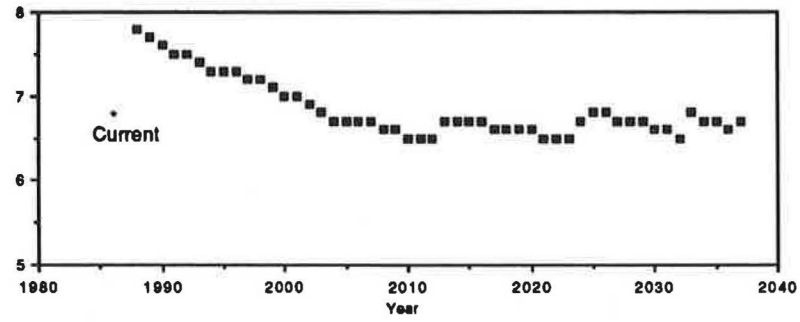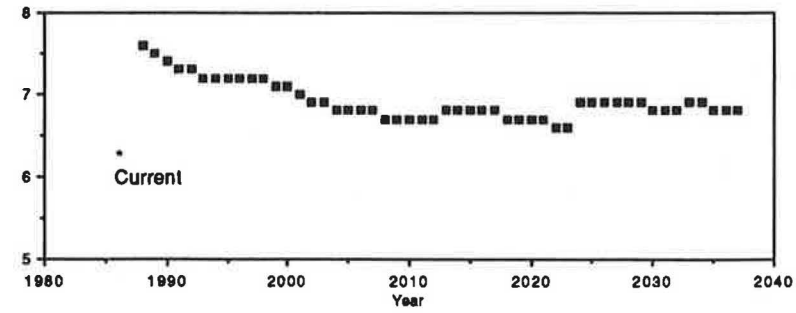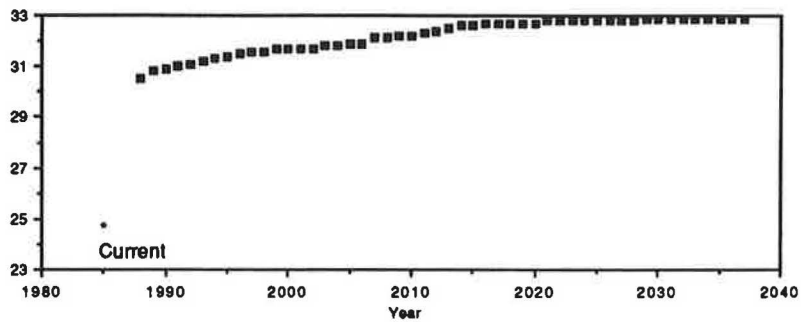
FIGURE 6   Predicted average element conditions and average single-vehicle posting versus year, if funded (Case 2).

otherwise deficient bridges on rural and low-ADT routes to remain in place. In fact, these bridges continue to lose capacity gradually over the years until replacement is mandated by closing.

However, the essence of government involvement in public services suggests that some level of service should be provided for life, safety, opportunity, and access. The acceptable level of service approach represented by Case 2 is somewhat more costly, but it provides reasonable service to all taxpayers, as a minimum. Furthermore, it prevents areas, counties, or regions from being limited in further development prospects because of an inadequate transportation system.

Providing the desirable level of service represented in Case 3 would be an alternate goal. However, the greater funding resources required are less likely to be available. Thus, an approach based on the acceptable level of service may be a reasonable alternative.

Fortunately, most deficient bridges would be selected for improvement under even the purely economic approach. Providing the acceptable level of service as a minimum, in addition, could be achieved for 6 percent more and the desirable level of service for 26 percent more than the purely economic approach for predicted actions over the 50 years.

Any of these approaches will require a substantial increase in funding. However, they can be justified because the user tax increase required would be more than offset by user savings from fewer accidents and detours. Regardless, many of the funding increases will occur as bridges deteriorate to a condition forcing replacement. To improve and maintain the bridge inventory is more cost effective.

CONCLUSIONS

On the basis of the research results presented, the following conclusions can be summarized:

1. A defendable analysis system was developed and implemented for bridge management decision making on the basis of economic analysis that considers both agency and user costs.

2. The analysis system uses engineering data from the NBI Structure Inventory and Appraisal file with some elements added by the North Carolina Department of Transportation (NCDOT) to predict needs on a bridge-by-bridge basis into the future.

3. System-wide needs can be predicted by adding individual bridge needs each year, while system-wide performance can be measured by averaging bridge condition parameters.

4. Future needs and performance are estimated through a bridge-by-bridge simulation of element deterioration and optimum improvement actions each year into the future.

5. Results of system-wide analysis for North Carolina indicate a large backlog of economically justifiable needs. These needs are likely to be even greater because delays in funding will cause increased costs for emergency actions. Additional funds will also be needed for culverts that are not included and for bridge improvements to accommodate additional lanes from traffic planning decisions.

6. The needs predicted would represent a significant increase over current funding levels. Nevertheless, the increased funding indicated represents the lowest cost solution to the public.

REFERENCES

1. Highway Bridge Replacement and Rehabilitation Program. 7th Annual Report of the Secretary of Transportation to the Congress of the United States, Bridge Division, Office of Engineering, FHWA, U.S. Department of Transportation, 1986.
2. *Recording and Coding Guide for the Structure Inventory and Appraisal of the Nation's Bridges.* FHWA, U.S. Department of Transportation, 1979.
3. D. W. Johnston and P. Zia. Level-of-Service System for Bridge Evaluation. In *Transportation Research Record 962*, TRB, National Research Council, Washington, D.C., 1984, pp. 1–8.
4. C. Chen and D. W. Johnston. *Bridge Management Under a Level of Service Concept Providing Improvement Action, Time and Budget Prediction.* Report FHWA/NC/88-004. Center for Transportation Engineering Studies, Department of Civil Engineering, North Carolina State University, Raleigh, Sept. 1987.
5. F. Hanssmann. *Operations Research Techniques for Capital Investment,* John Wiley, New York, 1968.
6. G. W. Smith. *Engineering Economy: Analysis of Capital Expenditures,* 3rd ed. The Iowa State University Press, Ames, 1979.

OPBRIDGE: An Integrated Bridge Budget Forecasting and Allocation Module at the State Level

KAMAL M. AL-SUBHI, DAVID W. JOHNSTON, AND FOAD FARID

An overview is provided of the optimum bridge budget forecasting and allocation module (OPBRIDGE), a decision support system for bridge management at the state level. OPBRIDGE has the capability of predicting funding requirements to achieve bridge system objectives specified by the bridge manager. Alternately, the program can optimally allocate limited budgets and predict performance of the bridge system.

A bridge management system (BMS) is a systematic framework that formalizes the decision-making process involving maintenance, rehabilitation, and replacement of bridges. The BMS applies systems engineering to assist decision makers in defining optimum strategies for maintaining bridges at predefined performance standards during a given period of time, called a horizon. The BMS attempts to gradually upgrade the entire inventory of bridges so that eventually condition ratings and user levels of service will not be deficient.

Decisions in a comprehensive BMS can be analyzed at two different levels—at the bridge (project) level and at the system level. A bridge system consists of a number of bridges under the jurisdiction of an agency. At the bridge level, the BMS prescribes the best action for a specific bridge. At the system level, the BMS supports decision makers in developing an agency-wide program of maintenance, rehabilitation, and replacement that will make optimum use of the available budget.

An overview of the optimum bridge budget forecasting and allocation module (OPBRIDGE), a decision support system for bridge management at the system level, is provided. OPBRIDGE, which was developed for the North Carolina Department of Transportation (NCDOT), can answer the following bridge-level question at the beginning of each year in the analysis horizon—What action should be selected for each bridge in the system: replacement, rehabilitation, major maintenance, or routine maintenance? OPBRIDGE may also answer the following system-level questions:

1. What are the annual budgets needed over the forecasting horizon?
2. How can budgets granted be allocated optimally at the state level?
3. What are the impacts of manager objectives and funds available on the estimated future user level of service (LOS) and condition ratings of the bridge system?

K. M. Al-Subhi, Construction Engineering and Management, King Fahd University of Petroleum and Minerals, Box 1468, Dhahran, Saudi Arabia 31261. D. W. Johnston and F. Farid, Department of Civil Engineering, North Carolina State University, Raleigh, N.C. 27695–7908.

OPBRIDGE adopts and improves a methodology for computing the user and agency costs associated with the different alternatives for a bridge, on the basis of the findings of Chen and Johnston (1). OPBRIDGE applies concepts of strategic planning for setting long-range bridge management objectives and policies that constitute the user input for the analysis module developed. The mathematical formulation for budget forecasting is adapted from the work of Chen and Johnston, while a budget allocation module is developed at the system level under constrained budgets. OPBRIDGE analysis procedures applied to an existing bridge data base are evaluated.

MATHEMATICAL FORMULATION AND APPROACH OVER HORIZON

OPBRIDGE attempts to resemble the real-life decision process. At the beginning of every year, OPBRIDGE analyzes the budget limitation that was entered by the user for that particular year. If the budget is limited (budget granted or limited maximum allowable budget), OPBRIDGE uses a 0–1 integer-linear programming formulation with multiple-choice constraints, also called "generalized upper bound" (GUB) constraints, to optimize budget allocation according to the decision criterion, thus maximizing overall reductions in equivalent uniform annual costs (EUAC). On the other hand, if the budget is unlimited, OPBRIDGE selects the alternative that has the highest reduction in EUAC for every bridge in the system. The routine maintenance alternative protects the bridges from accelerated deterioration. Therefore, the base alternative is provided if a major improvement alternative is not economical, not enforced by requesting immediate improvement for deficient bridges, or not possible because of budget limitation. Figure 1 shows the sequence of events in OPBRIDGE, as follows:

1. The user enters budgets, objectives, and policies into the file INPUT.DAT.
2. OPBRIDGE extracts data from the bridge database and the cost and parameter file.
3. OPBRIDGE optimizes decisions for every year in the analysis horizon. At the end of every year, OPBRIDGE ages bridges 1 year and predicts condition ratings, average daily traffic (ADT), etc. This process allows the system to repeat the analysis for the next year.
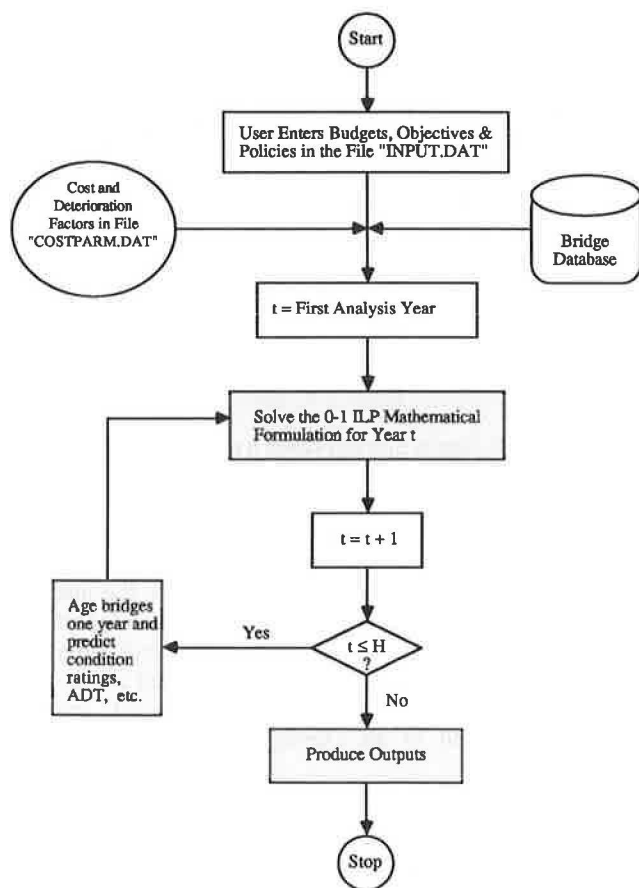
FIGURE 1 Flowchart for OPBRIDGE analysis.

4. OPBRIDGE produces detailed bridge-by-bridge output showing recommended current and future major actions, county-by-county output showing costs of major actions and budget required for each county, and tabular and graphical outputs showing the future performance level of the bridge system over the horizon, H.

INPUT DATA FOR USING OPBRIDGE

Figure 2 shows the OPBRIDGE user input computer screen layout. The input data consist of the following items.

1. *Horizon, H?* Enter the number of future years over which the analysis is made. This integer variable may have a value between 1 and 20.

2. *First-Analysis Year?* Enter the first year in the analysis horizon, H.

3. *Bridges for Analysis?* Specify whether all bridges or bridges with a certain federal-aid classification, a certain state system, or a certain division number are to be included in the analysis.

4. *Immediate Improvement for Deficient Bridges?* Specify whether improvement (rehabilitation or replacement) is mandatory for bridges that are deficient with respect to the requested user LOS goals as defined by Johnston and Zia (2). If the entry is N, then an improvement alternative is selected only

if it is economical. If the entry is Y and the bridge is deficient in meeting the user LOS goals, an action will be taken to correct the deficiency, even if the action is not economical. However, in this second case, bridges with economic alternatives will be improved first, and then noneconomic bridges, if there are funds remaining.

5. *User LOS Goals?* Assign 1 or 2, depending on whether the user LOS goals are (a) acceptable, or (b) desirable with respect to the following bridge characteristics: load capacity, clear deck width, and vertical roadway underclearance and overclearance. The goals vary depending on highway functional classification and traffic volume. At the beginning of each year, decision rules select appropriate alternatives for a bridge, if its LOS characteristics are below the user LOS goals. Acceptable levels are mainly applicable to existing bridges permitted to remain in service. Desirable levels are usually applied to new bridge construction.

6. *Minimum Allowable Condition Rating?* Enter any integer on the scale of condition rating. The 0-to-9 scale, from critical to new condition, has been used in the federal bridge inspection standard to record conditions of the bridge elements. Whenever the condition rating of a bridge element becomes lower than or equal to the minimum allowable element condition, that bridge should be recommended for rehabilitation, major maintenance, or replacement, depending on the economic attractiveness of each. Usually, the minimum element condition allowed is 3, 4, or 5.

7. *Highest Rehabilitation Condition Rating?* Define the condition rating at which a bridge element should be rehabilitated if its condition rating and LOS trigger a possible rehabilitation action. Generally, this variable is estimated as 7 or 8 on the scale of condition ratings.

8. *Real Required Rate of Return and Rate of Inflation?* Input the required rate of return (RRR) to be used in computing the EUAC of all possible improvement alternatives for a bridge. The RRR is the minimum acceptable rate of return on an investment after taking into account all the circumstances surrounding that investment. Inflation is a persistent increase in price levels that results in the decline of the purchasing power of future budgets. As shown in Figure 3, OPBRIDGE can take into account the effect of inflation on the output it produces (3). The nominal required rate of return (NRRR) is composed of two components—the real required rate of return (RRRR) and a component that is larger than the perceived rate of inflation (f), NRRR = RRRR + $(1 + $ RRRR$)f$.

9. *Factor to Transfer 1985/86 Dollars to Today's Dollars?* Enter index needed to convert cost tables (1) from 1985–1986 dollars to today's dollars (see Figure 3).

10. *Are Your Budgets in Constant (Today's) Dollars?* Enter N if the budgets are in future dollars and need to be transferred to the present time to account for inflation. This entry is needed to ensure that both the budgets and the cost estimation tables would have the same purchasing power. The inflation rate used in this case is entered by the user as the average yearly inflation rate expected over the analysis horizon.

11. *Enter Some or All of the Following Budgets:*

● Granted Budgets: The funding authority usually grants in advance certain budgets to be used during an allocation

```
ANALYSIS HORIZON
    HORIZON ? (YEARS) . . . . . . . . . . . . . . . . . . . . 20
    FIRST-ANALYSIS YEAR ? . . . . . . . . . . . . . . . . . . 1989

BRIDGES FOR ANALYSIS
    RANGE OF BRIDGE NUMBERS ? . . . . . . . . . . . . . . . . 00000-99999
    WHAT FEDERAL AID SYSTEM ? (F/N/A) . . . . . . . . . . . . A
    WHAT STATE SYSTEM ? (P/S/U/A) . . . . . . . . . . . . . . A
    WHAT DIVISION NUMBER ? (15 = ALL DIVISIONS) . . . . . . . 15

ANALYSIS PERFORMANCE REQUIREMENTS
    IMMEDIATE IMPROVEMENT FOR DEFICIENT BRIDGES ? (Y/N) . . Y
    USER LEVEL-OF-SERVICE GOALS ? (1 OR 2). . . . . . . . . 1
        1) ACCEPTABLE,
        2) DESIRABLE.
    MINIMUM ALLOWABLE CONDITION RATING ?. . . . . . . . . . 4

GENERAL SPECIFICATIONS
    HIGHEST REHABILITATION CONDITION RATING ? . . . . . . . 8
    REAL REQUIRED RATE OF RETURN ? (%). . . . . . . . . . . 5.00
    ARE YOUR BUDGETS IN CONSTANT (TODAY'S) DOLLARS? (Y/N) . Y
    RATE OF INFLATION ? (%) . . . . . . . . . . . . . . . . 3.00
    FACTOR TO TRANSFER 1985/86 DOLLARS TO TODAY'S DOLLARS ? 1.1

ENTER BELOW SOME OR ALL OF THE FOLLOWING  BUDGETS: BUDGETS GRANTED,
LIMITED OR UNLIMITED MAXIMUM ALLOWABLE BUDGETS.
INCLUDE DECIMAL POINTS IN BUDGETS.
  $ = BUDGET DISTRIBUTED BY DOLLARS.
  % = BUDGET DISTRIBUTED BY PERCENTAGE (MUST ENTER TOTAL BUDGET).
  T = ONLY TOTAL BUDGET IS ENTERED.
  U = UNLIMITED BUDGET.
```

YEAR	% $ T U	MAINTENANCE	REHABILITATION	REPLACEMENT	TOTAL BUDGET
1989	%	20.	30.	50.	80000000.
1990	$	15000000.	30000000.	45000000.	90000000.
1991	T	.	.	.	85000000.
1992	U	.	.	.	.
----	-	.	.	.	.
----	-	.	.	.	.
2008	U	.	.	.	.

```
OUTPUT SPECIFICATION
    DETAILED BRIDGE-BY-BRIDGE OUTPUT ? (Y/N). . . . . . . . Y
    TABULAR OUTPUTS (BUDGETS AND PERFORMANCE) ? (Y/N) . . . Y
        BY FEDERAL/NON-FEDERAL AID ? (Y/N). . . . . . . . . Y
        BY PRIMARY/SECONDARY/URBAN ? (Y/N). . . . . . . . . Y
    GRAPHICAL OUTPUTS (BUDGETS AND PERFORMANCE) ? (Y/N) . . Y
        BY FEDERAL/NON-FEDERAL AID ? (Y/N). . . . . . . . . Y
        BY PRIMARY/SECONDARY/URBAN ? (Y/N). . . . . . . . . Y
    COUNTY-BY-COUNTY OUTPUT OF ACTIONS ? (Y/N). . . . . . . Y
        UP TO WHAT YEAR ? . . . . . . . . . . . . . . . . . 1989

CURRENT NEW-BRIDGE COST PARAMETERS
    UNIT COST ? ($ / SF DECK AREA). . . . . . . . . . . . . 46.0
    FIXED COST ? ($) . . . . . . . . . . . . . . . . . . . 55000.
    DESIGN FEE ? (%) . . . . . . . . . . . . . . . . . . . 12.0
```

FIGURE 2 OPBRIDGE user input computer screen layout.
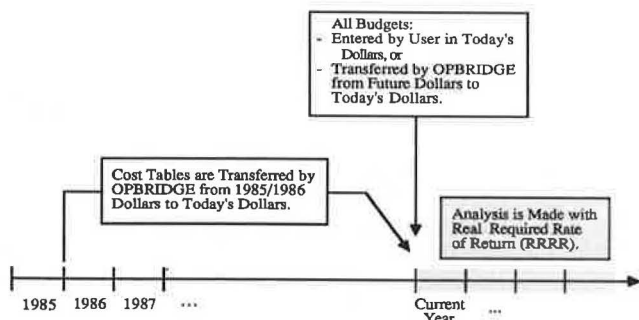
FIGURE 3 Dealing with inflation in OPBRIDGE analysis.

horizon, as shown in Figure 4. This allocation horizon may be 1 year or more.

● Limited Maximum Allowable Budgets: The decision maker does not know the budgets that will be granted during the years after the allocation horizon (see Figure 4). However, experience can be used to estimate the expected budgets granted to make reasonable forecasts about the bridge system performance. This term is the maximum allowable budget, $MAB(t)$, which serves as an upper limit to the budget computed for year t. This concept allows modeling of the system performance and behavior under realistic assumptions of future budgets.

FIGURE 4 Relationship between horizons.

● Unlimited Maximum Allowable Budgets: If the user elects to enter unlimited MAB(*t*), the OPBRIDGE analysis will be made for year *t* under the assumption of unlimited budget.

Granted budgets or limited maximum allowable budgets for year *t* can be entered in three ways: total budget only; budget distributed by percentage, for example, 20 percent for maintenance, 20 percent for rehabilitation, and 60 percent for replacement (in this case, the total budget must be entered to allow OPBRIDGE to internally compute the budgets in dollars available for maintenance, rehabilitation, and replacement activities); and budget distributed by dollars, for example, $15,000,000 for maintenance, $25,000,000 for rehabilitation, and $45,000,000 for replacement. In the $/%/T/U column, the user enters $ if the budget is distributed by dollars, % if the budget is distributed by percentage, T if only the total budget in dollars is limited, or U if the budget is unlimited.

12. *Detailed Bridge-by-Bridge Output?* Enter Y if output is desired showing the status and actions recommended for the first analysis year, and major actions (replacement and rehabilitations) and their timings recommended thereafter for every bridge in the system (see Figure 5). All dollars in the detailed bridge-by-bridge output are in constant (today's) dollars.

13. *Tabular and Graphical Outputs?* Enter Y if output is desired showing funding needs or budget limits and the behavior of the state-wide, system-level performance indicators over the horizon. The outputs can be listed by federal- or non-federal-aid bridges and by primary, secondary, or urban bridges. All dollars in the tabular and graphical outputs are in future (then-current) dollars.

14. *Yearly County-by-County Output?* Enter Y if output is desired showing a list of bridges needing major actions (replacement and rehabilitations), cost of the major actions, and total funds needed for each county in the state (see Figure 6). The total budget is also subdivided into federal-aid and state system funds. The county-by-county output is provided for each year up to the year (≤ horizon) specified by the user. All dollars in the county-by-county output are in constant (today's) dollars.

15. *Unit Cost?* Enter cost per square foot of deck area for constructing a new bridge, currently $46/ft².

16. *Fixed Cost?* Enter the fixed cost associated with new bridge construction, currently about $55,000.

Notes:
1. The output is under the assumption of a limited budget, immediate improvement for deficient bridges, a minimum allowable condition rating of 4, an acceptable user level-of-service goal, and a 20-year horizon.
2. If a bridge needs a major action or one of its major actions is the most economical, but was recommended for a routine maintenance (MN#1), then there is not enough budget to recommend the major action, e.g., bridge # 2.

FIGURE 5 Detailed bridge-by-bridge output.

```
COUNTY : ALAMANCE
YEAR   : 1989

BRIDGES NEEDING MAJOR IMPROVEMENTS:
------------------------------------------------------------------------------
BRIDGE  FED   SYS  REPLACEMENT   REHABILITAT   MAJOR-MAINT   ROUTINE-MAINT
NUMBER  AID         ($)           ($)           ($)           ($)
------------------------------------------------------------------------------
     1  SR    S         95103             0             0             0
     2  SR    S        342610             0             0             0
     3  SR    S             0         57084             0             0
     .  .     .             .             .             .             .
     .  .     .             .             .             .             .
     .  .     .             .             .             .             .
   102  SR    S             0             0         72050             0
   103  SR    S        119683             0             0             0
   104  FS    P             0         89098             0             0
     .  .     .             .             .             .             .
     .  .     .             .             .             .             .
     .  .     .             .             .             .             .
   313  SR    S             0         35725             0             0
   319  SR    S             0         37230             0             0
   326  SR    S        287252             0             0             0
   328  SR    S        138370             0             0             0
   329  SR    S             0         40344             0             0
   336  SR    S             0         44370             0             0
------------------------------------------------------------------------------

FEDERAL AID -- P      2917907       3703689             0          6632
FEDERAL AID -- S      5291855             0             0          3947
FEDERAL AID -- U      1257608             0             0           486
NON FED AID -- P      1551596             0             0           223
NON FED AID -- S     14644449        717812         76245          9627
NON FED AID -- U       828490             0             0           114
------------------    ----------    ----------    ----------    ----------
TOTAL       31010679   26491904       4421501         76245         21029

NOTE: BRIDGES NEEDING ROUTINE MAINTENANCE ONLY ARE NOT LISTED HERE
      (SEE THE DETAILED BRIDGE-BY-BRIDGE OUTPUT).
```

FIGURE 6 County-by-county output.

17. *Design Fee?* Enter the estimated design fee as a percentage of the basic construction costs for the new bridge, currently 12 percent.

FLOWCHART FOR USING OPBRIDGE

The OPBRIDGE decision-making process, shown in Figure 7, can be explained as follows:

1. The manager enters budgets as granted, limited, or unlimited maximum allowable budgets for each year in the analysis horizon. Other inputs include minimum performance requirements and other parameters.

2. The OPBRIDGE program is executed and, in the calculations, decisions are optimized for every year in the analysis horizon. Outputs include individual bridge performance, as well as tabular and graphical results, showing the trend of future performance of the bridge system over the analysis horizon, H.

3. If bridge managers are not satisfied with the results, they can revise the budget constraints and minimum requirements, reexecute the program, and analyze inventory performance again. This process is repeated as necessary to determine the effects of various strategies and options. Experience plays a major role in this process.

4. Once bridge managers have determined performance of the system under varying constraints, the results can support requests for adequate funding.

FINDINGS FOR THE NORTH CAROLINA BRIDGE INVENTORY

Ten different management cases were selected for analysis. Their analysis options are presented in Table 1, where the user LOS goals are those defined for bridges by Johnston and Zia (2). The sample bridges used for the analysis were the 14,100 conventional, state-owned bridges in the data base of the NCDOT. This list includes all structures in the North Carolina inventory except pipes and culverts, which are excluded internally by the program. Because all bridges in North Carolina are state owned except for approximately 300 municipal bridges, a full range of roadway functional classifications is represented. Constants for the analyses are shown in Figure 8.
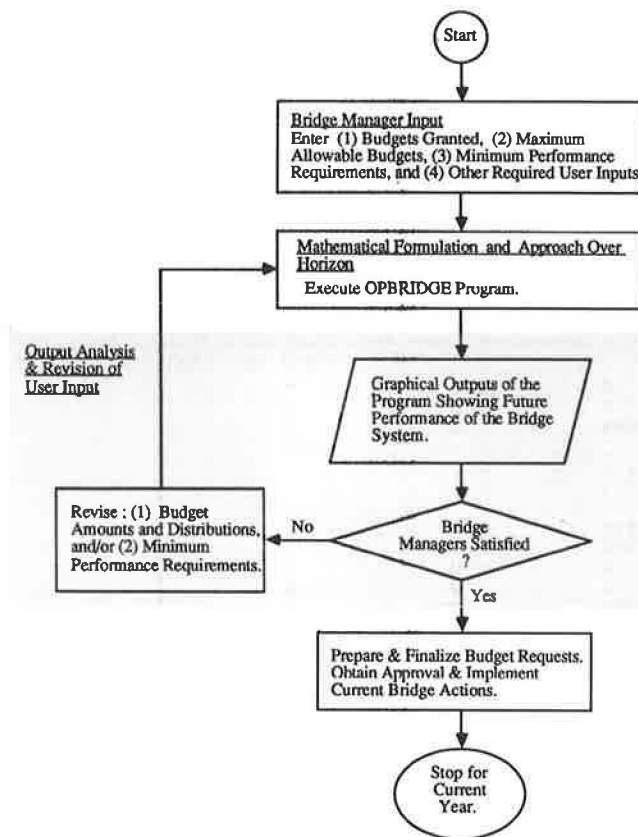
FIGURE 7   Flowchart for use of OPBRIDGE.

TABLE 1   ANALYSIS CASES

Case	Immediate Improvement for Deficient Bridges? (Y/N)	User Level-of-Service Goals	Total Budget
1	N	Acceptable	Unlimited
2	Y	Acceptable	Unlimited
3	Y	Desirable	Unlimited
4	N	Acceptable	Limited to $60,000,000/Year
5	Y	Acceptable	Limited to $60,000,000/Year
6	Y	Acceptable	Limited to $100,000,000/Year
7	N	Acceptable	Limited to $200,000,000/Year
8	Y	Acceptable	Limited to $200,000,000/Year
9	N	Acceptable	Limited to $400,000,000/Year
10	Y	Acceptable	Limited to $400,000,000/Year

Tables 2 through 5 present outputs showing the following results:

1. On the basis of the assumption of improvement only if economically viable (Case 1), the analysis indicated a backlog of $1.067 billion. If the funds were available, 3,377 bridges would be replaced, 424 bridges would be rehabilitated, and 144 bridges would receive major maintenance during the first year to eliminate the backlog.

2. On the basis of immediate improvement, if either economically viable or deficient in regard to acceptable criteria (Case 2), the analysis indicated a backlog of $1.874 billion. In this case, 5,512 bridges would be replaced, 1,814 bridges would be rehabilitated, and 144 bridges would receive major maintenance during the first year.

3. On the basis of immediate improvement if either economically viable or deficient based on desirable criteria (Case 3), the analysis indicated a backlog of $3.288 billion. In the desirable case, 8,881 bridges would be replaced and 2,292 bridges would be rehabilitated during the first year.

4. Eliminating the backlog under either economic or immediate approaches is unlikely to occur in 1 year. Funding for most agencies depends on revenue sources, which are received at fairly constant rates from year to year. Thus, performance of the bridge system under constrained levels of funding is of significant interest.

5. Under constrained budgets of $60 million/year (Cases 4 and 5), the analysis indicated a slight decrease in user costs and deficient bridges for approximately 5 years. However, average condition declines initially, and for the following 15 years there is a continued decline in condition and a significant increase in deficient bridges and user costs. Funding at $60 million/year, the current level, is insufficient to maintain the system and is not economical to the public.

6. Under constrained budgets of $100 million/year (Case 6), the analysis indicated a slight decrease in the number of deficient bridges with respect to LOS over the next 20 years. However, user costs, which initially decline for 5 years, thereafter gradually increase to higher than current levels because of increased traffic. Average condition ratings gradually decline with a significant increase in conditions that are less than acceptable because of insufficient funding to improve all bridges in need of repair.

7. Under constrained budgets of $200 million/year (Cases 7 and 8), the analysis indicated a gradual reduction of deficiencies over the next 20 years, which virtually eliminates bridge deficiencies versus acceptable LOS criteria. User costs are significantly reduced. Average condition ratings improve slightly with almost no bridges having less-than-minimum element conditions. The budget is fully used in each of the 20 years.

8. Under constrained budgets of $400 million/year (Cases 9 and 10), the analysis indicated a significant improvement in bridge performance indicators over the first 5 years. The full budget is used initially, but after 4 to 5 years, the full funding level is no longer needed and the system can be maintained with funding levels generally between $100 and $200 million/year.

9. From examination of the various cases, it appears that North Carolina needs could economically justify bridge improvement funding at the rate of $200 million/year over the next 20 years. This result is consistent with the findings of Chen and Johnston (1) who suggested $194 million/year for the next 10 years. However, because of the effects of delaying the improvements and needs for increasing numbers of bridge lanes, a reduction from that level after 10 years does not appear feasible.

```
ANALYSIS HORIZON
    HORIZON ? (YEARS) . . . . . . . . . . . . . . . . . . . . . . . . . . . 20
    FIRST-ANALYSIS YEAR ? . . . . . . . . . . . . . . . . . . . . . . . . . 1989

BRIDGES FOR ANALYSIS
    RANGE OF BRIDGE NUMBERS ? . . . . . . . . . . . . . . . . . . . . . . . 00000-99999
    WHAT FEDERAL AID SYSTEM ? (F/N/A) . . . . . . . . . . . . . . . A
    WHAT STATE SYSTEM ? (P/S/U/A) . . . . . . . . . . . . . . . . . A
    WHAT DIVISION NUMBER ? (15 = ALL DIVISIONS) . . . . . . . . 15

ANALYSIS PERFORMANCE REQUIREMENTS
    .

    .
    MINIMUM ALLOWABLE CONDITION RATING ? . . . . . . . . . . . 4

GENERAL SPECIFICATIONS
    HIGHEST REHABILITATION CONDITION RATING ? . . . . . . . . . . 8
    REAL REQUIRED RATE OF RETURN ? (%). . . . . . . . . . . . . . 8.00
    ARE YOUR BUDGETS IN CONSTANT (TODAY'S) DOLLARS ? (Y/N). . . Y
    RATE OF INFLATION ? (%) . . . . . . . . . . . . . . . . . . 0.00
    FACTOR TO TRANSFER 1985/86 DOLLARS TO TODAY'S DOLLARS ? . . 1.1
    .
    .
    .


OUTPUT SPECIFICATIONS
    DETAILED BRIDGE-BY-BRIDGE OUTPUT ? (Y/N). . . . . . . . . . . N
    TABULAR OUTPUTS (BUDGETS AND PERFORMANCE) ? (Y/N) . . . . . Y
        BY FEDERAL/NON-FEDERAL AID ? (Y/N). . . . . . . . . . . . Y
        BY PRIMARY/SECONDARY/URBAN ? (Y/N). . . . . . . . . . . . Y
    GRAPHICAL OUTPUTS (BUDGETS AND PERFORMANCE) ? (Y/N) . . . . Y
        BY FEDERAL/NON-FEDERAL AID ? (Y/N). . . . . . . . . . . . Y
        BY PRIMARY/SECONDARY/URBAN ? (Y/N). . . . . . . . . . . . Y
    COUNTY-BY-COUNTY OUTPUT ? . . . . . . . . . . . . . . . . . . N
        UP TO WHAT YEAR ? . . . . . . . . . . . . . . . . . . . . 1989

CURRENT NEW-BRIDGE COST PARAMETERS
    UNIT COST ? ($ / SF DECK AREA). . . . . . . . . . . . . . . . 46.00
    FIXED COST ? ($). . . . . . . . . . . . . . . . . . . . . . . 55000.
    DESIGN FEE ? (%). . . . . . . . . . . . . . . . . . . . . . . 12.0
```

FIGURE 8   Partial OPBRIDGE input screen indicating entries assumed constant for 10 cases.

On the basis of Cases 5, 6, 8, and 10, involving both economical and immediate improvements, results for selected parameters are shown in Figures 9 through 12. The funds of the yearly budget used are shown in Figure 9. As shown in Figure 10, user costs can be reduced initially if funds are directed at bridges with high user costs. However, if long-term funding is low, user costs will eventually climb rapidly. In Figure 11, deck condition ratings improve or remain stable under higher levels of funding but decline under low funding. The condition ratings of other elements respond similarly. In Figure 12, the average single-vehicle posting improves under higher levels of funding but remains low under lower levels of funding.

SUMMARY AND CONCLUSIONS

1. The economic decision-making model developed can be used in strategic planning to help bridge managers set objectives and policies, and forecast and allocate budgets required to maintain a state-wide bridge system. Bridge system objectives include a number of system-level performance indicators to be maintained over time. At a high managerial level, policies consist of distributions of available and potential funds among various bridge classifications. OPBRIDGE is a tool for assessing the impact of various funding levels and distributions.

2. Three improvement alternatives are assumed possible for a bridge at any point in time: replacement, rehabilitation, and major maintenance. Routine maintenance, if provided, is assumed to protect the bridge against accelerated deterioration in varying degrees, but it does not raise the bridge condition ratings or user LOS.

3. Techniques and data for estimating agency costs, user costs, and EUAC are implemented.

4. Two alternatives for two different bridges may have the same EUAC, but their impact in reducing the current bridge annual maintenance and user costs are usually different. For

Case 1

Economical Improvement; Acceptable Level of Service

YEAR	ROUTINE MAINT. COST	MAJOR MAINT. COST	NO.	REHABILITATIONS COST	NO.	REPLACEMENTS COST	NO.	TOTAL YEARLY BUDGET
1989	4965357.	7588001.	144	59614048.	424	994703616.	3377	1066870780.
1990	5021321.	10735712.	93	33425104.	140	161738208.	314	210920336.
1991	5240553.	5457473.	95	21750336.	125	105654032.	288	138102384.
1992	5320226.	6664511.	58	31242400.	129	107301696.	257	150528832.
1993	5777386.	3974461.	55	17011008.	109	81401584.	255	108164432.
1994	6134874.	4789402.	56	15369550.	85	62472800.	191	88766624.
1995	6040673.	18367472.	179	42614416.	230	117788384.	437	184810944.
1996	5894290.	21185840.	171	62617568.	247	117690048.	415	207387744.
1997	5700428.	19659264.	181	77936656.	242	122859744.	372	226156080.
1998	5490963.	17482240.	188	50540576.	260	89247184.	295	162760960.
1999	5630846.	14353487.	141	39933568.	205	74794240.	222	134712128.
2000	5660610.	15663039.	138	33331360.	183	80768416.	195	135423424.
2001	6052728.	17781680.	119	38137536.	199	48239488.	118	110211424.
2002	6265641.	15263466.	119	33433152.	158	53822528.	116	108784784.
2003	6471806.	14761956.	133	38165152.	201	50667392.	108	110066304.
2004	6627848.	13547097.	145	50307744.	218	58377520.	118	128860208.
2005	6581044.	12994815.	122	56724800.	220	75546304.	94	151846960.
2006	6627080.	12709186.	119	47165792.	236	49994080.	86	116496128.
2007	6748567.	10278602.	82	45496272.	219	30843040.	60	93366480.
2008	7038131.	13933733.	158	42999376.	248	18030464.	60	82001696.

Case 2

Immediate Improvement; Acceptable Level of Service

YEAR	ROUTINE MAINT. COST	MAJOR MAINT. COST	NO.	REHABILITATIONS COST	NO.	REPLACEMENTS COST	NO.	TOTAL YEARLY BUDGET
1989	3488013.	7588001.	144	311066624.	1814	1552334340.	5512	1874476800.
1990	3954589.	10735712.	93	37518640.	82	56678128.	124	108887056.
1991	4201249.	5457473.	95	10312592.	56	56458496.	92	76429808.
1992	4331535.	6664511.	58	20839312.	71	53641152.	107	85476496.
1993	4976562.	3974461.	55	19682992.	52	39863040.	84	68497040.
1994	5434614.	4789402.	56	15394375.	47	38019120.	77	63637504.
1995	5561729.	18367472.	179	52047712.	98	50785680.	123	126762592.
1996	5581043.	21185840.	171	36981712.	136	51688944.	141	115437536.
1997	5574434.	19659264.	181	30635728.	150	73462864.	137	129332288.
1998	5395930.	17482240.	188	50033424.	194	50750384.	129	123661968.
1999	5641173.	14353487.	141	27169776.	137	41308928.	96	88473360.
2000	5765154.	15663039.	138	29591856.	132	44164496.	79	95184544.
2001	6289930.	17781680.	119	26918672.	142	31048144.	54	82038416.
2002	6594817.	15263466.	119	34064848.	128	38686208.	74	94609328.
2003	6839733.	14761956.	133	34722848.	166	48261120.	74	104585648.
2004	7217678.	13547097.	145	43360528.	188	34088384.	84	98213680.
2005	7365423.	12994815.	122	46519024.	197	69223600.	99	136102848.
2006	7382101.	12709186.	119	51278656.	214	42579248.	115	113949184.
2007	7648110.	10278602.	82	42082608.	206	25125520.	60	85134832.
2008	7804030.	17428976.	296	44761264.	356	28578528.	107	98572784.

Case 3

Immediate Improvement; Desirable Level of Service

YEAR	ROUTINE MAINT. COST	MAJOR MAINT. COST	NO.	REHABILITATIONS COST	NO.	REPLACEMENTS COST	NO.	TOTAL YEARLY BUDGET
1989	1214663.	2849938.	18	768880128.	2292	2515520000.	8881	3288464640.
1990	2021307.	3506736.	20	17085488.	121	30186544.	55	52800064.
1991	2175912.	903686.	10	14562842.	83	23695440.	45	41337872.
1992	2306159.	1874651.	11	9972803.	60	13555536.	32	27709136.
1993	3028985.	790588.	12	13714163.	44	16819808.	25	34353536.
1994	3892941.	860448.	5	13481829.	37	8091966.	18	26327168.
1995	4175550.	3941115.	23	16059015.	48	17347952.	37	41521632.
1996	4275464.	7320168.	35	18532336.	64	20338880.	28	50466848.
1997	4323338.	9110234.	47	17270928.	54	22259744.	45	52964240.
1998	4249634.	6462658.	40	20234960.	62	64122432.	53	95069680.
1999	4392132.	6235563.	33	10443553.	41	23330128.	41	44401376.
2000	4562677.	6944057.	34	16614977.	44	11692852.	31	39814544.
2001	5397656.	6049120.	33	11134879.	49	9407896.	36	31989536.
2002	6127752.	8108084.	40	14412369.	51	14376552.	25	43024736.
2003	6481819.	8000053.	46	19331712.	66	18144608.	43	51958192.
2004	7228040.	7735232.	48	17618384.	71	6936907.	20	39518544.
2005	7410542.	7050124.	43	23776800.	86	37134704.	27	75372160.
2006	7609617.	6082785.	44	23373184.	77	11734301.	22	48799872.
2007	8359915.	6309981.	42	19754880.	64	3877593.	12	38302352.
2008	8637147.	14032047.	179	23318464.	146	62888960.	148	108876608.

TABLE 3 SYSTEM-LEVEL PERFORMANCE INDICATORS FOR UNLIMITED ANNUAL FUNDING ASSUMPTION CASES

Case 1

Economical Improvement; Acceptable Level of Service

END OF YEAR	AVERAGE CONDITION DECK	SUPER	SUB.	NMACR	AVG. SV POSTING	NSVA	NSVD	NLOSA	NLOSD	USER COST $MILLIONS
CURRENT	6.55	6.86	6.37	192	24.97	3234	8086	6697	11566	566.58
1989	7.18	7.46	7.10	0	28.51	1661	5131	3663	7952	61.93
1990	7.13	7.40	7.06	0	28.84	1489	4857	3380	7648	57.53
1991	7.07	7.33	7.02	0	29.12	1340	4613	3083	7340	53.05
1992	7.00	7.26	6.96	0	29.35	1247	4410	2855	7067	49.07
1993	6.95	7.21	6.93	0	29.59	1147	4212	2621	6814	42.97
1994	6.88	7.14	6.87	0	29.76	1105	4130	2468	6646	40.20
1995	6.92	7.17	6.93	0	30.22	882	3790	2014	6229	36.44
1996	6.96	7.19	6.99	0	30.62	690	3508	1628	5843	32.71
1997	6.99	7.21	7.03	0	30.97	494	3263	1289	5509	29.03
1998	7.01	7.21	7.06	0	31.24	364	3089	1054	5259	26.46
1999	6.98	7.18	7.05	0	31.42	284	2956	871	5049	23.99
2000	6.95	7.14	7.03	0	31.57	201	2854	702	4874	21.46
2001	6.91	7.09	6.99	0	31.65	150	2812	573	4753	20.24
2002	6.85	7.04	6.94	0	31.70	135	2798	505	4666	18.89
2003	6.80	6.99	6.90	0	31.75	117	2778	431	4580	17.60
2004	6.77	6.95	6.87	0	31.81	82	2740	355	4468	16.35
2005	6.72	6.91	6.83	0	31.84	82	2714	319	4396	15.43
2006	6.68	6.87	6.79	0	31.86	74	2695	275	4318	14.68
2007	6.62	6.82	6.74	0	31.87	82	2702	266	4283	14.05
2008	6.57	6.78	6.70	0	31.90	80	2697	246	4254	14.37

Case 2

Immediate Improvement; Acceptable Level of Service

END OF YEAR	AVERAGE CONDITION DECK	SUPER	SUB.	NMACR	AVG. SV POSTING	NSVA	NSVD	NLOSA	NLOSD	USER COST $MILLIONS
CURRENT	6.55	6.86	6.37	192	24.97	3234	8086	6697	11566	566.58
1989	7.78	7.97	7.78	0	31.30	27	3096	138	5290	36.75
1990	7.65	7.84	7.65	0	31.37	14	3014	103	5182	34.76
1991	7.53	7.71	7.53	0	31.41	10	2957	71	5091	32.53
1992	7.40	7.58	7.41	0	31.45	11	2897	51	4977	30.61
1993	7.30	7.49	7.32	0	31.48	15	2856	45	4907	25.70
1994	7.19	7.40	7.23	0	31.50	24	2863	44	4854	23.70
1995	7.13	7.33	7.17	0	31.55	24	2812	36	4761	22.47
1996	7.07	7.28	7.13	0	31.61	26	2771	35	4671	21.07
1997	7.02	7.22	7.09	0	31.65	17	2742	23	4583	19.49
1998	6.98	7.18	7.06	0	31.70	12	2707	20	4501	18.06
1999	6.91	7.12	7.00	0	31.73	20	2683	31	4432	17.20
2000	6.84	7.05	6.94	0	31.75	17	2677	29	4386	16.08
2001	6.76	6.97	6.87	0	31.76	9	2684	21	4356	15.76
2002	6.68	6.91	6.80	0	31.77	17	2696	25	4318	14.94
2003	6.62	6.84	6.74	0	31.78	22	2698	28	4275	14.18
2004	6.56	6.80	6.69	0	31.80	42	2677	49	4210	13.61
2005	6.51	6.74	6.64	0	31.84	66	2634	72	4138	13.12
2006	6.47	6.71	6.61	0	31.89	26	2574	31	4043	12.71
2007	6.40	6.65	6.55	0	31.91	71	2596	80	4042	12.29
2008	6.42	6.65	6.56	0	31.97	68	2600	76	4030	12.25

Case 3

Immediate Improvement; Desirable Level of Service

END OF YEAR	AVERAGE CONDITION DECK	SUPER	SUB.	NMACR	AVG. SV POSTING	NSVA	NSVD	NLOSA	NLOSD	USER COST $MILLIONS
CURRENT	6.55	6.86	6.37	192	24.97	3234	8086	6697	11566	566.58
1989	8.44	8.52	8.47	0	33.49	16	100	121	403	10.46
1990	8.26	8.35	8.30	0	33.52	7	60	89	292	9.09
1991	8.10	8.19	8.14	0	33.54	4	32	60	185	7.32
1992	7.93	8.03	7.98	0	33.56	1	11	35	117	6.64
1993	7.81	7.92	7.87	0	33.56	0	10	23	84	2.15
1994	7.70	7.82	7.76	0	33.57	2	26	17	77	0.87
1995	7.59	7.72	7.67	0	33.57	0	19	10	57	0.41
1996	7.49	7.64	7.58	0	33.57	2	28	9	60	0.36
1997	7.39	7.54	7.49	0	33.57	1	34	4	59	0.29
1998	7.29	7.46	7.40	0	33.57	1	30	4	49	0.18
1999	7.18	7.37	7.31	0	33.57	1	22	4	35	0.19
2000	7.09	7.28	7.21	0	33.57	0	27	3	39	0.09
2001	6.98	7.18	7.12	0	33.57	0	12	3	24	0.10
2002	6.87	7.10	7.03	0	33.57	0	24	3	37	0.09
2003	6.78	7.01	6.94	0	33.57	0	11	2	21	0.08
2004	6.68	6.92	6.85	0	33.57	0	8	2	19	0.08
2005	6.58	6.84	6.76	0	33.57	2	8	3	17	0.06
2006	6.48	6.76	6.67	0	33.57	0	6	0	16	0.03
2007	6.37	6.66	6.59	0	33.57	30	133	30	143	0.14
2008	6.34	6.63	6.56	0	33.57	7	102	7	116	0.03

NMACR	=	NUMBER OF BRIDGES WITH A CONDITION RATING LESS THAN THE MINIMUM ALLOWABLE CONDITION RATING, "4"
NSVA	=	NUMBER OF BRIDGES POSTED AT LESS THAN ACCEPTABLE
NSVD	=	NUMBER OF BRIDGES POSTED AT LESS THAN DESIRABLE
NLOSA	=	NUMBER OF BRIDGES WITH A LESS-THAN-ACCEPTABLE USER LEVEL OF SERVICE
NLOSD	=	NUMBER OF BRIDGES WITH A LESS-THAN-DESIRABLE USER LEVEL OF SERVICE

TABLE 4 BUDGET AND ACTION DISTRIBUTIONS UNDER LIMITED ANNUAL FUNDING ASSUMPTION CASES

Case 4

$60 million per year; Economical Improvement; Acceptable Level of Service

YEAR	ROUTINE MAINT. COST	MAJOR MAINT. COST	NO.	REHABILITATIONS COST	NO.	REPLACEMENTS COST	NO.	TOTAL YEARLY BUDGET
1989	7173180.	7392432.	130	10560176.	124	34872832.	184	59998608.
1990	7954772.	3663459.	47	12058970.	56	36322064.	124	59999264.
1991	8643612.	1908895.	36	1811465.	30	47635296.	118	59999264.
1992	9322319.	1938865.	28	12117855.	40	36620368.	88	59999392.
1993	9889559.	4657745.	85	12569841.	153	32880992.	179	59998128.
1994	10469515.	6957076.	108	10213602.	133	32358832.	201	59999008.
1995	11612815.	2968343.	46	9063271.	113	36354160.	208	59998576.
1996	12628462.	4099982.	39	9698856.	93	33570240.	204	59997536.
1997	13653629.	3975055.	30	7931333.	93	34434608.	233	59994608.
1998	14691874.	4137818.	74	11128765.	213	30039472.	199	59997904.
1999	15705378.	4445545.	77	10904580.	186	28942688.	195	59998176.
2000	17092848.	5927847.	100	9070261.	152	27900880.	198	59991824.
2001	18676896.	5086611.	72	9603459.	165	26618128.	182	59985088.
2002	20147856.	5220128.	76	8055802.	140	26555120.	185	59978896.
2003	21793184.	4164303.	61	8918457.	116	25091904.	178	59967808.
2004	23187936.	5001723.	57	9531038.	136	22245520.	151	59966192.
2005	24911824.	2688282.	45	9176861.	107	23184640.	146	59961584.
2006	26402448.	4444083.	55	7722696.	105	21388224.	139	59957440.
2007	27864400.	4065553.	55	7433537.	106	20592096.	136	59955584.
2008	29184160.	3498459.	53	7296580.	107	19969536.	121	59948720.

Case 5

$60 million per year; Immediate Improvement; Acceptable Level of Service

YEAR	ROUTINE MAINT. COST	MAJOR MAINT. COST	NO.	REHABILITATIONS COST	NO.	REPLACEMENTS COST	NO.	TOTAL YEARLY BUDGET
1989	7173180.	7392432.	130	10560176.	124	34872832.	184	59998608.
1990	7954772.	3663459.	47	12058970.	56	36322064.	124	59999264.
1991	8643612.	1908895.	36	1811465.	30	47635296.	118	59999264.
1992	9322319.	1938865.	28	12117855.	40	36620368.	88	59999392.
1993	9889559.	4657745.	85	12569841.	153	32880992.	179	59998128.
1994	10469515.	6957076.	108	10213602.	133	32358832.	201	59999008.
1995	11612815.	2968343.	46	9063271.	113	36354160.	208	59998576.
1996	12628462.	4099982.	39	9698856.	93	33570240.	204	59997536.
1997	13653629.	3975055.	30	7931333.	93	34434608.	233	59994608.
1998	14691874.	4137818.	74	11128765.	213	30039472.	199	59997904.
1999	15706162.	4581027.	76	10670266.	184	29040960.	196	59998400.
2000	17093984.	5931316.	101	9070261.	152	27898432.	198	59993984.
2001	18678144.	5086611.	72	9603459.	165	26648128.	182	59986336.
2002	20149104.	5220128.	76	8054486.	140	26555120.	185	59978832.
2003	21793744.	4164305.	61	8933127.	116	25075936.	178	59967088.
2004	23187872.	5099373.	58	9431856.	136	22245520.	151	59964608.
2005	24912672.	2688282.	45	9149842.	107	23210464.	146	59961248.
2006	26403616.	4444083.	55	7721380.	105	21388448.	139	59957520.
2007	27867136.	3950353.	54	7433151.	106	20701904.	137	59952528.
2008	29187792.	3498459.	53	7293958.	105	19970976.	121	59951168.

Case 6

$100 million per year; Immediate Improvement; Acceptable Level of Service

YEAR	ROUTINE MAINT. COST	MAJOR MAINT. COST	NO.	REHABILITATIONS COST	NO.	REPLACEMENTS COST	NO.	TOTAL YEARLY BUDGET
1989	6946043.	11109780.	130	15343713.	130	66598512.	262	99998032.
1990	7681723.	2381745.	45	10377024.	58	79557424.	206	99997904.
1991	8229275.	2155945.	41	13601678.	55	76009472.	231	99996368.
1992	8916991.	2323825.	30	11987707.	59	76768960.	209	99997472.
1993	9289178.	9580631.	111	22707456.	155	58420624.	269	99997888.
1994	9656729.	9072463.	120	15788903.	146	65479344.	325	99997424.
1995	10350127.	5852807.	80	27425872.	124	56389184.	245	99997984.
1996	11065676.	3921637.	69	38587664.	331	46420800.	231	99995776.
1997	11762377.	6529437.	77	13783308.	98	67922432.	308	99997536.
1998	12486888.	10483889.	154	26855616.	219	50169728.	315	99996112.
1999	13067825.	11787736.	103	28883424.	213	46255200.	303	99994176.
2000	13876480.	11585141.	104	13186708.	166	61344992.	420	99993512.
2001	14784690.	8459989.	85	15694221.	188	61054304.	346	99993184.
2002	15828223.	9645414.	89	13371290.	149	61147968.	375	99992880.
2003	16945616.	9578782.	82	16749520.	152	56722128.	328	99996032.
2004	17869712.	9900098.	81	14997986.	141	37222416.	294	99990208.
2005	18855072.	7214077.	64	21664480.	154	52252320.	262	99985936.
2006	19825280.	8429953.	63	17252240.	139	54472224.	233	99979696.
2007	20702672.	9355079.	70	21468608.	174	48450364.	217	99976736.
2008	21519888.	7352978.	61	22296240.	172	49004752.	193	99973856.

TABLE 4 (*continued*)

Case 7 $200 million per year; Economical Improvement; Acceptable Level of Service	YEAR	ROUTINE MAINT. COST	MAJOR MAINT. COST	NO.	REHABILITATIONS COST	NO.	REPLACEMENTS COST	NO.	TOTAL YEARLY BUDGET
	1989	6709899.	11789666.	131	22398336.	159	159097504.	521	199995392.
	1990	7296099.	2392983.	45	14409627.	116	175896848.	468	199995552.
	1991	7620156.	2121576.	38	19328048.	127	170924512.	675	199994288.
	1992	7985623.	2143363.	30	15820243.	110	174046672.	492	199995888.
	1993	7878643.	13729639.	115	42733712.	152	135452624.	302	199994608.
	1994	7964460.	11523774.	121	23220032.	157	157284672.	540	199992928.
	1995	8073357.	10568107.	88	26431664.	115	154923488.	357	199996528.
	1996	8361559.	9127456.	90	16696586.	114	165810768.	466	199996352.
	1997	8575208.	9438775.	69	19682064.	118	162298848.	580	199994880.
	1998	8741379.	18528768.	160	19893648.	170	152831456.	534	199995248.
	1999	8552481.	24884720.	209	60796800.	141	105759920.	375	199993920.
	2000	8410582.	31191472.	210	28469104.	157	131924320.	379	199995472.
	2001	8312836.	30742800.	206	30772592.	160	130165920.	394	199994144.
	2002	8335711.	24824784.	186	30311424.	137	136523536.	386	199995440.
	2003	8281142.	22392272.	172	36800512.	146	152518944.	347	199992864.
	2004	8188616.	21817072.	152	29656208.	114	140333600.	174	199995488.
	2005	8287672.	21855936.	139	19040384.	91	150813872.	181	199997856.
	2006	8201614.	23504464.	167	38609888.	185	129679168.	233	199995120.
	2007	8294037.	9158743.	88	35185264.	189	147356768.	225	199994800.
	2008	8024490.	22219072.	156	43408912.	135	126344688.	186	199997152.

Case 8 $200 million per year; Immediate Improvement; Acceptable Level of Service	YEAR	ROUTINE MAINT. COST	MAJOR MAINT. COST	NO.	REHABILITATIONS COST	NO.	REPLACEMENTS COST	NO.	TOTAL YEARLY BUDGET
	1989	6709899.	11789666.	131	22398336.	159	159097504.	521	199995392.
	1990	7296099.	2392983.	45	14409627.	116	175896848.	468	199995552.
	1991	7620156.	2121576.	38	19328048.	127	170924512.	675	199994288.
	1992	7986176.	2116710.	27	15845869.	111	174046672.	492	199995424.
	1993	7879054.	13729613.	114	42733712.	152	135452624.	302	199994992.
	1994	7964282.	11520317.	122	23225552.	158	157284672.	540	199994816.
	1995	8074061.	10563430.	86	26431664.	115	154926320.	357	199995472.
	1996	8362215.	9122578.	88	16696586.	114	165814816.	466	199996176.
	1997	8975537.	9449696.	71	19687400.	118	162201600.	581	199994320.
	1998	8741046.	18564256.	163	19859680.	168	152830160.	533	199995136.
	1999	8552056.	24890656.	211	60792752.	142	105759920.	375	199995376.
	2000	8410084.	31191472.	210	28469104.	157	131924320.	379	199994976.
	2001	8312114.	30749552.	207	30766400.	160	130165920.	394	199993904.
	2002	8335513.	24815080.	185	30417024.	138	136427888.	385	199995504.
	2003	8280881.	22393584.	172	38069920.	156	131251456.	341	199995040.
	2004	8216700.	21923328.	153	29864896.	116	139988704.	188	199993616.
	2005	8290277.	21847904.	140	23183520.	94	146676336.	170	199990032.
	2006	8363047.	13549777.	114	39151840.	172	138932592.	241	199997248.
	2007	8372266.	18031008.	131	32863488.	130	140724656.	194	199993600.
	2008	8152120.	22298768.	159	43507568.	132	126037232.	198	199995680.

Case 9 $400 million per year; Economical Improvement; Acceptable Level of Service	YEAR	ROUTINE MAINT. COST	MAJOR MAINT. COST	NO.	REHABILITATIONS COST	NO.	REPLACEMENTS COST	NO.	TOTAL YEARLY BUDGET
	1989	6323224.	11782886.	132	31683040.	258	350166272.	1094	399955200.
	1990	6607295.	2378051.	45	30067232.	266	360887296.	1401	399939840.
	1991	6027956.	14010448.	185	45506160.	237	334431232.	1045	399975680.
	1992	5397098.	13424122.	146	71831312.	246	248574896.	428	339227392.
	1993	5818429.	5122591.	58	18286080.	95	77712784.	265	106939872.
	1994	6149270.	5220405.	58	14561042.	84	67273568.	219	93204272.
	1995	6095660.	15799279.	167	38008960.	235	119632576.	425	179536464.
	1996	6029115.	18930224.	181	59773472.	234	117457840.	413	202190640.
	1997	5889749.	21822064.	175	79304432.	244	123270864.	394	230287104.
	1998	5687290.	17661408.	168	41492688.	253	143425120.	306	208266496.
	1999	5748438.	15165728.	152	39782608.	208	78470384.	224	139167152.
	2000	5673315.	18993840.	152	35496240.	187	92393840.	228	152557232.
	2001	5938534.	14726123.	126	28356896.	187	67500784.	142	116522356.
	2002	6150540.	13184694.	103	35706208.	156	65989616.	137	121031056.
	2003	6228328.	14132374.	127	41956128.	210	76482688.	110	138799504.
	2004	6389675.	13074331.	124	48164144.	226	50273408.	113	117901552.
	2005	6516185.	12586960.	125	60093120.	241	52666448.	95	131862704.
	2006	6541770.	15264622.	146	44425664.	217	50829344.	91	117061392.
	2007	6592551.	12535110.	103	46600608.	207	57030096.	93	122758352.
	2008	6780654.	11316391.	108	45037616.	230	21808768.	79	84943424.

Case 10 $400 million per year; Immediate Improvement; Acceptable Level of Service	YEAR	ROUTINE MAINT. COST	MAJOR MAINT. COST	NO.	REHABILITATIONS COST	NO.	REPLACEMENTS COST	NO.	TOTAL YEARLY BUDGET
	1989	6323224.	11782886.	132	31683040.	258	350166272.	1094	399955200.
	1990	6607295.	2378051.	45	30067232.	266	360887296.	1401	399939840.
	1991	6181279.	13999616.	184	29858672.	172	349934848.	1119	399974400.
	1992	5775728.	18185616.	155	68256000.	457	307747328.	1212	399964672.
	1993	5171684.	17677488.	169	102411376.	566	274723584.	779	399984128.
	1994	5108852.	6849685.	65	155090656.	334	133409488.	285	300458496.
	1995	5335529.	15799279.	167	15914826.	104	55672000.	136	92721616.
	1996	5402567.	18861088.	180	38523312.	138	56725168.	135	119512128.
	1997	5348337.	21954864.	176	32516192.	143	115447712.	153	175267104.
	1998	5467462.	17716208.	168	65136528.	183	72655552.	151	160975744.
	1999	5745587.	14990720.	151	30094016.	136	52339968.	104	103170080.
	2000	5773502.	18988224.	152	26981888.	135	56620192.	116	108363792.
	2001	6025087.	14453172.	117	24382416.	130	61712912.	84	106573584.
	2002	6117687.	13630078.	112	36077232.	132	66528960.	109	122353952.
	2003	6236061.	12923740.	121	36154384.	169	79400304.	91	134714480.
	2004	6348294.	13357929.	126	48078432.	203	40024400.	92	107809040.
	2005	6543085.	13291592.	128	45931296.	215	43699296.	81	109465264.
	2006	6649864.	14957370.	141	47621024.	195	39672768.	86	108901024.
	2007	6850516.	12541474.	106	48790128.	197	39720256.	73	107902368.
	2008	7117559.	11206768.	109	37687216.	208	22126368.	79	78137904.

TABLE 5   SYSTEM-LEVEL PERFORMANCE INDICATORS FOR LIMITED ANNUAL FUNDING ASSUMPTION CASES

Case 4

$60 million per year; Economical Improvement; Acceptable Level of Service

END OF YEAR	AVERAGE CONDITION DECK	SUPER	SUB.	NMACR	AVG. SV POSTING	NSVA	NSVD	NLOSA	NLOSD	USER COST $MILLIONS
CURRENT	6.55	6.86	6.36	192	24.97	3234	8087	6695	11567	566.60
1989	6.48	6.82	6.33	72	25.20	3167	7911	6441	11364	437.13
1990	6.37	6.73	6.24	40	25.30	3100	7798	6342	11282	412.50
1991	6.25	6.64	6.14	18	25.37	3099	7699	6238	11175	364.28
1992	6.13	6.54	6.02	10	25.39	3143	7666	6187	11097	357.48
1993	6.07	6.48	5.98	10	25.52	3166	7586	6002	10951	366.92
1994	6.01	6.43	5.93	192	25.70	3216	7602	5826	10780	382.71
1995	5.94	6.37	5.88	427	25.83	3255	7580	5689	10610	428.82
1996	5.87	6.30	5.82	663	25.95	3324	7580	5575	10476	452.11
1997	5.81	6.24	5.77	847	26.11	3363	7567	5447	10327	513.63
1998	5.77	6.21	5.74	993	26.18	3446	7606	5304	10226	562.20
1999	5.72	6.17	5.71	1639	26.21	3518	7612	5186	10085	598.56
2000	5.67	6.13	5.68	2280	26.23	3561	7603	5087	9937	645.81
2001	5.62	6.08	5.65	2866	26.22	3608	7606	4990	9810	707.03
2002	5.57	6.03	5.61	3375	26.21	3642	7581	4892	9669	765.80
2003	5.51	5.97	5.56	3808	26.18	3694	7602	4826	9550	817.98
2004	5.45	5.91	5.51	4111	26.10	3762	7694	4788	9492	902.02
2005	5.38	5.84	5.46	4346	26.03	3859	7785	4789	9427	973.67
2006	5.32	5.77	5.41	4546	25.95	3937	7909	4781	9395	1067.01
2007	5.26	5.70	5.37	4780	25.85	4005	7970	4789	9344	1159.89
2008	5.20	5.64	5.32	5009	25.72	4087	8068	4811	9319	1258.68

Case 5

$60 million per year; Immediate Improvement; Acceptable Level of Service

END OF YEAR	AVERAGE CONDITION DECK	SUPER	SUB.	NMACR	AVG. SV POSTING	NSVA	NSVD	NLOSA	NLOSD	USER COST $MILLIONS
CURRENT	6.55	6.86	6.36	192	24.97	3234	8087	6695	11567	566.60
1989	6.48	6.82	6.33	72	25.20	3167	7911	6441	11364	437.13
1990	6.37	6.73	6.24	40	25.30	3100	7798	6342	11282	412.50
1991	6.25	6.64	6.14	18	25.37	3099	7699	6238	11175	364.28
1992	6.13	6.54	6.02	10	25.39	3143	7666	6187	11097	357.48
1993	6.07	6.48	5.98	10	25.52	3166	7586	6002	10951	366.92
1994	6.01	6.43	5.93	192	25.70	3216	7602	5826	10780	382.71
1995	5.94	6.37	5.88	427	25.83	3255	7580	5689	10610	428.82
1996	5.87	6.30	5.82	663	25.95	3324	7580	5575	10476	452.11
1997	5.81	6.24	5.77	847	26.11	3363	7567	5447	10327	513.63
1998	5.77	6.21	5.74	993	26.18	3446	7606	5304	10226	562.20
1999	5.72	6.17	5.71	1639	26.21	3517	7611	5185	10084	598.56
2000	5.67	6.13	5.68	2280	26.23	3560	7602	5086	9936	645.81
2001	5.62	6.08	5.65	2866	26.23	3607	7605	4989	9809	707.03
2002	5.57	6.03	5.61	3375	26.21	3641	7580	4891	9668	765.80
2003	5.51	5.97	5.56	3808	26.18	3693	7601	4825	9549	817.68
2004	5.45	5.91	5.51	4111	26.10	3761	7695	4787	9491	901.72
2005	5.38	5.84	5.46	4345	26.03	3859	7784	4790	9427	973.68
2006	5.32	5.77	5.41	4545	25.95	3937	7909	4782	9396	1067.04
2007	5.26	5.70	5.37	4780	25.86	4004	7969	4789	9344	1159.67
2008	5.21	5.64	5.32	5009	25.72	4086	8067	4811	9319	1258.54

Case 6

$100 million per year; Immediate Improvement; Acceptable Level of Service

END OF YEAR	AVERAGE CONDITION DECK	SUPER	SUB.	NMACR	AVG. SV POSTING	NSVA	NSVD	NLOSA	NLOSD	USER COST $MILLIONS
CURRENT	6.54	6.87	6.36	193	24.97	3231	8085	6693	11567	566.56
1989	6.50	6.85	6.36	12	25.30	3099	7840	6362	11280	359.27
1990	6.41	6.78	6.28	2	25.47	3001	7659	6192	11115	272.59
1991	6.31	6.70	6.20	2	25.66	2934	7462	5977	10883	226.99
1992	6.22	6.63	6.12	2	25.81	2908	7331	5814	10671	206.07
1993	6.19	6.60	6.11	2	26.08	2815	7159	5505	10421	207.76
1994	6.18	6.57	6.11	63	26.44	2735	7006	5193	10123	212.59
1995	6.13	6.53	6.08	126	26.67	2700	6941	4965	9917	243.53
1996	6.11	6.51	6.07	232	26.82	2744	6915	4581	9634	250.87
1997	6.08	6.47	6.06	297	27.12	2693	6807	4350	9400	276.23
1998	6.10	6.48	6.09	372	27.41	2614	6697	4033	9164	335.73
1999	6.11	6.47	6.11	759	27.63	2603	6583	3843	8913	361.11
2000	6.14	6.49	6.16	1061	28.03	2446	6347	3573	8556	390.84
2001	6.16	6.50	6.19	1388	28.30	2346	6186	3339	8262	459.12
2002	6.17	6.49	6.22	1632	28.62	2192	5957	3098	7944	489.19
2003	6.18	6.49	6.24	1783	28.89	2094	5791	2896	7667	516.45
2004	6.17	6.48	6.25	1854	29.11	2048	5719	2763	7453	569.11
2005	6.17	6.46	6.26	1854	29.30	2018	5675	2640	7282	627.04
2006	6.15	6.43	6.25	1914	29.42	2025	5671	2586	7139	686.76
2007	6.14	6.41	6.25	1942	29.56	2006	5607	2506	6990	752.45
2008	6.12	6.39	6.24	2023	29.65	1985	5602	2433	6868	830.21

TABLE 5   (*continued*)

Case 7

$200 million per year; Economical Improvement; Acceptable Level of Service

END OF YEAR	AVERAGE CONDITION DECK	SUPER	SUB.	NMACR	AVG. SV POSTING	NSVA	NSVD	NLOSA	NLOSD	USER COST $MILLIONS
CURRENT	6.54	6.87	6.36	193	24.97	3231	8085	6693	11567	566.56
1989	6.56	6.90	6.42	2	25.56	2948	7624	6119	11012	229.11
1990	6.52	6.88	6.40	0	26.01	2719	7221	5676	10544	167.54
1991	6.54	6.90	6.44	0	26.72	2420	6610	5015	9819	122.00
1992	6.51	6.88	6.44	0	27.17	2245	6221	4583	9290	99.14
1993	6.48	6.85	6.43	0	27.49	2110	5998	4251	8994	94.84
1994	6.53	6.87	6.48	0	28.05	1910	5642	3782	8460	78.73
1995	6.51	6.85	6.49	0	28.39	1777	5452	3450	8128	83.13
1996	6.52	6.86	6.52	0	28.80	1626	5198	3096	7708	72.12
1997	6.57	6.89	6.58	0	29.32	1442	4835	2684	7179	69.98
1998	6.64	6.94	6.68	0	29.85	1170	4482	2222	6714	88.09
1999	6.67	6.95	6.72	0	30.23	972	4274	1893	6380	68.60
2000	6.71	6.97	6.77	0	30.62	756	4048	1568	6052	75.64
2001	6.75	7.00	6.83	1	30.94	577	3793	1262	5702	77.88
2002	6.79	7.01	6.88	2	31.24	411	3531	990	5357	64.13
2003	6.81	7.02	6.91	2	31.50	286	3321	734	5035	52.16
2004	6.77	6.97	6.87	1	31.60	262	3326	642	4926	52.28
2005	6.73	6.92	6.84	0	31.67	244	3313	566	4813	46.62
2006	6.73	6.92	6.84	0	31.76	214	3254	483	4652	48.23
2007	6.72	6.91	6.84	0	31.82	186	3153	420	4489	52.19
2008	6.69	6.89	6.82	0	31.88	157	3105	350	4357	53.67

Case 8

$200 million per year; Immediate Improvement; Acceptable Level of Service

END OF YEAR	AVERAGE CONDITION DECK	SUPER	SUB.	NMACR	AVG. SV POSTING	NSVA	NSVD	NLCSA	NLOSD	USER COST $MILLIONS
CURRENT	6.54	6.87	6.36	193	24.97	3231	8085	6693	11567	566.56
1989	6.56	6.90	6.42	2	25.56	2948	6119	11012		229.11
1990	6.52	6.88	6.40	0	26.01	2719	7221	5676	10544	167.54
1991	6.54	6.90	6.44	0	26.72	2420	6610	5015	9819	122.00
1992	6.51	6.88	6.44	0	27.17	2245	6221	4582	9289	99.14
1993	6.48	6.85	6.43	0	27.49	2110	5999	4250	8994	94.84
1994	6.53	6.87	6.48	0	28.05	1910	5643	3781	8460	78.74
1995	6.51	6.85	6.49	0	28.39	1777	5453	3449	8128	83.15
1996	6.52	6.86	6.52	0	28.80	1626	5199	3096	7708	72.13
1997	6.57	6.89	6.58	0	29.32	1442	4835	2683	7177	69.99
1998	6.64	6.94	6.68	0	29.84	1170	4483	2223	6715	88.10
1999	6.67	6.95	6.72	0	30.23	973	4275	1893	6382	68.61
2000	6.71	6.97	6.77	0	30.61	757	4049	1568	6054	75.65
2001	6.75	7.00	6.83	1	30.93	578	3794	1262	5703	77.89
2002	6.79	7.01	6.88	2	31.24	411	3532	989	5356	64.13
2003	6.81	7.02	6.91	2	31.49	285	3329	717	5029	50.32
2004	6.77	6.97	6.88	1	31.60	255	3320	617	4907	52.28
2005	6.73	6.92	6.84	0	31.67	241	3315	545	4801	46.77
2006	6.72	6.92	6.84	0	31.76	209	3259	460	4639	48.99
2007	6.69	6.89	6.81	0	31.82	175	3182	386	4500	49.96
2008	6.67	6.87	6.79	0	31.89	150	3126	319	4361	51.10

TABLE 5 (continued)

Case 9

$400 million per year; Economical Improvement; Acceptable Level of Service

END OF YEAR	AVERAGE CONDITION DECK	SUPER	SUB.	NMACR	AVG. SV POSTING	NSVA	NSVD	NLOSA	NLOSD	USER COST $MILLIONS
CURRENT	6.54	6.87	6.36	193	24.97	3231	8085	6693	11567	566.56
1989	6.69	7.02	6.55	0	26.17	2639	7132	5542	10376	149.00
1990	6.86	7.18	6.77	0	27.62	1986	5879	4244	8880	83.32
1991	7.01	7.29	6.96	0	28.76	1467	4940	3258	7756	58.52
1992	7.03	7.29	6.99	0	29.16	1247	4607	2835	7291	50.41
1993	6.96	7.22	6.94	0	29.41	1161	4404	2636	7033	46.33
1994	6.89	7.15	6.88	0	29.61	1093	4286	2472	6837	41.78
1995	6.92	7.18	6.94	0	30.05	876	3962	2036	6435	38.41
1996	6.97	7.19	6.99	0	30.45	694	3685	1670	6062	34.60
1997	7.00	7.21	7.04	0	30.83	499	3435	1310	5702	32.40
1998	7.02	7.21	7.06	0	31.09	368	3233	1069	5423	28.28
1999	7.00	7.18	7.06	0	31.28	285	3117	879	5212	26.17
2000	6.98	7.16	7.05	0	31.45	202	2986	706	4996	22.95
2001	6.93	7.11	7.01	0	31.53	155	2935	587	4864	21.54
2002	6.88	7.06	6.97	0	31.60	123	2898	499	4756	19.98
2003	6.84	7.01	6.93	0	31.65	112	2880	423	4659	19.10
2004	6.80	6.98	6.89	0	31.70	91	2846	359	4559	17.63
2005	6.75	6.94	6.86	0	31.73	96	2825	329	4484	16.25
2006	6.71	6.90	6.82	0	31.76	87	2803	291	4405	15.58
2007	6.66	6.86	6.77	0	31.78	91	2805	267	4351	14.66
2008	6.61	6.82	6.73	0	31.82	104	2775	253	4289	14.61

Case 10

$400 million per year; Immediate Improvement; Acceptable Level of Service

END OF YEAR	AVERAGE CONDITION DECK	SUPER	SUB.	NMACR	AVG. SV POSTING	NSVA	NSVD	NLOSA	NLOSD	USER COST $MILLIONS
CURRENT	6.54	6.87	6.36	193	24.97	3231	8085	6693	11567	566.56
1989	6.69	7.02	6.55	0	26.17	2639	7132	5542	10376	149.00
1990	6.86	7.18	6.77	0	27.62	1986	5879	4244	8880	83.32
1991	6.99	7.28	6.94	0	28.82	1474	4870	3212	7685	55.87
1992	7.21	7.44	7.18	0	30.25	716	3777	1690	6331	39.45
1993	7.56	7.55	7.36	0	31.17	178	3114	515	5405	31.57
1994	7.34	7.51	7.36	0	31.44	24	2943	44	4992	26.97
1995	7.26	7.44	7.29	0	31.50	14	2888	29	4886	26.04
1996	7.20	7.37	7.24	0	31.55	34	2858	44	4805	24.46
1997	7.15	7.32	7.20	0	31.61	28	2825	34	4699	22.69
1998	7.11	7.28	7.17	0	31.67	13	2759	21	4588	21.02
1999	7.04	7.21	7.11	0	31.70	19	2745	28	4511	20.25
2000	6.98	7.16	7.06	0	31.74	22	2706	33	4420	18.18
2001	6.91	7.09	6.99	0	31.75	20	2696	29	4361	17.35
2002	6.85	7.03	6.94	0	31.78	14	2695	19	4292	16.42
2003	6.79	6.97	6.89	0	31.80	15	2693	19	4235	15.54
2004	6.74	6.93	6.84	0	31.82	17	2671	25	4168	14.69
2005	6.68	6.88	6.80	0	31.84	30	2653	38	4115	14.04
2006	6.63	6.84	6.75	0	31.86	17	2625	27	4049	13.52
2007	6.57	6.79	6.70	0	31.88	26	2623	35	4008	12.75
2008	6.51	6.74	6.65	0	31.91	42	2596	49	3968	12.55

NMACR = NUMBER OF BRIDGES WITH A CONDITION RATING LESS THAN THE MINIMUM ALLOWABLE CONDITION RATING, "4"
NSVA = NUMBER OF BRIDGES POSTED AT LESS THAN ACCEPTABLE
NSVD = NUMBER OF BRIDGES POSTED AT LESS THAN DESIRABLE
NLOSA = NUMBER OF BRIDGES WITH A LESS-THAN-ACCEPTABLE USER LEVEL OF SERVICE
NLOSD = NUMBER OF BRIDGES WITH A LESS-THAN-DESIRABLE USER LEVEL OF SERVICE
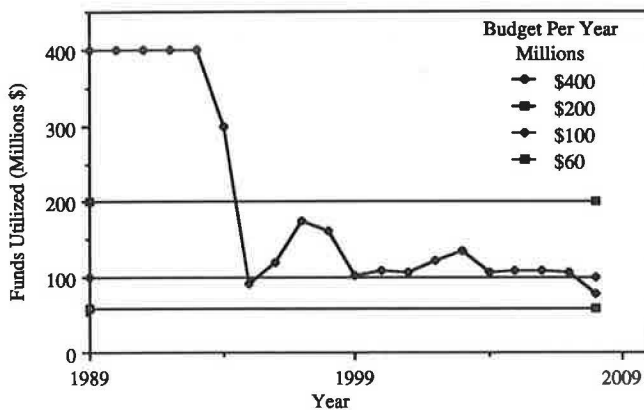
FIGURE 9   Funds of budget used per year.
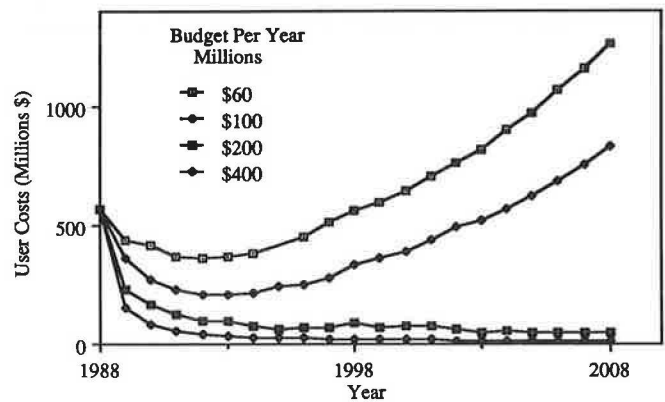
FIGURE 10   Budget impact on user costs.
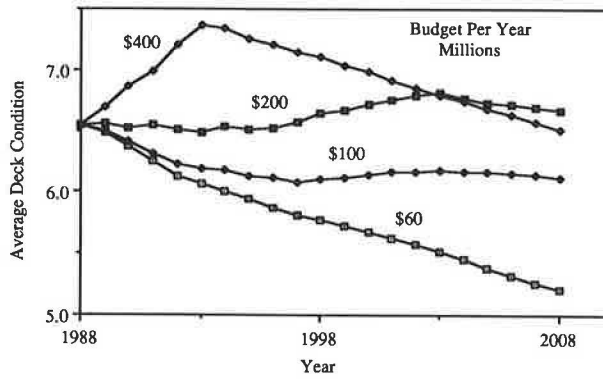
FIGURE 11 Budget impact on average deck condition.
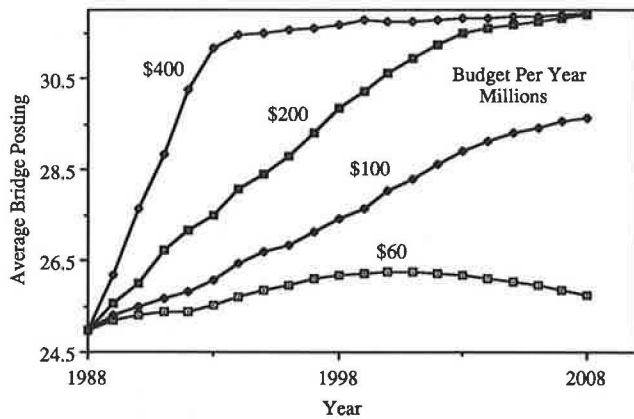
FIGURE 12 Budget impact on average bridge posting.

this reason, maximizing the EUAC reduction for improvement alternatives over routine maintenance is proposed for optimizing economic decisions at the system level.

5. A system-level optimization of bridge management decisions can be accomplished by 0–1 integer linear programming with multiple choice constraints.

6. The trial-and-error approach of OPBRIDGE allows managers to recognize the effect of their strategic user input on future budget needs and performance level of the bridge system. Revising user input is sometimes necessary to produce acceptable budgets and performance level.

7. The detailed bridge-by-bridge output provided by OPBRIDGE shows the status and actions recommended for first analysis year and major actions (replacement and reha-

bilitations) and their timings recommended thereafter for every bridge.

8. The tabular and graphical outputs provided by OPBRIDGE show funding needs or budget limits and the behavior of the state-wide, system-level performance indicators over the horizon. The outputs can be listed by federal- or non-federal-aid bridges and by state classification for primary, secondary, or urban system bridges.

9. The yearly county-by-county output provided by OPBRIDGE shows a list of bridges needing major actions (replacement and rehabilitation), cost of the major actions, and total funds needed for each county in the state. The total budget is also subdivided into federal-aid and state system funds. The county-by-county output is provided for each year up to the year ($\le$ horizon) specified by the user.

REFERENCES

1. C-J. Chen and D. W. Johnston. *Bridge Management Under a Level of Service Concept Providing Optimum Improvement Action, Time, and Budget Prediction.* Report FHWA/NC-88-004. FHWA, U.S. Department of Transportation, 1987.
2. D. W. Johnston and P. Zia. Level-of-Service System for Bridge Evaluation. In *Transportation Research Record 962*, TRB, National Research Council, Washington, D.C., 1984, pp. 1–8.
3. K. M. Isa Al-Subhi, D. W. Johnston, and F. Farid. *Optimizing System-Level Bridge Maintenance, Rehabilitation, and Replacement Decisions.* Report FHWA/NC/89-001. FHWA, U.S. Department of Transportation, 1989.

Resource-Constrained Capital Budgeting Model for Bridge Maintenance, Rehabilitation, and Replacement

KAMAL M. AL-SUBHI, DAVID W. JOHNSTON, AND FOAD FARID

A mathematical formulation is presented for optimal allocation of a granted budget among a system of bridges that are under the jurisdiction of a transportation agency. The formulation is based on a 0–1 integer-linear programming algorithm with multiple-choice constraints. Three improvement alternatives are assumed possible for a bridge at any point in time—replacement, rehabilitation, and major maintenance. Provision is also made for routine preventive maintenance. The optimal alternatives are selected on the basis of the criterion of maximizing reductions in equivalent uniform annual costs to the ultimate owner, the user-taxpayer.

A mathematical formulation is presented for optimal allocation of a granted budget among a system of bridges that are under the jurisdiction of an agency. The formulation is based on a 0–1 integer linear programming algorithm with multiple-choice constraints. The formulation is a part of Optimum Bridge Budget Forecasting and Allocation Module (OPBRIDGE), a computerized decision support system that was developed for the North Carolina Department of Transportation (NCDOT) for managing its 14,100-bridge system (1).

ANNUAL COST OF AN EXISTING BRIDGE

The annual cost of an existing Bridge i at the beginning of Year t, AMUC(i,t), consists of two types of costs: (a) annual user cost AURC(i,t), and (b) annual routine maintenance cost ARMC(i,t). These costs can be estimated by the methods developed by Chen and Johnston (2). Annual bridge user costs are caused by deficiencies related to narrow width, low vertical clearance, poor alignment, and low load capacity. Bridges having narrow width, low vertical clearance, or poor alignment have a higher accident-inducing probability. Bridges with low vertical clearance or low load capacity cause various proportions of vehicles to be detoured. As the volume of traffic increases, the number of accidents and detours also increases. Thus, the annual user cost increases over time because of continuous increase in average daily traffic, ADT(i,t), and continuous decline in bridge load capacity.

K. M. Al-Subhi, Construction Engineering and Management, King Fahd University of Petroleum and Minerals, Box 1468, Dhahran, Saudi Arabia 31261. D. W. Johnston and F. Farid, Department of Civil Engineering, North Carolina State University, Raleigh, N.C. 27695–7908.

The sum of the annual routine maintenance costs of the bridge components (e.g., deck, superstructure, and substructure) constitutes the total annual routine maintenance cost needed by a particular bridge. Annual routine maintenance cost also increases over time because of deterioration of element conditions. The resulting annual cost of an existing bridge because of user costs and routine maintenance costs increases with time as shown in Figure 1.

COST PARAMETERS FOR IMPROVEMENT ALTERNATIVES

Three types of improvement alternatives are usually available for a bridge: replacement, rehabilitation, and major maintenance. This section describes methods available to estimate their initial costs, IC(i,j,t), and their equivalent uniform annual costs, EUAC(i,j,t):

$$IC(i,j,t) = \text{initial cost of Improvement Alternative } j \text{ for Bridge } i \text{ at the beginning of Year } t; \text{ and}$$

$$EUAC(i,j,t) = \text{equivalent uniform annual cost of improvement alternative } j \text{ for Bridge } i \text{ at the beginning of Year } t.$$

Following the methods proposed in the literature (2–4), cost profiles of the different alternatives can be developed.

New Bridge Alternative

The first alternative is to replace the existing bridge with a new one having new condition ratings and desirable user levels of service. Conditions of various elements of a new bridge gradually deteriorate with age causing maintenance needs to increase over time. A major rehabilitation is assumed when one of the condition ratings drops below the minimum allowable condition rating. The rehabilitation alternative improves condition ratings to the highest rehabilitation condition ratings, and might improve load capacity, vertical clearance, and width of the bridge. As a result of rehabilitation, the service life of the bridge is extended for a few more years during which routine maintenance is needed.

NCDOT uses the following equations to estimate the initial cost, IC(i,NB,t), of a new bridge alternative for any existing Bridge i at the beginning of Year t (2):
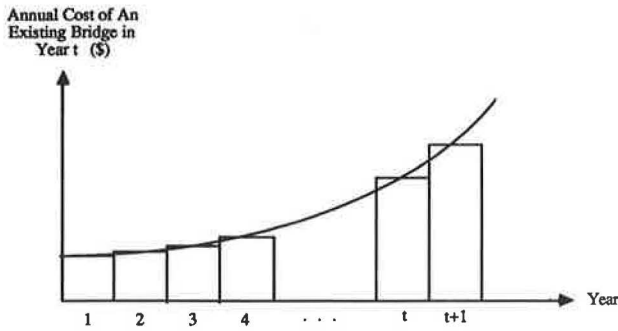
FIGURE 1 Annual cost of an existing bridge estimated discretely at the beginning of every year in the analysis horizon.

$$BASCOS(i,t) = NBLEN(i,t) * NBWID(i,t)$$
$$* UCDK(t) \qquad (1)$$

$$IC(i,NB,t) = BASCOS(i,t) * (1 + DESFEE/100)$$
$$+ FIXCOS(t) \qquad (2)$$

where

$BASCOS(i,t)$ = basic construction cost of the new bridge that will replace existing Bridge i at the beginning of Year t;

$NBLEN(i,t)$ = length (ft) of the new bridge to replace existing Bridge i at the beginning of Year t;

$NBWID(i,t)$ = width (ft) of the new bridge to replace existing Bridge i at the beginning of Year t;

$UCDK(t)$ = unit cost per deck area ($/ft²) of constructing a new bridge at the beginning of Year t;

$DESFEE$ = estimated design fee percentage; and

$FIXCOS(t)$ = fixed cost associated with new bridge construction at the beginning of Year t.

The cost profile for one replacement cycle of a new bridge is shown in Figure 2. The replacement cycle cost, $RCC(i,NB,t)$, of a new bridge alternative for bridge i at the beginning of Year t can be expressed as
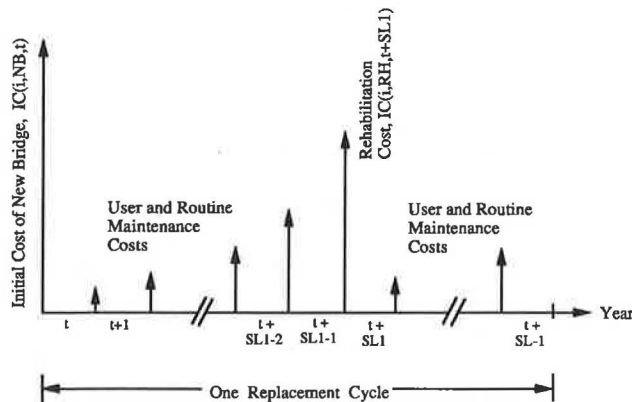
FIGURE 2 Cost profile for one replacement cycle.

$$RCC(i,NB,t) = IC(i,NB,t)$$
$$+ \sum_{tt=t}^{t+SL-1} [AMUC(i,tt)]$$
$$* (P/F,RRRR,tt-t)$$
$$+ IC(i,RH,t+SL1)$$
$$* (P/F,RRRR,SL1) \qquad (3)$$

where

$AMUC(i,tt)$ = annual routine maintenance and user costs of Bridge i at the beginning of Year tt;

$IC(i,RH,t + SL1 + 1)$ = initial cost of rehabilitation alternative for Bridge i at the beginning of year $(t + SL1 + 1)$;

$(P/F,RRRR,tt-t)$ = single-payment present-value factor;

$RRRR$ = real required rate of return;

$SL1$ = expected service life from new construction to rehabilitation; and

SL = expected service life of the bridge.

The initial cost, $IC(i,RH,t)$, of the rehabilitation alternative for Bridge i at the beginning of any Year t can be computed as

$$IC(i,RH,t) = \sum_{k=1}^{N} RHC(i,k,t) \qquad (4)$$

where $RHC(i,k,t)$ is the rehabilitation cost for Element Type k of Bridge i at the beginning of Year t and N is the total number of bridge components that may need rehabilitation (deck, superstructure, and substructure).

The equivalent uniform annual cost, $EUAC(i,NB,t)$, of the new bridge alternative for Bridge i, constructed at the beginning of Year t, over its service life can be estimated as

$$EUAC(i,NB,t) = RCC(i,NB,t) * (A/P,RRRR,SL) \qquad (5)$$

where $(A/P,RRRR,SL)$ is the capital recovery factor.

Because bridge service is assumed to be always required, the replacement cycle cost, $RCC(i,NB,t)$, would be repeated at SL intervals. The cost profile for repeated replacement cycles in perpetuity (i.e., forever) is shown in Figure 3. Thus,
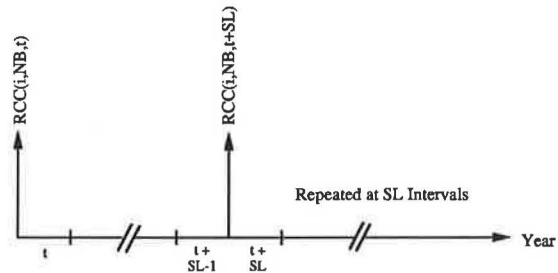
FIGURE 3 Life-cycle cost of the new bridge alternative in perpetuity.

the life cycle cost, LCC(i,NB,t), of the new bridge alternative in perpetuity for Bridge i at the beginning of Year t can be expressed as

$$\text{LCC}(i,\text{NB},t) = \frac{\text{RCC}(i,\text{NB},t)}{1 - (1 + \text{RRRR})^{-\text{SL}}} \qquad (6)$$

Rehabilitation Alternative

The second improvement alternative may be to rehabilitate the bridge. Rehabilitation may extend the life of the bridge by several years. Rehabilitation upgrades all bridge element conditions to a desirable rehabilitation condition rating. Thus, the extended service life E is estimated as the number of years until one of the condition ratings drops below the minimum allowable condition rating. At the end of the extended service life E, a new bridge is constructed to replace the rehabilitated bridge.

The life cycle cost, LCC(i,RH,t), of a rehabilitation alternative in perpetuity for Bridge i at the beginning of Year t (Figure 4), can be computed as

$$\text{LCC}(i,\text{RH},t) = \text{IC}(i,\text{RH},t)$$
$$+ \sum_{tt=t}^{t+E-1} \text{AMUC}(i,tt) * (\text{P/F,RRRR},tt - t)$$
$$+ \text{LCC}(i,\text{NB},t+E) * (\text{P/F,RRRR},E) \qquad (7)$$

Therefore, the equivalent uniform annual cost, EUAC(i,RH,t), of a rehabilitation alternative for Bridge i in perpetuity estimated at the beginning of Year t, is

$$\text{EUAC}(i,\text{RH},t) = \text{LCC}(i,\text{RH},t) * \text{RRRR} \qquad (8)$$

Major Maintenance Alternative

The third improvement alternative is major maintenance, which has also been termed an "interim rehabilitation" by Chen and Johnston (2). The intent is to improve the element in poor condition to a higher condition level compatible with the good elements as shown in Figure 5. All major maintenance cost parameters are estimated from the rehabilitation tables. However, its funding often comes from the maintenance budget.
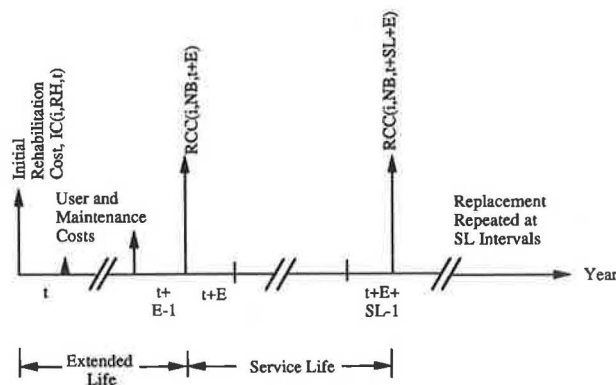
FIGURE 4 Life-cycle cost of the rehabilitation alternative in perpetuity.
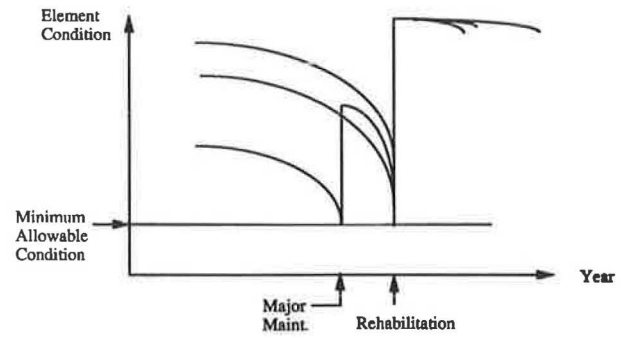
FIGURE 5 Major maintenance evaluation.

Following the approach of Chen and Johnston (2), one of two mutually exclusive cases is assumed:

● Case 1—If only one condition rating is less than 6, and the difference between the average of the two higher condition ratings and the lowest condition rating is greater than or equal to 2 points, then rehabilitate the bridge element with the lowest condition rating to the average of the other two higher ratings; or
● Case 2—If only one condition rating is greater than or equal to 6, and the difference of this highest condition and the lowest condition is greater than or equal to 2 points, then rehabilitate the bridge elements with the lowest two condition ratings to the single highest condition rating.

The extended service life produced by a major maintenance action, e, is assumed to be followed by a rehabilitation. Therefore, the equivalent uniform annual cost, EUAC(i,MN2,t), of a major maintenance alternative (MN2) for Bridge i at the beginning of Year t can be computed as

$$\text{EUAC}(i,\text{MN2},t) = [\text{IC}(i,\text{MN2},t)$$
$$+ \sum_{tt=t}^{t+e-1} \text{AMUC}(i,tt)$$
$$* (\text{P/F,RRRR},tt - t)$$
$$+ \text{LCC}(i,\text{RH},t+e) * (\text{P/F,RRRR},e)]$$
$$* \text{RRRR} \qquad (9)$$

REDUCTION IN EQUIVALENT UNIFORM ANNUAL COST

At the beginning of every year in the analysis horizon, the following question needs to be answered for every bridge: "Will the bridge be routinely maintained and retained in service for one more year, or will it be replaced, rehabilitated, or maintained with a major-maintenance alternative?"

At the bridge level and under unlimited budget assumption, the annual cost of the existing bridge, AMUC(i,t), is compared with the equivalent uniform annual cost, EUAC(i,j,t), of the three Improvement Alternatives j: major maintenance, rehabilitation, and replacement. The alternative with the minimum annual cost is selected (Figure 6).

The procedure suggested by Blank and Tarquine (5) requires that the equivalent uniform annual cost of routine maintenance over the remaining life of the existing bridge be
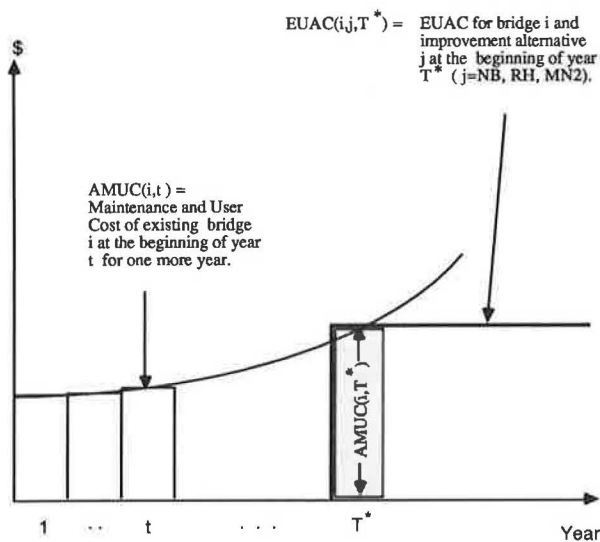
FIGURE 6   Comparison of AMUC(i,t) and EUAC(i,j,t) at the beginning of every year in the analysis horizon to determine optimal time for improving existing bridge.

computed and compared with EUAC(i,j,t) of other improvement alternatives, if AMUC(i,t) is greater than EUAC(i,j,t). However, this procedure is not necessary in this problem because it is always true that after T^*, AMUC(i,t) is smaller than the equivalent uniform annual cost of the routine maintenance alternative over the remaining life of the existing bridge. This could be concluded from the continuous increase in the annual cost of the existing bridge, as shown in Figure 1.

Minimizing EUAC(i,j,t) or AMUC(i,t) does not necessarily produce the optimal solution at the system level and under budgetary constraints, as can be concluded from the following example.

EXAMPLE

At the beginning of Year t, assume that two bridges have two alternatives, routine maintenance or replacement with a new bridge (NB), with the following values:

Bridge	AURC(i,t) ($)	ARMC(i,t) ($)	AMUC(i,t) ($)	EUAC(i,NB,t) ($)
1	30,000	1,000	31,000	15,000
2	21,000	500	21,500	15,000

Assume that the cost of replacing a bridge is the same for each. Further, assume that there is enough budget to replace only one bridge. Both bridges have a replacement alternative with the same minimum EUAC(i,NB,t), but only one of the two bridges can be replaced. To solve the problem, the analysis process computes reductions (savings) in annual costs as follows:

$$REUAC(i,j,t) = AMUC(i,t) - EUAC(i,j,t) \qquad (10)$$

where REUAC(i,j,t) is the reduction in EUAC for Bridge i produced by Improvement Alternative j at the beginning of Year t, and then maximizes the total amount of these reductions in annual cost under various constraints such as funding available for bridge improvements. Thus, in the example

for Bridge 1,

$$REUAC(1,NB,t) = \$31{,}000 - \$15{,}000 = \$16{,}000$$

and for Bridge 2,

$$REUAC(2,NB,t) = \$21{,}500 - \$15{,}000 = \$6{,}500$$

Bridge 1 should be selected because the reduction in user and agency costs will be greater than that for Bridge 2 for the same equivalent annual investment.

If REUAC(i,j,t) is negative in Equation 10, the routine maintenance alternative for Bridge i at the beginning of Year t is the optimum action (Figure 6). However, if the bridge is deficient with respect to the user level-of-service goals (6), a Major Improvement j for Bridge i at the beginning of Year t with a negative REUAC(i,j,t) can be selected if an immediate improvement for deficient bridges is requested by the decision maker and the budget is enough to allow such a selection.

It is important to understand the reasons for including AMUC(i,t) in Equation 10. AMUC(i,t) includes both current annual user and routine maintenance costs. Current annual user cost is included because users are the ultimate owners of the bridges. Current annual routine (preventive) maintenance cost is included because routine maintenance protects the bridge system against accelerated deterioration. Routine maintenance is generally recommended by modern maintenance systems for many types of facilities and plants. More importantly, all cost and deterioration tables were estimated on the basis of the assumption that routine maintenance is provided for all bridges.

The traffic parameters, cost factors, and deterioration relationships developed by Chen and Johnston (2) are used to estimate the initial and equivalent uniform annual costs (1).

MATHEMATICAL FORMULATION

The optimization problem, formulated at the beginning of every year in the analysis horizon, is a 0–1 integer linear programming algorithm with multiple-choice constraints, also called generalized upper bound (GUB) constraints. For every Year t in the analysis horizon, H, the yearly budgets are optimally allocated by maximizing the overall reductions in equivalent uniform annual costs.

$$\text{Maximize} \sum_{i=1}^{N_b} \sum_{j=1}^{NALT(i,t)} REUAC(i,j,t)\, X(i,j,t) \qquad (11)$$

subject to the following constraints:

1. Total budget constraint:

$$\sum_{i=1}^{N_b} \sum_{j=1}^{NALT(i,t)} IC(i,j,t)\, X(i,j,t) \le B(t,TOTAL) \qquad (12)$$

2. Maintenance budget constraint:

$$\sum_{i=1}^{N_b} IC(i,MN2,t) X(i,MN2,t) \le B(t,MN) \qquad (13)$$

3. Rehabilitation budget constraint:

$$\sum_{i=1}^{N_b} IC(i,RH,t)X(i,RH,t) \le B(t,RH) \qquad (14)$$

4. New bridge budget constraint:

$$\sum_{i=1}^{N_b} IC(i,NB,t)X(i,NB,t) \le B(t,NB) \qquad (15)$$

5. User level-of-service goals constraint:

$$LOS(i,g,t) + \sum_{j=1}^{NALT(i,t)} D(i,j,g,t)X(i,j,t) \ge MINREQ(1)$$

for $i = 1, 2, \ldots, N_b$ and

$$g = 1, 2, \ldots, N_g \qquad (16)$$

6. Minimum allowable condition rating constraint:

$$CR(i,c,t) + \sum_{j=1}^{NALT(i,t)} G(i,j,c,t)X(i,j,t) \ge MINREQ(2)$$

for $i = 1, 2, \ldots, N_b$ and

$$c = 1, 2, \ldots, N_c \qquad (17)$$

7. Multiple-choice decision variable constraint:

$$\sum_{j=1}^{NALT(i,t)} X(i,j,t) \le 1 \qquad for\ i = 1, 2, \ldots, N_b \qquad (18)$$

8. Decision variable constraint:

$$X(i,j,t) = 0,1 \qquad for\ i = 1, 2, \ldots, N_b\ and$$

$$j = 1, 2, \ldots NALT(i,t) \qquad (19)$$

where

N_b = number of bridges in the system;
$NALT(i,t)$ = number of improvement alternatives for Bridge i in Year t, or number of improvement alternatives in the ith GUB constraint for Year t, normally three, the new bridge (NB) alternative, major maintenance alternative (MN2), and rehabilitation (RH) alternative;
$REUAC(i,j,t)$ = reduction in equivalent uniform annual cost for Improvement Alternative j, Bridge i, and Year t, computed by Equation 10;
$X(i,j,t)$ = decision variable for Bridge i, Alternative j, and Year t. It is 1 if the alternative is selected and 0 otherwise;
$IC(i,j,t)$ = initial cost for Alternative j, Bridge i, and Year t;
$B(t,TOTAL)$ = total budget for Year t;
$B(t,MN)$ = budget for maintenance activities in Year t;
$B(t,RH)$ = budget for rehabilitation activities in Year t;
$B(t,NB)$ = budget for new bridge activities in Year t;
$LOS(i,g,t)$ = level of service of Bridge i with respect to Goal g at the beginning of Year t;
$D(i,j,g,t)$ = gain in level of service of Bridge i with respect to Goal g if Alternative j is selected for implementation during Year t;
$MINREQ(1)$ = user level-of-service goal selected as a part of the minimum performance requirements to be either (a) acceptable or (b) desirable;
N_g = number of user level-of-service bridge attributes measured on the scale of MINREQ(1), normally four, consisting of load capacity, clear deck width, vertical roadway underclearance, and vertical roadway overclearance;
$CR(i,c,t)$ = condition rating of Component c of Bridge i at the beginning of Year t;
$G(i,j,c,t)$ = gain in condition rating of Component c of Bridge i if Alternative j is selected for implementation during Year t;
$MINREQ(2)$ = minimum allowable condition rating; and
N_c = number of major bridge components, normally three, consisting of deck, superstructure, and substructure.

Budgets can be granted, limited, or unlimited maximum allowable budgets. The following actions are performed as parts of the problem preprocessing in order to simplify the problem solution:

1. Constraints 12 through 15 are eliminated if no budgetary constraints are imposed.
2. Constraint 12 is eliminated if the total budget is distributed by maintenance, rehabilitation, and replacement activities, because $B(t,TOTAL) = B(t,MN) + B(t,RH) + B(t,NB)$.
3. Constraints 13 through 15 are eliminated if the total budget is not distributed.
4. Constraints 16 and 17 are satisfied by including only improvement alternatives that can satisfy the minimum performance requirements.

The mathematical formulation of OPBRIDGE shows that the optimization is performed for each year independently.

ROUTINE MAINTENANCE: THE BASE ALTERNATIVE

The routine-maintenance alternative is considered to be essential, because it protects the bridges from accelerated deterioration. In a particular year, the load capacity deterioration and condition rating deterioration of those bridges that are not routinely maintained are accelerated by a multiplying factor of D_f ($D_f > 1.0$) compared with a factor of 1.0 for bridges that are routinely maintained. For this reason, routine maintenance is considered the base alternative that is provided if a major improvement alternative is not

economical, not enforced by requesting immediate improvement for deficient bridges, or not possible because of budget limitation.

However, there are two cases in which only part of the routine maintenance is provided: (a) the budget can be entered as a distributed budget in which the maintenance budget is not large enough to perform all the routine maintenance required; and (b) the budget can be entered as a total budget that is not large enough to perform all the necessary routine maintenance. Of course, no major improvement alternative can be considered for any bridge in the second case. To make the routine maintenance alternative the base alternative in the mathematical formulation, four steps are needed:

1. An initial sharing routine-maintenance factor, FACMN1, is computed as follows:

$$FACMN1 = Minimum\ (BA/BR,\ 1.0) \tag{20}$$

where BA is the budget available for routine maintenance and BR is the budget required adopting the routine maintenance alternatives for all bridges.

2. Each bridge is provided with an amount of routine maintenance dollars in Year t, AMCP(i,t), equal to FACMN1 multiplied by the routine maintenance dollars the particular bridge needs in Year t, AMC(i,t), that is,

$$AMCP(i,t) = FACMN1 * AMC(i,t) \tag{21}$$

3. The following variables are redefined in this formulation. If the budget is distributed,

$$IC(i,MN2,t) = IC(i,MN2,t) - AMCP(i,t) \tag{22}$$

$$B(t,MN) = B(t,MN) - BP(t,MN1) \tag{23}$$

If the total budget is used,

$$IC(i,MN2,t) = IC(i,MN2,t) - AMCP(i,t) \tag{24}$$

$$IC(i,RH,t) = IC(i,RH,t) - AMCP(i,t) \tag{25}$$

$$IC(i,NB,t) = IC(i,NB,t) - AMCP(i,t) \tag{26}$$

$$B(t,TOTAL) = B(t,TOTAL) - BP(t,MN1) \tag{27}$$

where

$$BP(t,MN1) = \sum_{i=1}^{N_b} AMCP(i,t) \tag{28}$$

4. After the problem is solved, certain bridges might be recommended for improvement alternatives. Therefore, if FACMN1 < 1, the routine maintenance budget is reallocated among those bridges that were not selected for an improvement alternative.

The deterioration multiplying factor, D_f, is evaluated as follows:

$$D_f = 1.0 + 0.2 * (1.0 - FACMN1) \tag{29}$$

In Equation 29, the constant 0.2 is assumed to be the factor for deteriorating bridges if no routine maintenance is provided at all (i.e., a 20 percent increase in deterioration rate). If a bridge is provided with all the routine maintenance budget required (i.e., if FACMN1 equals 1.0), then D_f will also equal 1. On the other hand, if a bridge is provided with only 60 percent of the routine maintenance required, D_f will equal 1.08. Further, if routine maintenance is provided for a bridge during a certain year, the bridge load capacity and condition ratings at the end of the year are computed as follows:

$$CE = CB - DY * D_f \tag{30}$$

where

CE = load capacity or condition ratings at the end of the year;

CB = load capacity or condition ratings at the beginning of the year;

DY = deterioration of the load capacity or condition ratings during the year; and

D_f = deterioration factor computed from Equation 29.

APPROACH OVER HORIZON

The analysis is illustrated by the flowchart in Figure 7. The sequence of events is as follows:

1. The user enters budgets, objectives, and policies;
2. OPBRIDGE extracts data from the bridge data base and the cost and parameter file;
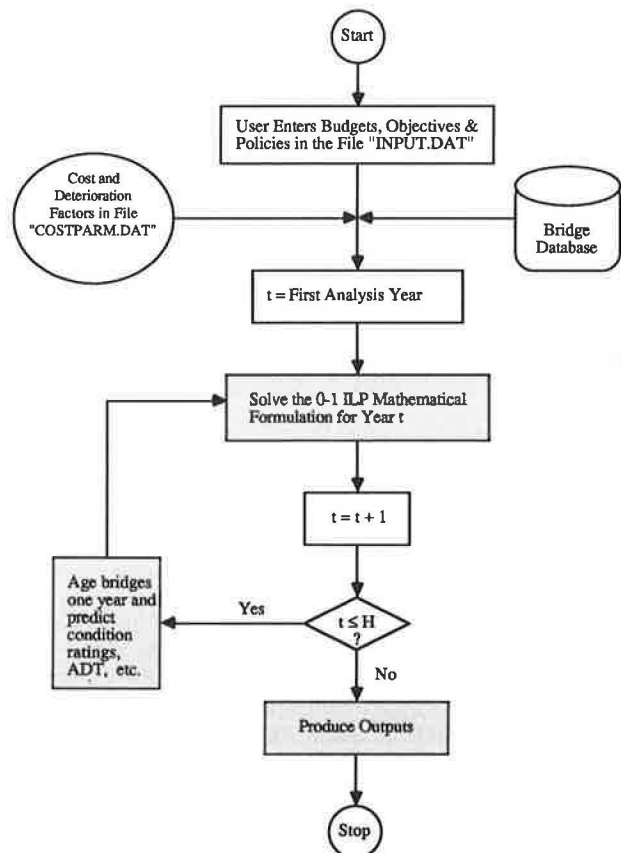
FIGURE 7 Flowchart for OPBRIDGE analysis.

3. OPBRIDGE optimizes decisions for every year in the analysis horizon. At the end of every year, OPBRIDGE ages the bridges 1 year and predicts condition ratings, ADT values, etc., allowing the system to do the analysis for the next year; and

4. Finally, OPBRIDGE produces detailed bridge-by-bridge output showing recommended current and future major actions, county-by-county output showing costs of major actions and budget required for each county, and tabular and graphical outputs showing future performance levels of the bridge system over the horizon, H.

SOLVING THE YEARLY BRIDGE OPTIMIZATION PROBLEM

The number of structures in North Carolina is almost 17,000. Approximately 2,600 pipes and culverts and 300 nonowned structures are not covered, leaving roughly 14,100 state-owned bridges. OPBRIDGE provides four possible actions per bridge—routine maintenance, major maintenance, rehabilitation, and replacement. Routine maintenance is the base alternative that is provided if other alternatives are not economical, are not enforced, or the budget is limited. Hence, there are a maximum of $14,100 * 3 = 42,300$ 0–1 decision variables. An average problem would have 25,000 to 30,000 0–1 decision variables. The numbers of constraints are as follows: (a) 14,100 multiple-choice constraints, one for each bridge; and (b) 3 or 1 budget requirement constraints, depending on whether or not the total budget is distributed, respectively. For the current state of the art in 0–1 integer linear programming, this problem is considered to be large.

The general-purpose branch-and-bound method, enumeration method, and cutting-planes method can solve only small to medium-sized (30 to 100 variables) 0–1 integer linear programming problems. If the number of variables and constraints becomes large (more than 100), then these methods become inefficient and in most cases even a good feasible solution (near optimal) may not be obtained (7).

Dynamic programming has also been used for solving the problem. However, dynamic programming, although fine for smaller problems (less than 50 variables), experiences degradation in efficiency as problem size increases (8).

For an algorithm to solve a large-scale knapsack problem, it should

1. Take advantage of the special structure of the problem;
2. Terminate in a finite number of steps—if it does not, then it should be able to generate a good feasible solution from the partial solution; and
3. Have reasonable computer storage requirements.

Nauss' algorithm and Ahmed's algorithm have been reported to satisfy these requirements. Nauss' algorithm uses branch and bound and an iterative procedure to calculate the optimum value of Lagrangian multiplier for arriving at an optimal solution of a knapsack problem with only one resource constraint (8). Ahmed mentioned that Nauss' algorithm is the most efficient algorithm developed to date for this type of problem (7, p. 13).

However, the knapsack formulation of the bridge problem has more than one resource constraint. Ahmed's algorithm initially uses the effective gradient concept by Senju and Toyoda (9) to solve a knapsack problem with more than one resource constraint (7). Senju and Toyoda (9) used the concept of effective gradient to design an algorithm for solving the multiconstrained knapsack problem. Briefly, the algorithm starts with an infeasible solution to the problem. It then computes the effective gradient of each variable whose value is equal to one (i.e., the variables that are in the solution). The variable with the smallest effective gradient is deleted and set equal to zero. The process is then repeated until feasibility is achieved. The whole procedure can then be repeated with the remaining (unused) capacities of the constraints. For details of this algorithm, see Senju and Toyoda (9). Ahmed (7) uses the concept of effective gradient to obtain an initial feasible solution for the 0–1 multiconstrained knapsack problem. Starting with this feasible solution, the algorithm switches to a ratio ranking procedure to tune in the solution, hence, hopefully obtaining a better feasible solution.

Senju and Toyoda (9, pp. B-196–B-207) proved numerically that the effective gradient concept can be applied satisfactorily for solving 0–1 integer linear programming problems. Ahmed (7, p. 51) tested his algorithm against another code, ILL1P–2, using 13 randomly generated test problems. The ILL1P–2 code uses the branch and bound and implicit enumeration technique. Therefore, the test problems were kept moderate in size so that the ILL1P–2 code can be applied. The ILL1P–2 code showed an average improvement of 0.258 percent in objective function values, compared to Ahmed's algorithm, which is insignificant for all practical purposes.

The algorithm was tested for use in OPBRIDGE and proved satisfactory for problems with a small number of bridges and alternatives. A problem with 25 bridges and approximately 3 alternatives each under a budgetary constraint was optimally solved by Farid et al. (4). Ahmed's algorithm (7) solved the same problem and achieved an objective function value of only 0.49 percent less than that of the optimum solution. The steps of Ahmed's algorithm (7) and the modifications made to speed up the process are described by Al-Subhi et al. (1).

SUMMARY AND CONCLUSIONS

A system-level optimization of bridge management decisions can be accomplished by 0–1 integer linear programming with multiple-choice constraints. Furthermore, the optimization is based on the objective of reducing overall costs to the ultimate owner, the user-taxpayer, the most defendable approach. Three improvement alternatives are assumed possible for a bridge at the beginning of every year—replacement, rehabilitation, and major maintenance. Routine maintenance, if provided, is assumed to protect the bridge against accelerated deterioration in varying degrees, but it does not raise the bridge condition ratings or user level of service. Two alternatives for two different bridges may have the same EUAC value. But, their impacts on reducing the current bridge annual maintenance and user costs are usually different. For this reason, maximizing the EUAC reduction for improvement alternatives over routine maintenance is used for optimizing economic decisions at the system level. The algorithm was programmed as OPBRIDGE and made operational at NCDOT

as part of its decision support system. Analysis results for the North Carolina bridge inventory have been determined (*1*) and used to support funding requests.

ACKNOWLEDGMENTS

REFERENCES

1. K. M. Isa Al-Subhi, D. W. Johnston, and F. Farid. *Optimizing System-Level Bridge Maintenance, Rehabilitation, and Replacement Decisions*. Report FHWA/NC/89-001. FHWA, U.S. Department of Transportation, 1989.
2. C-J. Chen and D. W. Johnston. *Bridge Management Under a Level of Service Concept Providing Optimum Improvement Action, Time, and Budget Prediction*. Report FHWA/NC/88-004. FHWA, U.S. Department of Transportation, 1987.
3. D. S. O'Connor and W. A. Hyman. *Bridge Management Systems*. Report FHWA-DP-71-01R, FHWA, U.S. Department of Transportation, Oct. 1989.
4. F. Farid, D. W. Johnston, C-J. Chen, M. A. Laverde, and B. S. Rihani. *Feasibility of Incremental Benefit-Cost Analysis for Optimal Allocation of Limited Budgets to Maintenance, Rehabilitation and Replacement of Bridges*. Report FHWA-DP-71-02. FHWA, U.S. Department of Transportation, 1988.
5. L. T. Blank and A. J. Tarquin. *Engineering Economy*, 2nd ed., McGraw-Hill, New York, 1983.
6. D. W. Johnston and P. Zia. Level-of-Service System for Bridge Evaluation. In *Transportation Research Record 962*, TRB, National Research Council, Washington, D.C., 1984, pp. 1–8.
7. N. U. Ahmed. *Optimization of Large Scale 0–1 Integer Linear Programming Problems with Multiple-Choice Constraints*. Ph.D. dissertation, Texas A&M University, College Station, 1978.
8. R. M. Nauss. The 0–1 Knapsack Problem with Multiple-Choice Constraints. *European Journal of Operational Research*, Vol. 2, 1978, pp. 125–131.
9. S. Senju and Y. Toyoda. An Approach to Linear Programming with 0–1 Variables. *Management Science*, Vol. 15, No. 4, Dec. 1968, pp. B-196–B-207.

Underwater Inspection of Bridges— Overview of a Statewide Program

R. Richard Avent and Marshall D. Whitmer III

A comprehensive statewide underwater bridge inspection program was conducted for the state of Mississippi. A total of 229 bridges on the federal-aid system were inspected. An overview of the inspection program is presented. The average number of bents or piers inspected per bridge was four, excluding four long bridges that averaged 235 bents or piers each. The type of inspection equipment, inspection methodology, and evaluation process used are described. The inspections were conducted by two three-man commercial diving teams under the on-site direction of a professional engineer. Before the project, the divers were required to take a 1-week course on bridge inspections that included a field dive. The overall condition of the underwater portions of the bridges on the federal-aid system was good. Less than 10 bents or piers out of nearly 1,900 inspected needed immediate attention. Only 6 percent were found to require remedial action over the next several years. Although a few scour problems were found, none were serious enough to immediately threaten the integrity of a bridge. To assist agencies in preparing for underwater bridge inspections, a method of rating six important aspects is given. This system would allow an agency to estimate the success of a proposed inspection process in terms of effectiveness as compared with cost.

The highway department of the state of Mississippi initiated a comprehensive underwater bridge inspection program in the spring of 1988. The program called for the inspection of all underwater portions of bridges on the federal-aid system from waterline to mudline. A total of 229 bridges was included in the inspection. An overview of the program is provided.

The Mississippi highway department is divided into six districts in terms of bridge inspection, maintenance, and rehabilitation. Under the supervision of the Bridge Division of the Mississippi State Highway Department (MSHD), each district has its own inspection teams that inspect the above-water portions of bridges on a regular basis. Inspections occur in 2-year intervals unless conditions of damage require more frequent inspections. In addition, each district has crews capable of providing maintenance and repair for routine damage. However, damage beyond the district's capability is handled by contract.

The approach used by MSHD was to have each district provide a list of bridges to be inspected underwater. The selection criteria were based on whether the underwater portions of the bridge could be inspected by the district inspection crews. Any bridge that did not allow for a dry season or shallow-water inspection by the state was included in the program. From a practical viewpoint, all bridges with a low water depth greater than 3 to 4 ft were included. Hardly any of

R. R. Avent, Civil Engineering Department, Louisiana State University, Baton Rouge, La. 70808. M. D. Whitmer III, Diving Services International, Inc., Hammond, La. 70804.

these bridges had ever been inspected underwater. Figure 1 shows a state map detailing the location of all bridges and districts. Characteristics of the rivers and bridges can also be observed from the map. District 1 is characterized by flat to rolling terrain with relatively small streams and rivers. One exception is the Tombigbee River that runs north to south through much of the district and is large enough for navigation in points. However, several years ago the Tennessee-Tombigbee Waterway was built, connecting the Tombigbee River to the Tennessee River through a canal with a series of locks and dams to create a navigable waterway from Tennessee to the Gulf of Mexico. The flow patterns and water levels of this river have changed significantly since completion of the waterway. Forty-seven bridges were inspected in this district. District 2 consists of terrain ranging from flat near the Mississippi River to rolling terrain over the majority of the district. There are few large rivers and, consequently, relatively few bridges with underwater bents or piers. Only 20 bridges were inspected in this district.

District 3 includes much of the flatlands of the Mississippi delta. Several large rivers run through the district as well as a number of smaller streams. Forty-one bridges were inspected in this district. There is no District 4. District 5 consists of rolling terrain with some major rivers. Of particular interest is the Pearl River that flows south and eventually into the Gulf. The river serves a large drainage basin in the district and is known for its heavy flows and flooding. Twenty-eight bridges were inspected in this district. District 6 includes a number of large rivers and the entire Mississippi Gulf Coast. It has the longest and largest number of bridges. A total of 78 bridges were inspected including 4 that had more than 100 bents. District 7 has few rivers and streams and only five bridges were inspected in this district. However, one bridge is worth noting—the bridge at Natchez across the Mississippi River.

The inspections began on May 16, 1988; all inspections were completed by October 16, 1988. The state had district representatives at the site during all inspections.

DIVING PROCEDURES

The diving inspection teams were headed by a registered professional engineer who was also a trained diver. This engineer was present at the site during inspections. The engineer generally dove personally to inspect any serious problems encountered. However, most of his time was spent monitoring the inspections from the surface.

Two dive teams were used simultaneously. Each team consisted of two divers and a tender. One diver performed the
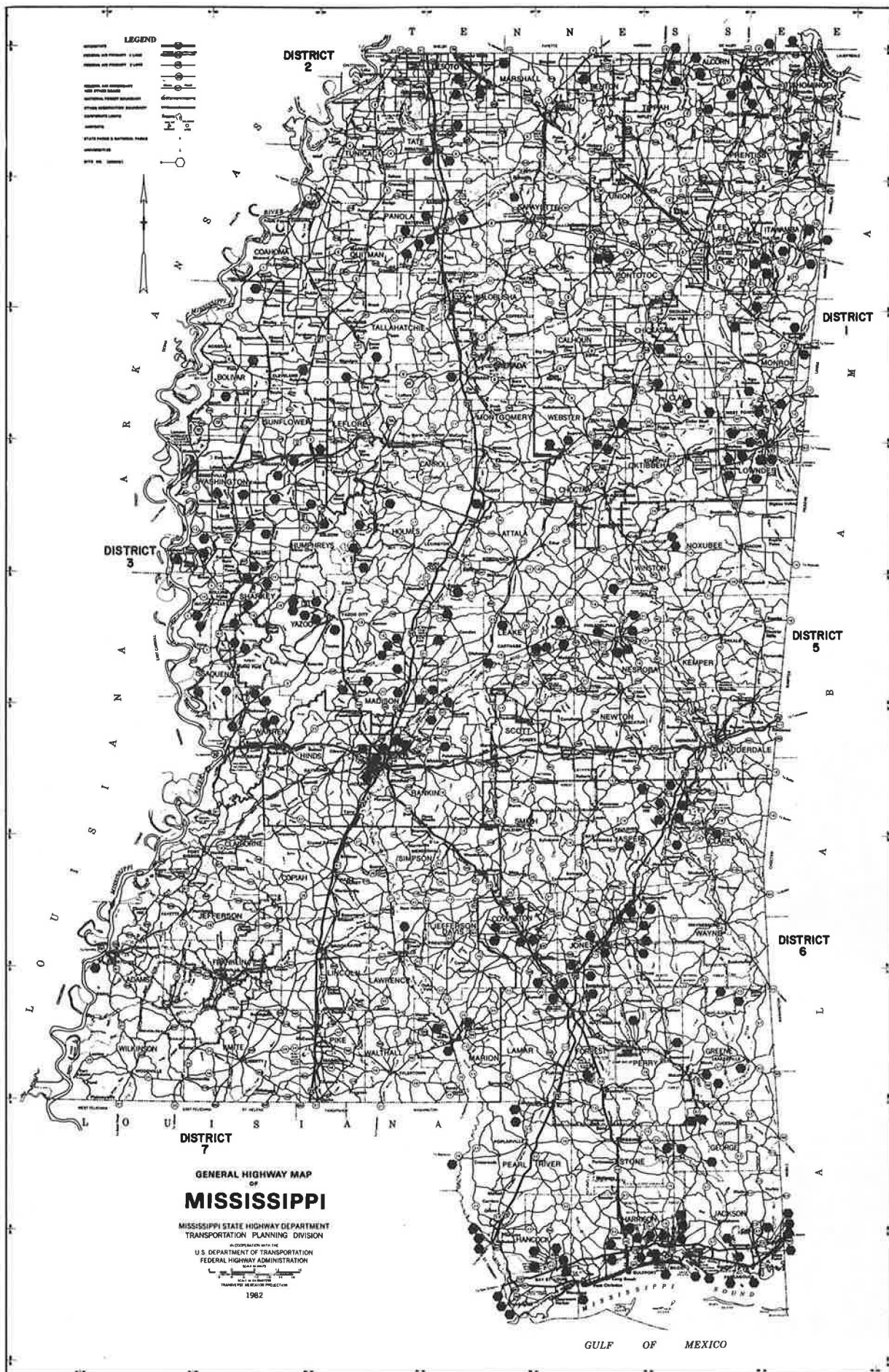
FIGURE 1 Location of bridges inspected.

actual inspection, while the other recorded the findings at the surface. The tender's responsibility was to maintain equipment and service the diver during a dive. The professional engineer alternated between the two dive teams as they moved from bridge to bridge.

The dive teams used commercial diving equipment. A compressor provided surface air to the diving hats. Two-way communication was maintained at all times through a communication line. A volume tank provided a reservoir of air and was connected with a pneumo tube that enabled the diver to measure water depths. The diver was equipped with various hand tools for inspection including a light, scraper, knife, calipers, incremental borer used for timber piles, and rule. In general, access to the bents or piers was from a motor launch. For some of the small streams, the access was from the shore. An outfitted diver and the launch equipment are shown in Figures 2 and 3.

The divers used for inspections were experienced commercial divers, particularly in offshore construction work, and also had some bridge inspection experience. In order to familiarize the divers with the requirements of the bridge inspection program, a two-part training program was developed. The program consisted of 18 hr of in-class instruction and a 1-day field dive for a bridge inspection. Also, during the course of

FIGURE 2   Outfitted diver entering water.
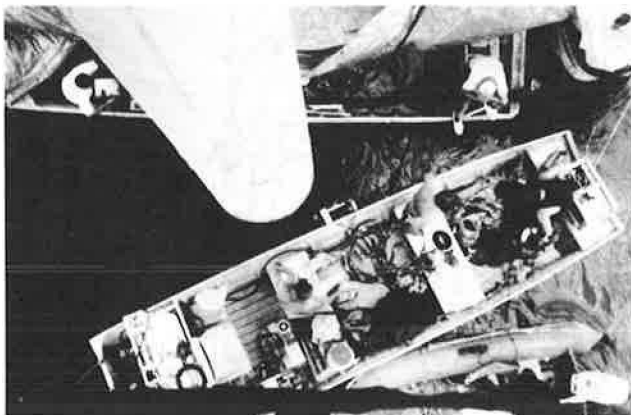
FIGURE 3   Aerial view of typical launch with three-man crew.

actual inspections, a weekly review session was held to ensure continued consistency in the inspection approach.

The specific items included in the inspection were

● inspection of steel, concrete, timber abutments, piers, pilings, fenders, and dolphins;
● identification of scour patterns in the stream bed adjacent to the foundation elements;
● identification and description of any cracks or erosion of concrete piers and abutments;
● identification and measurements of any voids beneath footings and abutments including a description of exposed piling;
● identification and description of any damage to the substructure that may have been caused by ship or barge collision or debris;
● description of piling on all pile-supported structures;
● identification and description of the condition of any pile protection, and
● identification of both location and description of condition of underwater power cables for any movable bridge.

A hands-on inspection was conducted of each bent or pier from waterline to mudline. For piles, each face was inspected from top to bottom in sequence. Visual inspections were not possible on many of the bridges because of muddy waters. So the inspection was done by feel. In addition to a hand inspection, a sharply pointed probe was also used to detect cracks, and dimensions were taken on all damaged sections found. Calipers were used to measure the flange thickness of steel piles, hammer soundings were used for concrete and timber piles, and a rule was used to measure damage to other types of bridge supports. Suspect timber piles were also cored with an incremental borer. For piers, the surface was inspected in 5-ft-wide vertical sections successfully moving around the perimeter of the pier.

In addition to the structural inspection, a bottom inspection was conducted to uncover evidence of scour. Depth elevations were taken at each pile of each bent. For piers, depths were taken around the perimeter. Depths were also taken 10 ft out from each bent or pier in each compass direction. If evidence of scour was found, additional depths were taken at 20 ft out. In cases where the scour could not easily be defined, a fathometer study was also conducted.

EVALUATION AND RATING

One of the key elements for reporting the inspection results was the bridge inspection and condition report form. A number of evaluations and rating schemes were reviewed for use in this project. The selected system is based on one used by the state of New York with some modifications. Each separate submerged structural element of the bridge was individually rated, as well as the overall unit. Elements typically identified were columns, footings, seals, piles, caps, and bracing. The overall unit was typically classified as pier, bent, or abutment. Fendering systems were classified as dolphins or bulkheads.

A numerical rating was used for the condition assessment with both the elements and the unit rated. The general rating scale was based on a 1 to 7 scale as follows.

1. Hazardous structure—The structure has lost practically all capacity to sustain the original design loads.

2. Potentially hazardous—Used to shade between a rating of 1 and 3.

3. Serious deterioration—The structure can no longer achieve its full original design capacity, while still maintaining the ability to react in a partially elastic manner retaining some degree of its original load-carrying capacity. However, extensive and serious material deterioration exists.

4. Major deterioration—Used to shade between ratings of 3 and 5.

5. Moderate deterioration—Isolated areas of light-to-moderate deterioration but not to the degree where there is any significant effect on the structure's ability to perform near the full original design capacity.

6. Minor deterioration—Used to shade between a rating of 5 and 7.

7. Undamaged—No evidence of decay or deterioration exists and the structure is performing at full design capacity.

These criteria were used for 26 rating categories under four headings: general, concrete and masonry, timber, and steel.

A detailed summary of how the rating criteria were applied in each category is given in the Appendix.

The ratings were recorded on the bridge inspection and condition report form shown in Figure 4. Although the inspection divers gave a preliminary rating, the final rating was given by the professional engineer after reviewing the field reports.

The other key element for reporting the inspection results was the diving inspection report. This report consisted of a running account of the diver's description of each element inspected. A sketch showing both a plan and an elevation was made of each pier, bent, or abutment inspected. For cases in which significant damage was found, a tape recording of the dive was made. Additional elevations or detail sketches were made as needed. A file of typical pier and bent types was produced using a computer-aided drafting (CAD) system. The diving team used the CAD drawings as applicable and produced hand sketches for atypical cases.

Key factors were recorded on the drawings or in accompanying notes. Specific items noted were bridge deck surface-to-waterline distance; depth from waterline to mudline at all piles, around piers and abutments, and 10 ft to each side of all elements; location, size, and depth of spalls and holes in

Date: _____   Year Built: _____   Bridge ID No: _____

Feature Crossed: _____   Feature Carried: _____

BENT/PIER/ABUTMENT	UNIT NUMBER			UNIT DESCRIPTION				General											Concrete/Masonry								Timber			Steel			UNIT RECOMMENDATIONS
								VOIDS	HOLES	IMPACT DAMAGE	LOSS OF SECTION	DISPLACEMENT	MISSING ELEMENTS	PREVIOUS REPAIRS	SCOUR/EROSION	LOSS OF FILL	MARINE GROWTH	DEBRIS	CRACKS	SPALLS	EXPOSED REINFORCING	LAITNT CONCRETE	SULPHATE ATTACK	HONEYCOMBING	RUST SPOTS	GROUT LOSS IN MASONRY	SPLITTING	MARINE BORERS	ROT	FASTENERS	DETERIORATION	CONNECTIONS	
20	21	22	23	24	25	26	27	28	29	30	31	32	33	34	35	36	37	38	39	40	41	42	43	44	45	46	47	48	49	50	51	52	53	54	55	56	57

Remarks:

REVIEWED BY: _____
TITLE: _____
DATE: _____

FIGURE 4   Underwater bridge inspection rating form.

concrete and steel; location, length, width, and depth of all cracks or breaks in concrete, steel, or timber; degree of section loss in corroded steel elements; degree of scaling on concrete surfaces; degree of checking on timber surfaces; level of decay (including core samples if necessary) for timber elements; misalignments or displacements; missing elements; details of previous repairs; description of scour or erosion around elements; level of marine growth; degree of drift and debris buildup; location of exposed reinforcing; location of laitent concrete; location and degree of honeycombing; type and degree of marine borer damage; and fastener deterioration.

These field reports were used by the professional engineer to prepare a final inspection report. A separate report was then prepared for each bridge that included CAD-generated drawings detailing all damage, condition rating forms, evaluation of the seriousness of damage found, and recommended repair alternatives.

SUMMARY OF BRIDGE TYPES INSPECTED

The dominant structural elements inspected were concrete pile bents. However, a variety of different structural systems were also inspected. A summary of the number and type of both bents and piers inspected is shown in Table 1. The largest number of bents were the concrete pile type. However, four long bridges on the Gulf Coast included half of all these bents.

OBSERVATIONS AND RECOMMENDATIONS

Condition Assessment of Mississippi System

The Mississippi system is in good condition overall. A summary of the inspection results is given in Table 1. Fewer than 1 percent of the bents and piers had what can be classified as major damage. Major structural damage refers to damage requiring significant structural repair within 1 year. Examples included timber piles that had completely rotted, buckled steel piling, and fractured concrete piles. In two cases, lane closures were initiated to reduce live loads with repairs immediately following.

Six percent of the bents had moderate damage. These defects require repair over the next several years but do not significantly reduce the structural integrity of the bent. Typical examples include spalls and cracks exposing reinforcing, corrosion of steel elements, and small areas of decay in timber elements.

Two percent of the bents and piers had scour or erosion to the extent that 5 ft or more of the element had become exposed since construction. Scour was not found to immediately threaten the integrity of any structure. However, additional multifrequency fathometer studies have been recommended to further evaluate a few of the more serious cases.

The final assessment given in Table 1 is recommendations for the frequency of future inspections. A recommendation is that an underwater inspection for most bridges be conducted

TABLE 1 SUMMARY OF BENT, PIER, AND ABUTMENT TYPES INSPECTED AND EVALUATION RESULTS

Type	Total Inspected	Repairs Required for Major Structural Damage	Repairs Required for Moderate Structural Damage	Significant Scour	Early Re-inspection Recommended
Bents					
Concrete Pile	1,330 (71%)	0	11 (0.8%)	5 (0.4%)	51 (3.8%)
Timber Pile	193 (10%)	8 (4.1%)	47 (24%)	0	40 (21%)
Steel or Concrete Encased Steel Pile	142 (7.5%)	0	27 (19%)	1 (0.7%)	15 (11%)
Column	58 (3.1%)	3 (5.1%)	10 (17.2%)	14 (24%)	2 (3.4%)
Pier					
Dumbbell	95 (5.1%)	1 (1.1%)	13 (14%)	9 (9.5%)	7 (7.4%)
Hammerhead	19 (1.0%)	0	0	2 (11%)	0
Wall/Solid	36 (1.9%)	0	1 (2.8%)	7 (19%)	10 (28%)
Abutments					
Concrete	4 (0.2%)	0	0	0	0
Timber	3 (0.2%)	0	2 (67%)	0	0
Steel	1 (0.05%)	0	0	0	0
Total	1,881	12 (0.6%)	111 (5.9%)	38 (2.0%)	125 (6.6%)

every 5 years. Depending on the age and degree of deterioration, more frequent inspections should be made. On the basis of these considerations, it was recommended that 7 percent of the bent or piers be reinspected at 1- or 2-year intervals. These reinspections, when compared with the initial inspection, will provide improved guidelines for determining the best frequency for future inspections.

The most important ramification of this statewide inspection was the establishment of a benchmark for the state system's underwater bridge components. Early stages of deterioration were discovered in a number of cases, allowing the opportunity for repair, rehabilitation, and preventive maintenance at a cost-effective stage.

Levels of Inspection

Although above-water bridge inspection procedures are now well established, underwater techniques are not nearly as well defined. The basic problem is visibility. A great deal of underwater bridge inspection is performed in zero or near-zero visibility. Cracks, defects, and misalignments that might be readily apparent above water are often difficult to detect in murky water. Maintaining diver orientation is also difficult. As a partial compensation, the underwater portions of most bridges are simple elements compared with superstructure design. The question arises as to how thorough an underwater inspection should be.

On the basis of experience, significant differences can exist in inspection programs. Some of these differences may be unavoidable, but many are a result of not considering the components that go into an inspection. In addition, an agency may desire to balance inspection costs and level of inspection. To provide some guidance in qualitatively evaluating the level of inspection, six basic underwater inspection characteristics are presented in Table 2. Basic characteristics are inspector qualifications, inspection thoroughness, inspection equipment used, level of record keeping, personnel preparing the final report and evaluation, and diving equipment. Associated with each of these characteristics are three levels of competence or quality. By evaluating the inspection characteristics to be used for a given bridge inspection, a numerical score can be obtained ranging from 18 to 6. The particular weightings assigned here are inessential, but this approach can be used as a general guide in evaluating the overall quality of the inspection. An overall rating of the quality of inspection could be classified as follows:

Inspection Quality Level	Sum of Numerical Rating from Table 2
0	5–7
1	8–11
2	12–14
3	15–18

TABLE 2 QUALITY RATING OF UNDERWATER INSPECTIONS

Inspection Characteristics	Numerical Rating		
	3	2	1
Inspector Qualifications	Engineer	Inspector trained diver with engineer at surface	Inspector trained diver
Inspection Thoroughness	Direct visible inspection of all elements	Limited visibility with hands-on inspection of all elements	Visible or hands-on spot sampling
Equipment Used	NDT	Coring/probes	Surface scrapers or hands only
Level of Record Keeping	Detailed sketches, field notes and rating sheets	Limited field notes and rating sheets	Overall rating only
Personnel Preparing Final Report and Evaluation	Engineer	Technician/Draftsman	Secretarial staff
Diving Equipment	Surface supplied air with communication line to surface and video equipment	Surface supplied air and communication line to surface	Scuba

Although subjective, this system allows an agency to evaluate the quality of an underwater inspection proposal. An agency may opt for a lower quality inspection based on such extenuating circumstances as age of bridge, track record of the specific bridge type, usage of bridge, and funds available. However, as the quality level of the inspection is reduced, the risk of missing damage may increase dramatically. To place the Mississippi inspection in perspective, the sum of the numerical ratings from Table 2 range from 14 to 17 placing the quality level at a high 2 to 3. This range occurred because judgment was used at the site by the professional engineer to decide which level of inspection was required. For example, although an engineer trained as a diver was present at the site, he only performed inspections when indications of damage were found. Thus, a rating of either 2 or 3 could be placed for inspector qualifications. Also, limited visibility required hands-on inspection approximately 50 percent of the time, giving a rating of 2 or 3 for inspection thoroughness. Video equipment was also available at the site but was only used when damage was found, given a rating of 2 or 3 on diving equipment.

Of particular attention is the differentiation of diving equipment between surface-supplied air and scuba. Actually, it is not just the equipment, but the training associated with use of the equipment that has prompted this delineation. The training and experience associated with commercial diving is generally greater than that required by scuba. The implication is not that there are not qualified scuba divers, but rather, there is a higher probability that a scuba diver will have less training and experience.

Considerations when Planning Inspections

Several additional aspects should be considered when setting up an underwater inspection program.

1. Drift removal should be an expected expense in many rivers. For the Mississippi job, a separate diving crew preceded the inspection team to remove drift and debris.

2. The need to remove marine growth should be evaluated and included as a cost item in coastal areas. This removal can be quite expensive and must be balanced against the inspection level desired.

3. The qualifications and training of the divers are of primary importance for a competent inspection. Both their training as divers and as inspectors carry equal weight. However, few have training in both. To use commercial divers trained to be bridge inspectors would be more effective than to train bridge inspectors or professional engineers to be divers. Commercial divers are required to have extensive training in all aspects of underwater operations. In addition, much of their experience is related to investigating damage. The additional training as a bridge inspector represents a relatively small step. However, diver training is a major undertaking requiring not just training but significant experience and physical conditioning to be qualified.

4. The time and cost of a bridge inspection will be affected by many aspects, which include the number of bridges to be inspected, cleaning (if necessary), level of inspection, structural type, number of underwater components per bridge,

water depth, water current, and drift removal required. The cost of the Mississippi inspection program averaged $1,750 per bridge.

CONCLUSIONS

An underwater bridge inspection program has been described in which 229 bridges were inspected. A summary of the inspection results was presented, indicating that the overall condition of these federal system bridges was quite good. A guide to subjectively rating the quality of an underwater bridge inspection proposal was also given to aid agencies contemplating bridge inspections.

ACKNOWLEDGMENTS

APPENDIX
Rating Criteria for Underwater Inspection of Bridges

The criteria for rating the conditions of the underwater portions of bridges for the Mississippi bridge inspection program were based on a rating system developed by the highway department of New York State. Each separate bent, pier, abutment, fendering system, or dolphin of the submerged substructure was identified and rated on 26 conditions as shown in the rating form (see Figure 4). In addition, these units were subdivided into individual structural elements (e.g., columns, footings, and piles), and each subunit was also rated.

The overall rating system has been previously outlined in this paper and is based on a numerical scale of 1 to 7 with 7 indicating excellent condition. The purpose of this appendix is to explain how the rating system was applied to specific categories of potential damage. For each category, the criteria are given for numerical ratings of 1, 3, 5, and 7. The even numbers between these ratings are used to shade between the odd-numbered ratings. Rated items are keyed to the rating form numbering as shown in Figure 4 and are classified under four headings: general, concrete and masonry, timber, and steel.

Item 32—Voids

Rating	Criteria
1	Given for a condition of massive voids that seriously jeopardize the stability of the unit. Included would be major loss of cross-sectional area, loss of masonry blocks or material, collapse, or settlement due to void-caused failure of a unit support.

Rating	Criteria

3   Given for a condition of serious voids that are beginning to threaten the stability of the unit, that are serious enough to warrant repair within the next 2 years, or that reduce the structural capacity of the unit, though not threatening to cause an immediate collapse or a sudden failure.

5   Voids are present, but are relatively minor, with either one major void or several small ones. These voids would not pose a major reduction in cross-sectional area of the unit but could develop into a problem in the future.

7   No voids present.

Item 33—Holes

1   Either a massive hole or many major holes in a unit that seriously jeopardize the integrity of the unit. Collapse of the unit may be possible because of the holes.

3   Major holes in the unit that are either in large enough numbers or large enough in size to significantly reduce structural capacity. The condition would merit monitoring and a probable repair within the next 2 years.

5   Holes are major enough or frequent in occurrence to warrant concern (such as smaller holes with minor loss of fill and no displacement or loss of members), although they do not pose a major threat to the structures.

7   No holes present.

Item 34—Impact Damage

1   Major impact damage with settlement of portions of the unit. The unit does not function as designed. If a fender system, the piles are cracked through or severed and would not protect the structural unit. If a structural unit, major damage exists with possible settlement and failure of the structural unit.

3   Significant impact damage that limits the effectiveness of the unit. In a fender system, this may reflect some cracked and broken piles but no settlement, and protection is still available to the structural unit. In a structural unit, loss of material or fallen blocks may exist, with an obvious condition that would warrant monitoring and possible repair within the next 2 years.

5   Impact damage is present and one or two members have signs of damage, but the unit

Rating	Criteria

is not significantly affected. A splintered fender system or cracked members on structural units are examples of this rating.

7   No impact damage present.

Item 35—Loss of Section

1   Extensive loss of section on supporting members of the unit or the substructure of the unit, possibly with signs of collapse or settlement that would require immediate repair. Loss of section may be a combination of several other conditions, but rating under this item should be limited to the actual loss of section condition in the range of 80 to 100 percent.

3   Significant loss of section, possibly allowing some settlement in the next 5 years if uncorrected. The section loss would be between 40 and 60 percent.

5   Minor to moderate loss of section. The unit is not in structural danger, but loss is present and continues. The section loss ranges from 10 to 20 percent.

7   No loss of original cross-sectional area.

Item 36—Displacement

1   Displacement of members of the unit, or the entire unit, that allows continued movement and potential collapse of the unit (e.g., downward crushing of supports due to loss of cross section).

3   Displacement of the unit, or parts of it, that is moderate and does not appear to be capable of continuing.

5   Minor displacement of the unit or portions of the unit that does not appear to be changing and does not pose a serious threat to the stability of the unit.

7   No displacement has occurred.

Item 37—Missing Elements

1   Many missing elements or members or a single missing element or member in a critical location that results in a serious loss of ability to support the unit as initially designed as well as possible settlement and shifting of the unit.

3   Moderate loss of elements or members that does not cause a major effect on the

Rating	Criteria
	structural unit (e.g., the loss of a member of a multimembered fender system).
5	Minor loss of elements or loss of a minor member that does not have a significant effect on the unit's ability to function as designed.
7	No missing elements.

Item 38—Previous Repairs

Rating	Criteria
1	Reflects total failure of the repair to achieve the desired result, allowing the initial deficient condition to continue and increase (e.g., a concrete patch used to stop the undermining of an abutment falls out resulting in a serious and potentially hazardous condition).
3	Reflects partial failure of the repair, but the original condition is partially protected and is not increasing.
5	Repair is deteriorated but is still in place and protecting the original condition.
7	Either the repairs made to the original construction are in excellent condition or no repairs have been made.

Item 39—Scour/Erosion

Rating	Criteria
1	Denotes a major loss of material with the footing exposed and undermined and with pilings, if present, exposed. The diver should be able to reach under the footing and locate piles.
3	Denotes a significant loss of material around the unit, although the pilings are not exposed. The difference in elevations between one end and the other, or between the channel and the unit, is within 4 to 5 ft.
5	Reflects that scour is minor and does not appear to pose a threat to the stability of the unit.
7	No scour activity at the unit.

Item 40—Loss of Fill

Rating	Criteria
1	Major loss of fill resulting in collapse of the ground behind the unit being inspected leading to major settlement to the roadway. Loss of material from the areas is continuing and threatening the unit if not stopped quickly.
3	Significant loss of fill that does not immediately threaten the unit, although there is

Rating	Criteria
	collapse of soil in the area. Repair suggested within the next few years to avoid future problems.
5	Minor loss of fill without signs of collapse of soil behind the unit being inspected. Probings reveal no major cavities due to missing material.
7	No loss of fill at the unit.

Item 41—Marine Growth

Rating	Criteria
1	Heavy marine growth, with thick growth of 4 to 6 in. or more in the tidal zone and below. Small voids could not be noted in the unit without cleaning the surface.
3	Moderate marine growth, with 2 to 4 in. of barnacles, and so forth, in the tidal zone and below. Small voids could be seen without cleaning, but exposed rebar or major cracks might be difficult to detect.
5	Minor growth, with only minimal cleaning actually needed to inspect the tidal zone and cleaning not needed on other areas of the unit.
7	No marine growth on the unit.

Item 42—Debris

Rating	Criteria
1	Extensive amount of debris covers the bottom of the waterway in the area of the unit. Debris in the surrounding area would hinder attempts to excavate for forms, should repairs be needed, and hinders the stream flow.
3	Significant debris located near the unit. Only part of the unit's area has debris.
5	Minor amount of debris around the unit. Much of the debris will be capable of being moved by the diver.
7	No debris around the unit.

Item 43—Cracks

Rating	Criteria
1	Major, deep cracks through the unit, usually combined with displacement of the sections, that cause major concern for structural integrity of the unit.
3	Significant set of cracks, possibly extensive or deep, that do not jeopardize the integrity of the unit to the point of possible failure. Damage may consist of many minor cracks

Rating	Criteria

or a few major cracks that would not be in a critical location.

5 — Minor set of cracks that are wide enough and deep enough to note but do not compromise structural integrity. Cracks rated 5 should be larger than hairline cracks.

7 — No cracks present in concrete and masonry unit.

Item 44—Spalls

1 — Extensive loss of material around reinforcing or at the corner of the unit. Spalling continues around reinforcing allowing the reinforcing to be totally exposed.

3 — Loss of concrete at reinforcing bars or at corners. Exposed reinforcing in spalls, possibly with some loss of section. Loss of concrete is structurally significant but does not threaten integrity of the unit to the point of potential failure.

5 — Spalling to the extent that reinforcing is exposed but not deteriorated. Loss of material is not yet structurally significant.

7 — No spalling present.

Item 45—Exposed Reinforcing

1 — Ten or more reinforcing bars exposed, with over 50 percent of each bar exposed. Possibly several bars that are totally exposed for some of the length.

3 — Five to nine bars either exposed less than 50 percent or fewer bars that are exposed more than 50 percent, but not for long distances.

5 — One to four reinforcing bars exposed with significant exposures or some minor exposure where the bar is just visible for an inch or so.

7 — No reinforcing bars exposed.

Item 46—Laitent Concrete

1 — The unit consists of over 50 percent laitent concrete, with probings over 1 ft into the material and the strength of the concrete seriously less than the original specifications. Possibly large voids in the material where erosion has occurred. A condition of imminent failure existing because of the unknown quality of the material.

Rating	Criteria

3 — The unit has distinct areas of laitent concrete, readily defined and probed back to solid material. The laitent concrete pockets do not pose an immediate threat to the structure, although the condition of the concrete is serious enough to warrant future inspection consideration or remedial work.

5 — The unit has a few small pockets of laitent concrete or there is a small layer of laitent concrete on the top of the substructure where a cold joint exists. The unit is not under any structural danger, but the condition does exist.

7 — No laitent concrete in unit.

Item 47—Sulphate Attack

1 — Extensive sulphate attack has reduced the section of the unit and is actively continuing in the deterioration of the unit.

3 — Active sulphate attack with only minor loss of section and the depth of the softer concrete is not more than 1 in.

5 — Signs of sulphate attack, although the depth and overall extent of the attack is minor.

7 — No sulphate attack of unit.

Item 48—Honeycombing

1 — Extensive honeycombing with voids that have loose material and can be excavated by hand. Usually a combination of honeycomb, void, and laitent concrete, with potentially large void that would jeopardize the unit structurally.

3 — Honeycombing exists in more than one location or at one major location, although the void caused by honeycombing is not structurally critical.

5 — Minor honeycombing exists, although the aggregate is solid in the void with good cement bonding, or the size of the void is very small.

7 — No honeycombing of unit.

Item 49—Rust Spots

1 — Unit has more than 20 major rust spots.

3 — Unit has between 10 and 20 major rust spots.

5 — Unit has less than 10 major rust spots or many very minor rust spots that are only a discoloration of the surface.

Rating	Criteria
7	No rust spots on unit.

Item 50—Grout Loss in Masonry

Rating	Criteria
1	Extensive loss of grout in joints, or granite blocks have fallen because of loss of grout between rows of blocks. Several sections have lost more than 50 percent of grout. Possibility of granite blocks falling from the unit because of the lack of binding grout.
3	Loss of grout in many locations, although the depth of the loss is less than 50 percent of the depth of the block or the loss is limited to a narrow bank, such as the lower tidal zone, possibly in only one horizontal joint.
5	Loss of grout noted in several locations, but extent of loss is minor, with shallow-depth sand and overall linear footage limited.
7	No loss of grout in masonry unit.

Item 51—Splitting

Rating	Criteria
1	Severe splitting of the pile or timber that causes the members to carry either no load or just a small fraction of their design load. Timber planking in a bulkhead that no longer retains fill due to splitting. Fender pile that has split at a fastener and no longer retains the fender system.
3	Splitting condition that affects the performance of the member but does not reduce the area by more than 30 percent or does not rule fasteners ineffective.
5	Minor splitting in the tidal zone due to ice action. Possibly minor impact damage on a fender system. The condition does not jeopardize the effectiveness of the unit at this time, but the condition does exist and is noteworthy.
7	No splitting of timber members in unit.

Item 52—Marine Borers

Rating	Criteria
1	Severe borer attack in the tidal zone with loss of section of the timber member that affects the ability of the member to operate as designed.
3	Several signs of marine borers in the tidal zone, or below, with some loss of section, but no major effect on the function of the members.
5	A few signs of marine borer activity, but no signs of major infestation and no significant loss of section at the tidal zone.
7	No signs of marine borers in timber members.

Item 53—Rot

Rating	Criteria
1	Severe rot of timber piles or planking that reduces the effective area of the members to less than 60 percent of the original member. Rot could be in the upper areas of the timber, caused by rain buildup, or in the tidal zone, caused by improper treatment or lack of treatment.
3	Significant rot noted in the members, with loss of section and reduction in the ability of the members to function as designed, although no structural problems. Not all members have rot, and not all members supporting a section of the unit have significant rot.
5	Some signs of rot in members, with no significant loss of the members' function. Usually just the outer inch of material is softer than a new pile, but still very solid.
7	No signs of rot in timber members.

Item 54—Fasteners

Rating	Criteria
1	Seriously deteriorated or missing fasteners that allow the timber members to carry little load.
3	Significant number of deteriorated or missing fasteners that reduce the capacity up to 50 percent.
5	Small number of deteriorated or missing fasteners with no significant loss of capacity.
7	No signs of fastener loss or deterioration.

Item 55—Deterioration

Rating	Criteria
1	Heavy corrosion with loss of section and possible signs of failure. Holes in the steel where the steel has been rusted through.
3	Moderate corrosion of the steel with heavy pitting, but no major holes. Only minor section loss.
5	Corrosion and oxidation on the steel surface, but only mild pitting, no holes, and no section loss.

Rating	Criteria
7	No corrosion or deterioration of steel members of unit.

Item 56—Connectors

Rating	Criteria
1	Missing or seriously deteriorated bolts or heavy section loss in welds. Effectiveness of the connector is seriously questioned. Splice welds in the piles would also be considered at this time.
3	Moderate deterioration of connectors or welds, with members still functioning, but capacity of the connector questioned.

Rating	Criteria
5	Some minor rusting of bolts but no section loss. Welds show signs of rusting, but no section loss found.
7	No deterioration of connectors or welds.

Item 57—Recommendation

This item represents the overall rating of the element or unit considering all of the separate items previously listed.

Inspection of the Substructure of the Chesapeake Bay Bridge-Tunnel Above and Below the Waterline

DONALD R. GRABER

The Chesapeake Bay Bridge-Tunnel, completed in 1964, was 24 years old when Wilbur Smith Associates, BTML Division, supplied engineering services as part of an in-depth, above-and-below water inspection of the substructure for the Chesapeake Bay Bridge-Tunnel District. As part of this inspection, a visual inspection of all substructure elements was conducted. A total of 60 bents were selected for a hands-on inspection. From these bents, 10 piles were selected for an in-depth evaluation. The 24-year-old substructure of the Chesapeake Bay Bridge-Tunnel was in fair condition. The splash zone and below-water portions of the piles were in good condition because of the protection provided by excessive marine growth. The above-water portions of the piles were found to be in generally fair condition. Almost all piles had hairline cracks; some piles had open cracks that allowed the ingress of corrosive agents. The prestressing strands were in good condition with no section loss. Corrosion generally began as the surface of the pile crack increased beyond $\frac{1}{4}$ in. Chloride ion presence in the concrete at the level of prestressing strand was almost negligible. The corrosion potential readings correlated with the rating of the crack tested. Caps were found to be in good condition with only isolated signs of deterioration. The report to the Chesapeake Bay Bridge-Tunnel District made the following recommendations: cracks open less than $\frac{1}{16}$ in. need only be monitored; cracks open $\frac{1}{16}$ to $\frac{1}{4}$ in. should be sealed by epoxy injection to prevent corrosion initiation; and piles with cracks open more than $\frac{1}{4}$ in. should be rehabilitated using a structural jacket or replaced.

The Chesapeake Bay Bridge-Tunnel facility, completed in 1964, was 24 years old when Wilbur Smith Associates, BTML Division, supplied engineering expertise, beginning in July 1988, as part of an inspection of the substructure of the facility above and below the waterline for the Chesapeake Bay Bridge-Tunnel District. Besides Wilbur Smith Associates, Crofton Diving Corporation of Portsmouth, Virginia, the prime contractor, supplied boats, divers, and access equipment, and Tidewater Construction Corporation of Newport News, Virginia, the original builder, supplied construction expertise. This ongoing project was originally scheduled for completion in early 1990. Its inspection procedures, inspection findings, and recommended repair-rehabilitation alternatives are described here. The Chesapeake Bay Bridge-Tunnel crosses the mouth of the Chesapeake Bay, which exposes the facility to a number of adverse conditions, including the full force of ocean storms and rough seas that they produce. The salinity of the water is roughly that of sea water. Tidal currents in the area are strong, averaging 3 knots and, under a worst-case

scenario, would exceed 6 knots because of the hydraulic constriction caused by the substructure units. In addition, some of the largest vessels in the world use the Hampton Road ports and have struck the facility on occasion.

The Chesapeake Bay Bridge-Tunnel is the longest facility of its type in the world. The facility, which is 17.6 mi in length, consists of 830 three-pile bents as shown in Figure 1, 18 two-column reinforced concrete piers, and 8 abutments that support a series of 75-ft, precast, prestressed-concrete girders, various steel girder spans, and a through-truss. The facility incorporates four man-made islands, providing access to two tunnels and one natural island.

Most of the substructure units consist of three piles supporting a cap. Piles are hollow, 5-in.-thick prestressed concrete cylinders, 54 in. in diameter. They were precast in 16-ft-long sections that were posttensioned together, grouted, then driven into the bay bottom. The piles were then filled with sand to approximately 4 ft below the bottom of the cap. Cylinders have either 12 or 16 prestressing strands, depending on the height of the bent above the point of fixity used in the design, and are laterally reinforced with No. 2 spirals that are not in direct contact with the prestressing strands.

The caps for these bents are precast, mild, reinforced concrete and set on top of the piles. They were cast with a protruding, reinforcing-steel cage that was inserted into each pile. The caps have 9-in.-diameter holes over each pile that allowed concrete to be placed inside the remaining hollow 4-ft sections of piling.

FINDINGS OF THE CURSORY ABOVE-WATER INSPECTION

The field work for this project was divided into four tasks: cursory and in-depth inspections both above and below the waterline. The cursory above-water inspection was quickly performed to summarize the general condition of the structure.

The first of the four tasks was to photograph and sketch both sides of each substructure unit. The sketches included a list of all deficiencies identified and an estimate of the quantities involved. An example of the data collected is shown in Figure 2.

Before the start of the inspection, guidelines were developed for assessing the condition of the substructure. These guidelines rated three types of deterioration found on the substructure—cracks, scaling, and impact damage—on a

FIGURE 1   General view of facility.

numerical scale based on the National Bridge Inspection Standards (NBIS). Rating guidelines are presented in Table 1. The cap and the three piles were rated separately. The condition with the lowest rating controlled the overall rating of that member. The conditions were defined as follows:

Scaling	*Characteristic*
None	No loss of surface mortar.
Minor	Slight loss of surface mortar.
Moderate	Aggregates exposed.
Advanced	Up to 1-in.-deep loss of section.
Severe	Steel exposed, greater than 1-in. loss of section; structural integrity appears OK.
Serious	Structural integrity questionable.

Impact Damage	*Characteristic*
None	No visible damage.
Minor	Surface scrapes or scars.
Moderate	Up to 3-in.-deep scrape or steel exposed.
Severe	Greater than 3-in.-deep scrape or steel damage; structural integrity appears OK.
Serious	Greater than 3-in.-deep scrape or steel damage; structural integrity questionable.
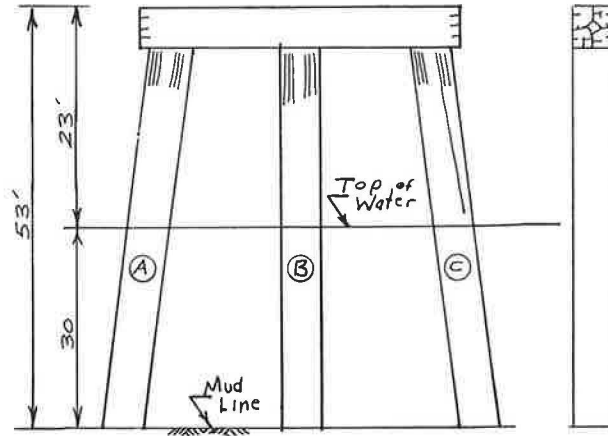
FIGURE 2   Data sheet.

Cracks	*Characteristic*
Minor	Visible hairline cracks.
Moderate	Cracks open $\frac{1}{16}$ in. or less, or hairline cracks with rust stains or efflorescence.
Advanced	Cracks open $\frac{1}{16}$ to $\frac{1}{4}$ in.
Severe	Cracks open $\frac{1}{4}$ to $\frac{1}{2}$ in. and structural integrity appears OK.
Serious	Cracks open 2 in. or more or structural integrity appears questionable, or both.

TABLE 1   RATING GUIDELINES

NBIS RATING	CONDITION	TYPE PROBLEM		
		SCALING	IMPACT DAMAGE	CRACKS
9	NEW			
8	GOOD	NONE	NONE	NONE
7		MINOR	NONE	NONE
6	FAIR	MINOR	NONE	MINOR
5		MODERATE	MINOR	MODERATE
4	POOR	ADVANCED	MODERATE	ADVANCED
3		SEVERE	SEVERE	SEVERE
2	SERIOUS	SERIOUS	SERIOUS	SERIOUS
1	CLOSED	--	--	--
0	--	--	--	--

In this rating system, the condition rated and the quantities involved have been separated. For example, moderate cracks are determined by their width and whether corrosion is apparent. The length and number of cracks are considered separately. The purpose of this system is to provide a means of grouping the condition categories. On a facility of the size of the Chesapeake Bay Bridge-Tunnel, this system is helpful in evaluating the magnitude of problems and planning a maintenance strategy.

Caps

The caps were found to be in good condition. As shown in Figure 3, open deck expansion joints wet the surfaces of the caps resulting in minor discoloration caused by moss, lichen, road oil, and light efflorescence. Many cap ends exhibited minor map cracks. Figure 3 also shows a cap with extensive map cracks.

Piles

The piles were in generally fair condition, typically having minor and moderate cracks over the prestressing strands around the uppermost 4 to 6 ft of each pile. Figure 4 shows this condition. Some piles had open cracks and some had minor scaling of the concrete surface, which would be expected of 25-year-old concrete.

Many piles in Trestle A have received impact damage. This damage is the result of a barge that came loose from its moorings in a storm and was driven against the exterior piles of the facility. The barge struck the facility repeatedly for a length of 2 mi, causing much damage.

A similar incident involved another vessel, which came loose from its moorings and destroyed four substructure units and five spans before drifting out to sea.

FINDINGS OF THE IN-DEPTH, ABOVE-WATER INSPECTION

In-depth test procedures were administered to determine the detailed condition of selected piles to draw conclusions for

FIGURE 4 Pile with typical cracks.

all piles and to develop recommended remedial actions. For these tests, 60 bents were selected for hands-on, above-water inspections, which consisted of sounding all concrete surfaces with a hammer and visually assessing all deficiencies at close range. During the course of these studies, 10 piles were selected for an in-depth inspection. This inspection consisted of four steps:

1. Locating all prestressing strands and the spiral reinforcing-steel cage in the vicinity of the test site,
2. Drilling the concrete surface with a rotary impact hammer to expose the prestressing strand for a visual assessment of the remaining cross-sectional area,
3. Collecting dust samples for determination of chloride content from a location adjacent to the exposed strand near the concrete surface and at a depth equal to that of the prestressing strand, and
4. Conducting a corrosion potential survey of an area adjacent to the exposed strand.

The 10 piles were selected to study damage associated with various condition categories. A pyramid-shaped design test group was selected, as shown in Figure 5, so that a spectrum of cracks would be investigated with emphasis placed on cracks with lower ratings.

All piles tested came from approximately the same location in Trestle A, Bents 30 to 42, except for one bent located in the surf zone and another bent located closer to the center of the bay. The test piles were grouped in this manner so that as many independent variables as possible could be held constant for the test group.

Remaining Cross-Sectional Area

The results of the visual assessment of the remaining cross-sectional area of the prestressing strand show that only three

FIGURE 3 Cap with map cracking.

RATING DESCRIPTION				
7 NO CRACK	1			
5 MODERATE CRACK	2	3		
4 ADVANCED CRACK	4	5	6	
3 SEVERE CRACK	7	8	9	10

FIGURE 5   Test group design.

FIGURE 7   Remaining steel area.

corrosion initiates halfway between a rating of 4 and 5 and progresses at a rate of 1.4 percent per rating-decrease squared.

test locations show any sign of corrosion (see Figure 6). Of these, two had minor corrosion and the other had heavy corrosion.

By grouping the test scores according to crack severity (crack rating), averages can be generated for each rating category. The result is that prestressing strands with no associated cracks, moderate cracks, advanced cracks, and severe cracks (rated 7, 5, 4, and 3, respectively), have an average percent remaining steel area of 100, 100, 99.7, and 85 percent, respectively. If the 50 percent datum value is discarded, the average value for severe cracks changes from 85 to 96.7 percent. A graph of these averages is shown in Figure 7. The plot is exponential, as might be expected.

A function describing the empirical data that were collected is

$$A = 100 \text{ for } R > 5, \text{ and} \tag{1}$$

$$= -1.4(4.5 - R)^2 + 100 \text{ for } R < 5 \tag{2}$$

where A is the area of remaining steel (in percent) and R is the rating of the crack severity. This function indicates that

Corrosion Potential

Data collected from the corrosion potential survey are shown in Figure 8. The values shown are the absolute maximum readings for each pile tested. Averages were taken of the data in each crack severity category, as previously discussed. The averages are -0.17, -0.41, -0.42, -0.50 for strands with no associated cracks, moderate cracks, advanced cracks, and severe cracks, respectively. If the datum value of -0.35 is discarded, the average of -0.50 changes to -0.54. A plot of this data is shown in Figure 9. A straight line has been plotted between the first and last average values, -0.17 and -0.54. This line falls close to the two intermediate average values. The graph has been extended to the left to show that the line plotted passes close to the origin of the graph, i.e., a rating of 9, which is defined as "new condition" under the NBIS guidelines, would have a corresponding corrosion potential reading of near zero.

The function that describes the line thus plotted is

$$P = 0.09(9 - R) + 0.02 \tag{3}$$

where P is the potential for corrosion in volts. This equation

RATING DESCRIPTION				
7 NO CRACK	100			
5 MODERATE CRACK	100	100		
4 ADVANCED CRACK	100	100	99	
3 SEVERE CRACK	90	50	100	100

FIGURE 6   Remaining steel area (percent).

RATING DESCRIPTION				
7 NO CRACK	-0.17			
5 MODERATE CRACK	-0.30	-0.51		
4 ADVANCED CRACK	-0.41	-0.47	-0.38	
3 SEVERE CRACK	-0.54	-0.35	-0.51	-0.58

FIGURE 8   Corrosion potential (volts).
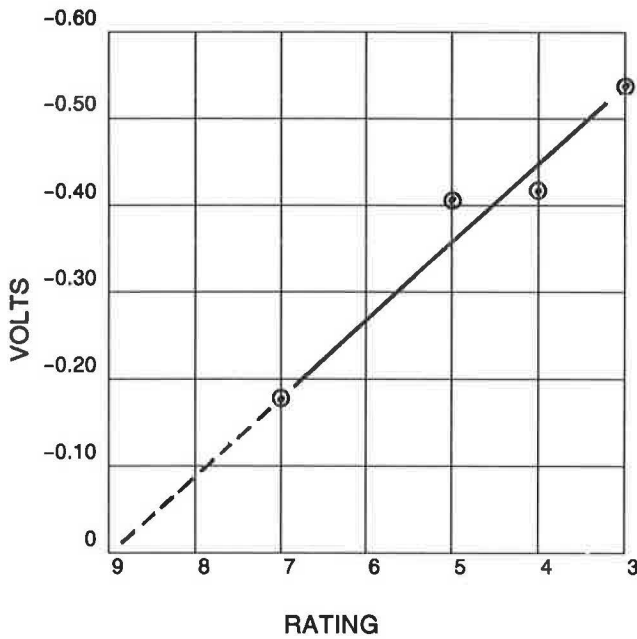
FIGURE 9   Corrosion potential.

FIGURE 10   Potential readings.

reveals that the potential for corrosion increases at a rate of −0.09 volt per rating decrease.

Half-cell corrosion potential readings correlated with the rating of the crack tested. The prestressing strand with no associated crack had a low potential for corrosion, the moderate and advanced cracks tested had a moderate potential, and the severe cracks had a high potential for corrosion. The categories for corrosion potential are based on FHWA guidelines for bridge decks, which use the values of −0.35 and −0.50 volt as breakpoints to separate low, moderate, and high potential readings.

In addition to the maximum values, readings were also taken on the pile surface in the vicinity of the test site. The widest point along the crack with the lowest rating on any given pile was selected. The readings showed that the location of the absolute maximum value for corrosion potential was about 1 ft below the location chosen from a visual inspection of the surface.

The additional potential readings have been mapped. A typical map is shown in Figure 10. The information reveals that (a) potential readings are greatest in the vicinity of the test site, (b) potential reading values decrease with distance above and below the test site, and (c) no trend exists to predict reading horizontally around the pile, as might be expected, because strands are electrically insulated.

Chloride Penetration Near the Concrete Surface

Figure 11 shows the data that resulted from the chemical analysis of dust samples, which shows a fair amount of scatter. Averages have been plotted in Figure 12. A correlation exists, however, between the crack severity and level of associated chloride ion content. After extensive data manipulation, the plot shown in the graph was developed. This plot passes to the right of the origin of the graph indicating that, near a
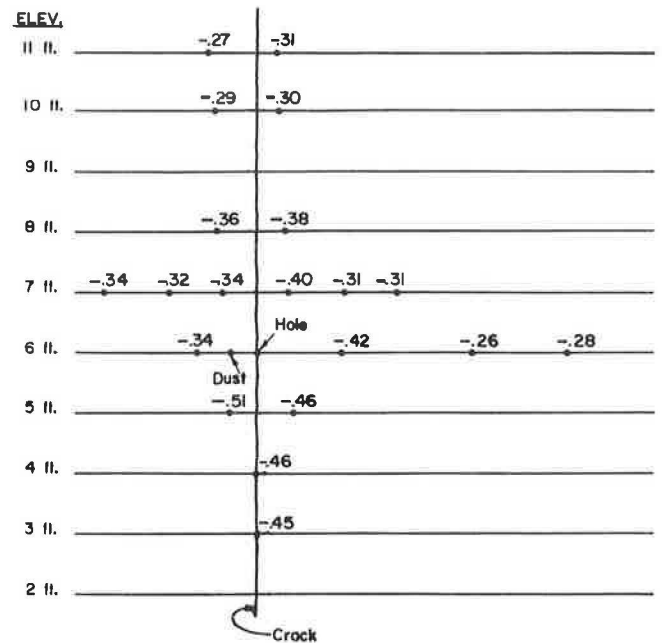
RATING DESCRIPTION				
7 NO CRACK	2.0			
5 MODERATE CRACK	0.8	2.0		
4 ADVANCED CRACK	3.1	7.4	4.7	
3 SEVERE CRACK	2.3	4.7	4.3	5.5

FIGURE 11   Chloride content near surface (lb/yd³).

rating of 8 (good condition), the chloride concentration should be near zero. This offset implies that chloride intrusion is not immediate. The equation that describes the plot is

$$[Cl] = 0.9(9 - R) - 0.8 \qquad (4)$$

where [Cl] is the chloride content near the concrete surface, in pounds per cubic yard.

Equation 4 indicates that the concentration of chloride ions increases at a rate of 0.9 lb/yd³ per rating decrease.

The chloride ion content measured near the concrete surface was in the contaminated range for cracks rated 6 or less on the basis of the FHWA breakpoint of 2 lb/yd³ for plain reinforced concrete bridge decks. It has been previously recommended that for prestressed-concrete beams, ". . . permissible water soluble chloride ion content . . . not exceed 0.10 percent by weight of portland cement" (1). This amount translates into a value of approximately 4 lb/yd³.
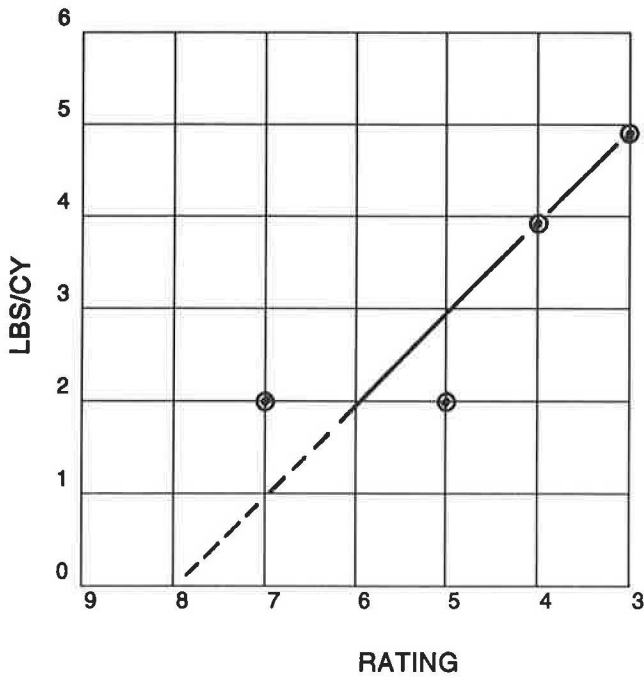
FIGURE 12 Chloride content near surface.

Chloride Content at the Level of the Prestressing Strands

Data from the chloride ion analysis of the dust samples collected at the level of the prestressing strand are shown in Figure 13. These data show that all values except one are extremely low. These values are, in fact, near the threshold of detection and are well below the level at which the concrete is considered contaminated with chlorides.

FINDINGS OF THE BELOW-WATER CURSORY AND IN-DEPTH INSPECTIONS

Almost all of the pilings were in good condition below the waterline with only occasional minor and moderate cracking,

RATING DESCRIPTION				
7 NO CRACK	<0.4			
5 MODERATE CRACK	0.4	0.4		
4 ADVANCED CRACK	0.8	0.8	2.3	
3 SEVERE CRACK	0.4	<0.4	0.4	0.4

FIGURE 13 Chloride content at depth of strand.

in part because the piles were encrusted with heavy biological fouling up to 3-ft thick as shown in Figure 14. This biological fouling consists of barnacles, oysters, mussels, and coral. Figure 15 shows an underwater inspector cleaning a pile. Bands 1 ft high were cleaned around the circumference of the piles to look for damage. These bands were located at the waterline, mudline, and at two intermediate points. Typical underwater cracks can be seen in Figure 16.
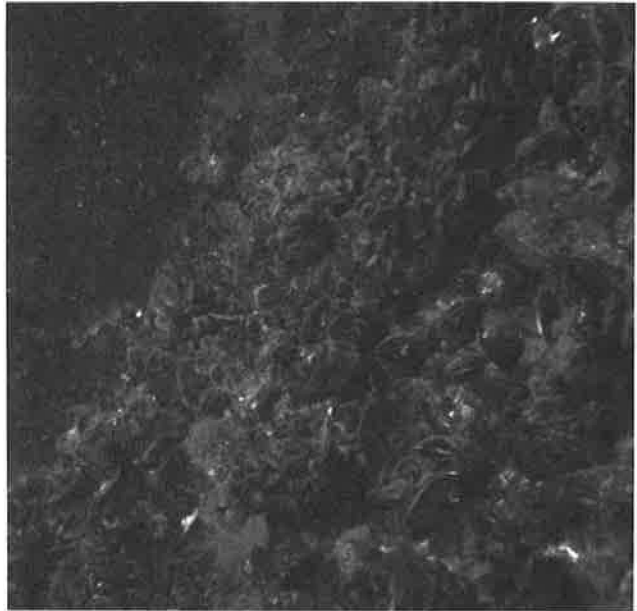
FIGURE 14 Pile surface before scraping.

FIGURE 15 Underwater inspector cleaning pile.

FIGURE 16 Two views of underwater cracks.

FIGURE 17 Contour map of first island vicinity (not to scale).

The bay bottom in the vicinity of each bent is overlaid with oyster beds—a process in which oysters, growing on the side of the pile, die and deposit their shells on the bottom, forming a mantle on which new oysters grow. This deposit protects the piles from abrasion by drifting sand.

A hydrographic survey was run parallel and perpendicular to the facility and showed the formation of a scour pocket beneath the approach trestle near one of the man-made islands. As shown in Figure 17, the scour pocket approaches 30 ft in depth and has compromised the structural integrity of the piling. This compromise occurs when scour lowers the bay bottom locally either to an elevation below the point of fixity assumed in the design or to an elevation near the pile tip elevation.

CONCLUSION

The Chesapeake Bay Bridge-Tunnel is in fair condition after 25 years of service in a marine environment.

The bent caps are wetted by rainwater because of the open deck slab expansion joints, which have been left open to help drainage. This wetting has resulted in moderate staining of the pier caps and in light efflorescence of the concrete surface by allowing aggressive agents to enter through the top of the cap, percolate through the concrete matrix, and leave through the bottom and side faces of the cap. This process weakens the concrete paste by removing soluble compounds. Future bridge projects should not allow open joints to continually wet the pier cap with salt-laden spray, contaminated rainwater, and road oils.

The results of the in-depth testing of the piles indicate that even though the potential for corrosion exists, chlorides have not penetrated the concrete cover to the level of the prestressing strands. Further, strands that are exposed in open cracks are not corroding, except for those exposed in the largest of the cracks. Chlorides do not penetrate the concrete cover because of the extremely dense concrete of strength 5,000 psi, which was cast in a spinning cylinder. In addition, strands exposed in open cracks may not have corroded because the vertical orientation of the crack allows water and corrosive agents to drain quickly. Therefore, the cracks are not the result of the expansive nature of corrosion byproducts. At and below the waterline, corrosion has not occurred because

of the protection provided by the heavy marine growth. This protection also extends to the adjacent bay bottom area and guards the pile at the bottom line from abrasion of drifting sands. Future bridge projects using these piles should place an emphasis on protecting the above-water portions of the concrete surfaces.

The scour pocket, which exists near one of the four man-made islands, is the result of tidal currents that must now flow around the islands. This pocket has formed on the trestle side of each island because the piles create a restriction that increases the flow velocity. In addition, this side of the island is not extensively overlaid with riprap for the tunnel tube cover. This scour pocket has compromised the structural integrity of the piles in the vicinity by increasing the unsupported length. It has either attained depths below the point of fixity assumed in the design of the pile or attained depths near the pile tip elevation. Future bridge projects under similar conditions should try to minimize any obstacles to tidal flow.

RECOMMENDATIONS

Although the joints on this type of superstructure are left open to increase drainage and neoprene bearing pads are provided, it is recommended that open bridge deck expansion joints not be used on a bridge subjected to large amounts of salt spray. Once the joints are sealed, a maintenance program should be established to ensure that the joints remain watertight.

Minor and moderate cracks require no remedial action at this time, because active corrosion is not the cause of cracking. However, it is recommended that these cracks be monitored during future inspection for any signs of progressive deterioration.

It is also recommended that advanced cracks be sealed by epoxy injection, because corrosion has yet to initiate. Such repair work is in progress.

It is recommended that piles with severe and serious cracks be replaced or rehabilitated with structural jackets. A structural jacket uses shear connectors embedded in the existing pile to transfer the pile load to the jacket for the length of the pile weakened by the crack. Corrosion has already initiated and the structural integrity of a 5-in. concrete shell has been compromised by these cracks.

Finally, it is recommended that the scour pocket that has formed near the man-made island be filled with riprap. This riprap should take the shape of a cone centered around the piles and slope away from each bent. This remedial work is now in progress.

REFERENCE

1. D. Stark. *Determination of Permissible Chloride Levels in Prestressed Concrete*. Technical Report 3, Prestressed Concrete Institute, Chicago, Ill., June 1983.

Repetitive Load Test on a Composite Precast-Decked Bridge Model

Roberto A. Osegueda and James S. Noel

The results of a repetitive load test conducted on a laboratory model to study the deterioration of connections designed to develop composite behavior in precast-decked steel bridges are presented. Two million sinusoidal load cycles at a frequency of 3.5 Hz at levels exceeding those of an equivalent HS 20-44 AASHTO truck were applied to a ⅓-scale laboratory model of a composite, precast-decked, simple-span bridge. Loads, deflections, strains, and relative deck-beam displacements were continuously monitored and recorded at several time windows. The dynamic measurements were approximated to the steady state response by curve-fitting 3.5 Hz sinusoidal wave functions from which the amplitudes of measurements were obtained. The amplitudes of deflections, composite moments of inertia of two sections, and relative deck displacements were analyzed and graphed versus the cycle number. A statistical test was conducted to establish the significance of the test results. The flexibility of the structure increased by less than 7 percent. The flexural properties of the two instrumented sections remained constant. The amplitude of relative deck-beam displacements remained negligible throughout the test. No evidence was found of any deterioration of the deck-beam interface connections.

The use of full-depth precast concrete panels for the replacement of bridge decks is expected to grow as deterioration problems on decks continue. Two major advantages offered by the precast replacement method over other methods are (a) on-site reconstruction is fast, and (b) traffic on the bridge during the reconstruction is allowed. These advantages were recognized as early as 1973 (1). Since then, several bridges have been replaced using precast concrete panels (2–6).

In the precast replacement method, the panels are connected to each other and to supporting longitudinal steel beams to form a monolithic unit. Connections between adjacent panels are usually accomplished with grouted keyways (1,2,4,6). Uniform bearing and vertical alignment of the panels of steel beams are obtained by the placement of a thick mortar before setting the panels (1), by use of bearing pads with the grout placed after setting the panels (4), or by use of bolt-leveling supports adjusted while the mortar bed is being placed (3).

All precast decks reconstructed to date can be classified according to their design as noncomposite or composite. In noncomposite designs, the applied loads are assumed to be resisted by the beams only; whereas in composite designs the loads are assumed to be resisted by the precast slab and beams combined. A difference between the construction of the two designs is that noncomposite bridges use tie anchors or bolts to connect the panels to the beams and composite bridges use

R. A. Osegueda, Department of Civil Engineering, University of Texas at El Paso, El Paso, Tex. 79968-0516. J. S. Noel, Department of Civil Engineering, Texas A&M University, College Station, Tex. 77843.

steel-headed studs housed in blockout holes filled with grout to ensure the transfer of horizontal shear between the deck and the beams by mechanical means.

Both designs typically include an adhesive layer of epoxy or polymer grout between the deck and the beams. The adhesive action of this material physically bonds the precast deck to the beams and may have sufficient strength to cause composite behavior at normal service load levels (2). Therefore, the use of shear connectors only ensures the composite interaction by mechanical means in the event of an adhesive bond failure.

The question that arises is what should be the fatigue design criteria for shear connectors used in this type of construction. There are two factors that should be considered. First, the AASHTO bridge design specifications (7) only allow for a composite design if mechanical shear connectors are provided (see Section 10.38.2). Second, AASHTO fatigue design equations for shear connectors (Section 10.38.5.1.1) were developed for connectors embedded in normal concrete (8–10) and not in other embedment materials.

The objectives are to report the results of a repetitive load test conducted on a scaled model of a precast-decked, simple-span bridge; to describe the performance of the model during a repetitive load test; and to discuss the adequacy of existing fatigue design criteria for shear connectors embedded in epoxy materials.

DESCRIPTION OF THE MODEL

The laboratory structure was a ⅓-scale model of a typical middle portion of a 60-ft steel stringer bridge decked with precast concrete panels. A layout of the model is shown in Figure 1. The details of the model beams are shown in Figure 2. The I-beams of the model were W 12 × 19 steel sections modified to scale W 36 × 150 section beams with cover plates at the top and bottom flanges. The modifications were necessary to scale the moments of inertia of the prototype beams by a factor of 1/81 and consisted of the cover plates and reductions of the flange width at the ends as shown in Figures 2a and 2d. The model beams also included pairs of ¼-in. steel studs welded at a 6-in. spacing. The laboratory model was designed using laws of similitude (11) to have the same live load stresses as the 60-ft prototype bridge. Concentrated loads and shear forces on the prototype scale by a factor of 1/9 to the model, and bending moments scale by a factor of 1/27. Modeling of dead weight was not considered because only live load stresses were of interest for this study.

The deck of the bridge model was made with 10 precast panels interconnected to each other and connected to the steel
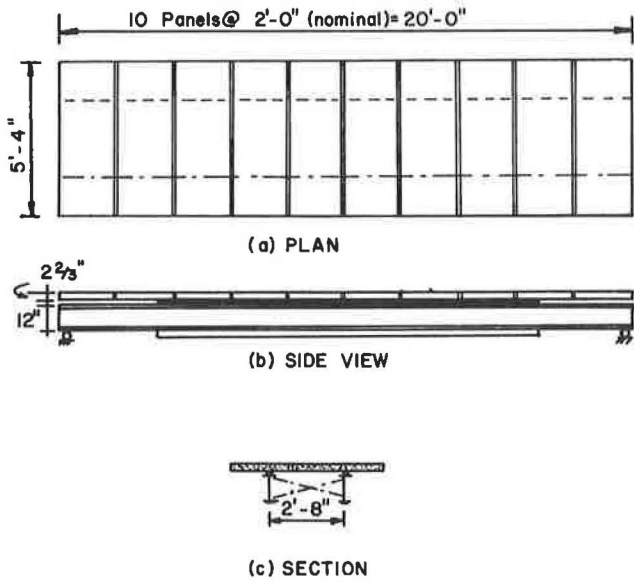
FIGURE 1 Layout of laboratory model: (a) plan view, (b) side view, and (c) typical section.
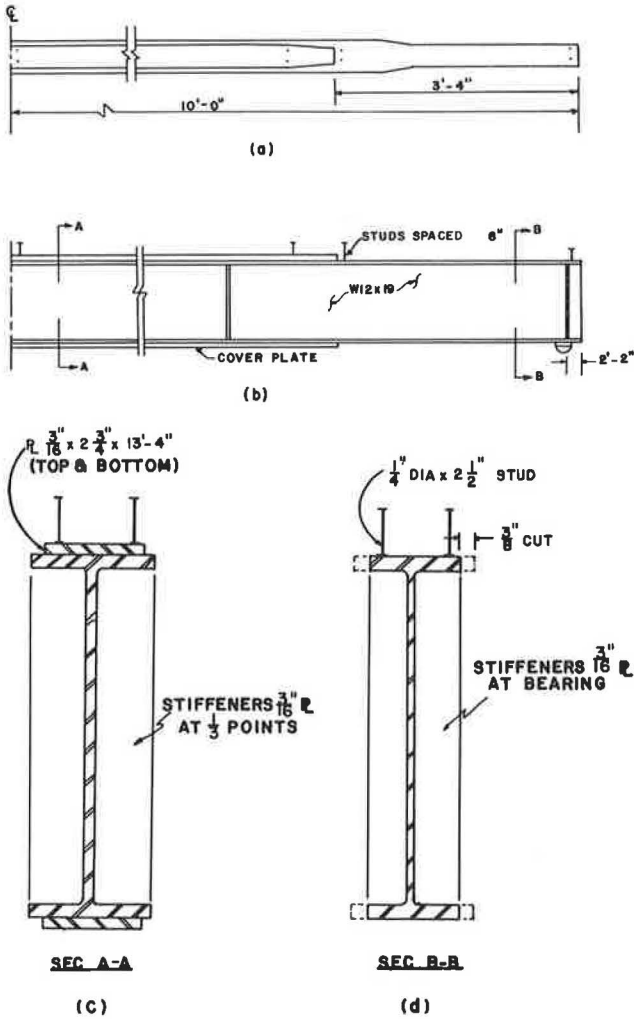

FIGURE 2 Details of model beams: (a) half-plan view, (b) half-elevation, (c) typical cover-plated section, and (d) typical end section.

beams. Each panel had nominal dimensions of 24 in. long and 64 in. wide. A typical panel is shown in Figure 3. Block-out holes were included to house shear connectors. Grooves were molded at the transverse sides so that shear keyways were formed between adjacent panels (Figure 3b). The block-out holes, the shear keyways, and the deck-beam interface gaps were grouted using an epoxy mortar obtained by mixing dry silica sand with epoxy binder THD–B–102 (similar to type VIII ASTM C–881) at a three-to-one proportion by weight. Tests conducted on epoxy mortar cylindrical samples at 7 days yielded a minimum compressive strength of 12,000 psi, split tensile strength of 1,500 psi, and an initial tangent modulus of 1.20×10^6 psi. The concrete mix for the panels consisted of typical volume proportions of scaled aggregates and cement. Results of concrete cylinder tests conducted at 28 days exhibited compressive strength values in excess of 6,000 psi. Welded wire fabric was used to simulate typical reinforcement. Complete details of the design and construction procedures of the model are described by Osegueda and Noel (11).

LOADING HISTORY OF THE MODEL

Before the repetitive load test, the model experienced two load test programs. In the first program (11), the model was statically tested up to bending stress levels equivalent to 150
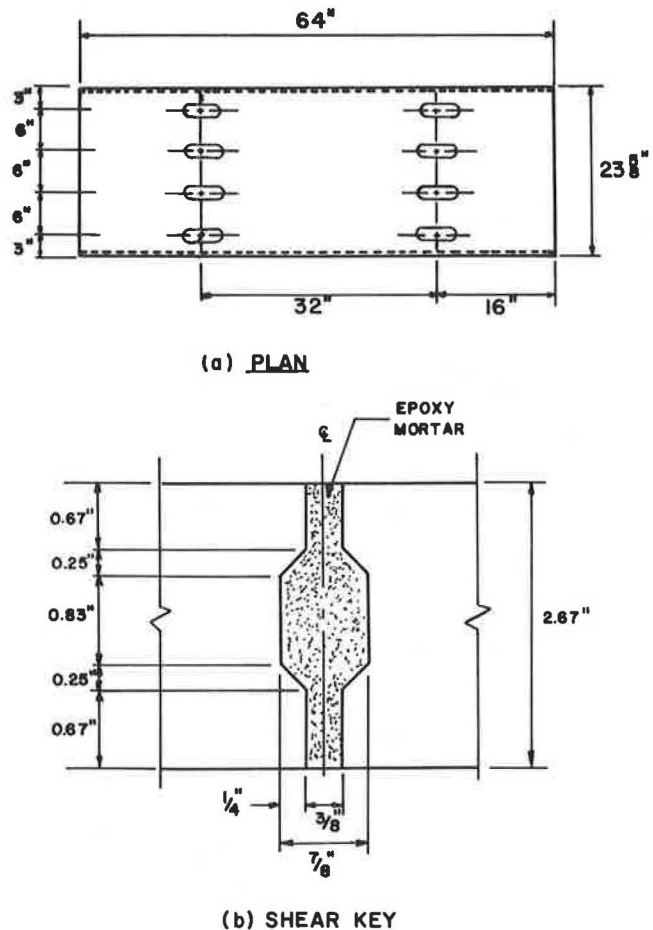
FIGURE 3 (a) Typical precast panels and (b) shear keyway.

percent of the stress levels caused by an HS 20-44 AASHTO truck. The load was applied at the third points of the model and the elastic range of the steel beams was never exceeded. The second test program consisted of evaluating the performance of the precast deck when subjected to negative moments (12). The model was anchored at the supports and was loaded with equal upward concentrated forces applied at the midspan of both beams. This loading sequence caused transverse cracking at the keyways and at the concrete mass in the vicinity of the midspan. This second test program led to the conclusion that the method is not adequate for redecking in negative-moment regions. However, no cracking or debonding was observed in the deck-beam interfaces. Thus, when the repetitive load test program started, the deck was severely cracked. However, because the cracks were formed by the application of negative moments, they were observed to close when the bridge model was subjected to positive moments.

INSTRUMENTATION AND TEST PROCEDURE

The set-up of the model for the repetitive load test is shown in Figure 4. Two equal cycling loads were applied to each beam while the centroid of the loads was located 36 in. from the midspan towards a high-shear side. The loading and instrumentation systems consisted of two closed-loop, 55-kip

hydraulic actuators and a computerized data acquisition and control system. A spreader beam attached to the bottom of each actuator was used to equally distribute the actuator load to two points per beam.

The instrumentation installed in the model consisted of strain gauges and displacement transducers. Figure 5 shows the location of the measuring points. Strain gauges were used to measure flexural strains at two different cross sections of the north beam of the model (Figure 5c). Displacement transducers were used to measure deflections at the inside quarter-points of the north beam (Figure 5b) and relative horizontal displacements between the precast deck and the beams at Locations 1 through 5 (Figure 5a). The instrumentation was complemented with the load cell and displacement transducer of each actuator. A total of 20 channels of information was used.

Two million cycles of sinusoidal loads were applied to the model at a frequency of 3.5 Hz. Each actuator was controlled to provide loading cycles oscillating between 1,700 and 9,900 lb in compression and to give a total load range of 8,200 lb per actuator. The test was executed continuously for about 8 days and was totally computerized. The computer was programmed to count cycles and to trigger the data acquisition equipment hundreds of times during the test. Each time the data acquisition system triggered, it sampled each of the 20 channels for a lapse time of 0.75 sec at a rate of 100 Hz per channel (one point every 0.01 sec). The data points were then stored along with their corresponding cycle number. When the cycle count was 2 million, the test stopped automatically.

FIGURE 4 View of test setup.
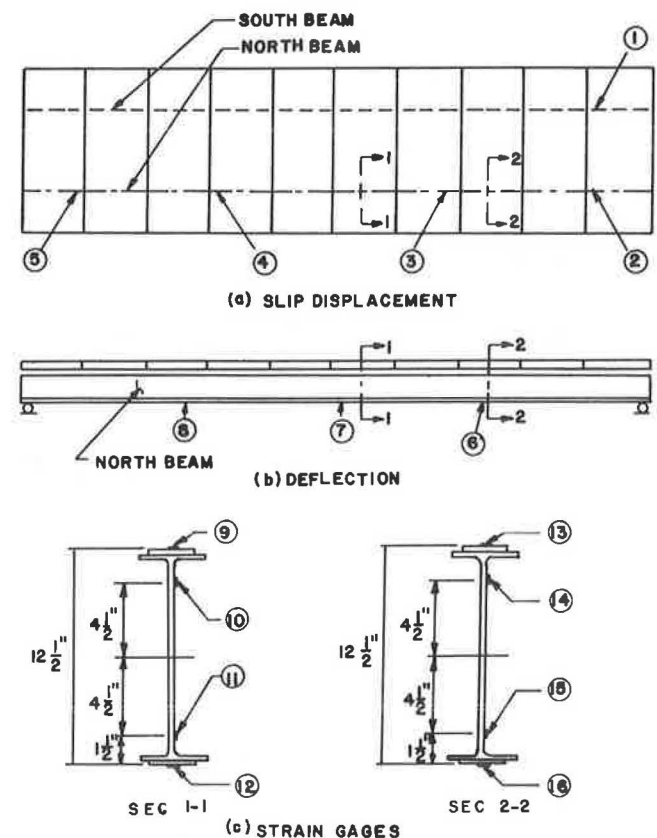
FIGURE 5 Instrumented locations: (a) deck-beam horizontal displacements, (b) deflections, and (c) strains.

EQUIVALENT LOAD LEVELS

In this section, the applied loads on the model are extrapolated to a 60-ft prototype bridge, and the extrapolated load levels of the prototype are compared to those produced by a single HS 20-44 AASHTO truck. The maximum and minimum shear and moment diagrams of the beams are shown in Figure 6. In these diagrams, dynamic amplifications have been conservatively neglected. The maximum end shear on the beams was 6.5 kips and the maximum shear range was 5.4 kips. The maximum moment and moment range were 32.8

FIGURE 6 Maximum and minimum shear and bending moment diagrams.

and 27.2 kip-ft, respectively, under the point load near the midspan. The maximum total load on the model was 18.4 kips and the load range was 16.4 kips. Because the model is at a scale of 1/3, shears and point loads extrapolate to the prototype with a factor of 9, and bending moments extrapolate with a factor of 27. Table 1 presents a comparison of the extrapolated load levels and the levels caused by an HS 20-44 AASHTO truck on the 60-ft prototype. The prototype HS 20-44 load levels were computed using procedures of the AASHTO bridge specifications (7). The loads applied to the model exceeded the levels of an equivalent HS 20-44 AASHTO truck. More important, the shear range levels, which may cause fatigue in the interface connections, were 128 percent of those expected from an HS 20-44 truck.

The maximum shear range in the model translates to a maximum horizontal shear range of 1.35 kips per connector or a shear stress range of 28 ksi if the adhesive action of the deck-beam interface material is totally neglected. In contrast, Section 10.38.5.1.1 of the AASHTO bridge specifications (7) only allows 10 ksi of shear stress range on the connectors if a design for 2 million cycles is considered.

TEST RESULTS

During the test, data from each channel were collected and recorded for 826 different time windows, each window lasting 0.75 sec. The results typify measured raw data for loads, strains, deflections, and relative deck-beam displacements. The signals measured at Cycle 10 are illustrated.

Figure 7 shows a typical measurement of the applied load signal as recorded from the load cells of one of the actuators. The load was oscillating between −1,700 and −9,900 lb (the negative sign indicates compression). Figure 8 shows the deflection measured at the midspan of the north beam. Similar deflection signals were measured at the other two quarter-points. Figures 9 and 10 show strain measurements made at

TABLE 1 EQUIVALENT PROTOTYPE LOAD LEVELS

	APPLIED IN MODEL	EQUIVALENT TO PROTOTYPE	PROTOTYPE HS 20-44 LEVEL	PERCENT LEVEL WRT HS 20-44
Total Live Load (kip)	19.8	178	91	196%
Total Live Load Range (kip)	16.4	148	91	162%
Max. End Shear (kip)	6.5	58.5	38	154%
Max. End Shear Range (kip)	5.4	48.6	38	128%
Max. Moment (k-ft)	32.7	885	727	122%
Max. Moment Range	27.2	734.4	727	101%
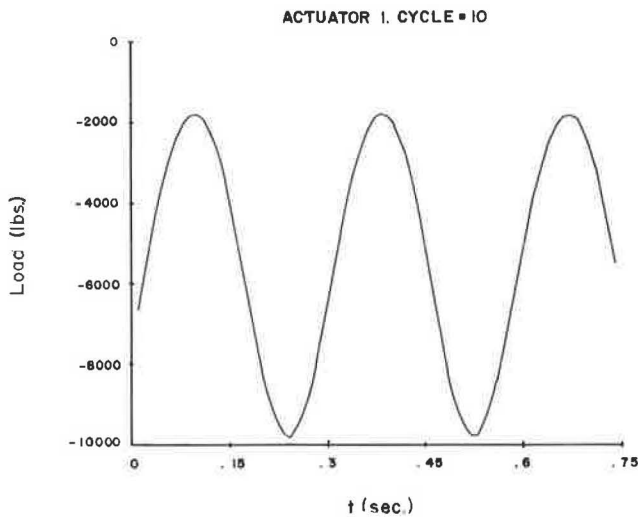
FIGURE 7   Typical load signal.
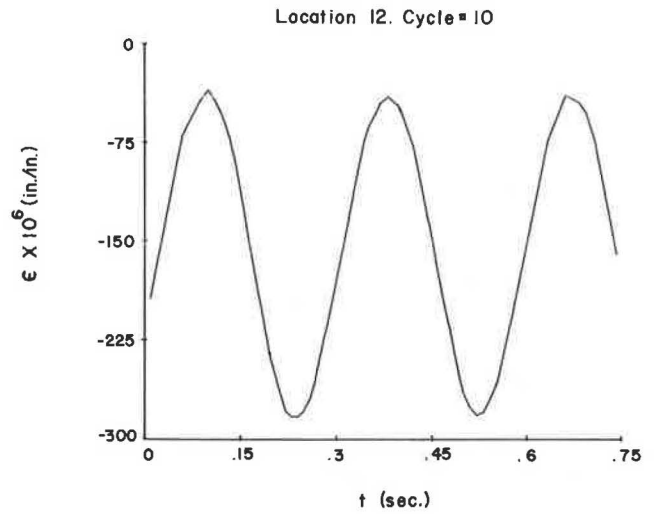
FIGURE 10   Typical strain signals at Section 1: bottom flange.
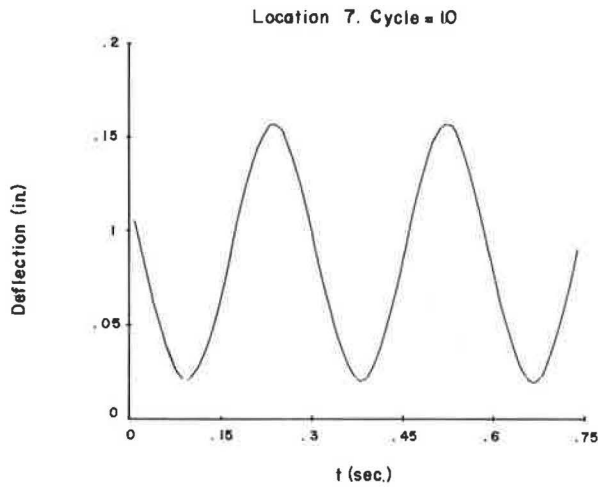
FIGURE 8   Typical deflection signal.

the top and bottom flanges, respectively, of Section 1 of the north beam. The strain measurements at the top flange (Figure 9) were contaminated with electronic noise. This problem was only typical for those measurements with small amplitudes. Similar signals were recorded from the other strain gauges bonded to Sections 1 and 2.

The measured relative deck-beam horizontal displacements were severely contaminated with noise because these displacements were of the order of 0.001 in. The major function of these measurements was to detect failure or debonding of the interface connection. Failure of the interface should have reflected dramatic increases in the relative deck-beam displacements. Figure 11 shows the relative displacement measured at Location 1 at the high-shear end of the south beam. The solid line represents a curve-fitted sinusoidal curve with a frequency of 3.5 Hz.

FIGURE 9   Typical strain signals at Section 1: top flange.
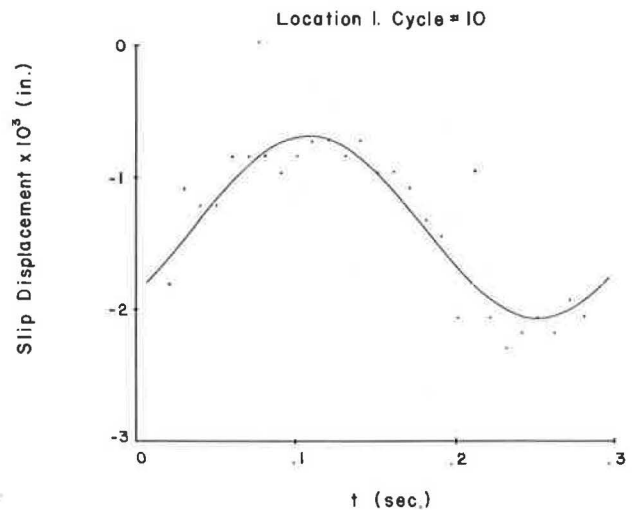
FIGURE 11   Typical relative deck-beam horizontal displacement.

ANALYSIS OF EXPERIMENTAL MEASUREMENTS

To correct the signals from noise, the measurement of load, strains, deflections, and relative displacements were curve-fitted using a sine wave function. The measured signals were assumed to have a predominant oscillating frequency of 3.5 Hz. The data were approximated to the steady state response by functions all of which had the form

$$g(t) = A + B \sin \omega t + C \cos \omega t \qquad (1)$$

where A, B, and C are regression constants and ω is the loading frequency of 7.0π rad/sec.

By minimizing the square of the errors between the functions $g(t)$ and the n measured points $f(t_i)$, the regression constants were determined by the equation

$$\begin{pmatrix} A \\ B \\ C \end{pmatrix} = \begin{pmatrix} n & \Sigma \sin \omega t_i & \Sigma \cos \omega t_i \\ \Sigma \sin \omega t_i & \Sigma \sin^2 \omega t_i & \Sigma \sin \omega t_i \cos \omega t_i \\ \Sigma \cos \omega t_i & \Sigma \sin \omega t_i \cos \omega t_i & \Sigma \cos^2 \omega t_i \end{pmatrix}^{-1}$$

$$\cdot \begin{pmatrix} \Sigma f(t_i) \\ \Sigma f(t_i) \sin \omega t_i \\ \Sigma f(t_i) \cos \omega t_i \end{pmatrix} \qquad (2)$$

Subsequently, Equation 1 was written as

$$g(t) = A + \frac{\alpha}{2} \sin (\omega t - \psi_0) \qquad (3)$$

where $\alpha = 2(B^2 + C^2)^{1/2}$ and $\psi_0 = \tan^{-1} (B/C)$.

In Equation 3, α is the total amplitude of the approximated function and ψ_0 is the phase angle.

This curve-fitting technique was performed to extract the amplitudes of loads, deflections, relative displacements, and strains for each recorded window of data. The extracted amplitudes were then normalized with respect to the load amplitude.

Deflections

The amplitude of deflections extracted for locations 6 through 8 of the north beam (see Figure 5) were normalized by obtaining the corresponding flexibility. The deflection amplitude at a given window was divided by the amplitude of load of the same window. The flexibility values were then plotted against the cycle number. These graphs are shown in Figures 12 through 14. The dynamic flexibility was slightly increasing as the number of load cycles increased.

Flexural Strains

The amplitude of the flexural strains recorded at Locations 9 through 12 and 13 through 16 were used to obtain the dynamical moments of inertia of Sections 1 and 2, respectively, as
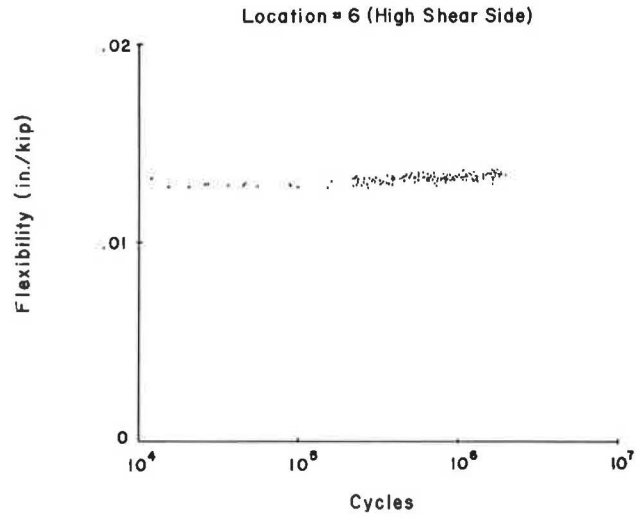
FIGURE 12   Flexibility at quarter points of north beam: high-shear side.
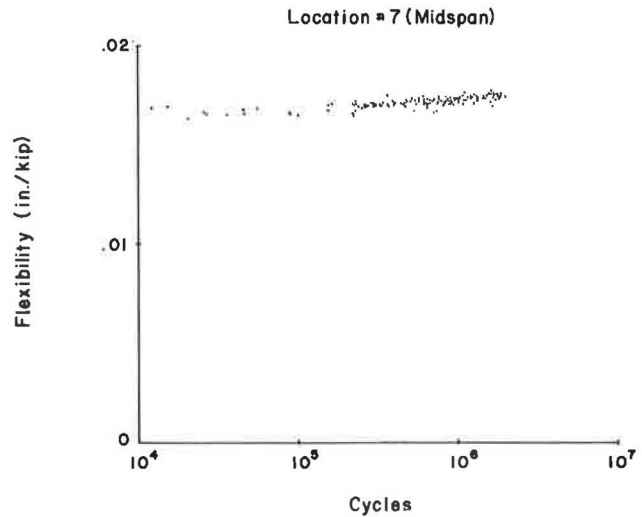
FIGURE 13   Flexibility at quarter points of north beam: midspan.
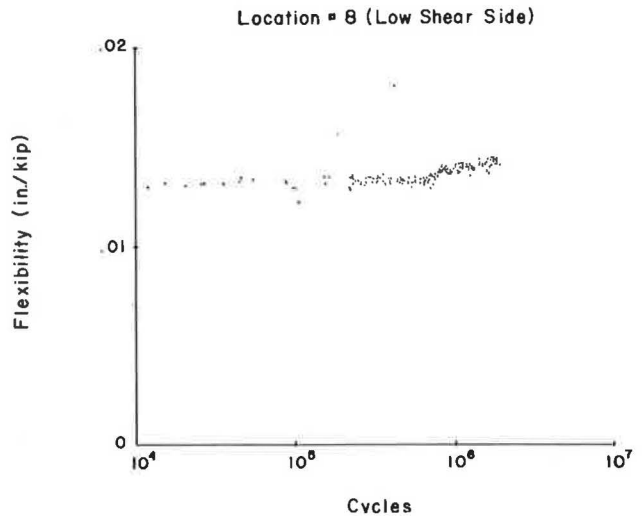
FIGURE 14   Flexibility at quarter points of north beam: low-shear side.

functions of the number of cycles. It is observed from Figure 15 that a straight-line fit of strain amplitudes corresponds to an equation of the form

$$\varepsilon(y) = \varepsilon_b + \phi y \qquad (4)$$

where

ε_b = strain amplitude at the bottom fibers,
ϕ = amplitude of curvature, and
y = vertical distance from the bottom fibers.

If the dynamic moment is known and linear elastic behavior is assumed, then the dynamic moment of inertia of the composite section can be determined from the equation

$$I = \frac{mP}{E\phi} \qquad (5)$$

where

P = load amplitude,
m = moment at the corresponding section caused by a unit load,
E = modulus of elasticity of steel (29,000 ksi), and
ϕ = amplitude of curvature.

The strain amplitudes extracted from Locations 9 through 12 were used to determine the curvature ϕ for Section 1 using Equation 4. Then, the moment of inertia was computed using Equation 5 for each time window. Figure 16 shows the composite moment of inertia of Section 1 plotted against the cycle number. The moment of inertia was almost constant with an average value of about 450 in.^{4}. Figure 17 shows a similar graph for Section 2 that was obtained using the strain amplitudes collected from Locations 13 through 16. The average moment of inertia of this section was about 500 in.^{4} and was higher than that of Section 1. However, the moment of inertia for Section 2 was also almost constant.

Relative Displacement Between Deck and Beams

The amplitudes of the relative deck-beam displacements measured at Locations 1 through 5 were normalized with respect to the amplitude of the load. Figure 18 shows the normalized displacement amplitudes measured at Location 2 corresponding to the high-shear side of the north beam. The scattering of the points can be noted, but all values remained negligible,

FIGURE 16   Dynamic composite moment of inertia of Section 1.
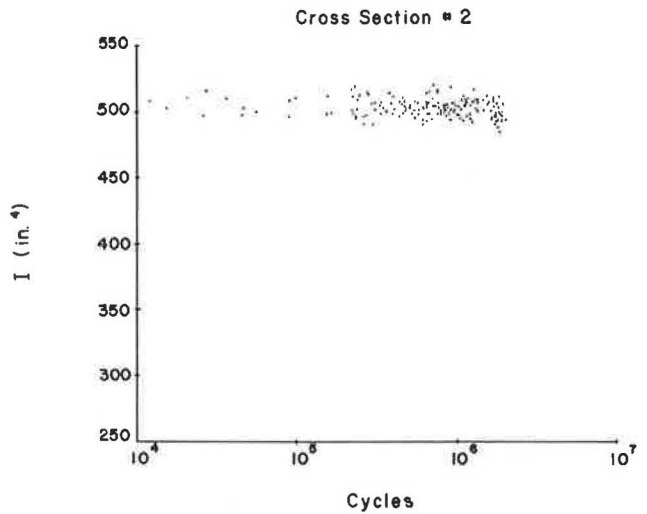
FIGURE 17   Dynamic composite moment of inertia of Section 2.

FIGURE 15   Straight-line fit of strain amplitudes at a section.
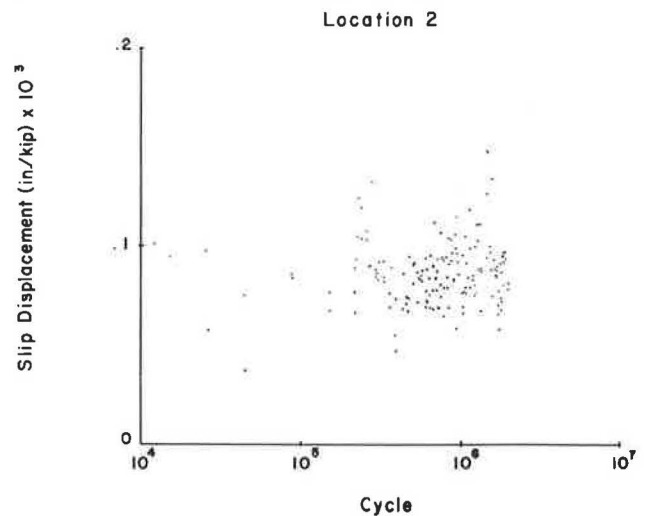
FIGURE 18   Relative normalized deck-beam horizontal displacement at Location 2.

so fracture or debonding of the interface connection between the deck and the beams was insignificant.

STATISTICAL SIGNIFICANCE OF TEST RESULTS

A statistical test was performed on the results to search for evidence of any deterioration of the bridge model during the load test. The statistical analysis was performed for the flexibilities at the quarter-points, the composite moments of inertia at Sections 1 and 2, and the relative displacements measured at the high-shear ends of the model (Locations 1 and 2). The following statistical assumptions were made:

- The relationships between the parameters involved and the logarithm of the cycle number were linear,
- The errors were statistically independent,
- The variance of the measurements was constant for each parameter, and
- The parameters were assumed normally distributed with means lying on a straight line.

The following procedure was adopted for this statistical test:

1. The flexibilities, the moments of inertia, and the relative displacement were assumed to be linear functions of the cycle number N, according to the expression

$$f(N) = \beta_0 + \beta_1 \log (N) \tag{6}$$

where

$f(N)$ = parameter function,
β_0 = intercept when $N = 1$, and
β_1 = slope of the regression equation.

2. After obtaining the linear regression coefficients, inferences about changes in the parameters were made by testing the null hypothesis (that the slope is zero) and its alternate hypothesis:

$$H_0: \beta_1 = 0 \tag{7}$$

$$H_a: |\beta_1| > 0 \tag{8}$$

When the null hypothesis is true, there is no statistical evidence of changes in the corresponding parameters. Alternately, H_a means that if the null hypothesis is not true, there is statistical evidence that the parameters changed.

3. The statistical test was made using the Student t-distribution, and the formula for the standard deviation of the slope β_1 was taken as

$$\sigma^2 = \left\{ \frac{\Sigma \left[f(N_i) - \beta_0 - \beta_1 \log N_i \right]^2}{n - 2} \right\} \tag{9}$$

4. An arbitrary probabilistic criterion was established to reject or accept the null hypothesis. The null hypothesis was rejected if there was a 90 percent probability that the magnitude of β_1 was greater than zero.

This statistical test was conducted on the data shown in Figures 11, 12–14, and 16–18, and also on the relative displacements at the high-shear ends of the beam (Locations 1 and 2). The results of the linear regression parameters and the probabilities that the slopes are not zero are presented in Tables 2–4.

Table 2 presents the results of the statistical test conducted on the flexibilities (Figures 12–14) obtained by measuring the deflections at the quarter-points of the north beam. From the

TABLE 2   STATISTICAL ANALYSIS RESULTS OF DYNAMIC FLEXIBILITIES

Location	β_0	β_1	$P[\,|\beta_1|>0]$
	(in./kip)	(in./kip)	
6, High Shear Side	0.0126	0.00020	0.99
7, Midspan	0.0156	0.00038	1.00
8, Low Shear Side	0.0113	0.00039	1.00

TABLE 3   STATISTICAL ANALYSIS OF COMPOSITE MOMENTS OF INERTIA

Section	β_0	β_1	$P[\,|\beta_1|>0]$
	(in^4)	(in^4)	
1	451.99	−1.589	0.98
2	506.99	−0.709	0.63

TABLE 4   STATISTICAL ANALYSIS OF RELATIVE DECK DISPLACEMENT

Location	β_O (in./kip)	β_1 (in./kip)	$P[\,|\beta_1|>0]$
1, South Beam	8.8×10^{-5}	8.6×10^{-6}	0.85
2, North Beam	6.4×10^{-5}	3.8×10^{-6}	0.75

last column of this table, it is observed that the values are near (or equal to) 1.0. Therefore, there is enough statistical evidence that the flexibilities increased during the 2 million cycles of load. If the flexibilities at cycle 10,000 are taken as initial values, their percent increases after 2 million cycles were less than 7 percent. However, because no physical deteriorations were observed on the model or at the interface connections, the causes of these changes could not be inferred.

Table 3 presents the results of the statistical tests for the composite moments of inertia of Sections 1 and 2 (Figures 16 and 17). The properties of Section 1 deteriorated but there was no evidence of deteriorations of Section 2. The total percent decrease of the moment of inertia of Section 1 during the test was about 2 percent.

Table 4 presents the statistics results of the relative displacement measurements at the high-shear side of the bridge model. The table indicates that there is no convincing evidence that the relative displacements increased.

SUMMARY AND CONCLUSION

Two million sinusoidal cycles of an equivalent HS 20-44 AASHTO truck load were applied to a scaled laboratory model of a composite precast decked simple span bridge. Loads, deflections, strains, and relative displacements between the precast deck and the beams were measured at 826 time windows during the test. The measurements within each window were curve-fitted with a 3.5-Hz sinusoidal wave function from which the amplitudes of the measurements were determined. The amplitudes of deflections and relative deck-beam displacements were normalized and graphed against the number of cycles. From the strain amplitudes, the composite moment of inertia of two sections was obtained and graphed against the number of cycles. A statistical test was then conducted to establish the significance of the test results.

The following conclusions can be stated:

• The epoxy mortar and steel stud connection resisting the horizontal shear between the precast deck and the steel beams did not show signs of deteriorations after 2 million cycles of applied load. This conclusion was also justified by the lack of statistical evidence that the amplitudes of relative deck-beam displacements increased.

• The composite integrity of two instrumented cross sections of the bridge model was maintained throughout the applied loads. The composite moments of inertia decreased by less than 2 percent.

• The amplitudes of the measured deflections increased with increasing number of cycles, but the total increase from 10,000 to 2 million cycles was less than 7 percent. This increase could not be attributed to deteriorations of the interface connections.

With respect to design, it was clear after this experiment that to fatigue the shear connectors, the bonding action of the deck-beam interface material must fail first. The number of load cycles and the load levels applied to the model, which exceeded equivalent HS 20-44 load levels, were not sufficient to cause any fracture or debonding failure in the deck-beam interface epoxy material. Therefore, the presence of a good bond between the deck and the beams is extremely beneficial because the bond action prolongs the fatigue life of the shear connectors. To obtain a good bond, it is always recommended to follow placement and mixing instructions supplied by the epoxy manufacturer as well as to clean the bonding surfaces.

REFERENCES

1. M. Biswas, J. S. B. Iffland, R. E. Schofield, and A. E. Gregory. Bridge Replacements with Precast Concrete Panels. *Special Report 148: Precast Bridge Deck Replacement Applications*, TRB, National Research Council, Washington, D.C., 1974, pp. 136–148.
2. C. V. Knudsen. Re-decking of a Bridge with Precast Concrete. *ASCE Civil Engineering*, Vol. 50, April 1980, pp. 75–77.
3. C. Slavis. Precast Concrete Deck Modules for Bridge Deck Reconstruction. In *Transportation Research Record 871*, TRB, National Research Council, Washington, D.C., 1982, pp. 30–32.
4. R. H. Berger. Full-Depth Modular Precast, Prestressed Bridge Decks. In *Transportation Research Record 903*, TRB, National Research Council, Washington, D.C., 1983, pp. 52–59.
5. J. G. Lutz and D. J. Scalia. Deck Widening and Replacement of Woodrow Wilson Memorial Bridge. *Journal of Prestressed Concrete Institute*, Vol. 29, No. 3, 1984, pp. 74–93.
6. M. M. Sprinkel. *NCHRP Synthesis of Highway Practice 119: Prefabricated Bridge Elements and Systems*. TRB, National Research Council, Washington, D.C., Aug. 1985, pp. 6–12.
7. *Standard Specifications for Highway Bridges*. AASHTO, Washington, D.C., 1983.

8. D. C. King, R. G. Slutter, and G. C. Driscoll. Fatigue Strength of ½-Inch Diameter Stud Shear Connectors. In *Highway Research Record 103*, HRB, National Research Council, Washington, D.C., 1965, pp. 78–106.

9. A. A. Toprac. Fatigue of ¾-Inch Stud Shear Connectors. In *Highway Research Record 103*, HRB, National Research Council, Washington, D.C., 1965, pp. 53–77.

10. R. G. Slutter and J. W. Fisher. Fatigue Strength of Shear Connectors. In *Highway Research Record 147*. HRB, National Research Council, Washington, D.C., 1966, pp. 58–65.

11. R. A. Osegueda and J. S. Noel. *Positive Moment Tests for Precast Concrete Panel-Decked Composite Bridges*. Research Report 324-1, Texas Transportation Institute, The Texas A&M University System, College Station, Sept. 1987.

12. F. E. Bonilla, R. W. James, R. A. Osegueda, and J. S. Noel. *Composite Action of Precast Panel Bridge Decks in Negative Moment Regions*. Research Report 324-2, Texas Transportation Institute, The Texas A&M University System, College Station, Sept. 1987.

Monitoring Steel Bridges by Acoustic Emission

AL GHORBANPOOR

The acoustic emission (AE) technique was used to locate fatigue crack initiation sites and to characterize signals related to fatigue cracks in bridge structural components. An experimental study that included a series of tests on welded and rolled beams was performed. Time and frequency domain analyses were performed on AE signals obtained during various life stages of each specimen. The effect on the AE signals of welding, which changed the material's microstructure, was studied. Two stress ranges and their effect on the AE signals were investigated. An in-service bridge was tested to study its general AE response. AE signals from growing fatigue cracks had distinct characteristics in both the time and frequency domains. Growing fatigue cracks were detected at relatively early stages of the fatigue lives and the corresponding AE signals were characterized throughout the experiments.

Fatigue crack behavior in structural steel components of highway bridges has been studied extensively through detailed theoretical and experimental investigations (*1–3*). The concept of fracture mechanics is used to evaluate fracture behavior and to predict the remaining fatigue lives of the structural members that contain cracks.

Using the fracture mechanics approach, the stress state adjacent to the tip of an existing crack, which is described by the stress intensity factor K, is normally examined. For example, the value of K for an infinite plate with a centrally located through-crack of size $2a$ and subjected to a remotely applied and uniformly distributed stress σ may be expressed as

$$K = \sigma(\pi a)^{1/2} \tag{1}$$

In general, Equation 1 can be written as

$$K = Y\sigma(\pi a)^{1/2} \tag{2}$$

where Y, a correction factor, is a function of the geometry of the crack and the cracked element under study.

The rate of crack growth per cycle (da/dN) increases exponentially with increased crack length (*4*), and is written as

$$\frac{da}{dN} = C(K_{max} - K_{min})^n \tag{3}$$

where C is the da/dN axis intercept in the da/dN versus fatigue life graph, and n is the slope of the crack growth rate curve.

Department of Civil Engineering and Mechanics, University of Wisconsin at Milwaukee, P.O. Box 784, Milwaukee, Wis. 53201.

Both C and n are material constants, and K_{max} and K_{min} are the stress intensity factors at the maximum and minimum applied stress levels, respectively.

It can be concluded from Equations 2 and 3 that, before an accurate fracture analysis or prediction of crack growth rate of a cracked element can be made, the crack size and shape, among other needed parameters, must be known precisely. More important, one should be able to detect small cracks because, as can be determined from Equation 3, most of the fatigue life is exhausted while a crack is small.

The presence of small cracks can have a significant influence on the remaining fatigue lives of structures. In steel highway bridge structures, various types of welded details are used. Most of these details contain discontinuities or imperfections that are created during the fabrication stage. Discontinuities of various sizes and frequencies, depending on the welding process, geometrical configurations of the welded details, and workmanship, are introduced in the welded structures. Previous fatigue studies of the welded components have shown that fatigue cracks were initiated from discontinuities with maximum depths of less than 0.016 in. (0.4 mm) at the toe of welds and from embedded defects, such as gas pockets, with a maximum radius of less than 0.08 in. (2 mm) (*1,3,5,6*). In many structures such as highway bridges, the structural members are normally subjected to cyclic loading, and the fatigue cracks are not visible until over 90 percent of the fatigue lives are expended. Clearly, to have a detection capability at a relatively early life stage that can provide adequate time for the necessary remedial work without compromising the safety of the public and producing traffic disruption is desirable.

Detection of small fatigue cracks by conventional nondestructive evaluation (NDE) techniques, such as visual, dye penetrant, magnetic particles, ultrasonic, and x-ray, is usually unreliable or costly, or both. The difficulty and cost of detection are significant because a majority of the discontinuities reside in regions of complex geometry. Past research studies (*7,8*) have shown that the probability of detection of such small discontinuities is low, even during the NDE of simple geometries and under controlled conditions.

To predict the remaining fatigue life of a component with an existing crack, the initial size of the crack is assumed to be the largest discontinuity that cannot be detected by the conventional NDE methods. Because the size of an undetectable crack or discontinuity can be relatively large, the assumption used here can result in an overly conservative estimate of the fatigue life or an uneconomical design of the component. Therefore, it is desirable to develop and use a more accurate and reliable NDE method capable of detecting

small fatigue cracks and of evaluating the status of a growing crack at various stages of its life.

The capability of acoustic emission (AE) for detection and evaluation of fatigue cracks is examined in two structural steels that are used in construction of highway bridge structures. An experimental laboratory investigation that included an AE study during fatigue testing of a series of full-sized beams was followed by an AE field test of an in-service steel bridge structure. The experimental procedures and results of the study are described herein.

ACOUSTIC EMISSION

AE consists of transient elastic waves that are generated by sudden releases of stored elastic energy from localized sources within a medium, e.g., by growth of a defect. In other words, they are produced by the occurrence of some dynamic processes at a micromechanism level in a material that is approaching a state of equilibrium. Normally, partitioning of the released energy takes place and only a fraction of this energy is converted into AE. These stress waves can be detected at various surface points of a component by highly sensitive transducers. The transducers convert the mechanical surface phenomenon to electrical voltage as a function of time, which may be evaluated to obtain information about the source.

Generation of AE results from large numbers of mechanisms or sources. These mechanisms include moving and piling up of dislocations, phase transformation, twinning, slippage at the grain boundaries, electrical discharges, and initiation and propagation of cracks. On the macromechanism level, these mechanisms generally include only plastic deformation and crack initiation and propagation.

EXPERIMENTAL PROGRAM

Constant cyclic loading was applied to full-sized beam specimens while the AE technique was used for detection and evaluation of fatigue cracks. The specimens were made of ASTM A588 weathering steel and A7 steel that are commonly found in existing steel bridges. The A588 beams were new, welded, plate girders; the A7 specimens were beams with extensive evidence of corrosion. The A7 beams were obtained from an old bridge that had been taken out of service before the beginning of the work. A total of seven A588 and seven A7 steel beams were included in this study. Each specimen was tested over a clear span of 15 ft. The geometrical configuration of the welded specimens and the AE transducer layout are shown in Figures 1 and 2. The A7 specimens had section properties similar to those of an S-type beam (S 15 × 42.9) (9). The AE transducer layout for the A7 beams was the same as that used for the A588 specimens (see Figures 1 and 2). The test values for the yield and ultimate strengths for the A588 steel were 455 MPa (66 ksi) and 606 MPa (88 ksi), respectively. Those values for the A7 steel were 227 MPa (33 ksi) and 448 MPa (65 ksi), respectively.

The constant cyclic loading of the specimens was performed by subjecting the beams to a four-point, bending-type load in a loading frame equipped with a 222.5-kn (50-kip) hydraulic load actuator. The specimens were divided into two groups
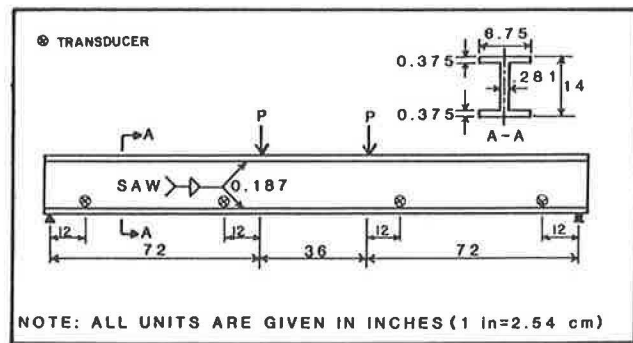

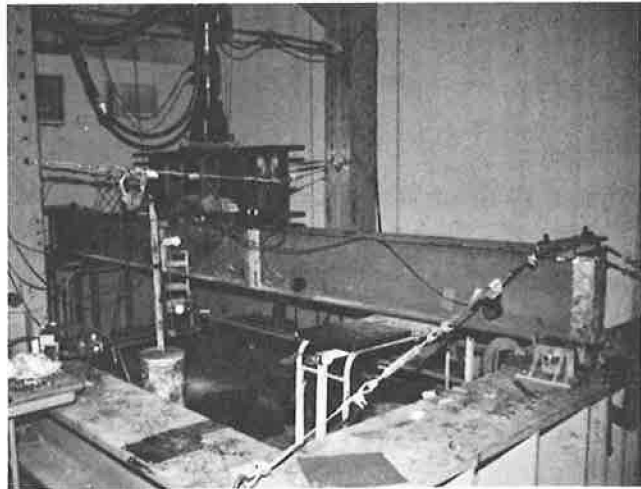**FIGURE 1** Geometrical configuration of welded beam specimens.

FIGURE 2 Loading frame assembly for testing of beam specimens.

and a different stress range was applied to the specimens in each group. The applied loading was sinusoidal and in a tension-tension fashion with a lower stress limit of 6.89 MPa (1.0 ksi) and a loading frequency of 2.5 Hz (see Tables 1 and 2).

The positions of fatigue crack tips, as indicated by AE, were examined carefully throughout the tests by using a traveling microscope, an ultrasonic unit, and a magnetic contour probe.

At the conclusion of the fatigue experiments, the fracture surfaces of the specimens were examined with a scanning electron microscope to determine the sources of crack initiation and to evaluate the material's microstructure for identification of various regions in the welded beams, namely, weld metal, heat-affected zone, and base metal. AE signals from fatigue cracks, with their tips advancing in these regions, were identified and characterized further at the conclusion of the tests.

A four-channel, acoustic emission testing system was used for this study. Time domain AE measurement was made by using 150-kHz resonant piezoelectric transducers and 100- to 300-kHz band-pass filters. Frequency domain AE data were obtained by using a wide-band filter and a contact piezoelectric transducer with a flat response point that was developed by the National Institute of Standards and Technology. The

TABLE 1   FATIGUE TEST RESULTS FOR A588 WELDED BEAMS

Specimens (1)	σrª (Ksi) (2)	Nt/1000 (cycles) (3)	Crack Detection % of Nt (4)
1	24	1,649	48
2	24	1,764	54
3	24	2,413	62
4	24	2,429	63
5	30	1,264	52
6	30	1,200	63
7	30	1,240	63

$^a\sigma_{min}$ = 1.0 Ksi.

Note: 1.0 Ksi = 6.89 MPa.

TABLE 2   FATIGUE TEST RESULTS FOR A7 ROLLED BEAMS

Specimens (1)	σrª (Ksi) (2)	Nt/1000 (cycles) (3)	Crack Detection % of Nt (4)
1	27	1,360	69
2	27	2,532	71
3	27	154	62
4	27	388	56
5	27	359	68
6	27	1,090	58
7	24	226	49

$^a\sigma_{min}$ = 1.0 Ksi

Note: 1.0 Ksi = 6.89 mpa.

total amplification of the AE system was set at 80 db and a threshold level of 30 db was used during the tests. Load values during each cycle were recorded at a time resolution of 10 msec and were correlated to the corresponding AE signals.

An AE study of an in-service bridge was also performed. Signal characteristics from various sources in the bridge, such as traffic and member rubbing, were determined by using the time and frequency domain information.

RESULTS AND DISCUSSION

Laboratory Tests

Test results from the fatigue study of the specimens are presented in Tables 1 and 2. In these tables, σ_r and N_t are the applied stress range and the total fatigue life, respectively.

The stress range is computed on the basis of the uncracked, cross-sectional area of each specimen. Fatigue life for each specimen was determined as the total number of load cycles from the beginning of each test to the specimen's failure. The last column of the tables presents the initial AE indication of fatigue crack activity as a percentage of the total fatigue life for each specimen. It is not clear that this initial AE indication of crack activity is from an actual crack initiation stage or from subsequent slow crack growth. However, it is of special interest to be able to detect fatigue crack activity at these early stages. The position for the tip of each fatigue crack, as indicated by AE, was marked and monitored throughout the test and was verified visually and by using the ultrasonic unit, traveling microscope, and magnetic contour probe. In all tests, verification of the indicated fatigue crack positions was successful.

All fatigue cracks in the rolled beams originated at the sites of the corrosion pits that were on the surface of the tension flanges. The large scatter observed in the fatigue lives of the rolled beams is attributed to the random orientation and severity of the corrosion pits that were formed on the beams.

In the welded beams, all fatigue cracks were initiated at discontinuities in the fillet welds at the junction of the tension flange and web. A typical source of fatigue crack initiation in a welded beam specimen is shown in Figure 3.

AE signals from the fatigue crack activities and noise sources were analyzed in both the time and frequency domains. Most mechanical noise sources during the laboratory and field investigations produced AE signals that contained predominant frequency components below 50 kHz. When the frequency components were larger than 50 kHz, the noise-related signal amplitudes were diminished by approximately 20 db or more. An average frequency spectrum for a typical signal related to mechanical noise in a beam specimen is shown in Figure 4. During the field testing of the steel bridge, similar spectra were obtained for signals from sources related to traffic noise (see Figure 5). As a result of this finding, band-pass electronic filters (100 to 300 kHz) were used in the AE system to minimize the signals related to undesirable noise. The upper frequency cut-off value for the filters was determined on the
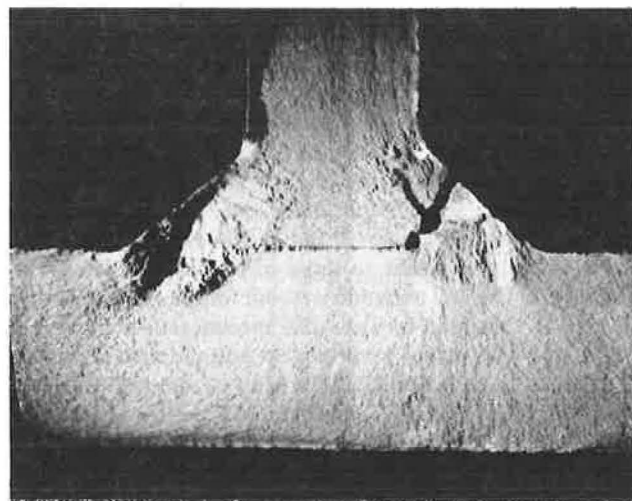

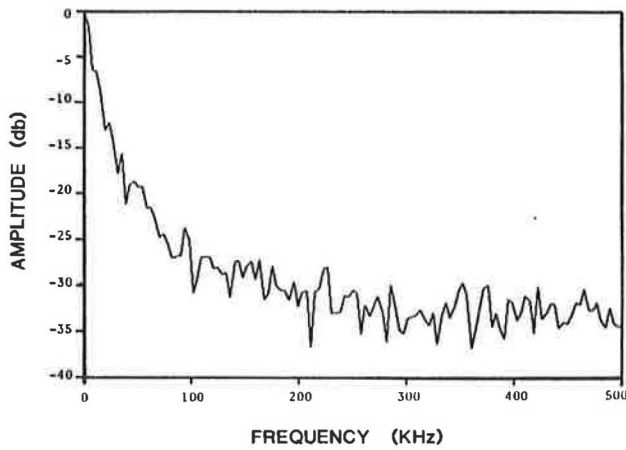FIGURE 3   A gas pocket in the longitudinal fillet weld of a welded beam.

FIGURE 4 Average frequency spectrum for mechanical noise in a beam specimen.
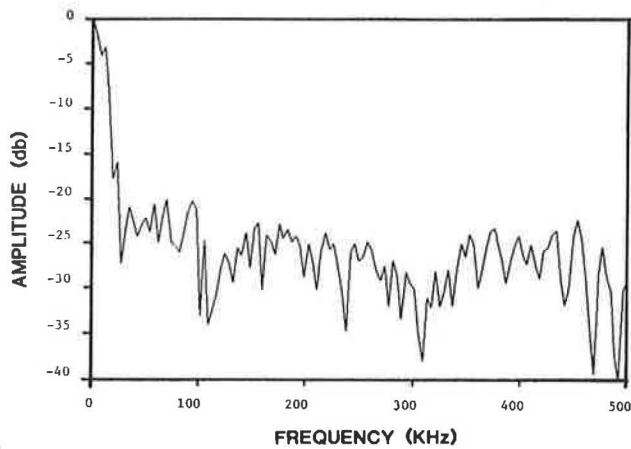

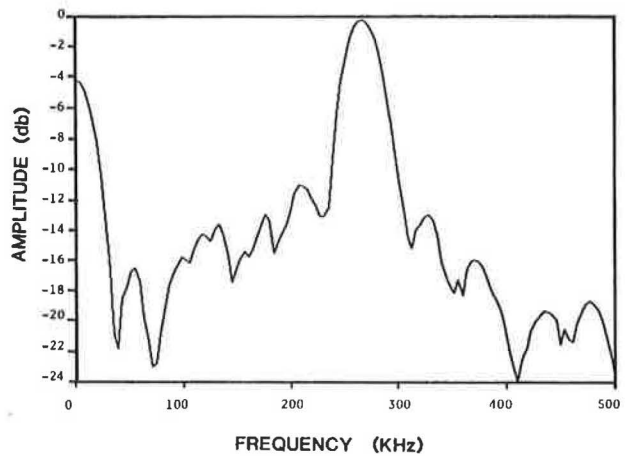**FIGURE 5** Average frequency spectrum for traffic noise in an in-service steel bridge (floor beam).

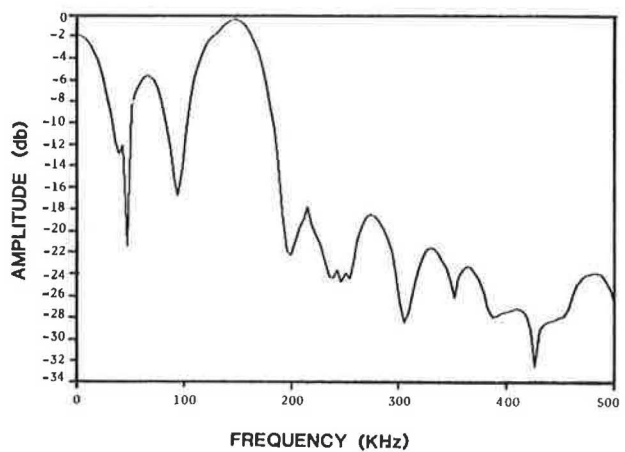**FIGURE 6** Average frequency spectrum for fatigue cracks at 62 percent of life of an A588 welded beam (Specimen 3).

FIGURE 7 Average frequency spectrum for fatigue cracks at 98 percent of life of an A588 welded beam (Specimen 3).

basis of the findings of the frequency analysis of AE signals from the active fatigue cracks in this study.

A significant finding of this work originated in the evaluation of the average frequency spectra for fatigue crack activities at various stages of the life of each specimen. The predominant frequencies in the spectra were higher at early stages of fatigue life and gradually moved towards lower values when the number of load cycles became greater. This observation was consistent for all experiments conducted in this study. Figures 6 and 7 show the average frequency spectra for a growing fatigue crack in one of the welded beams at an early stage (62 percent of total life) and at a late stage (98 percent of life), respectively. Both figures show average frequency values for 10 consecutive crack-related signals. Similar-frequency spectra were obtained for the A7 steel specimens. The change in the average frequency for the A588 steel specimens was from 280 to 152 kHz, and for the A7 steel specimens it was from 253 to 124 kHz. Tables 3 and 4 present the ranges of the average frequency values, listed at various percentages of the life for the A588 and A7 beams, respectively.

A simplified approach was also used to determine the frequency content of the acoustic waves. This approximate frequency analysis uses the time domain data and the following relationship to compute the various equivalent frequency components f:

$$f = \mu \cdot \frac{N}{T} \cdot 10^6 \tag{4}$$

where μ is a proportionality constant, initially taken as unity (1.0) and verified later in this study; and N and T are the total number of signal counts and duration, respectively, measured above a preset threshold level of 30 db. The constant 10^6 is a normalizing factor. Comparison of the frequency information obtained from Equation 4 and from the frequency domain data for the A588 specimens resulted in an average computed value for μ of 1.06, and a standard deviation of 0.03. The computed average value for μ was 1.04 and the standard deviation was 0.09 when the A7 specimens were considered. The earlier assumption of $\mu = 1.0$ may therefore be approximately justified.

The change in the predominant frequency components of the signals from the growing fatigue cracks may be rationalized from the point of view of dynamic fracture mechanics. Correlations have been established between the instantaneous

TABLE 3   RANGE OF FREQUENCY VALUES FOR A588 BEAMS

Specimens (1)	Frequency at Initial Crack Detection[a], KHz (2)	Frequency Just Before Fracture, KHz (3)
1	262	144
2	280	148
3	275	158
4	275	148
5	278	152
6	285	152
7	302	160
AVERAGE	280	152

[a]See Table 1 for percentages of life at the initial crack activity detection by AE

TABLE 4   RANGE OF FREQUENCY VALUES FOR A7 BEAMS

Specimens (1)	Frequency at Initial Crack Detection[a], KHz (2)	Frequency Just Before Fracture, KHz (3)
1	252	123
2	250	120
3	244	118
4	258	126
5	262	126
6	256	133
7	252	122
AVERAGE	253	124

[a]See Table 1 for percentages of life at the initial crack activity detection by AE

stress intensity factor K and the crack velocity V, by using dynamic photoelasticity (10,11). It has been shown that the crack velocity in a material suddenly increases from a stationary state to a relatively high value when K reaches a value representing the arrest toughness of the material K_{Ic}. Further increase in K beyond K_{Ic} results in a constant crack velocity subsequent to a small transition zone. Further, the frequency of an AE signal because of a crack growth increment with length sf may be determined from

$$f = \frac{v}{s} \tag{5}$$

With increase in the number of load cycles, during which length s of each crack growth increment becomes larger, and for a constant crack velocity v, it can be seen from Equation 5 that f gradually decreases.

The results from the frequency analysis of the AE signals from the specimens indicate that an effective signal

ination scheme may be used by performing a fast Fourier transformation (FFT) of an AE signal in a bridge member for its identification as a crack- or noise-related signal. Further, from the frequency analysis of a crack-related signal from a bridge member, it will be possible to estimate the remaining fatigue life of the member by comparing the computed peak-frequency component of the signal with the lower and upper frequency values obtained during the laboratory tests.

In the time domain, AE signal parameters, such as signal peak amplitude, counts, duration, rise time, and energy level, were measured. Signals in the laboratory and bridge studies related to mechanical noise showed a wide spread in the acquired time domain data. Signal duration values were on the order of 750 μsec and longer, and the rise time values were approximately 50 μsec and longer. The scatter in the data for the other parameters was large and therefore they were not used in developing a signal discrimination routine. Interference from the signals related to mechanical noise was somewhat minimized by using a front end filter, which incorporated the time domain information on the signal duration and rise time, as described.

In general, all AE signals from fatigue crack propagation in the tested specimens were of relatively low intensity. This was due to the high ductility of the materials used and the resulting low level of energy released at the crack tip for each crack growth increment. Two records of AE signals from a growing fatigue crack in a welded beam specimen at an early stage (54 percent of life) and late stage (98 percent of life) are shown in Figures 8 and 9, respectively. The figures also show the corresponding applied cyclic stress level as a function of time. In Figure 8, the occasional occurrence of low-level, crack-related, burst-type AE signals was produced near the maximum stress level. The continuous-type signals shown in Figures 8 and 9 were related to the plastic deformation associated with crack tip reversal, and the burst-type signals near the lower stress level were related to the hydraulic machine noise and were of no significance. At later loading cycles, the occurrence of the burst-type AE signals, with higher intensity levels, was observed at each cycle of the loading. Figure 9 shows a crack-related AE signal at the maximum stress level
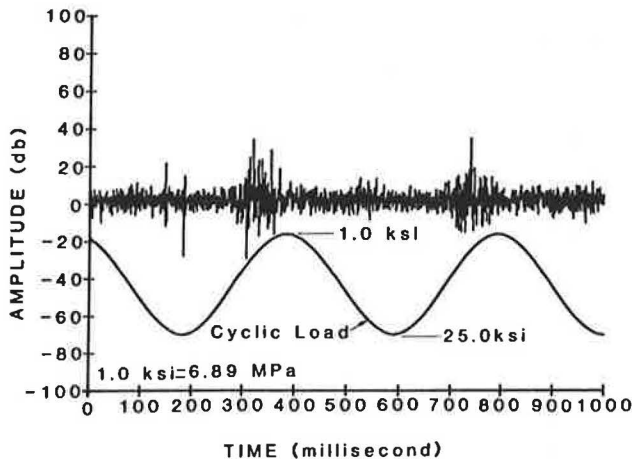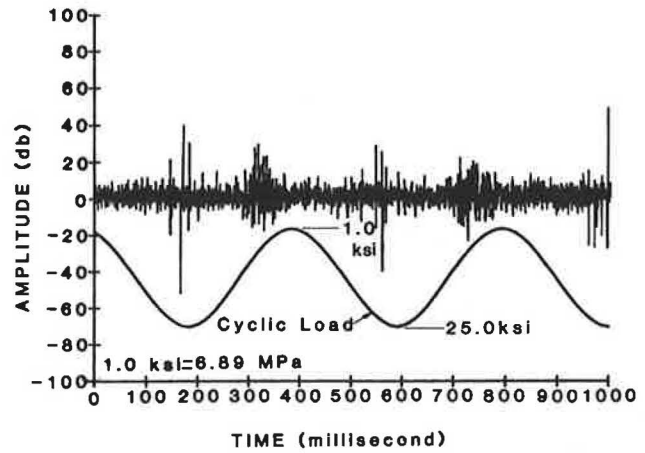

FIGURE 9 AE signals in the weld metal of a welded beam specimen at 98 percent of life (Specimen 2).

for each load cycle at 98 percent of the life of a welded specimen.

In the welded beam specimens, the characteristic features of AE signals were significantly changed as the crack tip, which had initiated in the weld metal, advanced into the heat-affected zone and the base metal. The signal amplitude levels and other AE parameters increased in values during the crack propagation within the weld metal. However, as the crack tip advanced into the heat-affected zone, and subsequently into the base metal, the signal amplitude and other AE parameters showed a decrease in their values. The variation of the signal amplitude (with 95 percent confidence level) with respect to the position of the fatigue crack tip in a welded beam and the rate of crack growth da/dN are shown in Figure 10. All crack tip locations during crack growth were verified by using the ultrasonic unit, traveling microscope, and magnetic contour probe. The signal intensity decreased in spite of the fact that the rate of crack growth da/dN was increased rapidly. Subsequent microscopic examination of the fracture surfaces demonstrated a combination of flat fractured facets with high reflectivity and some dimples that indicated a mix of brittle and ductile modes of fracture in the weld metal. Study of the fracture surfaces showed that in the heat-affected zone and
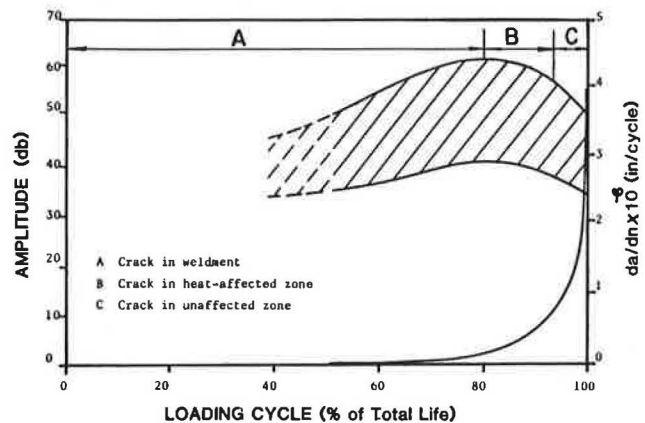

FIGURE 8 AE signals at incipient fatigue cracking in the weld metal of a welded beam specimen at 54 percent of life (Specimen 2).

FIGURE 10 Amplitude of AE signals and fatigue crack growth rate at various stages of life of a welded beam (Specimen 2).

the base metal the fracture was closer to a plastic type with numerous dimples, which were observed on the surfaces. This finding is in agreement with the results of the fracture toughness measurement of various welded bridge beams (*12*). The lower level signal intensities from the crack tip movement within the heat-affected zone and the base metal were the result of the void coalescent and plastic deformation in those regions. Lower signal intensity caused by plastic deformation was also observed by others (*13*). Except for final load cycles just before fracture of the A7 rolled beams, the values for the signal amplitude and other AE parameters were consistently increased with increasing number of loading cycles, because there were no changes in the material's microstructure, i.e., because of welding. Signal amplitude and other AE parameters decreased in magnitude for the final cycles of loading because of the presence of a large degree of plasticity at each crack tip. Generally, the signal amplitudes from crack growth in the weld metal were about 33 percent higher when compared to the results from the rolled beams.

Use of the information obtained during this investigation allowed for successful separation of fatigue-related AE signals from undesirable ones, namely, noise-related signals. The information also permitted detection of the incipient fatigue cracking at relatively early stages of the fatigue life (see Tables 1 and 2). For example, fatigue cracks in the welded beams were first detected by AE at stages ranging from 48 to 63 percent of the total fatigue lives of the beams. Locations of growing fatigue cracks were determined by measuring times of arrival of AE signals to two data transducers. The distance between the calculated position of each crack tip and the actual crack site, as determined by analyzing AE signals, was generally less than 2 percent of the distance between the two data transducers.

Field Test

An in-service steel highway bridge was tested for detection of fatigue cracking. The bridge was constructed from ASTM A373 steel, which is similar to the A7 steel used in the laboratory study during this work. A known fatigue problem area in the bridge was at the ends of floor beams where connections to main girders were made. The floor beams were coped at each end at a right angle and without a gradual transition, causing stress concentration (see Figure 11). Several fatigue cracks had been previously identified in the bridge and had been repaired by drilling a hole at each crack tip. An AE test of a segment of the bridge was performed during this study to evaluate the effectiveness of the previous remedial work and to examine other details that had not been identified with fatigue cracking. No fatigue crack activities were observed by AE in the details that had been repaired. A small fatigue crack, approximately 0.3 mm, was detected by AE at the coping of a floor beam at one of the end connections to a main girder. The presence of the crack was also verified by an ultrasonic evaluation of the area. From the frequency analysis of the AE signals emitted from the crack, a peak-frequency component of 255 kHz was determined, which indicated a fatigue crack activity at an early stage. Because cross-sectional dimensions in the bridge members are larger than those in the laboratory specimens, a plain-strain
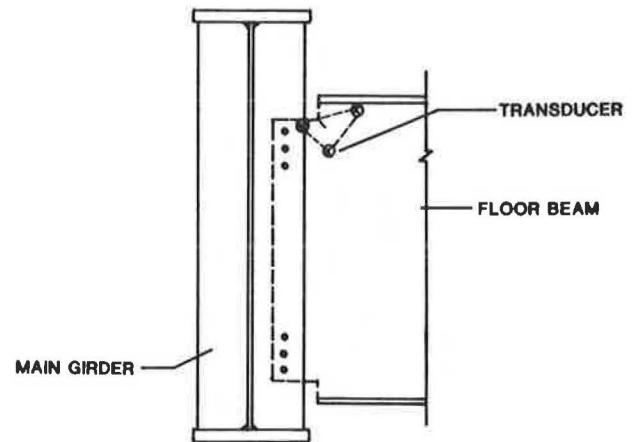

FIGURE 11 A typical detail for connection at a floor beam end and a main girder.

state of stress, which causes a brittle type of fracture, is expected. As a result, AE signals with lower durations, or higher frequencies, are produced. Tests of larger specimens must be performed to verify this effect and to develop the necessary data for use during field evaluation. Results from the time domain analysis of the AE signals from the fatigue crack in the floor beam are presented in Table 5. Because of the scatter in the time domain AE data, the lower and upper limits with 95 percent confidence levels are shown in the table.

CONCLUSION

Use of AE for early detection of active fatigue cracks in highway bridge structural components was discussed. An experimental study that included test specimens made of ASTM A588 and A7 steels was conducted. AE signals from growing fatigue cracks were analyzed for their time and frequency domain characteristics. AE signals from growing fatigue cracks at different stages of their lives contained distinct characteristic features, which can be used for identification of the sources of emission. Fatigue cracks, in all laboratory specimens, were detected at relatively early stages of fatigue lives of the corresponding specimens.

To detect active fatigue cracks at relatively early stages of the fatigue lives of steel highway bridge members by using AE is possible. Early detection in steel bridges can provide

TABLE 5 RANGE OF CRACK-RELATED AE PARAMETERS IN THE BRIDGE

AE Parameters (1)	Lower Limit (2)	Upper Limit (3)
Amplitude	32 dB	35 dB
Duration	15 µs	55 µs
Rise Time	3 µs	8 µs
Counts	5	25
Energy	3	20

adequate warning and ensure the safety of the traveling public. Additionally, a safe and economical remedial work with minimum disturbance of the traffic can be planned. AE may also permit, under normal traffic loading, the assessment of the behavior of existing bridge elements with known defects. By using AE, it is possible to accurately determine whether an existing crack is active. As a result, costly repairs may only be applied to areas with active fatigue cracking.

REFERENCES

1. J. W. Fisher, K. H. Frank, M. A. Hirt, and B. M. McNamee. *NCHRP Report 102: Effect of Weldments on the Fatigue Strength of Steel Beams*. TRB, National Research Council, Washington, D.C., 1970.

2. M. A. Hirt. *Fatigue Behavior of Rolled and Welded Beams*. Ph.D. dissertation. Lehigh University, Bethlehem, Pa., 1971.

3. J. W. Fisher, P. A. Albrecht, B. T. Yen, D. J. Klingerman, and B. M. McNamee. *NCHRP Report 147: Fatigue Strength of Steel Beams with Welded Stiffeners and Attachments*. TRB, National Research Council, Washington, D.C., 1974.

4. P. C. Paris, M. P. Gomes, and W. E. Anderson. A Rational Analytic Theory of Fatigue. *The Trend in Engineering*, Vol. 13, 1961, pp. 9–14.

5. E. G. Signes, et al. Factors Affecting the Fatigue Strength of Welded High Strength Steels. *British Welding Journal*, Vol. 14, No. 3, 1967.

6. F. Watkinson, et al. The Fatigue Strength of Welded Joints in High Strength Steels and Methods for its Improvement. *Proc., Conference on Fatigue of Welded Structures*, The Welding Institute, Brighton, England, 1970.

7. J. M. Barsom and S. T. Rolfe. *Fracture and Fatigue Control in Structures, Applications of Fracture Mechanics*. Prentice-Hall, Englewood Cliffs, N.J., 1987.

8. W. C. Clark. Some Problem in the Application of Fracture Mechanics. Scientific paper 79-1D3-SRIDS-P1, Westinghouse Research and Development Center, Pittsburgh, Pa., 1979.

9. *Manual of Steel Construction*. 8th ed., American Institute of Steel Construction, Inc., 1986.

10. T. Kobayashi and J. W. Dally. A System of Modified Epoxies for Dynamic Photoelastic Studies of Fracture. *Experimental Mechanics*, Vol. 17, No. 10, 1977, pp. 367–374.

11. T. Kobayashi and J. W. Dally. Dynamic Photoelastic Determination of the a-K Relation for 4340 Alloy Steel. *Crack Arrest Methodology and Applications, ASTM STP 711*. G. T. Hahn and M. F. Kanninen, eds., ASTM, Philadelphia, Pa., 1980, pp. 189–210.

12. J. U. Yung. *Mechanical Testing of Welds*. Report FHWA/RD-83/006. FHWA, U.S. Department of Transportation, 1984.

13. A. A. Pollock. Acoustic Emission: Basic Considerations and Energy Transfer and Some Structural Testing Results. Presented at the Institute of Physics Conference on Acoustic Emission, Imperial College, London, England, 1972.

Assessing Highway Field Maintenance Office Locations by the *p*-Median Model

Daniel S. Turner, Jerry R. Weaver, and William D. Gunther

Deciding when to establish a new highway maintenance office and where to put this new office is often a difficult process. A modeling technique may assist in making such difficult decisions. The *p*-median model is widely used in the business field to study the attractiveness between potential service facilities and the audience receiving these services. The model has proved successful in selecting optimum locations for business and government facilities, and it may be readily adapted to the highway field office problem. The theoretical basis, characteristics, and constraints associated with the *p*-median model are discussed. For any fixed number of service facilities, the model finds their optimum locations, such that total system travel is minimized between the facilities and the maintenance sites (adjacent nodes in the road network). The model can also be adapted to optimize two levels of maintenance offices, in which groups of offices at the lower level report to offices at an upper level. Several examples are used to show modeling methods for selecting the best number of field offices and their optimum locations. Weighting factors (lane-miles of pavement, population, maintenance budgets, etc.) are applied to travel distances to modify the attractiveness between nodes and facilities and thus improve the model. An example is given to illustrate calibrating the model in this manner.

State highway departments have widely differing philosophies about the number and locations of field maintenance offices. Deciding when to establish a new field office and where to put this new office is often a difficult process. The decision is usually subjective in nature, with no way to measure the efficiency of alternate locations. For any state, the existing configuration of offices may reflect the historical pattern of state development, political pressures, degree of control exerted by the central office, or all of these.

A statistical technique is used in Alabama to compare alternate locations of field maintenance offices. The technique is called the *p*-median model, and it may be applied either to existing or proposed locations.

NEED FOR MODELING

Sophisticated modeling has been widely accepted in the business world. Business managers use the modeling process to forecast trends, to evaluate various management scenarios, and to help make difficult decisions when there is insufficient data for direct evaluation of the situation. A number of models have been developed for such uses by the business community. As computers have increased in capacity and sophistication,

D. S. Turner, Department of Civil Engineering; J. R. Weaver, Department of Management Science; and W. D. Gunther, Center for Business and Economic Research; University of Alabama, P.O. Box 870205, Tuscaloosa, Ala. 35487.

the models have done likewise. At the current time, some models use extremely large data bases and apply increasingly complex statistical procedures to overcome incompleteness or irregularities of the data and to examine increasingly large numbers of scenarios.

Highway engineers have traditionally made good use of computers as part of the engineering design process, and for accumulation, use, and reporting of data. Increasingly, engineers are using computers as management tools. Maintenance management systems and bridge management systems are two good examples of highway management through computer applications. Several bridge management systems use sophisticated operations research techniques to analyze incomplete data sets (called fuzzy data) and to make complex decisions regarding optimization of funding for bridge treatment.

APPLICATIONS TO HIGHWAY FIELD OFFICES

Field offices are normally placed so that employees have reasonable access to all roadway locations, and so that the public has good access to a highway manager. Enough offices should be close together so that employee travel time to the work site is reasonably minimized. On the other hand, there should not be too many field offices because the administrative overhead becomes too large a portion of the overall highway budget. The most efficient arrangement usually has a minimum number of field offices located in the optimum locations so that employees can readily cover the entire roadway network.

It seems logical that modeling techniques could be used to pick the optimum locations of field offices. Because the problem involves multiple trips from field offices to different nodes in the transportation system, it lends itself to the *p*-median technique.

One use for modeling might be to choose where to place a new county-level maintenance office in a location where there had previously been none. Trial locations of the office could be modeled to determine which location minimized overall travel from the office to the various roadway sections. Similarly, the current offices in several counties could be studied for closure with the replacement by a single office serving several counties. In this case, the added expense of constructing the new office and the added expenses of longer employee travel routes could be balanced against the savings generated by the closure of the multiple existing field offices.

The modeling process can be customized to fit individual states or individual regions within a state. For example, measures of economic development and growth (population, income per capita, dollars of manufacturing per capita, etc.) can be

added to the model to evaluate the need for future offices in areas of high growth. It is also possible to use such models to devise plans for the highway agency for future reshaping of its field office network through additions, closures, and relocations of offices.

SIMPLIFIED DESCRIPTION OF THE *p*-MEDIAN MODEL

Several examples will illustrate the nature of the *p*-median model. This discrete model has been used to establish the optimum locations for medical facilities in rural India, to identify the best pattern for neighborhood schools, and to predict the best locations for commercial and merchandising outlets. In general, the model measures accessibility of a facility that is delivering a service to a widespread audience.

The *p*-median methodology attempts to find an optimum set of locations for facilities by minimizing the distances between these facilities and the audience that they serve. In the context of highway maintenance offices, the model has the following characteristics:

1. All demands for service are assigned to the closest facility.
2. Each demand for service is located at a node within the transportation network.
3. The number of facilities (maintenance field offices) is a fixed value for each scenario to be modeled.
4. The model attempts to reach equilibrium by minimizing the distances between the service facilities and the adjacent nodes.
5. Trial locations of service facilities are established and nodes are assigned to them. The nodes are then reassigned to various facilities until the optimum locations and patterns are identified.
6. The physical distances between nodes and service facilities can be weighted to reflect the attractiveness of one node over another.
7. The model calculates an objective function for each possible pattern and attempts to find the best configuration by optimizing this function.

The typical state highway agency has multiple levels of field offices. Typically, this involves several district offices reporting to one larger division office, which in turn reports to the headquarters of the agency. The *p*-median model has now been modified to handle multiple levels of facilities. The hierarchical facility version of *p*-median has several characteristics in addition to those for the normal version, as follows:

1. There are multiple levels of facilities such that each facility level provides different but related services.
2. The service levels form a nested facility hierarchy.
3. The presence of a higher-level facility in a region requires that more than one lower-level facility also be located in that region.
4. For a given number of facilities and for a given ratio of higher-order to lower-order facilities, the model selects the optimum locations of the higher-order facilities with an optimum pattern of lower-order facilities clustered around them.

The concept of the *p*-median technique is simple to grasp. Given a fixed number of facilities, it finds a set of locations that minimizes the total system of travel between the facilities and the network that they serve. The model operates by starting with trial locations and calculating the total travel. One at a time, the model then exchanges nodes in and out of the current solution set until the objective value is optimized. For the hierarchical problem with two levels of facilities, the model starts by calculating travel for a fixed set of primary offices. Then a level change procedure is used to find optimum locations for the lower-level offices. The model then switches levels and returns to find another optimum configuration of higher-level offices, then switches back to find a matching set of second-level offices. This procedure is repeated until the objective function is minimized for all locations of first-level and second-level facilities. Obviously for simulation of an entire state, this procedure can involve an extremely large number of manipulations and calculations.

The basic premise of trial-and-error location of offices to minimize travel can be enhanced through analytical techniques. In the next section, the theoretical basis for the *p*-median methodology and heuristic and bounding procedure techniques used to improve the modeling process are described.

THEORETICAL BASIS OF THE *p*-MEDIAN MODEL

The highway maintenance office location problem is a generalization of the *p*-median problem. It can be formulated as a binary linear programming problem as follows:

Minimize

$$\sum_{i=1}^{n} \sum_{j=1}^{n} a_i d_{ij} x_{ij} \tag{1}$$

subject to

$$\sum_{j=1}^{n} X_{ij} = 1 \qquad \text{for } i\varepsilon I \tag{2}$$

$$\sum_{j=1}^{n} Y_j = P \tag{3}$$

$$X_{ij} \leq Y_j \qquad \text{for } i\varepsilon I, j\varepsilon J \tag{4}$$

$$X_{ij}, Y_j \varepsilon \{0, 1\} \tag{5}$$

where

J = set of potential facility sites;
I = set of demand nodes ($I = J$);
n = number of demand nodes;
Y_j = 1 if a facility is located at Node j, 0 otherwise;
X_{ij} = 1 if the demand at Node i is assigned to a facility at Node j, 0 otherwise;
a_i = population (or weight) at Node i;
d_{ij} = distance traveled (cost incurred) if the demand at Node i assigns to a facility at Node j; and
P = number of facilities to be located.

This formulation is a slight modification of the ReVelle and Swain (*1*) formulation of the *p*-median problem. Implicit in this formulation is the assumption that all demand is located at the nodes of the transportation network. The objective function (Equation 1) of the formulation minimizes weighted distance. The constraint set (Equation 2) ensures that each demand node is assigned to one and only one facility node. Assignment is limited to open facilities (Equation 4). The number of open facilities is limited to *p* by constraint (Equation 3). The final constraint set (Equation 5) is the binary requirement. If the facility variables Y_j are binary, then it can be shown that the assignment variables X_{ij} are also binary, so the restrictions on the X_{ij} variables can be relaxed to nonnegativity requirements.

Some high points in the history of the *p*-median problem will now be noted. Hakimi (*2*) described the problem and gave a proof that if all demand is located at the nodes of the transportation network then an optimal facility set will exist consisting of nodes. Tietz and Bart (*3*) developed an exchange heuristic for the *p*-median problem that starts with an initial configuration and exchanges nodes not in the current configuration with nodes in the current configuration until no one-at-a-time exchange will reduce weighted distance. ReVelle and Swain (*1*) formulated the problem as a binary linear program and discovered that if the constraint set (Equation 5) is relaxed to nonnegativity conditions before the formulation is solved, natural binary solutions are obtained in many cases. Corneujols et al. (*4*) and Narula et al. (*5*) developed an efficient solution procedure for the *p*-median problem on the basis of subgradient optimization of a Lagrangian dual. In both cases, the Lagrangian dual was developed by multiplying each assignment constraint (Equation 2) by a nonnegative multiplier and appending it to the objective function (Equation 1).

The *p*-median problem is often used to analyze public sector locational decisions in which the cost of facilities or the benefits of services are difficult to estimate with precision. Sometimes, the actual number of facilities that should be established is one of the decisions to be made, in which case the formulation can be solved for various values of *p*, and a tradeoff curve can be drawn between the number of facilities and weighted distance. Weighted distance is used as a surrogate for the aggregate level of service in the locational system. Thus, a tradeoff curve between the number of facilities and weighted distance allows an evaluation of the improvement in service that results from additional facilities.

Hierarchical Median Model

The *p*-median problem has been applied in many different contexts; however, there are a number of situations that require extensions of the basic *p*-median model to allow for such factors as multiple time states, nonclosest facility service, a coverage objective, and facilities of different types. A more complete account of these generalizations of the *p*-median problem is given by Church and Weaver (*6*) and the references contained therein. The problem of locating district offices and division offices of a state highway department can be modeled as an extended median problem known as the "nested hierarchical median problem." The hierarchical median model was developed by Weaver and Church (*7*) as a general multiple-level model. The problem here is modeled as a two-level hierarchical locational system, and a two-level formulation will be given. Special-purpose solution procedures for the nested hierarchical median will be outlined for the two-level case. A more general formulation and more complete account of the solution procedures is given by Weaver and Church (*7*), who include an account of the nested hierarchical median model's relationship to other models in the location literature.

Two-level hierarchical facilities provide two types of services in a manner such that there is a hierarchical relationship between the first-level facilities and the second-level facilities. The location of a second-level facility at a site requires that a first-level facility also be located at the site. In the context of highway department district and division offices, first-level facilities are district offices and second-level facilities are division offices. Division offices are only located in counties with district offices so this problem can be modeled as a nested hierarchical median problem.

The two-level nested hierarchical median model can be formulated as a binary linear program as follows:

Minimize

$$\sum_{k=1}^{2} \sum_{i=1}^{n} \sum_{j=1}^{n} a_{ik} d_{ij} X_{ijk} \tag{6}$$

subject to

$$\sum_{j=1}^{n} X_{ijk} = 1 \qquad \text{for } i\varepsilon I,\ k = 1,\ 2 \tag{7}$$

$$\sum_{j=1}^{n} Y_{jk} = P_k \qquad \text{for } k = 1,\ 2 \tag{8}$$

$$X_{ijk} \le Y_{jk} \qquad \text{for } i\varepsilon I,\ j\varepsilon J,\ k = 1,\ 2 \tag{9}$$

$$Y_{j2} \le Y_{j1} \qquad \text{for } j\varepsilon J \tag{10}$$

$$X_{ijk},\ Y_{jk}\ \varepsilon\ \{0,\ 1\} \tag{11}$$

where

a_{ik} = demand at Node *i* for *k*-level service;
P_k = number of *k*-level facilities to be located ($P_2 \le P_1$);
Y_{jk} = 1 if a *k*-level facility is located at Node *j*, 0 otherwise; and
X_{ijk} = 1 if the demand for *k*-level service at Node *i* is assigned to a facility at Node *j*, 0 otherwise.

The objective function (Equation 6) again minimizes weighted distance, but here it is weighted to both first-level and second-level facilities. The constraint set (Equation 1) ensures that all demand nodes are assigned to exactly one first-level facility and one second-level facility. Assignment of demand nodes to facilities can take place only if a facility of the proper level is open as a result of the constraint set (Equation 9). Exactly P_1 first-level and P_2 second-level facilities will be opened because of the constraint set (Equation 8).

The constraint set also ensures that a second-level facility will not be opened at a site unless a first-level facility is also

opened at the site (Equation 10); Equation 11 is the binary requirement. The constraint that is required to enforce the nesting property makes the model more difficult to solve (Equation 10). Without the nesting constraint set (Equation 11), the formulation (Equations 6 through 9 and Equation 11) can be solved as two independent *p*-median problems.

Solution of the Nested Hierarchical Median Problem

The formulation for the two-level hierarchical median problem can be solved with commercial mathematical programming software such as IBM's MPSX/MIP. The difficulty of such a solution approach lies in the problem size. The formulation has $2n^2 + 2n$ decision variables of which $2n$ (the facility variables) must be explicitly required to be binary. The number of constraints is $2n^2 + 3n + 2$. For the problem of location of the highway district and division offices, when all 67 Alabama counties were considered potential facility sites, the resulting mixed-integer programming problem had 9,112 variables (of which 134 were required to be binary) and 9,181 constraints. Even with today's computing tools, this problem is large, especially when it is considered that in many cases one wants to solve the formulation for several different values of the parameters, such as the number of facilities (P_1, P_2) and demand weights (a_{ik}), so that not just one large mixed-integer linear program must be solved, but many such problems.

Efficient special-purpose solution procedures that have been developed for the *p*-median problem have been modified for the hierarchical median problem. Two approaches have been shown experimentally to generally obtain good results in a reasonable amount of computer time for the *p*-median problem. These approaches are the primal exchange heuristic and Lagrangian bounding. When both approaches are used together, optimal or near-optimal results are generally obtained for problems on the basis of actual spatial data sets. The modifications required for the *p*-median procedures are described later. A more complete account has been provided by Weaver and Church (7).

The exchange heuristic for the *p*-median problem was developed by Teitz and Bart (3). The heuristic, which starts with an initial facility set, partitions the nodes of the transportation network into facility nodes and nonfacility nodes. The effect of exchanging each node in the facility set with a node in the nonfacility set is determined. If an exchange reduces weighted distance, the change is made. After all nodes in the initial nonfacility set have been considered for exchange into the facility set, a cycle is complete. The heuristic then repeats the preceding steps, using the facility set of the first cycle as its starting set. This continues until no cycle produces an improvement in the model (i.e., no reduction in weighted travel distance). Modifying the exchange heuristic to solve the nested hierarchical median model proceeds by letting second-level facility locations be determined by their place in the facility list and by making the necessary changes in objective function evaluations. However, if these are the only modifications made, there is a possibility that facilities may be in the facility set at the wrong level. The heuristic can be improved by changing the level of facilities at the end of each cycle if such changes reduce weighted distance. This modified heuristic has been shown to obtain an optimal or near-optimal result for several moderately sized data sets (7).

Another solution approach that can be used alone or after the exchange heuristic is Lagrangian bounding. A Lagrangian dual (LD) (of Equations 6–11) is formed by multiplying each assignment constraint (Equation 7) by a nonnegativity multiplier μ_{ik} and appending the result to the objective function. After simplification and modification of the binary requirements (Equation 11), the following LD results:

Maximize

$$LD(\mu) = \text{Min} \sum_k \sum_i \sum_j (a_{ik} - \mu_{ik})X_{ijk} + \sum_i \sum_k \mu_{ik} \quad (12)$$

subject to

$$\sum_j Y_{ik} = P_k \quad \text{for } k = 1, 2 \quad (13)$$

$$X_{ijk} \leq Y_{jk} \quad \text{for } i \varepsilon I, j \varepsilon J, k = 1, 2 \quad (14)$$

$$Y_{j2} \leq Y_{j1} \quad \text{for } j \varepsilon J \quad (15)$$

$$(X_{ij2}, Y_{j2}) \, \varepsilon \, \{0, 1\} \quad (16)$$

$$(X_{ij1}, Y_{j1}) \, \varepsilon \, \{0, 1, 2\} \quad (17)$$

$$Y_{j1} \leq Y_{j2} + 1 \quad (18)$$

For any set of multipliers μ_{ik}, the formulation (Equations 12–18) determines a valid bound on the primal problem (Equations 6–11). The binary requirement for first-level assignments and facilities are relaxed in Equations 17 and 18 to make the dual easier to solve. For a fixed set of multipliers, the dual problem is solved as follows:

Define

$$E_{j1} = \sum_{i=1}^n \min(0, a_{i1}d_{ij} - \mu_{i1}) \quad \text{and} \quad (19)$$

$$E_{j2} = E_{ji} + \sum_{i=1}^n \min(0, a_{i2}d_{ij} - \mu_{i2}) \quad (20)$$

Determine the P_2 smallest E_{j2} values and $P_1 - P_2$ smallest E_{j1} values; add the sum of these E_{jk} values just determined to the sum of the multipliers, and the value of the dual is determined. The solution of the dual may not be primal feasible, but a feasible completion of this dual solution is easily constructed using E_{jk} values. For any set of multipliers μ_{ik}, a valid lower bound is determined and a feasible completion is available that can be compared to the best primal solution found so far (by the exchange heuristic or the bounding procedure). The task then is to determine a set of multipliers that maximizes the dual lower bound. This procedure can be accomplished by subgradient optimization as in Narula et al. (5) or Weaver and Church (8,9). The bounding procedure is terminated when the lower bound is within a specified tolerance of the best primal value identified or after a fixed number of interactions. When the exchange heuristic followed

by Lagrangian bounding was used to solve the highway district and division office location formulations, optimal or near-optimal solutions were always obtained.

APPLICATION OF *p*-MEDIAN METHODOLOGY

An example will be given to illustrate one use of modeling in examining the location of field offices. In this case, the *p*-median study was used for two purposes: (a) to evaluate the optimum number of division offices in Alabama and (b) to identify the best locations for these offices. In Alabama, the lower-level facilities are called district offices. Typically, three to six districts report to a division. Currently, the Alabama Highway Department has nine division offices.

Operation of the Model

For this study, the higher-level service facilities were division offices. The lower-level service facilities were district offices. The accessibility function was defined as the distance in miles between the various county seats in the state.

The physical distances between county seats were weighted by various factors that were felt to possibly influence highway maintenance costs and the level of service for maintenance. Factors that were examined in this trial study included centerline miles of state route, lane-miles of state route, vehicle-miles of travel, Alabama Highway Department historical maintenance cost records, population density, and income per capita. A series of constraints were also devised to simulate geographical and other real-world situations (indirect travel routes caused by rivers or mountains, spatial development patterns, etc.).

The model was operated separately with each of the parameters used to weight the accessibility of field office locations. The model was run many times for each parameter to determine the effect of increasing or reducing the number of field offices. Typically, scenarios were tested starting with four division offices around the state and progressing until 10 or 12 division offices had been studied. In each case, the optimum locations of division offices were plotted and the value of the objective function was tabulated for further study.

Results of *p*-Median Study

The *p*-median technique was used to establish an optimum number of division offices by tabulating the objective function from a series of computer runs. Adding more division offices reduces total travel because each district office becomes closer to a division office. At some point, so many division offices will have been added that there is almost no change in overall travel. This effect is shown in Table 1 and on Figure 1. The researchers examined the marginal change in the objective function as a technique for determining the best number of division offices. From Figure 1, a level of efficiency was noted after seven offices had been placed in the state because the marginal change reached a plateau. When there were seven, eight, or nine divisions in the state, the marginal change in objective value was relatively constant at about 4 percent. However, as a 10th office was added, the marginal change dropped drastically to about 2 percent, where it reached a new plateau. The drop from 4 to 2 percent indicates that exceeding nine division offices would not be as effective in minimizing travel as additions up to that time.

The effectiveness of adding additional division offices is highly dependent on the shape and density of the road network. Once the road network is in place, the optimum location for maintenance offices becomes a matter of minimizing travel over this network. In urban or semiurban locations where there are many miles of roads and alternate routes, the model will examine multitudes of locations to find the optimum travel configuration between offices. In underdeveloped rural areas, there will be few trial locations and the model can quickly choose the optimum locations.

When determining the optimum number of locations for offices, the marginal change curve (Figure 1) is usually balanced against the cost of division offices to find an optimum value for number of field offices, such that the cost for construction of the offices and the overhead for running them when combined with the operating cost of maintaining roads has reached a minimum value. This point may be found through an analytical analysis or by simply combining a plot of the change in objective value with a plot of the cost for adding new division offices.

TABLE 1   CHANGES IN OBJECTIVE VALUE FOR INCREASES IN THE NUMBER OF DIVISION OFFICES

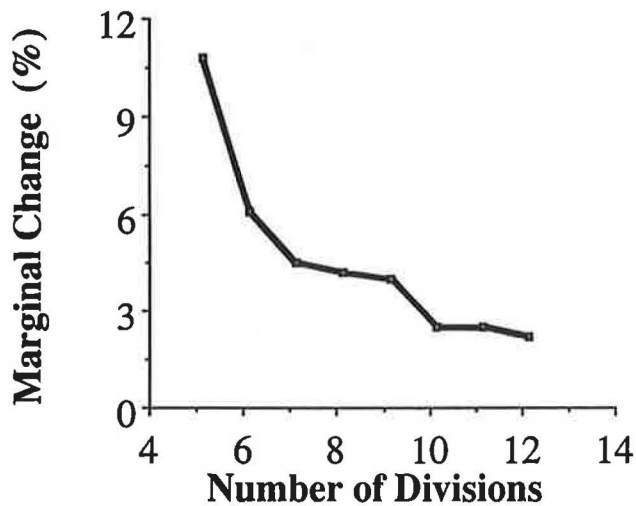| Number of Division Offices	Objective Value	Marginal Change
4	423,946	--
5	378,984	- 10.6%
6	353,995	- 5.9%
7	335,848	- 4.3%
8	318,685	- 4.0%
9	302,873	- 3.8%
10	291,821	- 2.3%
11	281,244	- 2.3%
12	271,919	- 2.0%

FIGURE 1 Marginal change in objective values.

Optimum Office Locations

Two figures indicate the results of *p*-median studies. Figure 2 shows the search for the optimum number of division offices. Figure 3 shows the effects of using several weighting factors to modify the distances between service facilities to reflect the attractiveness of some sites over others.
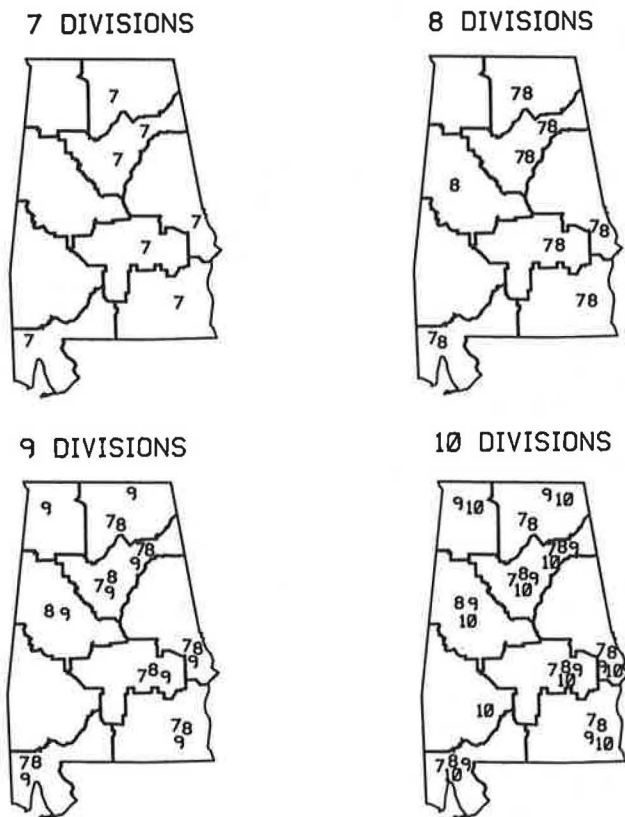

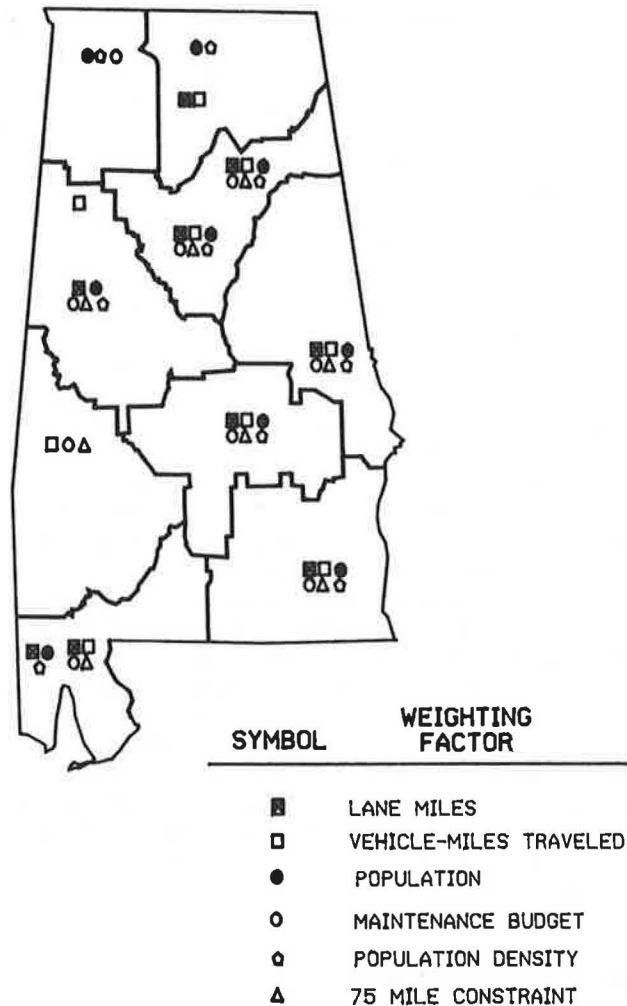FIGURE 2 Existing division boundaries and changes in optimum locations with increased offices.

SYMBOL	WEIGHTING FACTOR
▣	LANE MILES
□	VEHICLE-MILES TRAVELED
●	POPULATION
○	MAINTENANCE BUDGET
◑	POPULATION DENSITY
△	75 MILE CONSTRAINT

FIGURE 3 Existing division boundaries and optimum locations for nine division offices.

Number of Division Offices

The model can be used to determine the optimum locations for any given number of division offices. The number of offices can be varied through several scenarios to measure the effectiveness of various levels of field offices. This method can be used to find the best number of offices by examining marginal changes in objective value. Another use for such a study is to analyze the growth of field offices, in response to historical changes in population, miles of road, and other factors. This type of study is shown in Figure 2.

The fitness of any particular location for an office can be assessed by noting when it first appeared in the solution set, and how consistently the location remained in the solution set from scenario to scenario. Figure 2 shows a series of scenarios seeking the optimum locations for 7 to 10 division offices, using population as the weighting factor. After the modeling had been completed, six locations were found to have been assigned division offices for all scenarios. These sites might be considered excellent candidates for permanent division offices. One other location was assigned division offices in three of the scenarios and would also be considered a good

permanent site. Three additional locations received division offices in two of the scenarios, while one site was only assigned an office in one scenario. The modeling process could be extended by increasing or decreasing the number of offices until the user obtained a good feel for the situation being studied and the attractiveness of various sites as possible field office locations.

Adding division offices in consecutive scenarios provided a step-by-step picture of the expansion of the highway agency. Experienced highway managers assisted the research staff in understanding the results of the modeling by recalling the historical additions of offices and relating these changes to factors like population growth, construction of new roads, etc.

Each scenario must be examined in detail during the evaluation process. Drastic changes may occur between consecutive computer runs. For example, going from seven field offices to eight offices is not as simple as choosing the best site for the next office. It may involve changes to many of the previous locations in order to accommodate the added division office. For example, adding a new office at the north end of a state may squeeze the remaining offices toward the south end of the state to balance travel among all offices. If a state already had seven field offices, the model may indicate that six of the existing offices should be relocated to add an eighth office. Although the model showed eight offices to be the best number and the most efficient arrangement, the highway agency would have to close and reconstruct so many existing offices that the net result would not be cost effective. The user must interpret the model carefully to understand its limitations and implications.

Alternate Weighting Factors

It would be ideal if a single factor could be identified that always measured the effectiveness of alternate locations of maintenance offices. Where such a direct measurement or a surrogate measurement existed, it would be relatively simple to choose optimum locations. In the real world, a single factor can rarely be identified, and usually many possible influences (weighting factors) are considered for use in choosing office locations. Figure 3 shows one possible way to study surrogate measures of effectiveness both individually and in combination with other factors.

Figure 3 was prepared by formulating a scenario, then changing the weighting factors between consecutive computer runs. The optimum locations were plotted for each factor, then compared visually.

Figure 3 can be further analyzed to determine the role of each of the parameters used as weighting factors. For example, using current population values in each county as the weighting factor would yield a set of optimum locations. Next, miles of vehicle travel in each county could be used as the weighting factor and another set of offices identified. The two sets could be compared to each other and to the locations of existing field offices to evaluate the applicability of the factors and to calibrate the model. Large numbers of weighting factors could be tested to increase the effectiveness of the model.

When certain parameters are found to be reasonable surrogates for measuring the effectiveness of maintenance office locations, future values of the parameters could be investigated. The model could use estimated future values to show the effects of population growth, increased vehicle travel, or decreased maintenance budgets. The results of such scenarios can be used in planning future field office configurations of the highway agency.

A further illustration of the versatility of the model is shown on Figure 3. An artificial constraint was created to require that all district offices be located within 75 mi of a division office. This provided a way to reasonably minimize travel times for employees. For the case of nine division offices, the model was able to place the offices in locations that met the constraints. However, the constrained locations were in much different places from those selected by any other modeling effort. When the constraint was changed to 60 mi, finding nine locations that met the criteria was impossible. The model could have easily been expanded to study 100-mi constraints or other conditions. Such modeling provides background information to assist highway managers in making decisions regarding locating new field offices.

Summary of Examples

Two examples have been briefly presented to illustrate the modeling process and the types of results that may be expected. Both examples make it apparent that a scenario may be tailored to fit the local situation, and many conclusions may be drawn from the examples by careful study. Such adaptation may yield insights into the best locations for both existing and future field offices.

RESULTS

The purpose of the p-median modeling was to identify possible changes to increase efficiency in the location of high-level field maintenance offices of the Alabama Highway Department. The modeling was successful in defining one location that was a strong candidate for a new office, and in defining several existing offices that would be more efficient if relocated.

Following the p-median study, the researchers performed an intensive analysis of the travel savings provided through adoption of the new and relocated offices. This analysis was performed by an intensive, more conventional model that tracked travel to and from each roadway segment in a division. This second model provided quantitative estimates of travel savings; however, it was labor intensive and consumed huge amounts of computer time. The second model could not have been used to study all possible changes, but it did not have to be used in that manner because the p-median model had already defined the most realistic scenarios.

According to the final results of the research project, a new division office was not cost effective. Because a relocation of one division office with a consequent realignment of the boundaries of three affected divisions was found to be cost effective, the Alabama Highway Department is moving toward implementation of this latter recommendation.

CONCLUSION

The *p*-median model is widely used in the business industry to study the attractiveness between service facilities and the audience receiving services. The model has had demonstrated success in selecting optimum locations for business and government facilities, and it may be readily adapted to the highway field office problem.

The *p*-median model is easy to formulate, easy to calibrate, and relatively inexpensive to run. Many alternative scenarios may be examined quickly once the model has been formulated.

There are certain limitations to using the model. Surrogate measures must often be studied when directly measuring the effectiveness of office locations is impossible. The accuracy of conclusions drawn from use of the model may be limited by the appropriateness of the weighting factors and by the resourcefulness and experience of the persons interpreting the results.

ACKNOWLEDGMENTS

REFERENCES

1. C. ReVelle and R. Swain. Central Facilities Location. *Geographical Analysis*, Vol. 2, 1970, pp. 30–34.
2. S. L. Hakimi. Optimum Distribution of Switching Centers in a Communication Network and Some Related Group Theoretic Problems. *Operations Research*, Vol. 13, 1965, pp. 462–475.
3. M. E. Teitz and P. Bart. Heuristic Methods for Estimating the Generalized Vertex Median of a Weighted Graph. *Operations Research*, Vol. 16, 1968, pp. 955–961.
4. G. Corneujols, M. L. Fisher, and G. L. Nemhauser. Location of Bank Accounts to Optimize Float: An Analytic Study of Exact and Approximate Algorithms. *Management Science*, Vol. 23, 1977, pp. 789–810.
5. S. C. Narula, U. I. Ogbu, and H. M. Samuelsson. An Algorithm for the P-Median Problem. *Operations Research*, Vol. 25, 1977, pp. 709–713.
6. R. L. Church and J. R. Weaver. Theoretical Links Between Median and Coverage Location Problems. *Annals of Operations Research*, Vol. 6, 1986, pp. 1–20.
7. J. R. Weaver and R. L. Church. The Nested Hierarchical Median Facility Location Problem. *INFOR, Canada* (in press).
8. J. R. Weaver and R. L. Church. Computational Procedures for Location Problems on Stochastic Networks. *Transportation Science*, Vol. 17, 1983, pp. 168–180.
9. J. R. Weaver and R. L. Church. A Median Location Model with Nonclosest Facility Service. *Transportation Science*, Vol. 19, 1985, pp. 58–74.

Feasibility Study of Changes to the Highway Maintenance and Operations Cost Index

MICHAEL J. MARKOW, EDMOND L. SEGUIN, EUGENE F. IRELAND, AND DEBORAH M. FREUND

The highway maintenance and operations cost index, published annually by FHWA, was established in its current form in 1947 and has not been revised since. The purpose of this study was to evaluate the procedures used to develop the index, and to consider the feasibility of options—retaining it in its current form, revising, redeveloping, or discontinuing the index. This study included several tasks: a literature review of the theoretical aspects of price index development; a detailed survey of state department of transportation needs for the index, current uses, relationship to maintenance operations, preferences for change, and assessments of the utility of different options; a detailed review of other construction and maintenance indexes and related cost data; analyses of current maintenance index behavior, and comparison with construction indexes of various types; and recommendations to FHWA regarding the future of the index. On the basis of the findings of this study, the most favorable option is index redevelopment. A revised index will require collaboration between FHWA and the states for the critical tasks of identifying candidate items of labor, equipment, and materials for a simpler market basket; actually defining and building the market basket; redesigning forms (with clearer instructions) for states' submission of data; creating the weighting functions to translate state unit cost data into regional and national composites; and defining the regions that are to be encompassed. Furthermore, this collaboration must continue on a long-term basis to review the index periodically and revise it as needed.

Results of a study of the highway maintenance and operations cost index [hereafter referred to as "the maintenance (cost) index" or "the index"] are discussed. The objectives of the study were twofold:

- To evaluate the procedure now used to develop the maintenance index; and
- To perform a feasibility study of options: retaining the index in its current form, revising, redeveloping, or discontinuing it.

The index is published annually by FHWA (see Figure 1) (1). The index is based on a fixed market basket of 34 items of maintenance labor, equipment, materials, and overhead. Unit prices or costs are applied each year to these fixed quantities of maintenance items; the resulting total cost is compared to the equivalent cost in a reference base year to compute the value of the index.

The procedures now used to compute the index involve a cooperative effort between FHWA and the states, in which the states compile their average unit costs of the 34 market basket items. These data are submitted annually to FHWA, which checks them and removes nonconforming entries. The cost data are then processed to compute the composite maintenance index, as well as subsidiary indexes for labor, equipment, materials, and overhead items.

The maintenance index serves as a price index, measuring the purchasing power of a maintenance dollar over time. Because the index is tied to a market basket, it does not reflect other conditions that also affect maintenance costs in the field, such as

- Shifting composition of the road inventory, reflecting evolution of road design standards, materials usage, and construction practices;
- Changes in maintenance policy, standards, or levels of effort (e.g., deferred maintenance, stopgap maintenance);
- Evolution of maintenance technology and practice;
- Differences in management techniques and their effectiveness;
- Effects of safety-related or other regulatory requirements (e.g., those affecting crew composition or work performance);
- Adjustments in maintenance productivity resulting from one or more of the previously mentioned items;
- Changes in need for maintenance that arise from increasing traffic, age of facility, or unusual environmental conditions.

HISTORY

The structure, composition, and analytic basis of the current maintenance index were established in 1947 to help assess cost trends in road maintenance prior to and following World War II. The index was based on the costs of maintaining a hypothetical, 10,000-mi sample of highways. This sample was composed of five types of roads: portland cement concrete, bituminous concrete, low-type bituminous, gravel-stone-soil, and nonsurfaced. The percentages of each type of road in the sample matched the actual distribution of surface types on state highways nationally in 1947.

M. J. Markow, Cambridge Systematics, Inc., 222 Third St., Cambridge, Mass. 02142. E. L. Seguin, Institute for Research, 257 S. Pugh St., State College, Pa. 16801. E. F. Ireland, 221 S. Busch Place, Tucson, Ariz. 85710. D. M. Freund, FHWA, Office of Motor Carrier Standards, 400 Seventh St., S.W., Washington, D.C. 20590.

The annual maintenance requirements estimated for this 10,000-mi sample were decomposed into labor, equipment, materials, and overhead for six highway elements: road surface, shoulders and approaches, roadside and drainage, traffic services, snow and ice control by sand, and bridges. These maintenance requirements were then consolidated into 34 items of labor, equipment, materials, and overhead. These 34 items were priced each year, as discussed, using average costs provided by the states, with each state's cost weighted by FHWA to arrive at a national composite unit cost for each of the items. The result is the total cost of maintaining the hypothetical 10,000-mi road network. When this cost is divided by the corresponding cost computed in the reference base year, and the result multiplied by 100, the value of the maintenance index shown in Figure 1 is obtained.

In 1967, a report by NCHRP recommended changing the maintenance cost index to a unit maintenance expenditure index (*2*). The revised index was intended to track highway maintenance expenditures by centerline-mile and class of system.

A limitation of this proposed index was that it too would not reflect the potential variations in availability of maintenance funds, crew productivity, and other factors that affect actual maintenance performance. It would show the change in the states' expenditures from year to year, but would not take into account, for example, the reduced levels of service forced by insufficient resources. Thus, a substantial increase in the unit costs of labor, equipment, or materials might be hidden in the total yearly expenditures of the states if the levels of maintenance effort were reduced. For these reasons, FHWA management decided not to implement the recommended changes but rather to retain the maintenance cost index as originally established in 1947.

In 1987, FHWA determined that a new evaluation of the index was needed. As the era of Interstate highway construction draws to a close, the relative responsibilities of states has begun to shift from the construction of new facilities to the lifetime maintenance of facilities in place. Timely, effective maintenance is important to the ability of the highway system to safely and efficiently meet increasing traffic demands. Both the nationwide highway network and the maintenance methods used had evolved over 40 years; it was definitely time for a second look at the index. The result of this initiative was the feasibility study described herein.
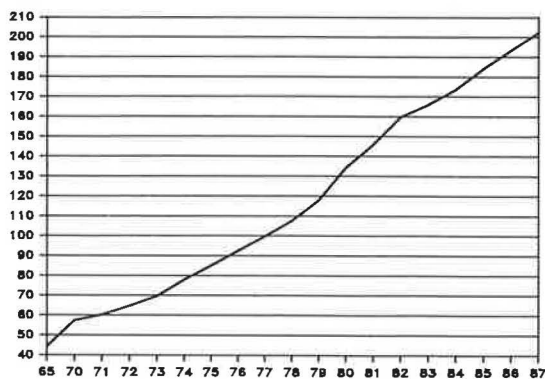

FIGURE 1 Trend of the highway maintenance and operations cost index.

OUTLINE OF STUDY

The scope of this study encompassed the current applications of the index, accuracy of its data, limitations of the data base, assumptions inherent in index calculations, and the degree to which the index reflects current maintenance and operations cost trends. Developments since 1947 in the road network itself, types and manner of data collection, changes in technical and financial record keeping, and maintenance management practices have provided the historical backdrop and current context within which revisions to the index were investigated.

This feasibility study addressed potential changes to the index to more accurately reflect prevailing conditions and trends. Data base development and data reporting requirements were examined to identify potential new sources of meaningful and measurable information, while not imposing a reporting burden on state highway agencies. Methods to assess this information for both statewide and nationwide perspectives were also examined. Costs and benefits were evaluated from perspectives of both data collection and analysis. From these findings, recommendations for future changes to the index were developed.

A close and continuing working relationship with highway maintenance practitioners was deemed necessary for the successful performance of this effort. A number of papers were prepared over the course of the study. A workshop was held to bring together representatives from state highway agencies and FHWA to exchange information and ideas on both the application of the current system and proposals for revision or redevelopment to better meet the needs of the highway maintenance community.

STATE PERSPECTIVES ON THE HIGHWAY MAINTENANCE INDEX

State departments of transportation (DOTs) represent the primary intended users of the FHWA maintenance cost index. Obtaining their opinions on the current use of the index, procedures for collecting and processing data, and options for revising the index was therefore important. Two mechanisms of contact with the states used were (a) survey of nine states, including site visits, and (b) establishment of a panel, or working group, of state representatives to offer advice and guidance during the course of this project. Both mechanisms proved to be extremely helpful and effective.

The survey of nine states constituted one of the major tasks of this project. In consultation with FHWA and the working group, nine states were included in the sample: California, Colorado, Florida, New Jersey, Ohio, Oregon, Pennsylvania, Texas, and Wisconsin. Each state designated a contact individual to oversee the completion of the survey forms and handle local arrangements for site visits. Limited by the small sample size permitted by survey guidelines, these states were not chosen randomly, but purposely, to obtain a mix of opinions regarding the index.

Two types of survey forms were prepared and distributed to each of the states:

1. A questionnaire soliciting information on the index regarding current uses, opinions, resources devoted to data

collection and processing, and elements of maintenance practice within that state that might affect the data provided for the index; and

2. A form allowing the states to assess the different options that might be taken in revising the maintenance index.

FINDINGS OF THE SURVEY

The results of the nine-state survey indicated divided opinions on the usefulness and retention of the current index. Those states that do not apply the index expressed apathy to its existence and use. Strong support came from those states that now use the index for a definite administratively or legislatively established purpose. The current composition of cost items that constitute the index remains controversial. Desired improvements suggested include (a) a simpler index, (b) regional or state indexes as well as a national statistic, and (c) updates in the labor, equipment, and materials items used to calculate costs.

Use and Usefulness of the Index

The sampled states were sharply divided on the use and perceived usefulness of the current maintenance index. The index is applied to some important functions (e.g., fuel tax determination); however, these applications appear to be limited to a few states. Four of the nine states reported not using the index at all. The other five indicated that they use it annually in various functions other than maintenance (e.g., planning, budgeting, finance, and construction). However, among these five, there are strong differences in the perceived usefulness of the index, with two of the five indicating that they could do without it. On the other hand, those favoring retention of the index identified it with important financial and budgetary responsibilities, such as its use in formulas to establish motor fuel tax rates, or in preparation and justification of maintenance budgets that, by implication, involve the state legislature as well as DOT.

Even though many states professed little or no use for the current index, they acknowledged the desire to be able to compare their cost trends with the composite trend nationwide. Thus, their position was not so much one of opposition, but more a judgment on the usefulness of the current index. This is evident in the questionnaire, where even those states suggesting elimination of the index acknowledged some uses of it, and are willing to contemplate potential changes.

The strengths of the current index, as seen by the reporting states, are the following:

- The index provides a mechanism for monitoring and comparing trends in maintenance costs.
- The index helps to prepare and defend maintenance budgets.
- The index is used in some states as a basis for road finance determinations (e.g., establishment of the fuel tax rate and apportionment of funds to local jurisdictions).

For one state, which uses the index to establish the motor fuel tax rate, the significant feature is that the index is outside the state's control, presumably lending an aura of objectivity and impartiality to the inclusion of the index in the taxation formula.

Among the weaknesses of the index, as viewed by the states, are the following:

- The index is based on an outdated mix of technology, labor, and materials.
- Its development does not address the lack of uniformity from state to state with respect to how maintenance functions are defined, organized, managed, and performed.
- The index may embody inaccurate materials prices because of differences in units of measurement and the type of price being quoted.

Also mentioned were problems interpreting what data are needed for the index. States have found difficulty in matching their own classifications of resources to those listed on FHWA Form 1521. (Form 1521 is used annually by the states to transmit maintenance unit cost data to FHWA for the maintenance index.)

Comments during the interviews also revealed that the units specified on Form 1521 do not always reflect current pricing methods. For example, the unit price of cement is requested on Form 1521 in dollars/barrel; however, cement today is shipped either by the sack or in bulk (priced by the ton). Because bulk unit costs differ from the unit price per sack, requesting a cost in dollars/barrel is both vague and potentially distorting (depending on how the instruction is interpreted). A further problem noted during the interviews concerns cost items that are too inclusive (e.g., lumber, which includes structural and common grades, and pipe, which includes diameters from 18 to 30 in.). With so many grades or sizes of an item, which averaging procedures should be used is not clear.

Utility of a Revised Index

A second component of the state survey sought opinions on what revisions to the maintenance index would be most beneficial, and for what reasons. The responses again varied widely by state; nevertheless, when the ratings were summed and averaged to yield a global utility, clear groupings of alternatives emerged.

Alternatives having strongly positive utilities:

- Generate values that can be adjusted regionally or locally,
- Develop an index based on a limited set of maintenance data,
- Develop a composite index comprising many activities,
- Update the index annually (as opposed to more frequently),
- Base the index solely on price or cost trends,
- Maintain a federally developed index based on state input, and
- Maintain a state-developed index based on state input.

Alternatives having strongly negative utilities:

- Retain the current index with no changes,
- Update the index monthly (as opposed to less frequently),
- Incorporate other factors in the index (e.g., standards, productivity),

- Maintain a state-developed index based on input from external sources, and
  - Abandon the index.

Alternatives having indifferent utilities:

- Maintain an index with a national composite value (as compared with allowing regional variations),
  - Update the index quarterly or semiannually, and
- Build a federally developed index on the basis of input from external sources.

These findings support the conclusions developed earlier from the questionnaire responses. The strongly positive results may be interpreted as follows: states are looking for a simple index that includes local or regional variation, retains the credibility of a federally developed measure, but does not unduly burden the states with frequent data collection. On the negative side, states do not want to retain the current index, nor do they wish to abandon the idea of a maintenance index. Also falling into disfavor were frequent updates of the index, complicated indexes, and use of cost data from external sources (e.g., published construction cost files, or other cost indexes).

DIFFERENT INDEX FORMULATIONS

To better understand the options available in redeveloping the maintenance index, the following tasks were also undertaken by the study team:

1. A literature review of the theoretical aspects of price index development, including basic index forms (Laspeyres and Paasche index forms), mathematical formulation and calculation, the difference between shifts in index base period versus rebasing, chaining of index values, accounting for local or regional variations, mathematical properties related to behavior, and accounting for changes in quality, technology, and tastes.

2. A detailed review of other construction and maintenance indexes and related cost data, including those published by FHWA, Engineering News Record (ENR), Department of Commerce, Bureau of Reclamation, Environmental Protection Agency, Dodge Reports, R. S. Means, Leonard McMahon, Construction Labor Research Council, and Bureau of Labor Statistics.

3. A corresponding review of general economic indexes, the system of producer price indexes, and other data from the Bureau of Labor Statistics.

4. Analyses of current maintenance index behavior, comparison with construction indexes of various types, and behavioral aspects of different indexes. A partial summary of these analyses is presented in the following section.

ANALYSES OF THE CURRENT MAINTENANCE INDEX

Two major types of analyses of the current maintenance index were conducted. The first analysis investigated the distributions of unit costs submitted by states to FHWA for each of

32 direct cost items used to build the index (the set of 34 items discussed earlier, excluding the two overhead cost items). The second investigated the relative contribution of each of these 32 items to the values of the labor, equipment, and materials components of the index.

Distributions of Unit Costs

Distributions of unit costs were prepared for each of the 32 items of labor, equipment, and materials used in developing the index. Examples of two such distributions are shown in Figures 2 and 3, for bituminous mix and snow plows, respectively. Strong peaking and central tendency are evident in Figure 2 for bituminous mix, demonstrating agreement among a majority of the reporting states on unit costs in the $20.00/ton to $30.00/ton range. On the other hand, the distribution of costs for snow plows in Figure 3 tends to be more dispersed. Distributions of the other cost items generally fell between these extremes.
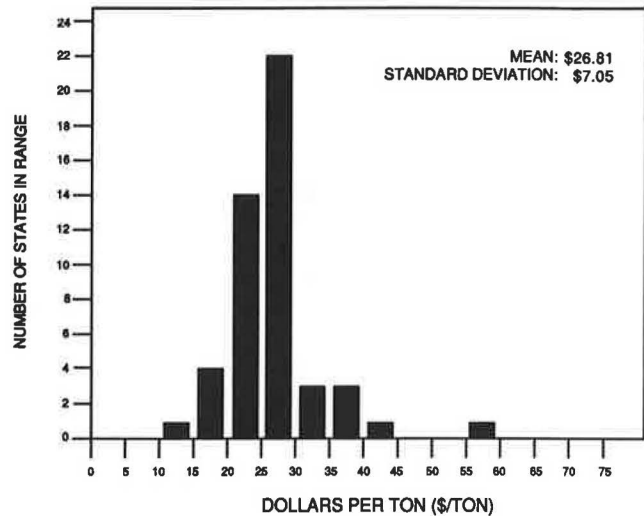
FIGURE 2   Distribution of unit costs of bituminous mix.
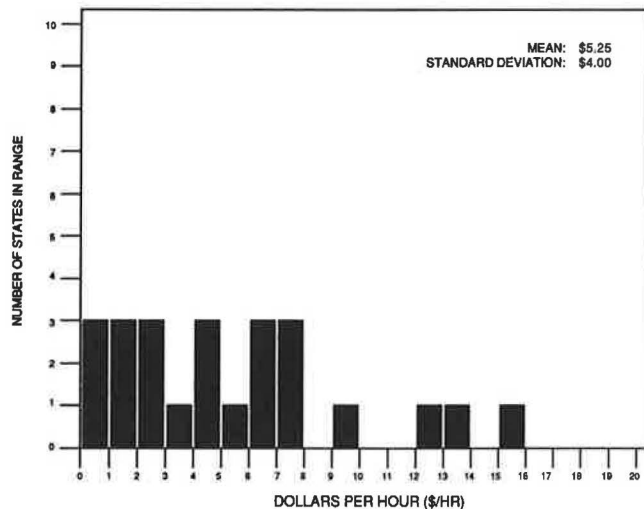
FIGURE 3   Distribution of unit costs of operating snow plows.

These data revealed patterns among the cost items. For example, those cost items whose distributions resembled Figure 2 indicated not only a similarity in unit cost values, but also agreement among states as to the description of the item for which costs must be provided, and the procedures of developing that cost. Cost items whose distributions resembled Figure 3 are either subject to greater variation in their unit costs or involve higher uncertainty or misinterpretation as to how these costs are calculated and reported. This finding indicates a need for greater uniformity in the submission of unit cost data, implying a need for clearer instructions and guidance in preparing and submitting unit cost data.

Relative Contributions of Cost Items

Cost items within each of the three major components of the index (labor, equipment, and materials) were analyzed to determine their relative contributions:

• The labor component of the index is dominated by the common labor class, whose contribution to the labor index value (about 55 percent) exceeds that of all other labor classes combined (despite the fact that common labor wages are the lowest of all labor unit costs). This dominance has remained fairly constant throughout the period analyzed (1974 to 1987), hence, the large weight given to common labor in the current index.

• The materials component of the index is dominated by three items: bituminous liquid, stone, and gravel. The dominance of these items, accounting for about 60 percent of the total materials index, has been sustained since 1974.

• The equipment component of the index is dominated by three classes: light trucks, heavy trucks, and graders, collectively accounting for 60 to 65 percent of equipment index value throughout this period. These items illustrate a fortuitous combination of weight and relative unit cost; for example, automobiles and pickups are assigned a much larger weight but their unit cost of operation is too low to influence the index by much.

The implication of these findings is that the value of the current maintenance index is essentially controlled by a handful of cost items. Rather than dealing with 34 items, the index could be based on the 10 to 20 most important items in highway maintenance, and still yield trends of comparable value and stability. Furthermore, the historical stability in the percentages, signifying the relative importance of items, implies a lack of volatility: within each index component, many of the items undergo price changes at approximately the same rate from year to year. If the most important maintenance cost items, or the ones that are trend setters in changing prices, could be identified, a reliable index based on this small set of items could be developed without sacrificing accuracy or credibility.

CONCLUSIONS AND RECOMMENDATIONS

Several of the basic assumptions around which the index has developed have evolved over time: the sample 10,000-mi network does not conform with the distribution of today's road-way surface types; some of the classes of maintenance equipment in the index are obsolete; and both the types and units of measurement of several materials items do not conform to current practice. Although the index has provided a relatively stable picture of inputs to maintenance activities over a long period of time, these significant changes suggest discontinuing the index in its current form. FHWA is now studying this topic.

Nevertheless, the highway maintenance and operations cost index is one of but a few indexes devoted specifically to the price or cost of facility maintenance. As such, it is used for a number of purposes in tracking or projecting maintenance costs by FHWA, state DOTs, researchers, consultants, and others.

The conclusions of this study are as follows:

1. There is no compelling reason to discontinue the maintenance index entirely. This option was explicitly rejected by state DOTs in the utility assessment. The costs of producing the index are not excessive, and its existence enables tracking of maintenance price trends not only by state DOTs, but also by researchers and consultants in public policy studies of highway infrastructure. If the index were eliminated, it would be difficult to find a substitute measure that did not entail distortions now filtered out by the index.

2. The index in its current form should not be retained. This form has served well for 40 years, as indicated by the stability and consistency of its price trends. Nevertheless, it is acknowledged to be obsolete, and therefore has limited support.

3. A revised index, consistent with the desires of the surveyed state DOTs, is feasible from a technical and a policy standpoint. This conclusion is based on analyses of current index behavior, comparisons with other price indexes in construction, and theoretical considerations of index formulation. The design of an index was beyond the scope of this project; yet the following conclusions are warranted:

• The market basket of a revised index can be reduced to 10 to 20 items while maintaining the desirable behavioral properties of the current index.

• The sample highway network, which was used in 1947 to develop market basket composition and quantities, is outdated. Moreover, its use is optional in the index redevelopment, because current data on labor, equipment, and materials quantities actually used in maintenance should be available directly from state management systems.

• The current index uses an arcane system of weights to convert the unit costs submitted by states for each item to a composite national unit cost, which is applied in the index calculation. This weighting procedure should be completely revised.

• The unit cost data now submitted by states appears to vary in quality. Greater attention must be given to clarifying the items to be priced and the content of the cost or price figures in terms of what they should or should not include.

• A set of regional indexes desired by the states is feasible computationally, and involves negligible incremental costs. The main issue is policy related; states desire comparisons among regions, as opposed to simply data on trends within a given region.

● Periodic checking of the index's market basket is advisable (i.e., every 5 to 10 years). If significant differences exist (or are anticipated), the index should be rebased or the weighting functions revised.

A revised maintenance index will require collaboration between FHWA and the states for the critical tasks of identifying candidate items of labor, equipment, and materials for the market basket; actually defining and building the market basket; redesigning Form 1521 and developing instructions to state DOTs for completing the unit cost form annually; creating the weighting functions to translate state unit cost input into regional and national composite; and defining the regions that are to be encompassed by the maintenance index. Furthermore, periodic reviews of both the market basket and the index's weighting functions are needed.

A potential mechanism to accomplish these items is a joint panel of state technical experts working in concert with FHWA technical experts. The structure and authority of this task force remain to be defined by both FHWA and the states. Having as wide a representation as possible would be useful, because this group would establish the broadest possible base for defining the market basket and the weighting functions. If this panel is untenable or unwieldly, then a sample of states or a hierarchical structure that grouped states by regions might be feasible.

The FHWA has taken these recommendations under advisement, and will consider the future of the index from three major perspectives:

1. Any redevelopment undertaken must be geared to producing an index that can be implemented and used by both the states and the FHWA.

2. The index inputs should reflect today's maintenance practices, and should not place an undue burden of data collection and analysis on state agencies.

3. As the index would still require information to be gathered from nonfederal sources, it must be defensible from both the technical and the administrative viewpoint.

ACKNOWLEDGMENTS

REFERENCES

1. *Highway Statistics*. FHWA, U.S. Department of Transportation, 1987.
2. Bertram D. Tallamy Associates. *NCHRP Report 42: Interstate Highway Maintenance Requirements and Unit Maintenance Expenditure Index*. TRB, National Research Council, Washington, D.C., 1967.

Abridgment

Maintenance Management on Gravel Roads

Vesa Männistö and Raimo Tapio

Management systems for unpaved roads are often neglected because of the low traffic density on those roads. However, unpaved roads constitute a large portion of the length of the road network and often a large portion of the administration's total maintenance budget. An efficient system for dividing and optimizing that expenditure is therefore justified. The Finland Roads Administration recognized the need for an analytical optimization method for setting up maintenance levels and standards, organizing the required road condition measurements and monitoring systems, and selecting and timing the most economical maintenance actions for gravel roads. A long history of developing management systems for paved roads, good experiences in collecting road condition data, and the availability of a very precise road data bank containing data on road structure, traffic, and costs formed a good background for the development of an analytical network-level maintenance management system for gravel roads. The final system will also include the project-level approach, organization of road condition measurements, and a monitoring system. The optimization model, based on semi-Markovian models, is divided into 1-year and multiyear models on the basis of condition variables and the maintenance actions taken. Although the model is mathematical, it can be used for dividing funds between maintenance districts and for setting up the objective maintenance standards for the gravel road network. The system is to be used in the central administration and district headquarters. A simpler, project-level system to be used by maintenance engineers will be developed and integrated with this system.

The Finland Roads Administration (RWA) has a long history of developing pavement management systems for the paved-road network. However, the RWA manages 32 000 km of gravel-surfaced roads, which is 42 percent of the length of the public-road network. More than 90 percent of these gravel roads are low-volume roads, with approximately 7 percent of the total vehicle mileage taking place on them.

The maintenance of gravel roads is much more essential than their share of vehicle mileage represents. In 1987, maintenance of the surface layer of the gravel roads constituted 13 percent of the total road maintenance cost. The maintenance cost of gravel roads per vehicle-kilometer is twice as high as the average maintenance cost of public roads. However, the maintenance program for gravel roads involves big appropriations, a long road network, and low vehicle mileage. The development of this management system aims at a more efficient allocation of these resources.

A network-level analytical optimizing method for determining the level of structural service on gravel roads is being developed. The main results of the system are identifying the most economical of the maintenance actions needed (to minimize costs) and determining the costs of those actions. The

results also include developing an overall level of maintenance standards and objectives for the gravel road network. The optimal timing of different maintenance actions is determined by the system.

One of the objectives for the management system was that it should be integrated with the existing pavement management systems. This objective brought with it the requirement that the software be run in microcomputers. The annual procedure for developing a capital program for maintenance work in the maintenance districts is currently time-consuming and complicated. The integration of all management systems will give maintenance engineers the opportunity to plan the maintenance in their own areas as a whole, including the maintenance of both paved and unpaved roads and other maintenance actions.

EVALUATION OF GRAVEL ROAD CONDITION

Variables of the System

Factors that describe the condition of a gravel road can be divided into state, condition, and control variables. State variables are factors that can be assumed to remain constant during the summer maintenance season. The effect of maintenance actions directed at these factors usually lasts more than 1 year. Condition variables are used to describe the condition of a gravel road during the summer maintenance season. The effect of the summer maintenance actions lasts at best only for that season. Control variables describe all other variables that affect the models needed.

The state variables for this system are (a) the thickness and quality of the wearing course (in centimeters) and (b) road structure (index). The quality of the wearing course was initially based on its thickness and the quality of materials used. After the first year's measurements, the wearing course was disqualified because most of the roads measured were near fraction curves. The condition of the road structure describes everything below the wearing course.

Condition variables have been chosen in such a manner that it would be easy and inexpensive to measure them reasonably often. The following variables were selected:

- Amount of loose aggregate (index, 1 to 5),
- Longitudinal roughness (subjective; index, 1 to 5), and
- Longitudinal roughness (bump integrator, in centimeters per kilometer).

Control variables will not change over time (except average daily traffic), but they have a strong effect on road structure and behavior. These variables are

V. Männistö, Viatek, Ltd., Alventie 4, SF-02170, Espoo, Finland. R. Tapio, Roads Administration, Helsinki, Finland.

- Average daily traffic (summer, vehicles per day),
- Geographical region (south or north), and
- Road geometry (good or poor).

The length of a frost season defines the geographical region. Road geometry is a combination of hilliness and curvature of road.

Measurements

A random sample of 360 km of gravel roads was drawn for the gravel road measurements in 1988 by means of simple random sampling from two geographically different districts and three traffic volume classes. The sample units are between 2500 and 3000 m long, and measurement data are recorded every 500 m. This sample is assumed to represent the whole gravel road network.

State Variable Measurements

The thickness and quality of the wearing course of the sample roads are measured at every sample kilometer twice a year, before the spring and fall maintenance seasons. In this way the deterioration over one summer season can be evaluated. Factors describing the road structure condition are assigned every spring, when roads are at their worst.

Condition Variable Measurements

During the summer maintenance season (May to September), the condition of sample roads is monitored through weekly measurements. The amount of loose aggregate on the road and road roughness are estimated by visual inspection according to RWA instructions. Road roughness is also measured with a bump integrator.

Other Measurements

All data for road geometry and traffic are supplied by RWA from the road data bank. In addition, highway residents record their maintenance and repair actions. The measurements necessary for road user cost estimation are executed with a driving analyzer along with condition measurements to reduce measurement errors.

SYSTEM DESCRIPTION

Overview

This system is based on the previously chosen state, condition, and control variables. To make the system as clear and simple as possible, all variables will be used as classified variables, for which one equals good, two equals fair, and three equals poor. The class limits have been chosen so that significant differences will occur between the classes for all variables and deterioration models used.

The system comprises the following state and condition variables.

Variable	Good	Fair	Poor
Roughness (cm/km)	<200	200–360	>360
Loose aggregate (1 to 5)	4 to 5	3	1 to 2
Thickness of wearing course	≥5 cm	—	<5 cm
Road structure (index)	4 to 5	3	1 to 2

In addition, gravel roads are classified according to control variables as follows.

Variables	Classification
ADT volume class (vpd)	<100, 100–200, >200
Road geometry	Good, poor
Region	North, south

A road can theoretically be in 54 (9 × 6) states in each of the 12 classes of the control variables. Thus, the total number of states is 648 (54 × 12), but in practice most of those can be discarded before optimization.

Road Deterioration and Maintenance Effect Modeling

The selection of the deterioration model family and its estimation is the most important part of this system, because the validity of the results received from the system is totally dependent on the validity of the deterioration models.

The use of the probability models in this system is straightforward. In the Finnish pavement management system (*1*), developed for paved roads, a Markovian approach with transition probability models has been successful. For gravel roads, it is more important to know the mean waiting time of the process in different condition states. For that reason, semi-Markov processes (i.e., Markovian renewal processes) (*2,3*) have been incorporated into the system.

The gravel road deterioration process can be evaluated through two types of models: those that experience normal deterioration without maintenance and those that receive maintenance actions.

To determine normal deterioration, all models are estimated separately for each condition and state variable. The estimated parameters for each variable are

- Transition probabilities [$p(i,j)$] from each Condition Class i to Condition Class j, when $i,j = (1,2,3)$, and
- Holding times [$h(i)$] in different condition classes, when $i = (1,2,3)$.

At the first stage, holding times are assumed to be exponentially distributed. This assumption does not restrict the scope, because the semi-Markov process can accommodate any holding-time distribution. The models estimated for each state or condition variable depend on control variables and are selected from the family of log-linear models (*4*).

A simple, nine-state, semi-Markov model can be estimated with assumptions that (a) only one variable will change its value in one transition, and (b) the holding times [$h(i,j)$] are exponentially distributed. The interval transition probabilities can be applied to compute the probabilities that a gravel road that started at time 0 in State i is at time t in a certain State j. If the initial condition distribution and transition parameters are known, the probability distribution of roads at any time t is easy to evaluate.

The other type of model describes gravel roads that have received some maintenance or repair actions. In this case, the condition distribution of roads after a certain maintenance or

repair action is estimated for each state and condition variable. After any maintenance, a road continues the normal deterioration process.

Maintenance and Repair Actions

Gravel road maintenance is divided into maintenance and repair actions. Maintenance is directed at 1-year factors, and repair actions are for multiyear factors.

Gravel road maintenance is made up of spring maintenance—blading and dust binding during the summer season—and fall maintenance. Five different maintenance strategies were defined for this system according to current RWA norms.

The multiyear repair involves adding the wearing course material and upgrading the structural condition of the road. The wearing course material is added during the spring or fall maintenance. The structural condition upgrades consist of repairing damaged base points, upgrading drainage, and upgrading the structure of the road.

Road User Costs

One of the most important targets of this system was to take road user costs into account. These costs are divided into three types: time, vehicle, and accident costs (5). Road user costs had to be made dependent on all the state and condition variables. An example of road user costs is presented in Table 1.

Optimization

Optimization in this system is executed at road network level. Budget and condition constraints and user-cost weights can be used. The objective of optimization is to find the minimum of societal costs, as follows:

Minimize SMC + RRC + VOC

where

SMC = Summer maintenance costs,
RRC = Multiyear repair costs, and
VOC = Vehicle operating costs.

TABLE 1 ROAD USER COSTS ACCORDING TO ROAD CONDITION INDEX

Cost Type	Road Condition Index				
	1 (Poor)	2	3 (Average)	4	5 (Good)
Vehicle	141	148	136	136	135
Time	67	57	48	42	42
Accident	6	8	10	13	13
Total	214	213	194	191	190

NOTE: Average daily traffic greater than 200 vehicles per day. Costs given in p/km.

In this system, optimization is basically a three-part process:

1. The total costs are defined for each of the five 1-year strategies.
2. The most economical summer maintenance strategy is selected. This strategy determines the road condition according to condition variables.
3. The most economical road repair strategy is selected on the basis of the best summer maintenance strategy.

A linear optimization method is used. The following results of optimization are gained:

- The optimal road roughness and loose aggregate class,
- The optimal road structure and wearing course class, and
- The optimal maintenance and repair strategies.

CONCLUSION

The results of using the semi-Markov process to optimize the maintenance of the gravel road network will be gathered from the maintenance districts in 1990. Those results will outline the future development needs of the system. The continuous use of the system, condition measurements, and results from the monitoring of the maintenance actions and their effects will also be used to modify and develop the system.

The interpretation of the measurement data and the estimation of the deterioration models must be done frequently in the future. Gravel road deterioration is a phenomenon that needs continuous research. The study of condition variables of the gravel roads, especially the condition of the road structure, must be continued.

The integration with the project-level system and other pavement management systems will also take place in 1990. The objective for the maintenance management in the maintenance district is to have one software program for the whole management work. The results gained from the integration of the sophisticated statistical software for the network-level system used by the central administration and district headquarters and the more straightforward, user-friendly, project-level system should be of interest to those working on developing maintenance management systems.

REFERENCES

1. *Finland Highway Investment Programming System.* Finland Roads Administration, Helsinki, 1988.
2. K. Tikka. *Semi-Markov Processes—An Introduction.* Helsinki, 1989.
3. D. Nesbitt and G. Sparks. A Computationally Efficient System for Infrastructure Management with Application to Pavement Management. *Proc., 2nd North American Conference on Managing Pavements,* Toronto, 1987.
4. P. McCullagh and J. Nelder. *Generalized Linear Models.* London, 1983.
5. *User Costs on Public Roads.* Finland Roads Administration, Helsinki, 1988.

Comparative Study of Undercutting and Disbondment Characteristics of Chemical Deicers

A. Dean McElroy, Robert R. Blackburn, and Henry W. Kirchner

A laboratory study was conducted to determine the undercutting and disbondment characteristic of 10 chemical deicers. The materials included six discrete deicing chemicals and four blends: calcium chloride pellets, calcium chloride flakes, two sodium chloride products, potassium chloride, pelletized urea, sodium chloride with a small amount of carboxymethocellulose, a blend of sodium chloride and potassium chloride sprayed with urea, a blend of sodium chloride and urea, and calcium magnesium acetate. In the undercutting tests, deicer particles were distributed on 6- × 9- × 2-in. concrete slabs covered with a ⅛-in. layer of ice. Tests were conducted at temperatures ranging from 0°F to 25°F in 5°F increments. Results were photographed and subsequently measured with a computerized stylus. The disbondment test apparatus measured and recorded the horizontal and vertical forces required to remove ice from a concrete specimen as it was drawn beneath a stationary blade. Each deicer was applied to the ⅛-in. ice samples and allowed to undercut for 30 min before disbondment forces were recorded. The tests showed that at least a 95 percent-complete undercutting is necessary for ice removal by mechanical disbondment forces of 2.8 lb per inch of blade width.

Removing a layer of ice from a roadway or sidewalk by plowing or shoveling is not an easy task when the ice is firmly bonded to the concrete surface. Only when the ice layer has been sufficiently undercut can it be removed easily. The difficulty holds true for ice bonded to any surface. The application of chemical deicers, however, can help initiate and accelerate the undercutting process and thus facilitate ice removal.

A previous study (*1*) revealed significant differences in the penetration and melt volume capabilities of several deicing chemicals over a range of selected temperature and time intervals. The goal of subsequent research was to determine the undercutting and disbondment characteristics of the same deicing chemicals.

Ten chemical deicers, including six discrete chemicals and four blends, were studied. The discrete chemicals included

- Calcium chloride ($CaCl_2$) pellets,
- $CaCl_2$ flakes,
- Sodium chloride (NaCl, two products tested),
- Potassium chloride (KCl), and
- Pelletized urea.

A. D. McElroy and R. R. Blackburn, Midwest Research Institute, Kansas City, Mo. 64110. H. W. Kirchner, Dow Chemical U.S.A., Midland, Mich. 48674.

The blended products consisted of

- NaCl with traces of carboxymethocellulose,
- Mixture of NaCl with KCl and urea,
- Mixture of NaCl and urea, and
- Calcium-magnesium acetate (CMA).

TEST PROCEDURES

Undercutting is a physically complex process dependent on a number of variables, including type of pavement surface, pavement porosities or irregularities, heat transfer rates, brine concentration, density gradients, and chemical species diffusion rates. The experimental procedures were designed to minimize as many of the variables as possible to elicit easily reproducible data.

Concrete test specimens measuring 6 in. wide, 9 in. long, and 2 in. thick were prepared according to ASTM specifications (ASTM C109–84). Figure 1 shows a typical specimen with an ice-leveling iron.

After setting for 60 to 90 min, each concrete specimen was lightly broomed along the 9-in. dimension to simulate the roughened surface of a highway or sidewalk. The surfaces were scribed with small grooves, approximately 0.2 cm apart and 0.1 cm wide at the top. All specimens were then cured for 28 days. Throughout the study, care was taken to prevent contamination of the cured specimens by dust or body oils, and specimens were handled without touching the broomed surface. To hold water on the surface, a ¼-in.-high lip of acrylic latex caulk and duct tape was applied along the outer perimeters of the concrete specimens, forming a leakproof dam.

A series of initial tests was conducted to determine the appropriate freezing rate and mode of freezing (bottom up or top down) to yield ice-and-concrete specimens with a uniform ⅛-in. ice thickness, a smooth ice surface, reasonably stress-free ice, and uniform and reproducible bonding between the ice and concrete. The tests revealed that the desired characteristics could be achieved in all disbondment and undercutting tests by using the following procedures.

ICE PREPARATION

A 17- × 18- × 15-in. freezing chamber was constructed to permit controlled, bottom-up freezing of the specimens. Before being placed in the freezing chamber, the concrete blocks
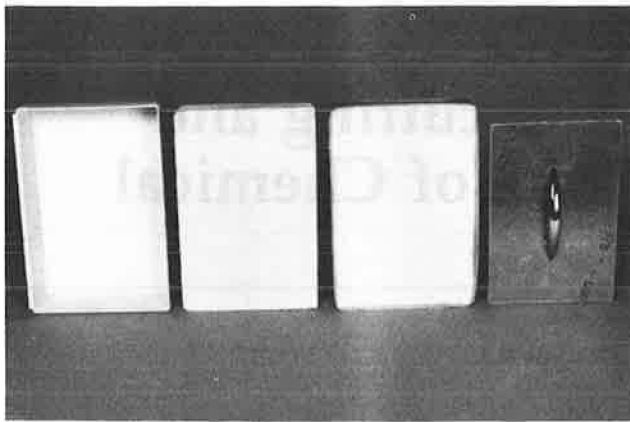
FIGURE 1 Concrete form, concrete block, duct-taped concrete block, and ice-leveling iron.

(with duct tape sidewalls in place) were flushed with deionized water, presoaked with approximately 50 ml of water, and placed in a refrigerator overnight at 35°F to 38°F. An inventory of deionized water was cooled to 35° to 38°F.

After precooling, specimens were removed and any excess water was poured off. Two or three concrete blocks at a time were placed in the freezing chamber, and 115 ml of cooled, deionized water was poured onto the surface of each. The blocks were then cooled from an initial temperature above 32°F to each test temperature. To prevent freezing at the surface of the water, the blocks were cooled from below and the air temperature was kept above 32°F until the ice was frozen from the bottom up.

Because the ice resulting from this process was uneven and granular, the surface was partially melted with a metal iron, and the specimens were returned to the cold room for refreezing. The ice-and-concrete specimens were then inserted in plastic bags, placed in a temperature-regulated cold box at the specified test temperature, and allowed to equilibrate.

UNDERCUTTING TESTS

Undercutting tests of the 10 deicers were conducted at six temperatures: 0°F, 5°F, 10°F, 15°F, 20°F, and 25°F. Dual-pellet tests were conducted for the blend of NaCl and urea. Pellets were separated and tested individually for the blend of NaCl and KCl sprayed with urea, resulting in a total of 11 undercutting tests, all replicated five times at each of the six test temperatures.

Particles from each of the 10 deicers were sieved and individually weighed before the tests. The average weights of the −6 mesh, +8 mesh fractions selected for use in the tests were as follows: the $CaCl_2$ flakes, urea, and CMA weighed 15 mg; the $CaCl_2$ pellets weighed 21 mg; the NaCl, KCl, NaCl-KCl blend, and NaCl with carboxymethocellulose weighed 31 mg; and the urea pellets from the NaCl-urea blend weighed 2.5 to 3.0 mg.

A 20-pellet grid pattern was laid out on each of three ice blocks and was marked with a small amount of dye. Weights of the individual deicer particles were recorded on data sheets numbered to correspond to the marked positions on the blocks

of ice. After allowing the deicer samples to equilibrate to the test temperature, the first set of 10 was placed on the ice and a timer was activated. The second set of 10 deicer particles was placed on the ice 5 min after the first. Figure 2 shows a typical pellet placement.

As melting commenced, a surface film spread over the surface of the ice. The initial dye pattern on the surface slowly faded in intensity at its extremities, leaving an intensely colored circular core denoting the path of penetration. After the deicer penetrated the ice, further melting yielded a roughly circular film of brine between the ice and the substrate.

The undercutting process for each set was recorded on slide film with a 35-mm camera 5, 10, 15, 20, 25, 30, 45, and 60 min after placement. After projecting the slides on a glass plate, the lens was adjusted to yield a 1:1 image. The researchers traced the undercut areas on onionskin paper, enlarged them to twice their original size on a copier, and took measurements with a computerized stylus.
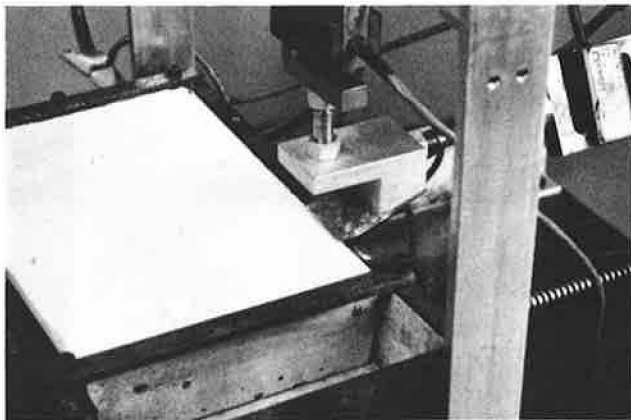
DISBONDMENT TESTS

The principal objective of the disbondment tests was to obtain reproducible data that would permit reliable comparisons between deicers and an evaluation of the effects of time or other variables on disbondment. An ice disbondment apparatus was constructed to measure the horizontal and vertical forces generated as an ice-covered concrete specimen was pulled beneath a stationary blade mounted close to the ice-concrete interface (Figures 3 and 4). The forces measured

| 1	2	3	4
5	6	7	8
9	10	1	2
3	4	5	6
7	8	9	10

FIGURE 2 Typical pellet placement.
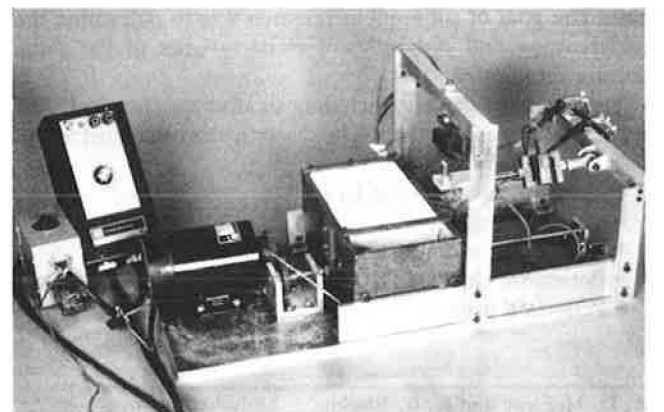
FIGURE 3 Ice disbondment apparatus.

FIGURE 4 Positioning of disbondment blade relative to concrete surface.

with the apparatus were the same as those that would be recorded if the ice-covered specimen were stationary and the blade was moved through the ice coating.

The disbondment apparatus was equipped with a 1.5-in.-wide blade mounted on two 200-lb-load cells (one horizontal and one vertical), which were connected to a two-pen recorder (Figures 5 and 6). The dimensions of the ice-and-concrete specimen and the blade permitted two tests per specimen.
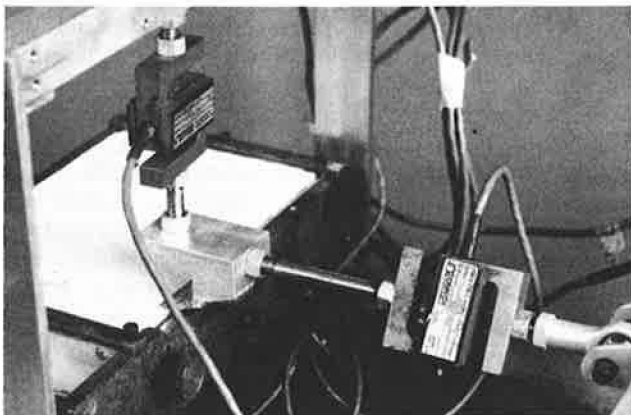
FIGURE 5 Load cell arrangement.
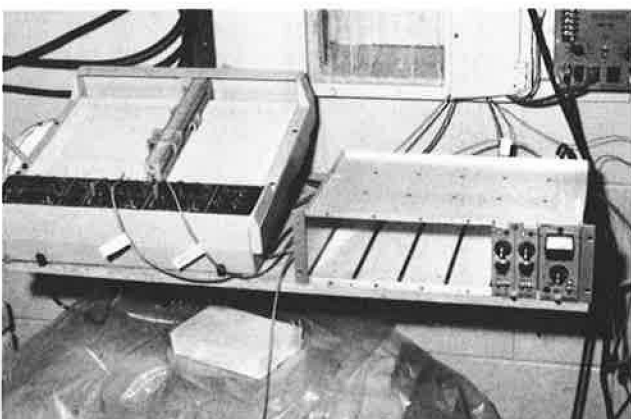
FIGURE 6 Disbondment force recorder.

A disbondment test procedure was developed from a study of deicer placement. These results are discussed in the following section.

DEICER PELLET PLACEMENT

In order to ensure reproducible results, the deicer pellets had to be of equal weights and spaced uniformly on the ice-and-concrete specimens. Accordingly, pellet dispensers were constructed to apply 3 oz/yd^2 of 15-, 21-, and 31-mg pellets. Hole dimensions were adjusted to permit pellets of varying dimensions to be dispensed.

Initial disbondment tests indicated that the application rate of 3 oz/yd^2 was not high enough for all deicers to complete undercutting at 25°F and substantially insufficient at lower temperatures. Therefore, the tests were reevaluated with the following guidelines: (a) pellet placement arrays should provide maximum opportunity to completely undercut the ice, and (b) pellet-loading rates should be adjusted upward and varied with temperature to permit the essentially complete undercutting required for ice removal with reasonable forces.

Because undercutting data for CMA indicated little undercutting after 60 min at 25°F and no undercutting at lower temperatures, CMA was excluded from disbondment testing. The second NaCl deicer and the NaCl deicer with a small amount of carboxymethocellulose added were excluded to avoid redundancy.

With pellets of equal weights and idealized perfect-circle undercutting patterns, the optimum pellet array involved the placement of pellets at the corners of equilateral triangles, in a pool ball rack arrangement (Figures 7 and 8). On the basis of data derived from the undercutting research, the loading rate required to completely fill void spaces was calculated to be 1.21 times an idealized loading rate.

With the preceding considerations in mind, the disbondment testing protocol was revised as follows:

● Thirty minutes was selected as the disbondment time.

● Areas undercut per unit weight of deicer at each temperature for 30 min were multiplied by 1.21 to determine loading rates and to calculate pellet spacings.
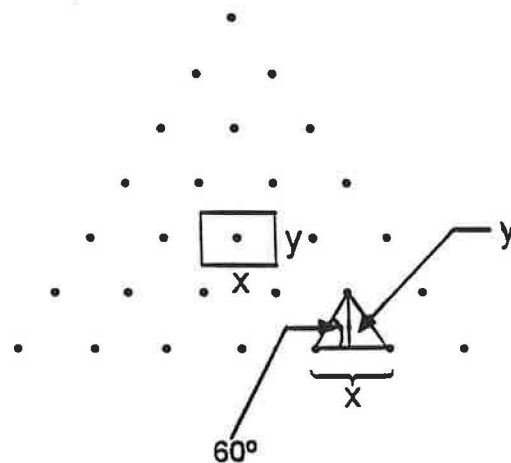
FIGURE 7 Schematic representation of pellet array for ice disbondment tests.
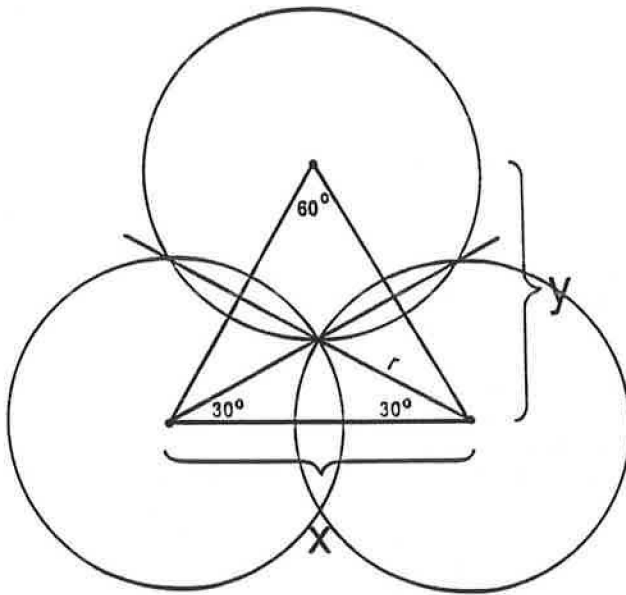
FIGURE 8 Idealized representation of undercutting with pellet arrays in ice disbondment test, with overlapping circular undercutting patterns.

- Pellet dispensers were constructed to permit application of deicers at the specified rates. The pellet arrangement was a pool ball rack configuration (see Figures 7 and 9).

DISCUSSION AND RESULTS

The deicer parameters (loading rates in ounces per square yard, pellet weights, and number of pellets) used in the disbonding tests are presented in Table 1. To permit visual observation of the undercutting, approximately 2 to 3 mg of Rhodamine B dye was added to each deicer sample and distributed by shaking. The $CaCl_2$ deicers (flake and pellet forms) were taken into the cold room, cooled, and loaded into dispensers
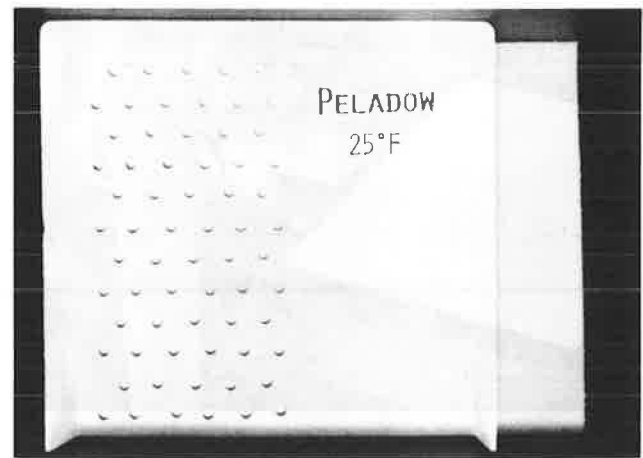

FIGURE 9 Pellet dispenser for disbondment tests.

immediately before the disbondment tests. The remaining deicers were loaded into dispensers in the laboratory and transferred to the cold room 15 to 20 min before the tests.

Pellet dispensers were positioned over the ice specimens and held in place with one hand. The dispenser tray was moved so that pellets dropped through the holes onto the ice surface. The timer was started immediately after the drop. Pellets that did not drop through their respective holes were forced through with forceps, and the dispensing tray was removed. Pellets that rolled or were dropped significantly out of position were repositioned. (Although considerable effort was expended in attempts to uniformly distribute the $CaCl_2$ flakes, distribution was judged to be less than satisfactory.)

Just before activating the disbondment blade, a visual estimate of the completeness of undercutting was made. When 30 min had elapsed, the recorder traverse mechanism was activated, and the forward switch for the blade drive of the disbondment apparatus was immediately activated. Typically, the blade was stopped when it reached the far edge of relatively nonundercut ice. The completeness of ice removal was

TABLE 1 DEICER PARAMETERS FOR DISBONDMENT TESTS

Deicer	Active Ingredient (% by wt)	Temperature (°F)	Time (min)	Application Rate (oz/yd²)	Average Pellet Weight (mg)	No. of Pellets per Test
1. $CaCl_2$ pellets	91.0 $CaCl_2$	25	30	4.36	21	66
		20	30	5.42	21	91
		15	30	6.93	21	113
		10	30	9.38	21	145
2. NaCl	99 NaCl	25	30	4.02	31	55
		20	30	6.20	31	72
		15	30	10.36	31	113
3. NaCl-urea blend[a]	92 NaCl, 8 urea	25	30	4.49	35	55
		20	30	7.24	36	72
		15	30	11.89	36	113
4. $CaCl_2$ flakes	77.5 $CaCl_2$	25	30	5.87	15	–
5. Urea	100 urea	25	30 and 60	9.00	15	190
6. KCl	99-100 KCl	25	30	6.42	31	72
7. NaCl-KCl-urea blend	44-45 NaCl, 54-55 KCl, 1 urea	25	30 and 60	5.36	26.8[b]	72

[a]Testing involved using equal numbers of rock salt and urea pellets and placing a rock-salt crystal next to a urea pellet.
[b]Testing involved using equal numbers of rock salt and potassium chloride—sprayed with urea—alternately placed on ice surface.

estimated visually, and the dislodged ice was then removed from the specimen.

Undercutting

Table 2 presents the average undercut areas (in square centimeters per gram) for the various deicers at each of the six test temperatures. The results express the average of five replicates.

Table 3 presents the application rates (in ounces per square yard) for complete undercutting of ⅛-in.-thick ice after 30 and 60 min at temperatures from 0°F to 25°F. The application rates presented in Table 3 are idealized, in that circular undercutting patterns and areas are mathematically converted to touching, but not overlapping, perfect squares. Several deicers were not tested at the lower temperature limits, because these limits are below the eutectic temperature of the chemical.

Undercutting Observations

1. At the highest temperature (25°F) and the longest time (60 min), the most effective deicers and a fixed application rate of 3 oz/yd² produced 85- to 90-percent–complete undercutting.

2. The undercutting process was essentially complete in 60 min, and little or no benefit was gained by extending the time period.

3. At all temperatures, the CaCl₂ pellets began undercutting the ice specimens more quickly than the other deicers tested.

4. The rapid undercutting action of the CaCl₂ pellets became more pronounced, comparatively, as the temperature was lowered.

5. At 25°F, NaCl-based deicers undercut more slowly than CaCl₂ pellets in short time intervals. At longer intervals (45 to 60 min), the NaCl deicers undercut more extensively by factors of 1.05 and 1.10.

6. Urea and KCl deicers exhibited no undercutting of ⅛-in. ice at temperatures lower than 20°F.

7. The undercutting behavior of CMA paralleled its ice penetration behavior (i.e., slight undercutting occurred at 25°F after 60 min, and none occurred at lower temperatures).

Disbondment

Table 4 presents disbondment results of deicers after 30 min at 10°F, 15°F, 20°F, and 25°F. Table 5 presents the average disbondment results for each deicer over all test temperatures and times.

Disbondment Observations

1. The CaCl₂ pellets exhibited the best disbondment results. Compared to the averages for NaCl (the deicer with the second-best performance), the averaged results for CaCl₂ pellets at each temperature and for all temperatures show that

CaCl₂ pellets yielded greater degrees of undercutting and ice removal, and that less force was required to remove the ice.

2. The average disbondment force (over all temperatures) for CaCl₂ pellets was 9 lb/in. The other average disbondment forces were as follows: NaCl, 16 lb/in.; NaCl-KCl-urea blend, 22 lb/in.; NaCl-urea blend, 27 lb/in.; KCl, 31 lb/in.; urea, 32 lb/in.; and CaCl₂ flakes, 56 lb/in.

3. At least 95-percent–complete undercutting is indicated as being necessary for ice removal by mechanical disbondment forces of 2.8 lb per inch of blade width.

4. The high disbondment forces required for CaCl₂ flakes, urea, KCl, and the blended products are attributed to extensive surface melting. The extent of surface melting appeared to be considerably greater with the closely spaced pellets in the disbondment tests than with isolated pellets in undercutting tests. Urea and CaCl₂ flakes exhibited the greatest surface melting, causing the disbondment blade to slide over large portions of the ice surface.

5. The data indicate that an increase of approximately 10 percent in nonundercut areas is accompanied by a 10-lb/in. increase in the average resultant force requirement for disbondment.

CONCLUSION

Although actual field conditions vary considerably from those of the controlled laboratory environment under which these tests were conducted (e.g., laboratory-developed ice-pavement bond strength may have been greater than that occurring on highways), some general conclusions regarding the undercutting and ice disbondment characteristics of the tested deicers can be drawn. The distinctly different undercutting and disbondment characteristics exhibited by different chemical deicers over a range of times and temperatures have important implications for personnel responsible for clearing ice and snow from roads and highways, sidewalks, and steps.

Clearly, the faster and more complete the degree of undercutting a deicer provides, the more efficiently road crews will be able to moderate hazardous conditions. For situations where rapid ice removal is critical to safety, CaCl₂ pellets appear to be the deicer of choice, regardless of temperature. At temperatures 25°F and higher, where time intervals of 45 to 60 min are available, NaCl can be expected to provide sufficient undercutting to facilitate ice removal. At the other extreme, on the basis of its poor performance in the undercutting tests at all times and temperatures, CMA can reasonably be characterized as an inefficient disbondment facilitator.

PRODUCT INFORMATION

Information on materials 3 through 8 obtained in 1986 in a study reported elsewhere (*1*).

1. PELADOW (registered trademark, Dow Chemical Company)

Manufacturer:	Dow Chemical U.S.A.
Principal ingredient:	Calcium chloride
Lot number:	ML861006
Assay:	91.0 percent CaCl₂ by ASTM Method E-449; 2.16 percent KCl; 1.7 percent NaCl; 0.03 percent MgCl₂

TABLE 2   UNDERCUT AREA COMPARISONS

| Time (min) | Undercut Area (cm²/g) | | | | | | NaCl-KCl-Urea Blend | | | | | |
	CaCl$_2$ Flakes	CaCl$_2$ Pellets	NaCl	NaCl with Carboxymetho-cellulose	NaCl + Urea	NaCl	NaCl	KCl	NaCl + KCl[a]	KCl	Urea	CMA
25°F												
60	63	86	93	91	88	89	94	66	79	68	51	21
45	62	82	95	92	85	86	94	61	76	65	46	0
30	61	82	89	87	79	79	85	48	65	56	40	0
·25	61	82	83	78	74	72	79	41	58	48	35	0
20	59	79	74	67	63	60	67	33	48	38	0	0
15	59	72	53	52	52	47	52	23	36	27	0	0
10	52	57	34	31	29	27	33	8	19	12	0	0
5	32	33	15	12	13	9	14	0	6	0	0	0
20°F												
60	49	70	68	61	61	63	71	32	49	31	33	0
45	46	67	66	56	60	61	67	27	45	25	27	0
30	46	66	58	45	49	50	58	18	36	18	21	0
25	47	63	50	37	41	44	53	16	33	14	0	0
20	43	59	41	30	35	36	42	14	27	13	0	0
15	43	53	30	22	27	28	31	3	16	0	0	0
10	38	40	20	17	21	24	18	0	8	0	0	0
5	8	17	0	0	12	0	7	0	3	0	0	0
15°F												
60	44	55	52	51	51	50	53	0	24	0	0	0
45	41	55	46	45	43	45	48	0	21	0	0	0
30	40	51	34	33	30	30	33	0	15	0	0	0
25	40	51	28	26	23	26	27	0	12	0	0	0
20	40	46	21	21	19	19	20	0	9	0	0	0
15	38	38	16	16	12	13	13	0	6	0	0	0
10	31	25	—	—	0	0	0	0	0	0	0	0
5	0	0	0	0	0	0	0	0	0	0	0	0
10°F												
60	31	40	29	24	26	26	28	0	13	0	0	0
45	27	38	23	19	22	20	21	0	10	0	0	0
30	24	38	16	14	15	14	18	0	8	0	0	0
25	21	36	15	10	12	12	17	0	8	0	0	0
20	24	34	15	11	10	12	15	0	7	0	0	0
15	10	29	14	4	13	9	12	0	5	0	0	0
10	0	20	5	0	0	0	0	0	0	0	0	0
5	0	0	0	0	0	0	0	0	0	0	0	0
5°F												
60	25	31	12	12	14	11	15	0	7	0	0	0
45	25	29	10	10	11	10	11	0	5	0	0	0
30	21	26	8	8	10	8	10	0	5	0	0	0
25	18	23	7	7	7	8	9	0	4	0	0	0
20	17	20	5	4	—	6	9	0	4	0	0	0
15	13	18	0	—	0	0	0	0	0	0	0	0
10	0	18	0	0	0	0	0	0	0	0	0	0
5	0	0	0	0	0	0	0	0	0	0	0	0
0°F												
60	21	25	11	8	10	9	11	0	5	0	0	0
45	22	25	10	6	9	9	9	0	4	0	0	0
30	22	21	8	5	8	6	8	0	4	0	0	0
25	14	17	—	0	—	0	—	0	0	0	0	0
20	23	16	0	0	0	0	0	0	0	0	0	0
15	—	14	0	0	0	0	0	0	0	0	0	0
10	—	—	0	0	0	0	0	0	0	0	0	0
5	0	0	0	0	0	0	0	0	0	0	0	0

NOTE: Data based on average of five replicates.
[a]Deicer, calculated undercutting, based on 45 percent NaCl and 55 percent KCl sprayed with urea.

TABLE 3 DEICER APPLICATION RATES FOR COMPLETE UNDERCUTTING, ⅛-IN.-THICK ICE

| | Application Rate (oz/yd²) by Temperature and Time | | | | | | | | | | | |
| | 25°F | | 20°F | | 15°F | | 10°F | | 5°F | | 0°F | |
Deicer	30 min	60 min	30 min	60 min	30 min	60 min	30 min	60 min	30 min	60 min	30 min	60 min
CaCl₂ pellets	3.6	3.4	4.4	4.2	5.7	5.3	7.8	7.4	11.0	10.0	14.0	12.0
NaCl	3.3	3.2	5.1	4.3	8.6	5.7	18.0	10.0	36.0	25.0	39.0	27.0
CaCl₂ flakes	4.9	4.7	6.4	6.0	7.3	6.7	13.0	9.5	14.0	12.0	13.0	13.0
NaCl with carboxymethocellulose	3.4	3.3	6.5	4.8	8.9	5.8	22.0	12.0	37.0	24.0	57.0	36.0
NaCl + urea	3.7	3.3	6.0	4.8	10.0	5.8	20.0	11.0	29.0	21.0	38.0	31.0
NaCl	3.7	3.3	5.9	4.7	10.0	5.9	22.0	11.0	39.0	27.0	54.0	32.0
NaCl	3.7	3.3	5.9	4.7	10.0	5.9	22.0	11.0	39.0	27.0	54.0	32.0
NaCl-KCl-urea	4.4	3.7	7.7	5.7	18.0	11.0	34.0	21.0	60.0	39.0	74.0	53.0
KCl	5.3	4.3	16.0	9.5	—	—	—[a]	—[a]	—[a]	—[a]	—[a]	—[a]
Urea	7.4	5.8	14.0	8.9	—	—	—[a]	—[a]	—[a]	—[a]	—[a]	—[a]
CMA	—	14.0	—	—	—	—	—	—	—	—	—[a]	—[a]

NOTE: Deicer application rates in this table are those (see Figure 8) for idealized perfect square undercutting.
[a] At 10°, 5°, and 0°F, urea and NaCl-KCl are below eutectic temperatures. At 0°F, CMA is approximately at the CMA eutectic temperature.

TABLE 4 DISBONDMENT TEST RESULTS

| | | | Average Force (lb/1.5 in.) | | Resultant Force | | | Visual Estimates | |
Deicer	Time (min)	Concentration (oz/yd²)	Horizontal	Vertical	Pounds per 1.5 in.	Pounds per Inch	Angle (degrees)	Percent Undercut	Percent Removed
25°F									
CaCl₂ pellets	30	4.36	2.1	4.8	5.3	3.5	66	95	95
CaCl₂ pellets	30	4.36	4.0	3.4	5.3	3.5	41	95	95
NaCl	30	4.02	10.2	16.7	19.6	13.0	59	80	85
NaCl	30	4.02	5.9	12.7	14.0	9.3	65	90	90
NaCl	30	4.02	7.2	13.4	15.2	10.1	62	90	90
NaCl + urea	30	4.49	8.3	21.1	22.7	15.1	68	80	70
NaCl + urea	30	4.49	19.8	28.0	34.0	22.7	55	70	75
KCl	30	6.42	22.4	42.4	48.0	32.0	62	75	60
KCl	30	6.42	20.0	41.0	46.0	31.0	64	80	85
NaCl-KCl-urea	30	5.36	15.0	30.0	33.0	22.0	64	75	80
NaCl-KCl-urea	60	5.36	6.8	8.5	11.0	7.3	52	90	95
CaCl₂ flakes	30	5.87	18.0	73.0	75.0	50.0	76	50[a]	50[a]
CaCl₂ flakes	30	5.87	28.0	89.0	93.0	62.0	72	50[a]	50[a]
Urea	60	9.0	25.5	55.0	61.0	41.0	65	50[a]	50[a]
Urea	30	9.0	24.0	42.0	48.0	32.0	60	50[a]	50[a]
20°F									
CaCl₂ pellets	30	5.42	12.4	8.3	14.9	9.9	34	90	90
CaCl₂ pellets	30	5.42	11.5	13.7	17.9	11.9	50	90	90
NaCl	30	6.20	11.0	17.1	20.3	13.5	57	85	90
NaCl	30	6.20	9.9	14.4	17.5	11.7	55	85	90
NaCl + urea	30	7.50	21.6	29.6	36.7	24.5	54	80	80
NaCl + urea	30	7.50	11.0	22.0	24.5	16.3	63	85	85
15°F									
CaCl₂ pellets	30	6.94	10.4	19.6	22.0	14.7	62	80	80
CaCl₂ pellets	30	6.94	18.8	22.7	29.5	19.7	50	85	85
CaCl₂ pellets	30	6.94	12.0	16.0	20.0	13.3	53	85	85
NaCl	30	10.36	18.2	21.5	28.2	18.8	50	60	60
NaCl	30	10.36	22.4	33.0	40.0	26.7	56	60	60
NaCl	30	10.36	21.0	40.0	45.0	30.0	62	80	85
NaCl	30	10.36	19.0	35.6	40.0	26.7	62	85	85
NaCl + urea	30	10.8	28.8	66.4	72.4	48.3	66	60	60
NaCl + urea	30	10.8	21.2	46.8	51.3	34.2	66	65	60
10°F									
CaCl₂ pellets	30	9.38	9.0	4.5	10.0	6.7	27	90	95
CaCl₂ pellets	30	9.38	6.5	4.0	7.6	5.1	32	95	95

[a] Approximate.

TABLE 5 DISBONDMENT RESULTS: AVERAGE OF ALL TESTS AT ALL TEMPERATURES WITH EACH DEICER

Deicer	Resultant Force (lb/in. blade)	Percent Undercut	Percent Removed
$CaCl_2$ pellets	9.0	90	91
NaCl	16.0	81	84
NaCl + urea	27.0	74	72
Urea	32.0	50	50
$CaCl_2$ flakes	56.0	50	50
KCl	31.0	78	72
NaCl-KCl-urea	22.0	75	80

2. DOWFLAKE (registered trademark, Dow Chemical Company)

Manufacturer:	Dow Chemical U.S.A.
Principal ingredient:	Calcium chloride
Lot number:	ML870925
Assay:	77.50 percent $CaCl_2$; 2.62 percent KCl; 1.49 percent NaCl; 0.04 percent $MgCl_2$

3. HALITE (1)

Manufacturer:	Diamond Crystal Salt Company
Principal ingredient:	Sodium chloride
Assay:	99 percent NaCl by chloride analysis

4. ICE FIGHTER PLUS (1)

Manufacturer:	Morgro Chemical Company
Principal ingredient:	Sodium chloride with Propolyice (registered trademark of Morgro Chemical Company)
Assay:	99 to 100 percent NaCl by chloride analysis

5. SAFE-STEP ICE MELTER (1)

Source:	Koos, Inc.
Principal ingredient:	Sodium chloride and potassium chloride
Assay:	44 to 45 percent NaCl, 54 to 55 percent KCl by chloride analysis; 51.5 percent KCl, 48.5 percent NaCl; 1.0 percent urea by physical segregation of particles

6. SUPERIOR SNO-N-ICE MELTER (1)

Manufacturer:	CP Industries (Chemopharm)
Principal ingredient:	Sodium chloride and urea
Assay:	92.0 percent NaCl by chloride analysis; 8.0 percent urea by urea nitrogen analysis

7. UREA (1)

Distributor:	Lange Stegmann
Assay:	Fertilizer grade, spherical particles 100 percent urea by nitrogen analysis
Principal impurity product specifications:	1.8 percent biuret

8. ZERO ICE MELTING CRYSTALS (1)

Source:	Howard Johnson Enterprises, Inc.
Principal ingredient:	Potassium chloride
Assay:	99 to 100 percent KCl by chloride analysis

9. CMA (CALCIUM MAGNESIUM ACETATE)

Manufacturer:	Chevron Chemical Company
Principal ingredient:	Calcium acetate and magnesium acetate
Assay:	49.25 percent calcium acetate; 46.42 percent magnesium acetate; 2.45 percent moisture; 1.88 percent water insolubles pH 8.97 at 20 percent weight solution.

10. PREMIERE ICE MELTER

Manufacturer:	CP Industries (Chemopharm)
Principal ingredient:	Sodium chloride
Assay:	99 percent NaCl

REFERENCE

1. A. D. McElroy, R. R. Blackburn, J. Hagymassey, and H. W. Kirchner. Comparative Study of Chemical Deicers. In *Transportation Research Record 1157*, TRB, National Research Council, Washington, D.C., 1988.

Development of a Corrosion Inhibitor for Reinforced Concrete

RÉJEAN BEAUDOIN, BERNARD MALRIC, AND CHANTAL BERTHELOT

Because of its highly alkaline concrete environment, reinforcing-steel surface is protected from corrosion by a thin oxide film. This film is maintained only in the absence of substances that form soluble complexes with iron. One of these substances is the chloride ion found in common deicing salt. Domtar Inc. established a research program to address the problem of rehabilitation of corroding reinforced-concrete structures. The experimental procedures and measuring techniques used to identify suitable corrosion inhibitors and typical results obtained with a selected inhibitor are presented. The inhibitor proved effective in reducing corrosion of steel embedded in concrete, and therefore it can be applied either as a curative or preventive means to protect reinforced-concrete structures.

In regions where winter brings snow and ice, both chemical and mechanical means are used to keep road surfaces clean and dry. The most popular deicing chemical is sodium chloride. Because it is a natural and abundant mineral, salt is economical. Difficulties arising from its use include its corrosiveness toward metals, particularly reinforcing steel in highway structures.

The widespread use of corrosion inhibitors in various situations suggested that a suitable inhibitor could be found to protect the reinforcing steel.

The purpose of this project was to find a chemical that, when added to deicing salt, would reduce the corrosion of the steel in reinforced-concrete structures. It was also hoped that in studying different inhibitors using a variety of experimental techniques it would be possible to determine the mechanism by which inhibitors can protect reinforcing-steel bars (rebars) in concrete.

The following selection criteria were established:

• The corrosion inhibitor must work in a concrete environment in which the pH is higher than 12, calcium hydroxide is present, and chlorides are often the aggressive ions;
• The corrosion inhibitor must work through concrete making the conditions favorable for the formation of a passive film;
• The corrosion inhibitor must retard further corrosion in actively corroding structures and minimize corrosion in new construction;
• The corrosion inhibitor must be a cost-effective solution to the problem of corrosion;
• The corrosion inhibitor must be environmentally acceptable;
• The corrosion inhibitor must be compatible with the materials that may come in contact with it. These include

Domtar Inc. Research Centre, P.O. Box 300, Senneville, Quebec, Canada H9X 3L7.

concrete, plastic, rubber, paint, and metals other than steel;
• The product must be readily available; and
• The corrosion inhibitor must not reduce the deicing effectiveness of salt.

Concrete normally provides an environment in which steel is passivated (1). A layer of Fe_2O_3 is formed on the surface of steel, which protects it from further corrosion. One of concrete's protective mechanisms is the pH control action of calcium hydroxide crystals located at the steel-concrete interface. Yonezarva et al. (2) concluded that for the protective mechanism to operate, adhesion between the steel and the concrete is necessary because formation of voids at the steel-concrete interface is essential for active corrosion to start (2). Reduction of the pH by carbonates and attack by aggressive ions can destroy this passive layer and lead to active corrosion (3,4).

The corrosion products of steel occupy a volume about four times that of the steel itself. The forces created because of this increase in volume cause cracking of the concrete and delamination as shown in Figure 1.

Figure 2 is a schematic illustration of the corrosion of reinforced steel in concrete. Depassivation of the steel by anions such as chlorides, that migrate through the concrete pore network or through hairline cracks and structural cracks in the concrete, triggers the anodic dissolution of iron. A local corrosion cell is created sustaining iron oxidation and oxygen reduction, the two corrosion reactions.

In the presence of chloride ions, iron reacts to form an intermediate iron chloride complex, as indicated by Equation 1.

$$Fe + 2Cl^- \rightarrow [Fe^{++} + 2Cl^-] + 2e^- \tag{1}$$
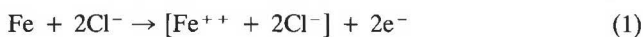
This complex reacts with moisture, as shown by Equation 2, to form ferrous hydroxide, and leaves chloride ions free to prevent further passive film formation (5).

$$[Fe^{++} + 2Cl^-] + 2H_2O \rightarrow Fe(OH)_2$$
$$+ 2H^+ + 2Cl^- \tag{2}$$
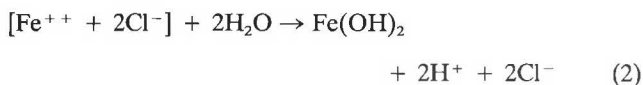
TESTING METHODOLOGY

Testing a Corrosion Inhibitor for Reinforcement Steel

As a rule, a corrosion test simulates service conditions. Thus in the case of a corrosion inhibitor designed to reduce the corrosion of reinforcing steel in concrete, a test begins by
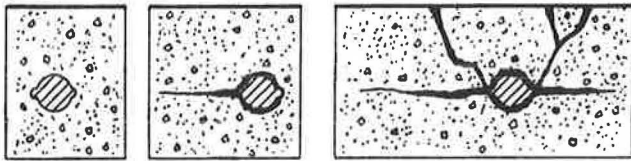
FIGURE 1 Cracking of concrete caused by the corrosion product of steel.
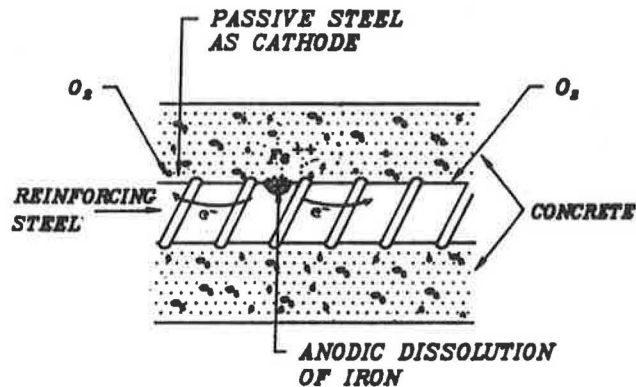

FIGURE 2 Schematic of corrosion of reinforcement steel in concrete.

simulating the chemical conditions in concrete, and progresses to the simulating of service conditions. The procedure includes the following:

- Immersion Test. A saturated calcium hydroxide solution containing sodium and potassium hydroxides simulates the concrete pore solution. Immersion of metal coupons in this solution is useful as a quick screening test because it does not require difficult specimen preparation and it allows for direct surface examination. However, it cannot be considered a sufficient test because it does not include all the limitations of a concrete cover.
- Lollipop Test. An embedded steel probe provides a closer simulation of service life conditions. The drawback of this procedure is the time required to prepare the specimens and the time required for the corrosion to start or to slow down (usually on the order of months). The results are also scattered and must be carefully interpreted.
- Macrocell Test. Specimens that create a macrocell effect to simulate service conditions must also be considered. This is also a time-consuming procedure and the results must be carefully interpreted.

A combination of these three testing procedures will give a realistic evaluation of corrosion inhibitor effectiveness.

Measurement Techniques

Electrochemical measurement techniques are important for the following reasons: (a) the corrosion rate of reinforcement steel is not high in normal conditions, and (b) weight loss determination implies destruction of the specimen and does not explain the corrosion evolution. The following techniques

are best suited in this case because they are nondestructive; the last two in particular can measure corrosion rates down to low levels.

1. Half-cell potential measurements give qualitative evaluation of the corrosion state of the reinforcing steel. Because half-cell potential is a thermodynamic parameter, it gives the probability for corrosion to happen but not the rate at which it progresses.
2. Linear polarization gives a reasonable estimate of the corrosion rate, and various instruments for its measurement are available in standard laboratories. Correction must be made for concrete resistance.
3. Electrochemical impedance spectroscopy also gives a reasonable estimate of the corrosion rate; moreover, it also gives clues about the corrosion mechanism. For example, the corrosion rate is often temporarily limited by the oxygen diffusion through the concrete. This behavior immediately shows on the impedance diagram.

A combination of these techniques must be used to determine the effectiveness of a corrosion inhibitor as a function of time. A variety of other electrochemical techniques is also available. Each method has its advantages and disadvantages. The most widespread technique, as far as corrosion of steel in concrete is concerned, is the method of linear polarization with current interruption, which compensates for concrete resistance.

Experimental Procedure

Immersed Rebar Steel (Immersion Test)

Steel samples were cut from one length of rebar, which is commonly used for construction. Initial sample preparation consisted of wet-grinding on SIC papers to a 600-grit (17-μm) finish, followed by a 3-μm diamond-paste polish. Electrical connection was made by spot-welding a 0.15-mm-diameter Pt wire to each specimen. The unpolished surfaces of the samples were coated with Lacomit varnish to prevent exposure to the solutions. The contact area and a portion of the Pt wire were also coated. The solutions were prepared from reagent-grade chemicals and distilled, deionized water. The pore solutions were KOH (0.6 M) + NaOH (0.2 M) + Ca(OH)$_2$ (saturated). The NaCl concentrations were 0 and 0.52 M (3 percent by weight). The inhibitor concentration was $\simeq$2.5 percent by weight of salt (0.074 percent by weight of solution). This last formulation, of salt plus the inhibitor, is named "TCI."

The electrochemical experiments were performed in beakers, open to air, containing $\simeq$200 ml of solution. The counter electrode was a 6-cm^2 Pt foil and the reference electrode was a saturated calomel electrode (SCE). The corrosion current measurements were made manually on a daily basis. Linear polarization measurements were made by manually changing the potential in 2-mV steps to $\pm$10 mV to the measured corrosion potential and recording the current response. The polarization resistance was then calculated from the slope of the overvoltage-current plot. Alternatively, a triangular voltage perturbation (10 mV$_{\text{peak-to-peak}}$) was applied at a sweep rate of 2.5 mHz, and the polarization resistance was calculated from the slope of the linear portion of the recorded curve.

Both of these methods gave similar results, and for most of the tests the manual technique was used. For the Tafel slope determination, anodic and cathodic scans of ±250 mV were performed with a generator at a scan rate of 20 mV/min.

Steel Embedded in Mortar (Lollipop Test)

Mortar specimens used in initial studies were cylinders of dimensions 50 mm (height) × 25 mm (diameter) as shown in Figure 3. The mortar mix design was 1 part portland cement, 1 part water, and 5 parts sand.

Rebars 70 mm in length and 11 mm in diameter were placed in the center of the mortar cylinder (one in each cylinder). Before placement, the top and bottom portions of each rebar were coated with wax to give a length of rebar exposed for 35 mm, or approximately an exposed surface area of 12 cm². The concrete cover to the surface of the steel was 7 mm thick. The concrete probes were allowed to cure for 2 days in their molds, demolded, and immersed in deionized water where they were allowed to cure for 28 days.

Several electrochemical techniques were used in this study. Linear polarization, current transient decay, and electrochemical impedance spectroscopy are complementary methods that were used. For clarify of presentation, results of electrochemical impedance only will be reported because each method gave similar results. The constant used for corrosion rate determination was 26 mV. This value was found by Gonzalez et al. (6) to give, in most cases, an acceptable agreement between the gravimetric weight loss and that calculated from polarization resistance values.

Electrochemical measurements were made using a Solartron 1286 potentiostat/galvanostat and a Solartron 1250 frequency response analyzer controlled by a Hewlett-Packard 9816 computer. The experimental apparatus was configured using the three-electrode measurement system. The rebar specimen was used as the working electrode, a series of interconnected graphite rods as the counter electrode, and a saturated calomel electrode as the reference electrode.
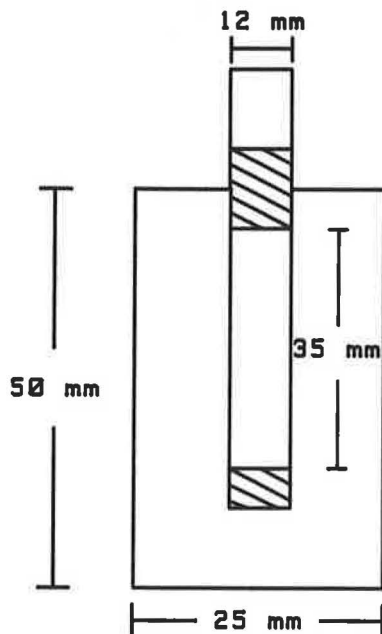
Simulated Macrocell

Small concrete slabs for laboratory-scale macrocell corrosion current measurements were built from construction-type rebars 11 mm in diameter, and concrete mix design in the proportions portland cement, 1.00; water, 0.52; sand, 1.76; and aggregate 2.36. The chloride concentration (as Cl⁻) was 9 kg/m³ (15 lb/yd³), and the unit weight of concrete was 2,235 kg/m³ (3,726 lb/yd³). This concrete mix design was used by FHWA to represent an average-quality concrete (7). (A lower ratio of water to cement and use of specialized admixture would significantly improve the concrete quality.)

Figure 4 is a schematic of the prism used in the laboratory-scale macrocell tests. The macrocell was a concrete block 9.5 cm (3¾ in.) high, 11.4 cm (4½ in.) wide, and 22.9 cm (9 in.) long. The two mats of rebars were cast in the concrete prisms using average-quality air-entrained concrete. The concrete cover was 1.9 cm (¾ in.) over the top mat of rebar. It was 1.3 cm (½ in.) over the lower mat of rebar to ensure good oxygen availability to the cathodic part of the macrocell. Sodium chloride was admixed into several of the top mat layers to accelerate corrosion and simulate the environment present in old bridge decks. A dam was placed on top of each slab and 6 percent solutions of deicer product or water were ponded to a depth of 1.9 cm (¾ in.). Solutions were replenished every 2 weeks.

The top and bottom sets of rebars were electrically connected and an on-off switch in series with a 1.0-ohm resistor was installed between the two mats.

The corrosion current flowing between the top and bottom mats was measured as the voltage drop across the 1.0-ohm resistor with the switch in ON (normal) position, or directly using a Hokuto Denko Corporation zero-shunt ammeter.

RESULTS OBTAINED WITH A SELECTED CORROSION INHIBITOR

Immersed Rebar Steel (Immersion Test)

The corrosion rate measured by linear polarization of rebar steel specimens immersed in simulated pore solution for 65 days is shown in Figure 5. Curve 3 represents the behavior
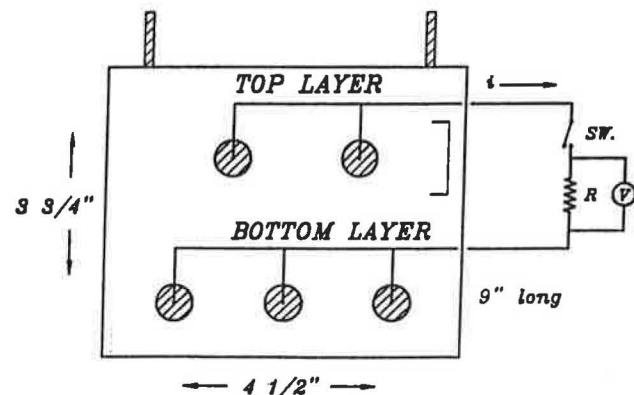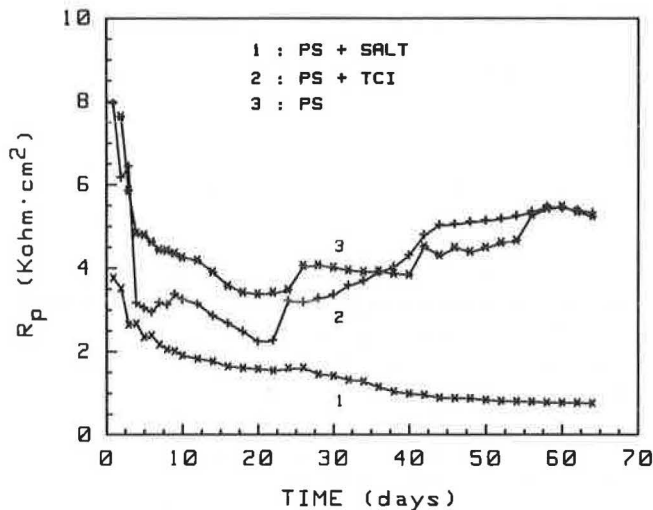
FIGURE 3 Schematic of a lollipop specimen.

FIGURE 4 Schematic of a laboratory-scale macrocell.

FIGURE 5 Polarization resistance of steel immersed in pore solution for 65 days.

FIGURE 6 Corrosion rate of mortar lollipops.

of steel in pore solution without aggressive ions. The polarization resistance was high for all the experiments, indicating a low corrosion rate. The polarization resistance in the solution containing NaCl decreased (Curve 1), then stabilized at the lower level over the 60-day period. Curve 2 shows the polarization resistance in the presence of TCI. The measured polarization resistance was in the same range as in straight pore solution after 25 days, indicating a low corrosion rate. These results demonstrate the ability of the inhibitor to reduce the corrosion rate, even in the presence of chloride ions, to its background level in pore solution without aggressive ions.

Steel Embedded in Mortar (Lollipop Test)

A rebar steel specimen of known surface area was embedded in mortar. The mortar cover was made small to accelerate the diffusion through it and, therefore, to reduce the response time for aggressive ions or for the inhibitor to affect the embedded steel. The mortar can also be made with chloride admixture to simulate a contaminated reinforced-concrete structure.

Figure 6 shows the corrosion rate of embedded rebar probes in salt solutions with and without inhibitor. The measurements were made by electrochemical impedance spectroscopy. In the absence of the inhibitor, the corrosion rate increased dramatically, then stabilized after 2 months. With the inhibitor, the corrosion rate never attained such magnitude and was still decreasing after 3 months.

This case indicates the effectiveness of the corrosion inhibitor with steel embedded in mortar.

Simulated Macrocell

One important behavior of reinforced-steel structures is the formation of a macrocell. Iron oxidation and oxygen reduction, the two corrosion reactions, happen at different locations on the structure. Because of the origin of the chloride contamination (sodium chloride for deicing), a bridge deck will
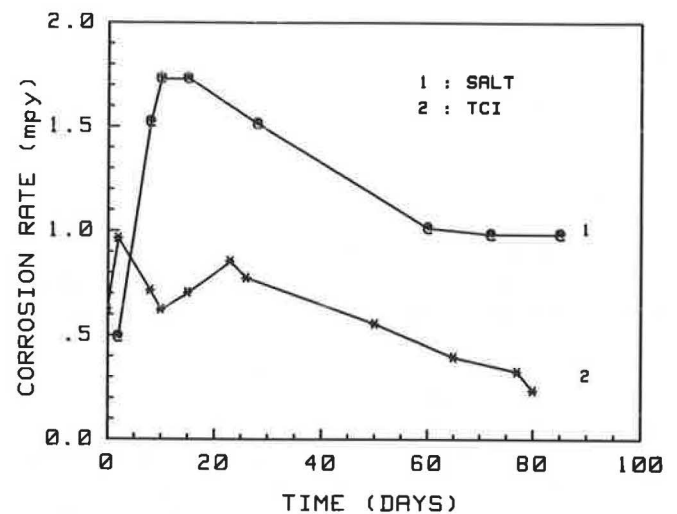
often form a macrocell where the iron oxidation occurs at the top mat of rebars (high chloride concentration) and the oxygen reduction occurs at the lower mat of rebars (availability of oxygen is higher because of dryer conditions). A simulated macrocell can be built in the laboratory by making a concrete prism where the top layer is contaminated with chloride. A macrocell will be established, giving rise to a macrocell current.

A total of 16 specimens were used in this study. The results with three slabs, for which the top layer of concrete was not contaminated with salt, are shown in Figure 7. The slabs were ponded with 6 percent NaCl solutions with and without inhibitor, and with distilled water only. At first, the current increased for the three slabs. After this initiation period, the slab containing the inhibitor showed a sharp decrease in current down to almost zero. With the brine solution only, the current slowed down but still stayed relatively high, indicating a well-established corrosion rate. Visual examination of the concrete specimens revealed extensive cracking in the absence of inhib-
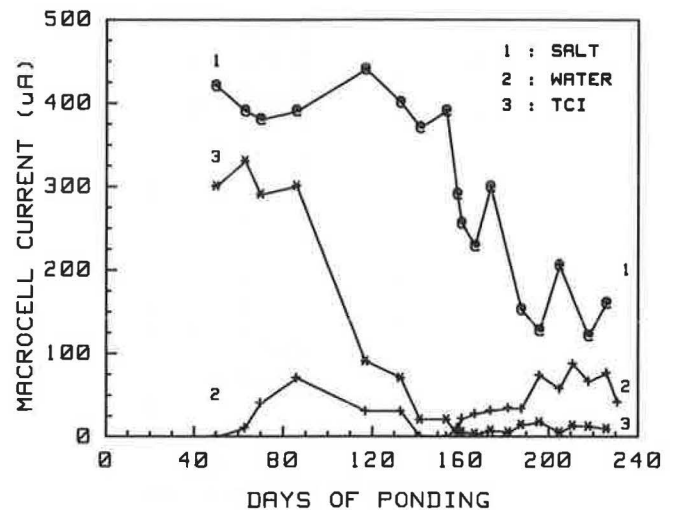

FIGURE 7 Macrocell current obtained with three slabs not contaminated with NaCl and ponded for 8 months.

itor. The slab ponded with water only had a small macrocell current, indicating little corrosion, as expected for a concrete specimen not contaminated with chloride ions.

A similar behavior was observed with a chloride-contaminated specimen as shown in Figure 8. After 5 months of ponding with the inhibitor in solution, the macrocell current was reduced to low values. The prism ponded with brine solution and with water only exhibited a high current throughout the experiment. This behavior was expected, because the concrete was contaminated with chloride ions at fabrication of the specimens. The break at 170 days happened when the electrical contacts of all the cells were redone, cleaned, and reassembled. The reduction in the macrocell current observed with the inhibitor proves its effectiveness in already-contaminated concrete where active corrosion is taking place.

Insight into the Mechanism

Passive Film Examination

Examination of the passive film on the steel surface indicated the mechanism by which this inhibitor can effectively reduce the corrosion of steel embedded in concrete. X-ray photoelectron spectroscopy (XPS) and scanning-electron microscopy (SEM) were used to investigate the surface chemistry and morphology. Steel specimens exposed to the simulated pore solution with TCI and parts of the rebar extracted from the TCI-treated slabs (macrocell test) were examined.

When the inhibitor was added to the pore solution, the surface morphology was different. Electron diffraction x-ray analysis indicated that the surface passive film was mainly composed of calcium and iron. The XPS analysis revealed a common feature of the film formed in simulated pore solution with TCI and of the film found on the rebar in the TCI-treated slabs (macrocell test). The calcium regions on both samples indicate that there may be significant differences in the chemical species formed when the inhibitor is added to the system. These early results demonstrate that the inhibitor is effective through concrete. A full research program is continuing to determine the exact mechanism and its limitations.

Concrete Examination

SEM examination of the slabs ponded with TCI (macrocell test) indicated little effect on the concrete. Accumulation of the inhibitor near the surface of the slab was observed. Compared with the noninhibited specimens, insignificant amounts of iron diffused in the concrete around the rebar. The fibrous outgrowths on the calcium silicate hydrate crystal appeared unusually long in the TCI-treated specimen.

CONCLUSION

The results demonstrate the ability of the inhibitor to eliminate most of the corrosive effect of chloride ions in a simulated concrete pore solution. Moreover, the corrosion inhibitor can work through concrete and create favorable conditions for the formation of a passive film on the reinforcing steel. Because this inhibitor can effectively reduce the corrosion rate of an already contaminated structure, it can be applied as a curative as well as a protective means for protecting reinforced concrete from corrosion.

REFERENCES

1. J. Holm. In *Corrosion, Concrete and Chloride.* ACI SP-102. American Concrete Institute, Chicago, Ill., 1987.
2. T. Yonezarva, V. Ashworth, and R. P. M. Procter. Pore Solution Composition and Chloride Effects on the Corrosion of Steel in Concrete. *Corrosion*, Vol. 44, 1988, p. 489.
3. C. Alonso, C. Andrade, and J. A. Gonzalez. Relation Between Resistivity and Corrosion Rate of Reinforcements in Carbonated Mortar Made with Several Cement Types. *Cement and Concrete Research*, Vol. 8, 1988, p. 687.
4. J. E. Slater. In *Corrosion of Metals in Association with Concrete.* STP 819. ASTM, Philadelphia, Pa., 1983.
5. Y. P. Virmani, W. P. Jones, and D. H. Jones. Steel Corrosion in Concrete: pH at Corrosion Sites. *Public Roads*, Dec. 1984, p. 96.
6. J. A. Gonzalez, A. Molina, M. Escudero, and C. Andrade. A Comparison of Linear Polarization and A.C. Impedance in the Determination of Corrosion Rates of Reinforcements Embedded in Concrete. *Proc., Corrosion '85*, National Association of Corrosion Engineers, Houston, Tex., 1985.
7. Y. P. Virmani, K. C. Clear, and T. J. Pasko. In *Time-to-Corrosion of Reinforcing Steel in Concrete Slabs*, Vol. 5, 1983.
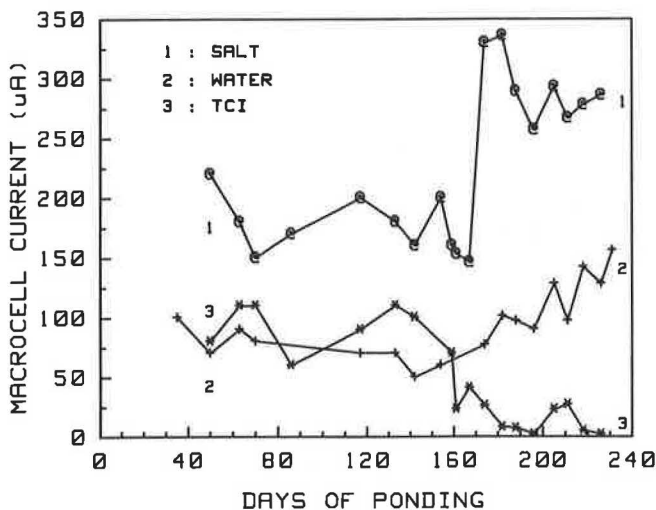

FIGURE 8   Macrocell current obtained with three slabs of which the top layer of concrete was contaminated with 15 lb/yd³ of chloride and ponded for 8 months.

Effects of Lignosulfonates in Deicing Salts on the Penetration of Chloride Ions into Concrete

RICHARD F. BUCHHOLZ

Lignosulfonates are being used as corrosion inhibitors in highway deicing salts. Corrosion reductions of 50 to 80 percent have been reported for mild steel. Lignosulfonates act as both cathodic and anodic inhibitors. They remove oxygen from solution, form insoluble material on the corroding surface, and use its reducing ability to prevent oxidation of ferrous iron to ferric. Although lignosulfonates in deicing salts would be expected to protect exposed rebar in concrete, experiments were run to measure corrosion inhibition on rebar exposed by microcracks in concrete, and in undamaged concrete where corrosion occurs by chloride diffusion. Mortar blocks with cracks leading to the embedded mild steel electrodes were soaked in 3 percent sodium chloride and 3 percent magnesium chloride solutions, with and without 0.75 percent lignosulfonate. After 6 weeks, electrochemical measurements showed a 70 percent reduction in corrosion for the solutions with lignosulfonates. Wiss-Janey concrete test blocks were treated weekly for 1 year with 15 percent sodium and magnesium chloride solutions, with and without 3.75 percent lignosulfonate. Chloride penetration data indicated substantially lower chloride levels for blocks treated with salt solutions containing lignosulfonate. This experiment was repeated using small mortar cylinders that were treated with 3 percent sodium, magnesium, and calcium chloride solutions, with and without 0.75 percent lignosulfonates. Significant reductions in chloride levels were observed for samples treated with lignosulfonates. The proposed mechanism is the precipitation of lignosulfonates on or with calcium hydroxide to seal the pores in the surface. Depending on conditions, the life span of undamaged reinforced concrete structures could substantially increase if lignosulfonates were added to deicing salts.

Lignosulfonates, which have been used for many years in concrete admixtures as a water reducer, are now being added to road deicing salts to reduce their corrosiveness to mild steel (*1–4*). Lignosulfonates, mixed with rock salt, small amounts of magnesium chloride, and liquid magnesium chloride, have been used as inhibited deicing salts in 14 states (*5–10*).

Corrosion rate reductions of 50 to 80 percent have been demonstrated by coupon methods, polarization resistance, potentiodynamic scans, and cyclic potentiodynamic scans by Dr. Hagar at the University of Washington (unpublished data). These results have been confirmed by several laboratories (*8–10*).

All these various methods yield similar percent reductions in corrosion rates even though the values obtained by the different measuring methods may vary. Typically, a 3 percent sodium chloride solution with 0.75 percent calcium lignosulfonate yields a 60 percent reduction in corrosion rate compared to untreated salt for an aerated system as might be found using periodic coupon dipping, stirring, or salt spray. If the corrosion environment had restricted oxygen transport, as would be found in an unstirred solution or in a crack in concrete, reductions up to 80 percent could be expected.

Lignosulfonates appear to act as corrosion inhibitors by a combination of three different mechanisms. In solutions, lignosulfonates react with dissolved oxygen, removing it from solution and thereby inhibiting the cathodic reduction reaction at the surface of the metal. Salt solutions with 1 to 2 percent lignosulfonate have low measured oxygen content. Lignosulfonates react with the forming corrosion products to give an insoluble layer that prevents the migration of ferrous ions from the reaction site and oxygen to the reaction site, which inhibits both the anodic and cathodic reactions. Infrared spectra of corrosion products scraped off the metal surface shows the presence of lignosulfonates. Cyclic potentiodynamic scans using mild steel electrodes in deicing salts with lignosulfonates have shown that lignosulfonates lower the pitting tendency by about 66 percent.

The ability of the lignosulfonate to coat the corrosion site is proposed to account for this action. The third mechanism is the result of the reducing properties of lignosulfonates, which inhibit the oxidation of ferrous iron to ferric (Dr. Hagar, unpublished data). This mechanism is readily observed in corrosion experiments where the coupons with the lignosulfonate have a black coating, whereas those without are red (indicative of ferric hydroxide). Lignosulfonates appear to act as rust converters changing red rust to black rust.

Lignosulfonates in deicing salts should inhibit corrosion of exposed rebar in concrete structures if the mixture has easy access to the metal surface, that is, to regions where bulk water can reach the metal surface. The objective of this work was to first determine the effectiveness of lignosulfonate in reducing corrosion when access is by microcracks in the surface, which travel to the rebar. The second objective was to find out if lignosulfonates would benefit undamaged concrete when corrosion of the rebar is the result of chloride ion diffusion.

CORROSION INHIBITION-CRACKED MORTAR

Mortar cylinders were prepared from one part Type I/II portland cement to two parts sand at a 0.4 w/c ratio and 6 percent air entrainment. The cylinders were 2.7 cm in diameter and 8 cm long with a 0.5-cm-diameter nail cast in each to simulate reinforced concrete. On curing, small hairline cracks formed,

Georgia Pacific Corporation, Chemical Division, 1754 Thorne Road, Tacoma, Wash. 98421.

that were assumed to travel to the embedded nail. The top half of the cylinder and all but the tip of the protruding nail were painted with epoxy paint. The 5-month-old mortar cylinders were submerged halfway into 15 percent sodium and magnesium chloride solutions, with and without 3.75 percent lignosulfonate at pH 7. The corrosion currents were measured using a potentiodynamic scan by the Tafel technique with an EG&G Princeton Applied Research Model 273 potentiostat with Model 342 computer system.

The results of the scans in Table 1 present approximately a 70 percent reduction in corrosion current for 15 percent magnesium chloride with 3.75 percent lignosulfonate after 2 and 6 weeks, and for 15 percent sodium chloride with 3.75 percent lignosulfonate after 6 weeks, compared with salts with no lignosulfonates. This is the amount of corrosion inhibition that was expected on the basis of previous coupon and electrochemical studies.

CORROSION INHIBITION ON UNDAMAGED CONCRETE

Lignosulfonates in deicing salts will inhibit the corrosion of rebar if the lignosulfonates can reach the surface of the metal. Using the Wiss-Janey test procedure (*11*), concrete blocks were prepared and treated with deicing salts, with and without lignosulfonates, to see if corrosion inhibition could occur when access to the rebar is by diffusion through the concrete.

The test blocks were prepared from a commercial sack concrete mix using the amount of water specified. They were 17.8 cm × 30.5 cm × 30.5 cm (7 in. × 12 in. × 12 in.) with two layers of rebar. The top set of rebar was 2.54 cm (1 in.) from the surface. Salt solutions (15 percent) with and without 3.75 percent calcium lignosulfonates were ponded on the blocks weekly for 1 year. The solutions were renewed on Mondays and removed on Fridays, and the surface was rinsed with plain water. The potential between the rebar layers, the copper to copper sulfate electrode potential between the surface and the first rebar level, and the ac resistance between rebar layers were measured weekly.

Only the test block treated with sodium chloride showed electrical activity. The potential between the rebar levels became more negative after the 1st week, maximizing at −700 mv in 5 weeks. In 12 weeks, the potential was almost back to zero. Because none of the other blocks changed, it was suspected that the sodium chloride test block had a passage to the rebar.

The test blocks were then analyzed after 1 year for chloride penetration. The blocks were cut in half and samples were then drilled out at different depths. The results for the 15 percent sodium chloride blocks, with and without 3.75 percent calcium lignosulfonate, are shown in Figure 1; the magnesium chloride blocks are shown in Figure 2. Although both sets of data show a large amount of scatter, the blocks with lignosulfonate present showed significantly decreased levels of chloride.

Chloride diffusion was reduced by about 50 percent. That degree of reduced penetration is significant in terms of lifetime of a bridge. Additional tests using mortar cylinders were run to confirm this effect.

The cylinders were 6 cm in diameter and 9 cm long. The mortar was prepared with one part Type I/II portland cement and two parts sand with a 2.4 fineness modulus at a 0.4 water/cement (w/c) ratio. Air entrainment was 6 percent. After sitting in the mold for 2 days, the mold was removed and the
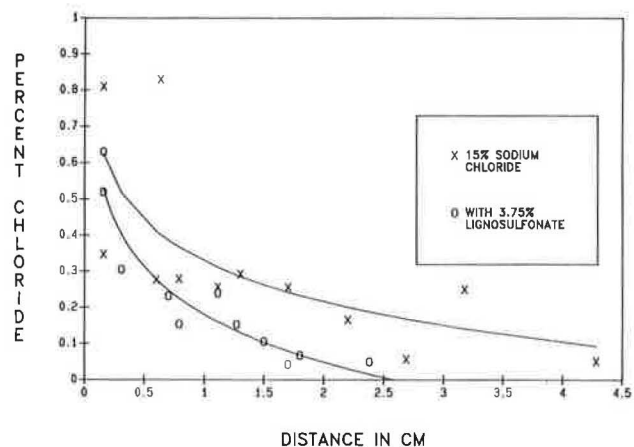
FIGURE 1   Chloride penetration into Wiss-Janey test blocks using 15 percent sodium chloride solutions.

TABLE 1   CORROSION INHIBITION OF LIGNOSULFONATES IN DEICING SALTS ON MORTAR BLOCKS WITH FINE CRACKS

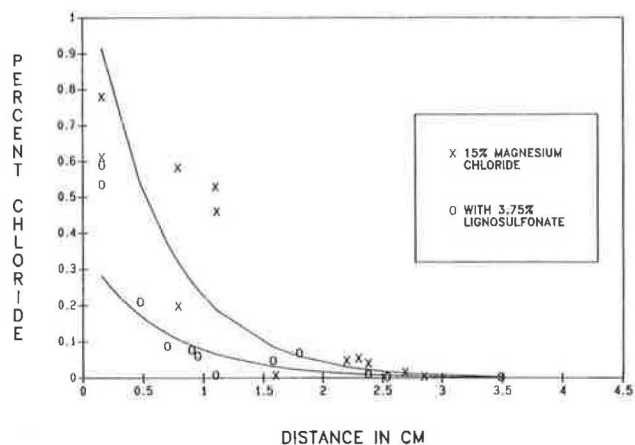| Sample	Time Weeks	Corr. Current microamps/cm^2
15% MgCl$_2$	2	3.3
w/3.75% lignosulfonate	2	1
15% MgCl$_2$	6	100
w/3.75% lignosulfonate	6	30
15% NaCl	6	60
w/3.75% lignosulfonate	6	15

FIGURE 2 Chloride penetration into Wiss-Janey test blocks using 15 percent magnesium chloride solutions.

cylinders were placed in 100 percent humidity at 20°C to 25°C for 15 days.

Only the sides of the cylinders were painted with epoxy paint 52 days later. A dam was attached to the top to hold the salt solutions. Fifty milliliters of 3 percent salt solutions, with and without 0.75 percent calcium lignosulfonate, were ponded weekly on the upper flat surface for 9 months and kept at 30°C. Solutions were put on each Monday and removed each Friday with the surface rinsed with 25 ml of fresh water.

The test cylinders were then analyzed for chloride content at different depths by cutting about 0.3-cm slices perpendicular to the cylinder axis with a rock saw having a 1.5-mm-thick diamond blade. The slices were then ground to a powder. A weighed amount of the powder, about 0.5 g, was put into 40 ml of deionized water and allowed to soak overnight. A portion of the solution was filtered, acidified, and then titrated with standard silver nitrate solution to determine the chloride content. Background chloride content of the mortar blocks was around 0.004 percent.

The chloride content of each slice was determined as percent of mortar and represented the average value of each slice. The mean distance the chloride ion traveled was from the top of the block to the middle of the slice.

The data for the 3 percent sodium chloride, 3 percent chloride with 0.75 percent calcium lignosulfonate, and 2.6 percent sodium chloride with 0.4 percent magnesium chloride and 0.75 percent calcium lignosulfonate are shown in Figure 3. The data for 3 percent calcium chloride with and without 0.75 percent calcium lignosulfonate are shown in Figure 4. In Figures 3 and 4, even though chloride concentrations of the test solutions are the same, the cylinders treated with lignosulfonate have lower chloride concentrations in the first slice of the blocks.

The data for the 3 percent magnesium chloride with and without 0.75 percent calcium lignosulfonate are shown in Figure 5. The solution with lignosulfonate did not perform as well in this experiment as indicated in the previous Wiss-Janey test. A partial explanation will be given later in the discussion of the mechanism of action.

DIFFUSION COEFFICIENTS

Fick's first law of diffusion was used to calculate the diffusion of chloride ion into the mortar blocks as expressed in the following equation:
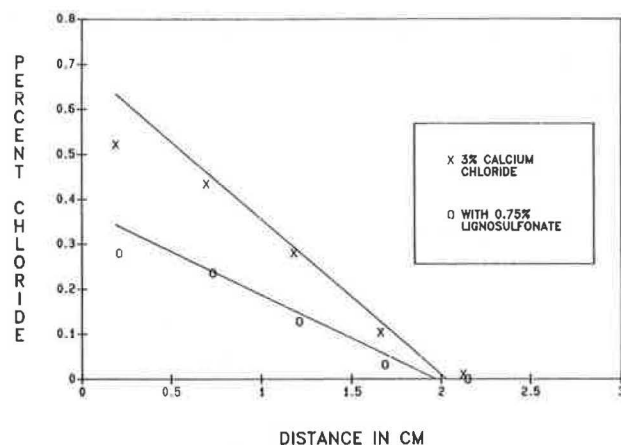
$$J = -D * dc/dx \qquad (1)$$

FIGURE 4 Chloride penetration into mortar test blocks using 3 percent calcium chloride solutions.

FIGURE 3 Chloride penetration into mortar test blocks using 3 percent sodium chloride solutions.
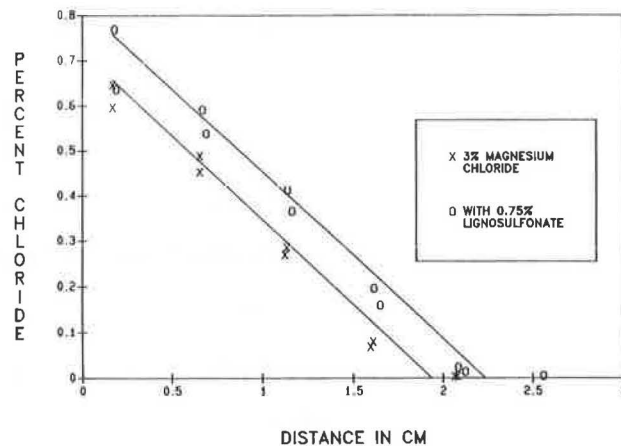

FIGURE 5 Chloride penetration into mortar test blocks using 3 percent magnesium chloride solutions.

where

J = flux of chloride ion,
c = concentration term,
x = distance traveled, and
D = diffusion coefficient.

Equation 2, which is a linear solution of Equation 1, shows the relationship of concentration of chloride c at depth x in time t with diffusion coefficient D and chloride apparent surface concentration c_0 (12).

$$c = c_0 * \left[1 - \frac{x}{2(D * t)^{1/2}} \right] \qquad (2)$$

Plotting c/c_0 versus x yields a straight line with intercept of 1. The slope of the line is then equal to the expression $-\frac{1}{2}(D * t)^{1/2}$. For each salt treatment, the diffusion coefficient D (in units of cm²/sec) was calculated from Equation 2 using the experimentally determined slopes. For these experiments, the ratio c/c_0 was the ratio of the percent chloride ion in each slice divided by the percent apparent surface concentration, and where the distance x from the top of each cylinder to the middle of each slice was in centimeters, and time t in seconds. The total time for these experiments was 9 months. The apparent surface concentration c_0 was obtained from Figures 3 through 5, by linearly extrapolating the percent chloride plots back to zero distance, which is the surface of the block.

The diffusion coefficients for the present experiments, calculated using Equation 2, are presented in Table 2. The values range from 3.2 to 6.0 * 10^{-8} cm²/sec. Typical values for high quality concrete are about 0.1 * 10^{-8} cm²/sec for high-quality concrete to 5 * 10^{-8} cm²/sec for low-quality concrete (12). The ability of chloride to penetrate to any depth in the concrete is a function not only of the diffusion coefficient, which is dependent on the quality of the concrete, but also the apparent surface concentration, which is a function of the interface between the bulk liquid and the concrete surface. For the cylinders treated with sodium chloride solution, the addition of lignosulfonate not only resulted in lowering the diffusion coefficient but also lower apparent chloride surface concentration, as presented in Table 2. When judged on the ability to give lower chloride concentrations at any depth, sodium chloride with lignosulfonate, and magnesium chloride and calcium chloride with and without lignosulfonate, all are better to use as a deicing salt than sodium chloride.

The effectiveness of these solutions to reduce chloride penetration can better be seen by calculating the time to corrosion onset. Corrosion of rebar in concrete usually starts when the chloride content at the rebar exceeds a given amount. The critical chloride concentration c_c at the rebar for corrosion to start is generally considered to be about 0.4 percent for cement or about 0.07 percent for concrete (12,13). By assuming the same linear relationship as in Equation 2, Equation 3 can be used to calculate the time for corrosion onset t_c, which is the time for the chloride concentration to reach the critical value.

$$t_c = \frac{1}{4D} \times \left(\frac{L}{1 - c_c/c_0} \right)^2 \qquad (3)$$

where

L = depth of the concrete cover over the rebar,

c_c = critical chloride content taken as 0.07 percent, and
c_0 = apparent surface concentration.

Using the apparent surface concentrations and diffusion coefficients in Table 2, the time t_c to reach a critical chloride concentration c_c of 0.07 percent at different covers over the rebar was calculated. Because the mortar for these tests was designed to be of low quality, the time t_c for sodium chloride treatment was only 1.0 year for 2.54-cm (1-in.) cover and 9.5 years for a 7.62-cm (3-in.) cover. In comparison, using the same apparent surface chloride concentration, a good-quality concrete with a diffusion coefficient of about 1 * 10^{-8} cm²/sec (12) and a 2.54-cm (1-in.) cover would have a life of about 6 to 7 years before corrosion onset.

The calculated times to corrosion onset t_c for all the test samples are presented in Table 3. Adding 25 percent lignosulfonate to the salt has the potential of increasing bridge life 70 percent over using plain salt. The use of a small amount of magnesium chloride with sodium chloride and lignosulfonate would slightly more than double the life of the bridge. The data clearly demonstrate the potential benefit of significant increased bridge life by adding lignosulfonate to deicing salts.

PROPOSED MECHANISM FOR LIGNOSULFONATE INHIBITION OF CHLORIDE DIFFUSION

The basic mechanism appears to be the same as what is commonly known as the Howard process for the precipitation of lignosulfonates (14). In this process, lime is used to precipitate lignosulfonates from solution. Lignosulfonates are adsorbed on the hydrated lime forming a bulky insoluble precipitate network. Calcium lignosulfonate is soluble at acid pH, but as the pH increases, a calcium lignosulfonate precipitate is formed. This process does not appear to occur to the same extent with magnesium ion.

If the presence of lignosulfonate in the deicing salt resulted only in an insoluble layer on the surface, then only the apparent surface concentration of chloride ion seen by the mortar would be affected. The interior of the mortar should remain the same in terms of pore solution concentration and composition, and the diffusion coefficient of the mortar towards chloride would not be affected. This result was not found to be the case, as demonstrated by significant changes in the calculated diffusion coefficient (see Table 2).

When sodium chloride solution is ponded on the surface of the mortar cylinder, hydroxide ion in the pore solution can diffuse, increasing the pH of the ponded salt solution. As pore solution diffuses out, the ionic strength of the pores decreases, which could result in increased diffusion of chloride ion. Also, some of the more soluble components could dissolve, increasing the pore size. When calcium lignosulfonate is present, it moves into the surface pores and adsorbs onto the hydrated lime in the alkaline environment, eventually sealing off the pores significantly. At the same time, hydroxide ion from the pores trying to diffuse would also react with calcium ion in solution, and an insoluble calcium hydroxide-lignosulfonate matrix could be deposited in the surface pores. With the weekly changes of the ponding solution containing

TABLE 2 SURFACE CONCENTRATIONS AND DIFFUSION COEFFICIENTS OF
CHLORIDE IONS IN TEST MORTAR CYLINDERS

Sample	Solution Concentration % Chloride	Surface[a] Concentration % on Mortar	Diffusion[b] Coefficient $*10^{-8}$ cm^2/sec
3% NaCl	1.82	0.70	6.0
3% NaCl + 0.75% Lig	1.82	0.50	4.0
2.6% NaCl + 0.75% Lig + 0.4% $MgCl_2$	1.89	0.40	3.2
3% $MgCl_2$	2.26	0.72	3.6
3% $MgCl_2$ + 0.75% Lig	2.26	0.82	4.7
3% $CaCl_2$	1.91	0.70	4.1
3% $CaCl_2$ + 0.75% Lig	1.91	0.38	3.6

a. Extrapolated value from Figures 3, 4, and 5.

b. Calculated using equation (2) in the text. Estimated
maximum variation 5%.

lignosulfonate, the pH of the salt solution would gradually
decrease as the diffusion of alkaline pore water is retarded.
The diffusion of chloride ion into the mortar is similarly
retarded. The pH of the salt solution was measured at the
end of each week and decreased when lignosulfonate was
present, as indicated in Table 4.

When 3 percent calcium chloride solution is added to the
surface of the mortar, the product of the concentration of the
calcium ion, 0.27 M, and the concentration of hydroxide (pH
13+) in the pore water exceeds the solubility product for
calcium hydroxide, which is 4.7×10^{-6} (15). Calcium hydrox-
ide is precipitated in the surface pores, reducing the perme-
ability to chloride ion. Because calcium hydroxide is reason-
ably soluble at 0.19 g per 100 ml, the pH of the solution
remains high, as indicated in Table 4.

When lignosulfonate is present, the precipitating calcium
hydroxide and lignosulfonate react as in the Howard process,
forming an insoluble material that appears to be much more

efficient at sealing the surface than calcium hydroxide alone.
This effect is confirmed by the low apparent surface concen-
tration of chloride ion. As the insoluble material builds up,
it results in slower diffusion of pore solution from the mortar
block into the salt solution, decreasing pH (see Table 4).

When 3 percent magnesium chloride is added to the cyl-
inder, the product of the concentration of magnesium ion,
0.32 M, and that of the hydroxide ion from the pore solution
exceeds the solubility product of magnesium hydroxide of 5.6
$\times 10^{-12}$ (15) and precipitated magnesium hydroxide forms
in the pores.

When lignosulfonate is present, the Howard process cannot
occur. The magnesium ion ties up almost all the hydroxide
from the pore solution and probably covers any of the calcium
hydroxide surfaces in the mortar matrix. Only a small amount
of calcium ion from the calcium lignosulfonate is available,
which is 6 percent of the 0.75 percent lignosulfonate, yielding
about 0.011 M calcium ion. From the calcium hydroxide

TABLE 3   CALCULATED TIMES TO CORROSION ONSET FOR DEICING
SALTS WITH AND WITHOUT LIGNOSULFONATE

Sample	Cover	2.54 cm	5.08 cm	7.62 cm
		t_c, Time in Years[a]		
3% NaCl		1.0	4.2	9.5
3% NaCl + 0.75% Lig		1.7	7.0	15.6
2.6% NaCl + 0.75% Lig + 0.4% $MgCl_2$		2.4	9.4	21.2
3% $MgCl_2$		1.7	7.0	15.7
3% $MgCl_2$ + 0.75% Lig		1.3	5.2	11.7
3% $CaCl_2$		1.5	6.1	13.5
3% $CaCl_2$ + 0.75% Lig		2.1	8.5	18.9

a.   Calculated using D and C_0 from Table 2 and equation 3.

TABLE 4   pH OF SALT SOLUTIONS AT THE END OF EACH WEEK

Week	NaCl	NaCl + Lig	NaCl + Lig + $MgCl_2$	$CaCl_2$	$CaCl_2$ + Lig	$MgCl_2$	$MgCl_2$ + Lig
1	11.82	11.54	11.64	11.82	11.54	9.32	9.78
3	11.68	10.04	11.73	11.46	10.06	9.51	9.46
5	11.34	9.18	10.20	11.28	9.48	9.39	9.40
7	11.26	8.54	9.45	11.03	8.81	9.41	8.81
9	11.52	9.18	9.94	10.44	8.16	9.57	9.72
11	11.13	8.68	8.71	11.08	7.78	9.58	9.27
13	10.91	8.57	8.20	11.08	8.00	9.40	9.11
15	11.15	8.64	8.16	11.05	7.86	9.54	8.88

a.   All solutions were 3% salt with 0.75% calcium lignosulfonate
    with the exception that one was 2.6% sodium chloride with
    0.4% magnesium chloride and 0.75% calcium lignosulfonate.

solubility product of 4.7×10^{-6}, the hydroxide concentration needed for precipitation is 4.3×10^{-4} M. As indicated in Table 4, the pH of the magnesium chloride solution is about 9.3, which is 2×10^{-5} M hydroxide, and is not high enough for precipitation.

In the previous Wiss-Janey experiment, the addition of lignosulfonate to magnesium chloride reduced chloride penetration (see Figure 2). These experiments were run at 15 percent salt and 3.75 percent calcium lignosulfonate. In this solution, the concentration of calcium from the lignosulfonate is five times greater at 0.066 M. Using the solubility product for calcium chloride, the hydroxide concentration needed for precipitation is 7.1×10^{-5} M, which is probably high enough at the mortar block surface to cause the Howard process to occur.

This effect can be demonstrated by adjusting the pH of 3 percent magnesium chloride with and without 0.75 percent calcium lignosulfonate and 15 percent magnesium chloride containing 3.75 percent calcium lignosulfonate to pH 9.5 with dilute caustic. The 3 percent magnesium chloride forms a fluffy gelatinous precipitate. The solution with lignosulfonate forms a smaller amount of precipitate, which did not appear as gelatinous. This result explains why the magnesium chloride solution with lignosulfonate was less effective at reducing chloride penetration at the 3 percent concentration. The supernatant has most of the lignosulfonate still in solution. The 15 percent solution has lots of precipitate with little lignosulfonate left in solution.

The reason, then, that the 3 percent magnesium chloride with 0.75 percent calcium lignosulfonate did not reduce chloride diffusion is that the Howard process could not occur because the concentration of calcium ion and hydroxide ion did not exceed the solubility product as it did in the original 15 percent salt experiments.

In actual practice, the magnesium chloride with lignosulfonate is generally added to roads as a solid or in a 28 percent solution. These are condensed sufficiently to produce high enough concentrations of calcium for precipitation by the Howard process to occur.

CONCLUSION

Calcium lignosulfonates, which are added to deicing salts as corrosion inhibitors toward exposed mild steel, have been shown to have additional advantages:

1. Lignosulfonates yield a substantial reduction in corrosion when fractures in concrete lead to the reinforcing bar—up to 70 percent reduction for a 3 percent salt solution with 0.75 percent lignosulfonate;

2. Lignosulfonates form insoluble precipitates in the surface pores that reduce the apparent surface chloride concentration; and

3. Lignosulfonates produce conditions that reduce the diffusion coefficient of chloride ion into the concrete and of alkalinity out of the concrete.

Reinforced concrete structures with exposed rebar, with cracks leading to the rebar, and with areas of undamaged concrete would benefit from calcium lignosulfonates in the deicing salts through the reduction in corrosion rates and reduced chloride penetration.

REFERENCES

1. J. Neal. A Lignosulfonate-Based Corrosion Inhibitor for Use with Deicing Salts. Presented at the Winter Maintenance Committee Meeting, TRB, National Research Council, Washington, D.C., 1985.
2. QWIKSALT® + PCI®. *Technical Bulletin*, Great Salt Lake Minerals and Chemicals Corporation, Ogden, Utah, undated.
3. FREEZGARD® + PCI®. *Technical Bulletin*, Great Salt Lake Minerals and Chemicals Corporation, Ogden, Utah, undated.
4. PCI® Corrosion Control Polymer. *Technical Bulletin*, Georgia-Pacific Corporation, Tacoma, Wash., undated.
5. The Great Salt Debate. *Better Roads*, June 1987, pp. 30–35.
6. D. Wheat. New Defense Against Winter Assault. *The Wenatchee World*, Jan. 15, 1988.
7. R. McCrum. CMA and Salt Mix Cuts Corrosion. *Better Roads*, June 1988, p. 32.
8. D. A. Komac. *Statewide Experiments with Chemical Deicers*. Washington State Department of Transportation, Olympia, 1989.
9. T. Wieman. *QWIKSALT® Plus PCI®, A Safer Deicer*. Washington State Department of Transportation, Olympia, undated.
10. M. Callahan. *Deicing Salts With and Without Corrosion Inhibitors*. Iowa Department of Transportation, 1988.
11. D. W. Pfeifer and M. J. Scali. *NCHRP Report 244: Concrete Sealers for Protection of Bridge Structures*. TRB, National Research Council, Washington, D.C., 1981.
12. E. Vesikari. *Service Life of Concrete Structures with Regard to Corrosion of Reinforcement*. Research Reports 553.53, Technical Research Center of Finland, Espoo, 1988.
13. O. A. Kayyali and M. N. Hague. Chloride Penetration and the Ratio of Cl^-/OH^- in the Pores of Cement Paste. *Cement and Concrete Research*, Vol. 18, 1988, pp. 895–900.
14. K. Sarkanen and C. Ludwig. *Lignins, Occurrence, Formation, Structure and Reactions*. Wiley, New York, 1971, p. 802.
15. *CRC Handbook of Chemistry and Physics, 68th Edition*. Chemical Rubber Publishing Co., Cleveland, Ohio, 1987, p. b–207.

Effectiveness of Epoxy Coatings in Minimizing Corrosion of Reinforcing Steel in Concrete

ALI AKBAR SOHANGHPURWALA AND KENNETH C. CLEAR

Corrosion characteristics of straight and bent epoxy-coated reinforcing steel were studied under accelerated southern exposure (SE) cycling as described in *NCHRP Report 244*. Variables included seven different suppliers, bend diameter, coating thickness, coating application before and after fabrication of the bar, rate of bending, temperature of steel during bending, and patching of damaged areas before installation into concrete slabs. Specimens with uncoated steel were included as controls. A total of 40 small-scale concrete slabs, each consisting of two independent specimens—one bent-bar and one straight-bar specimen—were tested. Results after completion of 47 SE cycles for some specimens and 70 cycles for others are reported. Results indicate that straight and bent epoxy-coated bars provide significantly better resistance to chloride-induced corrosion than uncoated bars. Out of the 36 sets of epoxy-coated specimens tested, only seven showed measurable macrocell corrosion currents. The macrocell corrosion currents on the control slabs were more than an order of magnitude higher than the epoxy-coated bar slabs. Corrosion rates calculated from three-electrode linear polarization data correlated with macrocell current data. Ac resistance data indicated that the coatings did not deteriorate or disbond with time. Autopsy testing revealed little corrosion damage on epoxy-coated rebars. Corrosion found on epoxy-coated rebars initiated only at damaged areas and at holidays. The effects of various coating parameters on the ability of the epoxy coating to provide corrosion protection was not distinguishable. There were no differences discernible between the bent and straight epoxy bars, other than visible coating damage.

One of the most important and costly maintenance problems faced by bridge owners is the damage caused by chloride-induced corrosion of reinforcing steel. For more than a decade, FHWA, state departments of transportation, National Bureau of Standards (NBS), Concrete Reinforcing Steel Institute (CRSI), Fusion Bonded Coders Association (FBCA), AASHTO, ASTM, and the private sector (*1*) have been working to find ways and means to prevent corrosion-induced damage in reinforced concrete.

The factors that initiate and sustain corrosion of reinforcing steel are chloride ions, oxygen, and water present at the steel-concrete interface. Therefore, to prevent, stop, or retard corrosion of reinforcing steel, access of some or all of these factors to the reinforcing steel should be minimized or eliminated. The characteristics of concrete that indirectly affect the phenomenon of reinforcing steel corrosion are permeability, which governs the access that water, chloride ions, and oxygen have to the steel; electrical resistivity, which determines the magnitude of corrosion current that can flow at a

Kenneth C. Clear, Inc., Sterling, Va. 22170.

given potential; and inherent alkalinity, which provides a passivating environment for the steel (*2*).

Many techniques and products, designed to completely stop or retard active corrosion of reinforcing steel or to prevent corrosion from initiating on new structures, have been identified and can be categorized as either mechanical or electrochemical. Most of these techniques and products are in experimental or developmental stages. However, some have gained acceptance in the bridge deck community.

The mechanical techniques are used to physically prevent the access of oxygen, chloride, and water to the steel. The electrochemical methods use an applied electrical current to either remove chlorides from the concrete (chloride removal) or alter the electrical characteristics of the reinforcing steel to make the steel less susceptible to corrosion (cathodic protection). The electrochemical category also includes additives called "inhibitors" that, when admixed into fresh concrete or combined with standard deicing salts, can prevent or minimize the formation of galvanic cells on the surface of steel. The mechanical category includes the use of silica fume admixtures and improvements in concrete mix designs and placement procedures to produce less-permeable concrete with higher electrical resistivity. Also included in this category are sealers and membranes used to prevent ingress of water and chloride ions into the concrete- and epoxy-coated reinforcing steel to isolate the steel from the aggressive environment. Early research performed by NBS for FHWA indicated that reinforcing bars, coated with select powdered epoxies using an electrostatic spray process after bar cleaning, performed well in salt contaminated concrete (*3*).

Epoxy resins are thermoset plastics belonging to the polyaddition plastics family. These resins are reported to have good long-term durability in concrete and against solvents, chemicals, and water (*4*). Epoxy resins also have desirable mechanical properties such as high ductility, small shrinkage in polymerization, and good heat resistance (*5*). Further, test results indicate that the chloride ion permeability of epoxy coatings is very low in the worst case (*3,5*).

One of the most important factors governing the performance of epoxy-coated bars is the quality control enforced during coating application and subsequent handling of the coated bars. If the coated bars are not handled properly, damage to the coating can result that could negate or reduce protection provided by the epoxy coating. ASTM specifications A775 and D3963, AASHTO specification M 284, and CRSI EDR 19 provide stringent guidelines to be followed

during coating application and subsequent handling and storage of the bars. However, laboratory research has indicated that even nonspecification epoxy-coated bars provide enhanced corrosion protection as compared to black (i.e. uncoated) steel (6).

Many states have used, and continue to use, epoxy-coated bars for construction of new bridge decks and full depth repair of old deck sections. Field performance studies have been conducted in Maryland, Minnesota, Virginia, and Pennsylvania (7–10). The Maryland and Minnesota studies did not provide unequivocal results because of early age evaluation and low chloride contamination levels in the concrete. The Virginia and Pennsylvania studies, however, found that epoxy-coated bars provided enhanced corrosion protection under extremely adverse conditions compared to uncoated bars.

In spite of positive laboratory and field studies, new concerns have been raised regarding the effectiveness of epoxy-coated bars in preventing corrosion and extending the life of structures as a result of recent failures in marine substructures of the Florida Keys (11). Some concerns are specifically targeted at the bent bar stirrups. When coated bars are bent into the required shape, there may be some loss of bond between the epoxy coating and the steel at the outer radius of the bend that may reduce the protection provided by the coating. Some researchers have also argued that a small imperfection in the coating may cause a small anode and large cathode situation that would be less desirable than using uncoated steel. Others are concerned that once corrosion starts at an imperfection in the coating it could spread underneath the coating (i.e., undercutting), leading to disbondment or—as suggested by Romano (12)—cathodic disbondment of epoxy coatings can occur adjacent to damaged areas because of the galvanic process occurring between the cathodic and anodic sites on the steel.

As a result, this research was undertaken to study the effectiveness of epoxy-coated bars in preventing or minimizing corrosion and to determine the influence, if any, the following variables have on the performance of epoxy-coated bars:

- Bend diameter,
- Thickness of the coating,
- Application of the coating before and after fabrication of the bar,
- Rate of bending,
- Temperature of steel during bending, and
- Patching of damaged areas before installation.

EXPERIMENTAL PROCEDURE

To evaluate the consistency of standard, present-day, epoxy coating practices, coated bars were obtained in 1988 from seven different suppliers located in all major geographical regions of the continental United States. A total of 15 variables, including two controls (black steel) were included in the study (see Table 1). Six sets of one bent and two straight coated bars, along with a set of uncoated bent and straight bars, were received for each variable from the appropriate supplier. Each supplier provided bars that had been blasted to a bright clean metal finish, heated to near 450°F, and passed through a bin fitted with electrostatic spray guns. During the

latter stage, epoxy powder was applied by spray to provide a coating of appropriate thickness. The coated bars were subsequently passed through a cooling bath and then through the holiday detection and thickness measurement systems used by the supplier. Scotchkote 213 epoxy coating was used in all instances and all bars were production line coated (e.g., no special fabrication procedures were followed other than those needed to obtain the variables presented in Table 1).

For the purpose of this research, bars referred to as standard were manufactured as follows:

- No. 4 and No. 5 bars were coated with a 9-mil-thick epoxy coating.
- For bent bars, bending was achieved at a fast rate (an average of 3 sec per 180-degree bend) with the steel at room temperature. Each bar contained two 180-degree bends (see Figure 1).
- No. 4 bars were bent to a 2-in.–diameter (herein referred to as the small-bend study).
- No. 5 bars were bent to a 3.75-in.–diameter (herein referred to as the large-bend study).
- No patching was applied after fabrication on either the bent or the straight bars.

The controls contain black steel of each size bar and bend diameter.

All pertinent physical property information for coatings was documented before placing the bars in the forms. Coating thickness was measured at six locations along each bar using a Mikrotest Model II thumbwell magnetic gauge calibrated to NBS standards. The number of holidays was determined using a 67.5 v Tinker-Rasor Model M–1 holiday detector. Additionally, any visible damage and its location were documented for each bar. The No. 5 bars were positioned in 13- × 14- × 7-in. wooden forms and the No. 4 bars were positioned in 10- × 12- × 7-in. wooden forms. Conventional concrete with a water/cement ratio of 0.47 was then placed. Clear concrete cover was 1 in. on all bars. The concrete mix design can be found in Table 2. The slabs were cured using wet burlap and polyethylene for 14 days, followed by laboratory air exposure through 45 to 52 days of age.

Three slabs were fabricated per variable. Each slab contained a coated set of one bent and two straight bars as top steel (see Figure 1). The bottom mat consisted of No. 5 and No. 6 black bars. The slabs were designed so that each slab effectively comprised two specimens. One-half of the slab was a bent-bar specimen and the remainder was a straight-bar specimen of the same variable. The bottom mat steel was sized to provide the same ratio of steel area between the top mat and the bottom mat for both halves of the slab. Thus, the ratio of epoxy-coated steel areas (top mat) to black steel areas (bottom mat) was the same for both halves of each epoxy-coated bar slab.

For the purpose of creating a macrocorrosion cell and to facilitate installation of instrumentation to measure macrocell currents, the bottom mat steel of each half of each slab was made electrically continuous (each bottom half remained discontinuous to the other bottom half within the same slab). The two straight bars in the top mat of each slab were also made continuous. All continuity was achieved outside the slab. A switch and a resistor were then installed between the

TABLE 1 DETAILS OF VARIABLES AND COATING PARAMETERS

VARIABLE SET	VARIABLE	# OF SLABS
V1	Control - Black, Uncoated Bars.	2
V2	Epoxy Coated After Fabrication - 6 mil Thick Coating.	2
V3	Epoxy Coated After Fabrication - 9 mil Thick Coating.	2
V4	Epoxy Coated After Fabrication - 12 mil Thick Coating.	2
V5	Standard Epoxy Coated Bar - 6 mil Thick.	2
V6	Standard Epoxy Coated Bar - 9 mil Thick, From sources 1,2,4,6, & 7.	10
V10	Standard Epoxy Coated Bar - 9 mil Thick, From source 5.	2
V12	Standard Epoxy Coated Bar - 12 mil Thick.	2
V13	Slow Bend Rate During Fabrication.	2
V14	Fabricated At High Temperature (approx. 125 F).	2
V15	100% Patch On The Outside Radius After Fabrication.	2
V16	Standard Epoxy Coated Bar - 9 mil Thick Coating, Small Bend Diameter.	4
V18	Fabricated At High Temperature (approx. 125 F), Small Bend Diameter.	2
V19	Epoxy Coated After Fabrication - 9 mil Thick Coating, Small Bend Diameter.	2
V20	Control - Black, Uncoated Bars, Small Bend Diameter.	2

NOTE: Except where noted all specimens were coated with a 9 mil thick Scotchkote 213 before fabrication. The bars were bent at a fast rate (an average of 3 seconds per 180 degree bend) with steel at room temperature. No patching was applied after fabrication. Variables V1 to V15 were fabricated from #5 steel with a bend diameter of 3.75 inches and the remaining variables were fabricated from #4 bar with a bend diameter of 2 inches.

top and bottom mats of each half of each slab. The sides of the slabs were then coated with epoxy to simulate an infinite slab. Finally, ponding dams were installed on all slabs that were to be subjected to southern exposure (SE) testing as per *NCHRP Report 244* (*13*). Figure 2 shows a typical slab with the ponding dam in place.

Following completion of the lab air cure, two slabs per variable were exposed to SE cycling. Weekly SE cycling consisted of four days of continuous ponding of the top surface with a 15 percent (by weight) sodium chloride solution followed by draining and 3 days exposure to an air temperature of 100°F and ultraviolet lights. The third slab of each variable was exposed in a northern Virginia climate at an outdoor exposure facility. These slabs served as controls for each variable.

Periodically, at the end of the ponding portion of SE cycling, top-surface half-cell potential surveys were conducted as per ASTM C–876 and the magnitude of the macrocell corrosion current was measured (*6*). The three-electrode linear polarization technique was periodically used, on an experimental basis, to monitor the polarization resistance as a function of time of the variable under test. Polarization resistance is used to calculate the rate of corrosion using the Stern-Geary equation (*14*). In addition, the ac resistance between the top and bottom mats was documented and visual and sounding surveys were conducted.

The slabs incorporating Variables 1 to 18 (excluding Variable 14) were subjected to a total of 70 SE cycles and have completed the accelerated test program, whereas the slabs incorporating Variables 14, 19, and 20 were subjected to a total of 47 SE cycles and are continuing accelerated testing. All control slabs (Variables 1 and 20) are presently demonstrating corrosion-induced staining on the top surface and on the sides of the slabs. To correlate the corrosion measurements on all slabs to the actual visible corrosion damage suffered by the coated bars, autopsy testing was conducted on 12 specimens after completing the accelerated test program.

RESULTS AND DISCUSSION

Visual Examination

Visual examination of all the control slabs exposed to SE cycling revealed stains of corrosion products on the surface
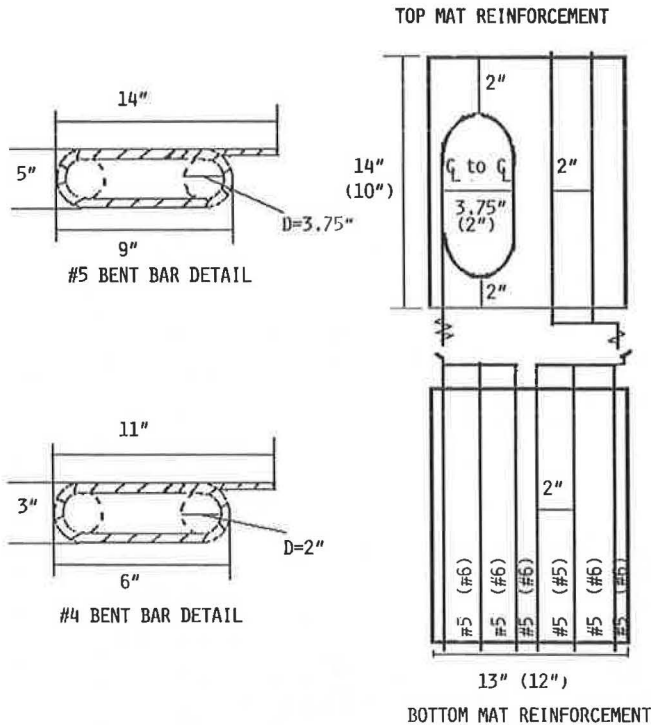
TOP MAT REINFORCEMENT

FIGURE 1 Slab and bent-bar fabrication details.

TABLE 2 CONCRETE MIX DESIGN

Materials	Amount
Cement, lb/cy	588
Coarse Aggregate, lb/cy	1915
Fine Aggregate, lb/cy	1250
Water, lb/cy	276
Daratard 17, ml	13
Air, %	7
Unit Weight., pcf	150
W/C=	0.47

of the slabs. Some corrosion products have also made their way out of the slabs adjacent to the bent and straight rebars protruding from the short side of the slabs. Some surface cracking parallel to the rebars was also seen. Sounding surveys did not reveal any delaminations at the end of 47 or 70 SE cycles on the slabs representing Variables 20 and 1 (control slabs), respectively, although detection of such is difficult on small-scale specimens. In comparison, epoxy-coated rebar slabs do not show any visible signs of corrosion-induced staining or cracking.

Corrosion Rate Data

Macrocell Corrosion Current Data

Corrosion of steel can occur in many forms. The type most damaging to bridge decks is termed macrocell corrosion. The top mat steel in bridge decks becomes anodic to the bottom
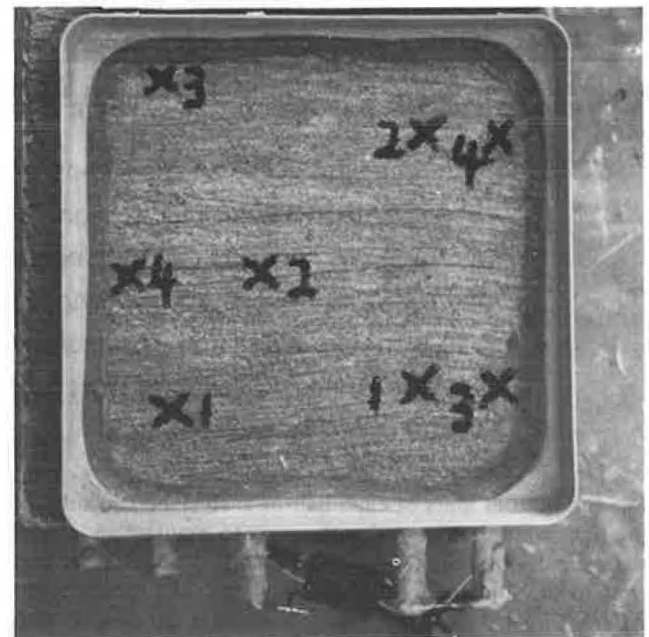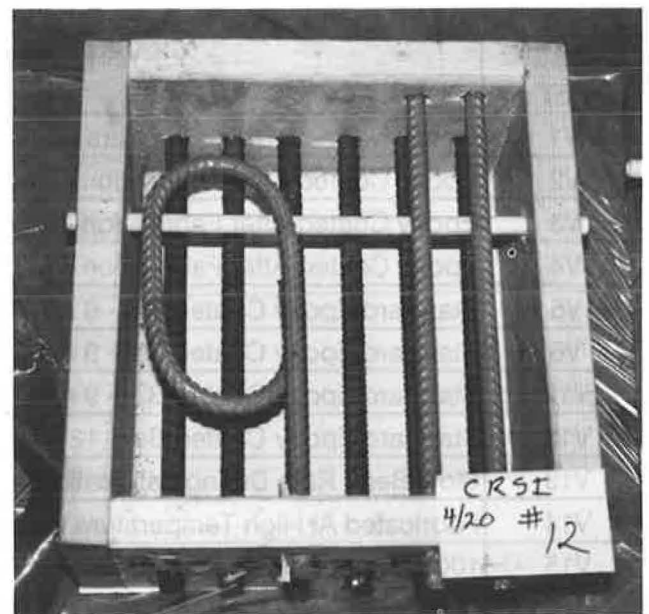
FIGURE 2 *Top*: epoxy-coated bars in forms before concrete placement. *Bottom*: completed slab before SE cycling.

mat because of the ingress of chlorides from deicing salts. A macrocell is then formed between the top and bottom mats and an electronic current flows from the top mat to the bottom mat through electrically continuous steel. An ionic current flows from the bottom mat to the top mat through the concrete. The ionic current is directly proportional to the loss of steel caused by corrosion and the algebraic sum of the ionic and electronic flow is zero. Therefore, the magnitude of the electronic macrocell corrosion current is directly proportional to the macrocell corrosion rate at the top mat steel.

Because the steel areas of the bent bar and the two straight bars in the top mat of the specimens are not equal, the macrocell currents have been analyzed in terms of milliamperes per

square foot of the top mat steel. Figures 3 and 4 present macrocell current data for all slabs that have values greater than 0.01 mamp/ft². Also, the data for each variable are an average of several slabs (see Table 1 for number of slabs representing each variable).

Out of the 36 sets of epoxy-coated specimens tested, only seven showed macrocell corrosion currents in excess of 0.01 mamp/ft². Of these seven sets, three (V10-Bent Bar, V13-Bent Bar, and V19-Bent Bar) had visibly identifiable coating damage such as nicks, scrapes, and cuts before placement in the concrete. The data in Figures 3 and 4 clearly highlight the difference in the rate of corrosion of the controls versus the epoxy-coated bars. The corrosion rate of the controls is more than an order of magnitude larger than the epoxy-coated bars (controls averaged 1.62 mamp/ft², and all the epoxy-coated bars averaged 0.018 mamp/ft² while the average of the 7 sets presented was 0.072 mamp/ft²). The data indicate that epoxy-coated rebars are less susceptible to corrosion than uncoated rebars under accelerated corrosion conditions. Work performed in Finland also indicated that electrostatically epoxy-coated bars provide corrosion protection even in an aggressive environment (*5*). Corrosion initiation in the control specimens occurred after only about a maximum of 20 SE cycles, whereas in the epoxy-coated bar specimens (with macrocell currents greater than 0.01 mamp/ft²) it occurred between 45 and 60 SE cycles except for one set of specimens (V19-bent) where it occurred at about 28 SE cycles.

The low corrosion rates of the epoxy-coated rebar specimens may be explained by theorizing that corrosion initiated in the coating defects and that because the size of the anodic (damaged) areas is small, the volume of corrosion products formed is not sufficient, at present, to cause corrosion-induced damage. When the autopsies are conducted, it will be possible to ascertain if the loss of steel cross section at the coating defects is significant or not. It may also be possible to evaluate whether corrosion initiated at a coating defect can lead to undercutting of the coating, although it may not be possible to determine whether coating disbondment around the coating defect is necessary for the spread of corrosion underneath the coating or if the corrosion process causes the disbondment.

Presently, there are no perceptible differences between the various coating parameters, such as speed of bending, temperature of bar during coating, bend diameter, coating thickness, and patching before or after fabrication. However, from the data collected, it appears that the bent epoxy-coated rebars are more likely to have coating damage.

Three-Electrode Linear Polarization Data

Until recently, it was not possible to determine the corrosion rate of steel embedded in concrete. Potential surveys and chloride analysis of concrete samples only indicated the areas where corrosion activity was most likely. The three-electrode linear polarization technique applies a small dc current to the steel and measures the response. The mathematical relationship between the applied current and the response (potential shift) has been defined by Stearn and Geary (*14*) and can be used to calculate the corrosion rate of uncoated steel embedded in concrete. This technique, however, has not been
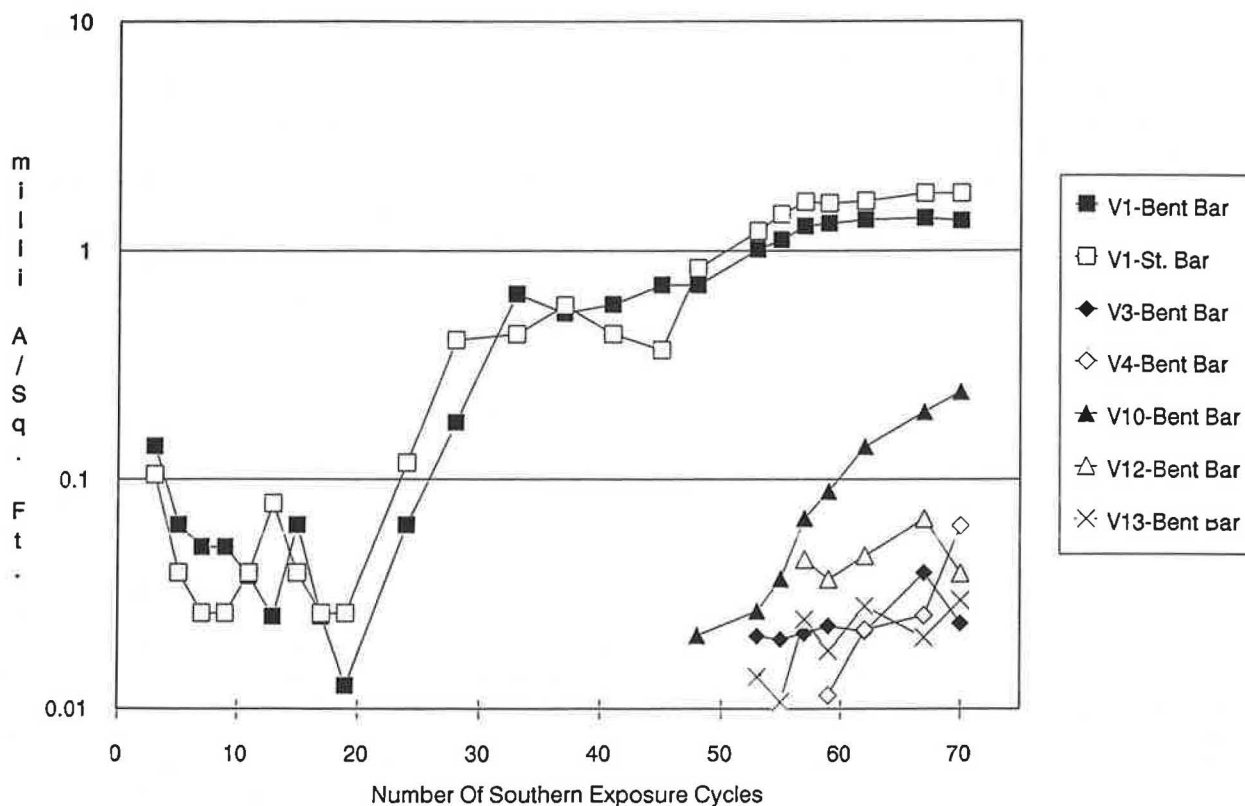

FIGURE 3 Large-bend study—controls and epoxy-coated bar specimens: macrocell current versus time.
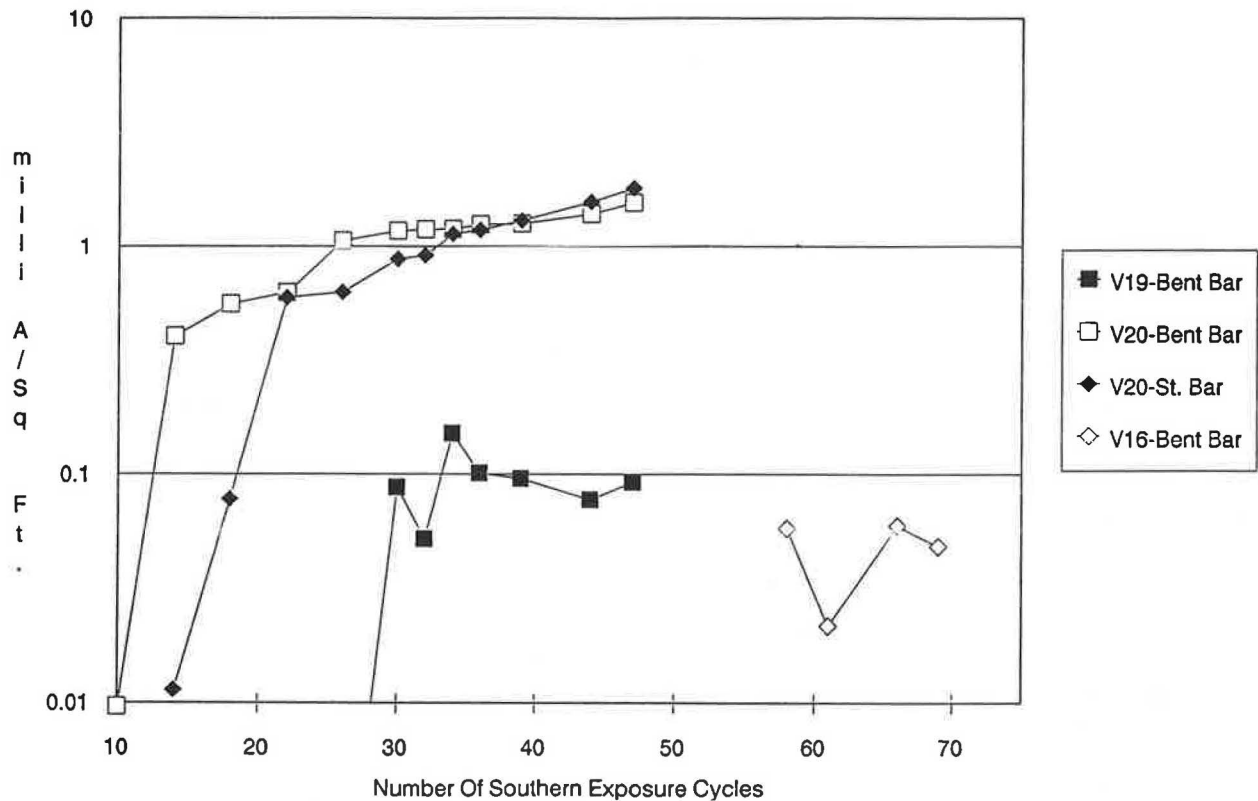
FIGURE 4   Small-bend study—controls and epoxy-coated bar specimens: macrocell current versus time.

validated for use on epoxy-coated bars. In this research, the technique was used to provide information on its suitability for use with epoxy-coated bars.

Corrosion rate data obtained from the same seven sets of specimens for which macrocell current data were presented are shown in Figures 5 and 6 and were calculated from the results of three-electrode linear polarization testing. The data reflect about an order of magnitude difference between the controls and the epoxy-coated bars, which was also indicated by the macrocell corrosion current data, but the data appear at present to fail to differentiate between epoxy-coated bar specimens.

Electrical Resistance Data

The electrical resistance between the top mat and the bottom mat through the concrete, with the mats electrically isolated from each other, significantly affects the phenomenon of macrocell corrosion. The magnitude of the ionic flow is inversely proportional to the electrical resistance between the mats. Also, the electrical resistance provides information regarding coating defects when epoxy-coated bars have been used in either or both mats. Figures 7 and 8 present typical resistance data obtained in this study. As expected, the epoxy-coated bars have a much higher electrical resistance between the mats, ranging from 1,300 to 129,500 ohms, compared to the controls that have electrical resistance in the range of a few hundred ohms. Although the mat-to-mat electrical resistance

of the epoxy-coated bars varies significantly from one specimen to another, the general trend is to remain constant with time. This observation indicates that the coating is not deteriorating or becoming disbonded with time. The concrete moisture content and temperature were about the same at the end of each SE ponding cycle when all data were collected. All epoxy-coated bars that had documented coating damage before installation in the concrete slabs demonstrated lower electrical resistance than those of the same variable with no damage. The epoxy-coated straight bars had a higher average electrical resistance (40,654 ohms) than the epoxy-coated bent bars (12,265 ohms). This difference may be partially because of the difference in geometry of the bars.

Potential Data

Figure 9 shows half-cell potential data for the control slabs and the coated bar specimens that exhibited the highest and lowest potentials. Except for the control slabs, the half-cell potentials are less negative than −350 mV for the copper sulfate electrode. Potential measurements on epoxy-coated rebars are difficult to interpret. In this case, the less negative potentials are probably the result of the large uncoated bottom mat and the lack of cathodic polarization thereon. One should, therefore, concentrate on within-variable changes with time rather than absolute magnitude. When this is done, these findings correlate well with the macrocell corrosion current data. A summary of all potential data is presented in Table 3.
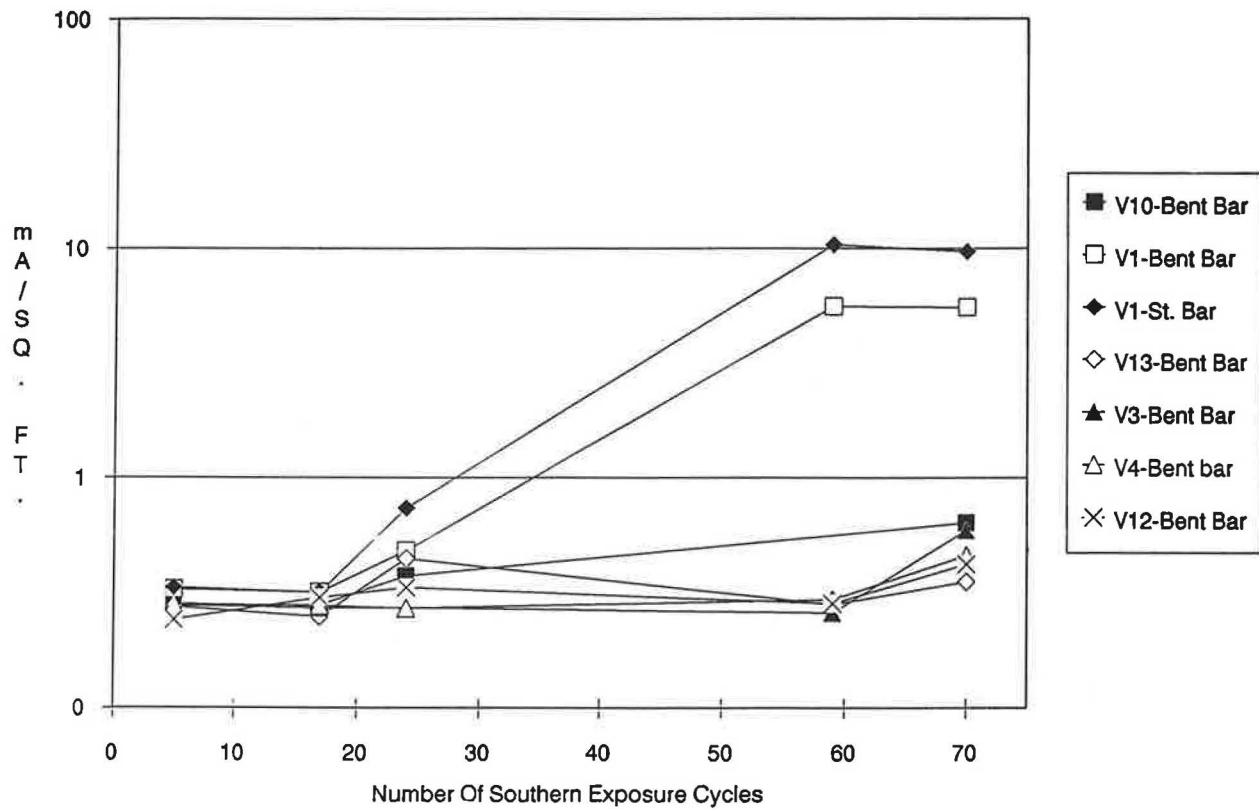
FIGURE 5 Large-bend study—controls and epoxy-coated bar specimens: corrosion rate versus time.
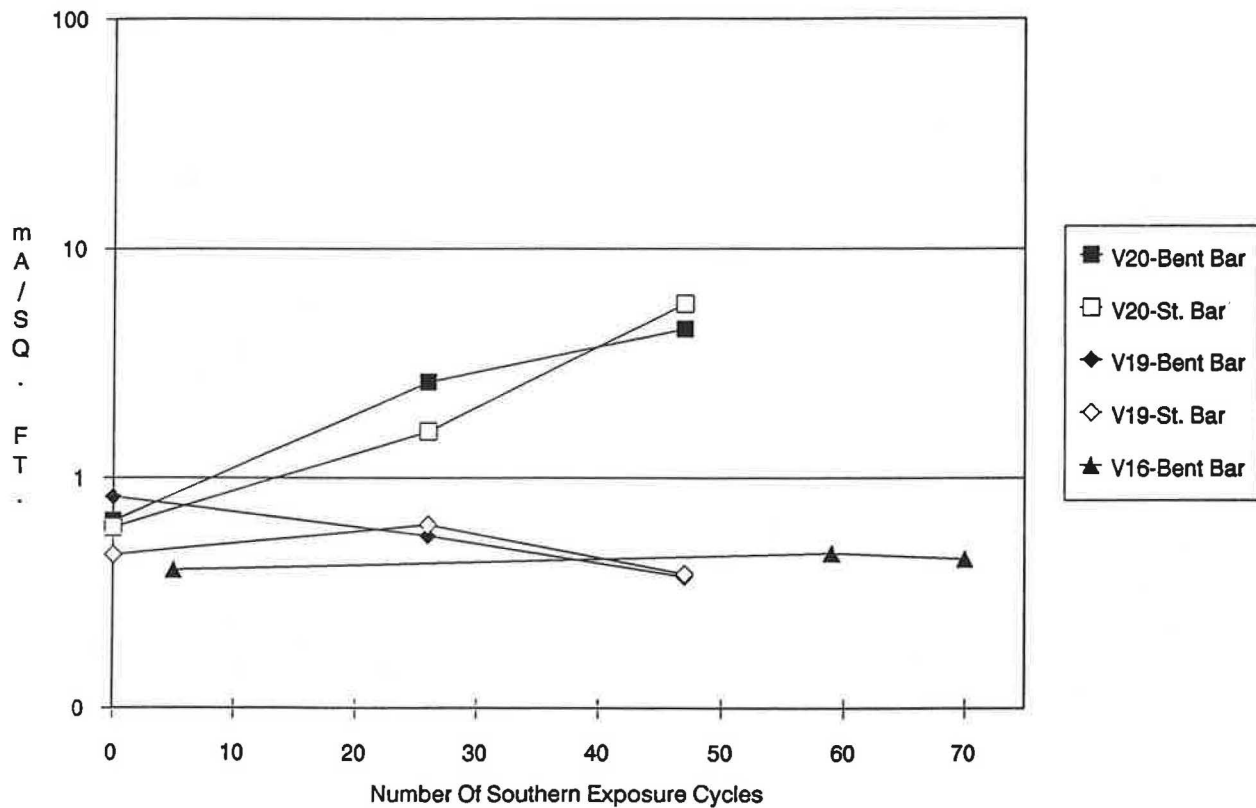

FIGURE 6 Small-bend study—controls and epoxy-coated bar specimens: corrosion rate versus time.
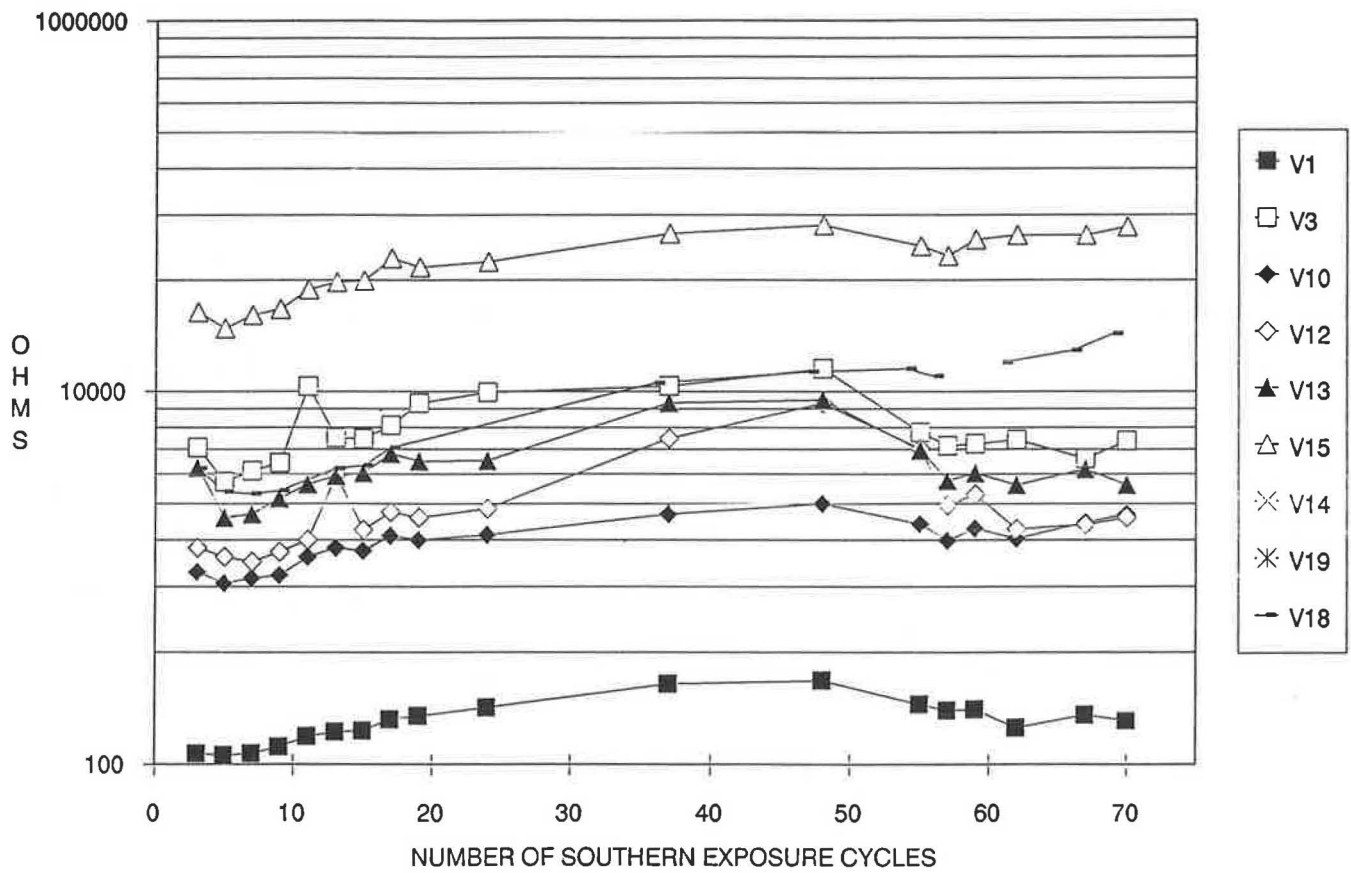
FIGURE 7   All bent bars—controls and epoxy-coated bar specimens: resistance versus time.
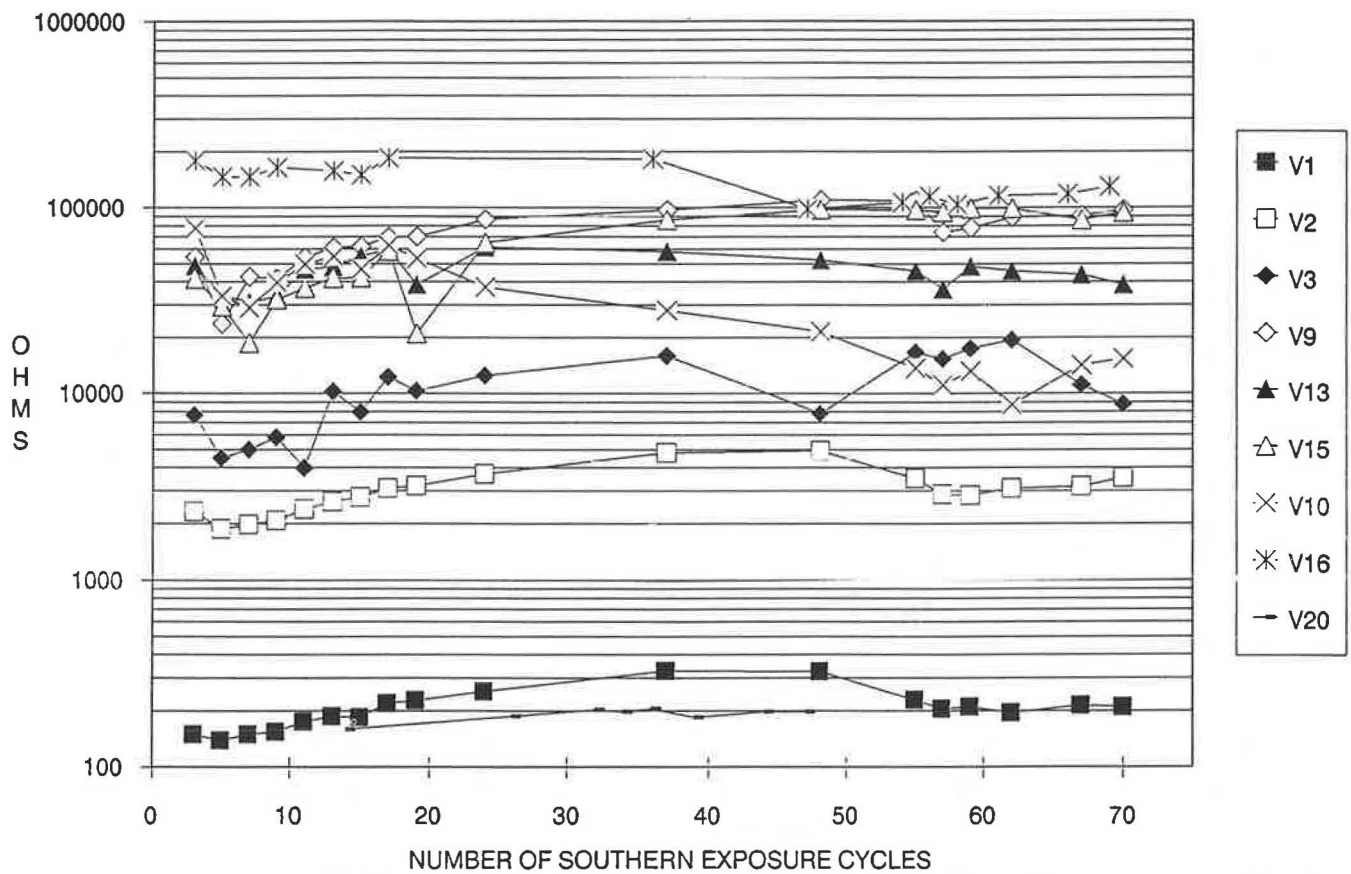

FIGURE 8   All straight bars—controls and epoxy-coated bar specimens: resistance versus time.
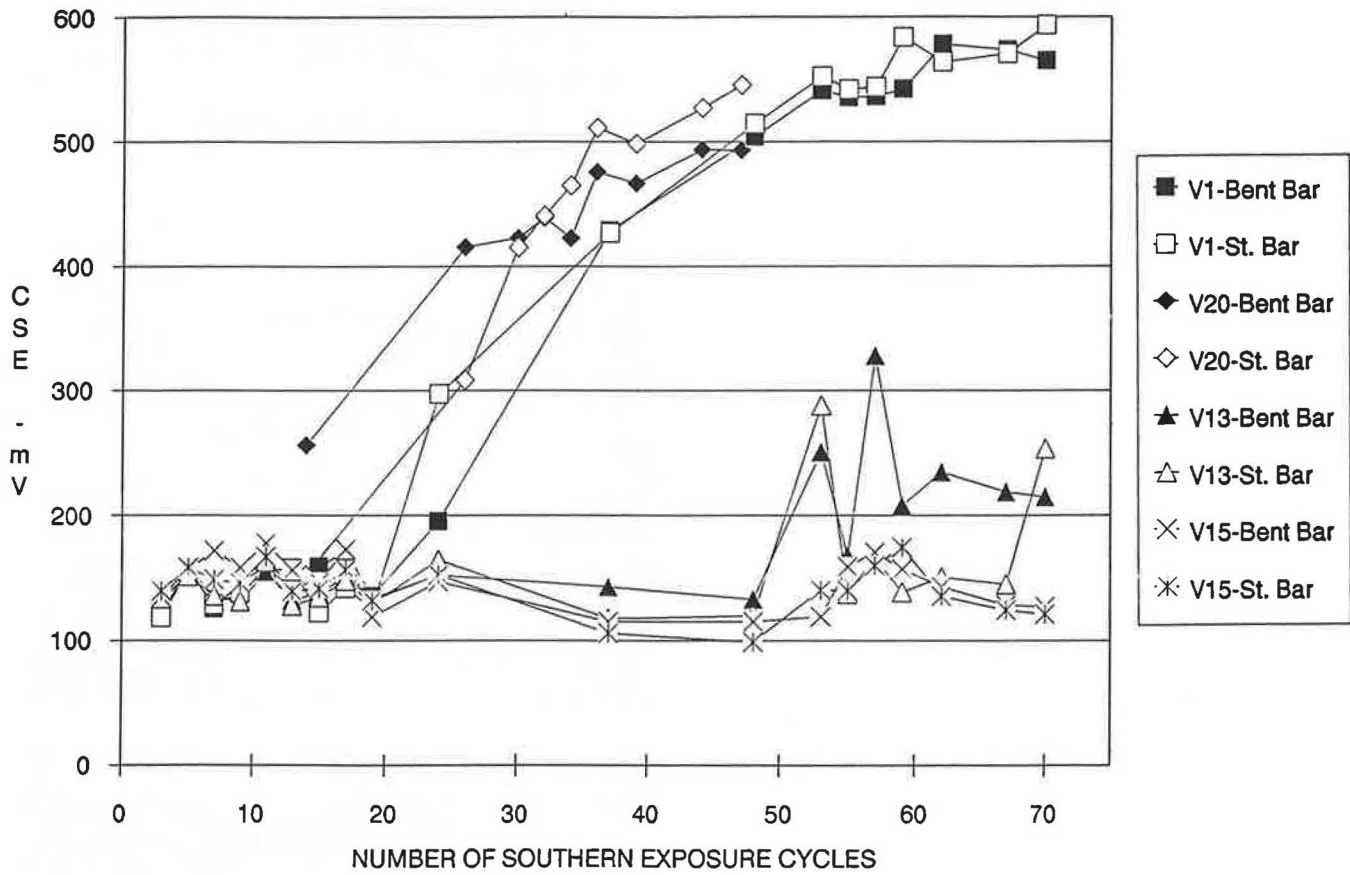
FIGURE 9 Controls and the highest and lowest epoxy-coated bar specimens: rebar potential versus time.

TABLE 3 REBAR HALF-CELL POTENTIAL DATA

Variable #	SE Cycles Completed	BENT BAR				STRAIGHT BAR			
		Initial Potential	Final Potential	Average Potential	Change in Potential. (Final - Initial)	Initial Potential	Final Potential	Average Potential	Change in Potential. (Final - Initial)
V1	77	-78	-565	-333	-487	-79	-594	-339	-515
V2	77	-113	-161	-145	-48	-117	-178	-152	-61
V3	77	-96	-236	-154	-140	-110	-201	-150	-91
V4	77	-94	-231	-170	-137	-95	-147	-158	-52
V5	77	-74	-210	-169	-136	-87	-201	-154	-114
V6	77	-77	-181	-154	-104	-78	-168	-148	-90
V10	77	-83	-262	-172	-179	-69	-201	-148	-132
V12	77	-70	-234	-167	-164	-71	-162	-139	-91
V13	77	-86	-215	-175	-129	-93	-253	-154	-160
V14	47	-96	-121	-127	-25	-106	-142	-132	-36
V15	77	-91	-127	-146	-36	-94	-121	-141	-27
V16	77	-91	-182	-152	-91	-115	-157	-155	-42
V18	77	-90	-169	-166	-79	-109	-169	-175	-61
V19	47	-101	-197	-198	-96	-128	-182	-182	-54
V20	47	-121	-493	-432	-372	-127	-545	-429	-418

NOTE : All potentials are expressed in negative mV CSE.

Autopsy

Autopsy testing was conducted on 1 black bar control slab and 11 epoxy-coated bar slabs. The epoxy-coated bar slabs were selected to represent all variables and to include the slabs that demonstrated the maximum and minimum macrocell corrosion currents from both the large-bend and small-bend studies.

Saw cuts were made along the sides of the slabs parallel to the top mat steel. The concrete was then chiseled along the saw cuts to force failure in the top mat rebar plane and expose the bars. Additional chipping allowed complete removal of the bars from the concrete without damaging the coating or the bars. Figure 10 shows a typical slab after completion of autopsy testing. After removal of the rebars from the concrete slabs, any visual coating damage, rusting, or changes in coating parameters (such as softening or disbondment) were documented. The visual condition of the bar traces left on the concrete was also documented.

In general, the epoxy-coated rebars exhibited insignificant corrosion damage as compared to the black bar controls. Corrosion that was found on epoxy-coated bars had initiated at sites where visual coating damage existed before placement of the rebar in concrete and at original holidays. Corrosion initiation at holidays was primarily limited to locations on the ribs of the bars. The increase in volume caused by corrosion product in the vicinity of holidays caused a bubble to form in the coating. In the later stages of corrosion, these bubbles ruptured causing a loss of coating. The diameter of the bubbles ranged from approximately $\frac{1}{16}$ to $\frac{1}{8}$ in. No bond loss around the bubbled areas was found and no deep pits or severe section loss from the small anode or large cathode effect was found.

Photographs of black bars from the control slab are presented in Figure 11. Figure 12 shows photographs of epoxy-coated rebars obtained from the slab representing Variable 10. This slab exhibited the maximum corrosion current for epoxy-coated rebar slabs at the end of 70 SE cycles. Figure 13 shows photographs of epoxy-coated rebars obtained from the slab representing Variable 11. This slab exhibited the minimum corrosion current for epoxy-coated rebar slabs at the end of 70 SE cycles.

CONCLUSION

Coated bars have performed significantly better than uncoated bars during the 70 and 47 SE cycles completed to date. Rust staining and cracking have occurred on the uncoated control slabs but not on any of the epoxy-coated rebar specimens.

Out of the 36 sets of epoxy-coated specimens tested, only seven showed macrocell corrosion currents greater than 0.01 mamp/ft². Of these 7 sets, three had visibly identifiable damage before placement in the slab. The macrocell currents on the control slabs were more than an order of magnitude higher than those on the epoxy-coated bars; the controls averaged 1.62 mamp/ft², all the epoxy-coated bars averaged 0.018 mamp/ft², and the average of the seven sets was 0.072 mamp/ft². Corrosion rates calculated from the three-electrode linear polarization data also correlated with the macrocell current data.
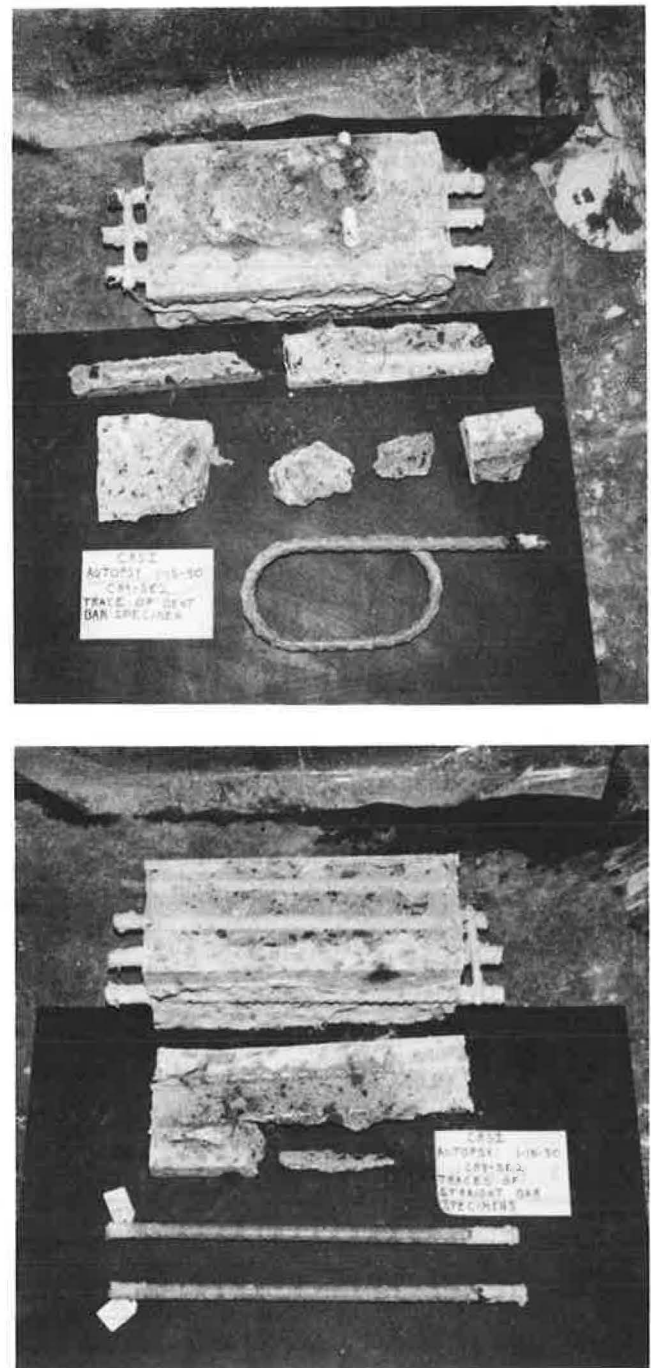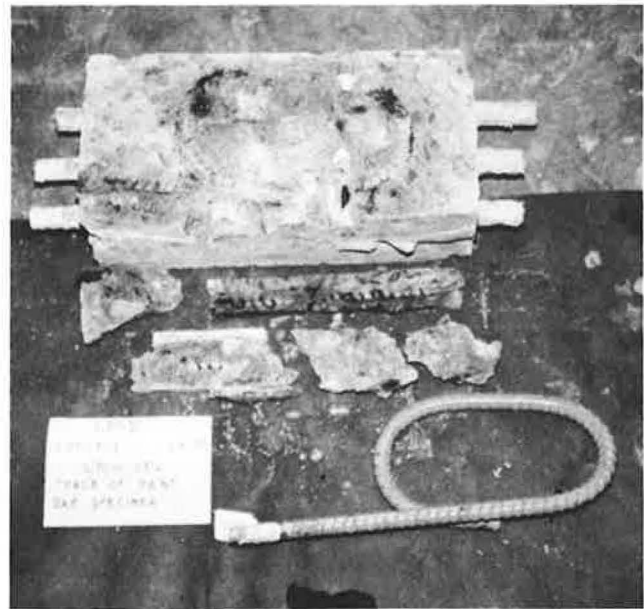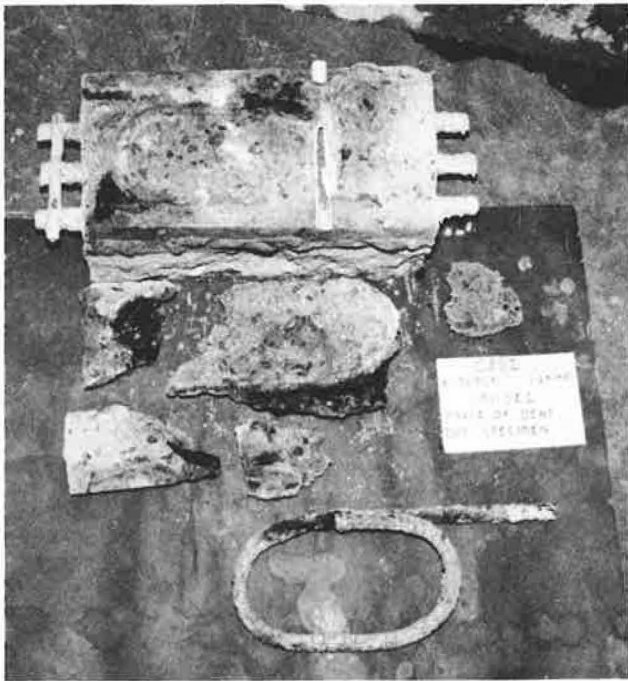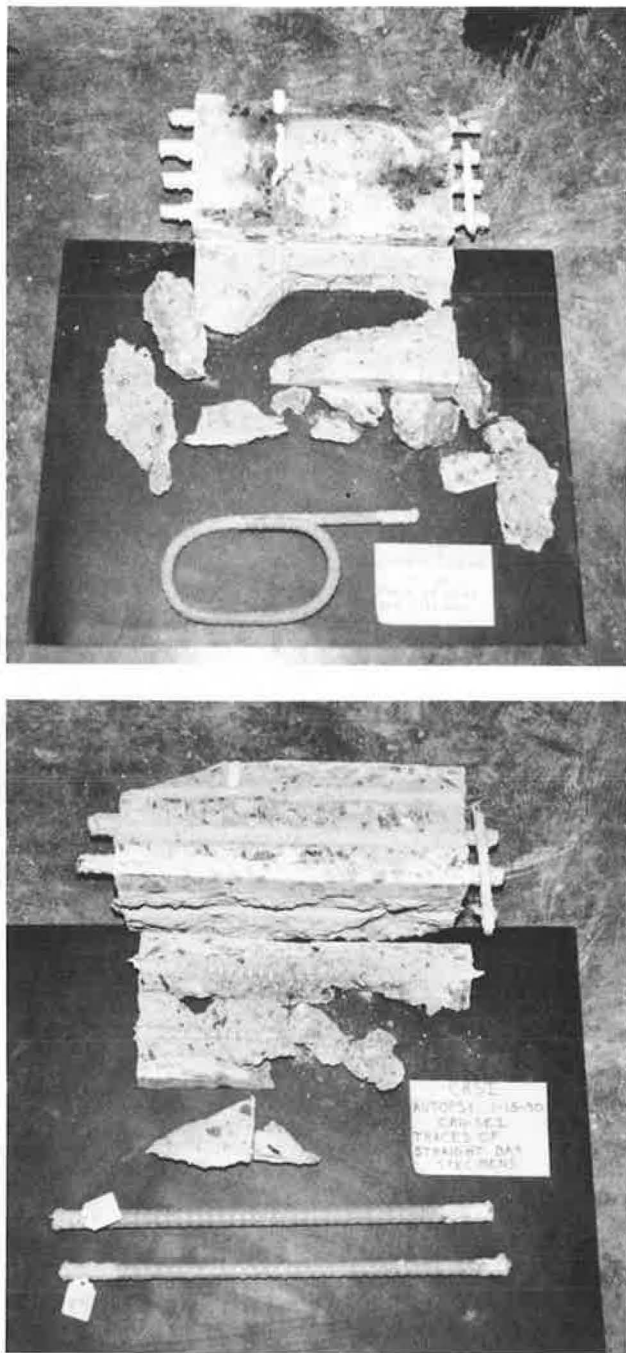

FIGURE 10 Rebars after completion of a typical autopsy.

The electrical resistance between the mats of the epoxy-coated bars ranged from 1,300 to 129,500. The average of epoxy-coated bent-bar specimens was 40,654 ohms, and that of epoxy-coated straight-bar specimens was 12,265 ohms. Although the mat-to-mat electrical resistance of the epoxy-coated bars varies significantly from one specimen to another, the general trend is to remain constant with time. This observation indicates that the coating is not deteriorating or becoming disbonded with time. A significant difference between the electrical resistance of coated straight and bent bars was noted.

FIGURE 11   Rebars after completion of autopsy of a slab representing black bar controls.

FIGURE 12   Rebars after completion of autopsy of a slab representing Variable 10.

FIGURE 13 Rebars after completion of autopsy of a slab representing Variable 11.

holidays, the volume of corrosion products caused a bubble to form in the coating, that eventually led to local coating loss as corrosion progressed and the bubble ruptured. No severe section loss or pitting caused by the small anode or large cathode effect was found.

Presently, the effects of the various coating parameters on the ability of the epoxy coating to provide corrosion protection are not distinguishable and no other differences between the bent and straight epoxy-coated bars, other than visible coating damage, are discernable.

ACKNOWLEDGMENT

This research was supported by the Concrete Reinforcing Steel Institute.

REFERENCES

1. R. T. Stafford. Epoxy Coated Rebars. *Parking*, March–April 1985, p. 39.
2. W. Whitman, R. Russell, and V. Altieri. *Industrial and Engineering Chemistry*, Vol. 16, 1924, p. 665.
3. J. R. Clifton, H. F. Beehgly, and R. G. Mathey. *Nonmetallic Coatings for Concrete Reinforcing Bars*. Report FHWA-RD-74-18. FHWA, U.S. Department of Transportation, Feb. 1974.
4. R. G. Pike. Nonmetallic Coatings for Concrete Reinforcing Bars. *Public Roads*, Vol. 37, No. 5, June 1973, pp. 185–197.
5. L. Salparanta. *Epoxy-Coated Concrete Reinforcements*. Research Report VTT-RR-525-88. Finland Technical Research Center, March 1988, p. 17.
6. Y. P. Virmani, K. C. Clear, and T. J. Pasko. Jr. *Time to Corrosion of Reinforcing Steel in Concrete*. Report FHWA-RD-83-012, Vol. 5. FHWA, U.S. Department of Transportation, Dec. 1982.
7. S. K. Manjal. *Evaluation of Epoxy Coated Reinforcing Steel Bridge Decks*. Report FHWA-MD-82-03. Maryland State Highway Administration, Brooklandville, March 1981.
8. M. G. Hagen. *Bridge Deck Deterioration and Restoration—Final Report*. Report FHWA-MN-RD-83-01. Minnesota Department of Transportation, St. Paul, Nov. 1982.
9. W. T. McKeel, Jr. *Evaluation of Epoxy Coated Reinforcing Steel, Milestone Report*. HPR Study 79. Virginia Highway and Transportation Research Council, Charlottesville, July 1984.
10. R. E. Weyers and P. D. Cady. Deterioration of Concrete Bridge Decks From Corrosion of Reinforcing Steel. *Concrete International*, Jan. 1987.
11. A. M. Zayed and A. A. Sagues. Corrosion of Epoxy Coated Reinforcing Steel in Concrete. *Proc., Corrosion/89*, National Association of Corrosion Engineers, New Orleans, 1989.
12. D. C. Romano. *Preliminary Investigation of Epoxy Coated Reinforcing Steel Disbondment; Cause and Effects*. Florida Department of Transportation, Materials Office, Gainesville, Nov. 1988.
13. D. W. Pfeifer and M. J. Scali. *NCHRP Report 244: Concrete Sealers for Protection of Bridge Structures*. TRB, National Research Council, Washington, D.C., Dec. 1981.
14. K. C. Clear. Measuring Rate of Corrosion of Steel in Field Concrete Structures. In *Transportation Research Record 1211*, TRB, National Research Council, Washington, D.C., 1989.

This may be partially because of the difference in geometry of the specimens.

Autopsy testing revealed little corrosion damage on epoxy-coated rebars. Corrosion that was found had initiated at sites where visual coating damage existed before concrete placement and at original holidays. Where corrosion initiated at

Abridgment

Economic Models for Setting Priorities for Road Maintenance and Rehabilitation in Israel

Moshe Livneh and Joseph Craus

Various general models have recently been used in an engineering-economic study to determine the road maintenance efficacy of the interurban road network in Israel. These models contain deterioration curves for various maintenance and rehabilitation policies, together with the preparation and overlaying costs, routine maintenance costs, and road users' costs, all as a function of overall pavement grade values. These models led, after the determination of an overlaying policy, to establishment of a purposive model for computing a priority ranking as a function of various parameters. The model obtained was found to be sensitive mainly to the annual average daily traffic.

Because of the poor condition of interurban roads in Israel, the Israeli Department of Public Works (DPW) decided to conduct an engineering-economic study that would respond to (a) analysis of the existing situation and scope of investment required to bring the interurban road network up to an acceptable level; and (b) economic justification, from the point of view of the national economy, of investing in road maintenance.

To respond to these points, a data bank was needed that would include the parameters of the condition of the pavements over time, in addition to models of agency and road user costs. Even in the absence of some of the required statistics, however, it is possible to determine the missing details on the basis of comparable work from other sources. This method leads to the construction of general fundamental models for pavement deterioration, and maintenance, rehabilitation, and road users' costs, and it enables, at a stage at which full data are needed, the calculation of a basic model for setting priorities for maintenance and rehabilitation work.

The answers obtained by this method are reported elsewhere (*1*). The derivations and results were given in a detailed report recently presented to the Israeli DPW (*2*). Because other authorities are also to be found at the stage before a full pavement management system (PMS) it will prove helpful to present the findings of the general models developed in this study.

NATURAL DETERIORATION CURVE

The deterioration curve of the pavement condition constitutes the key to any study dealing with the economic and engineering aspects of the maintenance of a given road system.

Transportation Research Institute, Technion-Israel Institute of Technology, Haifa 32000, Israel.

In Israel, the two parameters that show this condition are:

1. Distress grade (SN) from 1 to 5, or from a perfect condition of no surface cracks or other distress modes to a state of surface distress of great intensity; and
2. Level-of-service grade (PSI) from 5 to 0, or from best condition in terms of riding quality to a state of complete failure.

These two grades make up the overall pavement grade (PR) according to the following relationships, based on the PMS program of the state of Washington (*3*). Thus,

$$PR = DR \times RR$$
$$= (125 - 25SN)(1.06 - 0.30/PSI^{1.06}) \qquad (1)$$

where DR is the grade for a condition of pavement distress, from 100 (excellent condition) to 0 (worst condition), and RR is the grade for the ride quality of the pavement surface, from 1 (excellent quality) to 0 (worst quality).

The transitional expression from SN to DR, which expresses a simple linear transition, was empirically proven, whereas the transitional expression from PSI to PR was computationally derived.

Translation of the SN and PSI grades into the PR grade enables the use of the natural deterioration equation, that is, with no routine maintenance treatment of the Washington State program. In Israel, these PR statistics were in effect for one measurement year, 1985. It was necessary, therefore, to construct a single deterioration curve for the whole system, as follows:

$$PR = 100 - 0.25A^{2.301} \qquad (2)$$

where *A* is the number of years since the construction or rehabilitation of the pavement. This curve is based on the data analysis and on practical considerations for which a new pavement deteriorates to a grade of 50 PR after 10 years, or in other words for which the need for overlaying is manifested after 10 years of service.

DETERIORATION CURVE UNDER ROUTINE MAINTENANCE

In order to determine the economic advantages of a policy of routine maintenance, the effect of this policy on the natural deterioration curve must be known. This effect is derived from

a differential equation on the basis of data previously published [4,5]. From numerical integration of this differential equation, the following results were obtained (see Figure 1):

$$(PR)_m = 100 - 0.356A^{1.99} \tag{3}$$

$$(A_{50})_m = (A_{50}) \times 1.2 \tag{4}$$

$$(A_0)_m = (A_{50}) \times 1.7 \tag{5}$$

where

$(PR)_m$ = pavement condition grade for a pavement receiving routine maintenance;
$(A_{50})_m$ = time in years to reach $(PR)_m = 50$ in a pavement that is treated by routine maintenance;
$(A_0)_m$ = time in years to reach $(PR)_m = 0$ in a pavement that is treated by routine maintenance; and
A_{50} = time in years for reaching $PR = 50$ in an unmaintained pavement.

In Figure 1, Curve 1 is the natural deterioration curve, Curve 2 is the retarded deterioration curve as a result of routine maintenance operation, and Curve 3 is the retarded determination curve as a result of deferment of routine maintenance for d years. The effect on the deterioration curve of deferred routine maintenance can be found in the same way [i.e., the values of $(A_{50})_{md}$ and $(A_0)_{md}$ shown in Figure 1].

DETERIORATION CURVE FOR A REHABILITATED PAVEMENT

The deterioration curve of a rehabilitated pavement is naturally conditional on the following factors: the deterioration curve of the pavement before its rehabilitation, the pavement
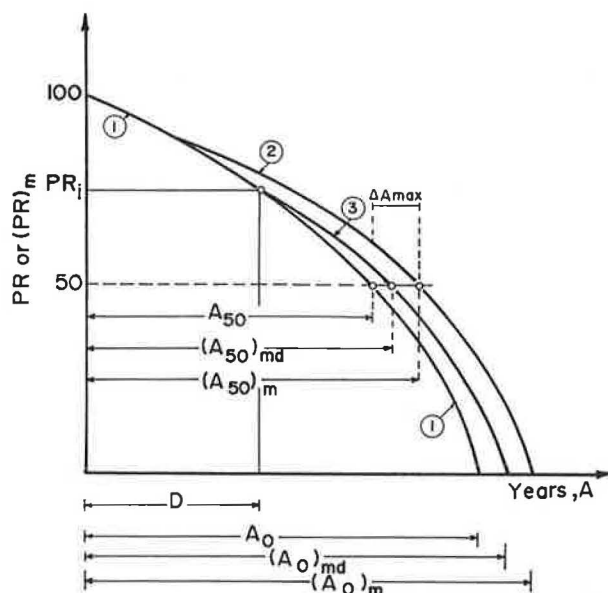

FIGURE 1 Deterioration curves as a result of immediate implementation of routine maintenance or as a result of deferment of routine maintenance work (2).

grade at the time of the rehabilitation work, and the rehabilitation solution itself. Generally, when rehabilitation is carried out with the pavement reaching a grade of $PR = 50$ or more, the rehabilitation is manifested in asphaltic overlaying at a thickness of d_a. For these cases, the deterioration curve for a rehabilitated pavement can be expressed as

$$(PR)_R = 100 - 0.25 A_R q_R \tag{6}$$

$$q_R = (\log 200)/[\log F + \log (A50)] \tag{7}$$

$$F = 0.20 + 0.16 d_a \tag{8}$$

where

$(PR)_R$ = the grade of the condition of the rehabilitated pavement;
A_R = the time, in years, since the last rehabilitation work; and
d_a = the asphaltic overlaying thickness, in centimeters.

Equation 6 is based on the assumption that an overlaying of 5 cm of asphalt renews the pavement to its starting condition, (i.e., $F = 1$, thus A_{50} for the rehabilitated pavement is equal to that for the original pavement). This condition happens only when the overlaying is carried out above the $PR = 50$ boundary line.

In pavements for which overlaying is undertaken at less than this value, an identical deterioration curve to that expressed in Equations 6 through 8 will be obtained, except for the relationship between d_a and F. Clearly, when the 5-cm overlaying, for example, is done after the pavement has deteriorated below $PR = 50$, this work cannot renew the pavement to its original condition, but only to a state in which F is smaller than 1. Rehabilitation of a condition in which $PR = 0$ necessitates an overlaying thickness of about three times the value required, had the rehabilitation been carried out at $PR = 50$ to attain the same operational level. The value of F in this condition is given by the following expressions:

$$F = 0.20 + \frac{0.16 \times 0.8}{Y}\left[(d_a)_e - 25\left(1 - \frac{Y}{0.8}\right)\right] \tag{9}$$

$$Y = 1 - 0.000\,406(100 - PR)^{1.585} \tag{10}$$

where $(d_a)_e$ is the overlaying thickness in centimeters, in cases for which $PR < 50$ (as opposed to the thickness of d_a for which $PR > 50$), and Y is the relative decline in the bearing capacity value of the pavement from a grade of $PR = 50$ (for which $Y = 0.8$), down to a grade of $PR = 0$ (for which $Y = 0.4$). Naturally, when $P = 100$, $Y = 1.0$.

Finally, the combination of routine maintenance work and overlaying leads to a deterioration curve that is calculated in accordance with the principles presented in this section.

AGENCY AND USERS' COSTS

To conduct economic and budgetary calculations, it is essential to know the agency and users' costs. The agency costs are

the total expenditures for the routine maintenance and rehabilitation work, and for the traffic delay caused by construction. On the other hand, the differences in the road users' costs (before and after upgrading) are the benefits gained from investment in the maintenance and rehabilitation work.

The examination of the agency's costs for various overlaying and rehabilitation work in Israel led to the relationship, shown in Figure 2. In Figure 2, the cost of the overlay is given by $C_a = 7.0 \times 1,000 (2.0 + 1.6 d_a)$ and $\$1 = 1.6\text{NIS}$. In Israel, the road user costs, which depend on the condition of the pavement, are found to stem principally from operating costs. The cost of the value of time is calculated only for professional drivers (about 40 percent of those on the road), and therefore this cost can be disregarded. For the same reason, the traffic delay time caused by construction is also disregarded. Operating cost was analyzed from various studies (2), and its value in Israeli prices was determined as

$$C_u = 2.455(\text{AADT}/1,000)I \tag{11}$$

$$I = 130.41 - 0.604\text{PR} + 0.000\ 018\ 5\text{PR}^3 \tag{12}$$

where

C_u = daily (varying expenses only) operating cost of all vehicle types per 1-km trip in NIS;

AADT = average daily traffic volume (both directions); and

I = operating cost index (varying expenses only).

PURPOSIVE MODEL FOR SETTING PRIORITIES

The various models that have been presented enable an examination of the purposive model for setting priorities in under-
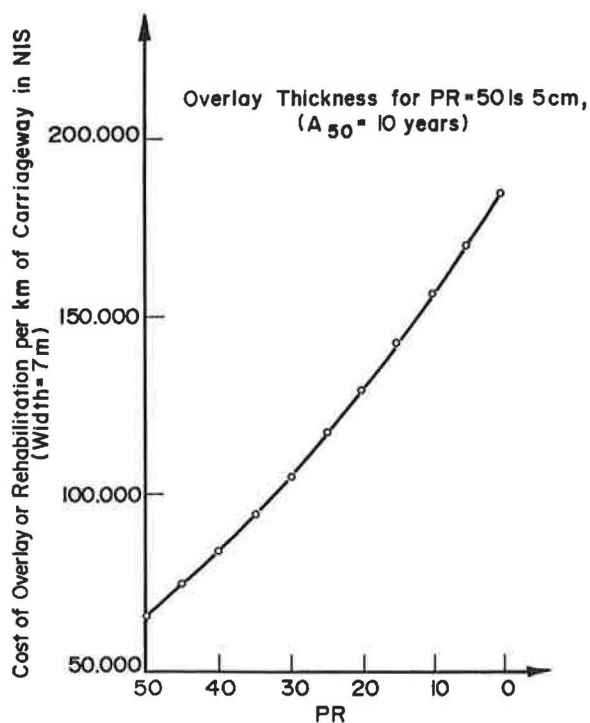

FIGURE 2 Relationship between pavement condition and the cost of overlay or rehabilitation C_a (2).

taking road maintenance and rehabilitation. This model must include the DR and RR grades or, alternatively in Israel, the SN and PSI grades, together with AADT, which is the traffic intensity traversing the given road. To find such a model, it is necessary to decide on the economic factor that dictates this order of priorities. In Israel, this factor is generally the first year rate of return (P percent) obtained for the given rehabilitation investment. Calculation of this rate of return for 1,219 additions of SN, PSI, and AADT through the available models led to the following regression expression (with coefficient R^2 equals to 0.76):

$$P\% = k \times \text{SN}^{3.72} \times (5 - PSI) \times (\text{AADT}/1,000) \tag{13}$$

The order of priorities is clearly set according to the P percent values computed from Equation 13 in which k is a numerical constant, the same for all cases. At the top of the priority list is found the project for which the P percent value is the highest. The striking feature of this order of priorities is the effect that AADT values have on P percent values. For example, for identical PSI values, a project with AADT = 10,000 and SN = 3 will have a priority identical to another project with AADT = 5,000 only when SN = 4. This means that roads with high traffic intensities supplant roads with lower intensities even when the condition of the latter is significantly worse. Furthermore, roads with low traffic intensities will be found in general at the bottom of the list of priorities, even when their condition is one of complete failure.

SUMMARY AND CONCLUSION

Various general models have recently served engineering economic studies for determining the efficacy of road maintenance of the interurban road network in Israel. These general models contain the deterioration curve for the following road conditions: without any maintenance at all, with only routine maintenance work, and after rehabilitation, with or without routine maintenance. This last condition depends on the PR value at the time of the rehabilitation work, which is manifested in the deterioration curve. In addition to this model, other models were presented, such as preparation and overlaying costs, routine maintenance costs, and of course, the road users' costs, depending on their PR values. These models can serve other agencies at their work in PMS phases before complete data are available.

The models mentioned herein enable, after the determination of an overlaying policy, the establishment of a purposive model for computing an order of priorities for carrying out the various maintenance projects. The model obtained was found to be affected mainly by the AADT value.

ven Yom-Tov and Eugen Stanescu. The authors thank these participants.

REFERENCES

1. M. Livneh, J. Craus, B. Ellenbogen, P. Thompson, R. Yom-Tov, and E. Stanescu. Economic-Engineering Survey of the Efficacy of Investing in the Maintenance of Interurban Road Network in Israel. *Proc., 11th IRF World Meeting*, Seoul, Korea, 1989.
2. B. Ellenbogen. *Pavement Management System—Stage A: Economic Engineering Survey of the Efficacy of Maintenance Investment of Interurban Road Network in Israel.* A report (in Hebrew) submitted to the Israeli Department of Public Works, L.C.I.- Transportation Engineering Consultants, Cambridge Systematics Inc., 1988.
3. T. L. Nelson and R. V. Leclerc. *Development & Implementation of Washington State's Pavement Management System.* Report WA-RD-50.1, Washington State Department of Transportation, 1983.
4. F. F. Humplick. *Predicting Pavement Expenditures in Highway Life Cycle Costing.* M.Sc. thesis, Massachusetts Institute of Technology, Cambridge, 1986.
5. M. J. Markow, R. Ramaswamy, and W. J. Renis. Optimal Maintenance and Rehabilitation Policies for Highway Pavements. Draft Report, Massachusetts Institute of Technology, Cambridge, 1986.